

# **The relationship between the adenovirus early region 1B55K (E1B55K) protein and the cellular DNA damage response**

*By*

**Tareq Mansour K. Abualfaraj**

A thesis presented to the College of Medical and Dental Sciences, the  
University of Birmingham, for the degree of Doctor of Philosophy

Institute of Cancer & Genomic Sciences

College of Medical and Dental Sciences

University of Birmingham

January 2023

UNIVERSITY OF  
BIRMINGHAM

**University of Birmingham Research Archive**

**e-theses repository**

This unpublished thesis/dissertation is copyright of the author and/or third parties. The intellectual property rights of the author or third parties in respect of this work are as defined by The Copyright Designs and Patents Act 1988 or as modified by any successor legislation.

Any use made of information contained in this thesis/dissertation must be in accordance with that legislation and must be properly acknowledged. Further distribution or reproduction in any format is prohibited without the permission of the copyright holder.

## ABSTRACT

Adenoviruses are members of the small DNA tumour virus family; there are more than 100 identified Human Adenovirus (HAdV) types which are assigned into 7 groups designated A to G. The adenoviral early region 1B55K (E1B55K) protein is essential for complete HAdV-mediated transformation of cells in culture and for efficient adenovirus replication. During infection, E1B55K forms a complex with early region 4 open reading frame 6 (E4orf6) protein; together they bind and target several cellular proteins, many of which are involved in the DNA damage response (DDR), for proteasomal-mediated degradation. This is the case for HAdV5 and HAdV12 although other HAdV types such as HAdV16 (group B), HAdV9 (group D), HAdV4 (group E), and HAdV40 (group F) do not cause degradation of many of the same proteins. Most previous research has focused on the activities of the HAdV5-E1B55K protein during viral infection while in collaboration with E4orf6 and functioning as part of the E3 ubiquitin ligase. Here, we examined effects of E1B55K both as part of the E3 ligase and in isolation. Furthermore, we have concentrated on the properties of the group A, B, D, E, and F E1B55K proteins rather than HAdV5. Initially, we confirmed the interactions between HAdV5-E1B55K, and proteins previously identified as part of mass spectroscopy screens and showed that some, but not all, are degraded during viral infection. We have further shown binding of the same proteins to HAdV12-E1B55K, although degradation during infection was more limited. Novel association of HAdV12-E1B55K with replisome components has also been demonstrated. In the second part of the study, we have confirmed that HAdV12-E1B55K can induce genome instability in human fibroblasts in the absence of any other viral proteins. We investigated the effects of HAdV12-E1B55K protein on the DNA damage response (DDR) and

on genomic stability, using human skin fibroblasts (HSF) expressing only HAdV12-E1B55K (55K<sup>+</sup>HSF). Our results show that HAdV12-E1B55K interferes with DNA replication dynamics, seen as a significant increase in stalled forks and R-loops, both of which are indicative of increased replication stress. We have also demonstrated that HAdV12-E1B55K expression sensitises cells to genotoxic agents, as shown by an increase in DNA damage foci formation and ATM activation. Furthermore, our findings are in line with previous observations which indicated that HAdV12 induces genomic instability in human cells, represented by an increase in chromosomal breaks. We hypothesise that interactions of HAdV12-E1B55K with different DDR and replication complex proteins is responsible for majority of these effects. Similarly, the expression of E1B55K protein from groups B, D, E and F HAdVs increased genomic instability in human tumour cells, seen as an increase in micronuclei formation. The viral proteins from these HAdV types associate with several homologous recombination DNA damage repair components, although with a limited effect, compared to HAdV12. Additionally, we have shown that HAdV-E1B55K from group B, D, E and F inhibits DNA double strand break repair as seen by the increased DNA damage repair foci after induced DNA damage. Using proteomic analysis, we have also identified novel E1B55K-interacting cellular substrates that bind these viral proteins, although the significance of these interactions is yet to be determined.



## **ACKNOWLEDGMENTS**

I would like to take this opportunity to offer my sincere thanks and appreciation to my supervisor, who has also been a great friend to me during my PhD, Dr. Roger Grand, for the guidance, encouragement, and helpful recommendations that he had provided me throughout the years of my study. I deeply appreciate his vast knowledge and experience, and I can honestly say that I have gained a lot of insight from him. I am thankful for his kindness, helpful nature and being there for me in the times of need. He constantly reminded me that I can do it and believed in me, I cannot be more thankful to have him as a supervisor.

Also, a very special thank you goes out to Prof. Grant Stewart for his insightful guidance and constructive conversations while I was pursuing my PhD. In addition, I would want to express my sincere gratitude to my coworker Nafiseh Hagkarim, whose scientific experience and continuous encouragement was invaluable to me, particularly when I worked in the lab, as well as supporting me and my wife throughout our journey during pregnancy. I also express a tremendous amount of gratitude to Taibah University as well as the Ministry of education in Saudi Arabia for providing me with this chance to pursue my studies to become a scientist and for providing me with financial assistance.

I am also immensely grateful to every member of the Stewart group, specially Satpal Jhujh, who was always there to provide me with advice and shared his knowledge with me while performing experiments and while writing my thesis.

Having the opportunity to pursue a PhD has been a remarkable adventure to me. My abilities have grown over the course of four years of hard work, not only as a scientist but also in life

in general, and I could not have arrived at this day and gained all this without the support of my family; they have been there for me from the very beginning of this journey. My most profound and heartfelt thanks, as well as my profound and genuine appreciation, for their love and support. I will never be able to adequately convey my heartfelt gratitude to my parents, and siblings for the endless love they have shown me, the emotional support they have provided me with, and the encouragement they have given me when times have been tough.

Finally, I would like to dedicate this work to my other half and spouse, Hala Khalil. Sincerity compels me to admit that I am unable to adequately convey in words the immense gratitude I feel toward her for the endless support that she provided me during the ups and downs of my PhD journey. Thank you, my lovely wife.

## PUBLICATIONS, CONFERENCES AND PRESENTATIONS

- **Abualfaraj, T.;** Grand, R.J. (2022). The effects of Human adenovirus early region 1B 55K protein (HAdV-E1B55K) on the cellular genome stability in the absence of protein degradation. Poster session presented at the DNA Tumour Virus conference 2022. The University of Cambridge, UK.
- **Abualfaraj, T.;** Hagkarim, N.C.; Hollingworth, R.; Grange, L.; Jhujh, S.; Stewart, G.S.; Grand, R.J. The Promotion of Genomic Instability in Human Fibroblasts by Adenovirus 12 Early Region 1B 55K Protein in the Absence of Viral Infection. *Viruses* **2021**,13,2444. [https://doi.org/ 10.3390/v13122444](https://doi.org/10.3390/v13122444).
- **Abualfaraj, T.;** Grand, R.J. (2021). The role of the Adenovirus 12 E1B55K protein as a cause of genetic instability in human cells. Oral presentation at the Annual ICGS PGR Festival 2021. The University of Birmingham, UK.
- **Abualfaraj, T.;** Grand, R.J. (2020). The role of the early region 1B55K protein in group B, D and E adenovirus infection. Oral presentation at the Annual ICGS PGR Festival 2020. The University of Birmingham, UK.

# TABLE OF CONTENTS

<b>CHAPTER 1: INTRODUCTION .....</b>	<b>21</b>
<b>1.1 DNA TUMOUR VIRUSES .....</b>	<b>22</b>
<b>1.2 ADENOVIRUSES.....</b>	<b>24</b>
1.2.1 Identification and classification.....	24
1.2.2 Clinical significance.....	26
1.2.3 Structure and genome.....	28
1.2.4 Cellular entry and replication.....	33
<b>1.3 ADENOVIRUS EARLY REGION PROTEINS.....</b>	<b>37</b>
1.3.1 Adenovirus early region proteins.....	37
1.3.1.1 Early region 1A (E1A) proteins.....	38
1.3.1.2 Early region 1B (E1B) proteins.....	42
1.3.1.2.1 Structure of E1B55K.....	45
1.3.1.2.2 The post-translational modifications of E1B55K.....	46
1.3.1.2.3 The role of E1B55K in cellular transformation.....	48
1.3.1.2.4 The role of E1B55K during viral infection.....	53
1.3.1.3 Early region 4 (E4) proteins.....	55
<b>1.4 DNA DAMAGE RESPONSE, DNA REPAIR AND REPLICATION STRESS .....</b>	<b>58</b>
1.4.1 Cell cycle checkpoints.....	58
1.4.1.1 The G <sub>1</sub> checkpoint.....	60
1.4.1.2 The S phase checkpoint.....	61
1.4.1.3 The G <sub>2</sub> /M checkpoint.....	62
1.4.2 Cellular DNA damage response.....	63
1.4.2.1 The ATM kinase pathway and double strand break repair.....	64
1.4.2.2 The ATR kinase pathway.....	66
1.4.3 DNA damage repair and genome integrity.....	68
1.4.3.1 Double-strand breaks repair.....	68
1.4.3.1.1 Non-Homologous End-Joining (NHEJ).....	69
1.4.3.1.2 Homologous Recombination (HR).....	70
1.4.4 DNA replication.....	73
1.4.4.1 DNA replication initiation and origin licensing.....	73
1.4.4.2 DNA replication stress.....	75
1.4.4.2.1 Stalled fork stabilisation.....	77
<b>1.5 ADENOVIRUSES AND THE DNA DAMAGE RESPONSE.....</b>	<b>80</b>
1.5.1 E1B55K/E4orf6-mediated regulation and degradation of DDR components during HAdV infection.....	81
1.5.1.1 Regulation of p53 during HAdV infection.....	83
1.5.1.2 Regulation of the ATM signalling pathway during HAdV infection.....	90
1.5.1.3 Regulation of the ATR signalling pathway during HAdV infection.....	92
1.5.1.4 Regulation of the DNA-PK pathway during HAdV infection.....	93
1.5.1.5 Degradation of additional proteins during HAdV infection.....	95
1.5.2 Relocalisation and inhibition of DDR proteins.....	96

1.5.3 Potential HAdV substrates not degraded by the E1B55K/E4orf6 complex. ....	100
<b>1.6 HYPOTHESIS AND AIMS .....</b>	<b>102</b>
<b>CHAPTER 2: MATERIALS AND METHODS.....</b>	<b>103</b>
<b>2.1 CELL CULTURE TECHNIQUES.....</b>	<b>104</b>
2.1.1 Human cell lines. ....	104
2.1.2 Cell culture media.....	105
2.1.3 Maintenance of human cell lines. ....	105
2.1.4 Cryopreservation of human cell lines. ....	105
<b>2.2 CELL BIOLOGY TECHNIQUES.....</b>	<b>106</b>
2.2.1 HAdV types. ....	106
2.2.2 Viral infections.....	106
2.2.3 Transfection of HeLa cells with siRNA. ....	107
2.2.4 Transient DNA transfections. ....	108
2.2.5 Irradiation of cells with ionising radiation. ....	109
2.2.6 Drug treatments and cytotoxic agents.....	109
2.2.7 Buffer recipes. ....	110
2.2.8 DNA fibre assay. ....	110
2.2.9 Metaphase spreads. ....	111
<b>2.3 PROTEIN BIOCHEMISTRY .....</b>	<b>112</b>
2.3.1 Whole cell lysate preparation. ....	112
2.3.2 Bradford assay (Protein determination). ....	113
2.3.3 SDS-Polyacrylamide Gel Electrophoresis (SDS-PAGE). ....	114
2.3.4 Electrophoretic transfer of proteins. ....	115
2.3.5 Preparation of proteins for Mass Spectrometry. ....	115
<b>2.4 IMMUNOCHEMISTRY TECHNIQUES.....</b>	<b>116</b>
2.4.1 Antibodies .....	116
2.4.2 Western blotting. ....	116
2.4.3 Co-immunoprecipitation assay. ....	120
2.4.4 Subcellular Chromatin Fractionation (SCF) assay.....	120
2.4.5 Immunofluorescence microscopy. ....	121
2.4.6 Immunostaining of DNA fibres. ....	122
2.4.7 R-loops analysis. ....	122
<b>2.5 MOLECULAR BIOLOGY TECHNIQUES .....</b>	<b>123</b>
2.5.1 Media preparation for bacterial growth. ....	123
2.5.2 Bacterial transformation. ....	123
2.5.3 Maxi-Prep plasmid DNA purification.....	124
<b>2.6 STATISTICAL ANALYSIS .....</b>	<b>125</b>
<b>CHAPTER 3: IDENTIFICATION OF MULTIPLE HUMAN ADENOVIRUS EARLY REGION 1B55K- INTERACTING PROTEINS DURING ADENOVIRUS 12 AND 5 INFECTIONS.....</b>	<b>126</b>
<b>3.1 Introduction.....</b>	<b>127</b>
<b>3.2 Results.....</b>	<b>131</b>

3.2.1 HAdV5 and HAdV12 E1B55K bind novel DDR and pre-replication complex proteins. ....	131
3.2.2 HAdV-mediated degradation of novel cellular targets during HAdV5 and HAdV12 infections. ....	136
<b>3.3 Discussion.....</b>	<b>140</b>
<b>CHAPTER 4: THE PROMOTION OF GENOMIC INSTABILITY IN HUMAN FIBROBLASTS BY ADENOVIRUS 12 EARLY REGION 1B55K PROTEIN IN THE ABSENCE OF VIRAL INFECTION</b>	<b>144</b>
<b>4.1 Introduction.....</b>	<b>145</b>
<b>4.2 Results.....</b>	<b>149</b>
4.2.1 Expression of HAdV12-E1B55K in human skin fibroblasts. ....	149
4.2.2 Genomic instability is induced by the expression of HAdV12-E1B55K in human skin fibroblasts. ...	151
4.2.3 HAdV12-E1B55K causes genomic instability as indicated by the formation of chromosomal gaps, breaks and radials in human skin fibroblasts. ....	154
4.2.4 HAdV12-E1B55K causes DNA replication stress, increased fork stalling, and decreased efficiency of replication fork restart in HSFs. ....	156
4.2.5 HAd12-E1B55K expression increases R-loop formation in HSFs.....	159
4.2.6 HAdV12-E1B55K affects DNA repair foci formation in HSFs after DNA damage. ....	161
4.2.7 HAdV12-E1B55K co-localisation with DNA repair foci following induced DNA damage. ....	166
4.2.8 Expression of HAdV12-E1B55K interferes with DNA repair in HSFs during the G <sub>2</sub> phase. ....	168
4.2.9 HAdV12-E1B55K causes sensitisation of HSFs to DNA damaging agents. ....	171
4.2.10 Expression of HAdV12-E1B55K in HSFs influences the DSB repair pathways by inactivating the MRN complex. ....	175
4.2.11 The presence of HAdV12-E1B55K impacts the ability of HSFs to undergo cell cycle arrest in response to DNA damage.....	177
4.2.12 HAd12-E1B55K associates with cellular chromatin. ....	179
4.2.13 HAd12-E1B55K affects the expression levels of proteins involved in DNA replication and DNA repair pathways.....	181
4.2.14 Co-localisation of HAdV12-E1B55K with cytoplasmic structures in 55K <sup>+</sup> HSFs. ....	183
4.2.15 HAdV12-E1B55K does not form or co-localise to cytoplasmic aggresomes in HSFs.....	186
<b>4.3 Discussion.....</b>	<b>189</b>
<b>CHAPTER 5: THE EFFECTS OF GROUP B, D, E AND F ADENOVIRUS EARLY REGION 1B55K PROTEINS ON CELLULAR GENOME STABILITY AND THE DNA DAMAGE RESPONSE .....</b>	<b>197</b>
<b>5.1 Introduction.....</b>	<b>198</b>
<b>5.2 Results.....</b>	<b>201</b>
5.2.1 E1B55K from group B, D, E and F HAdV types causes genome instability in human tumour cells. ...	201
5.2.2 E1B55K from group B, D, E and F HAdV types affects DNA repair foci formation in HeLa cells after DNA damage.....	206
5.2.3 E1B55K from group B, D, E and F HAdV types has a limited effect on double strand break repair pathways. ....	212
5.2.4 E1B55K from group B, D, E and F HAdV types binds to DDR components in transfected HeLa cells. .....	216
5.2.5 Isolation and identification of potential proteins associated with E1B55K from group B, D, E and F HAdVs. ....	218
5.2.6 HAdV5/12 infections have no effect on UBR5 expression.....	223

5.3 Discussion.....	225
<b>CHAPTER 6: FINAL DISCUSSION .....</b>	<b>230</b>
6.1 Conclusions.....	231
6.1.1 Introduction.....	231
6.1.2 Regulation of DDR pathways proteins during HAdV5/12 infections. ....	234
6.1.3 The potential effects of HAdV12-E1B55K on DDR pathways, DNA repair and replication stress. ....	239
6.1.4 The potential roles of HAdV-E1B55K from groups B, D, E, and F in the DDR, DNA repair and replication stress. ....	245
6.2 Unanswered questions and future work .....	250
<b>REFERENCES .....</b>	<b>252</b>
<b>APPENDIX.....</b>	<b>285</b>
<b>ORIGINAL PUBLICATION .....</b>	<b>315</b>

## LIST OF FIGURES

<b>Figure 1.1.</b> Structural depiction of the HAdV virion. ....	31
<b>Figure 1.2.</b> Schematic representation of HAdV5 transcriptional map. ....	32
<b>Figure 1.3.</b> Overview of HAdV life cycle. ....	36
<b>Figure 1.4.</b> Linear schematic representation of HAdV-E1A functional domains and protein interaction motifs. ....	42
<b>Figure 1.5.</b> Linear schematic representation of HAdV5-E1B55K functional domains and protein interaction motifs, along with their biological functions. ....	46
<b>Figure 1.6.</b> Activation of different protein complexes in response to DNA damage and their roles in ATM, ATR, and DNA-PK pathways. ....	67
<b>Figure 1.7.</b> HR repair pathway. ....	72
<b>Figure 1.8.</b> Representative model of ubiquitylation and degradation of cellular substrates by the host E3 Cullin-5 ring ligase complex. ....	90
<b>Figure 1.9.</b> Regulation of ATM and ATR signalling pathways by HAdVs. ....	94
<b>Figure 3.1.</b> E1B55K co-immunoprecipitations with DDR proteins and pre-replication complex components. ....	135
<b>Figure 3.2.</b> Degradation of novel binding partners during HAdV5 and HAdv12 infections is dependent on cullin function. ....	139
<b>Figure 4.1.</b> The morphological appearance of parental HSFs and 55K <sup>+</sup> HSFs and the expression of HAdV12-E1B55K protein in 55K <sup>+</sup> HSF. ....	150
<b>Figure 4.2.</b> Micronuclei formation in HSFs and 55K <sup>+</sup> HSFs. HSFs and 55K <sup>+</sup> HSFs were subjected to DNA damaging agents. ....	153
<b>Figure 4.3.</b> 55K <sup>+</sup> HSFs metaphase spreads. ....	155
<b>Figure 4.4.</b> Expression of HAdV12-E1B55K in HSFs affects DNA replication dynamics. ....	158
<b>Figure 4.5.</b> Expression of HAdV12-E1B55K in HSFs increases R-loops formation. ....	160
<b>Figure 4.6.</b> DNA repair foci formation is influenced by the expression of HAdV12-E1B55K in HSFs. ....	165
<b>Figure 4.7.</b> HAdV12-E1B55K does not co-localise with DNA repair foci following induced DNA damage. ....	167



<b>Figure 4.8.</b> Expression of HAdV12-E1B55K interferes with DNA repair in HSFs during the G2 phase. ....	170
<b>Figure 4.9.</b> HAdV12-E1B55K sensitises HSFs to DNA damaging agents. ....	174
<b>Figure 4.10.</b> Mirin affects the formation of micronuclei and $\gamma$ H2AX foci in HSFs and 55K <sup>+</sup> HSFs. ....	176
<b>Figure 4.11.</b> The expression of cyclins in 55K <sup>+</sup> HSFs and HSFs in response to DNA damage..	178
<b>Figure 4.12.</b> The nuclear fraction of HAdV12-E1B55K localises to the chromatin in 55K <sup>+</sup> HSFs and HAdV12-E1HER2 cells. ....	180
<b>Figure 4.13.</b> Comparative analysis of the expression of selected proteins in HSFs and 55K <sup>+</sup> HSFs. ....	183
<b>Figure 4.14.</b> HAdV12-E1B55K co-localises with some DDR binding partners following DNA damage. ....	185
<b>Figure 4.15.</b> HAdV12-E1B55K does not co-localise with tubulins. ....	188
<b>Figure 5.1.</b> Micronuclei formation in the presence of HAdVs 16, 9, 4 and 40 E1B55K proteins. ....	205
<b>Figure 5.2.</b> DNA repair focus formation is influenced by the expression of E1B55K from group B, D, E and F HAdVs. ....	211
<b>Figure 5.3.</b> The expression of E1B55K from group B, D, E and F HAdV types has no marked effects on the phosphorylation of HR pathway components. ....	215
<b>Figure 5.4.</b> E1B55K from group B, D, E and F HAdVs co-immunoprecipitate with some DDR and cellular proteins. ....	217
<b>Figure 5.5.</b> The expression of UBR5 in normally cycling and UBR5-depleted HeLa cells during wt HAdV5/12 infections. ....	224

## LIST OF TABLES

<b>Table 1.1.</b> Classification of human adenoviruses. ....	26
<b>Table 1.2.</b> Summary of HAdV early region proteins and their biological functions. ....	37
<b>Table 2.1.</b> List of human cell lines used throughout this study. ....	104
<b>Table 2.2.</b> List of siRNAs used in this study. ....	107
<b>Table 2.3.</b> List of DNA plasmids used throughout this study. ....	108
<b>Table 2.4.</b> List of cytotoxic agents used throughout this study. ....	109
<b>Table 2.5.</b> List of buffers used throughout this study. ....	110
<b>Table 2.6.</b> List of reagents used in polyacrylamide gel recipe. ....	114
<b>Table 2.7.</b> List of primary antibodies used throughout this study. ....	119
<b>Table 2.8.</b> List of secondary antibodies used throughout this study. ....	119
<b>Table 3.1.</b> Summary of HAdV5-E1B55K and HAdV12-E1B55K interactions with DDR components and their degradation patterns. ....	143
<b>Table 5.1.</b> Mass spectrometry analysis of proteins immunoprecipitating with E1B55K from HAdVs 16 (group B), 9 (group D), 4 (group E) and 40 (group F). ....	220

## LIST OF ABBREVIATIONS

53BP1	p53-binding protein 1
9-1-1	Rad9-Rad1-Hus1
AAV	Adeno-associated virus
AAV2	Adeno-associated virus 2
ADP	Adenovirus death protein
AdPol	Adenovirus DNA polymerase
ALCAM	Activated leukocyte cell adhesion molecule
APS	Ammonium Persulphate
ATCC	American Type Culture Collection
ATF	Activating transcription factor
ATM	Ataxia telangiectasia mutated
ATR	Ataxia telangiectasia and Rad3-related protein
ATRIP	ATR-interacting protein
BAK	BCL2 antagonist killer
BAX	BCL2-associated X
BLM	Bloom syndrome protein
BRCA1	Breast cancer type 1 susceptibility protein
BRCA2	Breast cancer type 2 susceptibility protein
BrdU	Bromodeoxyuridine
BRK	Baby rat kidney cells
BSA	Bovine serum albumin
C-terminal	Carboxy-terminal
CAR	Coxsackievirus and adenovirus receptor
CBF/NF-Y	Heterotrimeric transcription factor
CDC25	Cell division cycle 25

CDC45	Cell division cycle 45
Cdc6	Cell division cycle 6
Cdc7	Cell division cycle 7
CDK	Cyclin dependent kinase
Cdt1	Cell division cycle 10-dependent transcript 1
CHK1	Checkpoint kinase 1
CHK2	Checkpoint kinase 2
CldU	5-chloro-2'-deoxyuridine
CPT	Camptothecin
CR	Conserved Region
CRL	Cullin-RING ligase
CtBP	C-terminal binding protein
CtIP	CtBP interacting protein
Cul	Cullin
D-loop	Displacement loop
DAPI	4', 6-diamidino-2-phenylindole
Daxx	Death domain-associated protein
DBP	DNA binding protein
DDK	Dbf4-dependent kinase (Cdc7-Dbf4)
DDR	DNA damage response
DMEM	Dulbecco's modified Eagle's medium
DMSO	Dimethyl sulphoxide
DNA	Deoxyribonucleic acid
DNA-PK	DNA-dependent protein kinase
DNA2	DNA replication helicase/nuclease 2
dNTPs	Deoxyribonucleotides
DSB	Double-strand break

dsDNA	Double-stranded DNA
E1A	Early region 1A
E1B	Early region 1B
E1B-AP5	E1B55K-associated protein 5
E2A	Early region 2A
E2B	Early region 2B
E2F	Activation transcription factor
E3	Early region 3
E4	Early region 4
E4orf3	Early region 4 open reading frame 3
E4orf6	Early region 4 open reading frame 6
EBV	Epstein-Barr virus
EXO1	Exonuclease 1
ECL	Enhanced chemiluminescence
FCS	Foetal calf serum
G1	Gap phase 1
G2	Gap phase 2
GADD45	Growth arrest and DNA damage inducible 45 alpha
H2A	Histone 2A family member
H2AX	H2A histone family member X
H2B	Histone 2B family member
H3K9me3	H3 at lysine residue 9
HAdV	Human adenovirus
HAdV12	Human adenovirus type 12
HAdV16	Human adenovirus type 16
HAdV4	Human adenovirus type 4
HAdV40	Human adenovirus type 40

HAdV41	Human adenovirus type 41
HAdV5	Human adenovirus type 5
HAdV9	Human adenovirus type 9
HAT	Histone acetyltransferase
HBV	Hepatitis B virus
HCl	Hydrochloric acid
HCV	Hepatitis C virus
HEK	Human Embryonic Kidney cells
HER	Human Embryo Retinoblasts
HHV6B	Human herpesvirus 6B
HNRPU	Heterogeneous nuclear ribonucleoprotein U-like
HPV	Human papillomavirus
HR	Homologous recombination
HRP	Horseradish-peroxidase
HTLV-1	Human T-cell lymphotropic virus 1
HU	Hydroxyurea
IdU	5-iodo-2'deoxyuridine
IF	Immunofluorescence
IP	Immunoprecipitation
IR	Ionising radiation
ITR	Inverted terminal repeats
KAP1	KRAB domain-associated protein
Kbp	Kilo base pair
kDa	Kilo-Dalton
KSHV	Kaposi's sarcoma-associated herpesvirus
Ku70/80	Lupus Ku autoantigen protein p70/p80
LB	Luria Broth

Lys	Lysine
M	Mitosis
MCM	Mini chromosome maintenance
mDa	Megadalton
MDC1	Mediator of damage checkpoint 1
MDM2	Mouse double minute 2
MHC	Major histocompatibility complex
MLP	Major late promoter
MOI	Multiplicity of infection
MRE11	Meiotic recombination 11
MRN	MRE11-Rad50-NBS1
mRNA	Messenger ribonucleic acids
MTOC	Microtubule-organizing Centre
MUS81	Mus81 endonuclease homologue
NBS1	Nibrin
NEDD8	Neural precursor cell-expressed developmentally down-regulated 8
NES	Nuclear Export Signal
NF1	Nuclear factor 1
NF2	Nuclear factor 2
NHEJ	Non-homologous end-joining
NLS	Nuclear localisation signal
NRS	Nuclear retention signal
NTR	N-terminal region
ORC	Origin recognition complex
ORF	Open reading frame
pfu	Plaque forming unit
PARP	Poly (ADP-ribose) polymerase

PBS	Phosphate buffered saline
PCNA	Proliferating cell nuclear antigen
PFA	Paraformaldehyde
PI3K	Phosphoinositide 3-kinase
PML-NBs	Promyelocytic Leukaemia Nuclear Bodies
PP2A	Protein phosphatase 2A
pRB	Retinoblastoma protein
pre-RC	Pre-replication complex
PTM	Post Translational Modification
RBX1	RING-box Protein 1
RFB	Replication fork barrier
RNA	Ribonucleic acid
RNF8	RING finger protein 8
RNP	Ribonucleoprotein
RNR	Ribonucleotide reductase
ROS	Reactive Oxygen Species
RPA1	Replication Protein A 1
SD	Standard Deviation
SDS-PAGE	Sodium Dodecyl Sulphate polyacrylamide gel electrophoresis
siRNA	Small-Interfering RNA
SMC1	Structural maintenance of chromosomes protein 1A
SP1	Specificity protein 1
SSB	Single-strand break
ssDNA	Single-stranded DNA
SUMO	Small ubiquitin-like modifier
SV40	Simian virus 40
TAB182	Tankyrase 1 binding protein 1



TBST	Tris-buffered saline
TEMED	N, N, N', N' -tetramethylethylenediamine-1,2-diamine
Tip60	HIV-1 tat interacting protein 60kDa
TOPBP1	Topoisomerase II binding protein 1
TOPI	Topoisomerase I
Ub	Ubiquitin
USF	Upstream stimulatory factor
USP	Ubiquitin-Specific Protease
UTB	Urea-Tris HCl- $\beta$ -mercaptoethanol
VRC	Viral Replication Centre
wt	Wild Type
WB	Western blot
XRCC3	X-ray repair cross-complementing 3
XRCC4	X-ray repair cross-complementing 4
XRCC6	X-ray repair cross-complementing 6
$\gamma$ H2AX	H2AX phospho-serine 139

# **CHAPTER 1**

## **Introduction**

## 1.1 DNA TUMOUR VIRUSES

It has been a century since ground-breaking investigations showed that a 'filterable agent' was capable of causing sarcomas in chickens. Yet, it took a long time for researchers to demonstrate that this was the Rous sarcoma virus (RSV), an avian retrovirus and to understand the significance of this finding (Rous, 1911). Since then, several DNA viruses from the families Adenoviridae, Herpesviridae, Papillomaviridae, and Polyomaviridae have also been demonstrated to cause tumours in humans or other mammals, and by doing so, have proven to be important tools in the comprehension of tumour biology (Javier and Butel, 2008). It should be emphasised that, in 2018, around 2.2 million incidences of cancer, or 13% of all cancer cases worldwide, were caused by infectious agents, such as the human papillomavirus (HPV), human T-cell lymphotropic virus 1 (HTLV-1) retrovirus, hepatitis B and C viruses (HBV and HCV), the Epstein-Barr virus (EBV), and the Kaposi's sarcoma-associated herpesvirus (KSHV) (de Martel *et al.*, 2020). Although certain adenovirus species cause tumours in newborn rodents (group A viruses) or mammary tumours in mice (HAdV9) they have never been associated with tumours in *Homo sapiens*.

*In vivo*, DNA viruses may transform primary cells into neoplastic forms through a multiphase process that can take many years to complete. Similarly, these viruses, or their DNA, can transform mammalian and in most cases human cells in the laboratory. Characteristic morphological and growth alterations, including lack of contact inhibition, decreased adhesion, a need for less serum, disruption of the cytoskeleton, and immortalisation, are observed in the transformed cells (Hanahan and Weinberg, 2000). These changes are passed down heritably from parental to daughter cells to create an altered immortal, transformed

population or gives rise to a tumour *in vivo*. The fundamental mechanism of transformation frequently entails the integration of viral DNA into the cellular genome, where it either results in the permanent expression of early oncogenic viral genes (viral oncogenes) or activates nearby cellular oncogenes, disrupting the normal cellular gene expression and signal transduction pathways. The capacity of most DNA tumour viruses to block the inhibition of cell replication imposed by cellular tumour suppressors such p53 and the retinoblastoma gene product (pRB), as well as genetic, immunological, and environmental variables all contribute to this (Ludlow and Skuse, 1995; Hanahan and Weinberg, 2000). It is not surprising that DNA tumour viruses have been used experimentally to characterise the crucial molecular processes that take place during tumorigenesis given that p53 and pRB are the most often disrupted regulatory pathways in human cancer (Berk, 2005).

DNA tumour viruses have been used for the past four decades to investigate the molecular mechanisms of cell transformation and tumour development. These investigations have produced ground-breaking discoveries about the control of the cell cycle, transcription, and DNA replication (Javier and Butel, 2008). The discovery of p53 using Simian virus 40 (SV40)-transformed murine cells and the roles of pRB through its interactions with the HAdV early region 1A (E1A) gene product may be two of the most significant discoveries associated with DNA tumour viruses (Lane and Crawford, 1979; Linzer and Levine, 1979; Whyte *et al.*, 1988). However, a very important point which soon became apparent in these studies, was that all the 'small DNA tumour viruses' (Adenoviruses, Human Papilloma viruses and Polyoma viruses) inactivated or usurped the same cellular targets, such as p53, the Rb family of proteins and p300/CBP histone deacetylases. The mechanisms by which the other viruses which can cause human tumours (or transform human cells) vary. This is to be expected as they have

fundamental differences-HTLV-1 is a retrovirus and like HCV (an RNA virus) has a very small genome encoding just a few proteins whereas the Herpesviruses (EBV and KSHV) are much more complex expressing over 100 viral genes.

## **1.2 ADENOVIRUSES**

### **1.2.1 Identification and classification.**

The Human Adenoviruses (HAdVs) are a family of non-enveloped, double-stranded DNA (dsDNA) viruses with an icosahedral nucleocapsid and a small linear genome of approximately 36 Kbp. They were first described in 1953 by Rowe and colleagues as an unknown agent that provoked spontaneous impairment and destruction of adenoid gland tissue obtained from children, and as such they were termed “Adenoids degenerating agents” (Rowe *et al.*, 1953). Later, in 1954, Hilleman and Werner acquired an identical agent from tracheal cells of military personnel suffering from acute respiratory disease and they called it “RI-67”. Eventually, the two agents were shown to be related and were subsequently named “Adenovirus” (Hillman and Werner, 1954). Interest in HAdVs has grown ever since, especially when Trentin and colleagues determined that HAdV type 12 (HAdV12) possessed the ability to induce tumour formation in new-born rodents (Trentin, Yabe and Taylor, 1962). As a result, this was the first example of a human virus that causes cancer. Since their discovery, HAdVs have often been used as tools for studying molecular and cellular biology properties of normal and neoplastic human cells such as, cell cycle control, DNA replication and transcription, cellular transformation, and tumorigenesis. More importantly, HAdVs are now considered as the most widely used viral vectors for gene therapy, accounting for more than 18% of all viral

vectors used in gene therapy clinical trials with promising potential in vaccine development as well as, oncolytic therapy (Gao, Zhang and Ehrhardt, 2020).

HAdVs belong to the Mastadenovirus genus, one of the five recognized genera of the Adenoviridae family. Until recently, more than 103 HAdVs types have been identified and these were assigned into 7 species designated A to G (Table 1.1) (Gao, Zhang and Ehrhardt, 2020). Different types were originally classified on the basis of their hemagglutination and neutralization reactions. The agglutination of erythrocytes is inhibited using antibodies known to be designated to the same viral type but not by antisera against other types. Currently, genomic sequencing and bioinformatic analysis have become the gold standard of subclassifying new HAdVs types (Mennechet *et al.*, 2019).

HAdV5 and HAdV12 from groups C and A, respectively, are amongst the most extensively studied HAdVs. HAdVs are non-tumorigenic in humans; however, in tissue culture, it was shown that DNA from the non-oncogenic HAdV5 has the ability to transform human embryonic kidney cells (HAdV5-E1HEK293) (Graham *et al.*, 1977) and the oncogenic HAdV12 can transform human embryonic retinal cells (HAdV12-E1HER) (Byrd, Brown and Gallimore, 1982).

Group	Types	Target tissue	Tumorigenicity in new-born rodents	Tissue culture transformation
A	12, 18, 31, 61	Gastrointestinal tract	High	+

B	3, 7, 11, 14, <b>16</b> , 21, 34, 35, 50, 55, 66, 68, 72, 79	Lungs, Urinary tract, Eyes	Moderate	+
C	1, 2, <b>5</b> , 6, 57	Lungs, Eyes	Low/None	+
D	8, <b>9</b> , 10, 13, 15, 17, 19, 20, 22-30, 32, 33, 36-39, 42-49, 51, 53, 54, 56, 58-60, 62-65, 67, 69, 70, 71, 73-75, 81, 83-85, 90	Gastrointestinal tract, Eyes	Low/None	+
E	<b>4</b>	Lungs, Eyes	Low/None	+
F	<b>40,41</b>	Gastrointestinal tract	Unknown	+
G	52	Gastrointestinal tract	Unknown	Unknown
Unspecified	76-78, 80, 82, 86-89, 91-103	-	-	-

**Table 1.1.** Classification of human adenoviruses. HAdVs identified to date are classified into 7 groups (A-G). Their oncogenicity in new-born rodents, target tissue tropism and tissue culture transformation capability are indicated. Types used in this study are highlighted in red. An up to date list of all HAdVs is also found at (<http://hadvwg.gmu.edu>).

### 1.2.2 Clinical significance.

Clinically, different HAdV types have distinctive tissue tropisms that determine their pathogenicity and organ specificity (Ghebremedhin, 2014). HAdV groups B, C, D and E mainly cause ocular and respiratory symptoms such as, keratoconjunctivitis and pneumonia. Whereas groups G and F commonly produce gastrointestinal manifestations. Generally, HAdV viruses are transmitted via air droplets, faecal-oral route, contaminated surfaces and, less commonly, solid organ transplants. Infections are usually self-limited; however, they may cause serious complications depending on the immune status of the host. For instance, upper and lower respiratory infection may progress into acute respiratory distress syndrome (ARDS). Immunocompromised and organ transplant patients may also suffer from life-threatening disseminated infections (Radke and Cook, 2018). Recently, over one thousand healthy and

immunocompetent young children have been reported to suffer from severe acute hepatitis. A few fatalities have been reported, and a sizable percentage of the patients required liver transplants. Thus far, the majority of cases have been documented in the United Kingdom and North America, but it has also been reported in many other regions throughout the world. Surprisingly, most hepatitis-causing viruses, such as HBV and HCV have been ruled out. Nonetheless, most patients were found to be infected with adenovirus 41 (HAdV41). HAdV41 had not previously been linked to hepatitis and is usually thought to induce gastroenteritis in both immunocompetent and immunocompromised people (Grand, 2022). Adeno-associated virus 2 (AAV2) was found in virtually all patients in three recent investigations, along with HAdV types C and F and human herpesvirus 6B (HHV6B). It is still unclear how the hepatitis has arisen as AAV2 has, up to now, been considered harmless and no clinical have previously been linked to AAVs. It is possible that HAdV-41's tropism has changed, and its association with AAV2 may have a role in causing acute hepatitis in these individuals (Morfopoulou *et al.*, 2022; Ho *et al.*, 2023; Servellita *et al.*, 2023). All AAVs require a 'helper' virus in order to replicate and it is assumed that HAdVF41 (or HHV6B) provides this function in the infected children. It has also been suggested that because of 'COVID-19 lock-down' the children have not been exposed to the normal range of viruses and have, therefore, not developed the immunity that would previously been expected. Although the outbreak appears to be subsiding now, further work is needed to understand how two viruses, which have not been linked to liver disease, appear to have caused hepatitis in children (Grand, 2022).



### 1.2.3 Structure and genome.

HAdVs are about 70-100 nm in diameter with a molecular weight of approximately 150 Megadaltons (mDa). They are composed of two major components, the capsid and the core. The icosahedral capsid enclosing the virion consists of 252 capsomers of which, 240 are hexons (II), while 12 are pentons (III) dispersed around the summits of the icosahedron. Additionally, there are four minor structural proteins (IIIa, VI, VIII and IX) associated with the capsid and they are thought to provide structural integrity (Saban *et al.*, 2006). Small fibres (IV) are formed of rods which protrude from each of the 12 pentons, terminating in a knob-like structure. They mainly contribute to the binding of the virus to host cell receptors, which initiates infection (Brenner and Horne, 1959; Valentine and Pereira, 1965; Norkin, 2010). Interestingly, the variability between fibre knob proteins contributes to the hemagglutinating properties for each type, and this was previously used as the method of choice to distinguish different species *in vitro* (Russell, 2009; Mennechet *et al.*, 2019). The core consists of the viral genome and five proteins: V, VII, Mu, terminal protein and protease p23 (Figure 1.1). The core proteins are essential for efficient and stable viral infection (Norkin, 2010). Different viral types have distinctive inverted terminal repeat (ITR) sequences capping each end of DNA strands, and these are thought to associate with terminal proteins and act as primers for genomic replication (Rekosh *et al.*, 1977).

HAdVs have linear double stranded DNA formed of approximately 36 Kbp. The genome is organised into three regions which are expressed in a time-regulated manner as early, intermediate, and late regions, with multiple open reading frames (ORF's) encoding about 40 gene products (Figure 1.2). The transition from early to late region expression is dependent

on the commencement of DNA strand replication. The early region (E) genes are transcribed from five distinctive promoters (E1A-E1B-E2-E3-E4) into a set of a regulatory proteins, which are expressed before viral DNA replication. They mainly contribute to establishment of viral infection and facilitation of viral genome replication. For instance, expression of E1A gene begins after 6 to 8 hours of infection, and this, in turn, leads to the initiation of expression of other early region genes. The E1A protein inhibits cell-induced expression of interferons and limits the ability of the retinoblastoma family of proteins to control cell cycle progression, amongst other properties. E1B proteins (E1B55K and E1B19K) are the second proteins to be expressed after E1A; they are mainly responsible for suppressing the ability of tumor suppressor p53 and other cellular regulatory pathways to promote apoptosis induced by E1A. Additionally, E1B proteins are responsible for down-regulation of numerous cellular proteins through ubiquitin-proteasomal degradation, leading to alteration in viral and cellular protein expression and abrogation of apoptosis enacted by DNA damage response (DDR). This degradation is essential for efficient viral replication (Debbas and White, 1993; Lowe *et al.*, 1994; Cuconati *et al.*, 2002) (See sections 1.3.1.1 and 1.3.1.2 for a detailed discussion on HAdV-E1 proteins). The early region 2 (E2) region encodes three proteins that are crucial for viral replication; the precursor terminal protein (pTP), the single-stranded DNA (ssDNA) binding protein (DBP) and the adenovirus DNA polymerase (AdPol) (Holm *et al.*, 2002). The early region 3 (E3) region encodes multiple proteins that are primarily involved in immunomodulation and evasion of the host immune system. Principally, this is achieved by restricting antigen presentation of infected host cells through the binding of protein gp19k to MHC I particles and thus, protecting the primed cell against recognition by CD8<sup>+</sup> cytotoxic T lymphocytes (Wold, Tollefson and Hermiston, 1995). Furthermore, the E3 region encodes

adenovirus death protein (ADP); a protein that facilitates cytolysis and mature virion release (Tollefson *et al.*, 1996). The early region (E4) gene encodes multiple orf's (orf1, orf2, orf3, orf3/4, orf4, orf6 and orf6/7) through alternative splicing. E4-expressed proteins interact with various cellular proteins involved in DNA replication, transcriptional regulation, DDR and oncogenic transformation (See section 1.3.1.3 for a detailed discussion on HAdV-E4 proteins) (Nevels *et al.*, 2001; Tauber and Dobner, 2001; Ou *et al.*, 2012). Interestingly, E4orf6 was shown to interfere with cellular DDR proteins, such as the MRE11-Rad50-NBS1 (MRN) complex, by facilitating their proteasomal degradation in collaboration with E1B55K during HAdV infection (Berk, 2005). As such, specific attention is given to explain the role of these two proteins in the following sections.

Intermediate genomic region is expressed from two different transcriptional units (IX-Iva2), and they mainly control the transcriptional transition between early and late genomic regions by activating the two Major Late Promotor (MLP). In contrast, late region is transcribed from a single MLP after viral DNA replication, which transcribes into five late pre-mRNA transcripts (L1-L2-L3-L4-L5). Each late transcript encodes several different structural proteins (hexons, fibres and pentons) and DNA binding proteins (V, VII and Mu) through alternative splicing and polyadenylation (Russell, 2000; Ryu, 2016).

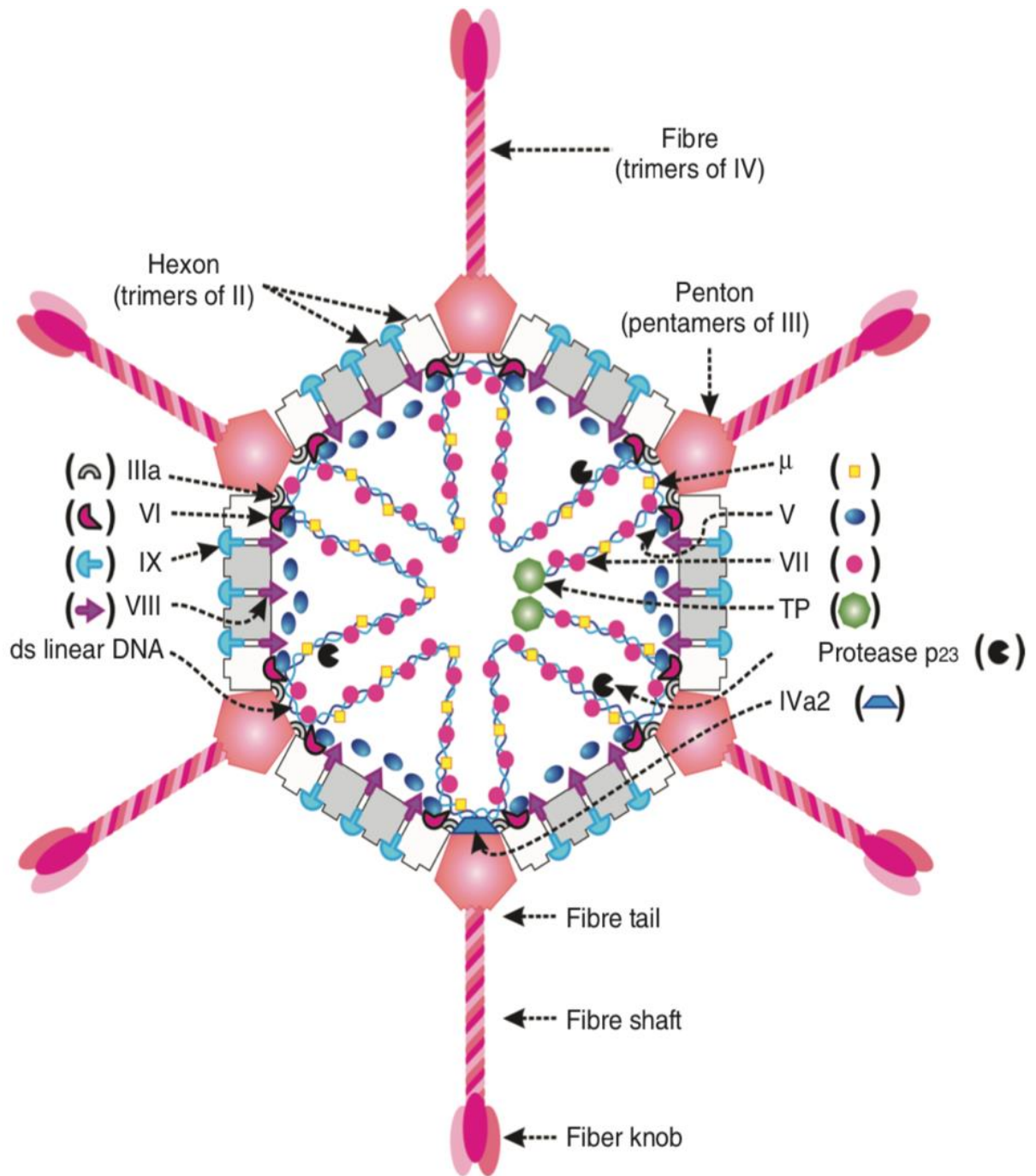


**Figure 1.1.** Structural depiction of the HAdV virion. The diagram depicts a cross section of the virion particle with capsid and core viral proteins. The dsDNA linear genome is also shown along with the core viral proteins associated with it. Taken from: (Echavarría, 2015).

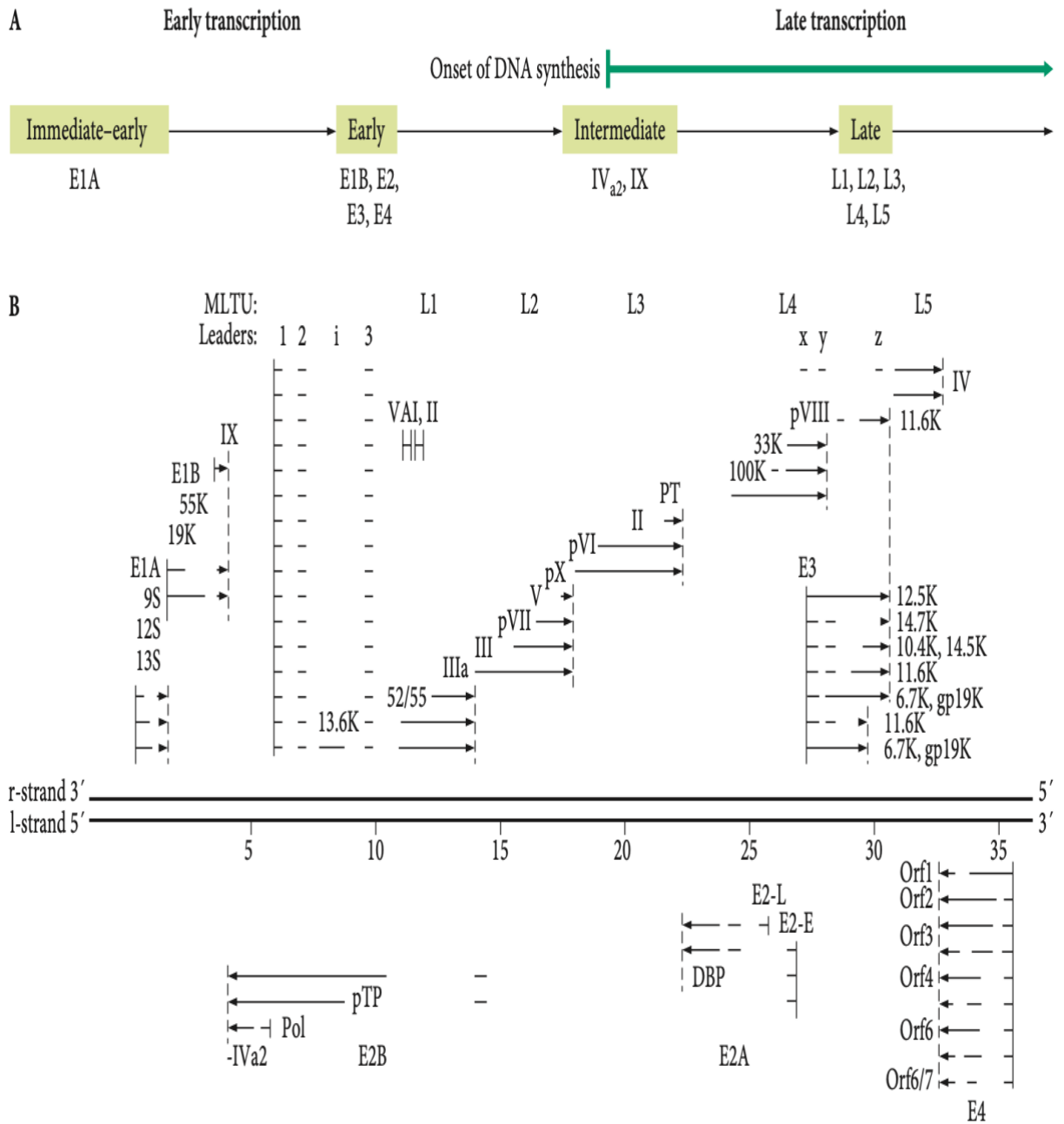


**Figure 1.2.** Schematic representation of HAdV5 genome and transcription map. (A) HAdV5 genome organisation and gene expression. (B) HAdV5 transcription map with introns indicated as gaps, individual mRNAs indicated as solid lines, and broken vertical lines indicate polyadenylation sites. The E1A, E1B, E2, E3, and E4 transcription units each have their own promoter. The E2 and E3 transcription units each have two alternative polyadenylation sites.

Five mRNA families, L1 through L5, are produced by the main late region. The same pre-mRNA serves as the processing source for all of the late mRNA families, which are all produced from the same promoter. Taken from: (Norkin, 2010)

#### 1.2.4 Cellular entry and replication.

The replication cycle of HAdVs involves viral-host cell attachment, entry by receptor-mediated endocytosis, endosomal escape by clathrin-dependent and dynamin-dependent endocytosis, dynein-mediated cytosolic transport of viral genomes to the nucleus, followed by viral gene expression, DNA replication and lytic viral release (Fig 1.3) (Luisoni and Greber, 2016).

The coxsackie-adenovirus receptor (CAR), which is expressed on epithelial cells, recognises the viral capsid fibre protein and allows the majority of HAdV species (A, C, D, E, and F) to enter the host cell (Ortiz-Zapater, Santis and Parsons, 2017), whereas group B HAdVs utilise CD46 (Marttila *et al.*, 2005), GD1a glycan (Nilsson *et al.*, 2011), Polysialic acid (Lenman *et al.*, 2018), and desmoglein-2 (Wang *et al.*, 2011) as cellular attachment receptors.

Following the binding of the penton base to  $\alpha v$ -integrin, entry into the cell is facilitated by Clathrin-dependent and dynamin-dependent endocytosis (Burckhardt *et al.*, 2011). Upon entry, uncoating of the capsid occurs via the viral p23 protein to release the virus particle into the cytosol through acidic endosomes, which is eventually transported to the nucleus, utilising the dynein-mediated cytosolic apparatus. p32 is part of the cellular machinery for transporting proteins that shuttle between the cytoplasm and the nucleus. Thus, it is hijacked by the virus in order to facilitate transportation of the virus particles towards the nucleus (Matthews and

Russell, 1998). Subsequently, the viral genome is imported into the host nucleus through special nuclear pore complexes and expression of early and late region genes then occurs (Shenk, 2001).

The replication of HAdV DNA commences approximately 6-8 hours post infection by the binding of pTP and Adv Pol to the ITR's *ori* sequence in each strand and using pTP as a Primer in a process called "Protein-priming" (Friefeld *et al.*, 1984; de Jong, van der Vliet and Brenkman, 2003). This progresses with the aid of two host cell transcription factors; the nuclear factor 1 (NF-I) and the octamer binding protein 1 (OCT-1), which associate with the TP-Adv Pol complex and the *ori* sequences. The nascent DNA synthesis then proceeds from the 5' to 3' direction and the non-template strand becomes disjointed and covered with the DBP. Correspondingly, Nuclear factor II (NF-II), which is a host cellular topoisomerase, is utilized to subdue the supercoiling of the DNA template and promote double strand elongation (Hoeben and Uil, 2013). The ITRs at each end of the strands are displaced to form a "panhandle" that simulates the end of a double stranded DNA; therefore, it may serve as a template sequence to initiate a new cycle of viral DNA synthesis. Eventually, during the termination of viral DNA replication, the pTP is cleaved at two sites by viral proteases, yielding a stable version of terminal protein (TP) and generation of viral DNA to be packaged in the nuclear matrix during final virion maturation. Interestingly, TP is covalently attached to the 5' end of viral DNA during genome replication to prevent the newly synthesised DNA from unfolding, thus protecting it from exonuclease activity and enhance its association with nuclear matrix (Dunsworth-Browne, Schell and Berk, 1980; Stillman *et al.*, 1981; Schaack *et al.*, 1990; Shenk, 2001).

The viral DNA replication process is accompanied by the expression and transcription of the intermediate (IX-lva2) and late (L1-L5) genes. This is necessary to synthesise structural proteins that are utilised in packaging virion particles, which is followed by cell lysis using the virally encoded adenovirus death protein (ADP) and the release of mature virions (Tollefson *et al.*, 1996; Echavarría, 2015). Indeed, it is crucial for HAdVs to avoid cellular antiviral responses by disrupting and controlling many cell-cycle checkpoints, modifying expression of various genes, and inhibiting apoptosis in order to achieve efficient replication and produce potent viral progeny. This is accomplished by several viral defensive strategies that will be addressed later in this chapter, with emphasis on the DDR (See section 1.5).





## 1.3 ADENOVIRUS EARLY REGION PROTEINS

### 1.3.1 Adenovirus early region proteins.

The following section will mainly describe the functions of the E1A, E1B55K, as well as E4orf6 proteins. The roles of E1B55K, both in collaboration with E1A during HAdV-mediated cellular transformation, and with E4orf6 during HAdV infection will be described in greater depth. In addition, the interactions of the E1B55K protein with key cell-cycle regulatory checkpoints, as well as the effects it promotes in causing cellular growth dysregulation will be discussed. Major biological functions of HAdV early region proteins are summarised below (Table 1.2).

Early region protein	Function
12S and 13S E1A	Cellular transformation, transactivation of viral early region genes, induction of forced S phase entry, modification of cellular transcriptional activity
E1B19K and E1B55K	Viral protein synthesis, inhibition of p53-dependent apoptosis, oncogenic transformation, proteasomal-dependent degradation of cellular targets, promotion of late viral mRNA export
E2A and E2B	Viral DNA replication
E3Gp18K and E311.6K	Host immunomodulation
E4 open reading frames	Transcriptional regulation, promotion of late viral mRNA expression and transportation, Viral DNA replication, virion assembly, oncogenic transformation

**Table 1.2.** Summary of HAdV early region proteins and their biological functions. The table illustrates the biological functions of HAdV E1A, E1B, E2, E3 and E4 viral proteins. See text for more detailed discussion.

#### 1.3.1.1 Early region 1A (E1A) proteins.

E1A is the first adenoviral gene to be expressed after infection. Its transcriptional units encode the 12S, 13S, 11S, 10S and 9S proteins through differential splicing of mRNAs (Boulanger and Blair, 1991; Gallimore and Turnell, 2001). It has been established that E1A is not a DNA-binding protein and has no enzymatic activities (Yousef, Brandl and Mymryk, 2009); however, it interacts indirectly with the chromatin in a modular fashion by binding and altering distinct cellular targets in order to regulate and exert control over both cellular and viral gene expression. As a consequence, E1A conditions the cellular environment to ensure the progression of a complete and stable HAdV infection by modulating the expression of other viral genes. This induces the cell to enter a pseudo S-phase of the cell cycle and modifies its transcriptional activity (Gallimore and Turnell, 2001).

E1A also plays a crucial role in HAdV-mediated cell transformation. In particular, it was shown that E1As on their own from Adenovirus type 5 (HAdV5) and type 12 (HAdV12), have the ability to partly transform rodent cells in culture, usually leading to their death, probably through p53-dependent apoptosis. Whereas its cooperation with E1B proteins yields complete and immortal transformed cells; this is, at least partly, due to E1B's inhibition of E1A-induced apoptosis (Shiroki *et al.*, 1979; Houweling, Van Den Elsen and Van Der Eb, 1980; Gallimore *et al.*, 1985). In rare cases, HAdV5 and HAdV12 DNA fragments containing E1A and E1B together were shown to transform human cells in culture (Graham *et al.*, 1977; Byrd, Brown and Gallimore, 1982). However, an etiological oncogenic role of these proteins in human cell tumorigenesis has not been established (Ip and Dobner, 2019).

The molecular weight of E1A proteins, as determined by SDS-PAGE, ranges from 35-48 kDa, depending on the encoded protein and post-translational modification (PTM). The two predominant isoforms of HAdV5-E1A are the 12S and 13S proteins (encoding proteins that are 243 and 289 amino acids in size, respectively) (Boulanger and Blair, 1991). Both isoforms are transcribed at the beginning of infection and they carry out most of E1A's known functions (Perricaudet *et al.*, 1979). Comparison of amino acid sequences of E1A proteins in different HAdV types shows the presence of four highly functional conserved regions (CR); CR1, CR2, CR3 and CR4, along with a less conserved N-terminal region (NTR) (Fig 1.4). These regions have been shown to be the primary interaction sites for most of the cellular targets. Indeed, both isoforms of the protein were shown to be identical, except for the presence of the CR3 region in the 13S E1A only, which functions as a transcriptional activator. On the other hand, 12S E1A possess only the CR1, CR2 and CR4, and is thought to act as a transcriptional repressor (Boulanger and Blair, 1991). Other variants of E1A (11S, 10S and 9S) are transcribed during late stages of infection and their functions are less well understood (Miller *et al.*, 2012).

The CR3 functional domain in 13S E1A drives the expression of other viral early region proteins and exhibits most of its functions as a transcriptional activator by modulating the cellular and viral transcriptional machinery through protein-protein interactions with their distinct promoters. The CR3 transactivation domain in HAd5V-E1A acts as a transcriptional activator for other early region promoters during HAdV infection, which encodes their gene products that perform essential functions necessary for viral replication, including suppressing the immune response, transporting viral mRNA and inhibiting premature apoptosis (Blackford and Grand, 2009; Pelka *et al.*, 2009). Studies have shown that the CR3 in HAdV5 consists of two important regions: a zinc finger motif that interacts with transcriptional regulators, and a

carboxyl region which facilitates the promoter-targeting capacity of E1A with distinct transcription factors (Webster and Ricciardi, 1991). The transcriptional activation capacity of zinc finger region resides in its ability to associate with MED32/Sur2 mediator complex subunits, TBP general transcription factor, CBP/p300 and PCAF transcriptional co-activators as well as, 19S, 20S and 26S proteasomes (Berk, 2005). Whilst the carboxy-terminal region mediates E1A interactions with several transcriptional factors such as, the TBP-associated factors (TAFs), activating transcription factors 1-3 (ATF1-3), upstream stimulatory factor (USF), the heterotrimeric transcription factor (CBF/NF-Y) and the specificity protein 1 (SP1) (Gallimore and Turnell, 2001; Berk, 2005).

One of the primary functions of E1A is to reprogramme cellular gene expression to promote cell cycle progression into the S-phase which initiates viral DNA synthesis in quiescent cells. The CR1, CR2 and NTR domains, present in both 12S and 13S E1A species, were shown to be required for inducing the entry of cells into the S-phase through short motif molecular recognition features (MoRFs) that direct E1A to interact with various cellular proteins. For instance, CR1 and CR2 are responsible for the activation of E2 transcription factor (E2F) dependent transcription by binding the retinoblastoma (pRB) protein tumour suppressor, along with p107 and p130 related proteins. This stimulates E2F-dependent transcription of E2 viral gene through HAdVE1A-mediated displacement of the pRB complex from E2F and induction of cell cycle progression into S-phase (DeCaprio, 2009). Whereas CR1 and NTR dependent binding to cellular histone acetyltransferases (HATs), such as CBP/p300, results in remodelling of histone acetylation (Howe *et al.*, 1990; Eckner *et al.*, 1994; Berk, 2005). It has been shown that E1A is involved in chromatin remodelling by binding and redistributing the CBP/p300 to distinct genomic loci during HAdV infection to enhance the acetylation of pRB

and modulate the H3K18 histones (Ferrari *et al.*, 2014). This causes the pRB at amino acids K873/874 to acetylate chromatin repressive enzymes and, in turn, represses the transcription of cellular genes that would otherwise inhibit productive viral replication and viral-induced cellular transformation (Jelsma *et al.*, 1989; Horwitz *et al.*, 2008). The roles of E1A binding proteins in HAdV-mediated cellular transformation will be considered later in more detail (See section 1.5.1.1).

The C-terminal region of E1A encompasses the CR4 functional domain which is encoded by the second exon of E1A and resides between the 240-288 amino acid residues (Yousef, Brandl and Mymryk, 2009) (Fig 1.4). CR4 exerts its roles by interacting with Carboxyl-terminal binding corepressors (CtBP-1, 2 and 3) through the PxDLS motif. CtBPs are known to associate with histone deacetylases (HDACs) and act as transcriptional repressors in a manner opposite to p300/CBP, to repress E1A's transcriptional activity. Interestingly, it was shown that acetylation of the 12S E1A protein by p300/CBP occurs adjacent to the consensus CtBP/PxDLS motif, which blocks transcriptional repression by disrupting E1A-CtBP complexes, resulting in disruption of repressor complexes in the cell and leading to gene activation (Zhang *et al.*, 2000).

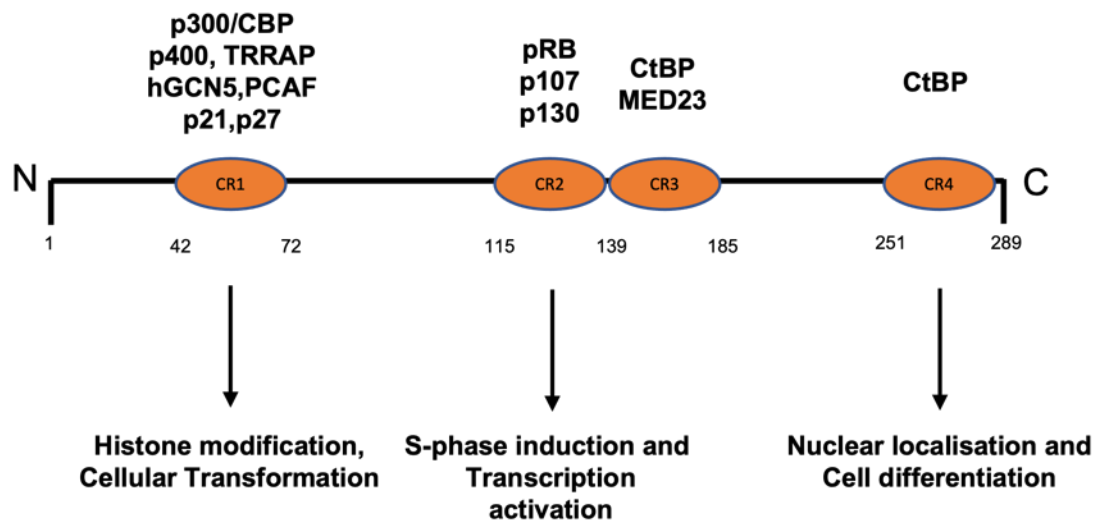


**Figure 1.4.** Linear schematic representation of HAdV-E1A functional domains and protein interaction motifs. Graphical representation of HAdV-E1A (13S variant) showing key binding proteins and their biological functions. Conserved regions (CR) are shown in orange circles. Adapted from: (Zheng, 2010).

### 1.3.1.2 Early region 1B (E1B) proteins.

Five genes are transcribed from the adenovirus early region 1B (E1B) by differential splicing; E1B-84R, E1B-93R, E1B-156R (E1B19K), E1B-176R, and E1B-496R (E1B55K), with E1B19K and E1B55K being transcribed from the same transcriptional unit but having different initiation codons and therefore different amino acid sequences. The two principal proteins that have been most widely investigated are the E1B55K and E1B19K, which were found to mainly function to inhibit cellular growth arrest, promote viral replication, and prevent premature apoptosis. The functions of other E1B splice variants remain largely unknown (Berk, 2005; Sieber and Dobner, 2007; Blackford and Grand, 2009).

The E1B19K shares amino acid sequence homology to the anti-apoptotic protein BCL-2. In infected cells, E1B19K counteracts the p53-induced apoptosis by imitating the action of MCL-1 through its binding to BAK/BAX oligomers irreversibly and keeping them inactive. Thus, it prevents mitochondrial pore formation and disrupts the activation of the caspase cascade, which forms the basis of the pro-apoptotic cellular pathway induced by E1A's stabilisation of p53 (Sundararajan and White, 2001; White, 2001).

The importance of the HAdV-E1B55K was brought to attention after it was found to interact with the tumour suppressor p53 in adenoviral transformed cells (Sarnow *et al.*, 1984). The protein binds p53, both during infection and transformation, and inhibits its transcriptional activation and causes its degradation during HAdV5 infection (Sarnow *et al.*, 1984; Yew and Berk, 1992). E1B55K impacts the host cell in several other ways. For instance, it complements the E1A-mediated cellular transformation by blocking E1A induced apoptosis, alters host cell proliferation by inducing host-cell shut off, as well as inhibiting cellular RNA export from the nucleus, while augmenting viral RNA export. Nonetheless, despite all the research conducted on E1B55K and its interactions with p53, relatively little is known about its association with other important cellular binding partners compared to E1A. Significantly, during HAdV infection, E1B55K collaborates with the E4orf6 protein to regulate host cell processes in favour of viral replication. In this regard, E1B55K is responsible for down-regulating numerous cellular proteins through proteasomal degradation by forming an E3 ubiquitin ligase complex with E4orf6, and the cellular protein Cullin (Cul2 or Cul5), Ringbox 1 (Rbx1) and Elongins B and C. The E1B55K and E4orf6 complex ubiquitinates specific antiviral targets to be degraded through ubiquitin-mediated proteolysis, where E1B55K serves as a substrate recognition unit while E4orf6 recruits the E3 ubiquitin ligase to E1B55K. Consequently, this leads to alteration



in viral and cellular protein expression, abrogation of apoptosis, and regulation of DDR and other cellular machinery in favour of viral replication (Blackford and Grand, 2009; Berk, 2013). It is also important to note that the E1B55K/E4orf6 complex ubiquitinates cellular targets which are not degraded (Herrmann *et al.*, 2020). This is considered in more detail in (Section 1.5.3). The complex also facilitates the transportation of late viral mRNA while inhibiting the translation and exportation of cellular mRNA (Querido, Blanchette, *et al.*, 2001; Harada *et al.*, 2002). Furthermore, it was reported that E1B55K requires E4orf6 for nuclear localisation and accumulation in cytoplasmic viral replication centres (VRC's) (Ornelles and Shenk, 1991). Interestingly, in the absence of E4orf6, E1B55K forms cytoplasmic aggresomes and acts as a co-operating oncogene, markedly increasing the frequency of transformation of cells (Gallimore *et al.*, 1985).

The cellular distribution of E1B55K protein varies throughout the viral replication cycle. Early during infection, HAdV5-E1B55K concentrates in cytoplasmic aggresomes and, as the infection progresses, it becomes readily distributed around the nucleus in association with ProMyelocytic Leukaemia Nuclear Bodies (PML-NBs) (Liu *et al.*, 2005). The perinuclear accumulation of E1B55K is thought to be linked to the expression of viral E4orf3 protein, which binds E1B55K and enhances its assembly in PML nuclear tracks and VRCs (Ornelles and Shenk, 1991). Interestingly, SUMOylation of E1B55K plays a role in its nuclear localisation, where it localises to VRCs with E4orf6 to be SUMOylated by E4orf3 SUMO E3-ligase during viral infection (Kindsmüller *et al.*, 2007).

#### 1.3.1.2.1 Structure of E1B55K.

Studies on HAdV5-E1B55K indicated that the protein has an elongated rather than a globular structure (Martin and Berk, 1998). However, no studies have demonstrated the exact modular structure of the protein although it is assumed to be highly structured. Due to its unpredictable shape, it is not clear whether E1B55K lacks distinctive structural domains; similarly, a delineation of specific binding sites for proteins is currently not possible. Additionally, further evidence that the protein may adopt a structured three-dimensional arrangement is based on the observations that it is susceptible to mutational inactivation. Thus, multiple small deletions or insertions into the protein render it incapable of binding either p53 or E4orf6, amongst other proteins, which might indicate that binding sites on the protein are composed of short sequences of amino acids dispersed over divergent areas. In contrast, E1A's modular shape allowed for its binding sites to be mapped precisely for protein partners (Pelka *et al.*, 2008). Interestingly, circular dichroism spectroscopy indicated that E1B55K is intrinsically disordered in the N-terminus (Sieber *et al.*, 2011). Sequencing of HAdV5-E1B55K revealed that it comprises a highly conserved cysteine and histidine zinc finger motif (C<sub>2</sub>H<sub>2</sub>) between amino acids 350-370, and a conserved hydrophobic centre between amino acids 215-345 that incorporates a ribonucleoprotein (RNP) binding motif, which was shown to interact non-specifically with viral RNA (Gonzalez and Flint, 2002; Tejera *et al.*, 2019). Nuclear export signal (NES) (amino acids 83-93), nuclear localisation signal (NLS) (amino acids 390-496), and C-terminal phosphorylation sites (serine 490,491 and threonine 495), were also reported as conserved sequences in HAdV5-E1B55K (Figure 1.5) (Hidalgo *et al.*, 2019; Tejera *et al.*, 2019). No evidence has demonstrated that any of the E1B55K interactions are enacted via its zinc finger motifs, although mutations in these regions may show some modifications

in substrate binding compared to the wild type (Blackford and Grand, 2009). Linear Schematic representation of E1B55K's functional domains is shown (Figure 1.5).

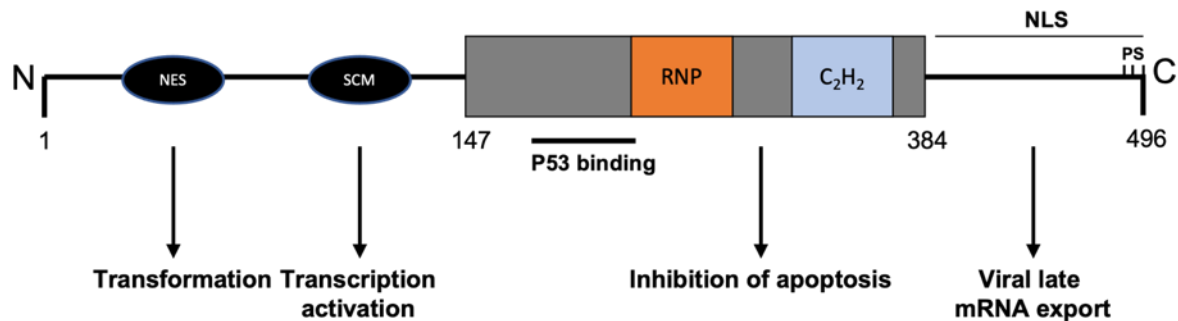


**Figure 1.5.** Linear schematic representation of HAAdV5-E1B55K functional domains and protein interaction motifs, along with their biological functions. The N-terminal nuclear export signal (NES) and SUMO conjugating motif (SCM), as well as the central region (amino acids 147-384) encompassing ribonucleoprotein (RNP) and C<sub>2</sub>H<sub>2</sub> zinc finger, are shown. Additionally, the C-terminal nuclear localisation signal (NLS) and the phosphorylation sites (PS) of Serine 490, Serine 491 and Threonine 495, are displayed. Adapted from: (Zheng, 2010; Hidalgo *et al.*, 2019).

#### 1.3.1.2.2 The post-translational modifications of E1B55K.

HAAdV5-E1B55K incorporates an intrinsic small ubiquitin-like modifier (SUMO) ligase activity, and it has been reported that the protein itself is SUMOylated at lysine 104 (Fig 1.5) (Endter *et al.*, 2001). This SUMOylation process conjugates SUMO modifiers to p53, which inhibits its activity. There are five SUMOs designated SUMO-1 to SUMO-5, where it was shown that SUMOs 1-3 attach covalently to a SUMO consensus motif ΨKXE-D, (where X is a random

residue and  $\Psi$  is a hydrophobic residue) (Härtl *et al.*, 2008; Wimmer *et al.*, 2013). HAdV5-E1B55K, but not HAdV12-E1B55K, is known to be SUMOylated and (post-translationally phosphorylated). As such further investigation is required to determine whether SUMOylation and phosphorylation are limited to certain HAdV types (Blackford and Grand, 2009).

A characteristic feature of HAdV5-E1B55K is shuttling between the nucleus and the cytoplasm, suggesting that the protein may be involved in late viral mRNA export from the nucleus through the chromosome region maintenance-1 (CRM-1) export pathway (Ornelles and Shenk, 1991; Dobbelstein *et al.*, 1997; Woo and Berk, 2007). After nuclear export of HAdV5-E1B55K, further degradation of p53 occurs (Muller and Dobner, 2008). However, an E1B55K protein with a mutated NES is expressed predominantly in the cytoplasm at perinuclear aggregates if the SUMO-1 conjugation is blocked. This may suggest that SUMOylation is of importance in directing *wt* HAdV5-E1B55K to shuttle between the cytoplasm and the nucleus independently of CRM-1 (Kindsmüller *et al.*, 2007). Thus, certain viral types like HAdV2 and HAdV5 that need their E1B55K to be transported to the nucleus, may require SUMOylation rather than other types. Significantly, it has been shown that SUMOylation of E1B55K induces its ability to localise p53 molecules to PML-NBs, leading to their successive deactivation (Pennella *et al.*, 2010). However, it is not yet well understood why some proteins bind to E1B55K independently of SUMO conjugation, even though protein conjugation may remarkably affect their localization (Sohn and Hearing, 2016). Nonetheless, evidence suggests that phosphorylation of E1B55K at its C-terminal region is required for SUMOylation (Kindsmüller *et al.*, 2007; Wimmer *et al.*, 2013). Additionally, it has been established that E4orf6 regulates E1B55K's SUMOylation, as it was shown that cells infected with an E4orf6 mutant virus have more SUMOylated E1B55K than cells that had been infected with the *wt*.

This reflects the importance of SUMOylation to E1B55K and the important role it might exert on the protein's binding affinity to different molecules and its ability to localise different virally encoded proteins and to mislocalize cellular proteins (Lethbridge, Scott and Leppard, 2003).

HAdV5-E1B55K is also post-translationally modified by phosphorylation at both threonine 495 and serines 490-491. In this regard, it was shown that mutation of serine 490-491 had a substantial negative impact on the potency of viral replication and on the efficiency of rodent cell transformation (Teodoro *et al.*, 1994). Additionally, these mutations affected the capability of the E1B55K protein to impede p53 transactivation (Querido *et al.*, 1997). As such, when threonine 495 and serine 490-491 were mutated *in vitro*, E1B55K failed to inhibit the p53-mediated apoptosis induced by E1A, as well as losing its capability to bind p53 and other known binding proteins, although its binding to E4orf6 was still possible (Schwartz *et al.*, 2008).

#### **1.3.1.2.3 The role of E1B55K in cellular transformation.**

Much of the interest in HAdVs, from a scientific point of view, stems from the early observations that group A viruses can cause tumours in new-born rodents (Trentin, Yabe and Taylor, 1962; Yabe, Trentin and Taylor, 1962; Huebner *et al.*, 1963). In these experiments, the whole virus was injected into the animals. However, in later experiments tumorigenicity was evaluated after introduction of transformed cells into the syngeneic host. Significantly, in immunocompetent animals, cells transformed with HAdV5-E1 region did not produce tumours, whereas those transformed with HAdV12-E1 were tumorigenic, consistent with the earlier experiments using 'whole' *wt* virus (A. E. Freeman *et al.*, 1967; McAllister *et al.*, 1969;

Gallimore, 1972; Mak *et al.*, 1979). Expression of HAdV-E1A in the transformed cells is essential for their tumorigenicity but this is enhanced by expression of E1B19K and to a greater extent by E1B55K (Houweling, Van Den Elsen and Van Der Eb, 1980; Van Den Elsen, Houweling and Van Der Eb, 1983; Gallimore *et al.*, 1985). In immunocompromised animals, HAdV5-E1 transformed cells will form tumours as will the HAdV12 equivalents. Interestingly, HAdV5-E1A, together with HAdV12-E1B expressing cells are as tumorigenic as HAdV12-E1 transformants when injected into athymic nude mice (Bernards *et al.*, 1982; Bernards, Schrier, Bos, *et al.*, 1983). It has been concluded on this basis that group A viral E1B55K proteins have properties not manifested in group C virus proteins, which contribute markedly to tumour formation. (This is discussed in detail, in relation to my data, in chapter 4).

In a more detailed analysis, it was shown that HAdV12-E1A was also important in determining the oncogenicity of transformed rat cell lines. In a study using chimeric HAdV5-E1A and HAdV12-E1A genes, it was found that cell lines were non-tumorigenic when transformed by E1A genes consisting of the N-terminal 80 amino acids from HAdV12 with the remainder from HAdV5. However, cell lines transformed by HAdV12-E1A sequences from the N-terminus to the CR3, or beyond, were tumorigenic. The region of HAdV12-E1A from amino acids 123-148, which is absent in non-oncogenic viruses has been termed the 'oncogenic spacer'. Although it has been shown that this region in HAdV12-E1A is essential to produce tumours in rodents, a further sequence at the N-terminus of the protein is also required (Jelinek and Graham, 1992; Jelinek, Pereira and Graham, 1994; Telling and Williams, 1994; Williams *et al.*, 1995).

An explanation for the ability of HAdV12 to cause tumours resides in its ability to downregulate cell-surface MHC I level in transformed rat and human cells (Bernards, Schrier,

Houweling, *et al.*, 1983; Schrier *et al.*, 1983; Eager *et al.*, 1985; Vaessen *et al.*, 1986). It appears that the HAdV12 13S-E1A can reduce mRNA levels of the class I heavy chain gene whereas the HAdV5 protein cannot. HAdV12-E1A also represses transcription of the transporters associated with class I antigen processing 1 (TAP1) and TAP2, as well as the proteasome-associated latent membrane proteins 2 (LMP2) and 7 (LMP7) (Rotem-Yehudar *et al.*, 1996).

Early studies determined that the E1 region from several HAdV types has the ability to transform baby rat kidney (BRK) and other rodent cells in culture (Yabe, Trentin and Taylor, 1962; Huebner *et al.*, 1963). Additionally, it was shown that human embryo cells could also be transformed by HAdV12-E1 and HAdV5-E1 regions DNA, although these were rare events when compared to rodent cell transformation (Graham *et al.*, 1977; Byrd, Brown and Gallimore, 1982; Whittaker *et al.*, 1984). The target cells in these experiments appear to all be of neuronal origin. More recently, a study have shown that human mesenchymal stem cells (hMSCs) derived from amniotic fluid are transformed by HAdV5-E1A/E1B oncogenes in a manner that is both reproducible and as effective as primary rodent cultures (Speiseder *et al.*, 2017). Abortive infection is associated with highly efficient transformation of nonpermissive rodent cells, suggesting that this may be a factor in the failure of many attempts to transform primary human cells in culture with HAdVs. However, compared to rodent cells, the efficiency with which human cells may be transformed by sub-genomic viral DNA fragments is quite low. This suggests that variations in permissivity to viral growth may not be the primary deciding factor in transformation efficiency (Graham, 1984; Endter and Dobner, 2004). Human embryo retinoblast (HER) cells (Fallaux *et al.*, 1996), human embryo kidney (HEK) cells (Graham *et al.*, 1977), human embryonic lung (HEL) cells (Van den Heuvel *et al.*, 1992), and amniotic fluid cells (AFC) (Speiseder *et al.*, 2017) are among the few main human cell types that have been

effectively transformed by HAdV12 and HAdV5 DNA fragments in culture. However, only AFC and HER are capable of undergoing transformation in an efficient and reproducible manner, but to a lesser extent than embryonic or kidney cells derived from rodents. It is not yet understood what the molecular foundation is for the disparities in the efficiency of transformation across the different kinds of primary human cell lines.

Transformation assays have shown that transformation of BRK cells was less efficient when E1A was expressed with either of the E1B proteins (E1B55K or E1B19K) rather than when the entire E1 region was expressed, suggesting that E1B55K has an imperative role in cellular transformation in addition to its antiapoptotic functions (Bernards *et al.*, 1986). Significantly, complete transformation of human cells is only possible if the entire E1 region proteins are present (Byrd, Brown and Gallimore, 1982). As stated earlier in section 1.3.1.1, E1A induces the cell cycle progression into a pseudo-S-phase, which promotes premature cellular apoptosis in the absence of the E1B cooperating oncogene. Evidence shows that the expression of the tumour suppressor gene p14<sup>ARF</sup> could be induced by HAdV-E1A (de Stanchina *et al.*, 1998). The expression and upregulation of p14<sup>ARF</sup> leads to the inhibition of the p53-antagonist Mdm-2, which promotes the stabilisation of p53 and mediates the subsequent activation of its downstream effectors, resulting in cellular apoptosis (Pomerantz *et al.*, 1998). The E1A oncogenic capacity to induce host cell transformation is due to its ability to associate with CBP/p300 and pRB family of proteins, as mutagenic studies have shown that E1A mutants are defective in causing transformation when they were not able to bind these proteins and coactivators (Jelsma *et al.*, 1989; Rasti *et al.*, 2005). Moreover, In order to influence cellular transformation, CR4 regulatory domain, located at the C-terminal of E1A, had been shown to associate with the CtBP co-repressor, DCAF7, and the dual specificity



tyrosine phosphorylation regulated kinase 1 (DYRK1A) (Schaeper *et al.*, 1995; Turnell *et al.*, 2000; Glenewinkel *et al.*, 2016). Furthermore, E1A was shown to promote cellular transformation through its interactions with chromatin modulators TRRAP and p400 through its N-terminal domain (Deleu *et al.*, 2001; Chan *et al.*, 2005).

Early studies on HAdV5 indicated that its ability to transform mammalian cells is dependent on the introduction of DNA fragments that incorporate the whole E1 region (Gallimore, Sharp and Sambrook, 1974; Graham, Van Der Eb and Heijneker, 1974). Indeed, later it was confirmed that, in addition to E1A, complete rodent cell transformation relied upon the presence of the E1B transcriptional units; E1B55K and E1B19K (Gallimore *et al.*, 1985). However, very occasional transformants were obtained after transfection of E1A alone although it seems likely they these cells have an additional mutation probably in p53 (Finlay, Hinds and Levine, 1989). In these experiments a limited number of transformants were obtained which expressed E1A and E1B19K; these cells were considered not to be fully transformed (Jones, 1990).

Expression of the complete HAdV-E1 region proteins was required to transform HER cells (Byrd, Brown and Gallimore, 1982; Whittaker *et al.*, 1984; Gallimore, Grand and Byrd, 1986). In this regard, inhibiting p53 activity and preventing premature cellular apoptosis were thought to be the key functions of the E1B proteins in cellular transformation, with E1B55K being able to associate directly with p53 and promote its transcriptional deactivation (Sarnow *et al.*, 1982), which depends on the HAdV type (Yew and Berk, 1992; Martin and Berk, 1998). While E1B19K, a homologue to the BCL-2 family of anti-apoptotic regulatory proteins, impairs p53 dependent and independent cell cycle arrest by preventing the activation of the caspase-

9 and caspase-3 cellular apoptotic pathways induced by E1A stabilisation of p53 (Sundararajan and White, 2001).

#### **1.3.1.2.4 The role of E1B55K during viral infection.**

The roles performed by the E1B55K protein during HAdV infection have been characterised mainly using HAdV5 as a model. Nevertheless, it appears that most of its functions are conserved in different HAdV types. During infection, E1B55K promotes viral DNA replication by relocating the cellular transcriptional factor (YB1) to VRCs, where it mediates the expression of viral E2 region genes and commencement of viral DNA replication (Holm *et al.*, 2002). Additionally, it was shown that the tumour suppressor p53 co-localises with E1B55K within the nucleus during both early and late phases of infection (Cardoso *et al.*, 2008). It has been shown that E1B mutants exhibited a substantial reduction in late viral mRNA accumulation and late viral protein synthesis compared to *wt*, suggesting that E1B55K indeed has an important role in promoting late viral mRNA stabilisation during infection (Babiss and Ginsberg, 1984; Babiss, Ginsberg and Darnell Jr., 1985). In cell lines infected with E1B55K null viruses, late gene transcription rates were also found to be drastically reduced (Leppard, 1993; Gonzalez and Flint, 2002). It has been suggested that E1B55K exploits the cellular mRNA export pathway by utilising nuclear RNA export factor (Nxf1/Tap) for selective export of late viral mRNAs (Yatherajam, Huang and Flint, 2011). E1B55K's role in late viral protein synthesis could be attributed to its interaction with the E1B-associated protein 5 (E1B-AP5), as it was shown that the association of the two proteins stimulates the selective export of viral late mRNAs, while repressing cellular mRNA export (Gabler *et al.*, 1998). Interestingly,

E1B55K/E4orf6-mediated degradation and regulation of heterochromatin associated factors (Spoc1) and (KAP1), respectively, were also shown to significantly increase viral late gene expression (Schreiner, Kinkley, *et al.*, 2013; Bürck *et al.*, 2016).

As previously mentioned in section 1.3.1.2, one of the major roles of E1B55K is promoting degradation of many cellular antiviral factors by forming an E3 ubiquitin ligase complex with E4orf6. E1B55K acts as the substrate recognition unit of the complex, which targets many cellular components that would otherwise inhibit efficient viral replication, such as the MRN complex (Harada *et al.*, 2002), the tumour suppressor p53 (Querido, Blanchette, *et al.*, 2001), Bloom helicase (BLM) (Orazio *et al.*, 2011), DNA ligase IV (Baker *et al.*, 2007), and others. Additionally, it has been shown that HAdV5-E1B55K can target the death domain associated protein (Daxx) for degradation in PML-NBs, independent of E4orf6 (Schreiner *et al.*, 2010). As stated earlier, some cellular proteins are targets for ubiquitination by E1B55K/E4orf6 without degradation. It is assumed that ubiquitination of cellular proteins has beneficial effects for viral replication (Herrmann *et al.*, 2020). The roles of E1B55K in collaboration with E4orf6 to regulate host cell processes and inhibit DDR and other antiviral pathways during infection will be considered later in more detail, with emphasis on DDR (See section 1.5.1).

An additional defined role for E1B55K during HAdV infection is the deregulation of cell cycle through repression of cyclin-dependent kinase inhibitor 1 (p21/Cip1), leading to the loss of host cell capacity to arrest in G<sub>1</sub> phase of the cell cycle (Steegenga *et al.*, 1995). It has been established that E1B55K upregulates CDC25A, cyclin E1 and E2, which are required for progression of cell cycle from G<sub>1</sub> to S phase, resulting in suppression of cell cycle checkpoints and facilitating viral DNA replication (Rao *et al.*, 2006; Zheng *et al.*, 2008). Additionally, the

level of viral progeny was observed to be dependent on the cell cycle phase in which the cells had been infected, such that cells infected with E1B55K-negative virus (*dl1520*) during the S phase have shown more efficient viral DNA synthesis in comparison to G<sub>0</sub> arrested cells (Goodrum and Ornelles, 1997; Zheng *et al.*, 2008). The comparable viral progeny of an E4orf6-negative virus in relation to an E1B55K-negative virus suggests that the E1B55K/E4orf6 complex indeed serves in regulating viral replication throughout the cell cycle. This indicates that there may be additional factors that affect the cell cycle restrictions which are regulated by the E1B55K/E4orf6 complex, as well as unknown cellular targets for the E3 ubiquitin ligase which has not been determined yet (Goodrum and Ornelles, 1999).

#### 1.3.1.3 Early region 4 (E4) proteins.

The E4 transcriptional unit is transcribed to produce a main transcript with a length of 2800 nucleotides, which encodes 18 different mRNAs that are alternatively spliced to create seven known open reading frames; E4orf1, E4orf2, E4orf3, E4orf3/4, E4orf4, E4orf6, and E4orf6/7 (Virtanen *et al.*, 1984; Täuber and Dobner, 2001). E4 encoded proteins carry out their biological functions through interactions with a variety of cellular proteins involved in cell cycle survival and genome stability, as well as, affecting transcriptional regulation, DDR, viral mRNA transport, virion assembly and HAdV-mediated transformation (Halbert, Cutt and Shenk, 1985; Weiden and Ginsberg, 1994). E4orfs collaborate functionally during viral infection, as it was shown that the deletion of the entire E4 region significantly impaired viral DNA replication and accumulation of late viral proteins, whilst mutations of individual orfs appeared to have a limited impact on viral growth (Halbert, Cutt and Shenk, 1985; Falgout and

Ketner, 1987). The roles of E4orf1 and E4orf2 during viral infections are still largely unknown; although HAdV9-E4orf1 was found to be highly oncogenic and induces the development of mammary neoplasm in rats (Thomas *et al.*, 2001). E4orf4 has been shown to exert a negative regulatory effect on viral replication. In particular, E1A promotes the expression of E4orf4, which in turn, suppresses E1A-dependent transactivation of viral promoters E2 and E4, as well as leading to hypophosphorylation of regulatory cellular proteins such as the protein phosphatase 2A (PP2A) (Kleinberger and Shenk, 1993; Mannervik *et al.*, 1999). It is believed that this negative regulatory role of E4orf4 increases viral infection efficiency by limiting the infection-induced toxicity to the host cell. In fact, E4orf4 has been proposed as a possible cancer treatment agent, since it was shown to bind PP2A regulatory B subunits to promote p53-independent apoptosis, exclusively in transformed cells (Kleinberger and Shenk, 1993; Shtrichman, Sharf and Kleinberger, 2000). E4orf6/7 is known as a viral transactivator, which binds and activates E2F-dependent transcription through associating with cellular E2F1 and viral E2 promoters (Schaley *et al.*, 2000).

During viral infection, E4orf3 protein performs a variety of functions that ultimately serve to inactivate the cellular antiviral response in the host such as, facilitating viral major late transcript's splicing (Nordqvist, Ohman and Akusjärvi, 1994). Additionally, E4orf3 re-localises several cellular proteins into distinct PML-NBs, which had been linked to the regulation of gene expression, sequestration of DDR components such as the MRN complex, and control of apoptosis (Doucas *et al.*, 1996). E4orf3 is also responsible for localisation of the tumour suppressor p53 to the PML-NBs, where it has been shown to function epigenetically by repressing p53's transactivity through formation of (H3K9me3) heterochromatin at p53 target promoter regions (Soria *et al.*, 2010). Moreover, E4orf3 relocates p53 from the nucleus into

the cytoplasm in order to separate it from E1B55K, allowing for its proteasomal-mediated degradation through the E1B55K/E4orf6 E3 ubiquitin ligase complex. E4orf3 possesses the ability to inhibit viral genome concatemerisation through recruitment of DDR components, such as MRE11, to VRCs, protecting the viral DNA from being recognised by the DDR machinery as double strand breaks (DSBs) and attempting to repair them (Stracker, Carson and Weitzman, 2002). As described earlier, E4orf3 also acts as a SUMO E3 ligase that SUMOylates E1B55K and promotes its localisation in the nucleus (Kindsmüller *et al.*, 2007).

E4orf6 mRNA encodes a 34 kDa protein that contains a highly conserved NLS in the N-terminal region and an amphipathic, arginine rich, nuclear retention signal (NRS) in the C-terminal region (Orlando and Ornelles, 1999). E4orf6 is a multifunctional protein that regulates late viral mRNA export, the DDR, viral late gene expression and p53 activity. During infection, E4orf6 exerts most of its function in cooperation with E1B55K by forming an E3 ubiquitin-ligase complex to degrade p53 and suppress DDR pathway components, as described in the previous section. Mutagenic analysis have shown that the NLS within the N-terminal domain of E4orf6 plays a role in re-localising E1B55K to the nucleus (Goodrum, Shenk and Ornelles, 1996), while the NRS in the C-terminal domain allows for nuclear recruitment of the two proteins (Dobbelstein *et al.*, 1997). E4orf6 also has a nuclear export site (NES), which is essential for cytoplasmic and nuclear shuttling of the E1B55K/E4orf6 complex, indicating that E4orf6 plays an important role in E1B55K localisation during infection (Weigel and Dobbelstein, 2000). Additionally, the two proteins collaborate in order to export viral mRNA from the nucleus to the cytoplasm (Dobbelstein *et al.*, 1997). Combined functions of both proteins will be addressed in detail later when discussing the relationship between HAdVs and the DDR pathways during infection (See section 1.5.1).

In isolation, HAdV5-E4orf6 is known to bind p53 directly through its C-terminal domain, which suppresses its transcriptional activity and prevents p53's N-terminal regulatory domain from interacting with cellular transcription factor (TAFII31) and, thus, inactivating p53-mediated transcriptional activity (Dobner *et al.*, 1996). In fact, it has been suggested that HAdV5-E4orf6 interactions with the C-terminal of p53 might induce conformational changes to its N-terminal domain which alters its regulatory functions. Consistently, it has been shown that the DNA binding activity of p53 is indeed affected when subjected to C-terminal modifications (Hupp *et al.*, 1992).

## **1.4 DNA DAMAGE RESPONSE, DNA REPAIR AND REPLICATION**

### **STRESS**

#### **1.4.1 Cell cycle checkpoints.**

The cell cycle is a complex mechanism that guides the cell through a predetermined series of events that ends in mitosis and division to produce two daughter cells. In mammalian cells, the cell cycle consists of four distinct phases as follows: gap-phase 1 ( $G_1$ ), synthesis of DNA (S), gap-phase 2 ( $G_2$ ) and mitosis (M). Cyclin-Dependent Kinases (CDKs) are central components in cell cycle progression and their catalytic activities are modulated through interactions with several activators (cyclins) and Cyclin-dependent Kinase Inhibitors (CKIs). Close coordination between these three components is required to ensure the progression of the cycle in an orderly manner. Three distinct classes of CDK activators have been identified:  $G_1$  phase cyclins (types D1, D2, and D3),  $G_1$ /S cyclins (types E1 and E2), S-phase cyclins (types A1 and A2), and

G<sub>2</sub>/M cyclins (types A1, A2, B1 and B2), whereas CDK inhibitors have been categorised into three groups comprising the CIP (p21<sup>cip1/waf1</sup>) and KIP proteins (p27<sup>kip1</sup>, p57<sup>kip2</sup>) that may inhibit all CDKs, as well as INK4a proteins (p16INK4a, p15INK4b, p18INK4c, and p19INK4d) which inhibit CDK4 and CDK6 (Sherr and Roberts, 1999; Lim and Kaldis, 2013). The cell cycle progression through various phases is facilitated by the expression of cyclins in different concentrations, depending on the phase of the cycle. In G<sub>0</sub> and G<sub>1</sub> phases, mitogenic factors induce the production of cyclin D proteins, which bind with CDK4 and CDK6, stimulating their kinase activity (Matsushime *et al.*, 1994; Meyerson and Harlow, 1994). This is followed by monophosphorylation of tumour suppressor proteins, pRB and its homologues p107 (Rb11) and p130 (Rb12) as a result of the active cyclin D-CDK4/6 complexes being formed. Hyperphosphorylated pRBs dissociate from members of the E2F transcription factors (Dyson, 1998; Harbour and Dean, 2000; Trimarchi and Lees, 2002). Free E2F then induces the transcription of cyclin E, a protein that binds CDK2. The cyclin E-CDK2 complex additionally phosphorylates pRB, which further dissociates it from E2F and causes transcriptional activation of S phase genes and G<sub>1</sub>/S phase transition in preparation for DNA synthesis (Ohtani, Degregori and Nevins, 1995; Harbour *et al.*, 1999). Expression of cyclin E is accompanied by an increase in cyclin A levels. Cyclin A association with CDK2 during the S phase of DNA replication, distinguishes the S/G<sub>2</sub> transition. The cyclin A2-CDK2 complex facilitates the transactivation of factors that stimulate the transcription of cyclin B1, which is required for progression into M phase. Cyclin A2 then binds CDK1 and promotes the G<sub>2</sub>/M transition before being subsequently degraded. Cyclin B1-CDK1 complexes are rendered inactive during G<sub>2</sub> as a result of phosphorylation of CDK1 on Tyr 15 and Tyr14 by the Wee1 and Myt1 kinases, respectively (Parker and Piwnicka-Worms, 1992; Liu *et al.*, 1997).



Subsequently, the G<sub>2</sub>/M transition is accelerated by the cell division cycle 25C (CDC25C) mediated dephosphorylation of CDK1. This, in turn, activates cyclin B1-CDK1 complexes and triggers G<sub>2</sub>/M transition (Malumbres and Barbacid, 2009; Lim and Kaldis, 2013). At the end of the G<sub>2</sub> phase, active cyclin B1-CDK1 complexes phosphorylate CDC25A/B/C, creating a positive feedback loop that stimulates further cyclin B1-CDK1 complex activity and triggers mitotic entry. The concentration of cyclin B1-CDK1 increases during the process of G<sub>2</sub> cells transitioning into mitosis, reaching its highest point during metaphase. When cells enter anaphase, the cyclin B1-CDK1 complex is degraded. This complex is thought to be responsible for promoting the construction of mitotic spindles as well as the alignment of sister chromatids (Izumi and Maller, 1993).

#### 1.4.1.1 The G<sub>1</sub> checkpoint.

The G<sub>1</sub> control checkpoint ensures that damaged DNA does not undergo replication in the succeeding S phase of the cell cycle. Two different mechanisms are proposed to initiate G<sub>1</sub> checkpoint arrest, the first is CHK1-mediated phosphorylation of CDC25A at various locations. CHK1 is a downstream effector of ATR, and it controls the phosphorylation and degradation of CDC25A, which inhibits aberrant or excessive replication firing during unperturbed S phase. This is accomplished by cyclin E-dependent downregulation of CDK2 (Sørensen *et al.*, 2004). CDC25A degradation prevents it from being loaded onto the pre-RC complex, as dephosphorylation of cyclin E-CDK2 complexes is blocked when CDC25A is absent. The second mechanism of G<sub>1</sub> checkpoint arrest is related to the upregulation of p21 and p27 in response to p53, which is accomplished through its direct phosphorylation by ATM and CHK1 (Banin *et*

*al.*, 1998; Shieh *et al.*, 2000; He *et al.*, 2005). Following this, p53 becomes transcriptionally active and is stabilised as a result of the phosphorylation-mediated disruption of p53/mouse double minute 2 (MDM2) binding. This, in turn, limits the MDM2-mediated nuclear export and degradation of p53 (Schon *et al.*, 2002). The stabilisation of p53 leads to the transcriptional activation of a variety of target genes, including p21, thus inhibiting G<sub>1</sub>/S transition via its Cyclin D-CDK4/6 and Cyclin D-CDK2 inhibitory role (He *et al.*, 2005).

#### 1.4.1.2 The S phase checkpoint.

The S phase cell cycle checkpoint, occurring between G<sub>1</sub> phase and G<sub>2</sub> phase, acts to preserve genomic integrity by preventing the replication of damaged DNA. The ATR/CHK1 signalling pathway activates the S phase checkpoint by inhibiting cyclin A-CDK2 and CDC7-DBF4 (DDK) protein complexes, which limit the firing of primed origins (Heffernan *et al.*, 2007; Zegerman and Diffley, 2010). Additionally, the S phase checkpoint acts to protect the replication forks if replication is disrupted. This allows DNA to be repaired before it is confronted by an ongoing replication fork. Furthermore, DSBs that occur during S phase, but are not linked to active replicons, are also identified by the S phase checkpoint. These DSBs are recognised by the ATM/CHK2 signaling pathway, which induces the degradation of CDC25A, a major promoter of the S phase checkpoint. The degradation of CDC25A enhances the inhibitory phosphorylation process of cyclin E/A-CDK2 complexes, which is typically eliminated by CDC25A. The inhibition of cyclins E/A-CDK2 complexes stops CDC45 from loading at pre-replication complexes, and as a result, it prevents firing of any remaining origins that have been prepared for replication initiation (Falck *et al.*, 2001). Ultimately, both ATM and ATR

signaling cascades contribute to the activation of the S phase checkpoint and stalling of cell cycle progression through proteasomal-mediated degradation of CDC25A, which eventually leads to inhibition of cyclin A-CDK2 and CDC7-DBF4 activities (Zhao, Watkins and Piwnicka-Worms, 2002; Gatei *et al.*, 2003; Sørensen *et al.*, 2004). (See section 1.4.4.2.1 for detailed discussion on ATR-mediated stabilisation of stalled forks).

#### 1.4.1.3 The G<sub>2</sub>/M checkpoint.

The G<sub>2</sub>/M cell cycle checkpoint exists to prohibit cells from initiating mitosis until any unrepaired or damaged DNA, or DNA that has been partially duplicated, has been repaired sufficiently. CDC25A/B/C phosphatases are mainly phosphorylated and inhibited by CHK1 and CHK2, which are downstream effectors of ATR and ATM kinases, respectively. This leads to the inhibition of the cyclin B1-CDK1 complex, which is crucial for the transition into M phase. The phosphorylation of CDC25B/C phosphatases facilitates their binding to the 14-3-3 proteins which causes their sequestration in the cytoplasm (Kumagai and Dunphy, 1999; Abraham, 2001). Proteins of the p38 mitogen-activated protein kinase (MAPK) pathway, in addition to, ATM/ATR-mediated phosphorylation of polo-like kinase 3 (Plk3), are responsible for the further phosphorylation and sequestration of CDC25B/C proteins in the cytoplasm, leading to further inhibition of CDC25 phosphatase functions during the G<sub>2</sub>/M checkpoint (Bulavin *et al.*, 2001; Bahassi *et al.*, 2004). The p53 protein is also implicated in G<sub>2</sub>/M checkpoint arrest through the suppression of CDK1 and by activating the transcription of cell cycle inhibitors such as p21, 14-3-3, and GADD45. CDK1 is inhibited directly by p21, relocated to the cytoplasm

by 14-3-3 proteins, and the binding of CDK1 to Cyclin B1 is prevented by GADD45 (Hermeking *et al.*, 1997; Wang *et al.*, 1999).

#### 1.4.2 Cellular DNA damage response.

The DNA damage response, also known as the DDR, is a cellular monitoring pathway that is responsible for detecting DNA damage and initiating cellular signalling pathways to either, halt the cell cycle and repair the DNA damage in an accurate manner, or to induce apoptosis if the damage is extensive. Therefore, it is an important surveillance system that protects genomic integrity in the face of exogenous genotoxic events like ionising radiation (IR), viral infections and toxic chemicals, or endogenous threats such as reactive oxygen species (ROS). Additionally, normal cellular processes involved in DNA replication may lead to replication stalling and DNA damage, which activate cellular DDR pathways (Cimprich and Cortez, 2008; Jackson and Bartek, 2009). These genotoxic events have the potential to produce DNA lesions such as, double strand breaks (DSBs) and single strand breaks (SSBs) (Ciccia and Elledge, 2010). These lesions need to be rapidly identified and repaired to protect the genome and ensure cell survival.

The DDR is dependent on a variety of cellular factors, including DNA damage sensors, mediators, signal transducers, and effectors, all of which work together to detect and repair damaged DNA, while also regulating the progression of the cell cycle. In some cases, apoptosis is triggered when the amount of DNA damage is deemed to be exceptionally severe. Principally, among the signal transducers and effectors involved in DDR, three

phosphoinositide 3-kinase (PI 3-K) like family protein kinases (PIKKs) play important roles in regulating the signalling pathways in response to DSBs and SSBs: Ataxia Telangiectasia Mutated (ATM), Ataxia Telangiectasia and Rad3-related (ATR), and DNA-dependent protein kinase (DNA-PK) (Figure 1.6) (Abraham, 2004; Blackford and Jackson, 2017). In light of the fact that HAdVs are known to interact with several different DDR components (See section 1.5), an overview will be given on the process of DNA damage detection and repair, as well as the cellular response to replication stress in the following sections.

#### 1.4.2.1 The ATM kinase pathway and double strand break repair.

ATM is a protein kinase with a molecular weight of 350 kDa that is involved in the homologous recombination (HR) repair pathway (See section 1.4.3.1.2) (Sancar *et al.*, 2004; Blackford and Jackson, 2017). ATM typically exists as an inactive homodimer in undamaged cells, and its activity is stimulated *in vivo* in response to DSBs, which causes its autophosphorylation at (S1981) and, in association with MDC1, causes its attachment to DSBs in a monomeric form (So, Davis and Chen, 2009). The detection of DSBs is facilitated by the MRN complex, which enhances the recruitment of ATM to the sites of the breaks. Additionally, the activation of ATM is mediated by the MRN complex, and its acetylation is regulated by the HIV-1 tat interacting protein (Tip60) once it has been activated (Sun *et al.*, 2005). Both steps are necessary for the full activation of ATM. Subsequently, ATM phosphorylates a number of DDR downstream substrates including TIF $\beta$ /KAP1, breast cancer type 1 susceptibility protein (BRCA1), p53-binding protein 1 (53BP1) and NBS1 (Sancar *et al.*, 2004; Blackford and Jackson, 2017). Additionally, phosphorylation by ATM activates effector proteins such as the histone

H2A variant (H2AX) and checkpoint kinase 2 (CHK2) that, in turn, regulate cell cycle signalling cascades, resulting in the initiation of the cell cycle checkpoint control and preventing the DNA from replicating until the damage has been accurately repaired (Hirao *et al.*, 2000).

Following DSB formation, the histone H2AX variant, constituting around 25% of the overall H2A pool, becomes phosphorylated by ATM and is termed ( $\gamma$ H2AX) (Rogakou *et al.*, 1998). This results in the recruitment of the DNA damage checkpoint mediator, MDC1, to the location of the DNA break, which also causes its phosphorylation by ATM (Goldberg *et al.*, 2003). Subsequently, MDC1 binds ATM,  $\gamma$ H2AX and the MRN complex, resulting in recruitment of more ATM to the site of DSBs and dissemination of the DNA damage signal by phosphorylation of more H2AX (Lou *et al.*, 2006). This is followed by recruitment of the E3 ubiquitin ligase ring finger protein 8 (RNF8) to the site of the break and binding to the phosphorylated MDC1 (Huen *et al.*, 2007; Kolas *et al.*, 2007). The interactions between RNF8, MDC1 and the E2 conjugating enzyme Ubc13, as well as the recruitment of E3 ubiquitin ligase (RNF168) to the site of damage leads to further amplification of the DNA damage signal by ubiquitination of  $\gamma$ H2AX through the addition of K63 ubiquitin chains (Wang and Elledge, 2007; Mattioli *et al.*, 2012). Collectively, in addition to its role in amplification of the damage signal,  $\gamma$ H2AX ubiquitination also leads to the recruitment of a number of DSB repair proteins such as, 53BP1, BRCA1 and others (Figure 1.6) (Wang *et al.*, 2002; Wang and Elledge, 2007). Significantly, HAdVs block the ATM repair pathway by targeting MRE11 for degradation (See section 1.5.1.2).

#### 1.4.2.2 The ATR kinase pathway.

ATR is a transducer kinase which has a molecular weight of around 300 kDa (Sancar *et al.*, 2004; Blackford and Jackson, 2017). It plays a major role in cellular proliferation by ensuring accurate chromosomal distribution throughout the mitotic phase of cell division (Kabeche *et al.*, 2018). ATR is also essential in sensing and repairing SSBs that occur as a result of either the processing of DSBs or due to stalling of DNA replication forks. ATR serves both as a sensor and transducer in the DDR cascade to phosphorylate Checkpoint Kinase 1 (CHK1) in order to activate the G<sub>2</sub>/M checkpoint of the cell cycle (Matsuoka *et al.*, 2007). In response to the presence of single strand DNA (ssDNA), replication protein A (RPA) coats exposed damaged regions, which attracts ATR in association with its regulator, ATR interacting protein (ATRIP) to the RPA-coated sites (Zou and Elledge, 2003; Binz, Sheehan and Wold, 2004). This is followed by full activation of ATR, which is mediated by the recruitment of topoisomerase II binding protein 1 (TOPBP1), along with its association with the Rad9-Rad1-Hus1 (9-1-1) and Rad17-replication factor C 2 (RFC2) clamp loader complexes (Kumagai *et al.*, 2006; Mordes *et al.*, 2008). Upon activation of ATR, a number of overlapping downstream effector substrates are phosphorylated, such as DNA repair proteins: H2AX, BRCA1 and BLM, as well as proteins involved in cell cycle checkpoint control: p53 and CHK1. By inducing cell cycle checkpoint arrest, ATR stabilises stalled replication forks and prevent their collapse (See section 1.4.4.2.1), as well as, allowing damaged DNA to be repaired (Cortez, 2015). HAdVs block the ATR repair pathway by targeting several DDR proteins, such as TOPBP1 for degradation (See section 1.5.1.3).

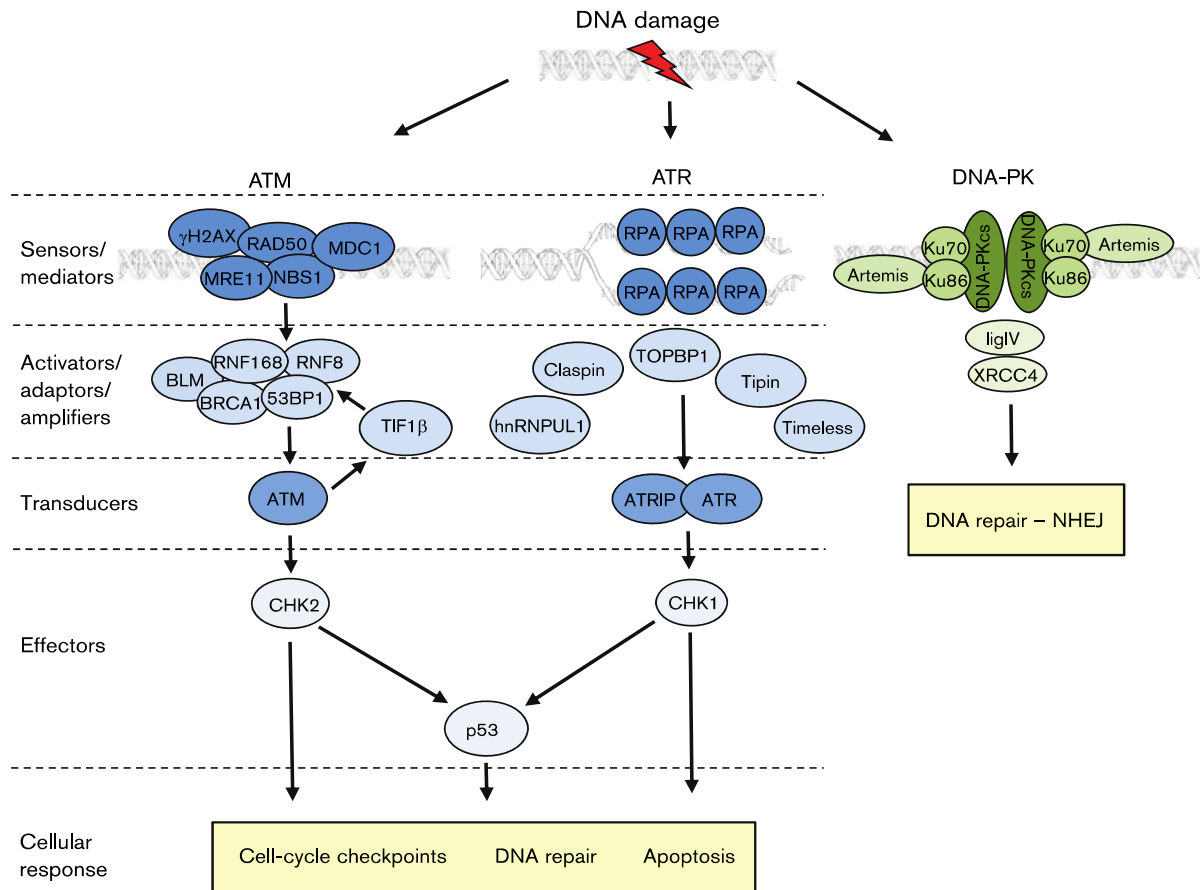


**Figure 1.6.** Activation of different protein complexes in response to DNA damage and their roles in ATM, ATR, and DNA-PK pathways. A schematic representing the ATM, ATR, and DNA-PK DDR signalling pathways. ATM facilitates HR DNA repair in response to DNA DSBs. The MRN complex is attracted to the locations of DSBs to facilitate the recruitment and subsequent activation of ATM and Tip60. ATM activation leads to cell cycle arrest by phosphorylating p53 and CHK2. In addition to phosphorylating MDC1 at the location of the break, activated ATM quickly phosphorylates H2AX (termed  $\gamma$ H2AX). To further disseminate the DNA damage signal, MDC1 recruits more ATM and RNF8 to the location of the break. In order to attach ubiquitin chains to  $\gamma$ H2AX, RNF8 and MDC1 act as catalysts. RNF168 is subsequently brought to the location of the break, where it causes further ubiquitination of H2AX. At this stage, repair proteins such as 53BP1 and BRCA1 are directed to the location of the break. ATR becomes



active as a result of the presence of ssDNA breaks. Through its collaboration with ATRIP, the binding of RPA to ssDNA results in the recruitment of the ATR kinase. The association with the 9-1-1 complex and the RFC2 clamp loader complex allows TOPBP1 to localise to the site of break. TOPBP1 then interacts with the 9-1-1 to activate ATR which stimulates downstream repair proteins and triggers cell cycle arrest through CHK1. DNA-PK participates in NHEJ repair, and it is recruited to DSB sites by the Ku regulatory proteins. It works in combination with two DNA-PKcs molecules in order to tie DNA ends together in a synaptic complex and attract the DNA ligase IV–XRCC4 complex to ligate damaged DNA ends. Taken from: (Turnell and Grand, 2012).

### **1.4.3 DNA damage repair and genome integrity.**

#### **1.4.3.1 Double-strand breaks repair.**

DSBs are defined as disruptions in both strands of the DNA double helix. They are the most fatal type of DNA damage which are commonly caused by Ionising radiation (IR). DSBs are processed and repaired either by Homologous Recombination (HR) or Non-Homologous End Joining (NHEJ) (Ciccia and Elledge, 2010). HR repair requires the complementary DNA strand, as such it can only take place during the S, G<sub>2</sub>, and early M phases of the cell cycle. In contrast, NHEJ may function at any time throughout the cell cycle; however, it is most active during the G<sub>1</sub> phase when DNA is haploid and there is no homologous template for recombination (Khanna and Jackson, 2001). Since direct ligation of broken DNA ends is required for NHEJ repair, there is a possibility that some genetic information might be altered or lost during the process due to the loss of nucleotides. Additionally, due to the fact that DNA ends may link in

an inaccurate manner, NHEJ can also cause chromosomal translocations (Heidenreich *et al.*, 2003). HR repair, on the other hand, involves DNA end-processing and is considered an error-free type of DSB repair because it does not result in the deletion or loss of any genetic material (Takata *et al.*, 1998; Rapp and Greulich, 2004).

#### 1.4.3.1.1 Non-Homologous End-Joining (NHEJ).

NHEJ DNA repair is initiated with the identification of DSBs by the Ku70/80 DNA-binding subunits, which form a ring-like structure with high affinity around DSB ends to prevent their degradation and allow other proteins involved in repair to access the break site (Figure 1.6) (Walker, Corpina and Goldberg, 2001). Significantly, the recruitment of 53BP1 to the site of damage promotes the repair process by inhibiting DNA resection, which is required for HR. The DNA-dependent protein kinase (DNA-PK) is a critical component of the NHEJ DNA repair. It has a molecular weight of 450 kDa and is involved exclusively in NHEJ. The DNA-PK holoenzyme is comprised of a large catalytic subunit (DNA-PKcs) along with the two regulatory DNA binding subunits; Ku70 and Ku86 (Smith and Jackson, 1999; Sancar *et al.*, 2004). Activation of DNA-PKcs is facilitated by DSBs and Ku70/86 along with a spectrum of downstream NHEJ proteins such as, Artemis and XRCC4 (Cary *et al.*, 1997; Gell and Jackson, 1999; Goodarzi *et al.*, 2006). Subsequently, the endonuclease activity of Artemis removes 5' and 3' DNA overhangs and DNA hairpins. This allows the DNA ends to return to their conventional 3'OH and 5'P DNA termini, followed by the recruitment of two DNA-PKcs molecules at each end of the DNA strand. This promotes tethering and re-ligation of the broken DNA ends via DNA ligase IV-XRCC4 complexes, which are necessary for the end processing and re-ligation phases

of NHEJ repair (Hsu, Yannonie and Chen, 2002; Ma *et al.*, 2002). HAdVs were shown to inhibit DNA-PK signalling pathway during infection by targeting DNA ligase IV for degradation (See sections 1.5.1 and 1.5.1.4).

#### **1.4.3.1.2 Homologous Recombination (HR).**

HR is the main mechanism for repairing DNA DSBs during the S and G<sub>2</sub> phases of the cell cycle due to the need for the homologous sister strand for the successful completion of the repair process, as opposed to NHEJ, which plays a major role in DSBs repair during all phases of the cell cycle (Figure 1.7) (Takata *et al.*, 1998). A significant amount of DNA end processing, also known as end-resection, is carried out during HR repair using homologous parts of the undamaged DNA strand as a template to fill in the gaps in the damaged sites. After the homologous region has been allocated in the undamaged strand, it is used as a template for the DNA repair process. The detection of DSBs is facilitated by the MRN complex, which senses and enhances the recruitment of ATM to the sites of blunt DNA ends (Williams, Williams and Tainer, 2007). 3'-ssDNA overhangs are then produced as a result of the 5'-3' nucleolytic destruction of DNA blunt ends. DNA end resection, an early stage in this process, is produced by the removal of short oligonucleotides from the ends of the DNA by the enzymes, 5'- MRE11-Rad50 nuclease-ATPase, and CtIP (Limbo *et al.*, 2007; Huertas and Jackson, 2009). DNA2, BLM helicase and Exo1 exonuclease then co-operate to produce a significant quantity of ssDNA stretches, which are coated and protected by RPA complexes (Zhu *et al.*, 2008). Subsequently, 3'-ssDNAs become accessible as substrates for the RAD51 recombinase, and the DNA structures that contain hairpins are eliminated (Baumann, Benson and West, 1996; Sugiyama

and Kowalczykowski, 2002). RAD51 removes RPA molecules from the ssDNA-RPA complex in a manner that is dependent on BRCA2 and subsequently joins ATP and ssDNA to create a presynaptic filament to catalyse DNA strand exchange. Although the specific function of the RAD51 ATPase activity in filament formation is still yet unclear, the ssDNA-RAD51-ATP complex executes homology searches and DNA strand exchange (Baumann, Benson and West, 1996). The formation of ssDNA-RAD51 nucleoprotein filaments allows it to invade the undamaged sister chromatid strand and use the homologous sequence as a template to synthesise DNA with the matching homologous region, forming a displacement D-loop structure (Alberts *et al.*, 2002; Sugiyama and Kowalczykowski, 2002). This structure may be resolved via standard recombination repair, whereby the newly formed D-loops are captured by the second DNA end. This leads to the development of double “Holliday junctions” which are then resolved by a variety of endonucleases to produce both cross-over and non-crossover products (Wu and Hickson, 2003; Ip *et al.*, 2008; Fekairi *et al.*, 2009). Alternatively, Holliday junctions can be resolved if D-loops are not captured by the second DNA end and the repaired DNA strand can then anneal to the opposite side of the DSB via synthesis-dependent strand annealing process (SDSA). As a result, this leads to the formation of a non-crossover product, exclusively (Adams, McVey and Sekelsky, 2003; Ira, Satory and Haber, 2006).

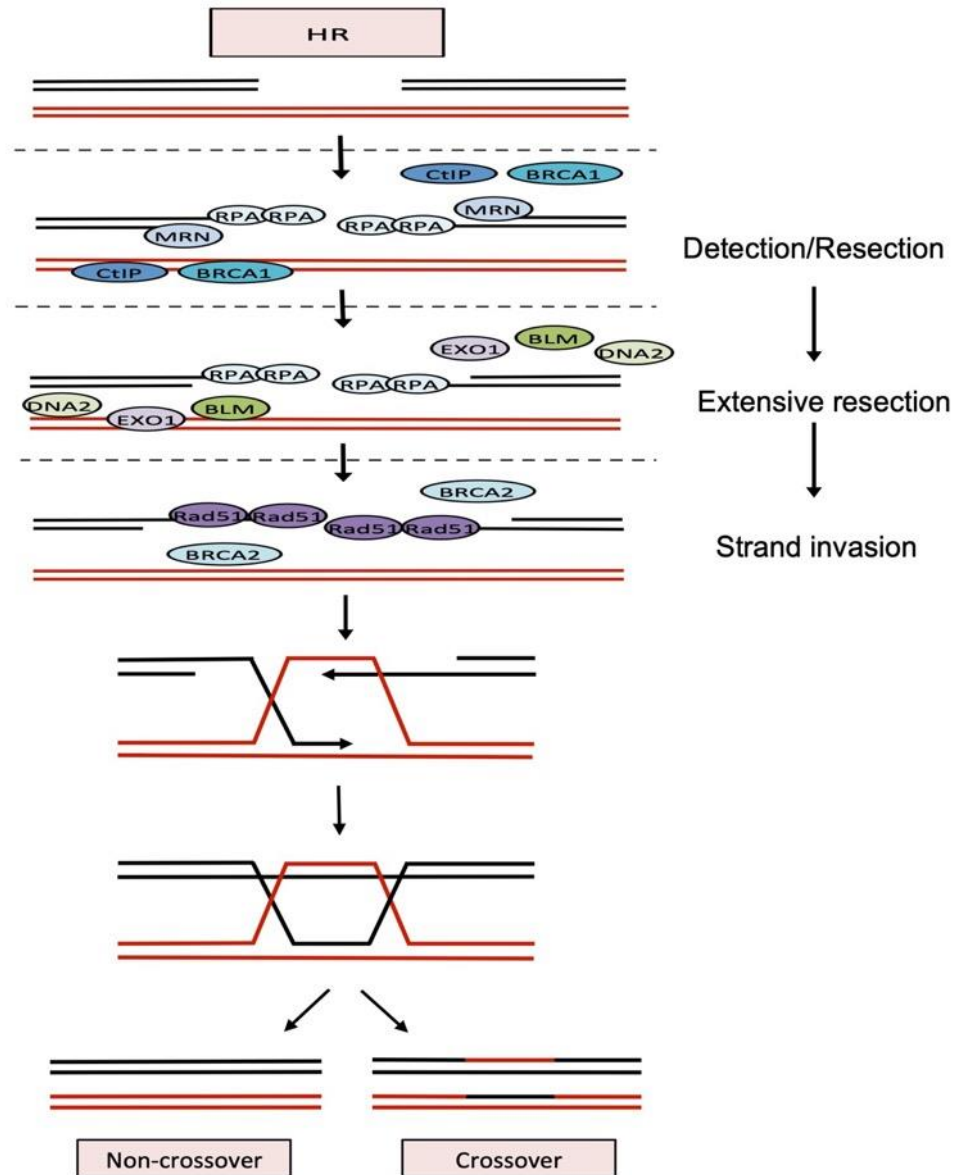


**Figure 1.7.** HR repair pathway. The initial detection and 5'-3' resection of the DNA at the location of the DSB is carried out by MRN, CtIP, and BRCA1, followed by extensive resection, which is executed by BLM, DNA2, and EXO1 proteins. The recombinase RAD51 in concert with BRCA2 displaces the 3' overhang ssDNA created by resection, and RPA quickly binds this ssDNA, producing a nucleoprotein filament. Homology searches are then initiated by the nucleoprotein filament, as is the process of exchanging DNA strands. HR intermediate

“Holliday junction” may be resolved afterwards by the endonucleases MUS81, EME1, SLX1/SLX4 and GEN1 (Ryan, 2016).

#### 1.4.4 DNA replication.

The cell cycle regulates all phases of DNA replication, including replication preparation, initiation, progression, and completion. All these steps are tightly regulated to maintain genome integrity.

##### 1.4.4.1 DNA replication initiation and origin licensing.

G<sub>1</sub> is the only phase of the cell cycle in which the components necessary for DNA replication are produced. This includes histones, dNTPs, and the pre-replication complex (pre-RC). The process of DNA replication begins in the late stage of mitosis and continues all the way through the G<sub>1</sub> phase of the cycle. The pre-RC is made up of the origin recognition complex proteins 1-6 (ORC1-6), cell division cycle 6 (Cdc6), cell division cycle 10-dependent transcript 1 (Cdt1), and the inactive mini chromosome maintenance (MCM) helicase complex, which is a hexamer consisting of six subunits (MCM2-7) (Piatti, Lengauer and Nasmyth, 1995; Nishitani *et al.*, 2000; Fragkos *et al.*, 2015). The activity of cyclin A-CDK2 denotes the transition from the G<sub>1</sub> to S-phase, where origin firing begins. Subsequently, Cdc6, a component of the pre-RC, undergoes phosphorylation at the beginning of S phase, which causes it to become detached from the pre-RC complex and enter the cytoplasm (Petersen *et al.*, 1999). Additionally, the activation of the MCM 2-7 hexamer takes place during the S phase of the origin firing process.

This is accomplished by the association of Cdc45 and MCM10 with the pre-RC complex, which subsequently binds the Sld5, Psf1, Psf2, and Psf3 (GINS) protein complex to form the active CMG (Cdc45-MCM-GINS) replicative helicase complex (Ilves *et al.*, 2010). The pre-initiation complex is formed via the binding of the pre-RCs with multiple replication proteins, such as TOPBP1-interacting protein (Treslin, also known as TICRR), TOPBP1, RECQL4 and MTBP (Kumagai *et al.*, 2010; Fragkos *et al.*, 2015). As the cell enters S phase and the origin fires, DDK protein kinase is activated, allowing it to phosphorylate a variety of proteins in the pre-initiation complex. Following this, the active MCM helicase is positioned to unwind the DNA at its origin point, leading to the formation of the replication fork (Heller *et al.*, 2011). The replication machinery, including the proliferating cell nuclear antigen (PCNA) factor, Pol primase subunits, RPA, TIPIN-TIMELESS-CLAPSIN, and DNA polymerases  $\alpha$ ,  $\epsilon$  and  $\delta$ , are proposed to be recruited to the origin site by GINS and Cdc45 (Aparicio, Stout and Bell, 1999; De Falco *et al.*, 2007). After the helicase has been loaded with the replication machinery, the replisome is formed, which is then able to travel in both directions along the DNA and continue to copy the DNA across the genome (Masai *et al.*, 2010).

Initiation of DNA replication begins with the synthesis of relatively short RNA fragments that are formed by the primase portions of Pol  $\alpha$ , and then elongated by Pol  $\epsilon$  and  $\delta$ . DNA replication only proceeds in one direction, as the CMG replicative helicase proceeds in a 3'→5' orientation because of the 5' to 3' polarity of DNA synthesis. The leading strand is the one that is synthesised without breaks, whereas the opposite strand, known as the lagging strand, is composed of Okazaki fragments, which are small, discontinuous pieces of nascent DNA. Okazaki fragments are replicated by the lagging strand polymerases in an opposite direction to the CMG helicase (Alberts *et al.*, 2002). While the Okazaki fragment is maturing, Pol  $\delta$  is

responsible for moving the RNA primer that is associated with the preceding Okazaki fragment into a 5' flap. Nucleases, such as DNA2 and FEN1 recognise the misplaced flap, bind to it, and then resolve it. A longer 5' flap is produced as a result of the interaction of Pol  $\delta$  with the 5'-3' helicase Pif1. This results in increased flap development in a subsequent Okazaki fragment. Following this, long flaps are coated by RPA, which makes them resistant to the action of FEN1 endonuclease and, as a consequence, the activity of DNA2 becomes necessary for the correct cleavage of RPA-associated flaps at several locations, leaving behind a shorter end-product. This shorter product is then removed by FEN1 to generate a nick, which is then ligated by DNA ligase I. It is only possible for the genome to be replicated once during each cell cycle because the replisomes detach from the DNA after the process of DNA replication is finished. This prevents the replisomes from interfering with the subsequent round of replication (Balakrishnan and Bambara, 2013).

#### **1.4.4.2 DNA replication stress.**

Any disruption in the sequence, coordination, or timing of DNA synthesis may be referred to as replication stress (RS). Replication stress can be induced when replication fork barriers (RFBs) interfere with DNA synthesis, causing replication forks to stall or collapse (Zeman and Cimprich, 2014). Fork stalling is known as a transient "halt" in the replication fork advancement in response to an RFBs and, as such, stalled replication forks may restart and resume their progression when RFBs are resolved. However, when replication forks are exposed to extended periods of fork stalling, they eventually become inactive and lose their ability to go through fork restart. In this particular situation, the replication of DNA is restarted



through a new global origin firing (Petermann *et al.*, 2010). Fork collapse describes a replication fork that, as a direct result of replication stress, is no longer able to finish the replication process. Fork collapse is often associated with the detachment of the replisome and the collapse of the replication fork into a DSB, both of which may occur either passively after prolonged replication stress, or actively by the cleavage of MUS81 endonuclease. Therefore, it is imperative for replication forks to be stabilised promptly to prevent their collapse (Hanada *et al.*, 2007).

Several RFBs, including unresolved DNA lesions, DNA-bound proteins, and secondary structures can cause replication stress. For example, R-loops, which are RNA-DNA hybrid structures with a misplaced ssDNA, may impede the replication mechanism, which cannot be copied in the presence of these structures. When the developing RNA anneals with the template DNA strand during transcription, the non-template DNA strand becomes displaced, forming R loops, which are non-B DNA structures (García-Pichardo *et al.*, 2017). R loops often compromise the integrity and function of the genome by interfering with DNA replication, repair, and transcription. As a result, cells have developed a variety of defences against such DNA-RNA hybrids. R loops constitute a threat to genome integrity and cell proliferation when one or more of these defence mechanisms fails, which increases the possibility of cellular anomalies. A growing body of evidence indicates that R-loop-mediated replication fork stalling is a key component of transcription-replication conflicts and R-loop-induced DNA damage. This is coupled with the fact that a ssDNA may be highly accessible to reactive oxygen species, DNA modifying enzymes, or nucleases, which would increase the incidence of DNA damage (Lindahl, 1993; Wellinger, Prado and Aguilera, 2006; Tuduri *et al.*, 2009; Boubakri *et al.*, 2010). Specialised RNA-DNA helicases may unwind RFBs and prevent the formation of R-loops, or

they can be resolved through the action of the enzyme RNase H1 that degrades the RNA fragment of R-loops and prevents their production in order to resolve the RS (Alzu *et al.*, 2012).

Exogenous chemotoxic agents are another important cause of replication stress. For instance, chemicals that limit DNA elongation, such as hydroxyurea (HU), which is a ribonucleotide reductase (RNR) inhibitor, are involved in depleting dNTP pools and eventually stall replication forks, causing their collapse after prolonged exposures or leading to their conversion into DSBs. RNR is involved in the conversion of NDPs to dNDPs, which is a crucial step in the synthesis of dNTPs (Elford, 1968; Jordan and Reichard, 1998). Another important drug that induces RS is camptothecin (CPT). CPT inhibits topoisomerase I (topo I), a nuclear enzyme that relieves torsional strain in supercoiled DNA during replication. Additionally, topo I can generate a temporary intermediate complex with ssDNA, which enables an intact single strand of DNA to pass through the nick and the broken section of DNA to be rotated around the rest of the DNA strand. It is thought that CPT attaches to and stabilises the normally transient DNA-topo I complex, which in turn, prevents any further breakage of the strand. Upon coming into contact with a replication complex, the SSB causes the formation of DSB, which leads to genomic instability and RS (Swamy, Purushotham and Sinniah, 2021).

#### **1.4.4.2.1 Stalled fork stabilisation.**

The most efficient way to avoid replication stress is to repair any damage to the DNA before encountering the replication fork. This may be accomplished through a variety of DNA repair pathways, depending on the type of the damage (See sections 1.4.3.1.1 and 1.4.3.1.2). However, if the damage is not repaired prior to its association with the replication fork,

replication checkpoints may temporarily stall the ongoing replication fork, which can then be stabilised and restarted when the damage has been repaired. In some cases, unresolved replication stress may eventually lead to fork collapse and defective DNA replication. Therefore, it is vital for the cell to be able to react appropriately to replication stress. Multiple cellular monitoring pathways that deal with RS have evolved in order to prevent genomic instability. The ATR/CHK1 pathway is central to genomic monitoring and plays a vital role in replication fork stabilisation. ATR and its downstream effector CHK1 are both activated in response to a broad variety of DNA damage types, such as SSBs, and together they control various cell signalling cascades that principally regulate cell cycle checkpoints, replication fork stabilisation, origin firing and HR repair (Figure 1.6).

The generation of large stretches of ssDNA is the most obvious consequence of replication stress, and this occurs as a result of the activity of the DNA helicase that continues to unwind the double helix even after the polymerase has ceased its work (Zeman and Cimprich, 2014). This may lead to DSB formation and/or fork collapse, which results from stalling of the replication polymerase when it meets a SSB in a template strand (Pfeiffer, Goedecke and Obe, 2000).

During ATR-mediated fork stabilisation, CDC25A/B/C are phosphorylated by CHK1, a downstream effector of ATR, and thus the replication checkpoint is activated when significant stretches of ssDNA are generated (See section 1.4.1.2) (Byun *et al.*, 2005). This prevents abnormal replication firing during S phase through the downregulation of E/A-CDK2 and Cdc7-Dbf4 complex, allowing for repair or restart of replication forks (Sørensen *et al.*, 2004). By preventing the association of Treslin and TOPBP1, CHK1 also blocks the formation of the CMG

replicative helicase, which limits dormant origin firing (Boos *et al.*, 2011). In addition, the association of ATR, ATRIP, and claspin contributes to the stability of replication forks by limiting the amount of ssDNA that is accessible for RPA (Lim and Kaldis, 2013). ATR kinase also regulates the RS response by facilitating the recruitment of RAD51 (Zellweger *et al.*, 2015), as well as the phosphorylation of numerous other cell cycle checkpoint proteins, including H2AX, RAD17, RPA2, BRCA1, FANCD2, and p53 (Petermann and Caldecott, 2006).

Increasing evidence suggests that HR also plays a crucial role in stabilising stalled forks. HR-mediated fork restart is different from HR-mediated DSB repair. Through the utilisation of DNA-end resection machinery, HR induces the repair of post-replicative SSBs. The MRN complex and CtIP catalyse a short-range resection of DSBs, followed by a long-range resection mediated by Cdk1-dependent phosphorylation of DNA nucleases Sae2 or DNA2, which results in the formation of larger ssDNA regions. This facilitates loading of RAD51 onto the single strand and increases the invasion of the 3' overhang into homologous sister chromatids by RAD51, which stimulates DNA synthesis before the endonuclease resolution of the D-loop intermediates, eventually leading to replication forks restart. Also, fork stability has been shown to be dependent on other HR proteins, including BRCA2/PALB2, BRAC1, and the RAD51 paralogue XRCC3 (Petermann *et al.*, 2010; Zellweger *et al.*, 2015). Additionally, nascent DNA is protected from MRE11-dependent DNA resection at stalled forks by BRCA2, which also facilitates RAD51 loading and the formation of nucleoprotein filaments during fork restart (Hashimoto *et al.*, 2010).

## 1.5 ADENOVIRUSES AND THE DNA DAMAGE RESPONSE

Viruses are known to trigger the DDR pathways in the same manner as other genotoxic agents. The first evidence suggesting a link between HAdVs and the DDR was shown after it was reported that HAdV12 infection induces certain chromosomal aberrations in human embryo kidney and human embryo lung cells, causing non-random damage and breaks in chromosomes 1 and 17 (zur Hausen, 1967; McDougall, 1971b). The sites of these breaks are known as HAdV12 modification sites, and are similar to classic fragile sites (Lindgren *et al.*, 1985; Durnam *et al.*, 1988). Infection with HAdV5, however, results in random chromosomal damage (Caporossi and Bacchetti, 1990; Caporossi, Bacchetti and Nicoletti, 1991). Significantly, mutational studies on HAdV12-E1 genes revealed that viral-induced chromosomal damage and modification of fragile sites is dependent upon the expression of the E1B55K protein, whereas E1A and E1B19K proteins had minimal effects (Schramayr *et al.*, 1990b).

The introduction of any viral DNA into an infected cell is likely to produce stress and the induction of the DDR, this is almost certainly the case for HAdVs. In addition, during HAdV infection, the viral linear dsDNA end resembles a DSB, whereas ssDNAs are produced during viral genome replication. These elements are probably recognised as DNA breaks by the host cell, which triggers DDR signalling pathways that would normally lead to cell cycle arrest and/or induction of apoptosis (Weitzman *et al.*, 2004). The activation of the host DDR would substantially restrict viral replication or lead to the formation of concatemers of viral DNA that can no longer be packaged into virions and is, therefore, considered as an anti-viral response. As a consequence, HAdVs were shown to have a greater ability to replicate in cancer cells as

opposed to primary cells. This is probably due to the fact that critical DDR proteins are often deactivated in cancer cells (Bischoff *et al.*, 1996; Heise *et al.*, 1997; Turnell, Grand and Gallimore, 1999; Johnson *et al.*, 2002; O'Shea *et al.*, 2004). Accordingly, comprehending the relationship between HAdVs and the cellular DDR is critical for understanding some aspects of the molecular basis of host cell and virus interactions (Weitzman and Ornelles, 2005; Turnell and Grand, 2012; Hollingworth and Grand, 2015). A number of HAdV's defence mechanisms that contribute to the effective evasion of cellular DDR will be described in more detail in the following sections (1.5.1, 1.5.2, and 1.5.3).

#### **1.5.1 E1B55K/E4orf6-mediated regulation and degradation of DDR components during HAdV infection.**

It has become apparent that, during infection, most of the E1B55K/E4orf6 complex functions are directly attributed to their ubiquitination activity (Sarnow *et al.*, 1984; Ornelles and Shenk, 1991; Querido, Blanchette, *et al.*, 2001; Harada *et al.*, 2002; Woo and Berk, 2007; Blanchette *et al.*, 2008; Herrmann *et al.*, 2020). This is supported by the observation that most of the viral E1B55K protein in infected cells was present in complexes with E4orf6 (Ornelles and Shenk, 1991). Interestingly, late viral mRNA expression was also shown to be associated with active proteasomal degradation induced by the E4orf6 protein (Corbin-Lickfett and Bridge, 2003). Furthermore, infecting Cul5-negative cells with HAdV5, where no degradation of p53 and the MRN complex is present, it has been found that the infection exhibits comparable behaviour to E1B55K mutants that are defective in promoting late viral mRNA export and protein synthesis (Woo and Berk, 2007). Accordingly, this suggests that most of the functions executed

by E1B55K and E4orf6 in the cell during infection pertain to their ubiquitination functions in ligase complexes.

The interaction between E1B55K and E4orf6 proteins is imperative for early and late functions of E1B55K and for successful viral replication. As previously mentioned, in the case of HAdV5 infection, E1B55K and E4orf6, together with cellular components, form an E3 ligase complex consisting of Cul5, Rbx1, elongins B and C (Querido, Blanchette, *et al.*, 2001). The core of this complex is recruited by E4orf6, while the E1B55K protein attaches to it and acts a recognition unit for different substrates and to enhance its affinity for recruitment of targets for subsequent ubiquitination, and in most cases, proteasomal-mediated degradation (Roth *et al.*, 1998; Arnberg *et al.*, 2000; Cathomen and Weitzman, 2000; Querido, Blanchette, *et al.*, 2001; Querido, Morisson, *et al.*, 2001; Blanchette *et al.*, 2004; Liu *et al.*, 2005; Schwartz *et al.*, 2008; Herrmann *et al.*, 2020). The E3 ligase complexes from six different HAdV groups, including HAdV12 (group A), HAdV16 (group B), HAdV5 (group C), HAdV9 (group D), HAdV4 (group E), and HAdV40 (group F), have been shown to exhibit heterogeneity in their structural composition and substrate specificity. Such that the E3 complex was shown to incorporate a Cul2 molecule in HAdV12 and HAdV40, while in HAdV4, HAdV5, and HAdV9 it was found to incorporate Cul5. However, HAdV16 was shown to bind both cullins (Blackford *et al.*, 2010; Cheng *et al.*, 2011; Forrester *et al.*, 2011). When the E3 ubiquitin ligase complex is assembled, several cellular DDR components that are unfavourable to viral proliferation and survival are targeted for ubiquitin-mediated proteasomal degradation. The following subsections (1.5.1.1, 1.5.1.2, 1.5.1.3, 1.5.1.4, and 1.5.1.5) will discuss some of these.

HAdVs from different groups show considerable variation in their ability to bind and degrade various substrates. For instance, HAdV5, HAdV12 and HAdV40 can induce rapid degradation of MRE11, whereas HaAVd9, HAdV16 and HAdV34 can only promote MRE11 degradation to a limited extent. Also, it was shown that HAdV4, HAdV5, HAdV12 and HAdV40 target integrin  $\alpha 3$  in infected cells, while DNA ligase IV was found to be completely degraded by most HAdV types (Cheng *et al.*, 2011; Forrester *et al.*, 2011). This might suggest that there is a considerable scale of target specificity and distinctive complex correlations between the E3 complex binding proteins among different HAdV types. Although these correlations were mostly attributed to the E1B55K-substrate binding affinity, adequate degradation was notable in many cases when there were weak or brief associations between the E3 complex and different substrates (Cheng *et al.*, 2013). Similarly, some proteins were demonstrated to bind effectively to E1B55K but not necessarily to be degraded, indicating that appropriate coordination of each substrate with the E3 ligase complex mapping locations is of importance (Herrmann *et al.*, 2020). Substantially, some studies revealed that HAdV5-E1B55K protein can, in fact, form a hybrid ligase complex with the E4orf6 from HAdV4 and HAdV9, which manifested substrate specificities similar to those of HAdV5 rather than that of HAdV4 or HAdV9. This confirms that the E1B55K molecule is undoubtedly the E3 ubiquitin ligase main substrate recognition unit (Cheng *et al.*, 2013).

#### **1.5.1.1 Regulation of p53 during HAdV infection.**

The tumour suppressor p53 was initially identified when it was detected in association with the large T antigen of Simian Virus 40 (SV40) (DeLeo *et al.*, 1979; Kress *et al.*, 1979; Lane and



Crawford, 1979; Linzer and Levine, 1979). Shortly afterwards, it was identified as a HAdV-E1B55K binding protein (Sarnow, Sullivan and Levine, 1982). p53 has been recognised as a tumour suppressor protein that regulates gene transcription processes that lead to cellular responses, such as G<sub>1</sub> and G<sub>2</sub> growth arrest, senescence, suppression of angiogenesis, or apoptosis in response to cellular genotoxic events such as IR, UV, or viral infections (Vogelstein, Lane and Levine, 2000; Surget, Khoury and Bourdon, 2014). p53 is a short-lived, inactive protein that is present at low levels in unstressed cells. However, in response to cellular stress, it is activated, stabilised, and plays a critical role in regulating cellular transcriptional activities (Meek, 2004; Surget, Khoury and Bourdon, 2014).

During HAdV infection, and in the absence of cooperating oncogenes, the expression of the 12S HAdV-E1A leads to an increase in p53 levels, which results in premature apoptosis (Lowe and Ruley, 1993). It is thought that HAdV-E1A elevates p53 protein levels by extending the cellular protein's half-life, which stabilises it (Sabbatini *et al.*, 1995; Turnell *et al.*, 2000; Li *et al.*, 2004). HAdV-E1A acts in different other ways to stabilise p53; however, it has been established that the NTR, CR1 and CR2 are all necessary for stabilising p53, consequently p300/CBP and pRB are thought to be involved in this activity (Querido, Teodoro and Branton, 1997; Turnell *et al.*, 2000).

Generally, during *wt* HAdV infection, the p53 protein has a limited half-life and is targeted for degradation through the ubiquitin-mediated pathway by the 26S proteasome. HAdV-E1A is able to associate with the 19S regulatory complex of the 26S proteasome through its NTR; an interaction that limits the direct degradation of p53 caused by the proteasome. HAdV-E1A selectively inhibits the 19S ATPase activity, which prevents the complex from effectively

directing ubiquitylated p53 to the 20S proteasome (Turnell *et al.*, 2000). The levels of p53 are thereby stabilised by HAdV-E1A.

Mdm2, a transcriptional target for p53, acts as a p53-specific E3 ubiquitin ligase that functions in a negative feedback loop to degrade and suppress p53's activity (Juven-Gershon and Oren, 1999). The p14<sup>ARF</sup> protein (known as p19<sup>ARF</sup> in mouse cells) is able to maintain stable levels of the p53 by acting as a negative regulator of Mdm2 (de Stanchina *et al.*, 1998). Normally, p53 is phosphorylated by ATM and CHK2 during DDR, which prevents Mdm2 from redirecting p53 out of the nucleus and inhibits its subsequent ubiquitylation (Shieh *et al.*, 1997; de Stanchina *et al.*, 1998). Although HAdV-E1A promotes DNA damage in cells, it stabilises p53 without inducing its phosphorylation (de Stanchina *et al.*, 1998). In this regard, it has been demonstrated that HAdV-E1A may stabilise p53 levels and induce cell cycle arrest or apoptosis by reducing Mdm2's capacity to degrade p53 through the activation of the E2F1-dependent transcription of p19<sup>ARF</sup> in mouse embryo fibroblasts. This is supported by the observation that HAdV-E1A fails to stabilise p53 levels in p19<sup>ARF</sup>-negative mouse embryo fibroblasts (de Stanchina *et al.*, 1998; Pomerantz *et al.*, 1998; Zhang, Xiong and Yarbrough, 1998; Ben-Israel and Kleinberger, 2002).

Through its interaction with p300/CBP, HAdV-E1A is also able to have an indirect influence on the stability of p53. It has been determined that HAdV-E1A blocks p53-dependent Mdm2 induction by interacting with p300/CBP, leading to p300/CBP inactivation (Grossman *et al.*, 1998; Thomas and White, 1998). It is interesting to note that p300/CBP is also capable of forming a trimeric complex with p53 and Mdm2 in order to facilitate the Mdm2-dependent ubiquitylation of p53 (Grossman *et al.*, 1998). Additionally, it is known that p300/CBP may

directly regulate p53 ubiquitylation, and as such, HAdV-E1A can limit p53 ubiquitylation and degradation via interacting with p300/CBP (Grossman *et al.*, 2003).

Finally, HAdV-E1A may also stabilise p53 by interacting with the Mdm2-related protein (known as Mdm4) (Li *et al.*, 2004). Even though Mdm4 lacks ubiquitin ligase function, it interacts with Mdm2 and activates Mdm2-mediated ubiquitin ligase activity against p53. It has been shown that the CR1 of HAdV-E1A associates with the NTR of Mdm4 and participates in the formation of a complex which binds p53 (Brooks and Gu, 2003; Li *et al.*, 2004). Accordingly, HAdV-E1A is able to stabilise p53 by limiting the nuclear export of p53 and preventing Mdm2-dependent polyubiquitylation of p53; however, HAdV-E1A is unable to stabilise p53 in the absence of Mdm4 and must work in conjunction with it in order to achieve this effect (Tanimura *et al.*, 1999; Li *et al.*, 2004).

The ability of HAdV-E1B55K to bind to p53 and repress its transcriptional activity is essential for viral-mediated cellular transformation (Yew and Berk, 1992; Yew, Liu and Berk, 1994). HAdV-E1B55K may interfere with p53 stabilisation, which is induced by HAdV-E1A in the early stages of infection, by two distinct strategies. The first strategy involves suppressing p53's transactivation domains. Transactivation of p53-responsive domains is inhibited when HAdV-E1B55K binds to the amino-terminal transactivation region of p53 (Kao, Yew and Berk, 1990; Yew, Kao and Berk, 1990; Yew and Berk, 1992; Yew, Liu and Berk, 1994). This suppression of p53 transactivation by HAdV-E1B55K is important for transformation of primary cells in conjunction with HAdV-E1A (Yew and Berk, 1992). The domain essential for p53 binding has been mapped to two core domains of HAdV-E1B55K situated between amino acids 180, 262 and 326 (Yew, Kao and Berk, 1990). Significantly, both *in vivo* and *in vitro* studies have shown

that HAdV-E1B55K does not bind cellular DNA but , instead, targets p53 sensitive promoters by direct interaction with DNA-bound p53 (Martin and Berk, 1998, 1999). However, it has been established that HAdV-E1B55K binding to p53 is required but not sufficient for the suppression of the protein (Teodoro *et al.*, 1994; Yew, Liu and Berk, 1994; Teodoro and Branton, 1997). HAdV-E1B55K might also restrict p53 transactivation by preventing acetylation of p53 by binding to both p300/CBP and the histone acetyl transferase (PCAF) (Liu *et al.*, 2000). The sequence-specific binding activity of p53 would be, otherwise, improved as a result of this acetylation (Gu and Roeder, 1997). Therefore, preventing this post-translational modification process may lead to a decrease in p53's DNA-binding activity and, as a consequence, hindering its ability to properly initiate transcription.

The second strategy by which HAdV-E1B55K modulates p53 function is via decreasing its half-life. When HAdV-E1A is expressed alone, it increases the level of p53. On the other hand, this rise in p53 levels is not observed following infection with the *wt* virus, indicating that the virus has the ability to degrade p53 in order to stop its accumulation. It was shown that this is accomplished by the formation of a complex which involves the viral E1B55K and E4orf6 proteins, as discussed in sections 1.3.1.2.4 and 1.5.1. It was shown that both proteins can independently associate with p53 to inhibit its functions. Collectively, the two proteins were found to collaborate to shorten p53's half-life and trigger its degradation (Querido *et al.*, 1997; Cathomen and Weitzman, 2000; Querido, Blanchette, *et al.*, 2001). Additionally, in HAdV-infected cells, both proteins were shown to collaborate to decrease p53 levels by shortening the half-life of p53 in Mdm2-negative cells via inhibiting its expression (Steegenga *et al.*, 1998). It has also been determined that E1B55K and E4orf6 mainly work together during infection to direct p53 to the ubiquitin-proteasome pathway for degradation (Steegenga *et al.*, 1998;

Querido, Blanchette, *et al.*, 2001). In this regard, it has been shown that E1B55K serves as the p53 receptor, and that E4orf6 serves to recruit the E3 cullin ring ligase to the E1B55K-p53 complex (Figure 1.8) (Querido, Morisson, *et al.*, 2001). It is also important to note that p53 can be stabilised by HAdV12-E1B55K in the absence of HAdV-E1A (Grand *et al.*, 1996), as reported in Chapter 4. This is presumably explained by the direct interaction between the viral protein and at the N-terminal region of p53, preventing its association with Mdm2 (Lin *et al.*, 1994).

Interestingly, it has been demonstrated that p53 is not degraded by all HAdV types. Despite the observation that E4orf6 can interact with p53, it is believed that the way in which p53 is able to associate with the E1B55K protein in various viral types plays a major role in its subsequent degradation by the E3 ligase complex (Blanchette *et al.*, 2004; Cheng *et al.*, 2011, 2013). Accordingly, p53 molecules were degraded during HAdV5 (group C), HAdV12 (group A) and HAdV40 (group F) infections, but not during infections with group B and D viruses (Forrester *et al.*, 2011). Additional *in vitro* studies have shown that p53 was degraded in the presence of E1B55K and E4orf6 from HAdV5, HAdV12 and HAdV40, but not in group B, D and E viruses (Cheng *et al.*, 2011). This was confirmed in many other studies performed on HAdV5 and HAdV12 by demonstrating that their E1B55K proteins bind p53 effectively (Sarnow *et al.*, 1982; Zantema, Schrier, *et al.*, 1985; Kao, Yew and Berk, 1990; Yew and Berk, 1992; Grand, Grant and Gallimore, 1994). Nonetheless, HAdV9, HAdV16, and HAdV34 E1B55K proteins were shown to interact efficiently with p53 with no apparent degradation (Cheng *et al.*, 2011).

Additional investigation revealed that some discrepancy in p53 degradation among different HAdV types might pertain to their ability to relocalise p53 by their respective E1B55K proteins during cellular infection and transformation. For instance, the E1B55K proteins from both

HAdV5 and HAdV12 are distinct from one another in a number of significant aspects. When HAdV12-E1B55K and p53 were co-immunoprecipitated, there was only a relatively weak (Grand, Grant and Gallimore, 1994) or negligible (Zantema, Schrier, *et al.*, 1985) interaction between the two proteins during infection, but HAdV5-E1B55K was shown to physically interact with p53 in transformed cells (Sarnow *et al.*, 1982). Additionally, E1B55K predominantly accumulates in the cytoplasm in HAdV5 transformed cells (Zantema, Fransen, *et al.*, 1985), while in HAdV12 it is largely present in the nucleus (Zantema, Schrier, *et al.*, 1985). On the basis of these variations, it has been hypothesised that HAdV12-E1B55K could control p53 activity in a way that is fundamentally distinct from the way in which HAdV5-E1B55K does (Wienzek, Roth and Dobbelstein, 2000). Similarly, many but not all HAdV types were shown to have their E1B55K proteins concentrated in juxtannuclear aggresomes or PML-NBs (Blanchette *et al.*, 2013). In the case of HAdV5 and HAdV16, E1B55K was shown to induce p53 relocalisation to juxtannuclear aggresomes, although in HAdV16 the relocalisation process was not as efficient as observed with HAdV5. HAdV9 and HAdV40 on the other hand, distinctively exhibited p53 relocalisation to PML-NBs, while in HAdV12, the viral protein displaced p53 into aggresome-like structures dispersed throughout the cytoplasm. However, HAdV4-E1B55K showed limited displacement of p53 into PML-NBs, even when it was highly expressed in infected cells.

As previously stated, the E1B55K protein binds p53 and blocks its transcriptional activity during HAdV5 and HAdV12 infections. Further investigation of other viral types revealed that HAdV9, HAdV16, HAdV34 and HAdV40 were also able to inhibit p53 transcriptional activity in a dose-dependent manner similar to HAdV5 and HAdV12, whilst HAdV4 showed no transcriptional repression of p53 at all (Forrester *et al.*, 2011; Cheng *et al.*, 2013). This might

suggest that HAdV4 may utilise a different way of repressing p53, as it is already known that E4orf6 protein can bind p53 independently and inhibit its transcriptional activation during HAdV5 infection (Dobner *et al.*, 1996; Nevels *et al.*, 1997; Querido *et al.*, 1997; Cathomen and Weitzman, 2000; Querido, Morisson, *et al.*, 2001). Significantly, when compared to HAdV9, HAdV16, and HAdV40, it has been shown that E4orf6 from HAdV4 and HAdV5 possesses the ability to bind and suppress p53 activity independently from E1B55K. This suggests that even though HAdV4 is not able to repress p53 by binding it with E1B55K, it could compensate for this through binding with it via the E4orf6 protein (Cheng *et al.*, 2013).

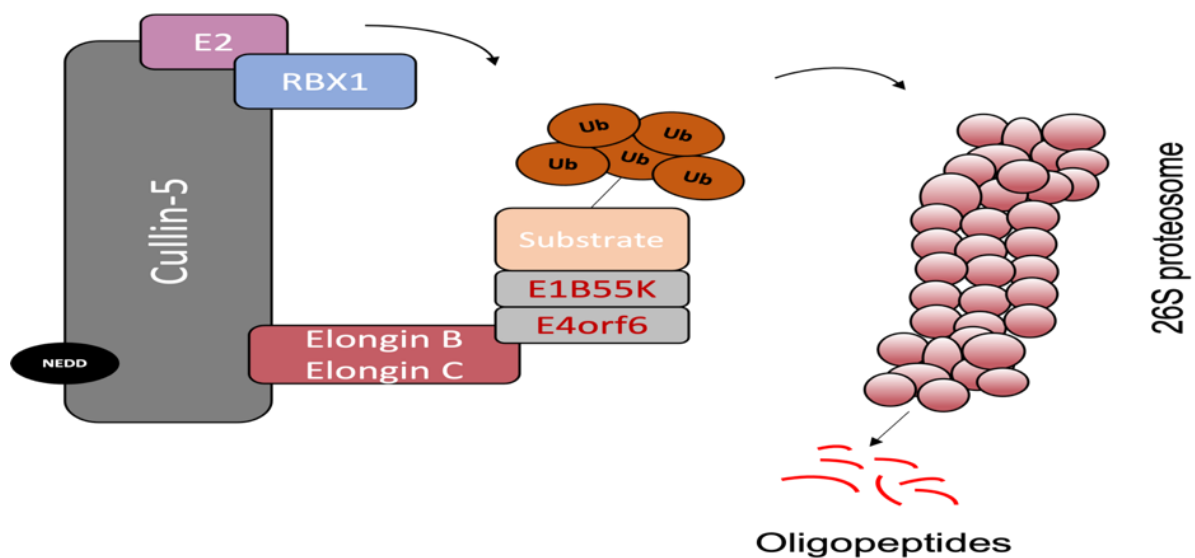


**Figure 1.8.** Representative model of ubiquitylation and degradation of cellular substrates by the host E3 Cullin-5 ring ligase complex. Adapted from: (Herrmann *et al.*, 2020).

#### 1.5.1.2 Regulation of the ATM signalling pathway during HAdV infection.

The MRN complex detects DSBs and activates the ATM signalling pathway to facilitate cell cycle checkpoint regulation and DNA repair (Uziel *et al.*, 2003). At least two different methods

are utilised by HAdVs to deactivate the MRN complex, which is a primary target for groups A and C HAdVs. These methods include relocating the complex away from VRCs to PML-NBs and juxtannuclear aggresomes (Section 1.5.2), as well as targeting components of the complex for proteasomal degradation.

Shortly after it was demonstrated that HAdV5 E1B55K/E4orf6 proteins 'hijack' the cellular E3 ligase components to promote p53 degradation (Querido, Blanchette, *et al.*, 2001), it was shown that HAdV5 can also deactivate the ATM pathway by targeting MRE11 for proteasomal-mediated degradation during infection, resulting in disruption of the cellular DDR (Figure 1.11). (Stracker, Carson and Weitzman, 2002). Significantly, Rad50 and NBS1 levels are also reduced in the absence of MRE11; however, it is possible that one or both of them are also targets for HAdV-mediated degradation (Stewart *et al.*, 1999; Zhong *et al.*, 2005). Later, it was reported that BLM, which is involved in the resection of DSBs, is also targeted for degradation by the E1B55K/E4orf6 complex during HAdV5 infection (Orazio *et al.*, 2011). E1B55K's binding to BLM was independent of its binding to MRE11, although it was not confirmed if BLM promoted viral replication before its degradation, nor whether its degradation facilitated viral replication (Orazio *et al.*, 2011).

Interestingly, heterogeneity was found amongst different HAdV types in their ability to degrade MRE11 (Cheng *et al.*, 2011; Forrester *et al.*, 2011). Whilst HAdV5-E1B55K was shown to interact efficiently with MRE11 and was necessary for its degradation, MRE11's association with E4orf6 was dependent on the presence of E1B55K (Blanchette *et al.*, 2004). Limited E1B55K binding and degradation of MRE11 was seen during HAdV9 and HAdV16 infections, compared to the efficient binding and rapid degradation seen in HAdV5. Additionally, weak



interactions between the E1B55K and MRE11 were evident in HAdV12 and HAdV40, although their degradation of MRE11 was shown to be comparable to that seen with HAdV5. In contrast, MRE11 was found to weakly bind HAdV4-E1B55K with no detectable degradation (Cheng *et al.*, 2013). Therefore, it appears that degradation of MRE11 is not solely dependent on its binding to E1B55K (Cheng *et al.*, 2013). Studies have also shown that relocalisation of MRE11 by E1B55K in different HAdV types may have an influence on its degree of degradation. For instance, during HAdV5, HAdV4 and HAdV16 infections, MRE11 accumulates in cytoplasmic aggresomes (Liu *et al.*, 2005). On the contrary, very limited MRE11 relocalisation was exhibited by HAdV9, HAdV12 and HAdV40 E1B55Ks (Section 1.5.2) (Cheng *et al.*, 2013).

#### **1.5.1.3 Regulation of the ATR signalling pathway during HAdV infection.**

ATR kinase is responsible for regulating many important cellular processes such as DNA replication, DDR, cell cycle arrest and induction of apoptosis (Section 1.4.2.2). Both HAdV5 and HAdV12 regulate the ATR signalling pathway during infection (Blackford *et al.*, 2008, 2010). It was shown that, during HAdV5 and HAdV12 infections, the E1B55K interacting protein, E1B-AP5 (hnRNPUL1) along with ATRIP, RAD9, and RAD17 were all recruited to VRCs. Although the role of their viral-mediated relocalisation to VRCs is not completely understood, it has been proposed that this relocalisation inhibits the functions of key DDR proteins by preventing their activation (Blackford *et al.*, 2008). Additionally, HAdV5 was shown to inhibit the ATR-mediated activation of CHK1 by inducing relocalisation of MRN to PML-NBs through viral E4orf3; however, many other viral types, including HAdV12 did not possess this ability (Carson *et al.*, 2009). HAdV12 was shown to suppress ATR-mediated activation of CHK1 by targeting the ATR activator protein, TOPBP1 for degradation in a Cul2-dependent manner that

requires HAdV12-E4orf6, but not HAdV12-E1B55K. This may indicate that E4orf6 can act both as a substrate adaptor and a recruiter of the Cul2 in the E3 ligase complex (Blackford *et al.*, 2010). Recent evidence shows that the E1B55K/E4orf6 E3 ligase complex from HAdV5 and HAdV12 also targets the ATR substrate, SMARCAL1 for degradation to modify cellular DNA replication (Nazeer *et al.*, 2019). Interestingly, it was established that claspin, which associates with CHK1 to induce its activity during replication stress, was restricted from associating with viral genomes that have recently undergone replication, suggesting that this checkpoint signalling protein might have a role in suppressing the replication of HAdVs (Reyes *et al.*, 2017). Additionally, the inhibition of CHK1 activation was also facilitated by HAdV5-mediated downregulation of MRE11 (Pantelidou *et al.*, 2016). These findings demonstrate that the ATR signalling pathway is indeed targeted by HAdVs to support viral genome replication (Figure 1.11).

#### **1.5.1.4 Regulation of the DNA-PK pathway during HAdV infection.**

During HAdV infection, DNA ligase IV is targeted by the E1B-55K/E4orf6 complex to block the DNA-PK-dependent NHEJ repair process (Baker *et al.*, 2007; Cheng *et al.*, 2011; Forrester *et al.*, 2011). The E4orf6 protein suppresses DNA-PK-dependent V(D)J-recombination by associating with DNA-PK independently to inhibit viral genome concatenation (Boyer, Rohleder and Ketner, 1999). Recent evidence indicates that the E4orf4 protein also interacts with DNA-PKcs during HAdV5 infection, and that these two proteins co-localise at VRCs (Nebenzahl-Sharon *et al.*, 2019). As such, it has been proposed that, early during infection, E4orf4 exploits DNA-PKcs to inhibit the ATM and ATR pathways by decreasing ATM

autophosphorylation and CHK1 activation, respectively. Whereas in late infection, the virus directly inhibits DNA-PK activity to promote viral genome replication (Nebenzahl-Sharon *et al.*, 2019).

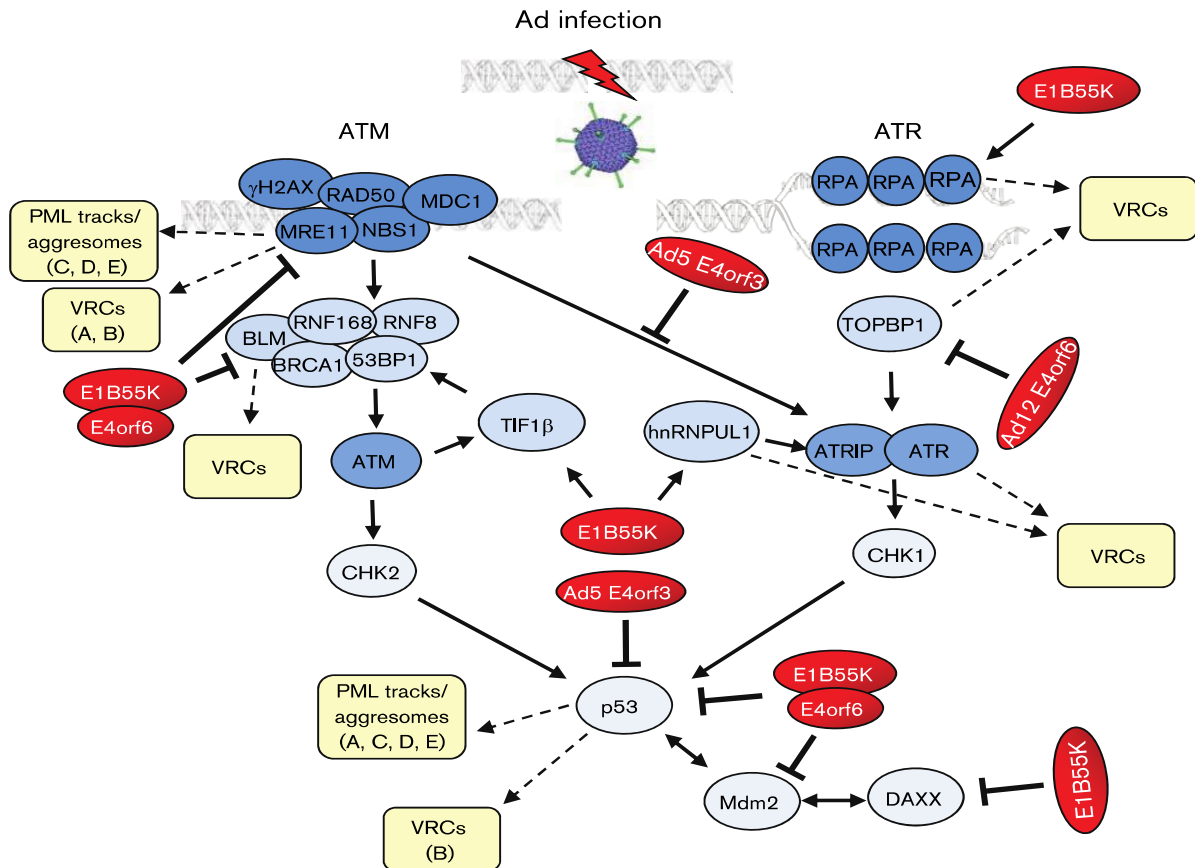


**Figure 1.9.** Regulation of ATM and ATR signalling pathways by HAdVs. The figure depicts the several strategies in which HAdV suppresses ATM and ATR signalling pathways during infection, including Cullin-Ring Ligase-targeted proteasomal degradation and recruitment to VRCs and E4orf3 nuclear tracks. Particularly, the functions that E1B55K/E4orf6 complexes from different viral types play in the regulation of p53, MRE11, and the BLM helicase is shown. It is also shown that HAdV12-E1B55K and E4orf6 may specifically target Daxx and TOPBP1 for proteasomal-mediated degradation. Additionally, the figure demonstrates that E1B55K binds RPA, TIFβ, and hnRNPUL1. It is also shown that HAdV5's E4orf3 has the ability to regulate p53

and ATR signalling. Viral proteins are shown in red circles and cellular proteins are shown in blue. Arrows indicate protein-protein interaction between viral and cellular proteins. Taken from: (Turnell and Grand, 2012).

#### 1.5.1.5 Degradation of additional proteins during HAdV infection.

Various other cellular proteins were shown to be targeted for degradation during HAdV infection by E1B55K and E4orf6, which, in some cases, facilitates viral replication and spread. For instance, during HAdV5 infection, the cell surface receptor (integrin  $\alpha 3$ ) associated with Cul5 (Dallaire *et al.*, 2009), along with other proteins involved in cellular adhesion, including ALCAM, EPHA2, and PTPRF, which were all substrates for E1B55K/E4orf6 dependent ubiquitination and proteasomal degradation (Fu *et al.*, 2017). The death-domain-associated protein (Daxx), involved in cellular transcription and apoptosis, has also been shown to be targeted by HAdV5-E1B55K during infection (Schreiner *et al.*, 2010).

BLM is a DNA helicase that is involved in maintaining genomic integrity and repair of DSBs during HR (W. Wang *et al.*, 2000; Y. Wang *et al.*, 2000; Cheok *et al.*, 2005). It has been established that BLM is targeted by different HAdV types for degradation via the E1B55K/E4orf6 complex, even though the specific role of its degradation during infection is still not yet fully understood (Orazio *et al.*, 2011). By analysing proteins that are targeted by HAdVs for degradation, our laboratory has recently identified a novel DDR protein, tankyrase 1 binding protein 1 (TNKS1BP1 also known as Tab182), which is degraded during HAdV5 and HAdV12 infections (Chalabi Hagkarim *et al.*, 2018). This degradation was shown to require viral E1B55K/E4orf6 proteins and is mediated by cullin-based E3 ligases and the 26S proteasome. The histone acetyltransferase (Tip60), involved in the activation of DDR and DNA

repair, is another target for E1B55K/E4orf6 proteasomal-mediated degradation. Tip60 also binds directly to the HAdV-E1A early promoter, limiting the protein's expression. Thus, degradation of Tip60 following viral infection is important to prevent the suppression of E1A expressing genes (Gupta *et al.*, 2013). Collectively, these reports show how important it is for HAdVs to inhibit and degrade key DDR proteins during infection through proteasomal-mediated degradation to promote viral replication.

### 1.5.2 Relocalisation and inhibition of DDR proteins.

HAdVs are capable of interfering with the DDR by mis-localising several DDR proteins. During infection, viral E4orf3 may induce the relocalisation of many DDR proteins to nuclear tracks that originate from PML bodies (Puvion-Dutilleul *et al.*, 1995; Everett, 2001). It is unclear what role this relocalisation serves; nevertheless, it is hypothesised that E4orf3-mediated relocalisation of p53 causes the development of heterochromatin at p53 target promoters, preventing p53-DNA binding and silencing p53 activated transcription (Soria *et al.*, 2010).

In addition to degrading MRN subunits, some HAdV types utilise the E4orf3 protein to relocalise the MRN complex to different cellular locations in order to inhibit MRN-dependent activation of the DDR at VRCs (Evans and Hearing, 2005; Stracker *et al.*, 2005). PML-NBs are multiprotein complexes that are seen in nuclei as punctate structures. These nuclear bodies have been implicated in the control of transcription, activation of apoptosis, repair of DNA damage, protein modification, and antiviral responses in cells (Lallemant-Breitenbach and de Thé, 2018). They include several DDR proteins to carry out their function in detecting DNA

damage (Lombard, 2001). A multimeric version of E4orf3 rearranges the punctate PML-NBs into "track-like" structures after HAdV infection (Carvalho *et al.*, 1995; Doucas *et al.*, 1996; Leppard and Everett, 1999; Ou *et al.*, 2012; Patsalo *et al.*, 2012). Thus, by counteracting PML-NBs function, HAdV replication is no longer inhibited. It has been shown that E4orf3 from HAdV2 and HAdV5 mis-localises the MRN complex, causing it to be sequestered in PML-NBs rather than VRCs, where it is unable to trigger the cellular DDR (Stracker, Carson and Weitzman, 2002; Evans and Hearing, 2005). The relocalisation process, seen following IR exposure, is thought to be responsible for inhibiting the activation of the ATR damage signalling pathway (Evans and Hearing, 2005). Significantly, during HAdV5 infection, MRN seems to be initially confined to PML-NBs, where it binds E1B55K; subsequently, E4orf3 or E4orf6 are needed in addition to E1B55K for aggresome formation; to which MRE11 is finally exported. Interestingly, proteasomal degradation of MRN complexes is accelerated by their export from the nucleus to E1B55K-containing aggresomes, as revealed in previous studies. However, It is important to note that, in a manner similar to the relocalisation of MRN to PML-NBs, infection with some HAdV types does not result in MRN mis-localisation to E1B55K aggresomes (Stracker *et al.*, 2005; Blanchette *et al.*, 2013). This finding suggests that different HAdVs employ a variety of mechanisms to inhibit MRN and the DDR. In this regard, it was reported that HAdV9 and HAdV12 may target MRN through both mis-localisation and degradation, but they still have impaired DNA replication, suggesting that these viral types are distinct from HAdV5 (Pancholi and Weitzman, 2018). It was also suggested that it is possible that different HAdVs have differing effects on the localisation of NBS1 to those seen with MRE11 (Pancholi and Weitzman, 2018). This is in line with the findings of earlier studies, which revealed that NBS1 colocalised with VRCs throughout the late phases of HAdV5 infection,

despite the fact that MRE11 was mis-localised to nuclear tracks or had been degraded (Evans and Hearing, 2005). Additionally, whether the MRN complex was present did not affect the replication of *wt* HAdV5. Similarly, the presence of NBS1 did not influence replication of HAdV5 mutants that were either E1B55K or E4orf3 negative (Babiss and Ginsberg, 1984). In contrast, in full E4-deleted HAdV5 (Bridge and Ketner, 1989), viral DNA replication was obstructed in cells that had functional NBS1 to produce the MRN complex, but was retained in cells lacking functional NBS1. This reveals that mis-localisation or degradation of MRN is sufficient to overcome the inhibitory effects of the MRN complex in *wt* HAdV5 infections, as was previously described (Lakdawala *et al.*, 2008). In a manner similar to that of HAdV5, neither HAdV2 nor HAdV4 were influenced by MRN, since the replication of each virus was unaltered in either NBS1-negative or NBS1-positive cells. This is in line with what was observed about the mis-localisation and degradation of MRN by the two viruses in other studies (Pancholi and Weitzman, 2018). It is also important to note that replication of HAdV9, which mis-localises MRN but does not degrade it, was significantly increased in the absence of functional NBS1 at several stages of infection. This effect was also seen in the absence of functional NBS1 (Pancholi and Weitzman, 2018). Similarly, replication of HAdV12, which degrades MRN but does not cause its mis-localisation, was shown to be greatly enhanced in the absence of a functioning MRN complex. Taken together, These findings point to the possibility that different HAdV types have varying degrees of sensitivity to inhibition by the MRN complex as it was observed that MRN does not have any effect on HAdV5, HAdV2, or HAdV4 (Pancholi and Weitzman, 2018). On the other hand, the MRN complex can inhibit the growth of both HAdV9 and HAdV12, despite being the primary target of both viruses. Based on these observations, it seems that, in contrast to HAdV5, neither mis-localisation of MRN by

HAdV9 nor the degradation of MRN by HAdV12 are sufficient to circumvent the inhibition of viral DNA replication imposed by the MRN complex during infection with wt HAdVs (Pancholi and Weitzman, 2018).

Several cellular activities, including transcription, replication, chromosomal segregation, and DNA repair, are regulated by protein modification with members of the ubiquitin/SUMO family of proteins (Gareau and Lima, 2010; Zhao, 2018). During HAdV infection, E4orf3 increases the recruitment of SUMOylated proteins to PML-NBs, leading to an increase in the SUMOylation of numerous host proteins. The majority of the E4orf3 SUMO targets are involved in DNA damage signalling and repair mechanisms (Sohn and Hearing, 2012; Sohn, Bridges and Hearing, 2015). This includes the MRN subunits MRE11 and NBS1. Significantly, both the production of PML-NBs and the recruitment of SUMO ligases are functions which are shared by E4orf3 proteins encoded by most but not all HAdV types (Sohn and Hearing, 2012). In this regard, SUMOylation of MRN components are not caused by HAdV types that do not induce MRN mis-localisation. In contrast, TIF-1 $\gamma$  is a protein that is mis-localised and SUMOylated by E4orf3 proteins of most HAdVs (Sohn and Hearing, 2012, 2019b). Interestingly, some targets that are SUMOylated by E4orf3 are degraded by the ubiquitin-proteasome pathway, whilst others, like MRE11 and NBS1, are not; the effect of this change on their function is still unknown (as reviewed in (Sohn and Hearing, 2019a)). Altogether, this suggests that HAdVs may utilise cellular aggresomes and PML-NBs to promote the degradation of key regulatory DDR proteins, which would otherwise restrict viral replication. Nonetheless, it was shown that relocalisation of E1B55K to aggresomes and PML-NBs is not essential for target protein degradation, based on the observation that cytoplasmic



aggresomes formation by E1B55K is not conserved amongst some HAdV types (Blanchette *et al.*, 2013).

### 1.5.3 Potential HAdV substrates not degraded by the E1B55K/E4orf6 complex.

As previously discussed, several host proteins, including p53, MRE11, Rad50, NBS1, DNA ligase IV, and BLM have been identified as candidates for proteasomal-mediated degradation by the HAdV5-E1B55K/E4orf6 E3 ligase complex (Querido *et al.*, 1997; Querido, Blanchette, *et al.*, 2001; Stracker, Carson and Weitzman, 2002; Baker *et al.*, 2007; Dallaire *et al.*, 2009; Orazio *et al.*, 2011). During viral infection, degradation of these proteins suppresses DNA damage signalling and apoptosis (Cathomen and Weitzman, 2000; Carson *et al.*, 2003; Schwartz *et al.*, 2008). Viral mutants lacking E1B55K or E4orf6 are likewise defective in late RNA processing and yield less late mRNA, viral protein, and viral progeny, with minimal effect on early phases of infection (Babiss, Ginsberg and Darnell Jr., 1985; Halbert, Cutt and Shenk, 1985; Pilder *et al.*, 1986; Bridge and Ketner, 1989, 1990; Sandler and Ketner, 1989). However, these defects are not entirely explained by most of the known E1B55K/E4orf6 target substrates (Babiss and Ginsberg, 1984; Babiss, Ginsberg and Darnell Jr., 1985; Halbert, Cutt and Shenk, 1985; Pilder *et al.*, 1986; Bridge and Ketner, 1989, 1990; Sandler and Ketner, 1989). The E1B55K/E4orf6 complex is known to facilitate ubiquitination and degradation of common DNA damage signalling pathway substrates (as reviewed in (Hidalgo *et al.*, 2019; Kleinberger, 2020)); however, a recent study has demonstrated that some putative ubiquitinated substrates, most of which are not involved in DDR, are not degraded in the presence of the E1B55K/E4orf6 complex (Herrmann *et al.*, 2020). These ubiquitinated substrates were left unaltered after

ubiquitylation. Correspondingly, it was shown that there was an increase in the abundance of host RNA-binding proteins (RALY and hnRNP-C) that are ubiquitinated in order to bypass constraints on the production of viral late transcripts. Significantly, these substrates emphasised the viral exploitation of non-degradative ubiquitination as a technique to control host pathways and suggest a putative mechanistic connection between E1B55K/E4orf6-redirected ubiquitination and late viral RNA processing (Herrmann *et al.*, 2020). In this regard, it was shown that the known viral targets MRE11 and Rad50 were among the substrates that displayed elevated ubiquitination as a result of the expression of the E1B55K/E4orf6 complex during infection. However, it was shown that 120 host proteins were also identified as potential targets of ubiquitination that was driven by the viral complex. Among these, 25 proteins were ubiquitinated, which resulted in a drop in their abundance, whereas another 91 proteins exhibited enhanced ubiquitination but without substantial change in their overall abundance. Thus, these proteins were projected to serve as non-degraded targets for the E1B55K/E4orf6 complex. Collectively, these findings imply that the E1B55K/E4orf6 complex is capable of facilitating non-degradative ubiquitination, and they also suggest that the majority of possible E1B55K/E4orf6 substrates might fall into this category (Herrmann *et al.*, 2020).

## **1.6 HYPOTHESIS AND AIMS**

Hypothesis: E1B55K proteins from different adenovirus types have broadly similar effects on the cellular DNA damage response.

The overall aim of this thesis is the further characterisation of HAdV-E1B55K proteins from different virus types to determine their role in the disruption of the cellular DNA damage response.

1. To isolate novel cellular (DDR) proteins which bind to HAdV5 and HAdV12 E1B55K proteins and determine their degradation patterns during viral infection.
2. To use the 55K<sup>+</sup>HSF cell line to characterize the relationship between HAdV12-E1B55K and the DDR in detail and to determine whether it impacts on DNA replication.
3. To determine the relationship between the E1B55K proteins from representative viruses from group B (HAdV16), group D (HAdV9), group E (HAdV4) and group F (HAdV40) HAdVs and the DDR.

# **CHAPTER 2**

## **Materials and Methods**

## 2.1 CELL CULTURE TECHNIQUES

### 2.1.1 Human cell lines.

The cell lines used in this study are summarised in Table 2.1. Transformed cell-lines (HAdV5-E1HEK293 and HAdV12-E1HER2) and cell strains (HSF and 55K<sup>+</sup>HSF) express either HAdV-E1 proteins or, in the case of 55K<sup>+</sup>HSFs only E1B55K. Interestingly, HeLa cells are known to have low levels of p53 due to the expression of the Human papillomavirus 18 (HPV18) E6 protein, which facilitates p53 degradation. The p53 gene in HeLa cells is wild-type and expression of the protein is induced by HAdV-E1A during viral infection as has been reported for other human cell lines (Grand, Grant and Gallimore, 1994).

Cell line	Supplier	Type	Information
HeLa S3	ATCC-CCL-2.2	Epithelial	Transformed epithelial cell line derived from Human cervical cancer cells expressing HPV-18 proteins
HAdV5-E1HEK293	ATCC-CRL-1573 or obtained from Invitrogen	Neuronal	HAdV5 E1-transformed neuronal cell line derived from human embryonic kidney cells
HAdV12-E1HER2	Produced in-house (Byrd, Brown and Gallimore, 1982).	Neuronal	HAdV12 E1-transformed neuronal cell line derived from human embryonic retinal cells
HSF	In-house donor (KS)	Connective tissue	Normal Human skin fibroblast cells
55K <sup>+</sup> HSF	Derived from the HSF cells	Connective tissue	Human skin fibroblast cell strain expressing HAdV12-E1B55K

**Table 2.1.** List of human cell lines used throughout this study.

### **2.1.2 Cell culture media.**

Cells were grown in Dulbecco's Modified Eagle Medium (DMEM) (Sigma-Aldrich) enriched with 8% foetal calf serum (FCS) (Sigma-Aldrich) and kept at constant humidity in 5% CO<sub>2</sub> at 37°C in an incubator. All cell culture media were stored at 4°C for up to 3 months. Prior to use, reagents were warmed to 37°C in a water bath.

### **2.1.3 Maintenance of human cell lines.**

When reaching 70-80% confluency, all cell lines were passaged and maintained by discarding existing media and washing the cells twice with pre-warmed 3ml phosphate buffered saline (PBS) (Sigma-Aldrich) followed by incubation with 0.05% trypsin (Invitrogen) at 37°C for 5 minutes in a humidified incubator. Detachment of cells was confirmed by light microscopy and detached cells were pelleted by centrifugation at 1500 rpm for 5 minutes and resuspended in fresh warm culture media which were replated at the appropriate density determined using a haemocytometer ( $5 \times 10^6$  cells in 10cm cell culture dishes). All cell lines were passaged in a sterile biological cabinet class 2/class 2 laminar flow hood and grown in a humidified incubator at 37°C supplied with 5% CO<sub>2</sub>.

### **2.1.4 Cryopreservation of human cell lines.**

For long time storage, cells were trypsinised as mentioned above and pellets were resuspended in 10% dimethylsulphoxide (DMSO) (Sigma-Aldrich) with DMEM supplemented with 20% FCS. Resuspended cells were transferred into cryovials and were gradually cooled

overnight to -80°C in an isopropanol freezing container. Frozen cryovials were then transferred into liquid nitrogen tanks for long-term storage at -180°C. When required, cells were retrieved from liquid nitrogen by thawing rapidly in water bath at 37°C followed by centrifugation at 1500 rpm for 5 minutes and pellets were resuspended again in fresh DMEM and then replated.

## 2.2 CELL BIOLOGY TECHNIQUES

### 2.2.1 HAdV types.

Human wild type HAdV5 (VR-5) and wild type HAdV12 (Huie; VR-863) were obtained from ATCC. Propagation of *w.t* Ad5 was performed on permissive HAdV5-E1 transformed HEK293, whilst *w.t* HAdV12 propagation was performed on HAdV12-E1 transformed HER2 cells.

### 2.2.2 Viral infections.

Stock titres of *w.t* Ad5 and *w.t* HAdV12 were previously determined by plaque assay on HAdV5 E1-transformed HER911 and HAdV12 E1-transformed HER3 cells (Turnell, Grand and Gallimore, 1999; Hutton *et al.*, 2000). Prior to HAdV infection, appropriate cells were grown to 80-90% confluency in 6cm dishes and were then infected with the appropriate virus in FCS-free DMEM media at a multiplicity of infection (MOI) of 5 plaque forming units (pfu) per cell; dishes were incubated in 5% CO<sub>2</sub> at 37°C for 2 hours with agitation at 15 minute intervals to ensure equal distribution and spread of virus-containing media around the dish. Subsequently,

media was replaced with fresh DMEM containing 8% FCS and infected cells were incubated at 37°C until harvesting.

### 2.2.3 Transfection of HeLa cells with siRNA.

24 hours before transfection, cells were plated onto 6cm dishes in DMEM with 10% FCS at 30–40% confluency. SMARTPool of ON-TARGETplus Human UBR5 (51366) siRNA was obtained from Dharmacon, and it was designed to reduce the expression of human UBR5. The siRNA transfection mixture was produced by mixing 1ml of Opti-MEM (Invitrogen) to 10µl of Oligofectamine (Invitrogen) and 1.8µl of siRNA (50uM stock). The media was removed from the cells that were plated the day before and cells were washed in Opti-MEM once, and then 1 ml of Opti-MEM was added to each dish. After an incubation period of 30 minutes, the transfection mixture was added to each dish, and then the dishes were incubated at 37°C for 16–18 hours. The Opti-MEM and transfection mixture was then removed and replaced with DMEM supplemented with 10% FCS. 48 hours post siRNA treatment, cells were infected with HAdV5 or HAdV12 and incubated at 37°C until harvested. A list of siRNAs used in this study is summarised in Table 2.2.

Target	siRNA	Sense sequence	Supplier
Non-silencing Control	Custom	CGUACGCGGAUACUUCGAdTdT	Dharmacon
UBR5	SMARTpool	GCACUUAUACUGGAUUA GAUUGUAGGUUACUAGAA GAUCAAUCCUACUGAAUU GGUCGAAGAUGUGCUACUA	Dharmacon

**Table 2.2.** List of siRNAs used in this study. The siRNA used to knockdown the expression of UBR5 in this study is shown.



#### 2.2.4 Transient DNA transfections.

Hela cells were transfected with plasmids that encode HAdV-E1B55K genes from representative HAdV types, (groups B, D, E and F). Prior to transfection, Hela cells were grown to approximately 80-90% confluence on 6cm dishes in DMEM supplemented with 8% FCS. The transfection mixture was prepared by adding 2 µg of plasmid DNA to 200 µl of Opti-MEM in a universal tube and incubated at room temperature for 5 minutes. Similarly, 10 µl of Lipofectamine 2000 (Invitrogen) were added to 200 µl of Opti-MEM in a separate universal tube and incubated at room temperature for 5 minutes. After Incubation, the contents of both tubes were mixed and incubated for another 20 minutes at room temperature. After incubation, plasmid DNA-Lipofectamine transfection mixture was added to cells in DMEM, without changing the media, in a drop-wise manner for overnight incubation at 37°C in 5% (v/v) CO<sub>2</sub> humidified incubator. On the following day, cells were washed once with PBS and the existing media was replaced with warm DMEM supplemented with 8% FCS and incubated at 37°C to be harvested when needed. All DNA plasmid constructs used in this study are listed below in Table 2.3.

Vector	Dose for 6cm dish	HAdV group	HAdV type	Supplier
pcDNA 3.1	2 µg	-	-	Invitrogen-V79020
pcDNA3.1 HA-HAdV4E1B55K	2 µg	E	4	A gift from Thomas Dobner
pcDNA3.1 HA-HAdV9E1B55K	2 µg	D	9	A gift from Thomas Dobner
pcDNA3.1 HA-HAdV16E1B55K	2 µg	B	16	A gift from Thomas Dobner
pcDNA3.1 HA-HAdV40E1B55K	2 µg	F	40	A gift from Thomas Dobner

**Table 2.3.** List of DNA plasmids used throughout this study.

### 2.2.5 Irradiation of cells with ionising radiation.

Cells subjected to induced irradiation damage were either mock-irradiated or irradiated with ionising  $\gamma$ -rays using a  $^{137}\text{Cs}$  source delivering approximately 1 Gy/20 seconds. Following irradiation, DMEM supplemented with 8% FCS was added to cells and they were placed in a 37°C incubator, before being harvested at appropriate times.

### 2.2.6 Drug treatments and cytotoxic agents.

As and when required in various experiments, cells were treated with different drugs and cytotoxic agents which are outlined below in Table 2.4. The working concentrations of drugs used are detailed in their appropriate figure legends.

Reagents	Working concentration	Supplier	Information
Camptothecin	1 $\mu$ M	Cayman	Topoisomerase I inhibitor which induces DNA replication arrest and formation of double-stranded breaks in DNA
Hydroxyurea	2mM	Sigma-Aldrich	Induces DNA replication stress by inhibiting DNA synthesis by depleting the cellular pool of dNTPs
MLN-4924	5 $\mu$ M	Cayman	Cell-permeable NEDD8-Activating Enzyme inhibitor used to inhibit Cullin Ring Ligase activation
Aphidicolin	3 $\mu$ M	Sigma-Aldrich	Anti-mitotic, DNA replication inhibitor used to achieve cell synchronization.
Nocodazole	200 ng/mL	Sigma-Aldrich	Inhibits mitosis by disruption of mitotic spindle function and arresting the cells in metaphase during cell division
Mirin	50 $\mu$ M	Sigma-Aldrich	Inhibits MRN-dependent activation of ATM and MRE11 exonuclease activity

**Table 2.4.** List of cytotoxic agents used throughout this study.

### 2.2.7 Buffer recipes.

All buffers used and their recipes used in this study are outlined in Table 2.5.

Buffer name	Recipe
DNA Fibre Spreading Buffer	0.2 M Tris-HCl pH 7.4, 50 mM EDTA and 0.5% SDS
DNA Fibre Blocking Buffer	1% BSA, 0.01% Tween 20 in PBS
NETN Buffer	1% NP-40, 0.15 M NaCl, 50 mM Tris-HCl pH 7.4, 5 mM EDTA
SDS Sample Buffer	5% SDS, 5 M urea, 20 mM Tris HCl pH 7.4 and 0.1 M $\beta$ -mercaptoethanol
Western Blot Running Buffer	100 mM Tris/Bicine and 1% SDS
Western Blot Transfer Buffer	200 mM Tris, 190 mM Glycine and 20% v/v methanol
TBST Buffer	50 mM Tris-HCl pH 7.4, 0.15 M NaCl, 1% Tween 80
UTB lysis buffer	9M urea, 50mM Tris HCl pH 7.4 and 150mM $\beta$ -mercaptoethanol
SCF Buffer A	0.34 M sucrose, 10% glycerol, 1.5 mM $Mg_2Cl$ , 10 mM KCl, 10 mM HEPES pH 7.9 and 1mM DTT
SCF Buffer B	3 mM EDTA, 5 mM EGTA and 1mM DTT

**Table 2.5.** List of buffers used throughout this study.

### 2.2.8 DNA fibre assay.

24 hours before DNA fibre labelling, HSF and 55K<sup>+</sup>HSF cells were seeded in 6cm dishes. At around 50% confluency, cells were pulse-labelled with 20  $\mu$ l (final concentration 25 $\mu$ M) of 5-Chloro-2'-deoxyuridine (CldU) (Sigma) for 40 minutes at 37°C. Excess CldU was removed by washing the cells 2 times with warm DMEM, followed by pulse- labelling the cells with 222  $\mu$ l (final concentration 250 $\mu$ M) of CO<sub>2</sub>-equilibrated 5-Iodo-2'- deoxyuridine (IdU) (Sigma) for 40 minutes at 37°C (when cells were treated with 2mM HU, the drug was added at the same time as the IdU). After incubation, DMEM/IdU solution was removed, and cells were washed 2 times with ice-cold sterile PBS. Cells were then trypsinised and resuspended in 1 ml PBS at a concentration of 5 $\times$ 10<sup>4</sup> cells/ml. DNA fibre spreads were prepared from harvested cells on

rectangular slides by adding 2  $\mu$ l drops of each resuspended sample near the frosted edge of the slide and left for 4 minutes until the edges of the drops became crinkly. The cells were subsequently lysed after 7  $\mu$ l of spreading buffer (Table 2.3) was added and the two were mixed and stirred 5 times and were left for 2 minutes at room temperature until lysis was completed. Glass slides were tilted to allow DNA to spread down the slide and excess liquid was allowed to run off the end of the slide and left to air-dry for 10 minutes. Fixation of DNA fibres was done by submerging the slides in methanol / acetone (3:1) for 15 minutes, followed by air drying for 10 minutes. Slides were then stored at 4°C until further processing.

#### 2.2.9 Metaphase spreads.

Sub-confluent HSFs and 55K<sup>+</sup> HSFs were treated with nocodazole (Sigma) at a final concentration of 200 ng/mL for 16 hours prior to harvesting by trypsinisation. Cells were pelleted by centrifugation at 900rpm for 5 minutes and then subjected to hypotonic shock by incubation in hypotonic solution (75 mM KCl) for 30 minutes at 37°C. Cells were then pelleted again by centrifugation at 900rpm for 5 minutes and resuspended in 2mls PBS, followed by fixation with ethanol: acetic acid (3:1) solution by adding the solution in a drop-wise manner with gentle agitation. The process of resuspending the cells in PBS followed by the drop-wise addition of 3:1 ethanol: acetic acid was repeated for a further 3 times. Two drops of fixed cells were dropped onto acetic acid-coated glass slides and allowed to dry overnight. The following day, slides were stained for 15 minutes in 5% Giemsa stain solution (5% v/v in H<sub>2</sub>O) (Millipore) and then immersed in H<sub>2</sub>O for 5 minutes to remove residual stain. Slides were allowed to dry

overnight and were mounted the following day using Etellan mounting medium (Millipore). Metaphase abnormalities were scored using a Nikon Eclipse Ni microscope.

## **2.3 PROTEIN BIOCHEMISTRY**

### **2.3.1 Whole cell lysate preparation.**

Whole cell lysates for western blotting were prepared by removing existing media and washing plates twice with 3 ml of ice-cold PBS. Cells were then scraped and solubilized in 200-500µl UTB lysis buffer (Table 2.3) depending on the cell confluency. Lysates were collected in 1.5 ml tubes. Sonication was performed on cell lysates using a Microson ultrasonic cell disruptor at 5 watts for 10 seconds, followed by centrifugation at 13000 rpm for 15 minutes at 4°C to remove any cell debris. The pellet was then discarded and the supernatant containing the proteins was transferred to new 1.5 ml tubes, which were either stored at -80°C or prepared for protein determination.

Whole cell lysates for co-immunoprecipitation (CIP) assays were prepared by removing existing media and washing plates twice with 3 ml of ice-cold PBS. Cells were then trypsinised as mentioned above; trypsin was removed, followed by resuspension of cells in PBS. Cells were then pelleted by centrifugation at 1500rpm for 4 minutes and PBS was removed. Cells were lysed in 1-5 ml NETN solution (Table 2.3) depending on the number of cells, followed by homogenization 20 times using a Wheaton-Dounce hand homogenizer. Afterwards, any remaining cellular debris was removed by centrifugation (2500-rpm for 5 minutes, followed by 13000-rpm for 5 minutes, and finally 44000-rpm for 20 minutes at 4°C using an Optima

MAX-TL Beckman Coulter ultracentrifuge). The supernatant was retained at every step of the preparation and the pellet discarded.

Whole cell lysates for Subcellular Chromatin Fractionation (SCF) assays were harvested by removing existing media and washing plates twice with 3 ml of ice-cold PBS. Cells were then trypsinised as mentioned above and trypsin was removed, followed by resuspension of cells in PBS. Cells were then pelleted by centrifugation at 1500rpm for 4 minutes and PBS was removed. Cells were incubated in 1ml Buffer A (Table 2.3) supplemented with 100 $\mu$ l of Triton X100 to a concentration of 0.1% and cells were left on ice for 10 minutes. After incubation, the cell suspension was centrifuged at 1300 x g for 5 minutes at 4°C. The supernatant collected comprises the cytoplasm and organelles. Whereas, the pellet was collected as the nuclear fraction and was washed with Buffer A (without Triton), followed by resuspension and incubation on ice in Buffer B (Table 2.3) for 10 minutes to lyse the nuclear membrane. The lysed nuclear fraction was then centrifuged at 1700 x g for 10 minutes at 4°C and the supernatant (Nucleoplasm) and nuclear lysate (Chromatin Fraction) were isolated. The Chromatin Fraction was solubilised in UTB Buffer (Table 2.5) and centrifuged at 1700 x g for 10 minutes at 4°C. The supernatant containing chromatin-bound proteins was collected into new tubes.

### 2.3.2 Bradford assay (Protein determination).

Bradford Assay was used to determine protein concentration of cell lysates. A standard curve was generated by adding 0, 2, 4, 6, 8 and 10  $\mu$ g of Bovine Serum Albumin (BSA) (Sigma) to 1ml

of Bradford reagent. 2 µl of each cell lysate was added to 1ml of Bradford reagent. Absorbance readings were determined at a wavelength of 595 nm using an Eppendorf Biospectrometer and final protein concentrations of cell lysates were calculated using the generated BSA standard curve.

### 2.3.3 SDS-Polyacrylamide Gel Electrophoresis (SDS-PAGE).

Typically, 40 µg of each protein lysate were fractionated on polyacrylamide gels based on their relative molecular weight. A 10% polyacrylamide gel was used for low molecular weight proteins (15 kDa-120 kDa), whereas an 8% polyacrylamide gel was used for high molecular weight proteins (> 120 kDa) (Table 2.6). Protein samples were denatured in an equal volume of SDS sample buffer (Table 2.5) and heated at 80°C for 5 minutes, followed by centrifugation at 13000rpm for 1 minute. Samples were then loaded onto the gel lanes along with the molecular weight ladder. Gels were run overnight at 10 mA until the desired separation of proteins had been achieved.

Ingredient	Manufacturer	8% Gel	10% Gel
H <sub>2</sub> O	----	42ml	39ml
40% Acrylamide (N, N' - methylene-bis- acrylamide)	Severn Biotech	12ml	15ml
10% SDS (sodium dodecyl sulphate)	Severn Biotech	1ml	1ml
1 M Tris 1MBicine	Sigma	6ml	6ml
TEMED (N, N, N' N'-tetra-methyl- ethylenediamine)	Severn Biotech	300 µl	300 µl
10 % APS (ammonium persulphate)	Sigma	300 µl	300 µl

**Table 2.6.** List of reagents used in polyacrylamide gel recipe.

#### 2.3.4 Electrophoretic transfer of proteins.

Following fractionation by SDS-PAGE, electrophoretic transfer of proteins onto nitrocellulose (NC) membranes (Biotrace) was performed in transfer running buffer (Table 2.5) at 300 mA for 6 hours at 4°C. The membranes were then cut according to the sizes of the proteins of interest.

#### 2.3.5 Preparation of proteins for Mass Spectrometry.

Samples were prepared by following the co-immunoprecipitation protocol to the point of washing the beads with NETN buffer (see Sections 2.3.1 and 2.4.3). Beads were washed twice in NETN without NP40 and then denatured by incubation in 0.5ml of 9M Urea/50mM ammonium bicarbonate at room temperature for 1 hour with constant shaking. Afterwards, samples were centrifuged at 3000rpm for 1 minute at 4°C and the supernatant was collected in new tubes. To reduce cystine residues, samples were incubated with 50mM dithiothreitol (DTT) in 50mM ammonium bicarbonate ( $\text{NH}_4\text{HCO}_3$ ) at 56°C for 30 minutes, followed by incubation in 100mM iodoacetamide in 50mM  $\text{NH}_4\text{HCO}_3$  at room temperature for 30 minutes in the dark. 300  $\mu\text{l}$  of denatured lysates were added to Filter-Aided Sample Preparation (FASP) filters (Amicon, 30K cut off) and centrifuged at 13000rpm for 10 minutes at room temperature. Filters were washed 4 times with 50mM ammonium bicarbonate, centrifuging at 13000rpm for 10 minutes in each wash and discarding the flow-through. Filters were transferred to new collection tubes and were subjected to digestion with 300  $\mu\text{l}$  of sequence-grade modified trypsin (Promega) (1  $\mu\text{g}$  per sample) diluted in 50mM ammonium bicarbonate,



at 37°C overnight. Tryptic peptides were collected by centrifuging the filters at 13000rpm for 10 minutes at room temperature. FASP filters were washed twice with 50mM ammonium bicarbonate and the flow-through was added to the previously collected filtrate. The peptides were dried in an Eppendorf vacuum centrifuge overnight and resuspended in 40 µl of (1% acetonitrile/ 1% formic acid/ H<sub>2</sub>O). Mass spectrometric analysis and protein identification was carried out by the University of Birmingham Advanced Mass Spectrometry Facility in the School of Biosciences.

## **2.4 IMMUNOCHEMISTRY TECHNIQUES**

### **2.4.1 Antibodies**

All Primary and Secondary antibodies used in this study are listed in Tables 2.5 and 2.6.

### **2.4.2 Western blotting.**

After electrophoretic transfer of proteins onto NC membranes (Section 2.3.4), nonspecific binding was blocked by incubating in 5% milk or BSA in TBST Buffer (Table 2.3) for 20 minutes, followed by multiple washes with TBST. The membranes were then incubated with the appropriate antibody, diluted in 3% (w/v) BSA at 4°C overnight with gentle agitation. On the following day, the membranes were washed repeatedly with TBST Buffer for 30 minutes to remove excess primary antibody. The membranes were then incubated with appropriate concentration of horseradish-peroxidase (HRP)-conjugated secondary antibody (diluted in 5% milk) for 2 hours with gentle agitation. Excess secondary antibody was removed by washing

repeatedly with TBST for 30 minutes. Antigen-antibody complexes were visualized by incubating membranes in enhanced chemiluminescence (ECL) reagent, followed by exposure to autoradiography films (Kodak) for different lengths of time in the dark room.

Primary antibody	Species	Dilution	Application	Clone\Cat#	Supplier
HAdV5 Hexon	Rabbit	1:1000	WB	-	Gift from Vivien Mautner
HAdV5-E1B55K (2A6)	Mouse	1:1000	WB	-	Gift from Arnold Levine
HAdV12-E1B55K (XPH9)	Mouse	1:1000	WB/IF	-	In house
HA (12CAS)	Mouse	1:1000	WB/IF	-	Monoclonal grown in house
p53 (DO1)	Mouse	1:2000	WB/IF/IP	-	Gift from David Lane
$\gamma$ H2AX (S139)	Mouse	1:1000	WB/IF	JBW301	Millipore
$\gamma$ H2AX (S139)	Rabbit	1:1000	WB/IF	938CT5.1.1	SantaCruz
H2B	Rabbit	1:2000	WB	EPR859	Abcam
TICCR	Rabbit	1:1000	WB/IP	HPA049454	Sigma-Aldrich
RPA1	Mouse	1:1000	WB	SAB1406399	Calbiochem
pNBS1 (S343)	Rabbit	1:1000	WB	EP178	Abcam
pKAP1 (S824)	Rabbit	1:1000	WB	A300-767A	Bethyl Laboratories
KAP1	Rabbit	1:1000	WB	600-401-FP2	Bethyl Laboratories
SMC1	Rabbit	1:1000	WB	BL-205-2G8	Bethyl Laboratories
BLM	Rabbit	1:1000	WB/IP	A300-110A	Bethyl Laboratories
TOPBP1	Rabbit	1:1000	WB/IP	A300-111A	Bethyl Laboratories
ATM	Rabbit	1:1000	WB/IP	A300-299A	Bethyl Laboratories
ATR	Rabbit	1:1000	WB/IF/IP	A300-137A	Bethyl Laboratories
pATM (S1981)	Rabbit	1:500	WB	600-401-398	R&D Systems
pCHK1 (S345 & S317)	Rabbit	1:1000	WB	133D3-D12H3	Cell Signalling
pCHK2 (T68)	Rabbit	1:1000	WB	C13C1	Cell Signalling
DNA-PKcs	Mouse	1:1000	WB/IF/IP	(G-4) SC-5282	SantaCruz
PARP1	Mouse	1:1000	WB	(F-2) SC-8007	SantaCruz

Ku80	Mouse	1:1000	WB	GTX109935	GeneTex
CHK1	Mouse	1:1000	WB/IP	(G-4) SC-8408	SantaCruz
CHK2	Rabbit	1:1000	WB	-	Gift from Steve Elledge
GAPDH	Mouse	1:500	WB	(0411) SC-47724	SantaCruz
NBS1	Rabbit	1:10000	WB/IF/IP	SC-11431	SantaCruz
MRE11	Mouse	1:1000	WB/IF/IP	(18) SC-135992	SantaCruz
MRE11	Rabbit	1:1000	WB	HL1385	GeneTex
MCM2	Mouse	1:500	WB/IP	(E-8) SC-373702	SantaCruz
MCM3	Mouse	1:500	WB/IF/IP	(E-8) SC-390480	SantaCruz
MCM5	Mouse	1:500	WB	(E-10) SC-165994	SantaCruz
MCM7	Mouse	1:500	WB/IP	(141.2) SC-9966	SantaCruz
ORC1	Rat	1:500	WB	(7A7) SC-23887	SantaCruz
ORC2	Rat	1:500	WB	(3G6) SC-32734	SantaCruz
ORC3	Rat	1:500	WB/IP	(1D6) SC-23888	SantaCruz
ORC6	Mouse	1:500	WB	(D-4) SC-390490	SantaCruz
cdc45	Mouse	1:500	WB/IP	(G-12) SC-55569	SantaCruz
DNA Polymerase $\delta$	Mouse	1:500	WB/IP	(D-7) SC-390583	SantaCruz
DNA Ligase IV	Rabbit	1:1000	WB/IP	HPA001334	Bethyl Laboratories
USP7	Mouse	1:500	WB/IP	(H-12) SC-137008	SantaCruz
USP9	Mouse	1:500	WB/IP	(5G-02) SC-100628	SantaCruz
USP15	Mouse	1:500	WB/IP	(B-5) SC-515688	SantaCruz
USP33	Mouse	1:500	WB	(1D7) SC-100632	SantaCruz
USP34	Mouse	1:500	WB	(3H9) SC-100631	SantaCruz
UBR5	Mouse	1:500	WB/IP	(B-11) SC-515494	SantaCruz
UBR5	Rabbit	1:5000	WB	22782-1-AP	Proteintech
Tankyrase 1/2	Rabbit	1:1000	WB	GTX117417	GeneTex
hnRNPUL1	Rabbit	1:1000	WB/IP	-	In house

DNMT1	Rabbit	1:1000	WB/IP	39905	Bethyl Laboratories
TOP3A	Rabbit	1:1000	WB/IP	14525-1-AP	Proteintech
Cullin 2	Rabbit	1:1000	WB	EPR3104(2)	Abcam
Cullin 5	Mouse	1:500	WB	(F-6) SC-373822	SantaCruz
P62	Mouse	1:1000	WB	(D-3) SC-28359	SantaCruz
LetM1	Mouse	1:1000	WB	(D-3) SC-271234	SantaCruz
Cyclin A	Rabbit	1:500	WB	(B-8) SC-271682	SantaCruz
Cyclin B1	Rabbit	1:500	WB	(GNS1) SC-245	SantaCruz
Cyclin D1	Mouse	1:500	WB	(A-12) SC-8396	SantaCruz
Cyclin E	Mouse	1:500	WB	(HE12) SC-247	SantaCruz
Lamin B1	Mouse	1:500	WB	(A-11) SC-377000	SantaCruz
53BP1	Rabbit	1:1000	IF	NB100-304SS	Novus Biologicals
RAD51	Rabbit	1:1000	IF	ABE257	Calbiochem
Mitotin	Rabbit	1:500	IF	A301-611A	Bethyl Laboratories
R-loops (S9.6)	Mouse	1:1000	IF	-	Gift from Angelo Agathangelou
Nucleolin	Rabbit	1:500	IF	N2662	BD Bioscience
IdU	Mouse	1:500	DNA fibres	OTI2F8	Becton Dickinson
CldU	Rat	1:500	DNA fibres	C6891	AbD SeroTec

**Table 2.7.** List of primary antibodies used throughout this study.

Secondary antibody	Species	Dilution	Application	Clone\Cat#	Supplier
Mouse IgG	Goat	1:2000	WB	P0447	DAKO Laboratories
Rabbit IgG	Swine	1:3000	WB	P0217	DAKO Laboratories
Rat IgG	Rabbit	1:2000	WB	P0162	DAKO Laboratories
Rabbit IgG Alexa fluor 488	Goat	1:1000	IF	A-11008	Invitrogen
Mouse IgG Alexa fluor 546	Goat	1:1000	IF	A-11030	Invitrogen
Rat IgG Alexa fluor® 555	Goat	1:500	DNA fibres	A-21434	Molecular Probes
Mouse IgG Alexa fluor® 488	Goat	1:500	DNA fibres	A-11001	Invitrogen

**Table 2.8.** List of secondary antibodies used throughout this study.

#### **2.4.3 Co-immunoprecipitation assay.**

CIP lysates (prepared as described in section 2.3.1) were divided into suitable aliquots and incubated with 10 µl of the appropriate primary antibody or control antibody at 4°C overnight. Cell lysates were centrifuged the following day at 44000 rpm at 4°C for 7 minutes and the supernatant collected in new tubes. Antigen–antibody complexes were isolated by adding 50 µl of Protein-G Sepharose beads (Generon) to the lysates and incubating at 4°C for 2 hours on a rotator. The samples containing immunocomplexes and beads were centrifuged at 3000 rpm for 1 minute at 4°C and the supernatant discarded, followed by 3 times washes in ice-cold NETN Buffer (Table 2.3) with repeated rounds of centrifugation at 3000 rpm for 1 minute at 4°C. The supernatant was removed between each wash. Washed beads were denatured in 50 µl of SDS sample buffer (Table 2.3) and heated at 80°C for 5 minutes, followed by centrifugation at 13000rpm for 1 minute. The supernatants were then fractionated by SDS-PAGE and co-immunoprecipitating proteins were identified by western blotting as described in section 2.3.3, 2.3.4 and 2.4.2, respectively.

#### **2.4.4 Subcellular chromatin fractionation (SCF) assay.**

The supernatant containing chromatin-bound proteins (prepared as described in section 2.3.1) was fractionated by SDS-PAGE and developed by western blotting as described in section 2.3.3, 2.3.4 and 2.4.2, respectively.

#### 2.4.5 Immunofluorescence microscopy.

Glass coverslips were placed in 24-well plates and submerged in 100% absolute ethanol for 1 hour. Afterwards, ethanol was removed, and cover slips were washed once with 1ml warm DMEM. Cells were aliquoted ( $25 \times 10^3$  cells/well) on the coverslips and incubated at 37°C overnight. Cells were then treated with 1µM CPT, 2mM HU or IR (2Gy-4Gy), depending on the experiment. After the appropriate times, growth medium was removed and coverslips were washed once with ice-cold PBS and cells were fixed with 500µl of 3.6% paraformaldehyde (PFA) in PBS for 10 minutes, followed by permeabilization using 0.5% Triton X100 in PBS for 5 minutes. After washing in PBS, cells were stained with appropriate primary antibodies diluted in 5% FCS/PBS (table 2.5) overnight. After washing twice with PBS, cells were stained with secondary antibodies diluted in 5% FCS/PBS (table 2.6) for 1 hour in the dark at room temperature with subsequent staining of DNA with 4',6-diamidino-2-phenylindole (DAPI) for 10 minutes in the dark. Coverslips were then washed with PBS twice to remove excess DAPI. Cover slips were mounted onto glass slides using a drop of mounting medium (Vector Laboratories) and applying gentle pressure to the edges of the cover slips to remove excess mounting medium, followed by sealing of the edges with colourless nail polish. Slides were stored at 4°C, and visualisation of fluorescence images was carried out using a Nikon E600 Eclipse microscope. Images were acquired using Volocity software and analysed using ImageJ software.

#### 2.4.6 Immunostaining of DNA fibres.

DNA fibres were fixed on glass slides (as described in section 2.2.7) and placed in a blackout chamber. Slides were washed twice in deionised H<sub>2</sub>O, rinsed once in 2.5M hydrochloric acid (HCl) and denatured in 2.5M HCl for 75 minutes. Following denaturation, slides were rinsed once with PBS, washed twice with DNA fibre blocking buffer (Table 2.3) and incubated for a further 30 minutes in blocking buffer. Slides were then incubated with 200 µl of rat anti-bromodeoxyuridine (anti-BrdU) to detect CldU and 200 µl of mouse anti-BrdU to detect IdU (Table 2.5) in blocking buffer for 1 hour. Slides were then washed 3 times with PBS and fixed with 3.6% PFA in PBS for 10 minutes. Slides were then washed 3 times with PBS, followed by three washes with blocking buffer and incubated for a further 1.5 hours with 200 µl anti-rat and 200 µl anti-mouse IgG secondary antibodies diluted at the required ratios in blocking buffer (Table 2.6). Slides were then washed three times with blocking buffer, followed by three washes in PBS. Rectangular coverslips were mounted onto glass slides using two drops of mounting medium (Vector Laboratories) and applying gentle pressure to the edges of the cover slips to remove excess mounting medium, followed by sealing of the edges with colourless nail polish. Visualisation of DNA fibres was performed using a Nikon E600 Eclipse microscope and images were acquired using Volocity software and analysed using ImageJ software.

#### 2.4.7 R-loop analysis.

Cells were fixed on coverslips as described above (section 2.4.5) and stained with the S9.6 antibody to visualise R-loops. Cells were counterstained against the nucleolar protein

nucleolin to pinpoint nucleoli, with subsequent staining of DNA with DAPI. The relative total intensity of S9.6 staining due to R-loops was calculated by subtracting the R-loops S9.6 staining in the nucleoli from the total nuclear staining intensities. The intensities of nuclear R-loops were quantified using a Nikon E600 Eclipse microscope and images were acquired using Volocity software and analysed using ImageJ software.

## 2.5 MOLECULAR BIOLOGY TECHNIQUES

### 2.5.1 Media preparation for bacterial growth.

Luria Broth (LB) (Sigma) was made at a concentration of 20g/litre in deionised H<sub>2</sub>O (pH 7.2), and the broth was autoclaved for sterilisation prior to use. LB-agar was prepared to final concentration of 1.2% (w/v) by the addition of 7.6g of LB-agar to 1 L of LB broth, followed by autoclaving. Prior to use, LB-agar was melted, cooled, and 50µg/ml of Ampicillin (Sigma) was added to the solution. The mixture was then poured into agar plates. The plates were left to set in a biological cabinet class 2/class 2 laminar flow hood and stored at 4°C for bacterial transformations of Amp-resistant clones.

### 2.5.2 Bacterial transformation.

Bacterial transformation was performed to introduce the DNA plasmid from different adenoviral E1B constructs (HAdV4-E1B55K, HAdV9-E1B55K, HAdV16-E1B55K and HAdV40-E1B55K) into competent *E.coli* strain (BL21- α-Select Bronze) (BioLine). Prior to transformation, competent bacterial cells were thawed on ice and 50ng of plasmid DNA was added to 50 µl of bacteria and the mixture was incubated on ice for 30 minutes and then heat-



shocked at 42°C for 1 minute to allow plasmid DNA to enter the bacteria and immediately placed back on ice for 5 minutes. 100 µl of Super Optimal broth with Catabolite repression (SOC) medium (Invitrogen) was added to the mixture, which was then incubated for 1 h in an orbital shaker at 37°C. 20 µl of the solution was then spread onto LB agar plates containing the Ampicillin antibiotic and plates were allowed to dry and incubated at 37°C overnight to allow antibiotic-resistant clones to grow.

### 2.5.3 Maxi-Prep plasmid DNA purification.

For large scale DNA plasmid purification, individual bacterial colonies were picked from agar plates and inoculated into 5ml of LB broth containing 50µg/ml of Ampicillin and incubated at 37°C for 8 hours in an orbital shaker. The total volume of the bacterial culture was then transferred to a flask containing 250 ml of LB supplemented with 50µg/ml of Ampicillin and incubated at 37°C overnight in an orbital shaker. Bacterial cultures were pelleted by centrifugation at 4000 rpm for 15 minutes at 4°C. Large scale DNA plasmid purification was performed using the NucleoBond Xtra Maxi kit (Macherey-Nagel) as follows. The bacterial pellet was resuspended in 35ml of resuspension buffer supplemented with RNase A. The solution was then lysed in 12ml of lysis buffer, mixed gently by inversion and incubated at room temperature for 5 minutes. 10mls of precipitation buffer was added to the mixture to neutralise the reaction. The precipitated lysate was then transferred to a maxi DNA-binding column that had been equilibrated with 30ml of equilibration buffer, and the mixture containing plasmid DNA was allowed to flow through by gravity. The column was washed twice with 25ml of wash buffer. Plasmid DNA was eluted into a clean tube by the addition of 15ml elution buffer. The eluted DNA was precipitated by the addition of 10.5ml isopropanol

and pelleted by centrifugation at 15000 rpm for 30 minutes at 4°C. The pelleted DNA was then washed once with 70% (v/v) ethanol to remove salts and air-dried in a biological cabinet class 2/class 2 laminar flow hood for 10 minutes. DNA pellets were resuspended and hydrated with the appropriate amount of TE buffer, and the plasmid DNA concentrations were measured in ng/μl using a Nanodrop 1000 spectrophotometer (Thermo-Fisher) at an optical density of 260nm /280nm.

## **2.6 STATISTICAL ANALYSIS**

DNA fibres assay and R-loops data were plotted by GraphPad Prism statistical software and represented in dot plot graphs (Significant differences between the means  $\pm$  SD were determined by unpaired student t tests \*p < 0.05, \*\*p < 0.01, \*\*\*p < 0.001 and \*\*\*\*p < 0.0001). Quantification of Micronuclei and DDR foci were plotted by MS Excel software and represented in clustered column bars (Significant differences between the means  $\pm$  SD were determined by unpaired student t tests \*p < 0.05, \*\*p < 0.01 and \*\*\*p < 0.001). Error bars represent the standard error of mean (SEM).

# **CHAPTER 3**

**Identification of multiple human  
adenovirus early region 1B55K (HAdV-  
E1B55K)-interacting proteins during  
adenovirus 12 and 5 infections**

### 3.1 Introduction

The E1B55K protein, expressed at early time during HAdV infection, is required for efficient viral replication and for full HAdV-mediated transformation of mammalian cells in culture. Its major role, during viral infection, has generally been seen as a partner for E4orf6. Together they act as part of a ubiquitin E3 ligase targeting certain cellular proteins for ubiquitylation and, often, for subsequent proteasome-mediated degradation (Querido, Blanchette, *et al.*, 2001; Herrmann *et al.*, 2020). A wide variety of biological regulatory processes, such as cell cycle progression, cellular differentiation, apoptosis, and the DDR, are all mediated by post-translational modifications, which do not end in protein degradation, by E3 ubiquitin ligases (Welchman, Gordon and Mayer, 2005). It seems possible that the E1B55K/E4orf6-containing ligase may have roles in protein ubiquitylation, during viral infection, which only result in modifications, affecting the activities of particular pathways, although this has yet to be established.

HAdV-E1B55K appears to protect infected cells against apoptosis, for example, by causing rapid degradation of p53 in the case of the group A and group C viruses, or by direct interaction with cellular proteins, resulting in the inhibition of their transcriptional activity in other viral types (Querido *et al.*, 1997; Steegenga *et al.*, 1998; Querido, Blanchette, *et al.*, 2001; Cheng *et al.*, 2011; Forrester *et al.*, 2011). The group A (HAdV12) and C (HAdV2 and HAdV5) HAdVs also target an appreciable number of other cellular proteins for degradation (Blackford and Grand, 2009; Schreiner, Wimmer and Dobner, 2012). Reports over the last two decades have shown that many of these are associated, directly or indirectly, with the DDR; for example, BLM, MRE11, DNA ligase IV, TNK1BP1, TOPBP1, and p53 have all been shown to associate with

HAdV5-E1B55K and, in most cases with HAdV12-E1B55K, which results in their degradation (Stracker, Carson and Weitzman, 2002; Baker *et al.*, 2007; Blackford *et al.*, 2010; Orazio *et al.*, 2011; Ching *et al.*, 2013; Chalabi Hagkarim *et al.*, 2018).

E1B55K-mediated protein degradation is accomplished by its association with HAdV-E4orf6, which recruits a cellular E3 ubiquitin ligase comprising a cullin (Cul5 in the case of HAdV5 and Cul2 in the case of HAdV12), elongins B and C and RING Box 1 (Rbx1), leading to ubiquitylation of substrates and degradation by the proteasome (Querido, Blanchette, *et al.*, 2001; Blanchette *et al.*, 2004; Blackford *et al.*, 2010). HAdV-E1B55K serves as the substrate recognition component of this ubiquitylating complex, whereas E4orf6 binds to elongin C. The ubiquitin-like polypeptide NEDD8 is attached covalently to the active site of the cullin by a mechanism known as NEDDylation, which controls the activity of all cullin-based E3 ubiquitin ligases (Pintard *et al.*, 2003). Little is known about how HAdVs regulate this activity, despite the fact that it allows conformational changes within the cullin and RBX1 domains necessary to induce ubiquitylation (Duda *et al.*, 2008).

A number of cellular proteins involved in chromatin remodelling, such as Daxx, ATRX and SPOC1, are also degraded in an E1B55K-dependent manner (Schreiner *et al.*, 2010; Schreiner, Bürck, *et al.*, 2013; Schreiner, Kinkley, *et al.*, 2013). However, it is interesting to note that there is no requirement for E4orf6 for the degradation of Daxx (Schreiner *et al.*, 2010). Interactions with many other proteins not associated with the DDR or chromatin remodelling, for example integrin  $\alpha 3$ , Fas and EPHA7, have also been reported (Dallaire *et al.*, 2009; Hung and Flint, 2017; Herrmann *et al.*, 2020). Some of these targets are degraded whereas others are not.

Research shows that distinct HAdV types have evolved in such a way that, despite the fact that homologous proteins from different viral types maintain many of the same activities, there are also functional changes between these proteins; this appears to be the case for the E1B55K and E4orf6 proteins in particular (Forrester *et al.*, 2011; Blanchette *et al.*, 2013). In light of the recent finding of possibly new HAdV5-E1B55K and HAdV5-E4orf6 interacting proteins (summarized in (Hidalgo *et al.*, 2019; Herrmann *et al.*, 2020)) and the observation that some of proposed interactions have only limited effects on viral replication (as far as we can tell up to now) (Dallaire, Blanchette and Branton, 2009; Orazio *et al.*, 2011; Chalabi Hagkarim *et al.*, 2018), we considered the possibility that ,despite their homology, HAdV5 and HAdV12 E3 ubiquitin ligase complexes may have diverse functional distinctions in their abilities to degrade various cellular DDR proteins. Therefore, our goals in this chapter were to determine whether HAdV12-E1B55K binds similar DDR proteins in comparison to HAdV5-E1B55K; we have also examined possible association of both viral proteins with novel DDR pathway and replication machinery components. Additionally, we have examined whether the novel E1B55K binding proteins were degraded during HAdV5 and/or HAdV12 infections.

It has now been shown here that ATR, CHK1, DNMT1, USP9, ATM, DNA-PKcs, and hnRNPUL1 all co-immunoprecipitate with HAdV5-E1B55K in the absence of E4orf6. Additionally, many of the well-characterised HAdV5-E1B55K binding proteins are shown to be degraded during HAdV5 infection. Similarly, the novel interactors CHK1, USP9, DNMT1, DNA-PKcs, and the previously identified binding proteins USP15 and SQSTM1 (p62), are also degraded in a cullin-dependent manner during HAdV5 infection (Table 3.1). Significantly, some of the HAdV5-E1B55K binding proteins, such as ATR and USP34, were not degraded during HAdV5 infection. We have also shown that HAdV12-E1B55K co-immunoprecipitates with novel and previously

characterised DDR proteins in the absence of E4orf6, such as ATM, DNA-PKcs, BLM, TOP3A, USP7, USP9, USP15, hnRNPUL1, TOPBP1, CHK1 and DNMT1 (Table 3.1). Our results show that some well-characterised HAdV12-E1B55K binding proteins are degraded during HAdV12 infection, such as MRE11, p53, and NBS1; however, many novel HAdV12-E1B55K binders such as, CHK1, ATR, USP9, USP15, DNMT1 were not degraded. Additionally, other proteins involved in DDR repair, such as p62 and USP33 were shown to be degraded following HAdV12 infection. Surprisingly, some of the target proteins were less stable during HAdV12 infection in the presence of the cullin inhibitor, MLN4924 rather than more stable as is the case with HAdV5, as would be expected.

## 3.2 Results

### 3.2.1 HAdV5 and HAdV12 E1B55K bind novel DDR and pre-replication complex proteins.

It has been demonstrated, or in some circumstances assumed, that the E1B55K protein serves as the binding component for cellular targets which are ubiquitylated by the E3 Ligase during HAdV infection and subsequent HAdV-mediated protein degradation (Blackford and Grand, 2009; Hidalgo *et al.*, 2019; Herrmann *et al.*, 2020; Kleinberger, 2020). In the past it was assumed that ubiquitylation of substrates led to degradation. However, more recently, it was shown that a number of proteins were ubiquitylated in the presence of HAdV5-E1B55K/E4orf6 but no degradation occurred (Herrmann *et al.*, 2020). Furthermore, numerous HAdV-E1B55K binding proteins have been identified, but with little evidence as to whether they are ubiquitylated or what function the interaction might serve (reviewed in (Hidalgo *et al.*, 2019)). It is also unclear whether E1B55K proteins expressed by viruses from types other than group C (i.e., HAdV5) associate with the same cellular components. Therefore, to answer some of these questions, we have conducted a limited number of co-immunoprecipitations to determine if HAdV5 and HAdV12 E1B55Ks interact with potential replication machinery and DDR pathways components previously not known to associate with the HAdV5-E1B55K (Figure 3.1 A and B). The basis for the proteins chosen for investigation was as follows: (summarised in Table 3.1). We concentrated on proteins linked, to some extent, to the DDR. Thus, interaction of MRE11, NBS1, and p53 are well established. USP15, USP34, and p62 (SQSTM1), had previously been identified as HAdV5-E1B55K binding proteins in a mass spec screen (Hung and Flint, 2017). The other proteins examined are all linked to the DDR but have not been investigated previously. We utilised HAdV5-E1HEK293 and HAdV12-E1HER2 cells for this



purpose because they are easy to culture in larger quantities and express E1B55K at high levels but not the viral E4orf6 protein.

Proteins were immunoprecipitated from HAdV5-E1HEK293 cells using either mouse or rabbit antibodies against HAdV5-E1B55K and western blotted for potential binding partners (Figure 3.1A). It can be seen that DNA-PKcs, USP9, CHK1, ATR, DNMT1, USP15, and proteins that participate in ATR-dependent signalling (hnRNPUL1) all co-immunoprecipitated with the viral protein. Co-immunoprecipitations of the well characterised binding partners MRE11, NBS1, p53, BLM, and USP7, are included for comparison; they have previously been identified in mass spectrometry screenings and co-immunoprecipitation experiments (Cheng *et al.*, 2013; Hung and Flint, 2017; Hidalgo *et al.*, 2019).

HAdV12-E1B55K has been shown to bind with p53, DNA ligase IV, as well as, MRE11 and NBS1, which is consistent with the fact that these proteins are degraded in response to HAdV12 infection as reported in previous studies (Cheng *et al.*, 2011; Forrester *et al.*, 2011). Moreover, there was additional evidence of co-immunoprecipitation between HAdV12-E1B55K and ATM, DNA-PKcs, BLM, TOP3A, USP7, USP9, USP15, hnRNPUL1, TOPBP1, CHK1 and DNMT1 (Figure 3.1B). However, only weak association was seen between the viral protein and ATR. These interactions are likely to have a significant impact on the DDR.

Figure 3.1C shows that when HAdV12-E1B55K is immunoprecipitated, MCM3, MCM7, and ORC3 co-precipitated. This suggests that the viral protein is associated to, at least some extent, with members of the ORC and MCM pre-replication complexes. However, there was no association found between ORC2, ORC6, MCM2, MCM4, or MCM4 and the viral protein (data not shown). Also, HAdV12-E1B55K has also shown a considerable binding affinity for

replisome components such as, DNA polymerase  $\delta$ , TICRR (also called as Treslin and SLD3), and cdc45 (Figure 3.1C). There was no evidence of an interaction with PCNA (data not shown). It is likely that some of the abnormalities seen in DNA replication in the presence of HAdV12-E1B55K (shown in detail in Chapter 4) are the result of the binding of the viral protein to the MCM complex, ORC1, and/or DNA Pol  $\delta$ . It is important to note that experiments to examine the association of HAdV5-E1B55K with members of the pre-replication complexes were not carried out due to lack of time. Given more time, we would have compared HAdV5-E1B55K and HAdV12-E1B55K interactions with all members of the ORC and MCM complexes.

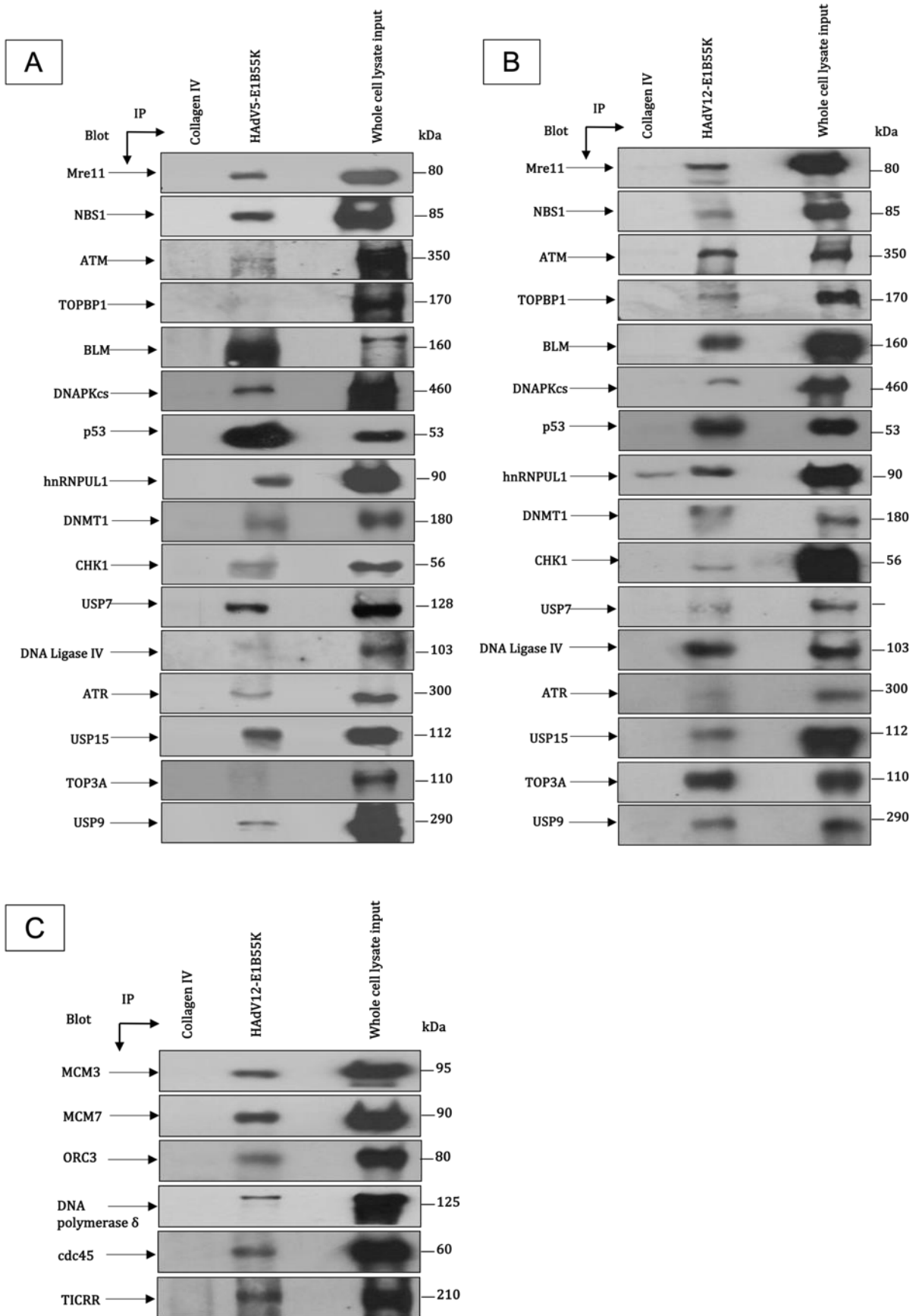


**Figure 3.1.** E1B55K co-immunoprecipitations with DDR proteins and pre-replication complex components. Collagen IV was used as a non-specific negative binding control in cellular aliquots to verify the pulldown of the prey protein of interest in the absence of viral protein antibodies. Lysates from HAdV5-E1HEK293 or HAdV12-E1HER2 cells were incubated with an antibody against collagen IV or antibodies against HAdV5-E1B55K or HAdV12-E1B55K overnight. Immunocomplexes were captured on protein G-agarose beads, and then they were fractionated using SDS-PAGE and western blotted using antibodies that were specific to the proteins shown. (A) HAdV5-E1B55K interactions with DDR proteins in HAdV5-E1HEK293. (B) HAdV12-E1B55K interactions with DDR proteins in HAdV12-E1HER2. (C) HAdV12-E1B55K interactions with pre-replication complex proteins in HAdV12-E1HER2.

### 3.2.2 HAdV-mediated degradation of novel cellular targets during HAdV5 and HAdV12 infections.

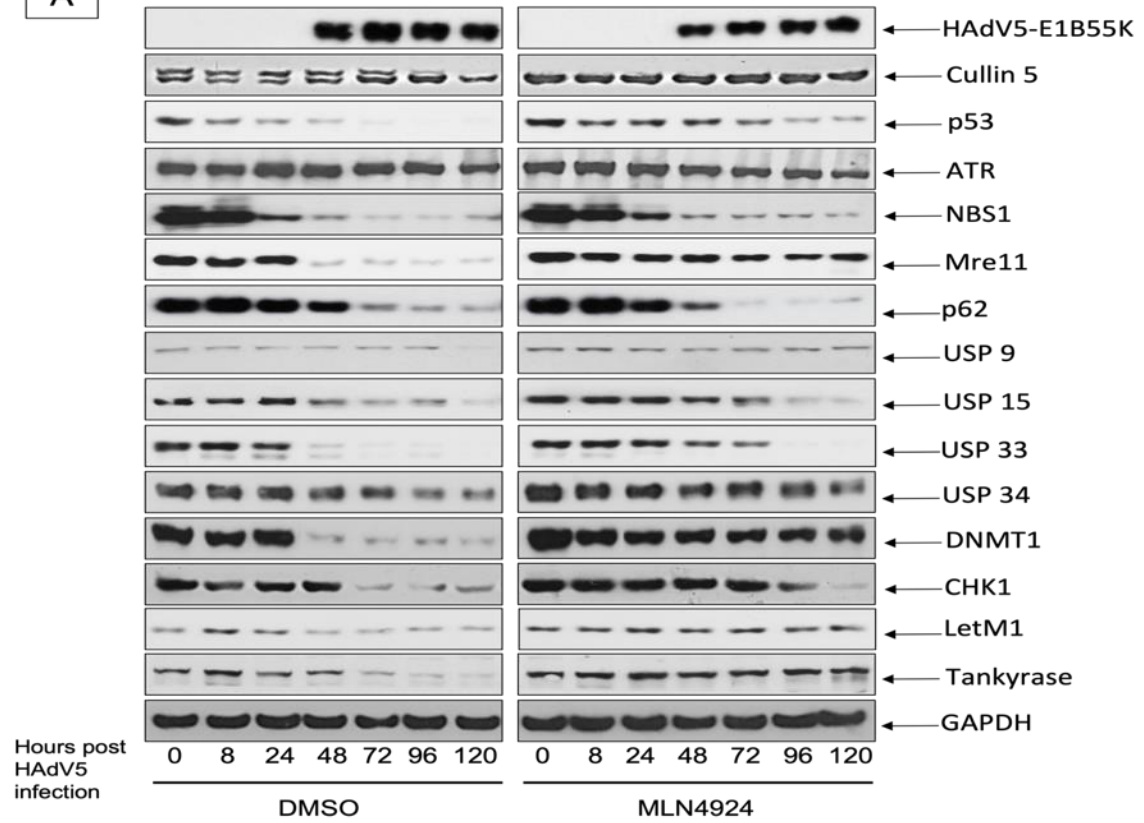
To date, the major consequence of HAdV5-E1B55K binding during viral infection has been shown to be rapid proteasome-mediated protein degradation (Querido, Blanchette, *et al.*, 2001; Schreiner, Wimmer and Dobner, 2012). With this in mind, the expression of the proteins, identified in (Figure 3.1 A and B), was assessed over an extended time course of HAdV5 and HAdV12 infections. A similar set of infections was carried out in the presence of the cullin inhibitor, MLN4924. It can be seen from (Figure 3.2A) that USP15, USP33, p62, Tankyrase 1/2 (the antibody used recognises both Tankyrase 1 and 2), LETM1, DNMT1 and CHK1 are all degraded during HAdV5 infection. The well-characterised HAdV5 targets p53, MRE11, and NBS1 are included for comparison. The rates of protein degradation vary, with some proteins being very rapidly degraded (for example, p53 and USP33), whereas others are more stable, such as p62 and Tankyrase 1/2. Our lab had previously noted that TAB182 (TNKS1BP1) is also degraded relatively slowly during HAdV5 and HAdV12 infections (Chalabi Hagkarim *et al.*, 2018).

It is interesting to note that some previously reported HAdV5-E1B55K binding proteins are not degraded at all during HAdV5 infection (Figure 3.2A). For example, there appears to be little or no reduction in the level of USP9, USP34 or ATR. This is consistent with recent observations by Herrmann *et al.*, (2020), who found that many proteins, although ubiquitinated by HAdV5-E1B55K/E4orf6, were also stable. To confirm that reduction in protein expression was due to cullin-based E3 ligase activity, viral infections were carried out in the presence and absence of MLN4924. MLN4924 is a potent and selective inhibitor of cullin NEDDylation with IC50 value

of 4nM and, thus, it inhibits protein degradation during HAdV infection (Querido, Blanchette, *et al.*, 2001; Xu *et al.*, 2022). It can be seen in Figure 3.2A that HAdV-induced protein degradation is generally reduced in the presence of the inhibitor although it is not completely negated (for example, Tankyrase 1/2, LetM1, USP15 and USP33). In the case of p62, however, inhibition of the cullins does not result in protein stabilisation; whether this indicates degradation by a different pathway is unclear at present. The western blot of cullins 2 and 5 shows that the higher molecular weight NEDDylated (active) band is absent in the cells treated with MLN4924 (Figure 3.2 A and B).

On the other hand, the expression of the same set of proteins during HAdV12 infection (Figure 3.2B) seems to show dissimilar results in some cases. For example, it can be seen from (Figure 3.2B) that the only proteins rapidly degraded during HAdV12 infection are p53, NBS1, and MRE11. The patterns of degradation of some other proteins seems contradictory to that seen in the case of HAdV5 infection or to what would be logically expected after the addition of MLN4924. For example, there is somewhat less degradation of NBS1, MRE11, USP15, USP33, DNMT1, and LetM1 during HAdV12 infection than is seen after the addition of the NEDDylation inhibitor MLN4924; the levels of HAdV12-induced protein degradation are not reduced in the presence of the inhibitor, and it appears that inhibition of the cullins does not result in protein stabilisation in this case; whether this indicates degradation by a different pathway is unclear at present. However, the levels of ATR, p62, USP9, USP34, CHK1, and Tankyrase 1/2 remain unchanged. This experiment was repeated multiple times but gave consistent results; no explanation is obvious at present.

A



B

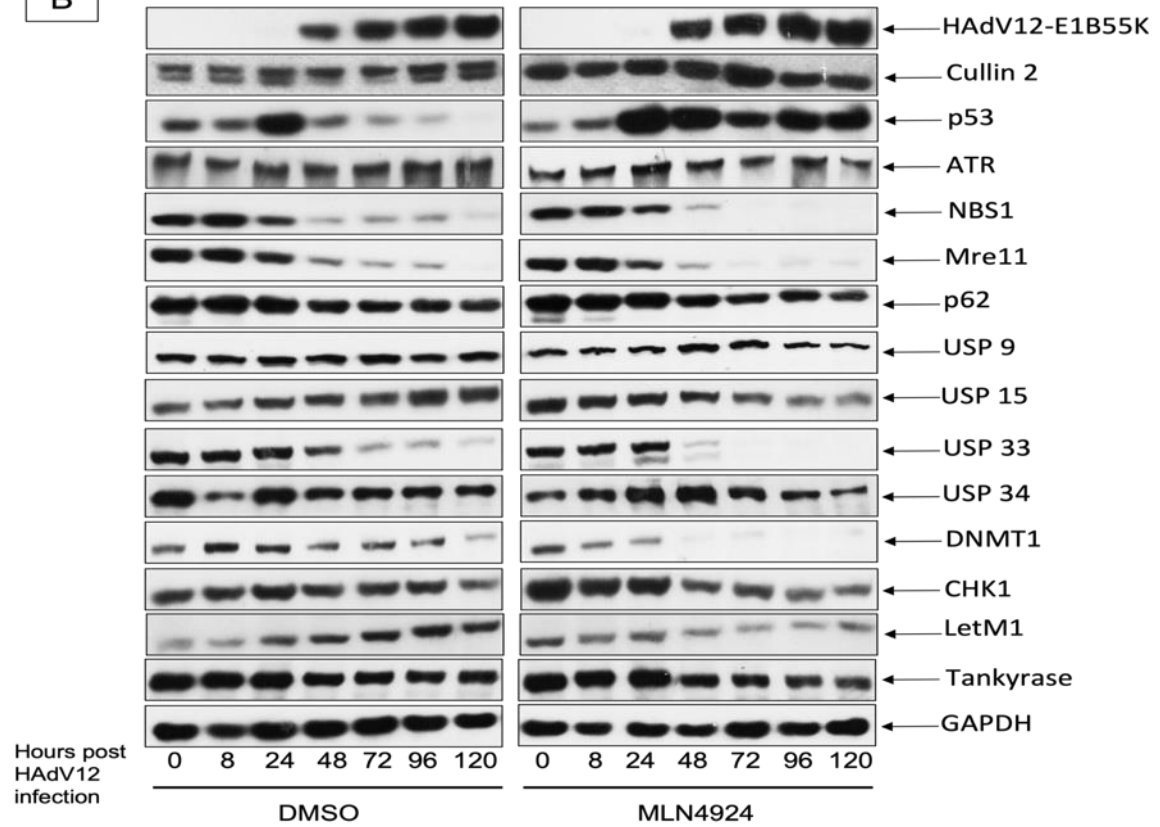


**Figure 3.2.** Degradation of novel binding partners during HAdV5 and HAdV12 infections is dependent on cullin function. HeLa cells were infected with *wt* HAdV5 or HAdV12 at an infectivity of 5pfu/cell, either in the presence or absence of 5mM MLN4924. Cells were harvested at the times shown post infection, fractionated by SDS-PAGE, and western blotted with the antibodies shown. (A) HAdV5 infection and (B) HAdV12 infection.



### 3.3 Discussion

The HAdV early region 1 proteins exert their effect on target cells, both during infection and cellular transformation, through a complex series of protein-protein interactions, as neither HAdV-E1A nor HAdV-E1B55K have enzymatic or DNA-binding activity. A large number of interacting proteins have been identified for both early region proteins from HAdV5 and, to a lesser extent, from HAdV12 (Pelka *et al.*, 2008; Blackford and Grand, 2009; King *et al.*, 2018; Hidalgo *et al.*, 2019; Ip and Dobner, 2019).

Large numbers of cellular proteins have been shown to interact with HAdV5-E1B55K and many more to be ubiquitinated by a HAdV5-E1B55K/E4orf6-dependent mechanism (Hung and Flint, 2017; Hidalgo *et al.*, 2019; Herrmann *et al.*, 2020). We aimed to identify novel potential E1B55K-interactors that associate with HAdV5-E1B55K or HAdV12-E1B55K, apart from their E3 ligase activities. However, a role for most of these associations has not been established.

We chose to examine novel E1B55K-interacting proteins picked predominantly based on their involvement in the DDR. Our results have shown that HAdV5-E1B55K from HAdV5-E1HEK293 cells co-immunoprecipitates with several novel DDR proteins, which had not been characterised before in the context of HAdV biology, such as DNA-PKcs, USP9, CHK1, ATR, and DNMT1 (Figure 3.1A). We included additional HAdV5-E1B55K interacting-proteins that were previously reported, such as MRE11, NBS1, USP15, p62, hnRNPUL1 and USP34, for validation (Figure 3.1A) (Hung and Flint, 2017). Correspondingly, several DDR repair proteins were examined from HAdV12-E1HER2 cells to check if HAdV12-E1B55K associates with the same set of DDR proteins in comparison to HAdV5-E1B55K. It was shown that HAdV12-E1B55K associates with MRE11 and NBS1, two members of the MRN complex, and DNA ligase IV. This

is consistent with the observation that MRE11 and DNA ligase IV are degraded after HAdV12 infection (Cheng *et al.*, 2011; Forrester *et al.*, 2011). Consistently, p53 has previously been reported to co-immunoprecipitate with HAdV12-E1B55K (Grand *et al.*, 1996). However, interactions of HAdV12-E1B55K with ATM and DNA-PKcs, constitute new targets that are likely to contribute to the DDR effects described in this study (Chapter 4). Interestingly, we have shown for the first time that HAdV12-E1B55K interacts directly (without its association with E4orf6 and, therefore, its role in the E3 ligase complex) with several other DDR proteins, such as BLM, TOP3A, USP7, USP9, USP15, hnRNPUL1, CHK1, and DNMT1. We have also observed a weak association between HAdV12-E1B55K and ATR. A full list of HAdV5-E1B55K and HAdV12-E1B55K interactions with DDR components and their degradation patterns is shown in (Table 3.1). It is currently unclear whether similar interactions take place with E1B55K proteins of other HAdV types. It is highly plausible that these interactions will be of significance during viral infection. However, it is also possible that some of these interactions of E1B55Ks from HAdV5 and HAdV12 with DDR proteins are fortuitous and may not be of biological significance. This does not, of course, mean that none are required for viral replication. Further work is needed to determine which is the case for each protein identified.

As HAdV12-E1B55K interferes with DNA replication, as shown in detail in Chapter 4, a further set of co-immunoprecipitations was carried out with members of the pre-replication complex proteins to acquire a more complete idea of the likely targets of HAdV12-E1B55K. It is possible that the interactions that were identified between HAdV12-E1B55K and MCM3, MCM7, ORC3, DNA polymerase, and cdc45 would be expected to impact 'normal' DNA replication and cause replication stress (Figure 3.1C). No interaction between the viral protein and any other MCM, ORC proteins or PCNA was observed (Data not shown). Unfortunately, due to lack of time we

could not perform the same experiment on HAdV5-E1B55K to look for its association with members of the pre-replication complexes and compare it to what had been observed with HAdV12-E1B55K.

It had seemed possible that interaction with HAdV5-E1B55K/E4orf6 during viral infection would always result in proteasome-mediated degradation, as has been observed for p53, DNA Ligase IV and BLM (Schreiner, Wimmer and Dobner, 2012). However, it was recently shown that some cellular proteins were ubiquitylated by the HAdV5 protein complex without degradation occurring (Herrmann *et al.*, 2020). With this in mind, we investigated whether novel HAdV-E1B55K interactors were also targeted to the proteasome during HAdV5 and HAdV12 infections.

Most of the proteins investigated were degraded during HAdV5 infection, although at varying rates (Figure 3.2A). For example, DNMT1 and USP33 were degraded at a similar rate to p53 and MRE11, whereas Tankyrase and LetM1 were much more stable (Figure 3.2A). Interestingly, however, ATR and USP34 were largely unaffected over a prolonged time course of infection. It would be interesting to examine whether these proteins were ubiquitylated (without degradation) as has recently been reported for an appreciable number of other proteins which are not degraded in the presence of HAdV5-E1B55k/E4orf6 (Herrmann *et al.*, 2020).

We have conducted a comparable series of infections when MLN4924, a cullin inhibitor, was introduced. Many of the targets were more stable in the presence of MLN4924, although the effect was more marked for some substrates than for others. For example, DNMT1 and MRE11 were hardly degraded at all in the presence of the inhibitor, whereas USP15 and NBS1 were

only slightly more stable. When the same assay protocol was applied to HAdV12 infected HeLa cells, the results were confusing. Whilst p53 was stabilised in the presence of MLN4924, several other proteins were appreciably less stable, for example, DNMT1 and USP33. We have no explanation for this, except to suggest that the effects of the drug on Cul2 are rather different to those on Cul5. Unfortunately, lack of time meant that we could not examine whether the pre-replication complex proteins which interact with HAdV12-E1B55K, were degraded during HAdV12 infection.

Protein	Substrate binding		Substrate degradation		Refs. for previously reported binding
	HAdV5-E1B55K	HAdV12-E1B55K	HAdV5-E1B55K	HAdV12-E1B55K	
MRE11	+	+	+	+	A
NBS1	+	+	+	+	A
ATM	+	+	ND	ND	B
TOPBP1	-	+	ND	ND	C
BLM	+	+	ND	ND	D
DNAPKcs	+	+	ND	ND	E
p53	+	+	+	+	F, G
hnRNPUL1	+	+	ND	ND	H, E
DNMT1	+	+	+	-	E
CHK1	+	+	+	-	E
USP7	+	+	ND	ND	I, E
DNA Ligase IV	+	+	ND	ND	J, K
ATR	+	+	-	-	E
USP15	+	+	+	-	L
TOP3A	-	+	ND	ND	E
USP9	+	+	+	-	E
P62	ND	ND	+	-	L
USP33	ND	ND	+	+	N/A
USP34	ND	ND	-	-	L
LETM1	ND	ND	-	-	N/A
Tankyrase	ND	ND	+	-	N/A

**Table 3.1.** Summary of HAdV5-E1B55K and HAdV12-E1B55K interactions with DDR components and their degradation patterns. (+), positive, (-), Negative, (ND), Not determined in this study, (N/A), not applicable. A, (Stracker, Carson and Weitzman, 2002), B, (Carson *et al.*, 2003), C, (Blackford *et al.*, 2010), D, (Orazio *et al.*, 2011), E, (This thesis), F, (Sarnow, Sullivan and Levine, 1982), G, (Grand, Grant and Gallimore, 1994), H, (Gabler *et al.*, 1998), I, (Ching *et al.*, 2013), J, (Baker *et al.*, 2007), K, (Cheng *et al.*, 2011), L, (Hung and Flint, 2017).

# CHAPTER 4

## **The promotion of genomic instability in human fibroblasts by adenovirus 12 early region 1B-55K protein in the absence of viral infection**

**Statement: Some of the Figures and Figure legends presented in this thesis have been published in Viruses, 2021 December 6, 13 (12), 2444, [Https://doi.org/10.3390/v13122444](https://doi.org/10.3390/v13122444). All of the Figures presented are my own work except for the metaphase spreads shown in Figure 4.3. The text from the Viruses publication has not been used 'directly' in this thesis although there might be some overlap or similarity between the text in the thesis and the text in the publication.**

## 4.1 Introduction

It was shown in early research that viruses from group A HAdVs, such as HAdV12, had the ability to generate tumours in new-born rodents, but viruses from species C, such as the widely researched HAdV2 and HAdV5, did not share this ability (Trentin, Yabe and Taylor, 1962; Yabe, Trentin and Taylor, 1962; Huebner *et al.*, 1963). When injected into a syngeneic host, rodent cells that had been transformed by HAdV12-E1 genes could also cause tumours. In contrast, cells that had been transformed by HAdV5 or HAdV2 could only cause tumours in athymic nude mice or animals with weakened immune systems (Freeman *et al.*, 1967; Gallimore, 1972; Gallimore, McDougall and Chen, 1977). HAdV12 has also been found to generate tumours that are similar to retinoblastomas in baboons, which is consistent with previous observations (Mukai *et al.*, 1980). Accordingly, HAdVs were categorised as DNA tumour viruses based on these observations.

Later studies of low dose HAdV12 infections showed that HAdV12-E1B55K promotes genomic instability in human cells, as it was reported that HAdV12 induces chromosomal aberrations in human embryo kidney and human embryo lung cells, causing non-random damage and breaks in chromosomes 1 and 17 (zur Hausen, 1967; McDougall, 1971b). The infection was found to affect primarily four chromosomal regions, commonly referred to as HAdV12 modification sites. Damage at these sites was shown as regions of uncoiled DNA and heterochromatic gaps from which breaks may result. Indeed, three of the HAdV12 modification sites were mapped on chromosome 1, specifically 1p36, 1q21, and 1q42-43, whereas 17q21-22 was mapped on chromosome 17 and all chromosomal regions were found to have distinct similarities to classic fragile sites (Stich, Van Hoosier and Trentin, 1964; zur

Hausen, 1967; McDougall, 1971; McDougall *et al.*, 1974; Lindgren *et al.*, 1985; Durnam *et al.*, 1988). A shared feature of the four loci is their correspondence to gene clusters encoding structural RNAs, such as the RN5S locus which comprises repeated genes encoding 5S RNA, the PSU1 locus that encodes U1 genes, and the RNU1-2 loci containing genes responsible for encoding U1 and U2 small nuclear RNAs (Lindgren *et al.*, 1985; Li *et al.*, 1993, 1998; Bailey *et al.*, 1995). Mutational studies on E1 genes from HAdV12 have shown that viral-induced chromosomal damage and modification of fragile sites is dependent upon the expression of the HAdV12-E1B55K protein, whereas E1A and E1B19K proteins had minimal effects (Durnam *et al.*, 1986; Schramayr *et al.*, 1990b). In light of these findings, we concluded that conducting additional research into the capability of HAdV12-E1B55K to cause DNA damage and its impact on host DDR would be of considerable interest. This is particularly relevant as our understanding of the pathways through which DNA damage is repaired has significantly improved since the initial studies on E1B55K proteins were conducted.

The majority of E1B55K activities during infection have been linked to its association with E4orf6 and the formation of the ubiquitin E3 ligase that incorporates cellular cullins, elongins b and C, and Ring box 1 (see section 1.3.1.2) (Querido, Blanchette, *et al.*, 2001). The cellular protein degradation that occurs is a consequence of the ubiquitylation by the E1B55K/E4orf6-containing E3 ligase (Blackford and Grand, 2009; Schreiner, Wimmer and Dobner, 2012; Hidalgo *et al.*, 2019; Herrmann *et al.*, 2020; Kleinberger, 2020); however, it has been established that some of the E1B55K-binding proteins that have previously been identified (reviewed in (Hidalgo *et al.*, 2019)) were shown not to be degraded during viral infection, whereas others remained intact (Hung and Flint, 2017; Herrmann *et al.*, 2020).

Inactivation and eventual activation of the DDR is seen after HAdV infection as a decrease and increase in the activity of DDR kinases and, more importantly, as a decrease in the ability of infected cells to produce viral concatemers (Stracker, Carson and Weitzman, 2002; Carson *et al.*, 2003; Karen *et al.*, 2009). Correspondingly, it has been established that a considerable number of regulatory proteins linked to the DDR, such as p53, BLM helicase, MRE11, DNA ligase IV and others, are degraded during HAdV5 and, in most cases, HAdV12 infections (Sarnow *et al.*, 1982; Stracker, Carson and Weitzman, 2002; Baker *et al.*, 2007; Blackford *et al.*, 2010; Orazio *et al.*, 2011; Gupta *et al.*, 2013; Chalabi Hagkarim *et al.*, 2018).

Most of the research carried out previously has focused on the activities of the E1B55K protein during viral infection while in collaboration with E4orf6 and functioning as a component of the E3 ubiquitin ligase complex. In this chapter, we aimed to characterise the unique roles of E1B55K in association with the DDR but distinct from its E3 ligase activities. We expected that this would allow us to throw light on its ability to cause genomic instability. With this in mind, we decided to look at the effects of HAdV12-E1B55K on DDR and DNA replication dynamics in primary human fibroblasts that express the HAdV12-E1B55K protein only. It was shown in earlier studies that the introduction of the gene extended the lifespan of human skin fibroblasts in culture, producing long lived (but not immortal or transformed) cells (Gallimore *et al.*, 1997). We compared results with normal HSFs obtained from the same donor. Our results show that HAdV12-E1B55K interferes with replication dynamics, seen as a significant increase in stalled forks probably due to collision of the replisomes with DNA lesions in cells expressing the viral protein, as well as a marked increase in the total number of R-loops, both of which are indicative of increased replication stress. Also, we demonstrate that HAdV12-E1B55K expression sensitises cells to a variety of genotoxic agents, as shown by a rise in DNA



damage foci formation and ATM activation. Furthermore, our findings are in line with previous observations which indicates that the viral protein induces genomic instability, represented by an increase in chromosomal breaks and micronuclei numbers. We hypothesise that interactions of HAdV-E1B55K with different DDR and replication complex proteins is responsible for majority of these effects.

## 4.2 Results

### 4.2.1 Expression of HAdV12-E1B55K in human skin fibroblasts.

To investigate the effects of HAdV-E1B55K protein on the DDR and its impacts on genomic stability, we used human skin fibroblasts (HSF) expressing the HAdV12-E1B55K protein (55K<sup>+</sup>HSF) in the absence of E4orf6, and consequently in the absence the E3 ubiquitin ligase complex activity (Gallimore *et al.*, 1997). The 55K<sup>+</sup>HSFs are clonal, as determined by IF. By staining for HAdV12-E1B55K, all cells were positive with the viral protein localised predominantly in the nucleus (data not shown but a single cell is shown in Figure 4.14). Results were compared to parental HSFs. The cells appear phenotypically similar under the microscope, and they have a considerably increased life span, but they are neither immortal nor transformed (Figure 4.1A). Cells were harvested, fractioned by SDS-PAGE, and western blotted to visualise the expression of the viral protein in 55K<sup>+</sup>HSFs using an antibody against HAdV12-E1B55K. It is interesting to note that they express HAdV12-E1B55K at a level that is much lower than that expressed by HAdV12-E1 transformed human cells (Figure 4.1B).

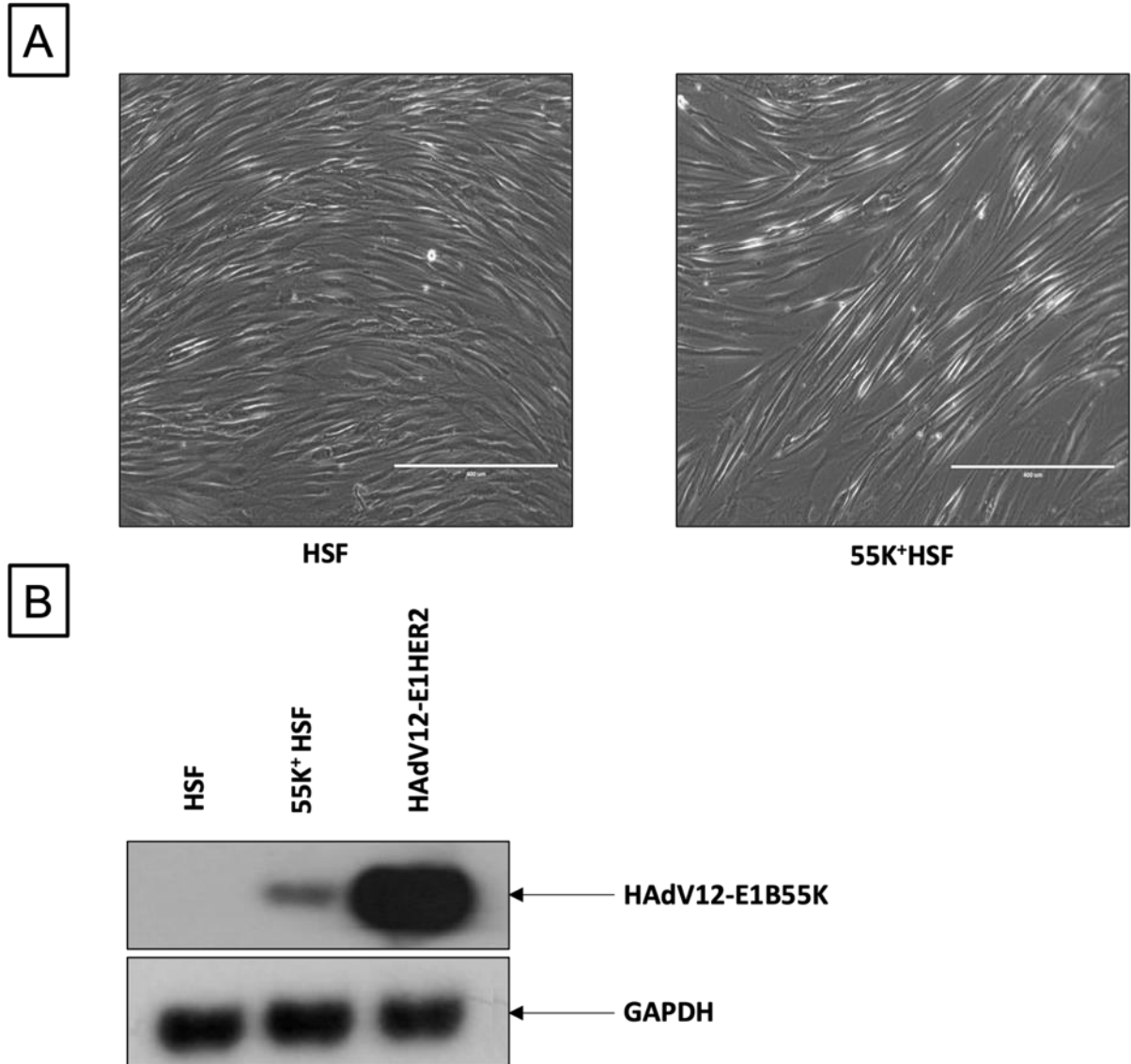


**Figure 4.1.** The morphological appearance of parental HSFs and 55K<sup>+</sup>HSFs and the expression of HAdV12-E1B55K protein in 55K<sup>+</sup>HSF. (A) Phase contrast microscopy images showing parental HSFs (left panel) and 55K<sup>+</sup>HSFs (right panel) (representative scale bar of 400  $\mu$ m). (B) Western blot of HSFs, 55K<sup>+</sup>HSF and HAdV12-E1HER2 cells showing the expression of HAdV12-E1B55K in 55K<sup>+</sup>HSF and HAdV12-E1HER2, probed using an antibody against HAdV12-E1B55K.

#### 4.2.2 Genomic instability is induced by the expression of HAdV12-E1B55K in human skin fibroblasts.

As previously stated, most studies have indicated that HAdV12-E1B55K causes chromosomal breaks at designated fragile sites in human cells, and that these breaks are comparable to those caused by exposure to low concentrations of DNA-damaging agents (zur Hausen, 1967; McDougall, 1971a; McDougall *et al.*, 1974; Durnam *et al.*, 1988; Schramayr *et al.*, 1990a; Caporossi, Bacchetti and Nicoletti, 1991). However, most of those studies examined the HAdV12-E1B55K effects in the context of viral infection when the whole virus was present. Micronuclei formation usually arises from cytotoxic events and chromosomal instability and they are often induced by the combined effects of accumulated DNA damage and defects in the cell repair machinery (Krupina, Goginashvili and Cleveland, 2021). In order to acquire a direct indication of the influence of the viral protein on the stability of the genome, the number of micronuclei in normally dividing HSFs, as well as 55K<sup>+</sup>HSFs was counted (Figure 4.2B). In addition, counting of micronuclei was also carried out 24- or 48-hours following treatment with Hydroxyurea (HU), Camptothecin (CPT), or ionising radiation (IR) (Figure 4.2C-E). Interestingly, although micronuclei are generally uncommon in untreated HSFs, they can be seen in 5-10% of cells expressing the viral protein (Figure 4.2A, B). Whereas in cells treated with DNA damage agents (1 $\mu$ M CPT, 2mM HU or IR (4Gy)), the numbers of micronuclei are again remarkably higher in cells expressing HAdV12-E1B55K in comparison to normal HSFs (Figure 4.2C-E). This suggests that the viral protein interferes with DDR and promotes defects in the cellular repair machinery, apart from its well-known ability to degrade DDR proteins with E4orf6.

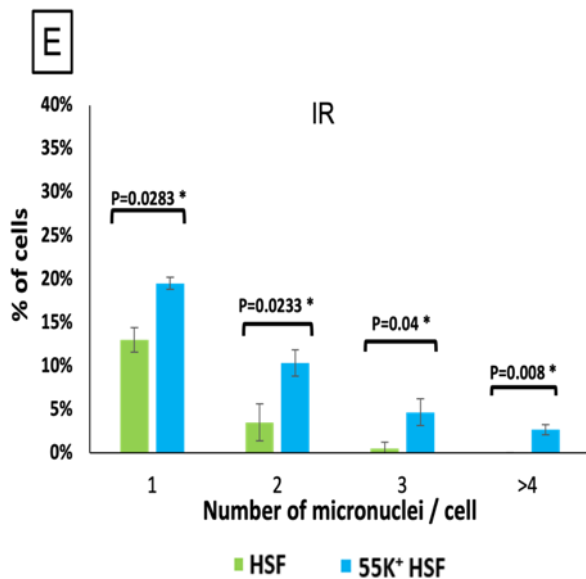
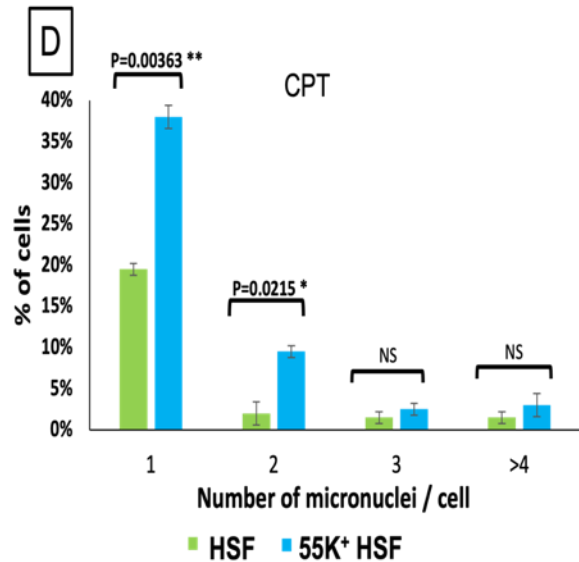
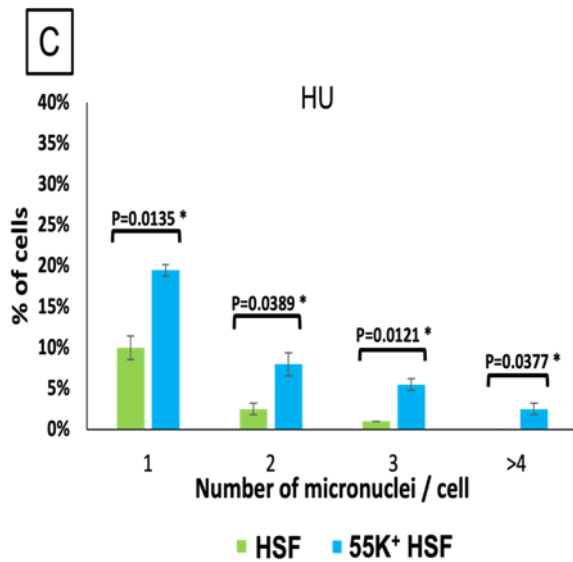
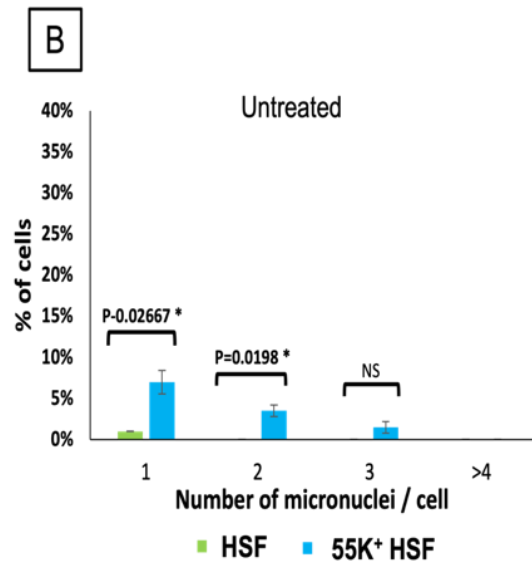
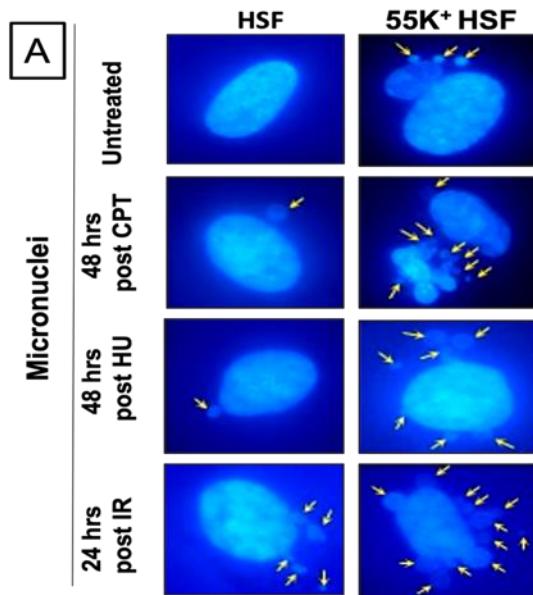


**Figure 4.2.** Micronuclei formation in HSFs and 55K<sup>+</sup>HSFs. HSFs and 55K<sup>+</sup>HSFs were subjected to DNA damaging agents. After 24 or 48 hours the cells were fixed and stained with DAPI. (A) Representative images showing DNA staining of HSFs and 55K<sup>+</sup>HSFs with DAPI, arrows indicate micronuclei. (B) Number of micronuclei per cell in untreated cells. (C) Number of micronuclei per cell observed after 48 hours of treatment with 2mM HU. (D) Number of micronuclei per cell observed after 48 hours of treatment with 1 $\mu$ M CPT. (E) Number of micronuclei per cell observed after 24 hours of irradiation with IR (4Gy). (n=3 independent experiments, >100 cells were counted for each replicate). Mean  $\pm$  SD, \*p < 0.05, \*\*p < 0.01, NS, not significant.

#### 4.2.3 HAdV12-E1B55K causes genomic instability as indicated by the formation of chromosomal gaps, breaks and radials in human skin fibroblasts.

(This experiment was kindly performed by Dr Rob Hollingworth)

Initial investigations that examined the impact of HAdV12 on human chromosomes have established that the virus causes chromosomal gaps and breaks at certain fragile sites, specifically at chromosomes 1 and 17 (zur Hausen, 1967; McDougall, 1970, 1971a). To see whether the 55K<sup>+</sup>HSF cells had a higher rate of chromosomal abnormalities, metaphase spreads were prepared from HSFs and 55K<sup>+</sup>HSFs. Gaps, breaks, and radials may be observed in the 55K<sup>+</sup>HSF metaphase spread depicted in (Figure 4.3). Consistent with other data presented in this chapter, HAdV12-E1B55K caused appreciable chromosomal damage which was not seen in parental HSFs (Figure 4.3).

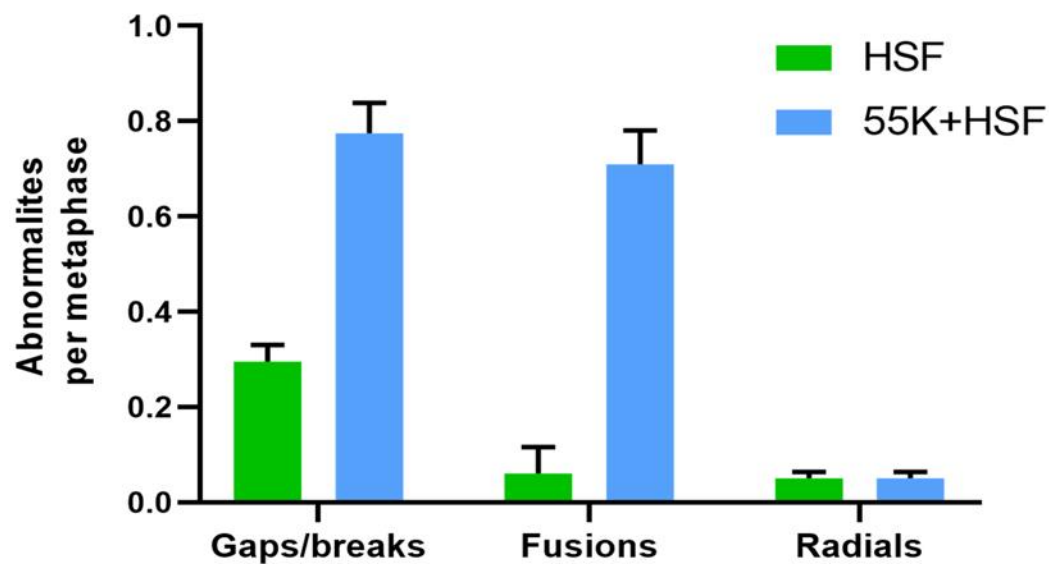
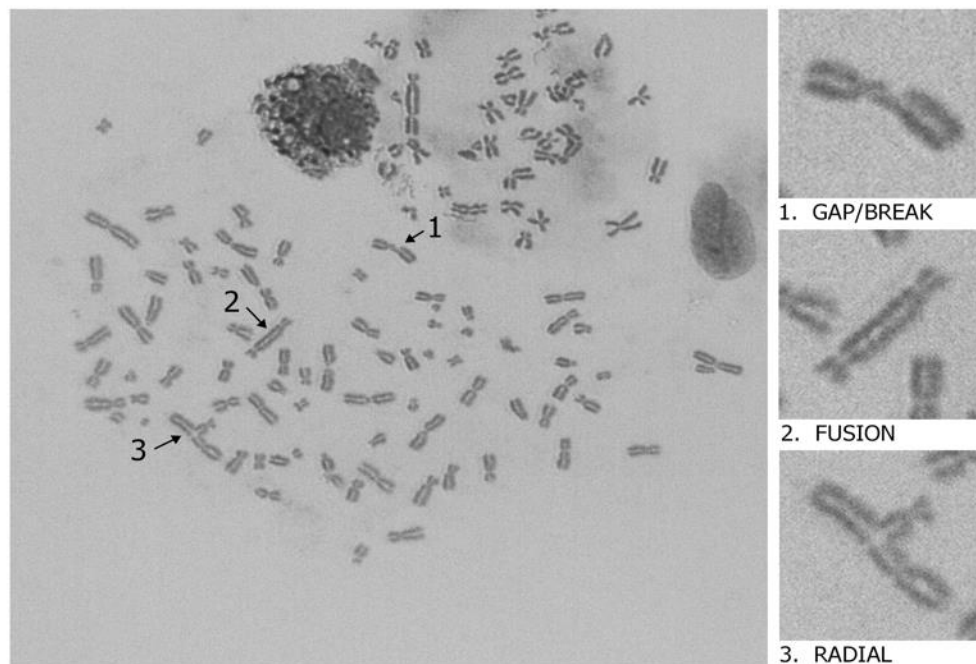


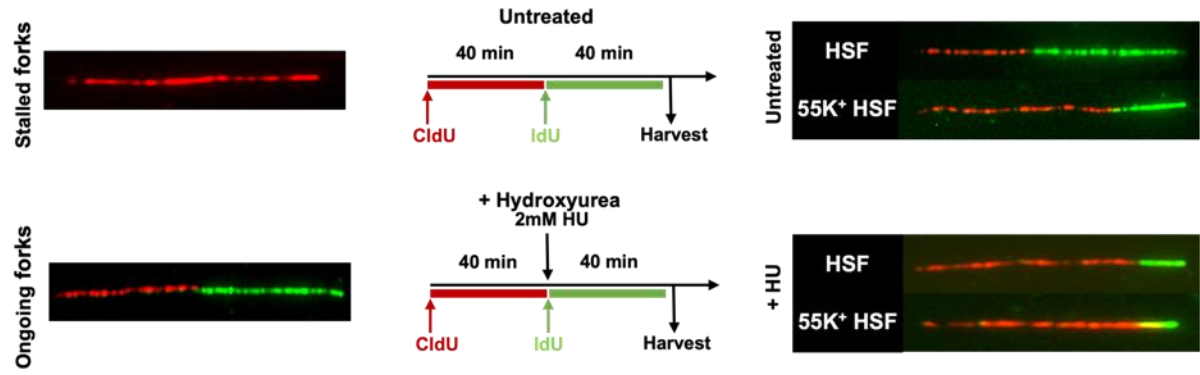
**Figure 4.3.** 55K<sup>+</sup>HSFs metaphase spreads. Metaphase spreads from HSFs and 55K<sup>+</sup>HSFs were prepared as outlined in the materials and methods section. (A) A sample metaphase spread from 55K<sup>+</sup>HSFs is shown. (B) The bar chart displays the average number of chromosomal anomalies obtained by analysing metaphase spreads from each cell group (n=2 independent experiments, >50 metaphase spreads were counted for each replicate).



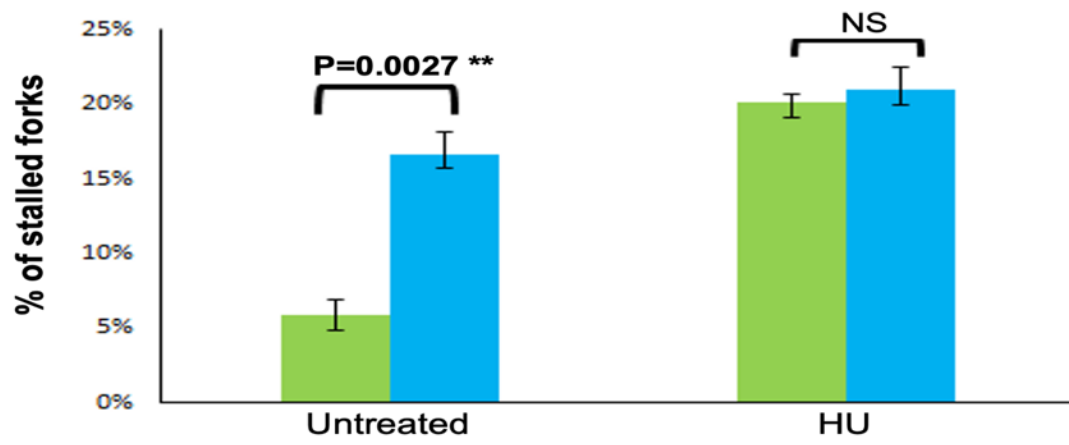
#### 4.2.4 HAdV12-E1B55K causes DNA replication stress, increased fork stalling, and decreased efficiency of replication fork restart in HSFs.

In light of the fact that treatment with the replication inhibitor HU has a marked impact on the genomic stability of 55K<sup>+</sup>HSFs (Figure 4.2C), we have investigated DNA replication dynamics in both cell populations using DNA fibre assays (Nieminuszczy, Schwab and Niedzwiedz, 2016), as outlined in the materials and methods chapter. In untreated cells, the expression of the viral protein resulted in a significant increase in the number of stalled forks in comparison to normal HSFs (Figure 4.4B). Replication fork speed and fork restart efficiency are also noticeably lower in 55K<sup>+</sup>HSFs (Figure 4.4C, D). The cells were treated with 2 mM HU, which induces depletion of the nucleotide pool (dNTP) and ultimately results in global replication fork stalling. This was done to investigate the influence that HAdV12-E1B55K has on the response to DNA replication stress. As anticipated, the HU treatment led to a considerable increase in the number of stalled forks in both cell populations (Figure 4.4B); although there was only a slight increase in the number of stalled forks caused by HU in 55K<sup>+</sup>HSFs. Additionally, the capacity of the 55K<sup>+</sup>HSFs to restart replication in an efficient manner was considerably impaired after HU treatment (Figure 4.4C). DNA fibre examples acquired throughout the study are shown (Figure 4.4A).

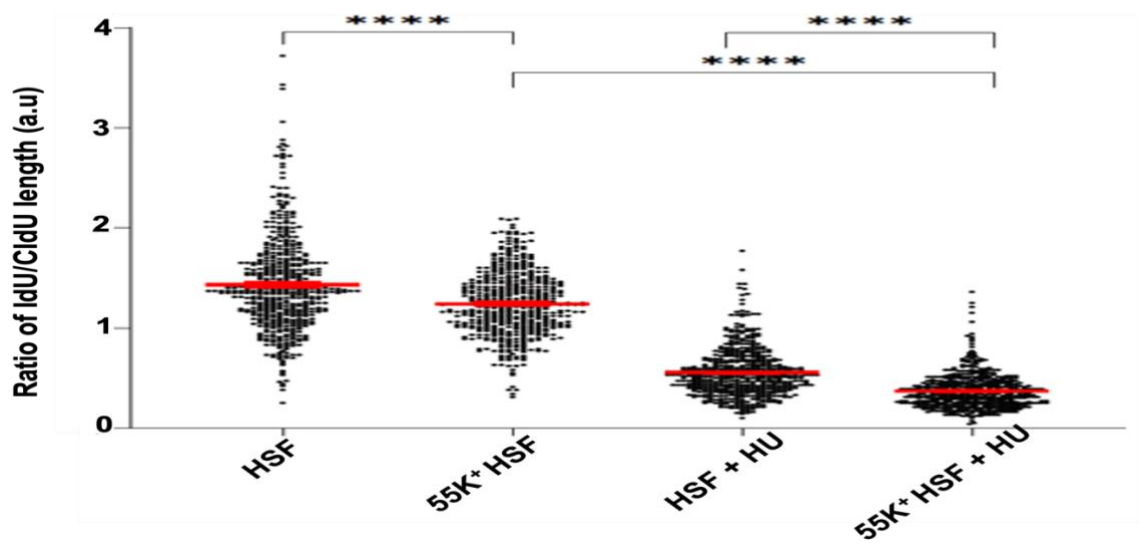
**A**



**B**



**C**



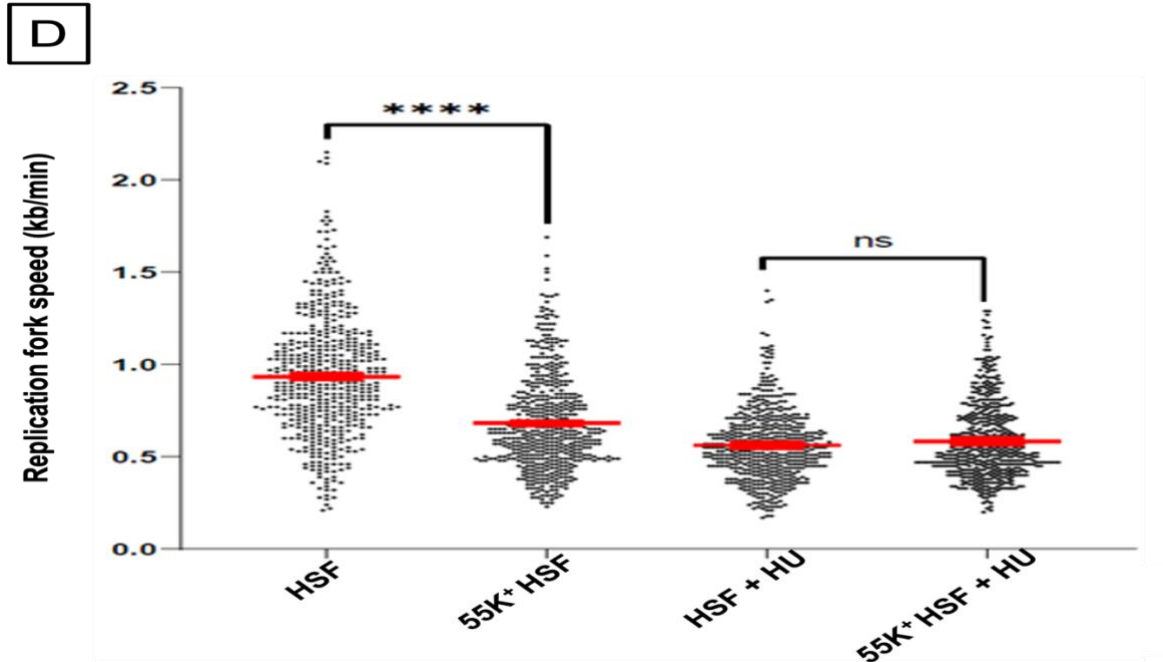


**Figure 4.4.** Expression of HAdV12-E1B55K in HSFs affects DNA replication dynamics. (B, C and D) HSFs and 55K<sup>+</sup>HSFs were analysed by DNA fibre assays as described in materials and methods with and without 2mM HU. (A) Representative examples of DNA fibres obtained throughout the study showing labelling protocol with CldU and IdU along with examples of fibres observed in HSFs and 55K<sup>+</sup>HSFs, in the presence and absence of HU. (B) Percentage of stalled forks before and after HU treatment of both cell populations, HSFs, the green bars and 55K<sup>+</sup>HSFs, the blue bars. (C) The ratio of the lengths of the IdU/Cldu tracts before and after HU treatment (to measure the replication fork restart efficiency after fork stalling). (D) Replication fork speeds before and after treatment with HU of both cell populations. (n=3 independent experiments, >175 DNA fibres were analysed for each replicate). Unpaired *t*-test, \*\*  $p < 0.01$ , \*\*\*  $p < 0.001$  and \*\*\*\*  $p < 0.0001$ , NS, not significant.

#### 4.2.5 HAd12-E1B55K expression increases R-loop formation in HSFs.

The presence of DNA-RNA hybrid R-loops is considered a sign of DNA replication stress (Fournier *et al.*, 2021). To assess whether HAdV12-E1B55K affected R-loop formation, HSFs expressing the viral protein and normal HSFs were stained with the S9.6 antibody (Boguslawski *et al.*, 1986) to visualise R-loops. The cells were counterstained with nucleolin antibody with subsequent staining of DNA (taken as the nucleus) with DAPI. The relative total nuclear intensity of S9.6 staining due to 'significant' R-loops was determined by subtracting the means of the R-loop intensities of the nucleolin staining bodies (nucleoli) from the total nuclear staining as described (Sollier *et al.*, 2014). Results showed a significant increase in the intensity of R-loop formation in 55K<sup>+</sup>HSFs in comparison to parental HSFs (Figure 4.5A). Additionally, following irradiation of the cells with IR, the S9.6 antibody staining was more intense in 55K<sup>+</sup>HSFs when compared to normal HSFs (Figure 4.5A). Examples of R-loop staining acquired throughout the study are shown (Figure 4.5B).

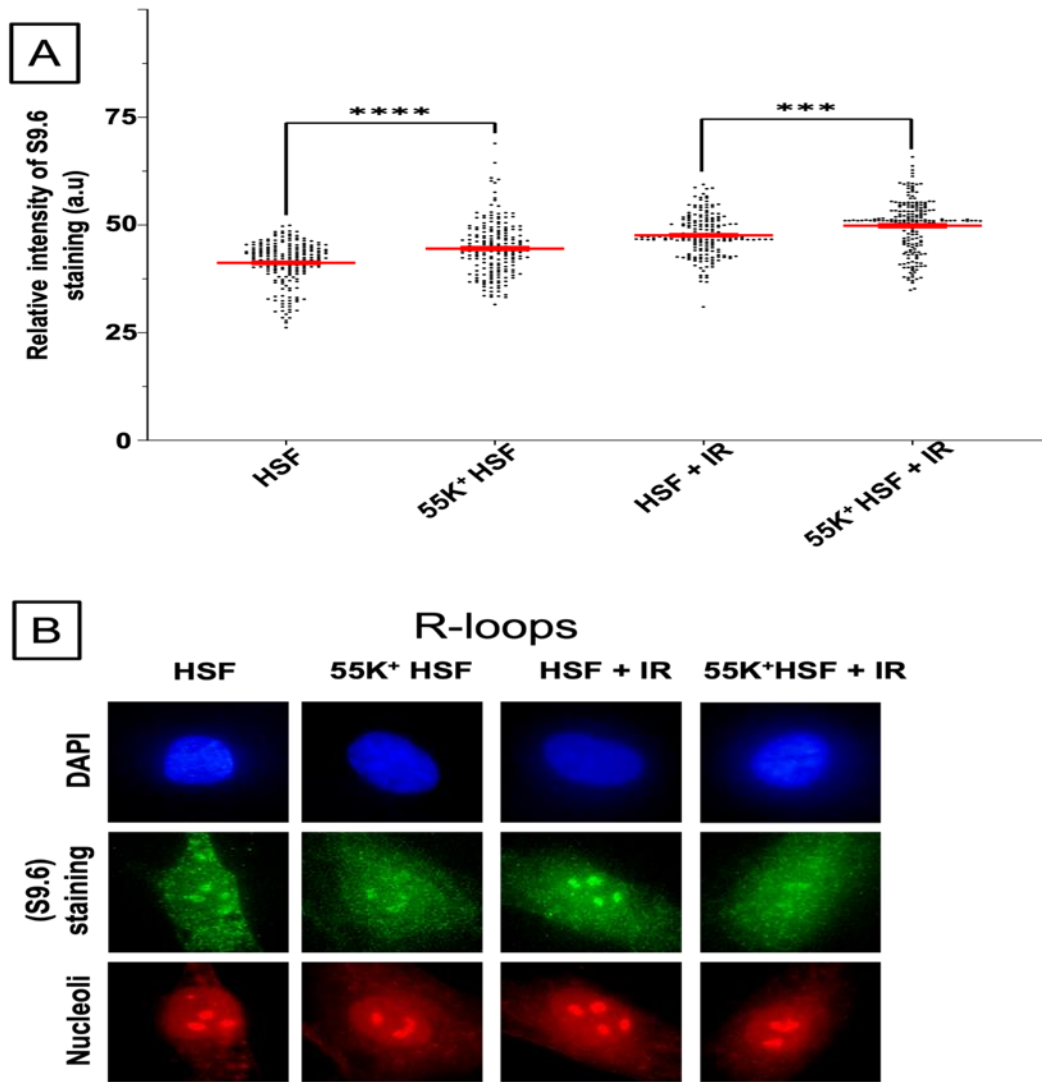
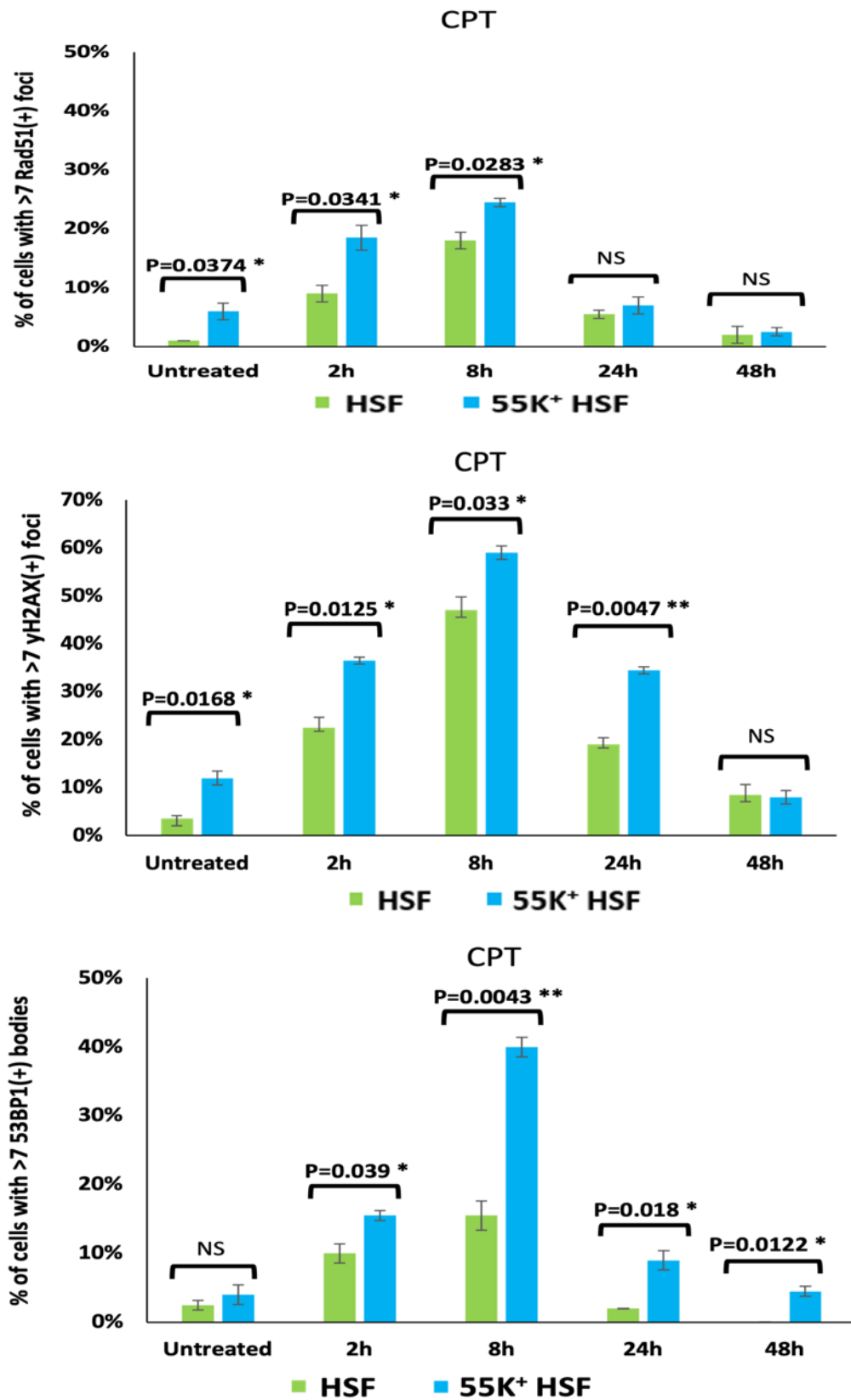


**Figure 4.5.** Expression of HAdV12-E1B55K in HSFs increases R-loops formation. Cells were fixed and stained with the S9.6 antibody to visualise R-loops and were counterstained with nucleolin antibody with subsequent staining of DNA with DAPI. (A) The relative intensity levels of R-loop staining calculated within the nucleus but outside the nucleoli in both cell populations before and after treatment with IR (4 Gy). (B) Representative examples of R-loops obtained throughout the study. (n=3 independent experiments, >200 cells were analysed for each replicant per cell strain). Unpaired *t*-test, \*\*  $p < 0.01$ , \*\*\*  $p < 0.001$  and \*\*\*\*  $p < 0.0001$ , NS, not significant.

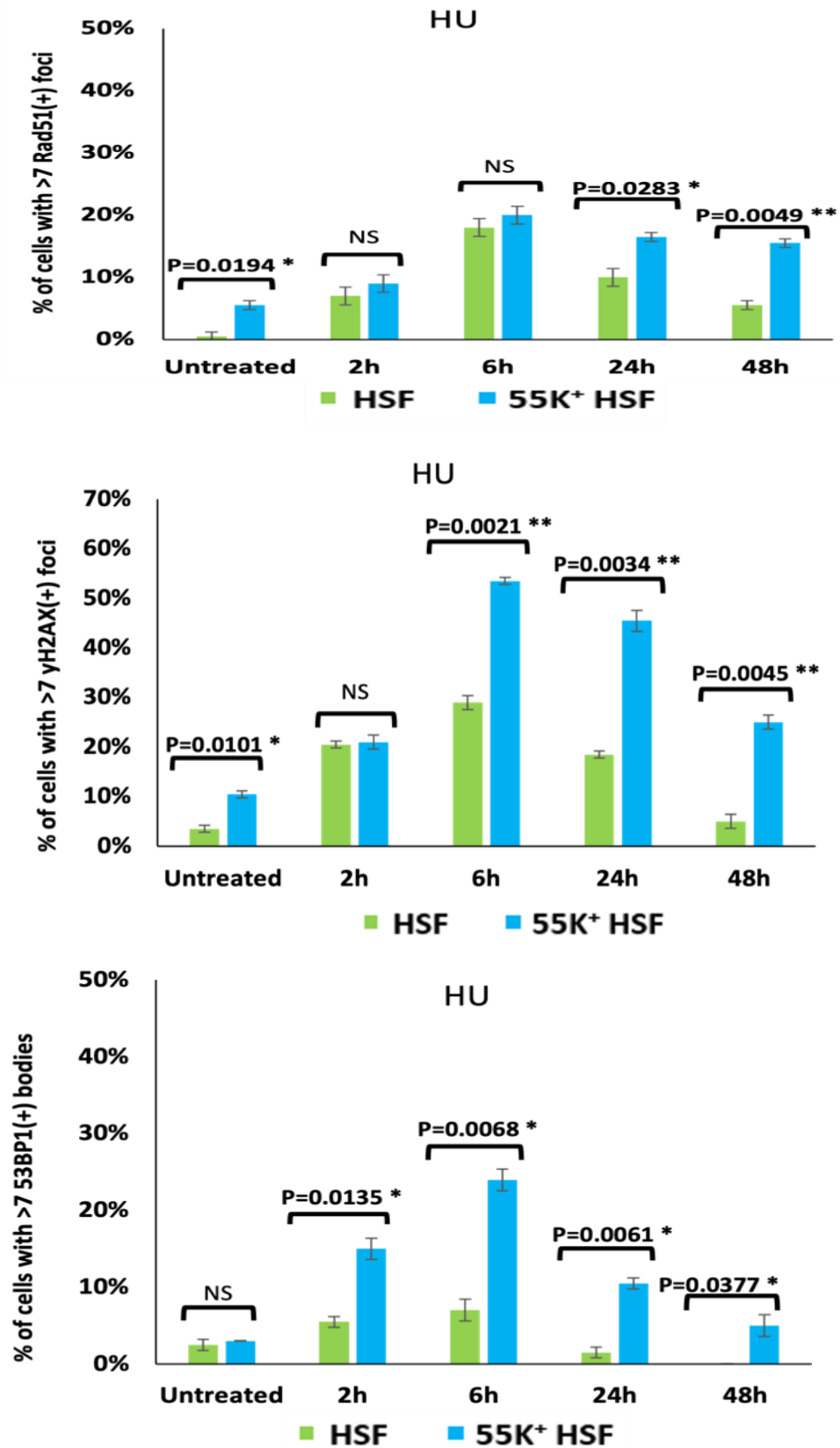
#### 4.2.6 HAdV12-E1B55K affects DNA repair foci formation in HSFs after DNA damage.

To understand the effect of HAdV12-E1B55K protein on the DDR, 'normal' and viral-protein expressing HSFs were exposed to different DNA damaging agents and DNA damage repair foci were counted over 24 or 48 hours. Foci stained for RAD51, 53BP1 and  $\gamma$ H2AX are shown (Figure 4.6). Results showed an overall increase in DNA foci formation in 55K<sup>+</sup>HSFs in comparison to the normal parental HSFs, both before and after treatment of the cells with CPT, HU, or IR (Figure 4.6). These results show an increase in DNA damage in cells expressing the viral protein and are consistent with the previously shown increase in micronuclei formation and stalled forks in 55K<sup>+</sup>HSFs.

A

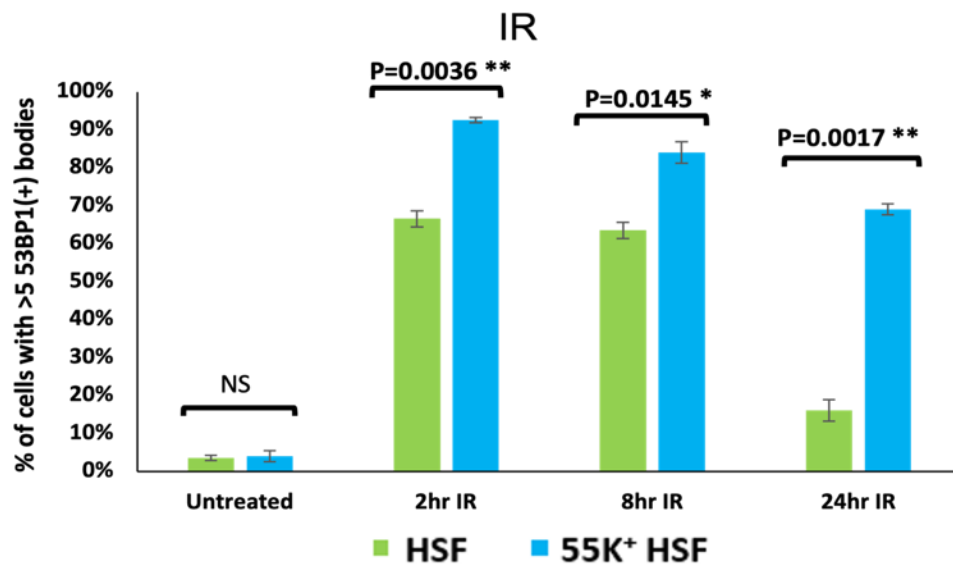
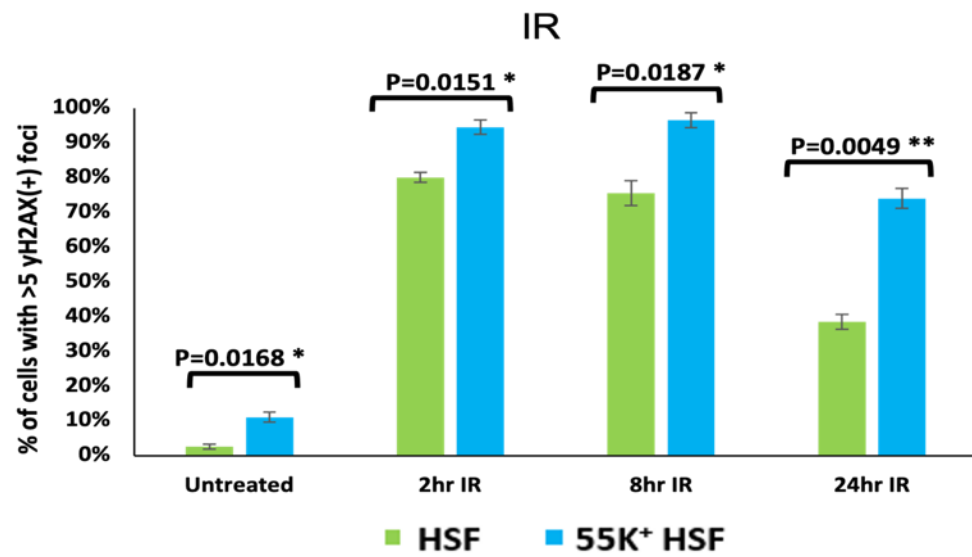
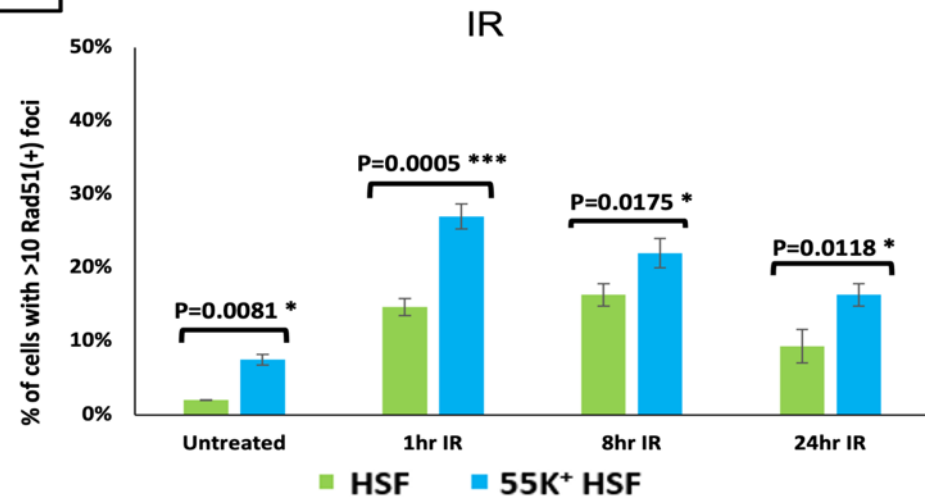


B





C



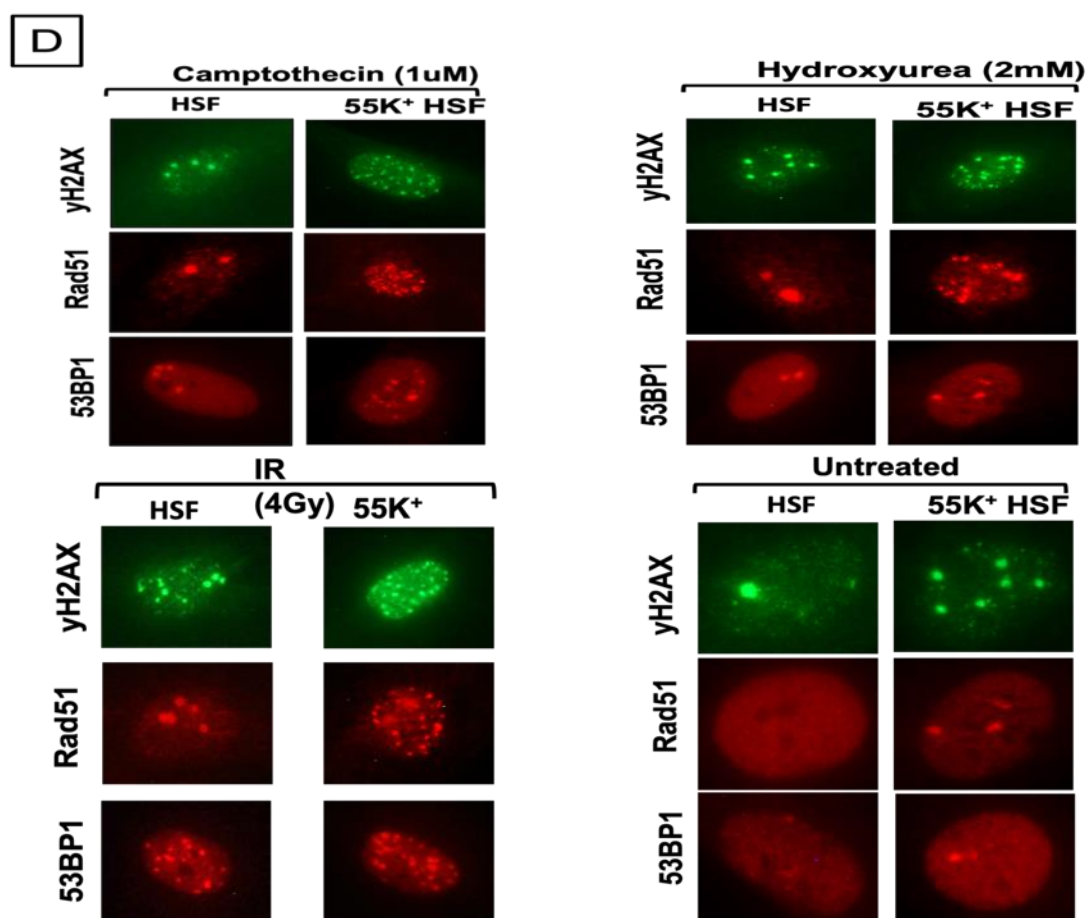


**Figure 4.6.** DNA repair foci formation is influenced by the expression of HAdV12-E1B55K in HSFs. Following treatment of HSFs and 55K<sup>+</sup>HSFs with DNA-damaging agents, cells were fixed and stained with antibodies against  $\gamma$ H2AX, RAD51 and 53BP1 at increasing times after treatment. DNA repair foci were counted before and after treatments with 1 $\mu$ M CPT, 2mM HU and IR(4Gy). (A) percentages of DNA repair foci in cells exposed to CPT in different time sets. (B) percentages of DNA repair foci in cells exposed to HU in different time sets. (C) percentages of DNA repair foci in cells exposed to IR in different time sets. (D) Representative images of stained repair foci before treatment and after exposure to CPT, HU, or IR. (n=3 independent experiments, >100 cells were counted for each treatment per replicant for each cell strain at each time point). Mean  $\pm$  SD, \* p < 0.05, \*\* p < 0.01 and \*\*\* p < 0.001, NS, not significant.

#### 4.2.7 HAdV12-E1B55K co-localisation with DNA repair foci following induced DNA damage.

In a further investigation, we examined the possibility that HAdV12-E1B55K may become localised to DNA repair foci. Although results have shown a marked effect of HAdV12-E1B55K on the DDR and focus formation after induced DNA damage (Figure 4.6A-C), in most cases, there was no evidence of co-localisation between the viral protein and either 53BP1 or  $\gamma$ H2AX (Figure 4.7). It appears that a few of the  $\gamma$ H2AX foci may be found in proximity to more concentrated HAdV12-E1B55Ks (marked with yellow arrows in Figure 4.7A). At this point, it is not possible to determine whether this has any biological significance. On the other hand, the viral protein was not recruited to 53BP1 bodies; it was seen as tracks within the cytoplasm and homogenous nuclear staining irrespective of induced DNA damage (Figure 4.7B).

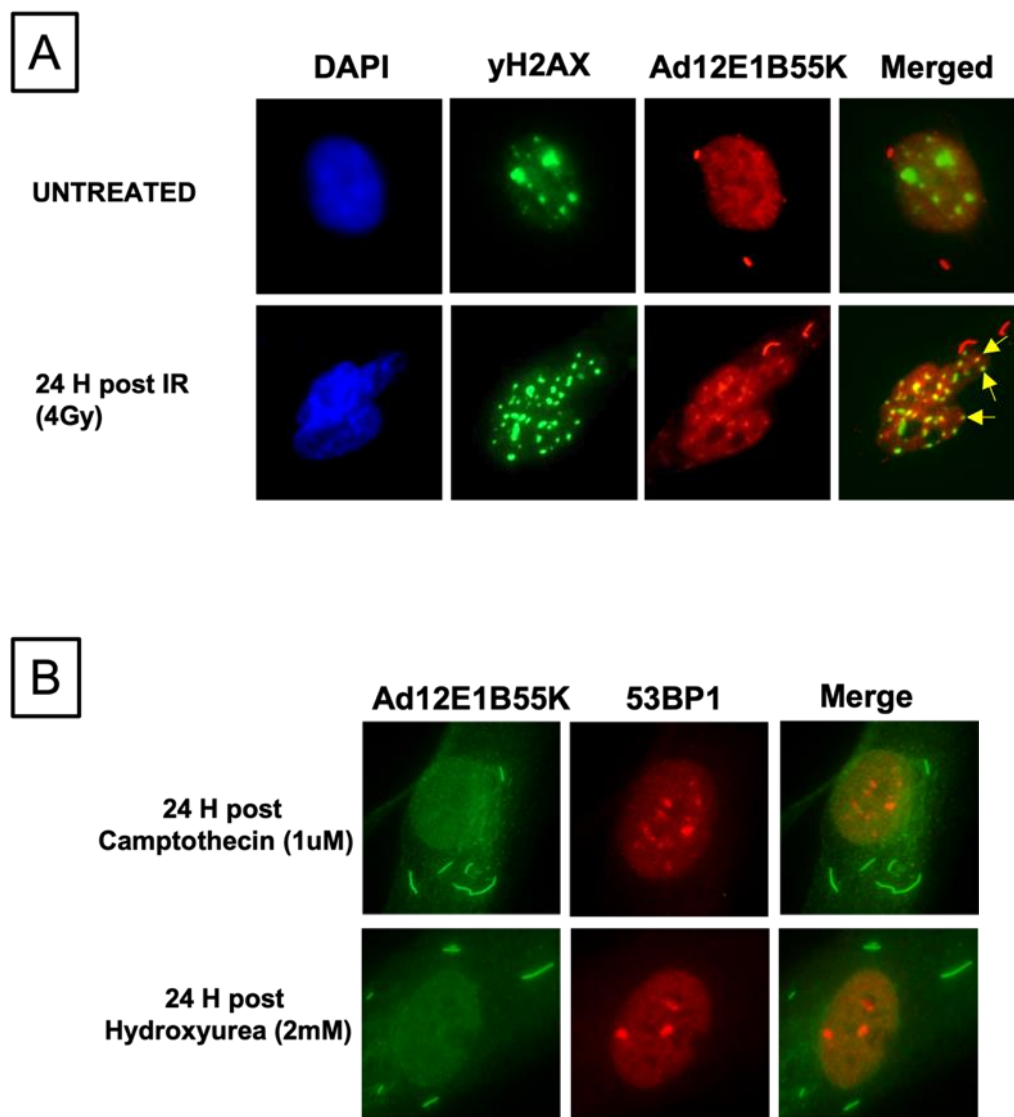
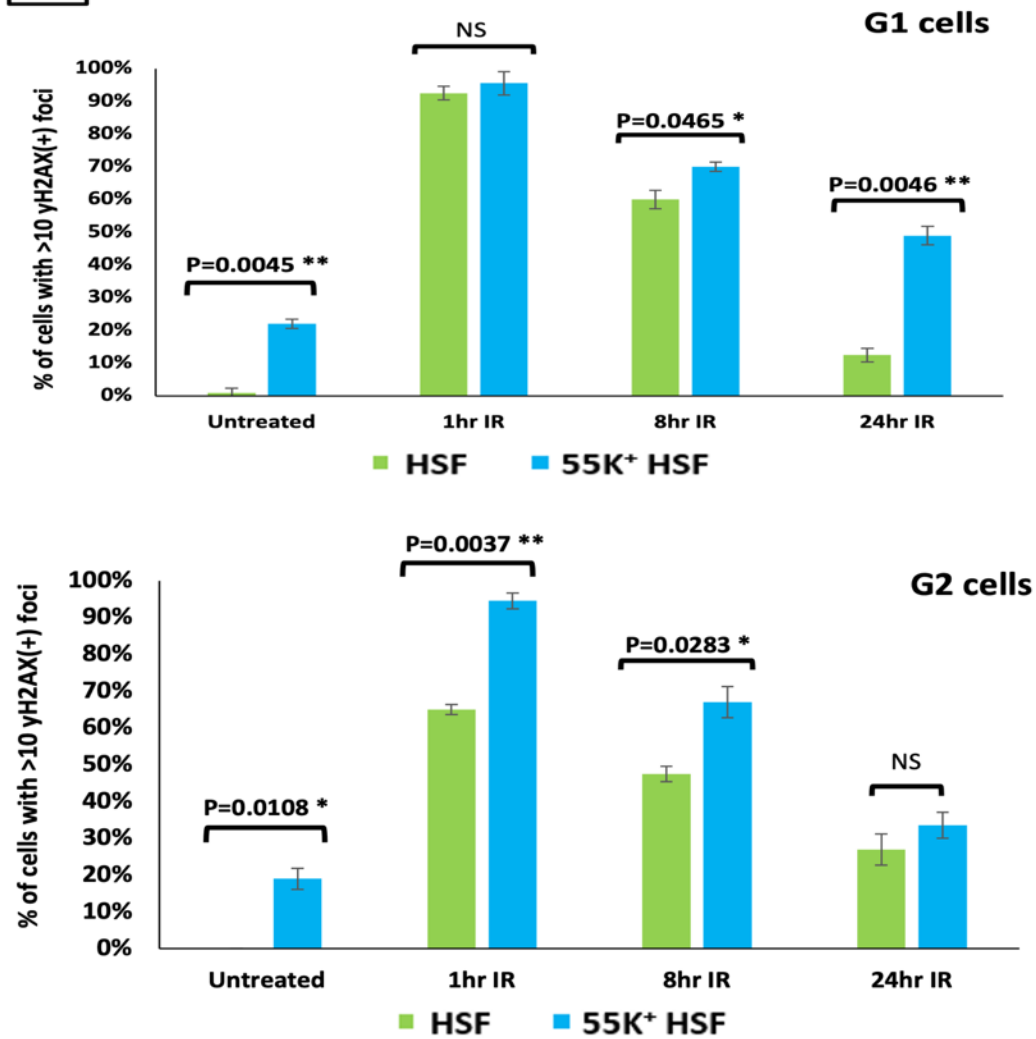


**Figure 4.7.** HAdV12-E1B55K does not co-localise with DNA repair foci following induced DNA damage. 55K<sup>+</sup>HSFs were exposed to CPT (1 $\mu$ M), HU (2mM), or IR (4 Gy) to induce DNA damage. After 24 hours, the cells were fixed, stained with HAdV12-E1B55K antibody, and counterstained with either (A),  $\gamma$ H2AX or (B), 53BP1 antibodies. Yellow arrows point to rare instances where HAdV12-E1B55K and  $\gamma$ H2AX may have been found to co-localise. No evidence of co-localisation between HAdV12-E1B55K and 53BP1 could be found.

#### 4.2.8 Expression of HAdV12-E1B55K interferes with DNA repair in HSFs during the G<sub>2</sub> phase.

We have analysed DNA damage focus formation in various stages of the cell cycle. Following treatment with 3  $\mu$ M aphidicolin (APH) for 45 minutes to induce cell cycle arrest, the cells were irradiated with 2 Gy and then fixed after either 1, 8, or 24 hours. The cells were stained with an antibody against Mitosin, which is expressed throughout the S, G<sub>2</sub>, and M phases of the cell cycle, and counter stained for  $\gamma$ H2AX. This allowed for the differentiation of foci created in the G<sub>1</sub> phase from those formed in the G<sub>2</sub> and S phases (Figure 4.8). In Mitosin-positive cells it was feasible to discriminate between G<sub>2</sub> cells (which had a limited number of highly distinct  $\gamma$ H2AX foci) and S phase cells (which had a large number of  $\gamma$ H2AX foci that were more diffuse). At 1 and 8 hours after irradiation, the numbers of foci in 55K<sup>+</sup>HSFs and HSFs are comparable in the irradiated G<sub>1</sub> cells that are negative for Mitosin. However, at 24 hours after irradiation, there was a marked increase in the number of foci in cells expressing HAdV12-E1B55K. On the other hand, in G<sub>2</sub> cells, the 55K<sup>+</sup>HSFs showed a distinctly higher number of foci at both 1 and 8 hours, although, the difference between the two cell populations was negligible at 24 hours after irradiation, when the cell cycle block may have possibly broken down. These findings lead us to hypothesise that cells expressing HAdV12-E1B55K have deficits in the HR pathway, which controls the majority of DNA repair during G<sub>2</sub> phase of the cell cycle.

**A**



**B**

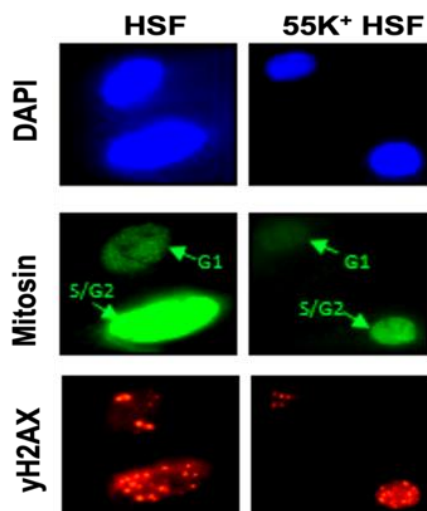


**Figure 4.8.** Expression of HAdV12-E1B55K interferes with DNA repair in HSFs during the G2 phase. Cells were treated with 3 $\mu$ M aphidicolin for 45 minutes and exposed to IR (2Gy). Following the periods indicated, cells were stained with antibodies against  $\gamma$ H2AX, Mitosin, and DAPI. (A) Quantification of cells with  $\gamma$ H2AX foci present in G<sub>1</sub> (Mitosin negative) and G<sub>2</sub> (Mitosin positive). (B) Representative images of cells stained with  $\gamma$ H2AX and Mitosin, as well as DAPI in normal parental and viral protein expressing HSFs. (n=3 independent experiments, >100 cells were counted for each replicant in each cell strain at each time point). Mean  $\pm$  SD, \* p < 0.05, \*\* p < 0.01, NS, not significant.

#### 4.2.9 HAdV12-E1B55K causes sensitisation of HSFs to DNA damaging agents.

We used western blotting with antibodies against recognised substrates of the PI-3-kinase-like kinases, ATM and ATR, to assess the activation of the DDR throughout a 24-hour's time course after exposing HSFs and 55K<sup>+</sup>HSFs to different DNA damaging agents. Cells were exposed to HU to induce replication stress. The replication stress generated by HU will produce SSBs in the DNA, which will then lead to DSBs formation. Similarly, CPT, a topoisomerase 1 inhibitor, also causes DSBs. Results demonstrated that, in all three treatments, the activation of the ATM pathway components is far more pronounced in 55K<sup>+</sup>HSFs than it is in the parental cells, with CHK2, KAP1, and  $\gamma$ H2AX being markedly more highly phosphorylated in cells expressing the viral protein (Figure 4.9). These findings provide evidence that HAdV12-E1B55K interferes with DSB repair mechanisms. Consistently, previous research has demonstrated that cells infected with HAdV5 undergo E1B55K/E4orf6-dependent degradation of the MRN complex, BLM, DNA Ligase IV, and TIP60 (Stracker, Carson and Weitzman, 2002; Orazio *et al.*, 2011; Gupta *et al.*, 2013). In addition, these findings are in agreement with previous reports which indicated that several of these proteins are degraded after HAdV12 infection (Cheng *et al.*, 2011; Forrester *et al.*, 2011), with HAdV12-E1B55K being most likely the binding component. There was just a marginal increase in DNA-PKcs phosphorylation that was detected in IR treated cells (Figure 4.9C). Unexpectedly, despite being exposed to HU, very limited CHK1 phosphorylation was detected. Because the cells would be under replication stress, a far more pronounced reaction was anticipated. The current explanations for these findings are unclear. (The blots in Figure 4.9 do not reveal p53 in parental HSFs because the autoradiographs were exposed for very brief periods of time to



make the images of 55K<sup>+</sup>HSFs clearer). It is interesting to note that there does not seem to be an increase in the expression of p53 when DNA damage is induced.

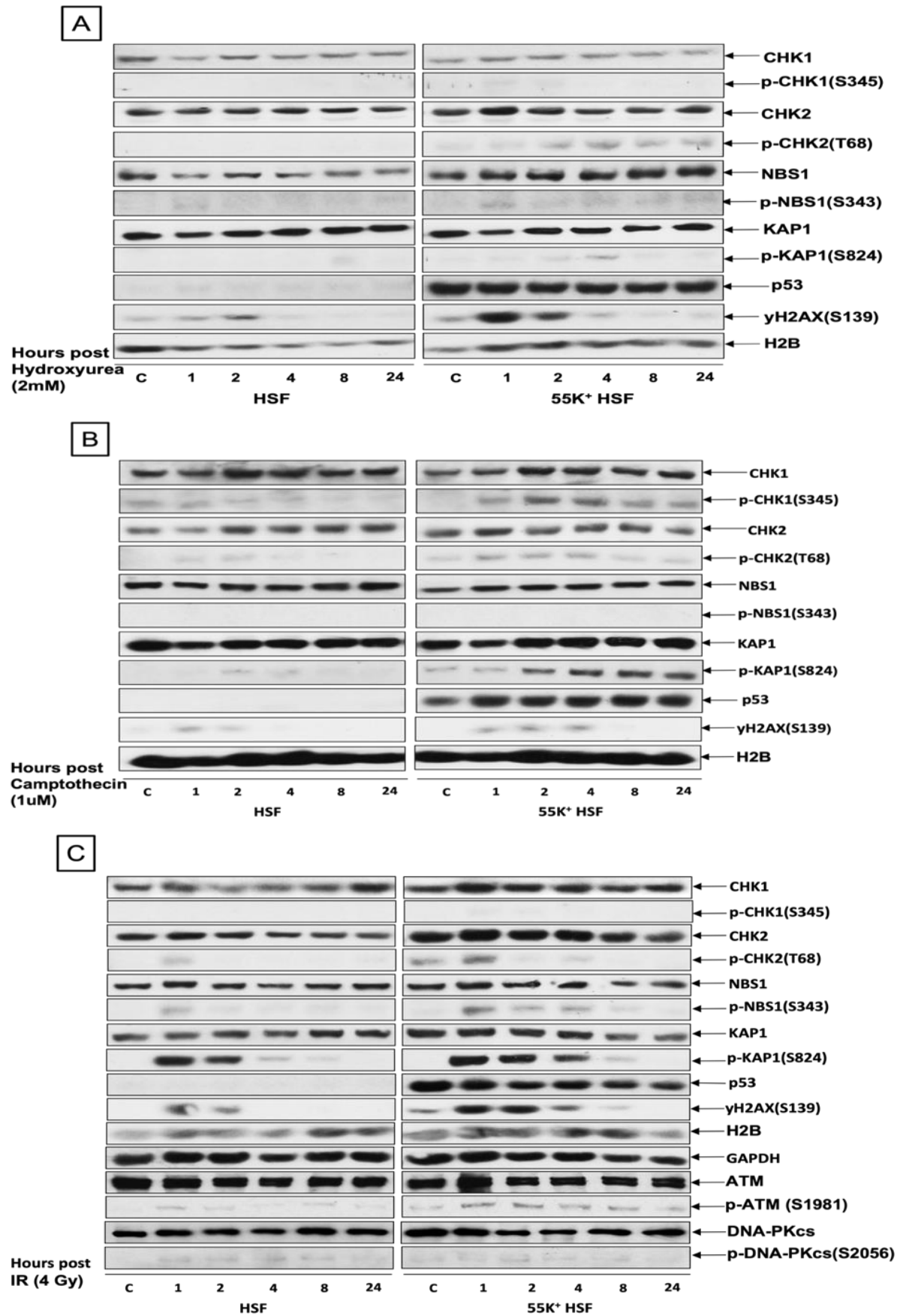


**Figure 4.9.** HAdV12-E1B55K sensitises HSFs to DNA damaging agents. HSFs and 55K<sup>+</sup>HSFs were exposed to CPT (1 $\mu$ M), HU (2mM), or IR (4 Gy) to induce DNA damage and harvested over a time course of 24 hours. Lysates were then fractioned by SDS-PAGE and western blotted with antibodies that recognised different known substrates of the DDR. (A) Western blots of HSFs and 55K<sup>+</sup>HSFs following treatment with HU (2mM). (B) Western blots of HSFs and 55K<sup>+</sup>HSFs following treatment with CPT (1 $\mu$ M). (C) Western blots of HSFs and 55K<sup>+</sup>HSFs following treatment with IR (4Gy). "C" untreated controls.

#### 4.2.10 Expression of HAdV12-E1B55K in HSFs influences the DSB repair pathways by inactivating the MRN complex.

It is evident from results in Figures 4.6 and 4.9 that HAdV12-E1B55K has a significant impact on the DDR, most likely compromising the process of repairing DSBs and possibly other pathways as well. We wanted to determine whether the same effects of HAdV12-E1B55K would be seen in the parental HSFs if MRE11 was inhibited using the inhibitor mirin. HSFs and 55K<sup>+</sup>HSFs were incubated with 50  $\mu$ M mirin for 45 minutes before being treated with 1  $\mu$ M CPT. After the indicated time points, the cells were fixed and the number of  $\gamma$ H2AX foci was counted (Figure 4.10A). Although there was not a significant change in the number of foci in 55K<sup>+</sup>HSFs due to the presence of mirin at the earlier time points, there was a significant rise in the total number of foci after 48 hours. On the other hand, there were greater numbers of foci in parental HSFs when they were subjected to mirin. Interestingly, after 24 hours, the number of  $\gamma$ H2AX foci in the two cell populations were relatively comparable while mirin was present; however, in its absence, there were 1.7 times as many foci in the 55K<sup>+</sup>HSFs cell population. Based on these findings, we propose that HAdV12-E1B55K affects the cellular DDR, at least partially, by inactivating the MRN complex. Furthermore, the number of micronuclei seen 48 hours after induced damage was considerably more comparable in the two cell groups when mirin was present, as opposed to when it was absent (Figure 4.10B). Therefore, in the absence of mirin, there were about four times as many cells in 55K<sup>+</sup>HSFs that had two micronuclei per cell as there were in the parental cells; but, in its presence, the number in these cells was equivalent in both populations. Additionally, there were almost no HSFs with more than three micronuclei in the absence of mirin, but when MRE11 was inactivated, identical numbers were seen in both cell populations.

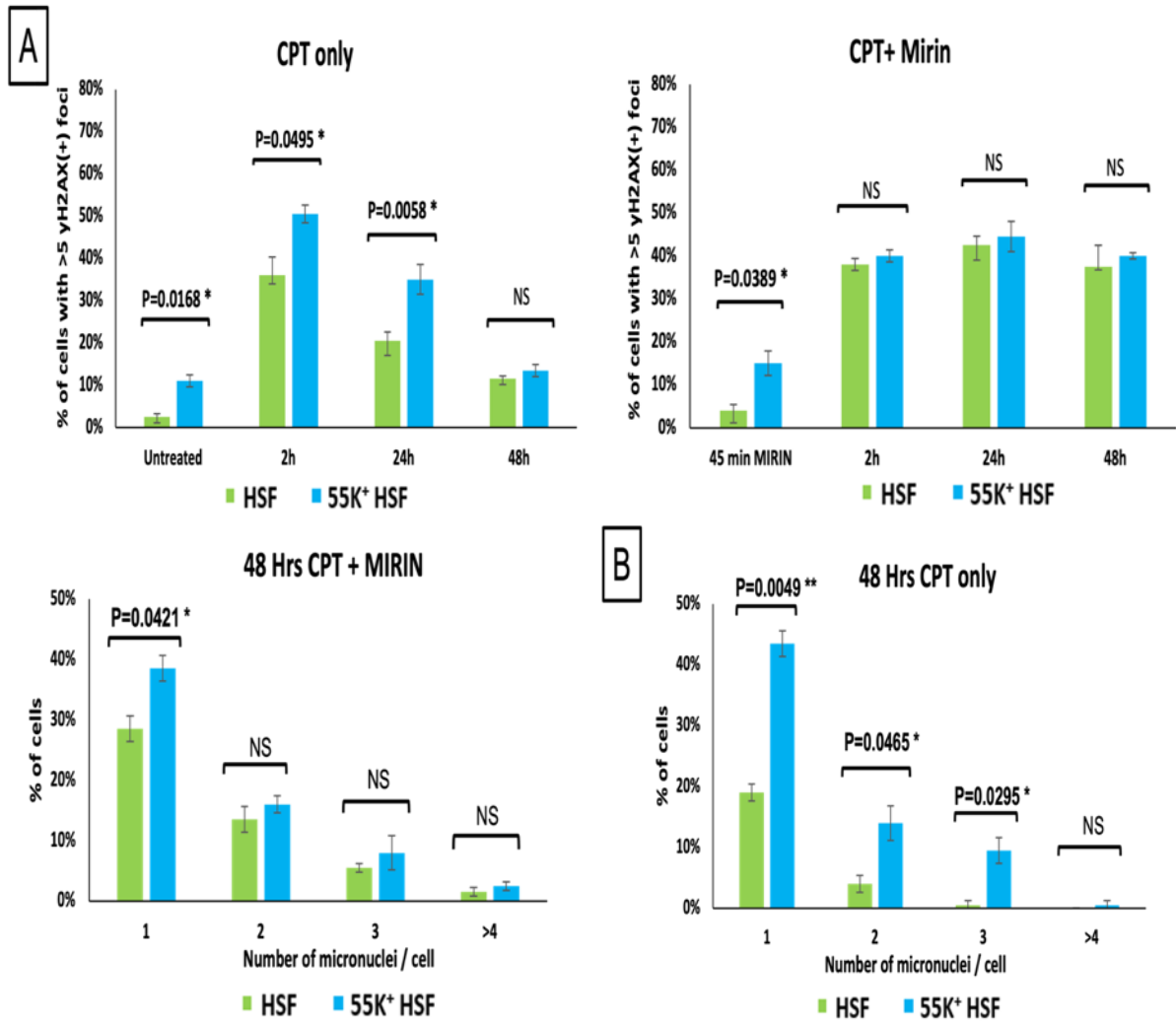


**Figure 4.10.** Mirin affects the formation of micronuclei and  $\gamma$ H2AX foci in HSFs and 55K<sup>+</sup>HSFs. After 24 hours of growth on glass coverslips, the cells were subjected to a 45-minute treatment with 50  $\mu$ M mirin. The cells were subsequently treated with 1  $\mu$ M CPT while mirin was present to induce DNA damage. (A) After the indicated time points, cells were fixed, stained for  $\gamma$ H2AX, and the number of foci was counted. (B) After 48 hours, the number of DAPI-stained micronuclei was counted. (n=3 independent experiments, >100 cells were counted for each replicant in each cell strain at each time point). Mean  $\pm$  SD, \* p < 0.05, \*\* p < 0.01, NS, not significant.

#### 4.2.11 The presence of HAdV12-E1B55K impacts the ability of HSFs to undergo cell cycle arrest in response to DNA damage.

In light of the profound effects that HAdV12-E1B55K has on the DDR and on DNA replication, we investigated whether or not there were any variations between the two cell populations in their ability to undergo cell cycle arrest in response to DNA damage. Both cell populations were treated with 1  $\mu$ M CPT before being harvested at different time points up to 48 hours. To evaluate the progression of the cell cycle in each cell population, cyclins were detected by western blotting (Figure 4.11). It appears that there is a decreased level of expression of cyclins A, B1, and D1 in parental HSFs, indicating an arrest of the cell cycle shortly after DNA damage. The expression of cyclin D1 increases after 8 hours, suggesting that cells are re-entering the cell cycle at this point. After 24 hours, there is a rise in the levels of cyclins A and B1 as the cells progress through the S and G<sub>2</sub> phases. However, in 55K<sup>+</sup>HSFs, the expression of cyclins stays high throughout the time course, indicating that the cells do not experience cycle arrest, likely as a result of the inactivation of p53 (despite that p53's expression is considerably much higher in cells expressing E1B55K than in parental cells, as shown in Figure 4.13).

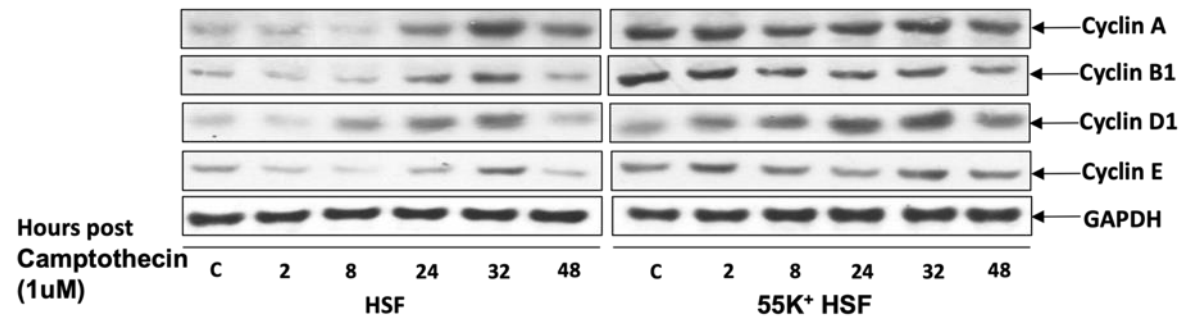


**Figure 4.11.** The expression of cyclins in 55K<sup>+</sup>HSFs and HSFs in response to DNA damage. Both HSFs and 55K<sup>+</sup>HSFs were treated with 1 μM CPT for 1 hour, followed by removal of the drug and incubation of the cells for another hour in normal media. Cells were harvested at the times indicated and cell lysates were fractioned using SDS-PAGE and blotted using the antibodies shown.

#### **4.2.12 HAd12-E1B55K associates with cellular chromatin.**

The images in Figure 4.7 clearly demonstrate that HAdV12-E1B55K is primarily nuclear. As a result, our objective was to determine if the viral protein was associated with cellular chromatin. 55K<sup>+</sup>HSFs and HAdV12-E1HER2 cells were fractionated as described in the materials and methods section and aliquots of each fraction were subjected to SDS-PAGE and western blotting. Figure 4.12 demonstrates that the nuclear fraction of the viral protein co-localises with the chromatin rather than the nucleoplasm. Additionally, a considerable amount of the viral protein was also present in the cytoplasmic fraction (Figure 4.12).



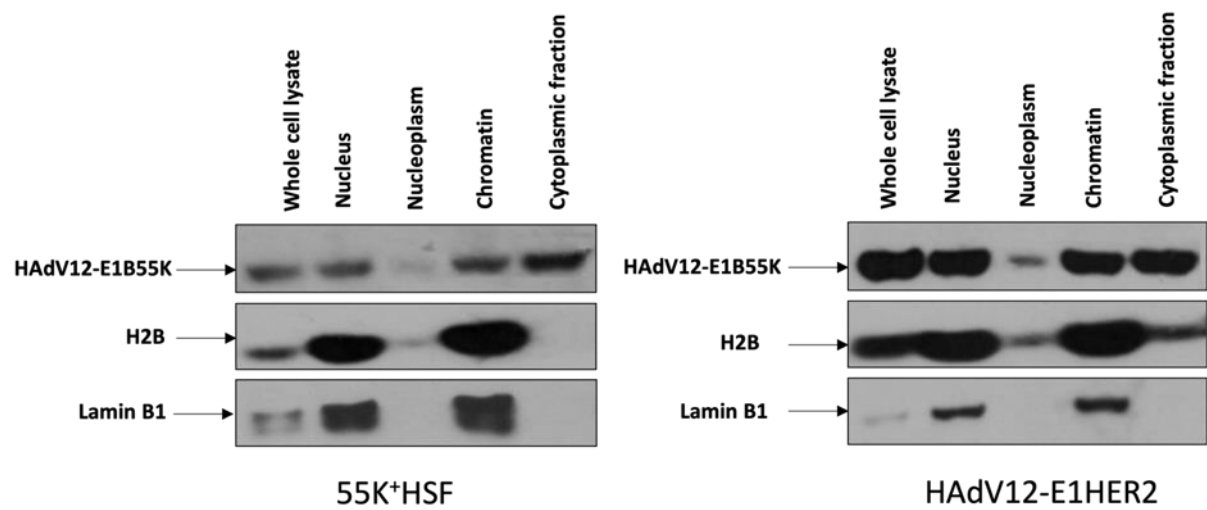
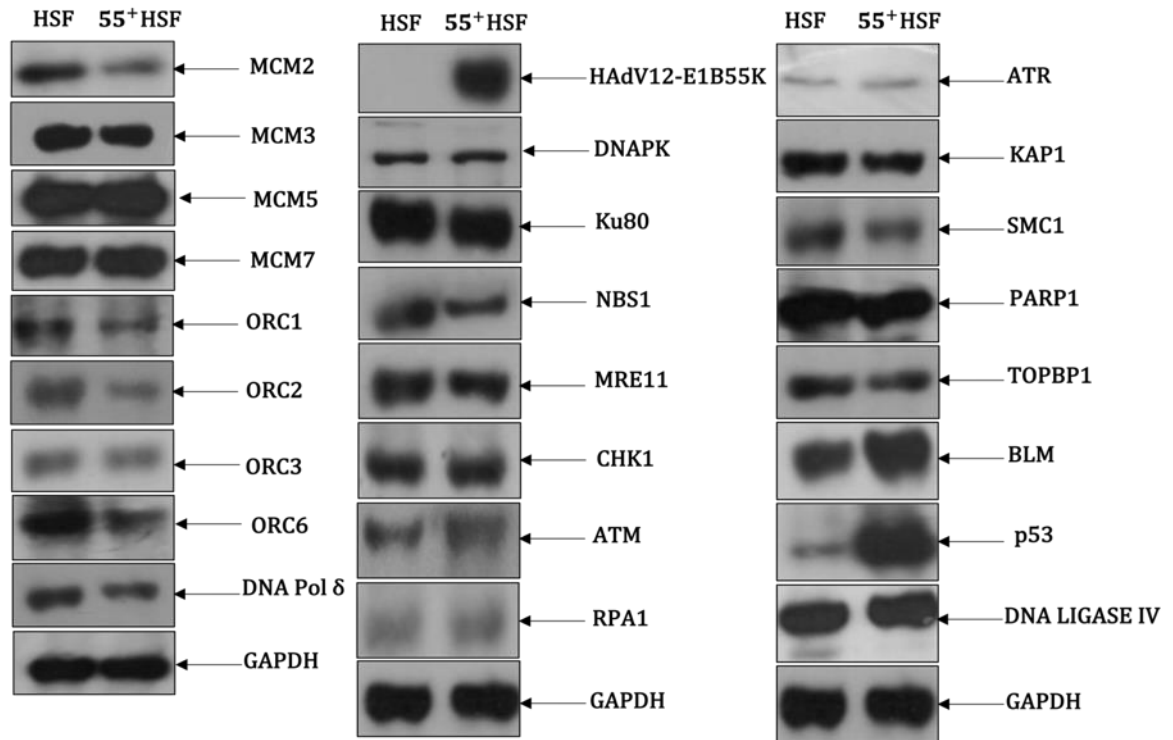


**Figure 4.12.** The nuclear fraction of HAdV12-E1B55K localises to the chromatin in 55K<sup>+</sup>HSFs and HAdV12-E1HER2 cells. Cells were harvested and treated in accordance with the procedures outlined in materials and methods. Western blotting was performed on fractions using the indicated antibodies. Other organelles were also included in the cytoplasmic fraction.

#### 4.2.13 HAd12-E1B55K affects the expression levels of proteins involved in DNA replication and DNA repair pathways.

Using a range of antibodies, samples of 55K<sup>+</sup>HSFs and parental HSFs were western blotted to determine if HAdV12-E1B55K affects the levels of expression of key proteins involved in DNA replication and repair pathways (Figure 4.13). As the experiment was not repeated three times, we only considered a 2-fold change to be significant. In 55K<sup>+</sup>HSFs, there was a large increase in p53's expression in comparison to control cells, yet it is presumed that it is transcriptionally inactive due to its interaction with HAdV12-E1B55K, as has been previously reported (Grand *et al.*, 1996). Additionally, the expression of replication-related proteins, such as ORC1, ORC2, and MCM2 was appreciably decreased in 55K<sup>+</sup>HSFs, with a 2-fold reduction. This could impact on DNA replication and possibly contribute to the differences we observed. Also, BLM and RPA expression in 55K<sup>+</sup>HSFs is increased, and this could be biologically significant. There are only minor changes observed in the expression levels of the other DDR proteins that were analysed between the two cell types. Reasons for the viral proteins' effects on different cellular proteins expression are not entirely clear at present.

**A**



**B**

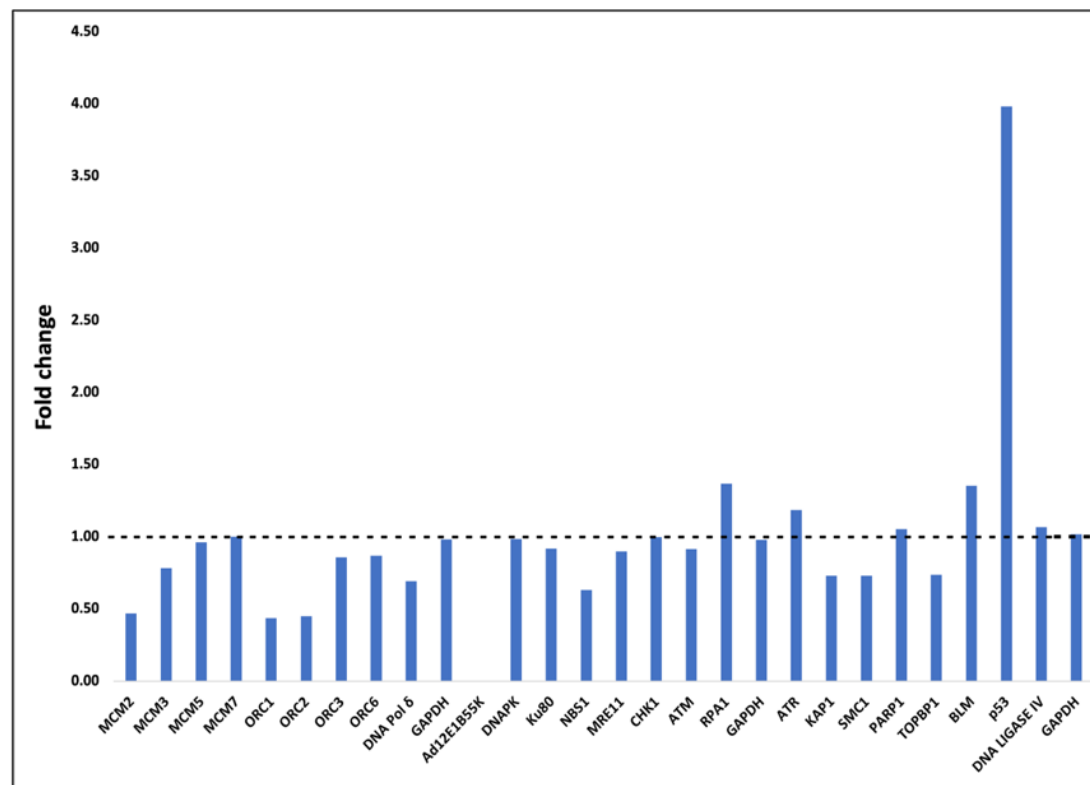


**Figure 4.13.** Comparative analysis of the expression of selected proteins in HSFs and 55K<sup>+</sup>HSFs.

After harvesting the cells, they were solubilised in a 9M urea solution, and the lysates were fractionated using SDS-PAGE. (A) Western blots of selected proteins using the antibodies shown. (B) Intensities of different proteins' bands were measured using ImageJ, and the ratio of relative protein densities of 55K<sup>+</sup>HSF to HSFs was blotted.

#### 4.2.14 Co-localisation of HadV12-E1B55K with cytoplasmic structures in 55K<sup>+</sup>HSFs.

It is interesting to note that in 55K<sup>+</sup>HSF cells, a portion of the HAdV12-E1B55K protein is seen as bright cytoplasmic staining 'tracks' that seem unaffected by DNA damage, as shown in the images provided in Figure 4.7, and in the original study (Gallimore *et al.*, 1997). We considered the possibility that some of the HAdV12-E1B55K binding proteins shown in (Figure 3.2B in chapter 3), may co-localise and interact with a fraction of the viral protein at these sites. However, co-staining of several of DDR proteins revealed that only MRE11 exhibited weak co-localisation with viral E1B55K tracks in some instances (marked with yellow arrows in the left upper hand section of Figure 4.14). None of the other binding partners in the 'tracks' were detectable except for NBS1, which occasionally seemed to form foci that co-localised with HadV12-E1B55K after IR treatment (marked with yellow arrows in the right upper hand section of Figure 4.14).



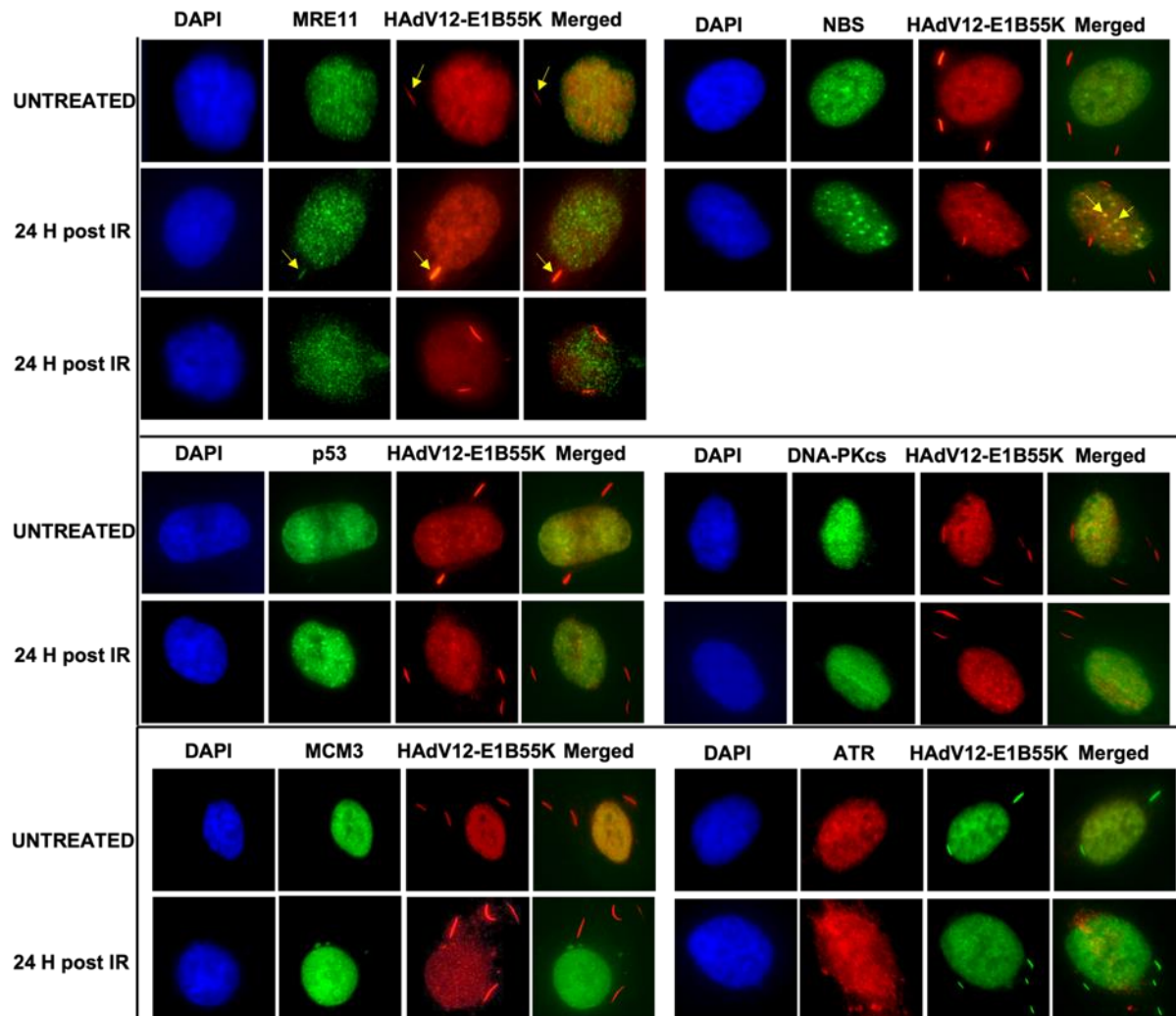


**Figure 4.14.** HAdV12-E1B55K co-localises with some DDR binding partners following DNA damage. 55K<sup>+</sup>HSFs were grown on glass coverslips over a period of 24 hours, followed by IR (3Gy) treatment or mock-treatment and fixation of cells. The antibodies that are indicated were used to stain the cells. In the images in the left upper hand side, the arrows show where HAdV12-E1B55K (red) and MRE11 (green) have localised within the cytoplasmic tracks. There is a possible co-localisation of NBS1 and HAdV12-E1B55K at DNA repair foci, as shown by the arrows in the set of images in the right top hand side.

#### 4.2.15 HAdV12-E1B55K does not form or co-localise to cytoplasmic aggresomes in HSFs.

The subcellular localisation of HAdV5-E1B55K has received a great amount of attention and research. It has been shown that when HAdV5-E1B55K is expressed in the absence of additional viral proteins, the majority of the protein may be found in the cytoplasm, while there is often juxtannuclear concentrations of the protein associated with structures identified as cellular aggresomes (Liu *et al.*, 2005). There is a variable but typically low level of the protein in the nucleus (Zantema, Fransen, *et al.*, 1985). When HAdV5-E1B55K is co-expressed with E4orf6, however, it migrates to the nucleus, where it becomes concentrated, although a sizeable portion remains associated with the cytoplasmic aggresomes (Goodrum, Shenk and Ornelles, 1996). In the case of HAdV12, E1B55K distributes throughout the cell with oval-shaped aggresome-like structures being apparent (Wienzek, Roth and Dobbstein, 2000; Zhao and Liao, 2003; Blanchette *et al.*, 2013). In the presence of E4orf6 again the protein becomes predominantly nuclear although some cytoplasmic protein is still present. However, even though the HAdV12-E4orf6 protein was present, the aggresome-like structures that contains HAdV12-E1B55K were still detectable in the nucleus and the cytoplasm (Blanchette *et al.*, 2013). This raises two important questions about the nature of the intracellular structures that include HAdV12-E1B55K. The first is that it has to be determined whether or not HAdV12 has a constant presence of E1B55K in aggresomes during infection. The second involves the make-up of these aggresomes-like structures that include E1B55K.

Important characteristics of aggresomes include their placement at, or close to microtubule organising centres (MTOC), as well as the need of retrograde transport for the completion of their construction (Johnston, Ward and Kopito, 1998; García-Mata *et al.*, 1999). Co-

immunofluorescence studies of E1B55K proteins with the MTOC marker  $\gamma$ -tubulin were performed in order to determine whether or not the localisation of E1B55K in aggresome structures is conserved in HAdV12-E1B55K expressing cells. In a previous study, H1299 cells were transfected with E1B55K-expressing plasmids. After fixation, cells were stained with anti-HA and anti  $\gamma$ -tubulin antibodies (Blanchette *et al.*, 2013).

In the original publication describing the 55K<sup>+</sup>HSFs, it was noted that some of the HAdV12-E1B55K localised to cytoplasmic structures which were termed 'cytoplasmic flecks' (Gallimore *et al.*, 1997). Similar structures have also been reported although no evidence for their origin or function has been presented (Zhao and Liao, 2003; Blanchette *et al.*, 2013; Cheng *et al.*, 2013). We considered that they resembled primary cilia which can be distinguished by staining for acetylated tubulin in co-localisation with SMO (Stiff *et al.*, 2016). However, it can be seen in Figure 4.15 that although the two structures appear similar, there is no co-localisation and, thus, we concluded that the cytoplasmic flecks are not primary cilia (Figure 4.15, row 4 and 5).

A further structure which has been associated with HAdV proteins are PML-NBs (Hoppe *et al.*, 2006; Wimmer *et al.*, 2010; Berscheminski *et al.*, 2013). Both HAdV5 and HAdV12 E1B55Ks localise to PML bodies in the nucleus to a limited extent (Blanchette *et al.*, 2013). Unfortunately, there was insufficient time to examine possible co-localisation of E1B55K with PML bodies in 55K<sup>+</sup>HSF cells.



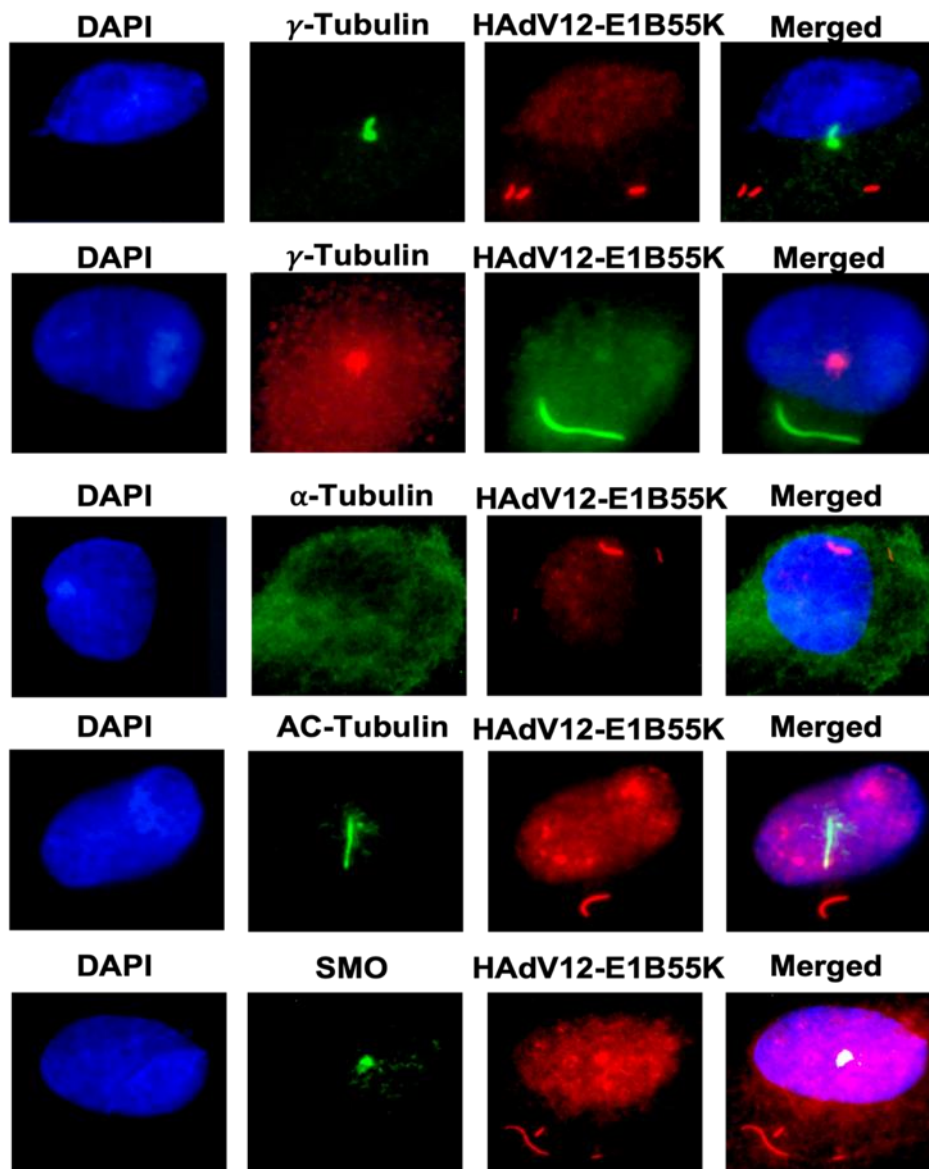


**Figure 4.15.** HAdV12-E1B55K does not co-localise with tubulins. 55K<sup>+</sup>HSFs were grown on glass coverslips over a period of 24 hours, followed by fixation of cells. Cells were stained with antibodies against  $\alpha$ -tubulin,  $\gamma$ -tubulin, acetylated (AC)-tubulin, SMO, and co-stained with HAdV12-E1B55K antibody as shown.

### 4.3 Discussion

It is already well known that during viral infection, group A and group C HAdVs target several important DDR components (reviewed in Blackford and Grand, 2009; Hidalgo *et al.*, 2019; Kleinberger, 2020). This has been shown to be accomplished, in the majority of instances, by ubiquitylation and proteasome-mediated degradation, which is triggered by a complex involving E1B55K, E4orf6, as well as cellular Cullins, Elongins, and Rbx1. However, we examined the possibility that, in the absence of E4orf6, the E1B55K protein may affect DDR pathways. Based on historical observations, it was determined that HAdV12-E1B55K caused non-random damage to chromosomes 1 and 17 at low viral concentrations and probably with no contribution from additional viral proteins (zur Hausen, 1967; McDougall, 1971a; Lindgren *et al.*, 1985; Schramayr *et al.*, 1990a; Gargano *et al.*, 1995; Li *et al.*, 1998; Liao, Yu and Weiner, 1999). It has also been shown that the combination of HAdV12 with DNA damaging agents results in a synergistic action that leads to the production of breaks (Caporossi, Bacchetti and Nicoletti, 1991). It is important to note that expression of E1B55K is necessary for HAdV12-mediated transformation of human cells in culture, in which it is plausible that inactivation or modification of the DDR might play a role (Byrd, Brown and Gallimore, 1982; Whittaker *et al.*, 1984). In this study we have used HSFs expressing HAdV12-E1B55K (55K<sup>+</sup>HSFs) and compared them to their parental cells to examine the relationship between the viral protein and the DDR (Gallimore *et al.*, 1997).

Genomic instability is triggered by HAdV12-E1B55K expression in HSFs, as shown by the increase in micronuclei numbers, both before and after treating the cells with DNA damaging agents (Figure 4.2). In agreement with previous observations (Stich, Van Hoosier and Trentin,

1964; zur Hausen, 1967; McDougall, 1970, 1971a; McDougall *et al.*, 1974), we also found an increased number of chromosomal anomalies in metaphase spreads produced from 55K<sup>+</sup>HSFs (Figure 4.3). Since treatment with HU significantly increases the number of micronuclei in 55K<sup>+</sup>HSFs in comparison to parental cells, we hypothesised that HAdV12-E1B55K may lead to DNA replication stress. Figure 4.4 shows that replication is inhibited by the viral protein in untreated cells, as shown by a significant increase of stalled forks, reduction in the efficiency of replication fork restart, and reduction in replication fork speeds. Both cell populations exhibited an equivalent increase of stalled forks and a comparable decrease in replication fork speeds after HU treatment, as might be expected. In contrast, parental HSFs were more efficient at fork restart than 55K<sup>+</sup>HSFs. Our findings imply that the HAdV12-E1B55K protein significantly affects DNA replication by promoting fork stalling and interfering with the process of fork restart, following induced DNA replication stress. These effects will probably contribute to genomic instability (as reviewed in, (Zeman and Cimprich, 2014; Wilhelm, Said and Naim, 2020)). It is possible that these effects are caused by the interactions between HAdV12-E1B55K and constituents of the replisome (ORC1, MCM3, MCM7, DNA polymerase, and cdc45) as discussed in more detail in Chapter 3.

HAdVs disrupt many elements of DSB repair pathways during viral infection by degrading and/or translocating MRN components, BLM, DNA Ligase IV, and TIP60 (Stracker, Carson and Weitzman, 2002; Baker *et al.*, 2007; Schwartz *et al.*, 2008; Orazio *et al.*, 2011; Gupta *et al.*, 2013). Cells were subjected to various genotoxic agents and the development of repair foci, and the phosphorylation of PI3K-related kinase substrates was observed in the two cell populations. This was done to determine if the HAdV12-E1B55K protein in isolation would also have an impact on the cellular response to DSBs. The increased phosphorylation of ATM

substrates in 55K<sup>+</sup>HSFs suggests the presence of defects with DNA damage repair and possibly the existence of extra damage related to checkpoint dysfunction (Figures 4.9 and Figure 4.11). At varying time points after induced DNA damage, 55K<sup>+</sup>HSFs were found to have more foci staining positive for  $\gamma$ H2AX, RAD51, and 53BP1 than control cells, again pointing to potential inefficiencies in DDR pathways and/or extra damage brought on by HAdV12-E1B55K (Figure 4.6). (The proportionate contributions of increasing damage and issues with repair may have been determined by a more in-depth investigation of DNA repair and resolution). Remarkably, a significant number of DNA repair foci were detectable in untreated 55K<sup>+</sup>HSF cells, adding credibility to the notion that HAdV12-E1B55K contributes to genomic instability even in the absence of exogenous DNA-damaging agents (Figures 4.2 and Figure 4.3).

To identify which DNA repair pathways were likely to be targeted, we looked at  $\gamma$ H2AX foci formation (in response to a low dose of IR) across the cell cycle using APH and distinguishing G<sub>1</sub> and G<sub>2</sub> cells using Mitosin staining (Figure 4.8). Up to 8 h, the formation of  $\gamma$ H2AX foci was comparable in both cell groups during G<sub>1</sub> phase of the cycle, where NHEJ is the primary repair mechanism; however, there were significantly more foci in 55K<sup>+</sup>HSFs during G<sub>2</sub> phase, where HR is the predominant DNA repair mechanism. The fact that there was a bigger difference between controls and 55K<sup>+</sup>HSFs in G<sub>1</sub> cells at 24 hours than in G<sub>2</sub> cells is likely due to a breakdown in the APH-induced cell cycle arrest (Figure 4.8). At 8 hours, on the other hand, there are many more foci in 55K<sup>+</sup>HSFs G<sub>2</sub> cells, which indicates that the cell cycle block is most likely present.

Examining the cell cycle following DNA damage in 55K<sup>+</sup>HSFs reveals that there is a possibility that the checkpoints have been disrupted (Figure 4.11). This is in line with the expectation

that HAdV12-E1B55K interacts directly with p53 to inactivate it (Yew and Berk, 1992; Grand *et al.*, 1996; Forrester *et al.*, 2011). If p53 is not transcriptionally active, the G<sub>1</sub>/S and G<sub>2</sub>/M checkpoints will not function appropriately. Therefore, if one or more checkpoints are disrupted, it is very probable that greater damage will be sustained to the DNA because of a particular treatment, which will result in the formation of more DNA repair foci and most likely an increased activation of ATM (Figures 4.6 and 4.9).

To study HAdV12-E1B55K further, we investigated the level of expression of numerous DDR proteins to rule out the idea that variations detected are due to protein degradation, since inactivation of Daxx during HAdV5 infection needs just E1B55K but not E4orf6 (Schreiner *et al.*, 2010). Since HAdV12-E1B55K seems to interfere with DNA replication, we looked at how it could alter the expression of some of the origin recognition complex (ORC) and the pre-replicative complex components (Figure 4.13). ORC protein expression was found to be distinct between the two cell groups, as was MCM2 expression, both of which might have an impact on DNA replication. Additionally, some DDR proteins, like BLM, have different levels of expression in the two cell groups. Furthermore, p53 is substantially overexpressed in 55K<sup>+</sup>HSFs; nonetheless, it is probable that it is transcriptionally inactive, as was previously addressed (Figure 4.13) (Yew and Berk, 1992; Grand *et al.*, 1996). We reasoned that the observed differences in the expressions of DDR proteins were probably insufficient to account for the obvious distinctions in characteristics that were found between the two cell groups, although this suggestion would need to be verified by more research. In addition, the implications of having high levels of transcriptionally inactive p53 are not entirely understood (Grand *et al.*, 1996). It is likely, however, that the appreciable differences seen in the levels of

replisome components could be, at least in part, responsible for differences seen in DNA replication.

We have investigated the subcellular localisation of E1B55K in 55K<sup>+</sup>HSFs. Even though most of the protein is found in the nucleus with much of it bound to chromatin, a sizeable portion of it may also be found in the cytoplasm in the form of 'tracks' (Figure 4.7B and Figure 4.14). In earlier research on HAdV5, it was shown that E1B55K was present in large cytoplasmic juxtanuclear aggresomes in cells that had been transformed by HAdV5-E1 region (Zantema, Fransen, *et al.*, 1985; Araujo *et al.*, 2005; Liu *et al.*, 2005). Both p53 and the MRN complex were present in the aggresomes. Similar aggresomes are formed during an infection with HAdV5, and these contain HAdV5-E4orf3 and/or orf6 in association with E1B55K. It is believed that these are the location where MRN degradation occurs (Araujo *et al.*, 2005; Liu *et al.*, 2005). Because of their position and general appearance, we do not believe that the 'tracks' or 'Flecks' seen in 55K<sup>+</sup>HSFs represent aggresomal structures. In addition, we were unable to find any evidence of p53 co-localising with any of these structures (Figure 4.14). We currently have no more information on their origin or composition.

In a further investigation, we attempted to determine whether HAdV12-E1B55K nuclear tracks seen in Figure 4.7 and Figure 4.14, are aggresomal bodies that are formed in 55K<sup>+</sup>HSFs (since they share a resemblance in shape). No co-localisation was seen between any proportion of the viral protein tracks and  $\gamma$ -tubulin in 55K<sup>+</sup>HSFs. This was also the case in a previous study that examined HAdV12-E1B55K's ability to form cytoplasmic aggresomes in H1299 cells (Blanchette *et al.*, 2013). According to the findings of that study, the process of forming an aggresome is not conserved in HAdV12 and the oval-shaped aggresome-like structures

(Flecks) stained with HAdV12-E1B55K do not display the recognised properties of aggresomes, and in fact, those structures do not develop close to MTOC in the case of HAdV12 infection, nor they are necessarily close to the nucleus. Furthermore, the addition of nocodazole, which should prevent MTOC formation and the creation of aggresomes, did not result in the disruption of the formation of these structures (Blanchette *et al.*, 2013). Therefore, after conducting our investigation here, we still do not know what these structures are yet, this needs further investigation in the future.

Due to the absence of E4orf6 and, therefore, the fact that the target proteins will not be ubiquitinated as may occur during HAdV12 infection, the effects of E1B55K on host cell pathways as detailed above may not be particularly relevant to viral infection. It has not yet been determined whether this would lead to proteasome-mediated degradation (Herrmann *et al.*, 2020). On the other hand, it is very probable that interference with DNA replication, an increase in the development of R-loops, and disruption of the DDR will all combine to render cellular transformation and tumour formation more probable when HAdV12-E1 is present. The interaction of HAdV2/HAdV5 or HAdV12-E1B55K with p53 is well known to block its transcriptional activities, which is thought to be important for successful transformation (Löber, Lenz-Stöppler and Döbelstein, 2002). However, in addition to its interaction with p53, E1B55K has been shown to have additional characteristics that lead to the transformation of rodent cells by HAdV-E1 (Löber, Lenz-Stöppler and Döbelstein, 2002; Sieber and Dobner, 2007; Härtl *et al.*, 2008; Ip and Dobner, 2019). It was hypothesised that the viral protein's capability of forming multi-protein complexes, as well as associating with the MRN complex might be characteristics that support the transformation process (Härtl *et al.*, 2008). However, in that investigation it was not determined if E1B55K proteins generated any of the DNA

replication or DDR effects described here. In spite of multiple impacts of HAdV-E1B55K on host cells, it is not possible for it to transform mammalian cells on its own; HAdV-E1A is required for the transformation process, even in rodent cells (Houweling, Van Den Elsen and Van Der Eb, 1980; Van Den Elsen, Houweling and Van Der Eb, 1983). Transformants are generated infrequently when HAdV-E1A is expressed alone, suggesting that an extra mutational event inside the cells is necessary for cellular immortalisation (Houweling, Van Den Elsen and Van Der Eb, 1980; Gallimore *et al.*, 1985).

While previous studies gave insight on the characteristics of HAdV12-E1B55K, it is unclear whether those findings extend to E1B55K from other HAdV types. Moreover, the situation is, of course, different during viral infection when E4orf6 is present, constituting the E3 ligase. In HAdV-infected cells, the association between HAdV5-E1B55K and constituents of the MRN complex, as well as other proteins involved in DSB repair, has been comprehensively analysed; however, the degree to which the protein itself influences the DDR is considerably less well characterised. HAdV12 and HAdV5 E1B55Ks would be assumed to have many of the same features, due to the fact that infection of human cells by both viruses leads to degradation of many of the same DDR components. However, this is not the case with HAdVs from groups B, D, E, and F (Cheng *et al.*, 2011; Forrester *et al.*, 2011). Moreover, even though HAdV5 and HAdV12 share just approximately 50% homology, it's probable that they each have their own distinct properties, one of which may be the tendency of HAdV12-E1B55K to promote genomic instability. The HAdV variant of the E1B55K protein has been shown to be the determining factor in E1-mediated tumour development in athymic nude mice, as demonstrated by the fact that HAdV5-E1A/HAdV12-E1B transformed rat cells were just as oncogenic as HAdV12-E1A/HAdV12-E1B transformed cells, whereas HAdV5-E1A/HAdV5-



E1B55K transformed cells were noticeably less oncogenic (Bernards *et al.*, 1982; Bernards, Schrier, Bos, *et al.*, 1983). Interestingly, group B HAdVs can induce tumours but to a lesser extent than group A (Javier *et al.*, 1991). It is, therefore, interesting to investigate the characteristics of E1B55K from group B HAdVs and compare them to the ones from group A, which is done in a part of Chapter 5 of this research.

In conclusion, proteins known to bind with E1B55K but not examined here likely contribute to some of the reported effects in this research (some of these interactions are analysed in Chapter 3); since the E1B55K interactome is substantially larger than the DDR (reviewed in (Hidalgo *et al.*, 2019)). However, it is likely that the effects of HAdV12-E1B55K on DNA replication and its interference with HR, as well as possible additional DNA repair processes, might account for the genomic instability initially observed in human cells exposed to this viral protein.

# **CHAPTER 5**

**The effects of group B, D, E and F  
adenovirus early region 1B55K  
proteins (HAdV-E1B55K) on cellular  
genome stability and the DNA damage  
response**

## 5.1 Introduction

Most previous scientific investigations on HAdVs have concentrated on viral members of group C (HAdV5 and to a lesser extent HAdV2) and group A (HAdV12), whereas studies on the more numerous groups B and D viruses have been much less frequent and relatively limited. In this chapter we have investigated properties of the E1B55K protein from representatives of groups B, D, E and F HAdVs in the context of host DDR and induction of cell genome stability. We have already shown that HAdV12-E1B55K can induce genome instability in human fibroblasts in the absence of any other viral proteins (See Chapter 4). We have determined that this is likely to be due to its impact on DNA replication and DNA repair pathways, probably through direct interaction with multiple cellular targets. In this chapter we examined whether E1B55K proteins from groups B, D, E and F HAdVs have comparable effects.

Since host cell proteins may act as barriers to infection, viruses have had to develop ways to circumvent these natural defences. Previous research has shown that the DDR response can halt HAdV DNA replication, late protein synthesis, and viral progeny production; it has been proposed that the MRN complex can interrupt viral replication, either directly or indirectly via downstream DDR effectors in different HAdV types (Evans and Hearing, 2005; Mathew and Bridge, 2007; Shah and O'Shea, 2015; Pancholi and Weitzman, 2018). Additionally, it has been shown that different HAdV types interact with MRN and other DDR proteins in distinct ways (Stracker *et al.*, 2005; Cheng *et al.*, 2011, 2013; Forrester *et al.*, 2011; Blanchette *et al.*, 2013). In this chapter, we analysed the effect of E1B55K on the activation of host DDR pathways, the induction of host genome instability, and the effect of the viral protein on DSB repair. We used HA-tagged E1B55K constructs from representative members of groups B, D, E and F HAdVs.

We have examined if the HAdV-E1B55K proteins induce genomic instability in HeLa cells and how their presence impacts on the ability of the cells to respond to DNA damaging agents in the absence of any other viral proteins. The effect these constructs have on HR repair activity was also studied by analysing DNA damage repair focus formation, both before and after introducing DNA damaging agents.

Most previous studies performed on E1B55K from different representative HAdV types have concentrated largely on its roles in the context of infection, while in collaboration with E4orf6 and functioning as a component of the E3 ubiquitin ligase complex (Cheng *et al.*, 2011, 2013; Forrester *et al.*, 2011; Blanchette *et al.*, 2013). In this chapter, we aimed to characterise the unique roles of E1B55K linked to the DDR but distinct from its E3 ligase activities to allow a comparison with the data presented in Chapter 4 on HAdV12.

For this study we have used HeLa cells. They suffer from obvious disadvantages, in that they have been in culture since the 1950s and, as such, they have almost certainly accumulated several mutations in different DDR components. In addition, it is well known that HeLa cells express the HPV18-E6 protein which is able to bind directly to and degrade p300 (Patel *et al.*, 1999; Zimmermann *et al.*, 1999; Thomas and Chiang, 2005). Furthermore, HeLa cells have reduced levels of p53 due to the action of the E6 protein. Nonetheless, they have proven to be reliable for use in HAdV research and in medical research generally; they have been used up to this day, even in Covid-19 research, despite having many mutations in their genome (Zhou *et al.*, 2020).

Through proteomic analysis, an increasing number of novel HAdV targets have been recognised among the DDR pathway members. Significantly, by using Mass Spectrometry

(MS), our lab identified the E3 ubiquitin-protein ligase 5 (UBR5) as a novel E1B55K-binding protein in groups B, D, E and F HAdVs. The protein had been shown to bind HAdV5-E1B55K previously (Hung and Flint, 2017) and, therefore, in this chapter we were interested to investigate its roles in more depth. UBR5 is an E3 ubiquitin-protein ligase that recognises and binds cellular proteins bearing certain N-terminal residues, such as CDK9, which ultimately results in their ubiquitination and eventual degradation. As such, by polyubiquitinating CDK9, UBR5 also regulates mRNA transcription, cell cycle progression, and functions as a tumour suppressor (Cojocaru *et al.*, 2011). It is also involved in the DDR by regulating TOPBP1, as well as, protecting against the uncontrolled proliferation of ubiquitinated chromatin at damaged chromosomes by suppressing the activity of RNF168; an E3 ubiquitin-protein ligase that promotes the accumulation of K-63'-linked histone H2A and H2AX at DNA damage sites (Gudjonsson *et al.*, 2012).

Data presented in this chapter also shows that the expression of E1B55K protein from groups B, D, E and F HAdVs increased the genomic instability in human tumour cells, seen as an increase in the number of cellular micronuclei formation. Also, we have shown that the viral protein from these HAdV types associates with several HR repair components, although with a limited effect seen in the phosphorylation of these components, with the exception of  $\gamma$ H2AX which might likely implicate a major effect on other DDR pathways. Additionally, we have shown that HAdV-E1B55K from group B, D, E and F inhibits DSBs repair as seen by the increased foci formation after induced DNA damage. We have also identified a plethora of novel E1B55K-interacting cellular substrates that bind the viral protein in these viral groups, although the significance and reliability of most of these observed interactions is yet to be determined.

## 5.2 Results

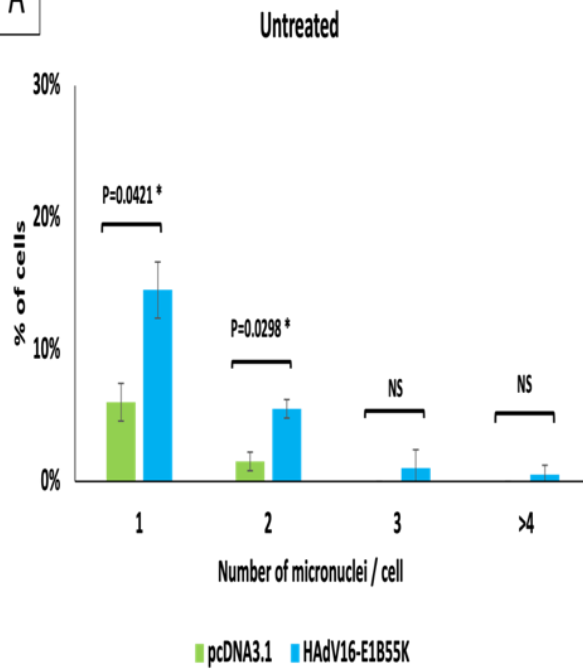
### 5.2.1 E1B55K from group B, D, E and F HAdV types causes genome instability in human tumour cells.

Previous studies on HAdVs only examined the roles of HAdV12 (group A) and HAdV5 (group C) infections in inducing chromosomal aberrations in human cells, with HAdV12 causing non-random damage and breaks in chromosomes 1 and 17 (zur Hausen, 1967; McDougall, 1971b), whilst, infection with HAdV5 resulted in widespread random chromosomal damage (Caporossi and Bacchetti, 1990; Caporossi, Bacchetti and Nicoletti, 1991). To the best of our knowledge, no cytogenetic studies have described the impacts of E1B55Ks from other HAdV types on genomic stability.

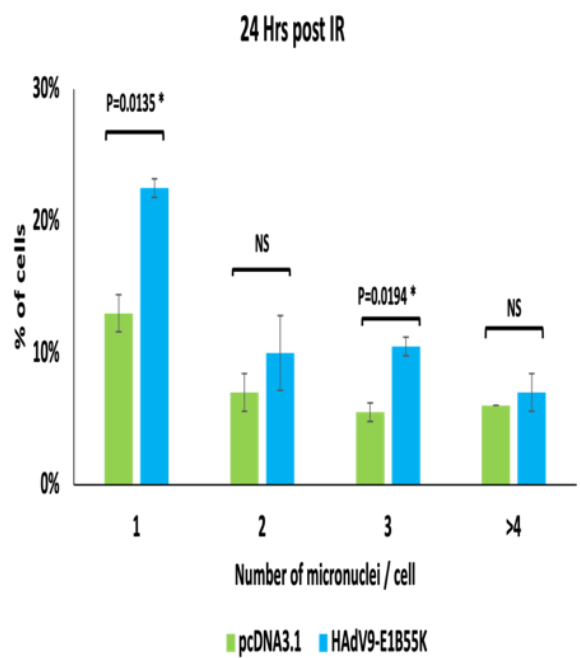
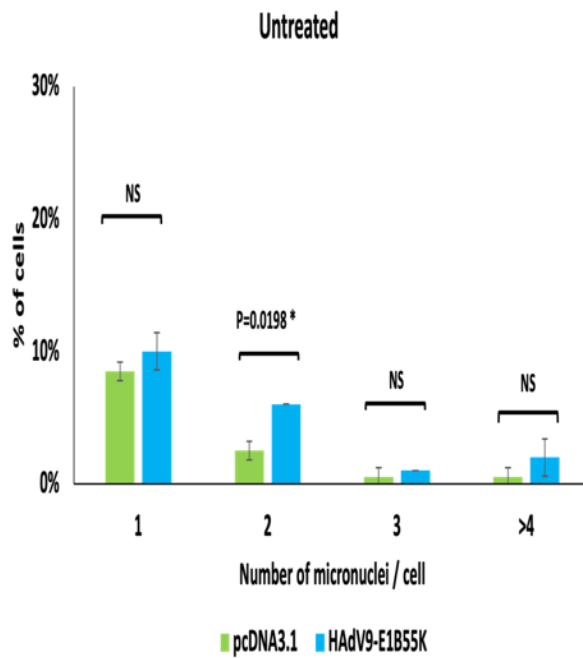
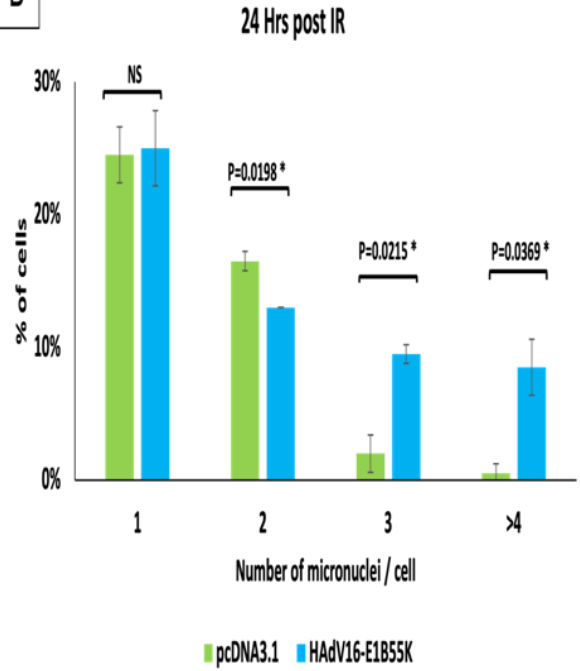
To obtain a better indication of how E1B55K from representative HAdVs affects the stability of the cellular genome, the number of micronuclei in normally dividing HeLa cells and E1B55K-transfected HeLa cells was counted (Figure 5.1A). Additionally, micronuclei were counted 24 hours after cells were exposed to IR (Figure 5.1B). In undamaged control HeLa cells, up to 10% usually contained micronuclei; however, the proportion significantly increases in cells transfected with E1B55K constructs without induced DNA damage (Figure 5.1A). The micronuclei grouped closely to the DAPI-stained nucleus and tended to be around the same size in both cell populations, even though there were some micronuclei that were much larger than others (Figure 5.1C). In all cell populations, micronuclei levels increased significantly after IR-induced DNA damage, with cells transfected with each viral protein having more than 3 micronuclei per cell (Figure 5.1B). Indeed, this indicates that E1B55K from groups B, D, E, and

F HAdVs interferes with the cellular response to DNA damage in a manner that is completely distinct from its well-characterised capacity to degrade DDR proteins with E4orf6.

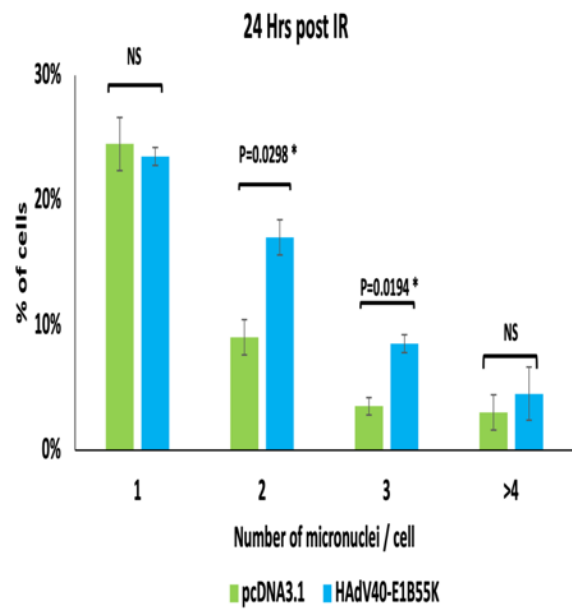
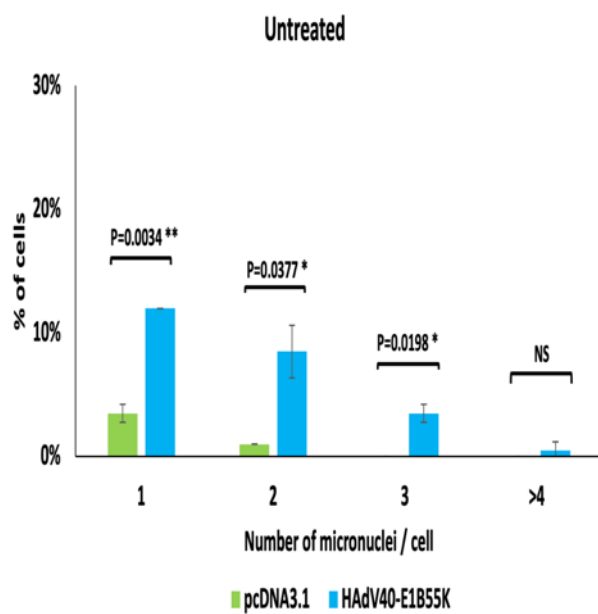
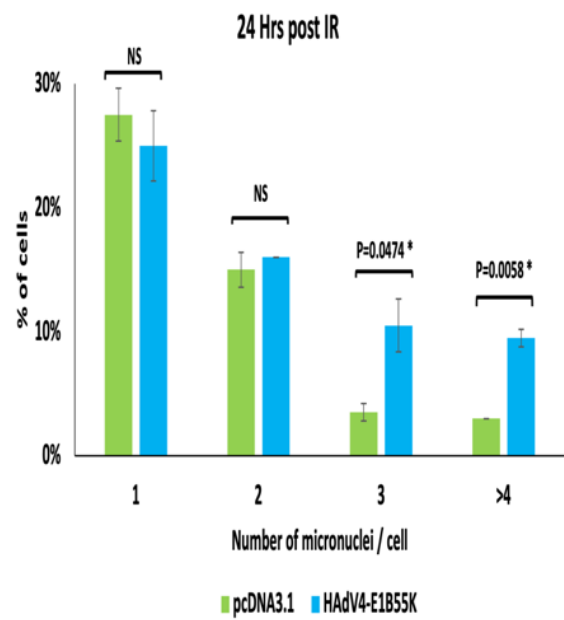
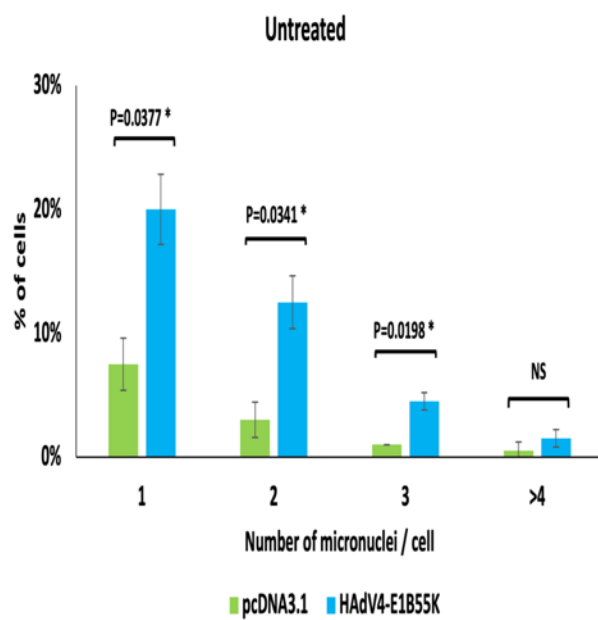
A



B







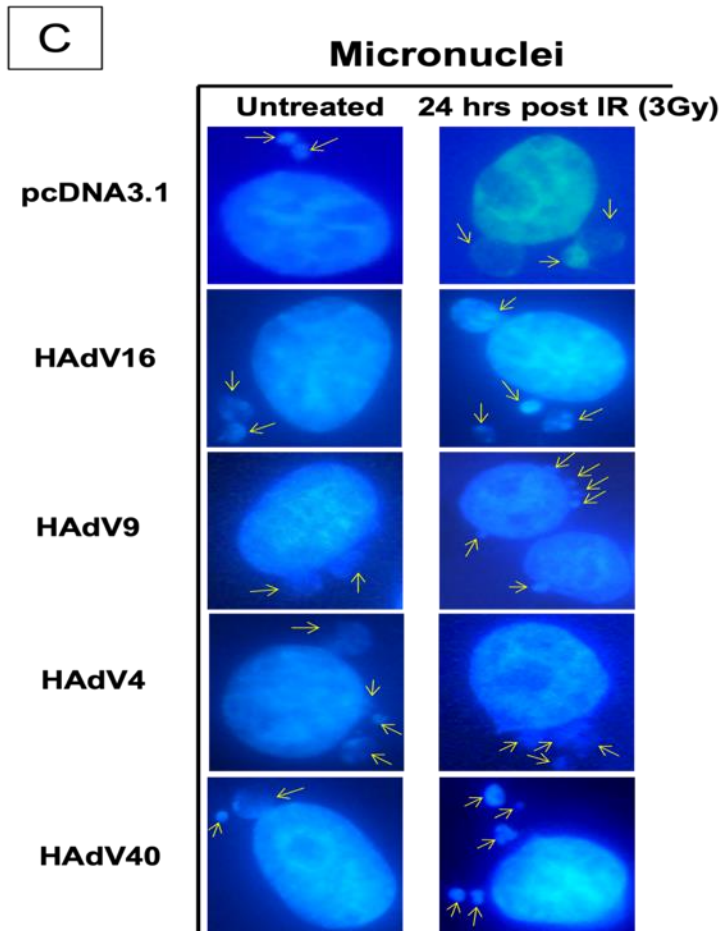
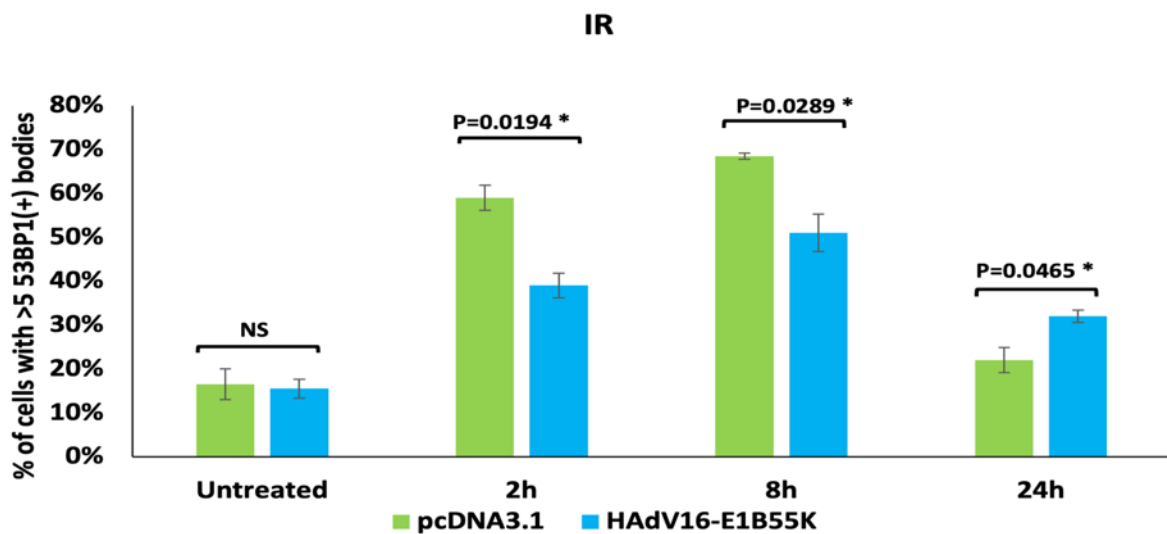
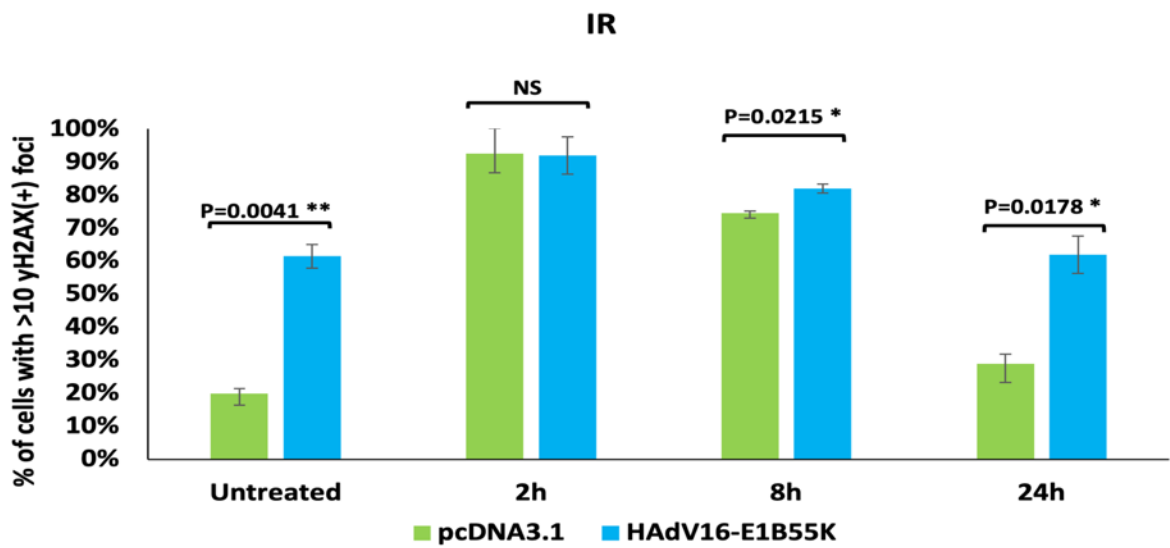
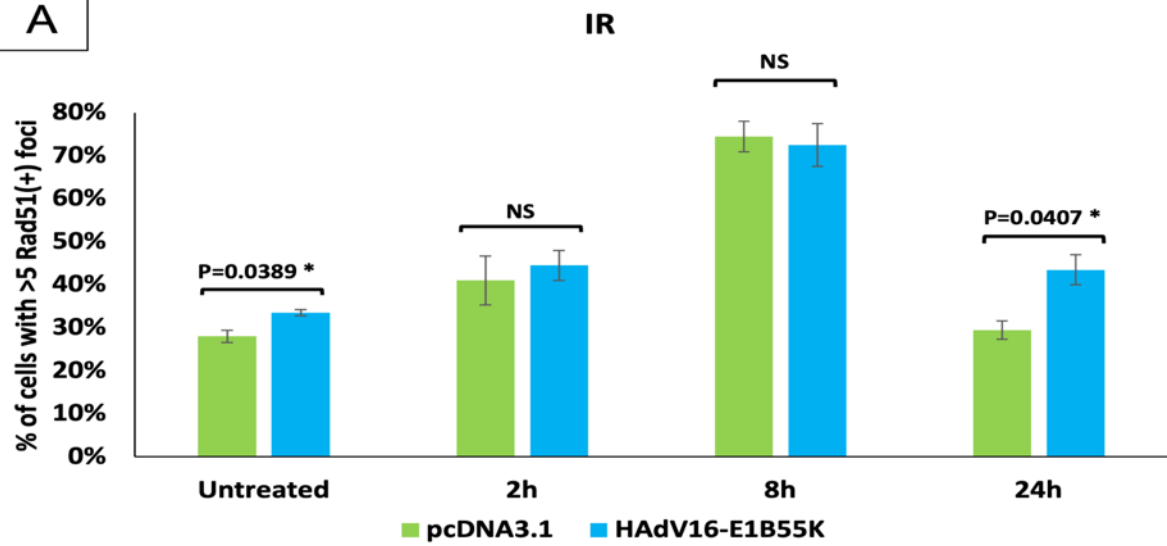


**Figure 5.1.** Micronuclei formation in the presence of HAdVs 16, 9, 4 and 40 E1B55K proteins. HeLa cells were transfected with constructs encoding E1B55K from HAdV16 (group B), HAdV9 (group D), HAdV4 (group E) and HAdV40 (group F), as well as pcDNA3.1 as a control. After 48 hours, cells were fixed, and DNA stained with DAPI. (A) Number of micronuclei per cell in untreated cells. (B) Number of micronuclei per cell after 24 hours of irradiation with IR (3Gy). (C) Representative images showing DNA staining of cells with DAPI, arrows indicate micronuclei. (n=3 independent experiments, >100 cells were counted for each replicant). Mean  $\pm$  SD, \*p < 0.05, NS, not significant.

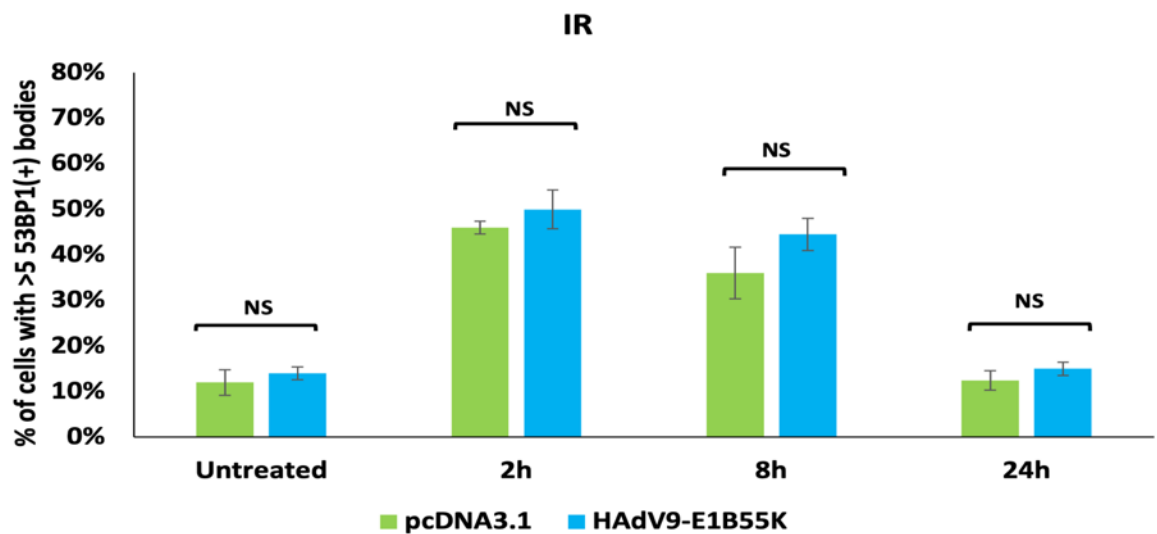
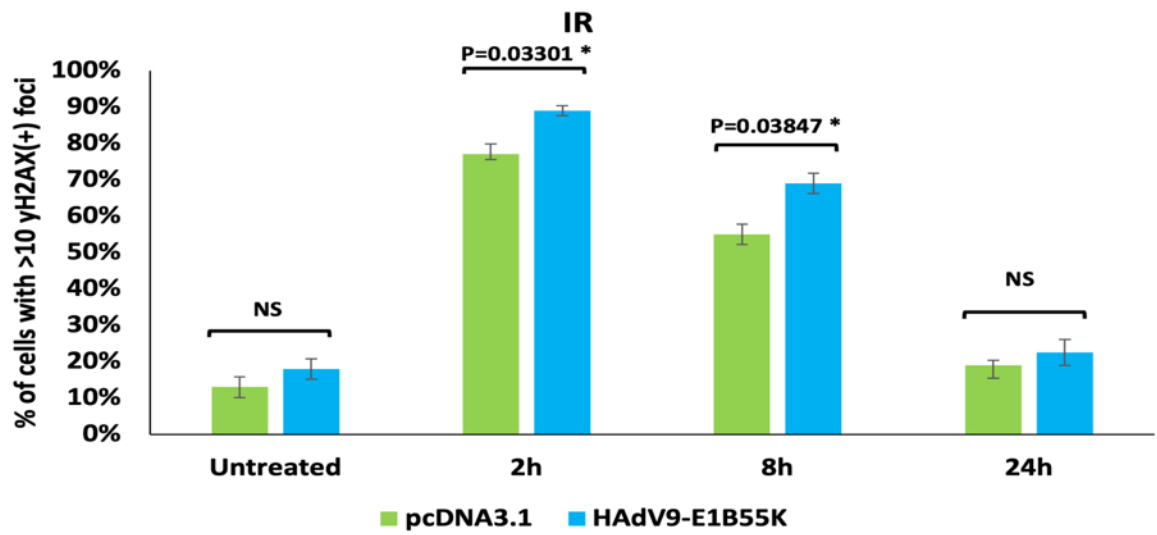
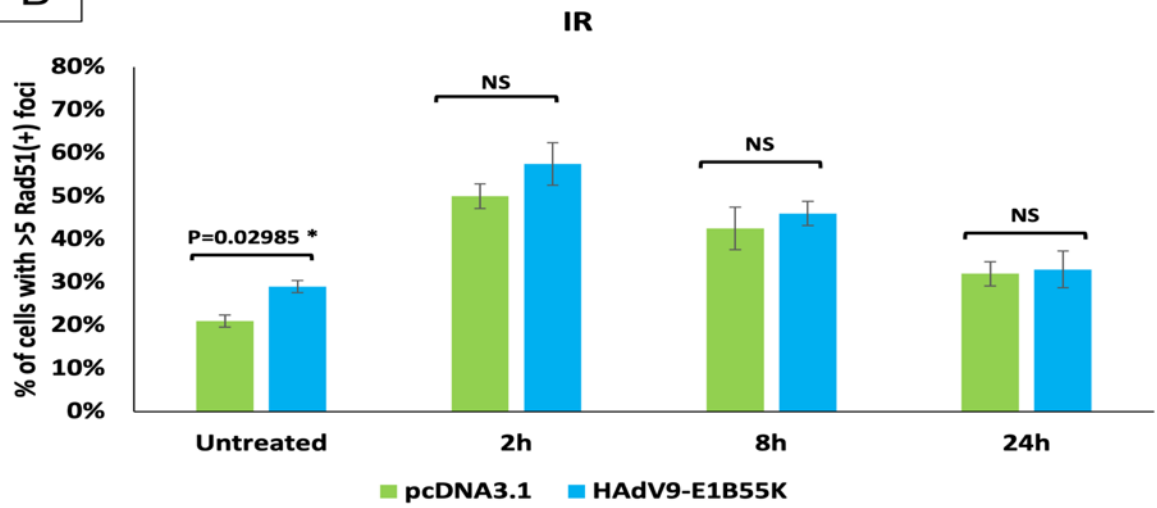
### 5.2.2 E1B55K from group B, D, E and F HAdV types affects DNA repair foci formation in HeLa cells after DNA damage.

To understand the effect of E1B55K protein from groups B (HAdV16), D (HAdV9), E (HAdV4) and F (HAdV40) HAdVs on the DDR, we exposed normally dividing transfected HeLa cells to IR (3Gy) and examined DNA damage repair foci formation over a 24-hour time course, looking at recruitment of RAD51, 53BP1 and  $\gamma$ H2AX foci. Results showed an overall increase in DNA repair foci formation in all cells expressing E1B55K constructs in comparison to the normal HeLa cells, with appreciably more foci being seen in transfected cells, both before treatment and at later time points (Figure 5.2A-D). However, in some cases (HAdV16 and HAdV4) we have seen less 53BP1 bodies formation at 2 and 8 hours after cell irradiation in comparison to controls. The 53BP1 nuclear bodies are generally considered to accumulate at sites of DNA damage as a result of replication stress (Lukas *et al.*, 2011), which suggests that the viral proteins, in the case of HAdV4 and HAdV16, may protect against replication stress. This obviously needs further investigation. These results indicate either an increase in DNA damage in cells transfected with the viral protein or an inhibition of the cell's ability to repair damaged DNA. Foci stained for RAD51, 53BP1 and  $\gamma$ H2AX in all cell populations are shown (Figure 5.2E).

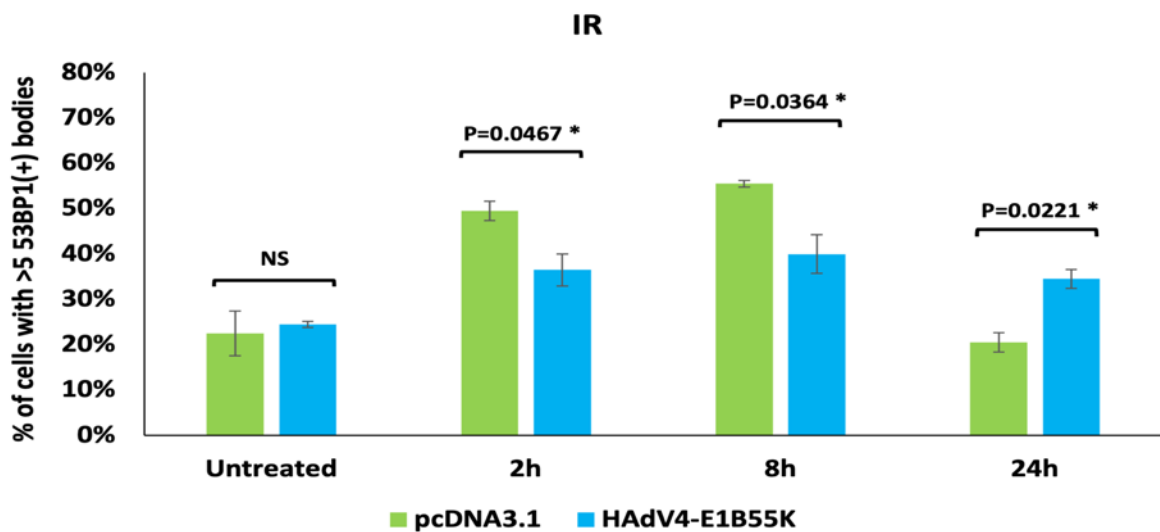
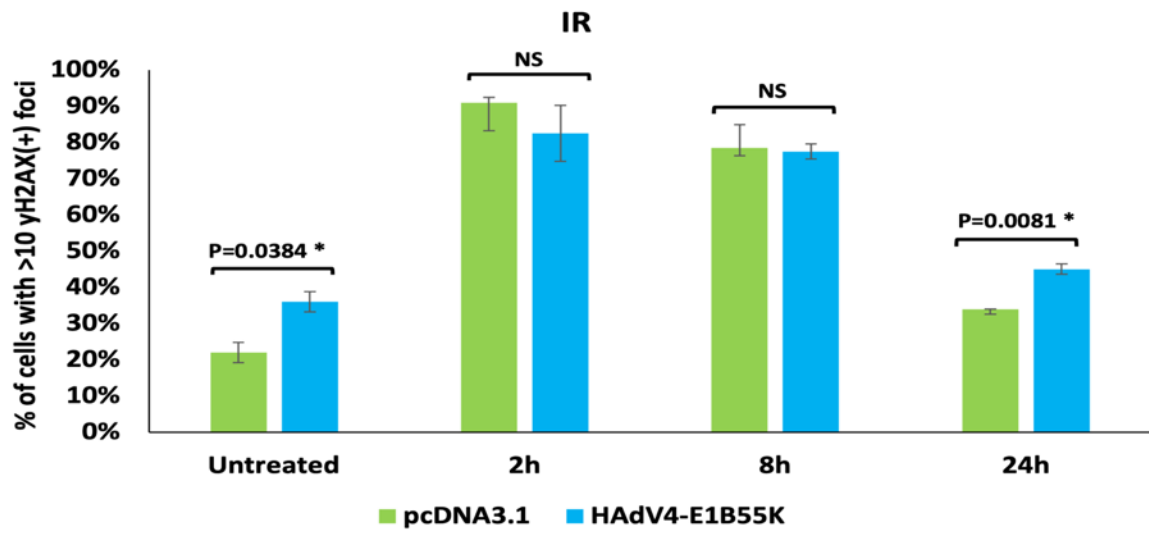
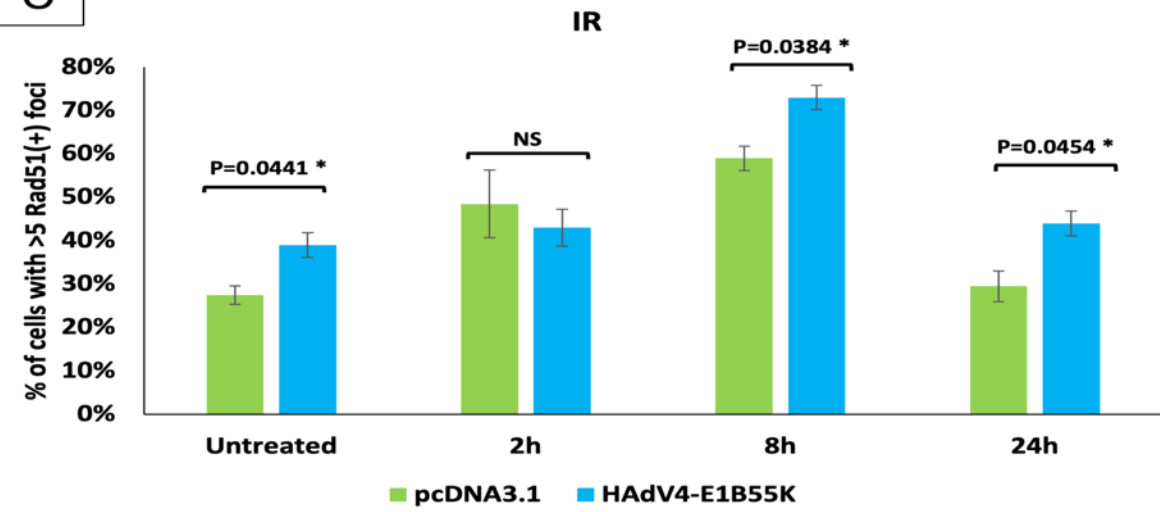
A

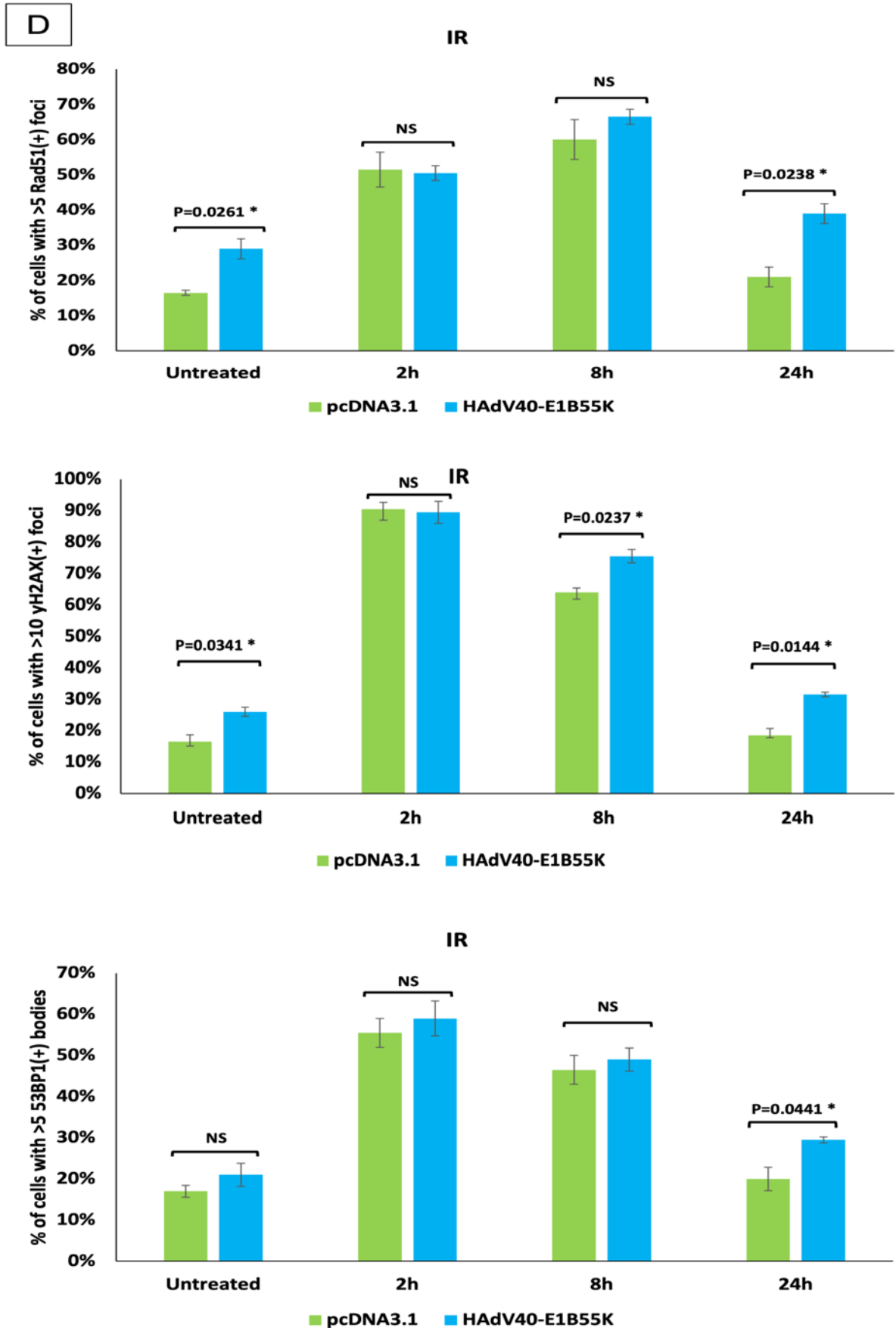


B



C





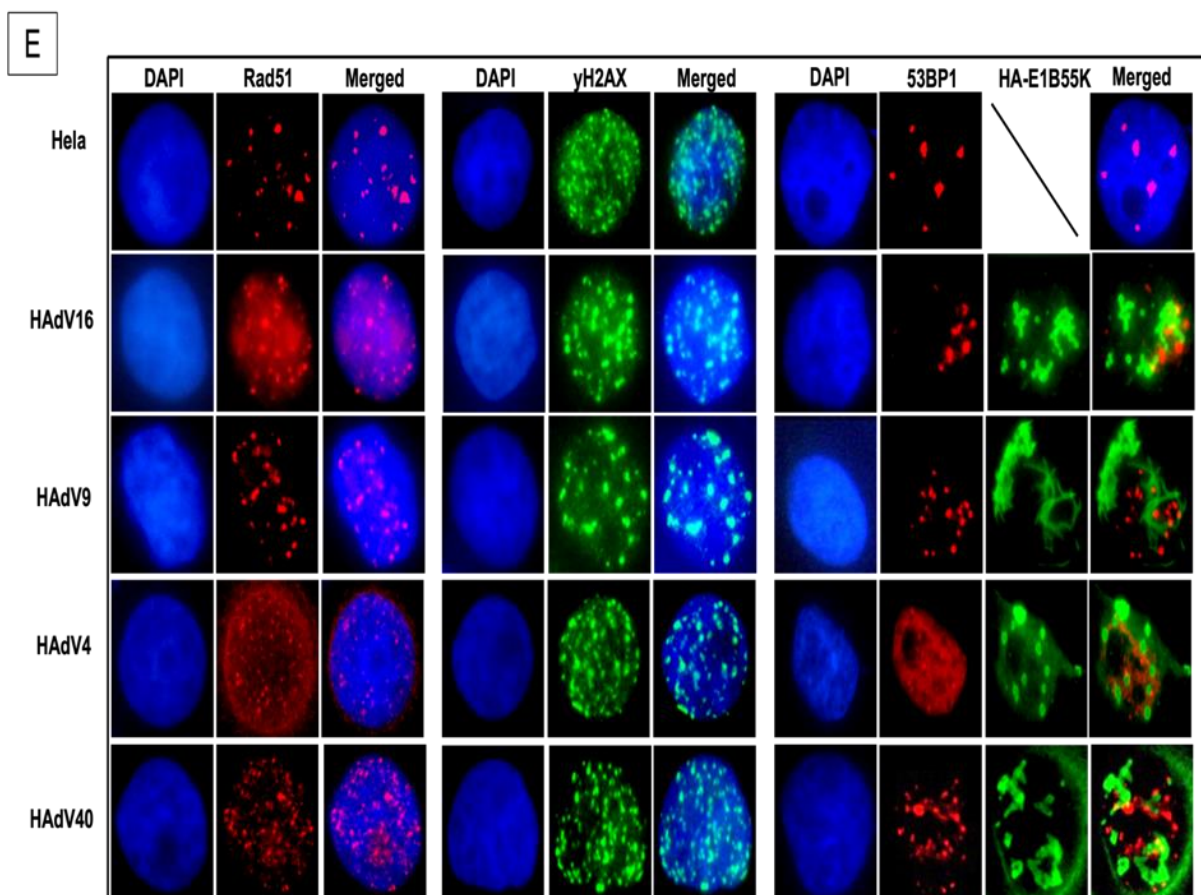


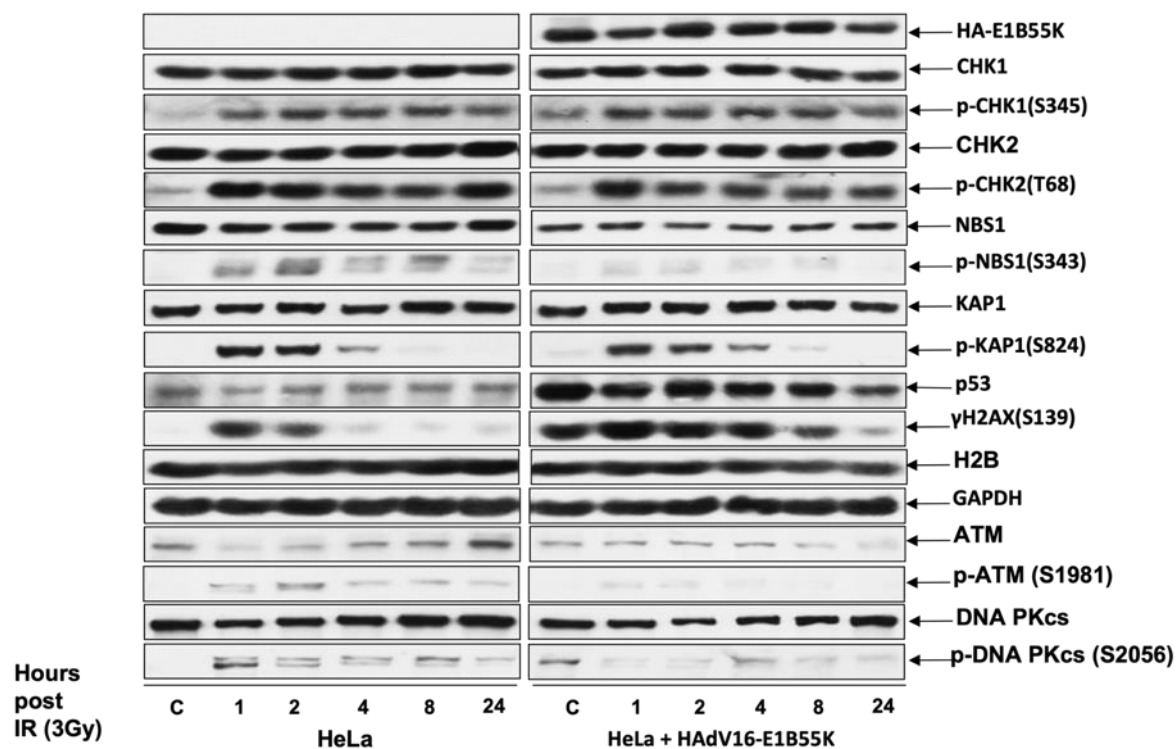
**Figure 5.2.** DNA repair focus formation is influenced by the expression of E1B55K from group B, D, E and F HAdVs. HeLa cells were transfected with constructs encoding E1B55K from HAdVs 16 (group B), 9 (group D), 4 (group E) and 40 (group F), as well as pcDNA3.1 as a control. After 24 hours cells were irradiated with IR (3Gy) and then fixed after increasing times. RAD51,  $\gamma$ H2AX and 53BP1 foci were counted. Percentages of DNA repair foci are shown; (A) HAdV16, (B) HAdV9, (C) HAdV4, and (D) HAdV40. (E) Representative example images of stained repair foci in transfected cells with pcDNA3.1, and with HAdV-E1B55Ks from group B, D, E and F HAdV types. (n=3 independent experiments, >100 cells were counted for each treatment per replicant for each cell strain at each time point). Mean  $\pm$  SD, \*  $p < 0.05$ , \*\*  $p < 0.01$ , NS, not significant.



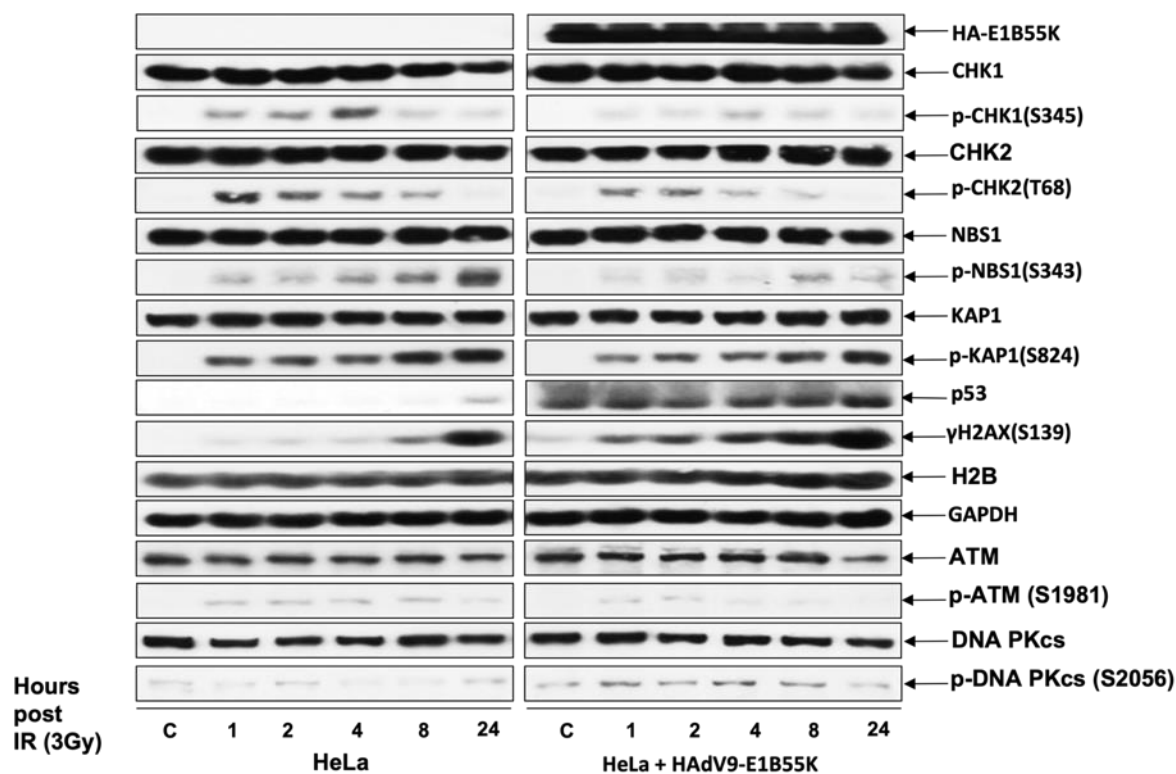
### 5.2.3 E1B55K from group B, D, E and F HAdV types has a limited effect on double strand break repair pathways.

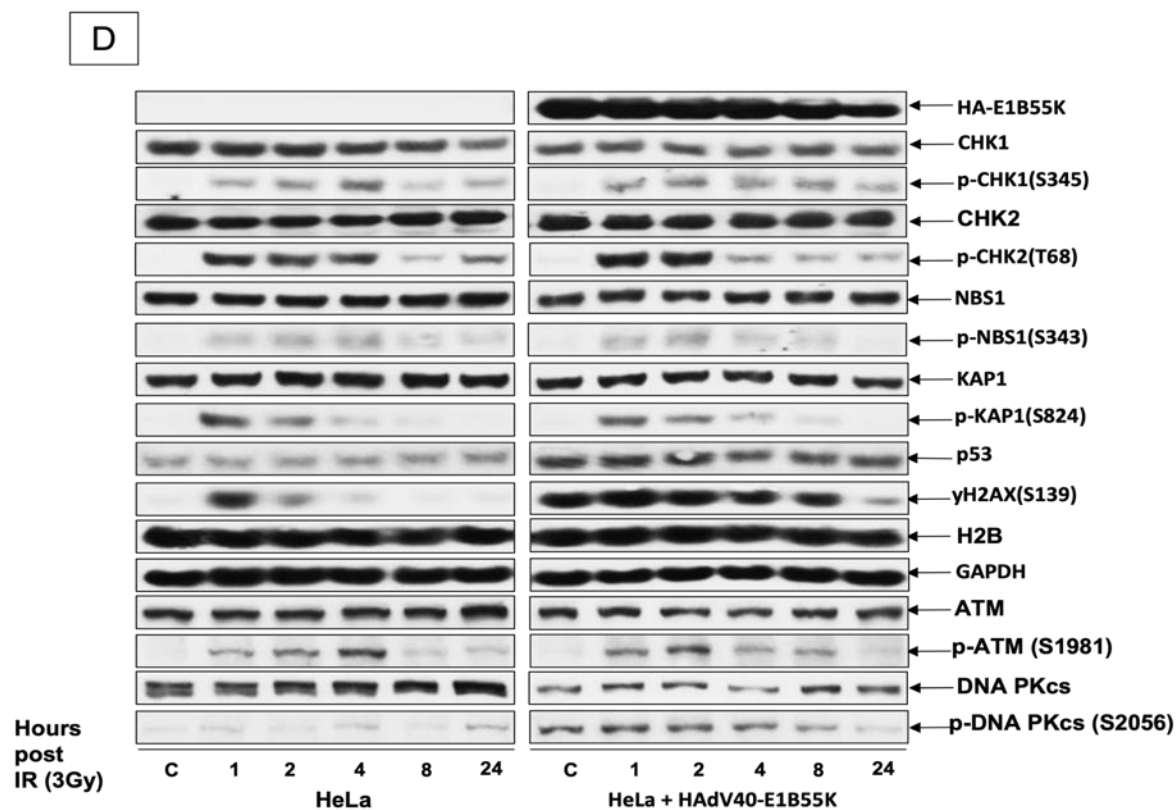
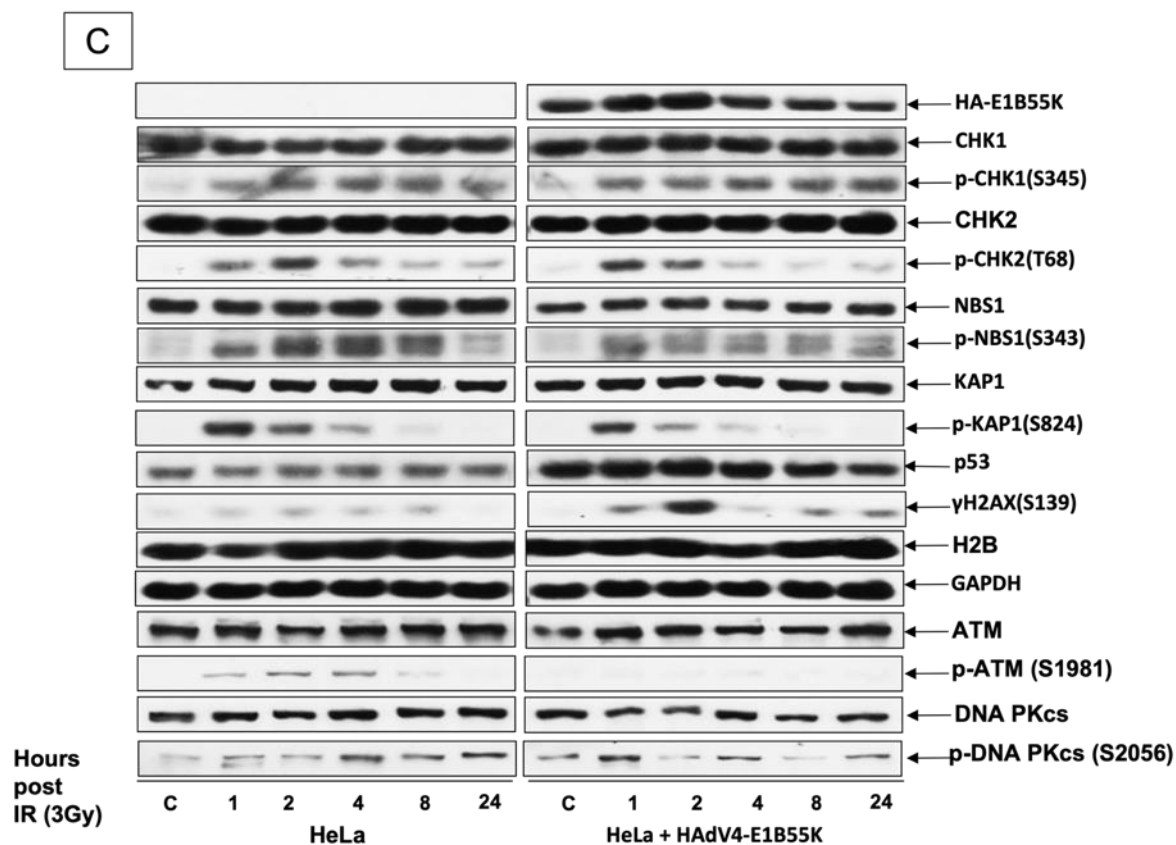
We used western blotting with antibodies against recognised substrates of the PI-3-kinase-like kinases, ATM and ATR, to assess the activation of the DDR throughout a 24-hour time course after exposing normally dividing and E1B55K-transfected HeLa cells to IR. The DNA damage induced by IR leads to DSB formation. Results demonstrated that the activation of the ATM pathway components is similar in all cells transfected with E1B55K from different constructs when compared to normally cycling HeLa cells, except for  $\gamma$ H2AX which was markedly more highly phosphorylated in all cells transfected with the viral gene (Figure 5.3A-D). These findings provide evidence that E1B55K from group B, D, E and F HAdVs has a limited effect on DSB repair pathways and that the difference seen in phosphorylation of the HR pathway component,  $\gamma$ H2AX, between control and transfected cells may be due to effects on other DDR pathways. These findings are in agreement with previous reports which indicated that, although several DDR proteins were degraded after associating efficiently with E1B55K from group B, D, E and F HAdVs during infection, there were several examples of DDR substrates that bound efficiently to E1B55K but were not degraded, and other examples in which substrates were degraded despite binding to E1B55K being low or undetectable in these HAdV types (Cheng *et al.*, 2011, 2013; Forrester *et al.*, 2011; Herrmann *et al.*, 2020). Interestingly, even before irradiating the cells with IR to induce DNA damage, phosphorylation of  $\gamma$ H2AX was evident in HAdV16 and HAdV40 E1B55K-transfected cells, and less markedly with HAdV4 and HAdV9 E1B55K-transfected cells, which is likely to reflect the ability of E1B55K from these HAdV types to trigger an important component of the DDR immediately after transfection (Figure 5.3E).

A



B





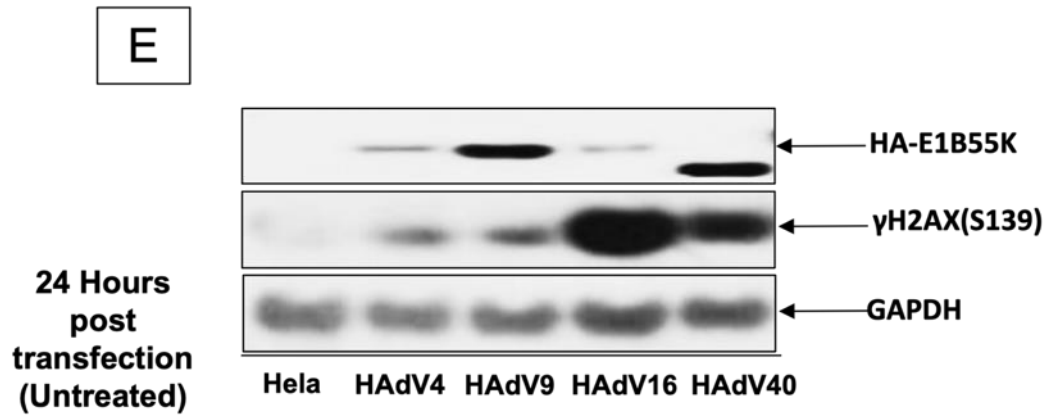


**Figure 5.3.** The expression of E1B55K from group B, D, E and F HAdV types has no marked effects on the phosphorylation of HR pathway components. HeLa cells were transfected with constructs encoding E1B55K from HAdVs 16 (group B), 9 (group D), 4 (group E) and 40 (group F), as well as pcDNA3.1 as a control. After 48 hours cells were irradiated with IR (3Gy) to induce DNA damage, and then harvested at increasing times. Cell lysates were subjected to western blotting using the antibodies shown, “C” untreated controls. (A) HAdV16, (B) HAdV9, (C) HAdV4, and (D) HAdV40. (E) western blot showing γH2AX levels in HeLa cells 24 hours after transfection but without IR.

#### 5.2.4 E1B55K from group B, D, E and F HAdV types binds to DDR components in transfected HeLa cells.

It has been demonstrated that, during infection, the E1B55K serves as the binding component for many cellular targets to be ubiquitinated by the E3 Ligase during HAdV-mediated protein degradation (Blackford and Grand, 2009; Hidalgo *et al.*, 2019; Herrmann *et al.*, 2020; Kleinberger, 2020). When E1B55Ks from group B, D, E and F HAdVs were immunoprecipitated with an antibody against the HA-tag, several cellular proteins such as ATR, ATM, USP7, UBR5, MRE11 and DNA ligase IV co-precipitated (Figure 5.4). This suggests that E1B55K proteins from these viral groups associate with some members of the DDR components, as well as, with UBR5 which is involved in the ubiquitination machinery. In previous studies, HAdV-E1B55K proteins have also been shown to bind with p53 in different HAdV types, with the exception of HAdV4-E1B55K (Cheng *et al.*, 2013). Similarly, the viral protein also bound MRE11 and NBS1 in several HAdV types (Cheng *et al.*, 2013). This is consistent with the fact that these proteins are sometimes degraded in response to HAdV infection with these viral species as reported in previous studies (Forrester *et al.*, 2011). These interactions might have a significant impact on the DDR. However, it is likely that the limited effect exerted by E1B55K from these viral constructs on the DDR activation and DSB repair are seen here since viruses from various HAdV species have developed different strategies to circumvent host cells' defences and promote viral replication, regardless of their ability to bind DDR components. This needs further examination in future studies.

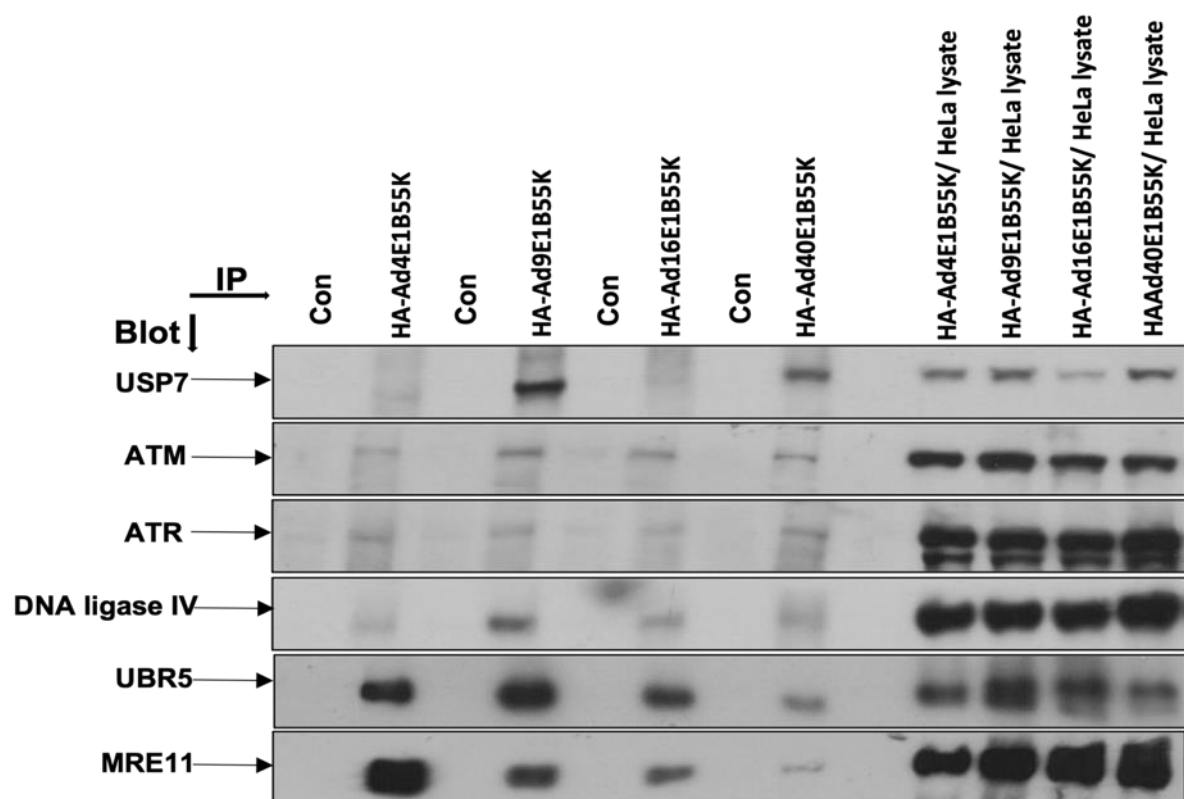


**Figure 5.4.** E1B55K from group B, D, E and F HAdVs co-immunoprecipitate with some DDR and cellular proteins. HeLa cells were transfected with constructs encoding HA-tagged E1B55K from HAdVs 16 (group B), 9 (group D), 4 (group E) and 40 (group F). After 48 hours lysates were immunoprecipitated with an antibody against the HA-tag or an irrelevant control (Collagen IV) antibody (labelled 'Con'). Immunoprecipitated proteins were fractionated by SDS-PAGE and identified by western blotting using the antibodies shown. Expression of the proteins in whole cell lysates is also shown.

### 5.2.5 Isolation and identification of potential proteins associated with E1B55K from group B, D, E and F HAdVs.

HAdV-E1B55K is a multifunctional protein, although only three molecular activities have been linked to it up to now: as an E3 SUMO-1 ligase of p53 (Pennella *et al.*, 2010), as the substrate recognition component of a Cullin 5-based E3 ubiquitin-ligase complex (Querido, Blanchette, *et al.*, 2001), and as a transcriptional repressor (Yew, Liu and Berk, 1994; Martin and Berk, 1998; Miller *et al.*, 2009; Chahal, Qi and Flint, 2012). However, it is still unclear if these three roles can fully explain how E1B55K affects productive infection or complements E1A-mediated transformation. It is now well established that E1B55K interacts with in excess of 90 cellular and viral proteins (Hung and Flint, 2017; Hidalgo *et al.*, 2019; Herrmann *et al.*, 2020), in addition to viral mRNA (Tejera *et al.*, 2019). Only a few of these interactions have been linked to the activity of E1B55K in the polyubiquitylation of target proteins, SUMO-1 ligation, or control of gene expression. The relevance of many of these interactions on the regulation of E1B55K activities has not been fully described yet (Hidalgo *et al.*, 2019). Furthermore, very few of these interactions have been shown to affect viral replication and/or cell transformation.

In a further study we have gone on to examine E1B55K-interacting proteins by performing Liquid Chromatography–Mass Spectrometry (LC-MS) in order to identify potential substrates that might interact with E1B55Ks from group B, D, E and F HAdVs. This, in turn, could provide important information on novel substrates that associate with the viral protein.

Many proteins were identified in the co-immunoprecipitants, and it is reasonable to assume that many were false positives. This could have been resolved, at least to some extent, by

repeating the study. Unfortunately, lack of time precluded this. However, a selection of binding proteins, relevant to the known activities of E1B55K, are shown in Table 5.1. (The complete list is included in the Appendix to this thesis in Table A1.1). Although our results show several proteins already identified as potential E1B55K-binding substrates, a large number of those proteins were considered as non-specific binders (as was determined by comparing the data to MS datasets of negative controls for immunoaffinity purification of target proteins from human cells). Additionally, many proteins identified with less than 2 peptides or present in controls have been eliminated from further consideration. Significantly, the recovery of previously reported E1B55K-interacting proteins (Table 5.1, section B) gives some confidence as to the reliability of the presented results. Furthermore, our results show that some of the listed proteins that we found to associate with E1B55K in these viral groups had been shown previously to associate with HAdV5-E1B55K in human tumour cell lines (Querido, Morisson, *et al.*, 2001; Harada *et al.*, 2002). Also, several previously unreported E1B55K-interacting proteins involved in mRNA metabolism are listed (Table 5.1, section C). It is worth noting that the final list of E1B55K-associated proteins represents only candidates which have high or medium peptide-spectrum match (PSM) levels as determined by assessing the false discovery rate (FDR) confidence ratios (Table 5.1). The total number of identified E1B55K-interacting proteins were 243 for HAdV16, 465 for HAdV9, 287 for HAdV4, and 367 for HAdV40.



**Table 5.1.** Mass spectrometry analysis of proteins immunoprecipitating with E1B55K from HAdVs 16 (group B), 9 (group D), 4 (group E) and 40 (group F).

Protein/gene name	MW [kDa]	# PSMs (Spectral counts)			
		HAdV16	HAdV9	HAdV4	HAdV40
(A) Novel proteins that bind some E1B55Ks from group B, D, E and F					
E3 ubiquitin-protein ligase UBR5	309	1	73	4	5
E3 ubiquitin-protein ligase UBR4	574	0	43	0	1
E3 ubiquitin-protein ligase HUWE1	482	0	0	2	3
(B) Known proteins to bind HAdV5 or HAdV12					
DNA-dependent protein kinase catalytic subunit PRKDC	469	1	52	6	9
Ubiquitin carboxyl-terminal hydrolase 7 USP7	128	0	18	1	18
Probable ubiquitin carboxyl-terminal hydrolase FAF-X USP9X	292	3	4	9	34
DNA replication licensing factor MCM3	91	1	9	1	1
DNA replication licensing factor MCM5	82	0	2	0	0
DNA replication licensing factor MCM7	81	0	4	0	0
Double-strand break repair protein MRE11	81	0	3	4	0
DNA repair protein RAD50	154	0	7	12	0
X-ray repair cross-complementing protein 6 XRCC6	70	0	1	0	0
182 kDa tankyrase-1-binding protein TNKS1BP1	182	0	1	0	9
Heterogeneous nuclear ribonucleoprotein U-like protein 1 HNRNPUL1	96	6	20	7	10

**(C) RNA binding proteins or splicing factors**

ATP-dependent RNA helicase DDX24	96	0	0	0	2
Poly(U)-binding-splicing factor PUF60	60	15	16	16	16
Ubiquitin conjugation factor E4 A UBE4A	123	12	0	15	15
Heterogeneous nuclear ribonucleoprotein H HNRNPH1	49	10	16	10	14
Heterogeneous nuclear ribonucleoprotein H2 HNRNPH2	49	0	8	0	0
RNA-binding protein FUS	53	10	10	9	8
RNA-binding protein 25 RBM25	100	9	19	19	14
Heterogeneous nuclear ribonucleoprotein A1 HNRNPA1	39	0	0	1	0
Heterogeneous nuclear ribonucleoprotein A3 HNRNPA3	40	0	1	0	1
Heterogeneous nuclear ribonucleoprotein K HNRNPK	51	5	12	6	6
Heterogeneous nuclear ribonucleoprotein F HNRNPF	46	5	7	5	8
Heterogeneous nuclear ribonucleoprotein H3 HNRNPH3	37	3	5	1	0
Heterogeneous nuclear ribonucleoprotein D-like HNRNPDL	46	3	4	2	2
Heterogeneous nuclear ribonucleoprotein L-like HNRNPDL	60	0	0	0	4
Heterogeneous nuclear ribonucleoproteins A2/B1 HNRNPA2B1	37	2	5	2	3
Heterogeneous nuclear ribonucleoprotein R HNRNPR	71	0	0	1	1
Heterogeneous nuclear ribonucleoproteins C1/C2 HNRNPC	34	0	0	0	3
Pre-mRNA-processing factor 40 homolog A PRPF40A	109	3	13	6	8
Cleavage and polyadenylation specificity factor subunit 5 NUDT21	26	4	5	2	2
Cleavage and polyadenylation specificity factor subunit 6 CPSF6	59	9	12	9	9
RNA-binding protein 39 RBM39	59	2	3	6	5
Heterogeneous nuclear ribonucleoprotein D0 HNRNPD	38	2	0	0	0
Heterogeneous nuclear ribonucleoprotein U HNRNPU	91	2	2	6	4
Heterogeneous nuclear ribonucleoprotein U-like protein 1 HNRNPUL1	96	6	20	7	10
RNA-binding protein with serine-rich domain 1 RNPS1	34	1	1	1	1
Splicing factor 3B subunit 1 SF3B1	146	1	6	8	7
Splicing factor 3B subunit 2 SF3B2	100	1	8	4	0
Splicing factor 3B subunit 3 SF3B3	136	4	4	1	1

Splicing factor 3B subunit 4 SF3B4	44	0	0	1	1
Splicing factor 3B subunit 5 SF3B5	10	1	1	1	1
Splicing factor 3B subunit 6 SF3B6	15	0	1	0	1
Heterogeneous nuclear ribonucleoprotein M HNRNPM	78	1	3	2	3
Small nuclear ribonucleoprotein-associated proteins B and B' SNRPB	25	0	1	0	1
Small nuclear ribonucleoprotein F SNRPF	10	1	1	1	1
Small nuclear ribonucleoprotein Sm D1 SNRPD1	13	1	1	1	1
Small nuclear ribonucleoprotein Sm D2 SNRPD2	14	1	2	1	0
Small nuclear ribonucleoprotein Sm D3 SNRPD3	14	2	3	1	0
RNA-binding protein EWSR1	68	1	1	1	0
Pre-mRNA-splicing factor 38B PRPF38B	64	0	3	2	1
Pre-mRNA 3'-end-processing factor FIP1L1	67	1	1	1	1
Pre-mRNA-splicing factor ATP-dependent RNA helicase DHX15	91	1	2	3	7
Splicing factor, proline- and glutamine-rich SFPQ	76	1	2	0	1
DNA topoisomerase 1 TOP1	91	1	1	0	0
Splicing factor 1 SF1	68	0	1	0	0
Splicing factor U2AF 35 kDa subunit U2AF1	28	1	2	0	0
Splicing factor U2AF 65 kDa subunit U2AF2	54	1	5	3	3
Splicing factor 3A subunit 1 SF3A1	89	1	9	5	3
Splicing factor 3A subunit 2 SF3A2	49	0	1	0	0
Splicing factor 3A subunit 3 SF3A3	59	2	1	1	2
Splicing factor, suppressor of white-apricot homolog SFSWAP	105	0	1	0	0
U1 small nuclear ribonucleoprotein 70 kDa SNRNP70	52	1	2	1	1
E3 ubiquitin-protein transferase MAEA	45	0	2	0	0
DNA-directed RNA polymerase II subunit RPB3 POLR2C	31	0	1	0	0
BRCA1-associated RING domain protein 1 BARD1	87	0	0	0	1
Next to BRCA1 gene 1 protein NBR1	107	0	1	0	0
Serine/arginine-rich splicing factor 11 SRSF11	54	2	4	3	3
Activated RNA polymerase II transcriptional coactivator p15 SUB1	14	1	1	1	1

### 5.2.6 HAdV5/12 infections have no effect on UBR5 expression.

Through proteomic analysis, UBR5 was reported recently as a potential target of HAdV5-E1B55K (Hung and Flint, 2017). We performed LC/MS on HeLa cells transfected with HAdV-E1B55K proteins from groups B, D, E and F HAdVs and we found that the cellular protein scored a high number of spectral counts but was not found in the HeLa controls (Table 5.1, section A). We considered UBR5 as an interesting candidate for further examination, especially as we have found that it is a major binding protein for HAdV9-E1B55K (represented by the number of peptide spectrum matches in Table 5.1). Here we show some interactions between UBR5 and HAdV5/12 E1B55Ks and the effects of the viral proteins on UBR5 in the context of viral infections with *wt* HAdV5 or *wt* HAdV12. No degradation of UBR5 was observed during infection of HeLa cells with either virus, either before or after the addition of the NEDDylation inhibitor (MLN4924), which acts as an indirect inhibitor of Cullin ring ligase by blocking Cullin NEDDylation (Figure 5.5A, B). Additionally, we depleted UBR5 via UBR5-siRNA and observed the effects on HAdV5 hexon expression throughout the course of infection. This was taken as an indication of viral replication. The effects on hexon expression were slight although there is limited reduction in expression of hexon in the UBR5-depleted cells (Figure 5.5C). This suggests that, although HAdV5-E1B55K might associate with UBR5 (as reported previously in (Hung and Flint, 2017)), this association does not necessarily lead to ubiquitin-mediated proteasomal degradation of the protein. Furthermore, the knockdown of UBR5 does not affect the course of HAdV5 infection to a marked extent. Nonetheless, this might raise the possibility for the need of conducting further investigation on the role of UBR5 association with E1B55K in other HAdVs infections.

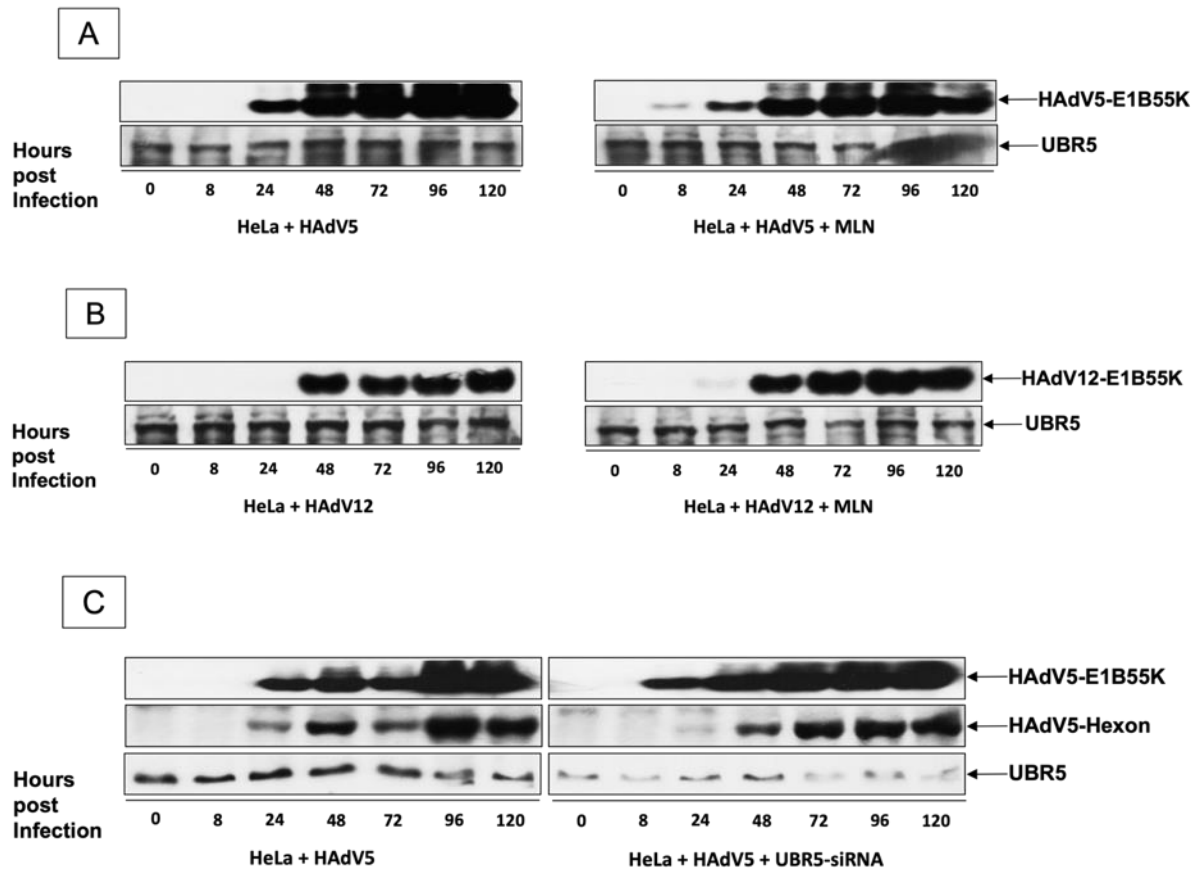


**Figure 5.5.** The expression of UBR5 in normally cycling and UBR5-depleted HeLa cells during wt HAdV5/12 infections. (A, B) HeLa cells were infected with wt HAdV5 or wt HAdV12 at an infectivity of 5 pfu/cell and cell lysates were harvested at increasing times after infection, either before or after the administration of MLN. Lysates were subjected to western blotting using the antibodies shown. (C) Western blots showing the degradation patterns of HAdV5-hexons in HeLa cells infected with wt HAdV5 at an infectivity of 5 pfu/cell, either with or without UBR5-siRNA transfection.

## 5.3 Discussion

Previous reports have determined that HAdVs from groups A to F neutralise host cell DDR by targeting certain cellular proteins for ubiquitin-mediated proteasomal degradation, and that these viruses are also able to differentially control the pathways involved in this process (Cheng *et al.*, 2011, 2013; Forrester *et al.*, 2011; Pancholi and Weitzman, 2018). Additionally, many previous investigations on HAdVs have concentrated on the properties and interactions of the E1B55K proteins from members of the relatively small groups C (HAdV5) and A (HAdV12) viruses and their established effects on the host cellular DDR and genomic instability. E1B55K has been shown to be the substrate-binding component in the E3 ubiquitin ligase recruited by these viruses (Blackford and Grand, 2009; Hidalgo *et al.*, 2019; Herrmann *et al.*, 2020; Kleinberger, 2020). However, those studies have generally concentrated on the roles of the protein in the context of viral infections. Here we have expanded this and investigated the properties of the E1B55K proteins from representative HAdVs from groups B, D, E, and F, to examine whether the viral protein from these types has comparable effects when expressed in isolation. All HAdV types studied here had minor effects on the phosphorylation of host cellular DDR proteins, after IR treatment, and induction of genomic instability, although to a lesser extent than was seen in the case of HAdV12 (group A) in chapter 4. Additionally, results shown here may demonstrate a limited effect exerted by viral E1B55K from groups B, D, E, and F on the expression of DSB repair pathways components, suggesting that these viral types might utilise more diverse tactics in the absence of DDR proteins degradation to impinge cellular DDR than what has been described for HAdV5 and HAdV12.

Our results demonstrate that E1B55K from groups B (HAdV16), D (HAdV9), E (HAdV4) and F (HAdV40) HAdVs causes genomic instability in human tumour cells, seen as an increase in micronuclei formation in undamaged growing cells, as well as, after irradiation of the cells with IR. These effects are less marked than those seen in HSF cells expressing HAdV12-E1B55K (see Chapter 4). The viral protein also caused inhibition of DNA DSB repair; seen by the increased formation of repair foci formation after IR-induced DNA damage. Again, the effect was less marked than we have seen in HSF cells expressing HAdV12-E1B55K. However, the E1B55K from group B, D, E and F exhibited only a limited effect on DSB repair pathways. The only significant difference seen in phosphorylation of HR pathway components between control and transfected cells after IR was in the levels of  $\gamma$ H2AX, possibly suggesting major effects on DDR pathways other than HR.

Interestingly, our results have also revealed that E1B55K from these viruses associates with some novel components of the DDR, such as, ATR, ATM, USP7, and UBR5 in co-immunoprecipitation experiments. MRE11 and DNA ligase IV were also shown to co-immunoprecipitate with E1B55K in these viral types; these interactions have already been described before (Cheng *et al.*, 2013).

A large number of binding proteins have been identified for HAdV5-E1B55K (reviewed in (Hidalgo *et al.*, 2019)). To determine whether similar proteins associated with E1B55K from the group B, D, E, and F viruses, a mass spectrometry analysis was undertaken. By applying LC/MS and analysing MS data of proteins that co-immunoprecipitate with E1B55K from transfected human tumour cells, we have identified a large list of novel E1B55K-associated proteins, which had not been described previously (Table 5.1). This list was thoroughly

examined and filtered to exclude proteins that routinely contaminate proteomic analysis samples from human cells in culture (Mellacheruvu *et al.*, 2013). However, as the experiment was only performed once we cannot rule out artefactual interactions. Caution should be exerted when considering the proteins listed in Table 5.1, particularly the RNA binding proteins, which are notoriously 'sticky'. However, HAdV5 has long been linked to RNA transport during viral infections (Pilder *et al.*, 1986; Leppard and Shenk, 1989; Mathews and Shenk, 1991). Additionally, it has recently been shown that hnRNPC and RALY, two RNA binding proteins, are ubiquitinated but not degraded during HAdV5 infection (Herrmann *et al.*, 2020). Our list also includes some E3 ubiquitin ligase subunits and their substrates, protein candidates that are involved in the regulation of mRNA metabolism, as well as, previously reported HAdV5-E1B55K interacting proteins, such as MRE11 and RAD50, which helps to give credibility to the results.

A few proteins were found to be present in the immunoprecipitates from E1B55K from all four types in relatively high yield. For example, the RNA binding proteins hnRNPK, H1, H3 and UL1 (also known as E1B55K-AP5), as well as FUS and RBM25 (Table 5.1). Significantly, hnRNPUL1 was previously identified as a protein that associated with HAdV5-E1B55K, which plays a role in mRNA transport (Gabler *et al.*, 1998).

A novel binding protein which occurred in all four co-immunoprecipitants was UBR5 (Table 5.1). We examined this relationship in HAdV5 and HAdV12 in slightly more detail. UBR5 is not degraded during infection with either of these viruses (Figure 5.5). Furthermore, depletion of UBR5 with siRNA did not have a marked effect on the time course of HAdV5 infection although



there appeared to be somewhat less hexon produced in the depleted cells. These experiments should be repeated to verify these observations.

Taken together, the observations that HAdV-E1B55K proteins from group B, D, E and F HAdVs have less effect on genome stability and the DDR than HAdV12-E1B55K, is consistent with the observations that HAdV12 is oncogenic whereas the other viruses are not, although it is important to note that factors other than E1B55K properties will help to determine transformation, such as the properties of the HAdV-E1A protein. In conclusion, our investigation into whether different HAdV types vary in their ability to inhibit DDR revealed that, in contrast to HAdV12, certain viral types are unable to bypass this inhibition, but may imply that different HAdV types might adopt entirely different tactics to repress cellular proteins by binding them with E1B55K proteins rather than inducing their degradation. In regards to this, it was shown that although the majority of E1B55K functions in infected cells are linked to its association with E4orf6 (Sarnow, Sullivan and Levine, 1982; Harada *et al.*, 2002), the E1B55K protein also has functions that are independent of the E4orf6 protein, and thus, its E3 ubiquitin ligase activity. For example, interaction of E1B55K with p53 strongly increases SUMOylation of the p53 protein in the absence of other viral proteins (Muller and Dobner, 2008). Also, even though UBR5 has been shown to co-immunoprecipitate with HAdV5-E1B55K in an earlier study, our results show that the cellular protein is not degraded during *wt* infections with either HAdV5 or HAdV12, suggesting the possibility that these viruses may interact with this protein in order to modify its activity rather than its degradation. Furthermore, the knockdown of UBR5 in HeLa cells infected with HAdV5 and transfected with UBR5-siRNA shows relatively slight effect on the expression of HAdV5 hexon. Hence, more

work needs to be done to establish the precise roles of this protein during HAdV infection and the significance of its interactions with HAdV-E1B55Ks.

# **CHAPTER 6**

## **Final Discussion**

## 6.1 Conclusions

### 6.1.1 Introduction.

DNA tumour viruses have long served as helpful research tools for examining cellular transformation and comprehending the biology of cancer. Oncoproteins produced by the majority of DNA tumour viruses specifically target the pRB family tumour suppressor proteins and p53, which are all crucial cellular proteins. By the actions of viral oncoproteins, many other cellular regulatory and transcriptional proteins are similarly dysregulated. For example, HPV-E6 specifically targets the p53 pathway and eliminates the transcriptional repression and pro-apoptotic effects of p53 by targeting it for very fast ubiquitin-dependent degradation in conjunction with the HPV-E6 associated protein cellular protein (Scheffner *et al.*, 1993). As we have discussed in detail, HAdV-E1B55K and E4orf6 similarly target p53 for ubiquitin-dependent degradation (Steegenga *et al.*, 1998; Querido, Blanchette, *et al.*, 2001; Harada *et al.*, 2002; Blanchette *et al.*, 2008). Furthermore, HPV, HAdV, and SV40 activate pRB signalling through their oncoproteins to cause quiescent cells to enter the proliferative state, enabling replication of the viral genomes (Dyson *et al.*, 1989; Münger *et al.*, 1989; Massimi and Banks, 1997). The SV40 T antigen binds to and disables p53's capacity for transcriptional transactivation (Lane and Crawford, 1979; Linzer and Levine, 1979; Mietz *et al.*, 1992). Moreover, it attaches to and deactivates the pRB, promoting cell cycle progression (Lee and Cho, 2002). Similar to this, the LXCXE motif found on the major T-cell antigen of Merkel Cell Polyomavirus targets pRB function by directly interacting with it, freeing E2F from Rb's inhibitory action (Feng *et al.*, 2008). It is clear that a variety of DNA cancer viruses alter DDR pathways during infection to encourage viral replication. Certain viruses selectively activate

or repress DDR pathways for viral development and/or oncogenesis, while others employ or exploit DDR pathways and others adversely regulate DDR pathways (Turnell and Grand, 2012; Pancholi, Price and Weitzman, 2017). Similar to adenovirus, other viruses frequently interact with the ubiquitin proteasomal system to control DDR pathways (Dybas, Herrmann and Weitzman, 2018). As a result, it appears that some overlap may be detected in how most of these DNA tumour viruses employ their oncoproteins to spread the virus, similar to how the HAdV-E1B55K oncoprotein functions.

HAdVs are promising and effective models for investigating the molecular processes behind infection-related metabolic alterations, cell transformation, and malignancy (Miller *et al.*, 2007; Ip and Dobner, 2019). Currently, they are also one of the most widely-employed viral vectors in anti-cancer oncolytic virus therapeutic applications and in vaccine research (Gao *et al.*, 2019; Hensen, Hoeben and Bots, 2020). The cellular pathways altered by the virus that lead to HAdV-induced pathogenesis, cellular transformation, or metabolic alterations have not yet been completely characterised and, in some cases remain poorly understood. This is despite advances in elucidating key elements of the functions of important viral proteins that are modulated by HAdV. A notable example is the HAdV oncoprotein E1B55K, which has been shown to enhance viral genome replication and expression while suppressing host gene expression and antiviral host responses. The E1B55K protein is, therefore, a major focus in HAdV research up to now due to its critical roles in viral replication and host cell transformation.

HAdV-E1B55K is multifunctional, with three molecular activities linked to the HAdV5 protein: it acts as an E3 SUMO-1 ligase that represses p53's transcriptional activity (Pennella *et al.*,

2010), it serves as the substrate recognition component of a Cullin 5-based E3 ubiquitin-ligase complex that ubiquitylates and, in many cases, leads to degradation of multiple cellular substrates (Querido, Blanchette, *et al.*, 2001; Herrmann *et al.*, 2020); the E1B55K/E4orf6 E3 ligase complex also facilitates the transportation of late viral mRNA while inhibiting the translation and exportation of cellular mRNA (Leppard and Shenk, 1989; Gabler *et al.*, 1998; Querido, Blanchette, *et al.*, 2001; Harada *et al.*, 2002). During viral infection, HAdV5-E1B55K acts in concert with E4orf6, this is particularly notable when it acts as an E3 Ligase. It has been reported that E1B55K requires E4orf6 for nuclear localisation and accumulation in viral replication centres (Ornelles and Shenk, 1991). Interestingly, in the absence of E4orf6, E1B55K acts as a co-operating oncogene, markedly increasing the frequency of transformation of rodent cells (Graham and Van der Eb, 1973; Bernards and Van der Eb, 1984; Gallimore *et al.*, 1985). Its expression is also essential for transformation of human cells in culture (Byrd, Brown and Gallimore, 1982; Whittaker *et al.*, 1984). E1B55K was also shown to control the gene expression of other cellular proteins (Yew, Liu and Berk, 1994; Martin and Berk, 1998; Miller *et al.*, 2009; Chahal, Qi and Flint, 2012). However, it is still unclear if these roles can fully explain how E1B55K affects productive infection or complements E1A-mediated transformation.

It is now well established that HAdV5-E1B55K interacts with in excess of 90 cellular and viral proteins (Hung and Flint, 2017; Herrmann *et al.*, 2020; this thesis Chapter 3), in addition to viral mRNAs (Tejera *et al.*, 2019). Only a few of these interactions have been linked to the activity of E1B55K in the polyubiquitylation of target proteins, SUMO-1 ligation, or control of gene expression. The relevance of many of these interactions to E1B55K's activities has not been fully described yet (Hidalgo *et al.*, 2019). Furthermore, very few of the interactions have

been shown to influence viral replication and/or cell transformation. E1B55K impacts the host cell in several other ways. For instance, it complements the E1A-mediated cellular transformation by blocking E1A induced apoptosis, alters host cell proliferation by inducing host-cell shut off, and it inhibits cellular RNA export from the nucleus, while augmenting viral RNA export. Consequently, this leads to alteration in viral and cellular protein expression, abrogation of apoptosis, and regulation of DDR pathways and other cellular machinery in favour of viral replication (Blackford and Grand, 2009; Berk, 2013). Whether these interactions of unidentified effect are necessary for the properties of E1B55K is still unknown. For example, HAdV5-E1B55K has been linked to RNA transport during viral infection (Pilder *et al.*, 1986; Leppard and Shenk, 1989; Mathews and Shenk, 1991). In this regard, hnRNPUL1, which plays a role in mRNA transport, was previously identified as a protein that associated with HAdV5-E1B55K (Gabler *et al.*, 1998). Recently, it has been shown that hnRNPC and RALY, two RNA binding proteins, are targeted by E1B55K/E4orf6 proteins for ubiquitylation, but not degradation, during HAdV5 infection (Herrmann *et al.*, 2020). It is possible that some, or perhaps all of the E1B55K binding proteins will be linked to known viral properties.

### **6.1.2 Regulation of DDR pathways proteins during HAdV5/12 infections.**

It is well established that, during infection with HAdV5 and HAdV12, the viral E1B55K protein (with E4orf6) appears to protect infected cells against apoptosis by causing rapid degradation of the tumour suppressor p53 protein (Querido *et al.*, 1997; Steegenga *et al.*, 1998; Querido, Blanchette, *et al.*, 2001; Cheng *et al.*, 2011; Forrester *et al.*, 2011). E1B55Ks from HAdV5 and HAdV12 also target an appreciable number of other cellular proteins for degradation, many

of which are associated, directly or indirectly, with the DDR. For example, BLM, MRE11, DNA ligase IV, TNK1BP1, and TOPBP1 have all been shown to associate with HAdV5-E1B55K and, in most cases with HAdV12-E1B55K, which results in their degradation (Stracker, Carson and Weitzman, 2002; Baker *et al.*, 2007; Blackford *et al.*, 2010; Orazio *et al.*, 2011; Ching *et al.*, 2013; Chalabi Hagkarim *et al.*, 2018; this thesis Chapter 3).

In this thesis we have shown that HAdV5-E1B55K associates with several novel DDR proteins, which had not been reported before in the context of HAdV biology, such as DNA-PKcs, USP9, CHK1, ATR, and DNMT1. Similarly, a number of DNA repair proteins were examined, using HAdV12-E1HER2 cells, to check if HAdV12-E1B55K associates with the same set of DDR proteins as HAdV5-E1B55K. Interestingly, we have shown for the first time that HAdV12-E1B55K interacts directly (without its association with E4orf6 and, therefore, its role in the E3 ligase complex) with several other DDR proteins, such as BLM, TOP3A, USP7, USP9, USP15, hnRNPUL1, CHK1, and DNMT1. We have also observed weak association between HAdV12-E1B55K and ATR. Significantly, interactions of HAdV-E1B55K with ATM and DNA-PKcs, constitute new targets that are likely to contribute to the DDR effects described in Chapter 4 of this study. It is highly plausible that these interactions will be of significance during viral infection. However, it is possible that some of these interactions of E1B55Ks from HAdV5 and HAdV12 with DDR proteins are fortuitous and may not be of biological significance. This does not, of course, mean that none are required for viral replication. Further work is needed to determine which is the case for each protein identified. It would be interesting to establish whether similar interactions take place between E1B55K proteins of other HAdV types in future studies, although binding to ATR, ATM, UBR5 and USP7 has been confirmed (Chapter 5).



As HAdV12-E1B55K was shown to interfere with DNA replication (See Chapter 4), we thought that it is possible that interactions could be identified between the viral protein and some members of the pre-replication machinery and origin recognition complexes. Those shown in Chapter 3, could account for the some of the anomalies seen with DNA replication dynamics in cells expressing HAdV12-E1B55K (Chapter 4). It would be interesting to look at HAdV5-E1B55K interactions with members of the pre-replication complex and compare it to those observed with HAdV12-E1B55K. In addition, it would be interesting to examine whether these pre-replication complex proteins which interact with HAdV12-E1B55K, were degraded during HAdV12 infection. Unfortunately, time limitation has hindered our efforts to do this.

Our investigation into whether novel E1B55K interactors that we have identified were also targeted to the proteasome has revealed that most of the cellular proteins investigated are degraded during HAdV5 infection, although at varying rates, with the exception of ATR and USP34 (Figure 3.2A). The presence of the cullin inhibitor MLN4924 has markedly increased the stabilisation of many proteins that were shown to be degraded in the absence of the drug; suggesting that these proteins are indeed targeted by the HAdV5-E1B55K/E4orf6 E3 ligase complex for degradation. As previously stated, some cellular proteins are ubiquitylated by the HAdV5 protein complex without being degraded, and this ubiquitylation is thought to be beneficial for viral replication (Herrmann *et al.*, 2020). Therefore, it would be interesting in future to examine whether ATR and USP34 were ubiquitylated (without degradation), as has recently been reported for an appreciable number of other proteins in the presence of HAdV5-E1B55k/E4orf6.

When we investigated the degradation patterns of DDR proteins that were shown to interact with HAdV12-E1B55K, results were rather confusing. p53 and MRE11 were the only proteins that became stabilised in the presence of MLN4924, several other proteins were appreciably less stable, such as, DNMT1 and USP33 (Figure 3.2B). We have no explanation for this, except to suggest that the effects of the drug on Cul2, or the Cul2-containing E3 ligase, are rather different to those on Cul5.

An important question to consider is, why would E1B55Ks from HAdV5 and HAdV12 bind so many DDR proteins and, whether these bound proteins serve functional activities needed for viral replication? Additionally, as some bound proteins are shown not to be degraded, does this imply that only their ubiquitylation is needed in these cases. Ubiquitylation, one of the most prevalent PTMs, occurs when a ubiquitin polypeptide, consisting of 76 amino acids, is covalently linked by an isopeptide bond between a Gly76 carboxyl group and either a Lys sidechain primary amino group (Lys6, Lys11, Lys27, Lys29, Lys33, Lys48, or Lys63) or the ubiquitin amino terminus by an E3 ubiquitin ligase enzyme that catalyses the transfer of ubiquitin to the target substrate. A single ubiquitin can be linked but ubiquitin chains can be formed when multiple ubiquitins are linked to a target. Linkage through Lys 48 is generally considered to be involved in targeting to the proteasome. The substrate is frequently degraded by proteasomes as a result of this process (Dye and Schulman, 2007; Kulathu and Komander, 2012; Yau and Rape, 2016; Dybas, Herrmann and Weitzman, 2018). Lysosomal targeting, DDR pathway activity, protein interactions, functioning, or localisation, as well as mono-ubiquitylation depend on polyubiquitylation through lysine binding other than Lys48, which is generally responsible for driving proteasomal degradation (Kulathu and Komander, 2012; Yau and Rape, 2016). The cellular functions that have been given to each of the links

that make up the ubiquitin polymers, as well as the specific cellular functions for Lys6, Lys27, give ubiquitin its versatility (Kulathu and Komander, 2012). In order to facilitate a successful infection, HAdVs take advantage of the cellular ubiquitylation/degradation pathway. It has been demonstrated that many DNA tumour viruses can modify the ubiquitylation of particular target proteins by encoding viral E3 ligases, integrating into cellular ubiquitin ligase complexes to alter E3 activity and specificity, and altering the enzymatic activity of pre-existing cellular E3 ligases to alter E3 activity and specificity (Dybas, Herrmann and Weitzman, 2018).

HAdV E1B55K and E4orf6 hijack the host ubiquitin ligase system in order to redirect ubiquitination and promote viral late RNA nuclear export and late protein synthesis. Modulation of the host ubiquitin machinery during HAdV infection has typically been examined in terms of proteasomal degradation, with few cases of non-degradative ubiquitination identified (Isaacson and Ploegh, 2009; Luo, 2016; Dybas, Herrmann and Weitzman, 2018). Nonetheless, it has been proposed that many substrates of the E1B55K/E4orf6 complex are ubiquitinated without significant changes in abundance, suggesting that non-degradative ubiquitination plays a significant role during viral infection (Herrmann *et al.*, 2020). However, in that study they did not determine if the ubiquitylation was the modification aimed at the proteasome or merely changing the properties of the target protein, as the linkage between ubiquitin and the target which determines whether it is a signal for degradation was not determined. This discovery emphasises the need of analysing both the ubiquitinome and the whole-cell proteome when predicting substrates. We argue that using ubiquitination without proteasome-mediated degradation allows for greater flexibility and faster methods to modify cellular pathways and host responses. Additionally, ubiquitylation may not be intended to target protein for degradation but as a post

translational modification altering their activity, which is very common in DDR proteins (Dybas, Herrmann and Weitzman, 2018). Therefore, it would be interesting to determine if degradation of a certain protein is somehow blocked or not recognised by the proteasome even though carrying ubiquitin modification or if the ubiquitylation process is a post translational modification altering the properties of the target protein. As such, further elucidation is needed in future studies to show whether this applies to other infections from groups B, D, E, and F HAdVs, as it has been assumed that inactivation of the DDR during HAdV infection was so that concatemers of viral DNA were not formed (Stracker, Carson and Weitzman, 2002). However, other evidence has suggested that concatemer formation is not important (Lakdawala *et al.*, 2008; Karen *et al.*, 2009). Therefore, it is possible that other effects of the DDR pathways need to be inhibited/inactivated for optimal viral replication- what these might be are not clear at present.

### **6.1.3 The potential effects of HAdV12-E1B55K on DDR pathways, DNA repair and replication stress.**

It was shown in early research that group A HAdVs, such as HAdV12, had the ability to generate tumours in new-born rodents (Trentin, Yabe and Taylor, 1962; Yabe, Trentin and Taylor, 1962; Huebner *et al.*, 1963; Freeman *et al.*, 1967). Later studies of low dose HAdV12 infections showed that HAdV12-E1B55K promotes genomic instability in human cells, as it was reported that HAdV12 induces chromosomal aberrations in human embryo kidney and human embryo lung cells, causing non-random damage and breaks in chromosomes 1 and 17 (zur Hausen, 1967; McDougall, 1971b). The infection was found to affect primarily four chromosomal

regions, commonly referred to as HAdV12 modification sites. Damage at these sites was shown as regions of uncoiled DNA and heterochromatic gaps from which breaks may result (Stich, Van Hoosier and Trentin, 1964; zur Hausen, 1967; McDougall, 1971; McDougall *et al.*, 1974; Lindgren *et al.*, 1985; Durnam *et al.*, 1988). Mutational studies on E1 genes from HAdV12 have also shown that viral-induced chromosomal damage and modification of fragile sites is dependent upon the expression of the HAdV12-E1B55K protein, whereas E1A and E1B19K proteins had minimal effects (Durnam *et al.*, 1986; Schramayr *et al.*, 1990b). In light of these findings, we concluded that conducting additional research into the capability of HAdV12-E1B55K to cause DNA damage and its impact on host DDR would be of considerable interest. This is particularly relevant as our understanding of the pathways through which DNA damage is repaired has significantly improved since the initial studies were performed.

The majority of research carried out previously has focused on the activities of the E1B55K protein during viral infection while in collaboration with E4orf6 and functioning as a component of the E3 ubiquitin ligase complex. However, we examined the possibility that, in the absence of E4orf6, the E1B55K protein may also affect DDR pathways in isolation.

In this study, we aimed to characterise the unique roles of E1B55K in association with the DDR but distinct from its E3 ligase activities. We expected that this would allow us to throw light on its ability to cause genomic instability. With this in mind, we decided to look at the effects of HAdV12-E1B55K on DDR and DNA replication dynamics in primary human fibroblasts that express the HAdV12-E1B55K protein only.

The data presented in this thesis shows that genomic instability is triggered by HAdV12-E1B55K expression in HSFs, as shown by the increase in micronuclei numbers, both before and

after treating the cells with DNA damaging agents. Furthermore, in agreement with previous observations (Stich, Van Hoosier and Trentin, 1964; zur Hausen, 1967; McDougall, 1970, 1971a; McDougall *et al.*, 1974), we also found a significant increase in chromosomal anomalies in metaphase spreads in cells expressing the viral protein. Since treatment with HU significantly increases the number of micronuclei in 55K<sup>+</sup>HSFs in comparison to parental cells, we hypothesised that HAdV12-E1B55K expression may lead to DNA replication stress. We have shown that replication is inhibited by the viral protein in untreated cells, as shown by a significant increase of stalled forks, reduction in the efficiency of replication fork restart, and reduction in replication fork speeds. In contrast, normally cycling HSFs were more efficient at fork restart than 55K<sup>+</sup>HSFs. Our findings imply that the HAdV12-E1B55K protein significantly affects DNA replication by promoting fork stalling and interfering with the process of fork restart, either before or after induced DNA replication stress. These effects will probably contribute to genomic instability seen in cells that express the viral protein (as reviewed in, (Zeman and Cimprich, 2014; Wilhelm, Said and Naim, 2020)). It is also possible that these effects are caused by the interactions between HAdV12-E1B55K and constituents of the replisome (ORC1, MCM3, MCM7, DNA polymerase, and cdc45), as we have shown that the viral protein associated with these proteins in Chapter 3.

We have also subjected the cells expressing HAdV12-E1B55K to various genotoxic agents and observed the development of DNA repair foci, and the phosphorylation of PI3K-related kinase substrates. This was done to determine if the HAdV12-E1B55K protein, in isolation, would also have an impact on the cellular response to DSBs. The increased phosphorylation of ATM substrates in 55K<sup>+</sup>HSFs suggests the presence of defects in DNA damage repair and possibly the existence of extra damage related to checkpoint dysfunction. At varying time points after

induced DNA damage, 55K<sup>+</sup>HSFs were found to have more foci staining positive for  $\gamma$ H2AX, RAD51, and 53BP1 than control cells, again pointing to potential inefficiencies in DDR pathways and/or extra damage brought on by HAdV12-E1B55K. Of course, the proportionate contributions of increasing damage and issues with repair may have been determined by a more in-depth investigation of DNA repair and resolution. Remarkably, a significant number of DNA repair foci were detectable in untreated 55K<sup>+</sup>HSF cells, adding credibility to the notion that HAdV12-E1B55K contributes to genomic instability even in the absence of exogenous DNA-damaging agents.

We looked at  $\gamma$ H2AX foci formation (in response to a low dose of IR) across the cell cycle using APH and distinguishing G<sub>1</sub> and G<sub>2</sub> cells using Mitosin staining to identify which DNA repair pathways were likely to be targeted by the viral protein. The formation of  $\gamma$ H2AX foci was comparable in both cell groups during G<sub>1</sub> phase of the cycle, where NHEJ is the primary repair mechanism; however, we have seen significantly more  $\gamma$ H2AX foci in 55K<sup>+</sup>HSFs during G<sub>2</sub> phase, where HR is the predominant DNA repair mechanism. Our findings lead us to hypothesise that cells expressing HAdV12-E1B55K have deficits in the HR pathway, which controls the majority of DNA repair during G<sub>2</sub> phase of the cell cycle, as we have seen more  $\gamma$ H2AX foci recruitments in Mitosin-positive cells which express HAdV12-E1B55K. It would be important to examine whether HAdV5-E1B55K has similar effects when expressed in primary human cells; we would predict that it would not, as the early reports showed that only HAdV12 caused chromosomal instability. However, the experiments should be undertaken. As HAdV12-E1B55K interacts directly with p53 to inactivate it (Yew and Berk, 1992; Grand *et al.*, 1996; Forrester *et al.*, 2011), we examined the expression levels of different cyclins following DNA damage in 55K<sup>+</sup>HSFs to check the possibility that cell cycle checkpoints had been

disrupted. If p53 is not transcriptionally active, the G<sub>1</sub>/S and G<sub>2</sub>/M checkpoints will not function appropriately. Therefore, if one or more checkpoints are disrupted, it is very probable that greater damage will be sustained to the DNA, which will result in the formation of more DNA repair foci and most likely an increased activation of ATM. It appears that there is a decreased level of expression of cyclins A, B1, and D1 in parental HSFs after induced damage, indicating an arrest of the cell cycle. However, in 55K<sup>+</sup>HSFs, the expression of cyclins remains high throughout the time course following DNA damage, indicating that the cells do not experience cycle arrest, likely as a result of the inactivation of p53 by the viral protein. It seems probable that inactivation of p53 could have occurred in the original HAdV12 experiments with human cells but in that case possibly due to p53 degradation as they were carried out using whole virus.

We have also investigated the level of expression of numerous DDR proteins to rule out the idea that variations detected are due to protein degradation, since inactivation of Daxx during HAdV5 infection needs just E1B55K but not E4orf6 (Schreiner *et al.*, 2010). As HAdV12-E1B55K seems to interfere with DNA replication, we looked at how it could alter the expression of some of the origin recognition complex (ORC) and the pre-replicative complex components. ORC proteins expression was found to be distinct between the 'normal' and viral protein expressing cells, as was MCM2 expression, both of which might have an impact on DNA replication. Additionally, some DDR proteins, like BLM, have different levels of expression in the two cell groups. Furthermore, p53 is substantially overexpressed in 55K<sup>+</sup>HSFs; nonetheless, it is probable that it is transcriptionally inactive (Yew and Berk, 1992; Grand *et al.*, 1996). We reasoned that the observed differences in the expressions of DDR proteins were probably insufficient to account for the obvious distinctions in characteristics that were found



between the two cell groups (except p53), although this suggestion would need to be verified by more research. In addition, the implications of having high levels of transcriptionally inactive p53 are not entirely understood (Grand *et al.*, 1996). It is likely, however, that the appreciable differences seen in the levels of replisome components could be, at least in part, responsible for differences that we observed in DNA replication dynamics.

Consequently, proteins known to bind with E1B55K but not examined here likely contribute to some of the reported effects in this research (some of these interactions are analysed in Chapter 3); since the E1B55K interactome is substantially larger than the DDR (reviewed in (Hidalgo *et al.*, 2019)). However, it is likely that the effects of HAdV12-E1B55K on DNA replication and its interference with HR, as well as possible additional DNA repair processes, might account for the genomic instability initially observed in human cells exposed to this viral protein.

Most, if not all, cellular pathways are regulated at some level through protein-protein interactions and interaction networks. Proteins at the centre of a network form a 'protein hub' (Maslov and Sneppen, 2002; Rual *et al.*, 2005; Stelzl *et al.*, 2005). There is now considerable evidence to show that HAdV5-E1A forms such a 'hub', which, in turn, interacts with many cellular hub proteins (Pelka *et al.*, 2008; King *et al.*, 2018). Interactions of this kind can target the cellular protein interaction networks and monopolise the cell. Moreover, viral proteins often target cellular "hub" proteins to appropriate a particular cellular network, indicating the mechanism by which the virus takes control of the cell, facilitating viral replication. It has been suggested that through 32 primary interactions, HAdV5-E1A can make over 2000 secondary interactions (King *et al.*, 2018). Based on the observed multiple and diverse interactions, it

seems possible that HAdV-E1B55K could also form a protein hub and target cellular hubs as is the case for HAdV-E1A. For example, it is clear that HAdV5-E1B55K has a propensity for components of the DDR and proteins involved in RNA metabolism; these cellular pathways could be seen as forming protein hubs. Previous studies suggested that the multiple interactions of HAdV-E1A were through SLiMs (short interaction motifs) which tend to be intrinsically disordered but contain a protein binding site within a short linear amino acid sequence (Pelka *et al.*, 2008; Davey, Travé and Gibson, 2011; Davey, Cyert and Moses, 2015). Although the central region of E1B55K is predicted to be structured, its N and C-terminal regions are probably random coil. It is possible that these could be the sequences forming multiple interactions and impacting on cellular protein hubs.

#### **6.1.4 The potential roles of HAdV-E1B55K from groups B, D, E, and F in the DDR, DNA repair and replication stress.**

Over the past two decades there has been considerable interest in the possibility of using mutant HAdVs as anti-tumour agents (oncolytic adenoviruses) (Larson *et al.*, 2015; Duffy, Fisher and Seymour, 2017). Originally the HAdV5-E1B55K negative virus *d1/1520* (also termed 'Onyx-015') was used, based on the assumption that it could replicate in p53-mutant or p53 negative tumour cells but could not replicate in surrounding 'normal' cells where p53 was functional (Bischoff *et al.*, 1996). Later a significant number of oncolytic viruses have been developed (based, for example, on HSV, vaccinia and adeno-associated viruses), but there is appreciable evidence to suggest that HAdVs have advantages as therapeutic agents. More recent oncolytic HAdVs have had modifications to genes other than E1B55K and have been

based on types other than HAdV5. For example, *Enadenotucirev*, which is a chimera of group B viruses (HAdV3 and HAdV11) with a complex series of deletions is in Phase I/II clinical trials (Chia *et al.*, 2017). However, our understanding of the properties of the group B, D, E, and F viruses is much more limited than is the case for those from group C (HAdV5) and group A (HAdV12). Relevant to this thesis, this is the case for E1B55K proteins as well as most other homologues. Therefore, characterisation of the E1B55K proteins is necessary to fully understand the mode of action of these potentially important anti-tumour agents.

In the past, scientific investigations on groups B, D, E, and F HAdVs have been much less frequent and relatively limited. In this thesis we have already shown that HAdV12-E1B55K can induce genome instability in human fibroblasts in the absence of any other viral proteins (see Chapter 4). We have determined that this is likely to be due to its impact on DNA replication and DNA repair pathways, probably through direct interaction with multiple cellular targets. Therefore, we examined whether E1B55K proteins from groups B, D, E and F HAdVs have some comparable properties. We analysed the effects of E1B55Ks from these viral groups on the activation of host DDR pathways, the induction of host genome instability, and on DSB repair. We have examined if the HAdV-E1B55K proteins from these viral types induces genomic instability in human tumour cells and how their presence impacts on the ability of the cells to respond to DNA damaging agents in the absence of any other viral proteins. The effect these E1B55K constructs have on HR repair activity was also studied in this thesis by analysing DNA damage repair focus formation, both before and after introducing DNA damaging agents.

We have determined that all HAdV types studied here had effects on the phosphorylation of host cellular DDR proteins and induction of genomic instability, although to a lesser extent

than was seen in the case of HAdV12 (group A). Additionally, results shown here may demonstrate a limited effect exerted by viral E1B55Ks from groups B, D, E, and F on the expression levels of DSB repair pathways components, suggesting that E1B55K from these viral types might utilise more diverse tactics in the absence of DDR proteins degradation to impinge cellular DDR than has been described for HAdV5 and HAdV12 (Chapter 3). We have also shown that E1B55K from groups B, D, E, and F HAdVs causes genomic instability in human tumour cells, seen as an increase in micronuclei formation in undamaged cycling cells, as well as after treatment of the cells with IR. These effects are, again, less marked than those seen in HSF cells expressing HAdV12-E1B55K. Indeed, this may indicate that E1B55K from groups B, D, E, and F HAdVs interferes with the cellular response to DNA damage in a manner that is distinct from its well-characterised capacity to degrade DDR proteins with E4orf6, as was shown in past studies (Cheng *et al.*, 2013). It must be remembered, however, that protein degradation during HAdV3, 7, 9 and 11 infections is much more limited than is the case for HAdV5 (Forrester *et al.*, 2011). The viral proteins also exhibited only a limited inhibition on DSB repair pathways; seen by the increased formation of HR repair foci after IR-induced DNA damage. Again, the effect was less marked in comparison to HSF cells expressing HAdV12-E1B55K. The only significant difference seen in phosphorylation of HR pathway components between control and transfected cells after IR was in the levels of  $\gamma$ H2AX, possibly suggesting major effects on other DDR pathways. The results from the experiments with the 55K<sup>+</sup>HSFs and HeLa cells transfected with E1B55K constructs are not directly comparable but do give an indication that HAdV12-E1B55K is more potent at disruption of the DDR; this might be explained by a different set of interactions with cellular targets, but this will require further investigation.

The observations that HAdV-E1B55K proteins from group B, D, E and F HAdVs have less effect on genome stability and the DDR than HAdV12-E1B55K, is consistent with the observations that HAdV12 is oncogenic whereas the other viruses are not, although it is important to note that factors other than E1B55K properties will help to determine transformation, such as the properties of the HAdV-E1A protein. In conclusion, our investigation into whether different HAdV types vary in their ability to inhibit DDR revealed that, in contrast to HAdV12, certain viral types are unable to bypass this inhibition, but may imply that different HAdV types might adopt different tactics to repress cellular proteins by binding them to E1B55K proteins rather than inducing their degradation. In regard to this, it was shown that although the majority of E1B55K functions in infected cells are linked to its association with E4orf6 (Sarnow, Sullivan and Levine, 1982; Harada *et al.*, 2002), the E1B55K protein also has functions that are independent of the E4orf6 protein, and thus, its E3 ubiquitin ligase activity. Hence, more work needs to be undertaken to establish the precise roles of this protein during HAdV infection and the significance of its interactions with HAdV-E1B55Ks.

Interestingly, we have identified several novel E1B55K-interacting DDR proteins in these viral types, such as ATR, ATM, USP7, and UBR5. Mre11 and DNA ligase IV were also shown to co-immunoprecipitate with E1B55K in these viral types; however, these interactions have already been described previously (Cheng *et al.*, 2013).

A large number of binding proteins have been identified for HAdV5-E1B55K (reviewed in (Hidalgo *et al.*, 2019)). Therefore, we applied mass spectrometry analysis to determine whether some of the same proteins associated with E1B55Ks from groups B, D, E, and F viruses in human tumour cells. Significantly, we have identified a large list of novel E1B55K-interacting

proteins, which had not been described previously. Our list also identified some E3 ubiquitin ligase subunits and their substrates, proteins that are involved in the regulation of mRNA metabolism, as well as, previously reported HAdV5-E1B55K interacting proteins, such as MRE11 and RAD50. Unfortunately, lack of time meant that this experiment could not be repeated to confirm these initial findings. Furthermore, it must be remembered that 'mass spec analysis' tends to produce an appreciable number of false positives.

It is well established that E1B55K serves as the binding component for many cellular targets which are ubiquitylated and degraded by the E3 Ligase complex during HAdV infection (Blackford and Grand, 2009; Hidalgo *et al.*, 2019; Herrmann *et al.*, 2020; Kleinberger, 2020). In a past study, where cells were transfected with E1B55K and E4orf6 only, viral types were shown to differ significantly in their ability to associate with and/or degrade different DDR substrates, with some causing either minimal or negligible degradation, while others caused exceptionally efficient degradation (Cheng *et al.*, 2013). For instance, in that study there were examples of DDR proteins that bound efficiently to E1B55K but were not degraded, such as p53 in the case of HAdV16 (group B) and HAdV9 (group D). Other examples demonstrated that substrates were degraded despite binding to E1B55K being low or undetectable, such as BLM during HAdV40 (group F) E1B55K/E4orf6 transfections. Furthermore, it has been shown that p53 does not distinctly associate with E1B55K, nor it is degraded in cells transfected with HAdV4 (group E) E1B55K/E4orf6 (as shown by co-immunoprecipitation assays). Therefore, it is not enough to only attribute the degradation of targets by E4orf6/E1B55K E3 ubiquitin ligases to the degree of stable binding of these targets to E1B55K, the assumed substrate recognition protein; hence, those results imply a degree of complexity in the mode of action of the E1B55K/E4orf6 complex itself and the specificity of substrate choice among HAdVs. In

this thesis we have shown that multiple novel DDR substrates associated with E1B55Ks from groups B, D, E, and F HAdVs in transfected HeLa cells. Previously, our lab reported that degradation of MRE11, p53 and TOPBP1 only occurred during HAdV5 and HAdV12 infection and not with group B, D, E and F viruses (Forrester *et al.*, 2011). Therefore, this might suggest that stable interaction of a substrate with E1B55K is not the only factor that determines how effectively it degrades; as a result, efficient degradation of a substrate might also depend on other unknown factors, such as transient binding or proper positioning of the substrate to the viral ligases as demonstrated in previous studies (Zheng *et al.*, 2002; Cheng *et al.*, 2013). In conclusion, an interesting question that comes to mind is, since many E1B55K proteins from different viral groups share a significant homology in sequences (as demonstrated by (Hidalgo *et al.*, 2019)), why would HAdV5, and to a lesser extent, HAdV12 go to all the trouble of degrading several DDR proteins during infection when viral types from other groups clearly do not share this feature (Cheng *et al.*, 2011, 2013)? This may partly be explained by determining whether all these viruses bind the same cellular and DDR targets as HAdV5 and HAdV12; however, this is not examined in the current study and, thus, needs further elucidation in future studies.

## **6.2 Unanswered questions and future work**

Throughout this thesis I have mentioned further experiments which could have been carried out with more time (the COVID-19 pandemic reduced my time in the lab appreciably) or in future investigations. I will briefly summarise these suggestions here.

1. DNA fibre assays should be performed on HeLa cells transfected with E1B55K from the group B, C, D, E and F viruses to see if similar effects are observed to those, we have seen with HAdV12 in Chapter 4.
2. Experiments outlined in Chapter 5 should be repeated using transfected HAdV5 E1B55K to give a more complete picture of the relationship between all E1B55K proteins and the DDR, and replication stress.
3. The mass spec analysis described in Chapter 5 should be repeated to confirm the observations. It should also be carried out with HAdV5 and HAdV12 E1B55K proteins.
4. Some of the proteins shown to bind HAdV5, and more specifically HAdV12, E1B55Ks are not degraded during infection-we should examine whether they are ubiquitylated.
5. Following on from this the role of ubiquitylation, in the absence of degradation, (as reported by (Herrmann *et al.*, 2020)) is likely to be important for viral infection-this should be investigated in detail.
6. A more detailed investigation of the relationship of HAdV12-E1B55K to the replication machinery would be interesting; for example, ChIP-sequencing analysis to see if it is present at replication forks could be illuminating.



## REFERENCES

- Abraham, R. T. (2001) 'Cell cycle checkpoint signaling through the ATM and ATR kinases', *Genes & development*, 15(17), pp. 2177–2196.
- Abraham, R. T. (2004) 'PI 3-kinase related kinases: 'big' players in stress-induced signaling pathways', *DNA repair*, 3(8–9), pp. 883–887.
- Adams, M. D., McVey, M. and Sekelsky, J. J. (2003) 'Drosophila BLM in double-strand break repair by synthesis-dependent strand annealing', *Science*, 299(5604), pp. 265–267.
- Alberts, B. *et al.* (2002) 'DNA replication mechanisms', in *Molecular Biology of the Cell. 4th edition*. Garland Science.
- Alzu, A. *et al.* (2012) 'Senataxin associates with replication forks to protect fork integrity across RNA-polymerase-II-transcribed genes', *Cell*, 151(4), pp. 835–846.
- Aparicio, O. M., Stout, A. M. and Bell, S. P. (1999) 'Differential assembly of Cdc45p and DNA polymerases at early and late origins of DNA replication', *Proceedings of the National Academy of Sciences*, 96(16), pp. 9130–9135.
- Araujo, F. D. *et al.* (2005) 'Adenovirus type 5 E4orf3 protein targets the Mre11 complex to cytoplasmic aggresomes', *Journal of Virology*, 79(17), pp. 11382–11391. doi: 10.1128/JVI.79.17.11382-11391.2005.
- Arnberg, N. *et al.* (2000) 'Initial Interactions of Subgenus D Adenoviruses with A549 Cellular Receptors: Sialic Acid versus  $\alpha$ vIntegrins', *Journal of virology*, 74(16), pp. 7691–7693.
- Babiss, L. E. and Ginsberg, H. S. (1984) 'Adenovirus type 5 early region 1b gene product is required for efficient shutoff of host protein synthesis', *Journal of Virology*, 50(1), pp. 202–212.
- Babiss, L. E., Ginsberg, H. S. and Darnell Jr., J. E. (1985) 'Adenovirus E1B proteins are required for accumulation of late viral mRNA and for effects on cellular mRNA translation and transport', *Molecular and Cellular Biology*, 5(10), pp. 2552–2558. doi: 10.1128/MCB.5.10.2552.
- Bahassi, E. L. *et al.* (2004) 'Cdc25C phosphorylation on serine 191 by Plk3 promotes its nuclear translocation', *Oncogene*, 23(15), pp. 2658–2663.
- Bailey, A. D. *et al.* (1995) 'Adenovirus type 12-induced fragility of the human RNU2 locus requires U2 small nuclear RNA transcriptional regulatory elements', *Molecular and cellular biology*, 15(11), pp. 6246–6255.
- Baker, A. *et al.* (2007) 'Adenovirus E4 34k and E1b 55k oncoproteins target host DNA ligase IV for proteasomal degradation', *Journal of Virology*, 81(13), pp. 7034–7040. doi: 10.1128/JVI.00029-07.
- Balakrishnan, L. and Bambara, R. A. (2013) 'Okazaki fragment metabolism', *Cold Spring*

*Harbor Perspectives in Biology*, 5(2), p. a010173.

Banin, S. *et al.* (1998) 'Enhanced phosphorylation of p53 by ATM in response to DNA damage', *Science*, 281(5383), pp. 1674–1677.

Baumann, P., Benson, F. E. and West, S. C. (1996) 'Human Rad51 protein promotes ATP-dependent homologous pairing and strand transfer reactions in vitro', *Cell*, 87(4), pp. 757–766.

Ben-Israel, H. and Kleinberger, T. (2002) 'Adenovirus and cell cycle control', *Frontiers in Bioscience-Landmark*, 7(4), pp. 1369–1395.

Berk, A. J. (2005) 'Recent lessons in gene expression, cell cycle control, and cell biology from adenovirus', *Oncogene*, pp. 7673–7685. doi: 10.1038/sj.onc.1209040.

Berk, A. J. (2013) 'Adenoviridae, p 1704–1731', *Fields virology*, 6th ed. Lippincott Williams & Wilkins, Philadelphia, PA.

Bernards, R. *et al.* (1982) 'Characterization of cells transformed by Ad5/Ad12 hybrid early region I plasmids', *Virology*, 120(2), pp. 422–432. doi: 10.1016/0042-6822(82)90042-3.

Bernards, R., Schrier, P. I., Bos, J. L., *et al.* (1983) 'Role of adenovirus types 5 and 12 early region 1 b tumor antigens in oncogenic transformation', *Virology*, 127(1), pp. 45–53. doi: 10.1016/0042-6822(83)90369-0.

Bernards, R., Schrier, P. I., Houweling, A., *et al.* (1983) 'Tumorigenicity of cells transformed by adenovirus type 12 by evasion of T-cell immunity', *Nature*, 305(5937), pp. 776–779.

Bernards, R. *et al.* (1986) 'Role of the adenovirus early region 1B tumor antigens in transformation and lytic infection', *Virology*, 150(1), pp. 126–139. doi: 10.1016/0042-6822(86)90272-2.

Bernards, R. and Van der Eb, A. J. (1984) 'Adenovirus: transformation and oncogenicity', *Biochimica et Biophysica Acta (BBA)-Gene Structure and Expression*, 783(3), pp. 187–204.

Berscheminski, J. *et al.* (2013) 'The adenoviral oncogene E1A-13S interacts with a specific isoform of the tumor suppressor PML to enhance viral transcription', *Journal of Virology*, 87(2), pp. 965–977.

Binz, S. K., Sheehan, A. M. and Wold, M. S. (2004) 'Replication protein A phosphorylation and the cellular response to DNA damage', *DNA repair*, 3(8–9), pp. 1015–1024.

Bischoff, J. R. *et al.* (1996) 'An adenovirus mutant that replicates selectively in p53-deficient human tumor cells', *Science*, 274(5286), pp. 373–376. doi: 10.1126/science.274.5286.373.

Blackford, A. N. *et al.* (2008) 'A role for E1B-AP5 in ATR signaling pathways during adenovirus infection', *Journal of Virology*, 82(15), pp. 7640–7652. doi: 10.1128/JVI.00170-08.

Blackford, A. N. *et al.* (2010) 'Adenovirus 12 E4orf6 inhibits ATR activation by promoting TOPBP1 degradation', *Proceedings of the National Academy of Sciences*, 107(27), pp. 12251–

12256.

Blackford, A. N. and Grand, R. J. A. (2009) 'Adenovirus E1B 55-Kilodalton Protein: Multiple Roles in Viral Infection and Cell Transformation', *Journal of Virology*, 83(9), pp. 4000–4012. doi: 10.1128/jvi.02417-08.

Blackford, A. N. and Jackson, S. P. (2017) 'ATM, ATR, and DNA-PK: The Trinity at the Heart of the DNA Damage Response', *Molecular cell*, 66(6), pp. 801–817.

Blanchette, P. *et al.* (2004) 'Both BC-box motifs of adenovirus protein E4orf6 are required to efficiently assemble an E3 ligase complex that degrades p53', *Molecular and Cellular Biology*, 24(21), pp. 9619–9629. doi: 10.1128/MCB.24.21.9619-9629.2004.

Blanchette, P. *et al.* (2008) 'Control of mRNA export by adenovirus E4orf6 and E1B55K proteins during productive infection requires E4orf6 ubiquitin ligase activity', *Journal of Virology*, 82(6), pp. 2642–2651. doi: 10.1128/JVI.02309-07.

Blanchette, P. *et al.* (2013) 'Aggresome formation by the adenoviral protein E1B55K is not conserved among adenovirus species and is not required for efficient degradation of nuclear substrates', *Journal of virology*, 87(9), pp. 4872–4881.

Boguslawski, S. J. *et al.* (1986) 'Characterization of monoclonal antibody to DNA· RNA and its application to immunodetection of hybrids', *Journal of immunological methods*, 89(1), pp. 123–130.

Boos, D. *et al.* (2011) 'Regulation of DNA replication through Sld3-Dpb11 interaction is conserved from yeast to humans', *Current Biology*, 21(13), pp. 1152–1157.

Boubakri, H. *et al.* (2010) 'The helicases DinG, Rep and UvrD cooperate to promote replication across transcription units in vivo', *The EMBO journal*, 29(1), pp. 145–157.

Boulanger, P. A. and Blair, G. E. (1991) 'Expression and interactions of human adenovirus oncoproteins.', *Biochemical journal*, 275(Pt 2), p. 281.

Boyer, J., Rohleder, K. and Ketner, G. (1999) 'Adenovirus E4 34k and E4 11k inhibit double strand break repair and are physically associated with the cellular DNA-dependent protein kinase', *Virology*, 263(2), pp. 307–312.

Brenner, S. and Horne, R. W. (1959) 'A negative staining method for high resolution electron microscopy of viruses', *Biochimica et biophysica acta*, 34, pp. 103–110.

Bridge, E. and Ketner, G. (1989) 'Redundant control of adenovirus late gene expression by early region 4', *Journal of virology*, 63(2), pp. 631–638.

Bridge, E. and Ketner, G. (1990) 'Interaction of adenoviral E4 and E1b products in late gene expression', *Virology*, 174(2), pp. 345–353.

Brooks, C. L. and Gu, W. (2003) 'Ubiquitination, phosphorylation and acetylation: the molecular basis for p53 regulation', *Current opinion in cell biology*, 15(2), pp. 164–171.

- Bulavin, D. V *et al.* (2001) 'Initiation of a G2/M checkpoint after ultraviolet radiation requires p38 kinase', *Nature*, 411(6833), pp. 102–107.
- Bürck, C. *et al.* (2016) 'KAP1 is a host restriction factor that promotes human adenovirus E1B-55K SUMO modification', *Journal of Virology*, 90(2), pp. 930–946.
- Burckhardt, C. J. *et al.* (2011) 'Drifting motions of the adenovirus receptor CAR and immobile integrins initiate virus uncoating and membrane lytic protein exposure', *Cell host & microbe*, 10(2), pp. 105–117.
- Burgert, H.-G. *et al.* (2002) 'Subversion of host defense mechanisms by adenoviruses', in *Viral Proteins Counteracting Host Defenses*. Springer, pp. 273–318.
- Byrd, P., Brown, K. W. and Gallimore, P. H. (1982) 'Malignant transformation of human embryo retinoblasts by cloned adenovirus 12 DNA', *Nature*, 298(5869), pp. 69–71. doi: 10.1038/298069a0.
- Byun, T. S. *et al.* (2005) 'Functional uncoupling of MCM helicase and DNA polymerase activities activates the ATR-dependent checkpoint', *Genes & development*, 19(9), pp. 1040–1052.
- Caporossi, D. and Bacchetti, S. (1990) 'Definition of adenovirus type 5 functions involved in the induction of chromosomal aberrations in human cells', *Journal of general virology*, 71(4), pp. 801–808.
- Caporossi, D., Bacchetti, S. and Nicoletti, B. (1991) 'Synergism between aphidicolin and adenoviruses in the induction of breaks at fragile sites on human chromosomes', *Cancer genetics and cytogenetics*, 54(1), pp. 39–53.
- Cardoso, F. M. *et al.* (2008) 'An early function of the adenoviral E1B 55 kDa protein is required for the nuclear relocalization of the cellular p53 protein in adenovirus-infected normal human cells', *Virology*, 378(2), pp. 339–346. doi: 10.1016/j.virol.2008.06.016.
- Carson, C. T. *et al.* (2003) 'The Mre11 complex is required for ATM activation and the G2/M checkpoint', *EMBO Journal*, 22(24), pp. 6610–6620. doi: 10.1093/emboj/cdg630.
- Carson, C. T. *et al.* (2009) 'Mislocalization of the MRN complex prevents ATR signaling during adenovirus infection', *The EMBO journal*, 28(6), pp. 652–662.
- Carvalho, T. *et al.* (1995) 'Targeting of adenovirus E1A and E4-ORF3 proteins to nuclear matrix-associated PML bodies', *Journal of Cell Biology*, 131(1), pp. 45–56. doi: 10.1083/jcb.131.1.45.
- Cary, R. B. *et al.* (1997) 'DNA looping by Ku and the DNA-dependent protein kinase', *Proceedings of the National Academy of Sciences*, 94(9), pp. 4267–4272.
- Cathomen, T. and Weitzman, M. D. (2000) 'A functional complex of adenovirus proteins E1B-55kDa and E4orf6 is necessary to modulate the expression level of p53 but not its transcriptional activity', *Journal of virology*, 74(23), pp. 11407–11412.

- Chahal, J. S., Qi, J. and Flint, S. J. (2012) 'The human adenovirus type 5 E1B 55 kDa protein obstructs inhibition of viral replication by type I interferon in normal human cells', *PLoS pathogens*, 8(8), p. e1002853.
- Chalabi Hagkarim, N. *et al.* (2018) 'Degradation of a Novel DNA Damage Response Protein, Tankyrase 1 Binding Protein 1, following Adenovirus Infection', *Journal of Virology*, 92(12). doi: 10.1128/jvi.02034-17.
- Chan, H. M. *et al.* (2005) 'The p400 E1A-associated protein is a novel component of the p53→ p21 senescence pathway', *Genes & development*, 19(2), pp. 196–201.
- Cheng, C. Y. *et al.* (2011) 'The E4orf6/E1B55K E3 ubiquitin ligase complexes of human adenoviruses exhibit heterogeneity in composition and substrate specificity', *Journal of virology*, 85(2), pp. 765–775.
- Cheng, C. Y. *et al.* (2013) 'Role of E1B55K in E4orf6/E1B55K E3 Ligase Complexes Formed by Different Human Adenovirus Serotypes', *Journal of Virology*, 87(11), pp. 6232–6245. doi: 10.1128/jvi.00384-13.
- Cheok, C. F. *et al.* (2005) 'Roles of the Bloom's syndrome helicase in the maintenance of genome stability'. Portland Press Limited.
- Chia, S.-L. *et al.* (2017) 'Group B adenovirus enadenotucirev infects polarised colorectal cancer cells efficiently from the basolateral surface expected to be encountered during intravenous delivery to treat disseminated cancer', *Virology*, 505, pp. 162–171.
- Ching, W. *et al.* (2013) 'A ubiquitin-specific protease possesses a decisive role for adenovirus replication and oncogene-mediated transformation', *PLoS pathogens*, 9(3), p. e1003273.
- Ciccia, A. and Elledge, S. J. (2010) 'The DNA damage response: making it safe to play with knives', *Molecular cell*, 40(2), pp. 179–204.
- Cimprich, K. A. and Cortez, D. (2008) 'ATR: an essential regulator of genome integrity', *Nature reviews Molecular cell biology*, 9(8), pp. 616–627.
- Cojocaru, M. *et al.* (2011) 'Transcription factor IIS cooperates with the E3 ligase UBR5 to ubiquitinate the CDK9 subunit of the positive transcription elongation factor B', *Journal of Biological Chemistry*, 286(7), pp. 5012–5022.
- Corbin-Lickfett, K. A. and Bridge, E. (2003) 'Adenovirus E4-34kDa requires active proteasomes to promote late gene expression', *Virology*, 315(1), pp. 234–244. doi: 10.1016/S0042-6822(03)00527-0.
- Cortez, D. (2015) 'Preventing replication fork collapse to maintain genome integrity', *DNA repair*, 32, pp. 149–157.
- Cuconati, A. *et al.* (2002) 'Bak and Bax function to limit adenovirus replication through apoptosis induction', *Journal of virology*, 76(9), pp. 4547–4558.
- Dallaire, F. *et al.* (2009) 'Identification of integrin  $\alpha 3$  as a new substrate of the adenovirus

E4orf6/E1B 55-kilodalton E3 ubiquitin ligase complex', *Journal of virology*, 83(11), pp. 5329–5338.

Dallaire, F., Blanchette, P. and Branton, P. E. (2009) 'A proteomic approach to identify candidate substrates of human adenovirus E4orf6-E1B55K and other viral cullin-based E3 ubiquitin ligases', *Journal of virology*, 83(23), pp. 12172–12184.

Davey, N. E., Cyert, M. S. and Moses, A. M. (2015) 'Short linear motifs—ex nihilo evolution of protein regulation', *Cell Communication and Signaling*, 13(1), pp. 1–15.

Davey, N. E., Travé, G. and Gibson, T. J. (2011) 'How viruses hijack cell regulation', *Trends in biochemical sciences*, 36(3), pp. 159–169.

Debbas, M. and White, E. (1993) 'Wild-type p53 mediates apoptosis by E1A, which is inhibited by E1B', *Genes and Development*, 7(4), pp. 546–554. doi: 10.1101/gad.7.4.546.

DeCaprio, J. A. (2009) 'How the Rb tumor suppressor structure and function was revealed by the study of Adenovirus and SV40', *Virology*, 384(2), pp. 274–284.

DeLeo, A. B. *et al.* (1979) 'Detection of a transformation-related antigen in chemically induced sarcomas and other transformed cells of the mouse.', *Proceedings of the National Academy of Sciences*, 76(5), pp. 2420–2424.

Deleu, L. *et al.* (2001) 'Recruitment of TRRAP required for oncogenic transformation by E1A', *Oncogene*, 20(57), pp. 8270–8275.

Dobbelstein, M. *et al.* (1997) 'Nuclear export of the E1B 55-kDa and E4 34-kDa adenoviral oncoproteins mediated by a rev-like signal sequence', *EMBO Journal*, 16(14), pp. 4276–4284. doi: 10.1093/emboj/16.14.4276.

Dobner, T. *et al.* (1996) 'Blockage by adenovirus E4orf6 of transcriptional activation by the p53 tumor suppressor', *Science*, 272(5267), pp. 1470–1473.

Doucas, V. *et al.* (1996) 'Adenovirus replication is coupled with the dynamic properties of the PML nuclear structure', *Genes and Development*, 10(2), pp. 196–207. doi: 10.1101/gad.10.2.196.

Duda, D. M. *et al.* (2008) 'Structural insights into NEDD8 activation of cullin-RING ligases: conformational control of conjugation', *Cell*, 134(6), pp. 995–1006.

Duffy, M. R., Fisher, K. D. and Seymour, L. W. (2017) 'Making oncolytic virotherapy a clinical reality: the European contribution', *Human gene therapy*, 28(11), pp. 1033–1046.

Dunsworth-Browne, M., Schell, R. E. and Berk, A. J. (1980) 'Adenovirus terminal protein protects single stranded DNA from digestion by a cellular exonuclease', *Nucleic acids research*, 8(3), pp. 543–554.

Durnam, D. M. *et al.* (1986) 'The E1 region of human adenovirus type 12 determines the sites of virally induced chromosomal damage', *Cancer cells*, 4, pp. 349–354.

- Durnam, D. M. *et al.* (1988) 'A fragile site in the human U2 small nuclear RNA gene cluster is revealed by adenovirus type 12 infection', *Molecular and cellular biology*, 8(5), pp. 1863–1867.
- Dybas, J. M., Herrmann, C. and Weitzman, M. D. (2018) 'Ubiquitination at the interface of tumor viruses and DNA damage responses', *Current opinion in virology*, 32, pp. 40–47.
- Dye, B. T. and Schulman, B. A. (2007) 'Structural mechanisms underlying posttranslational modification by ubiquitin-like proteins', *Annu. Rev. Biophys. Biomol. Struct.*, 36, pp. 131–150.
- Dyson, N. *et al.* (1989) 'The human papilloma virus-16 E7 oncoprotein is able to bind to the retinoblastoma gene product', *Science*, 243(4893), pp. 934–937.
- Dyson, N. (1998) 'The regulation of E2F by pRB-family proteins', *Genes & development*, 12(15), pp. 2245–2262.
- Eager, K. B. *et al.* (1985) 'Expression of histocompatibility antigens H-2K,-D, and-L is reduced in adenovirus-12-transformed mouse cells and is restored by interferon gamma.', *Proceedings of the National Academy of Sciences*, 82(16), pp. 5525–5529.
- Echavarría, M. (2015) 'Adenoviruses', in *eLS*. Chichester, UK: John Wiley & Sons, Ltd. doi: 10.1002/9780470015902.a0000409.pub2.
- Eckner, R. *et al.* (1994) 'Molecular cloning and functional analysis of the adenovirus E1A-associated 300-kD protein (p300) reveals a protein with properties of a transcriptional adaptor.', *Genes & development*, 8(8), pp. 869–884.
- Elford, H. L. (1968) 'Effect of hydroxyurea on ribonucleotide reductase'.
- Van Den Elsen, P., Houweling, A. and Van Der Eb, A. (1983) 'Expression of region E1b of human adenoviruses in the absence of region E1a is not sufficient for complete transformation', *Virology*, 128(2), pp. 377–390.
- Endter, C. *et al.* (2001) 'SUMO-1 modification required for transformation by adenovirus type 5 early region 1B 55-kDa oncoprotein', *Proceedings of the National Academy of Sciences of the United States of America*, 98(20), pp. 11312–11317. doi: 10.1073/pnas.191361798.
- Endter, C. and Dobner, T. (2004) 'Cell transformation by human adenoviruses', *Current Topics in Microbiology and Immunology*, pp. 163–214.
- Evans, J. D. and Hearing, P. (2005) 'Relocalization of the Mre11-Rad50-Nbs1 complex by the adenovirus E4 ORF3 protein is required for viral replication', *Journal of Virology*, 79(10), pp. 6207–6215. doi: 10.1128/JVI.79.10.6207-6215.2005.
- Everett, R. D. (2001) 'DNA viruses and viral proteins that interact with PML nuclear bodies', *Oncogene*, 20(49), pp. 7266–7273.
- Falck, J. *et al.* (2001) 'The ATM–Chk2–Cdc25A checkpoint pathway guards against radioresistant DNA synthesis', *Nature*, 410(6830), pp. 842–847.

- De Falco, M. *et al.* (2007) 'The human GINS complex binds to and specifically stimulates human DNA polymerase  $\alpha$ -primase', *EMBO reports*, 8(1), pp. 99–103.
- Falgout, B. and Ketner, G. (1987) 'Adenovirus early region 4 is required for efficient virus particle assembly', *Journal of virology*, 61(12), pp. 3759–3768.
- Fallaux, F. J. *et al.* (1996) 'Characterization of 911: a new helper cell line for the titration and propagation of early region 1-deleted adenoviral vectors', *Human gene therapy*, 7(2), pp. 215–222.
- Fekairi, S. *et al.* (2009) 'Human SLX4 is a Holliday junction resolvase subunit that binds multiple DNA repair/recombination endonucleases', *Cell*, 138(1), pp. 78–89.
- Feng, H. *et al.* (2008) 'Clonal integration of a polyomavirus in human Merkel cell carcinoma', *Science*, 319(5866), pp. 1096–1100.
- Ferrari, R. *et al.* (2014) 'Adenovirus small E1A employs the lysine acetylases p300/CBP and tumor suppressor Rb to repress select host genes and promote productive virus infection', *Cell host & microbe*, 16(5), pp. 663–676.
- Finlay, C. A., Hinds, P. W. and Levine, A. J. (1989) 'The p53 proto-oncogene can act as a suppressor of transformation', *Cell*, 57(7), pp. 1083–1093.
- Forrester, N. A. *et al.* (2011) 'Serotype-Specific Inactivation of the Cellular DNA Damage Response during Adenovirus Infection', *Journal of Virology*, 85(5), pp. 2201–2211. doi: 10.1128/jvi.01748-10.
- Fournier, L.-A. *et al.* (2021) 'Global prediction of candidate R-loop binding and R-loop regulatory proteins', *bioRxiv*, p. 2021.08.09.454968. doi: 10.1101/2021.08.09.454968.
- Fragkos, M. *et al.* (2015) 'DNA replication origin activation in space and time', *Nature reviews Molecular cell biology*, 16(6), pp. 360–374.
- Freeman *et al.* (1967) 'Adenovirus type 12-rat embryo transformation system', *Journal of Virology*, 1(2), pp. 362–367.
- Freeman, A. E. *et al.* (1967) 'Transformation of primary rat embryo cells by adenovirus type 2.', *Proceedings of the National Academy of Sciences of the United States of America*, 58(3), pp. 1205–1212. doi: 10.1073/pnas.58.3.1205.
- Friefeld, B. R. *et al.* (1984) 'The in vitro replication of adenovirus DNA', in *The Molecular Biology of Adenoviruses 2*. Springer, pp. 221–255.
- Fu, Y. R. *et al.* (2017) 'Comparison of protein expression during wild-type, and E1B-55k-deletion, adenovirus infection using quantitative time-course proteomics', *The Journal of general virology*, 98(6), p. 1377.
- Gabler, S. *et al.* (1998) 'E1B 55-kilodalton-associated protein: A cellular protein with RNA-binding activity implicated in nucleocytoplasmic transport of adenovirus and cellular mRNAs', *Journal of Virology*, 72(10), pp. 7960–7971.



- Gallimore, P. H. (1972) 'Tumour production in immunosuppressed rats with cells transformed in vitro by adenovirus type 2', *Journal of General Virology*, 16(1), pp. 99–102.
- Gallimore, P. H. *et al.* (1985) 'Properties of rat cells transformed by DNA plasmids containing adenovirus type 12 E1 DNA or specific fragments of the E1 region: comparison of transforming frequencies', *Cancer research*, 45(6), pp. 2670–2680.
- Gallimore, P. H. *et al.* (1997) 'Adenovirus type 12 early region 1B 54K protein significantly extends the life span of normal mammalian cells in culture', *Journal of virology*, 71(9), pp. 6629–6640.
- Gallimore, P. H., Grand, R. J. and Byrd, P. J. (1986) 'Transformation of human embryo retinoblasts with simian virus 40, adenovirus and ras oncogenes.', *Anticancer research*, 6(3 Pt B), pp. 499–508.
- Gallimore, P. H., McDougall, J. K. and Chen, L. B. (1977) 'In vitro traits of adenovirus-transformed cell lines and their relevance to tumorigenicity in nude mice', *Cell*, 10(4), pp. 669–678.
- Gallimore, P. H., Sharp, P. A. and Sambrook, J. (1974) 'Viral DNA in transformed cells. II. A study of the sequences of adenovirus 2 DNA in nine lines of transformed rat cells using specific fragments of the viral genome', *Journal of Molecular Biology*, 89(1), pp. 49–72. doi: 10.1016/0022-2836(74)90162-4.
- Gallimore, P. H. and Turnell, A. S. (2001) 'Adenovirus E1A: remodelling the host cell, a life or death experience', *Oncogene*, 20(54), pp. 7824–7835.
- Gao, J. *et al.* (2019) 'State-of-the-art human adenovirus vectorology for therapeutic approaches', *FEBS Letters*, 593(24), pp. 3609–3622. doi: 10.1002/1873-3468.13691.
- Gao, J., Zhang, W. and Ehrhardt, A. (2020) 'Expanding the Spectrum of Adenoviral Vectors for Cancer Therapy', *Gao, J.; Zhang, W.; Ehrhardt, A. Expanding the Spectrum of Adenoviral Vectors for Cancer Therapy. Cancers* 2020, 12, 1139.
- García-Mata, R. *et al.* (1999) 'Characterization and Dynamics of Aggresome Formation by a Cytosolic Gfp-Chimera<sup>+</sup>', *The Journal of cell biology*, 146(6), pp. 1239–1254.
- García-Pichardo, D. *et al.* (2017) 'Histone mutants separate R loop formation from genome instability induction', *Molecular cell*, 66(5), pp. 597–609.
- Gareau, J. R. and Lima, C. D. (2010) 'The SUMO pathway: emerging mechanisms that shape specificity, conjugation and recognition', *Nature reviews Molecular cell biology*, 11(12), pp. 861–871.
- Gargano, S. *et al.* (1995) 'The transcriptionally competent U2 gene is necessary and sufficient for adenovirus type 12 induction of the fragile site at 17q21-22.', *Molecular and cellular biology*, 15(11), pp. 6256–6261.
- Gatei, M. *et al.* (2003) 'Ataxia-telangiectasia-mutated (ATM) and NBS1-dependent

phosphorylation of Chk1 on Ser-317 in response to ionizing radiation', *Journal of Biological Chemistry*, 278(17), pp. 14806–14811.

Gell, D. and Jackson, S. P. (1999) 'Mapping of protein-protein interactions within the DNA-dependent protein kinase complex', *Nucleic acids research*, 27(17), pp. 3494–3502.

Ghebremedhin, B. (2014) 'Human adenovirus: Viral pathogen with increasing importance', *European Journal of Microbiology and Immunology*, 4(1), pp. 26–33. doi: 10.1556/eujmi.4.2014.1.2.

Glenewinkel, F. *et al.* (2016) 'The adaptor protein DCAF7 mediates the interaction of the adenovirus E1A oncoprotein with the protein kinases DYRK1A and HIPK2', *Scientific reports*, 6(1), pp. 1–15.

Goldberg, M. *et al.* (2003) 'MDC1 is required for the intra-S-phase DNA damage checkpoint', *Nature*, 421(6926), pp. 952–956.

Gonzalez, R. A. and Flint, S. J. (2002) 'Effects of mutations in the adenoviral E1B 55-kilodalton protein coding sequence on viral late mRNA metabolism', *Journal of Virology*, 76(9), pp. 4507–4519. doi: 10.1128/JVI.76.9.4507-4519.2002.

Goodarzi, A. A. *et al.* (2006) 'DNA-PK autophosphorylation facilitates Artemis endonuclease activity', *The EMBO journal*, 25(16), pp. 3880–3889.

Goodrum, F. D. and Ornelles, D. A. (1997) 'The early region 1B 55-kilodalton oncoprotein of adenovirus relieves growth restrictions imposed on viral replication by the cell cycle', *Journal of Virology*, 71(1), pp. 548–561.

Goodrum, F. D. and Ornelles, D. A. (1999) 'Roles for the E4 orf6, orf3, and E1B 55-kilodalton proteins in cell cycle-independent adenovirus replication', *Journal of Virology*, 73(9), pp. 7474–7488.

Goodrum, F. D., Shenk, T. and Ornelles, D. A. (1996) 'Adenovirus early region 4 34-kilodalton protein directs the nuclear localization of the early region 1B 55-kilodalton protein in primate cells', *Journal of Virology*, 70(9), pp. 6323–6335.

Graham, F. L. *et al.* (1977) 'Characteristics of a human cell line transformed by DNA from human adenovirus type 5', *Journal of general virology*, 36(1), pp. 59–72.

Graham, F. L. (1984) 'Transformation by and oncogenicity of human adenoviruses', in *The adenoviruses*. Springer, pp. 339–398.

Graham, F. L. and Van der Eb, A. J. (1973) 'Transformation of rat cells by DNA of human adenovirus 5', *Virology*, 54(2), pp. 536–539.

Graham, F. L., Van Der Eb, A. J. and Heijneker, H. L. (1974) 'Size and location of the transforming region in human adenovirus type 5 DNA', *Nature*, 251(5477), pp. 687–691. doi: 10.1038/251687a0.

Grand, R. J. (2022) 'A link between severe hepatitis in children and adenovirus 41 and adeno-

associated virus 2 infections', *Journal of General Virology*, 103(11), p. 1783.

Grand, R. J. A. *et al.* (1996) 'Control of p53 expression by adenovirus 12 early region 1A and early region 1B 54K proteins', *Virology*, 218(1), pp. 23–34. doi: 10.1006/viro.1996.0162.

Grand, R. J. A., Grant, M. L. and Gallimore, P. H. (1994) 'Enhanced Expression of p53 in Human Cells Infected with Mutant Adenoviruses', *Virology*, 203(2), pp. 229–240. doi: 10.1006/viro.1994.1480.

Grossman, S. R. *et al.* (1998) 'p300/MDM2 complexes participate in MDM2-mediated p53 degradation', *Molecular cell*, 2(4), pp. 405–415.

Grossman, S. R. *et al.* (2003) 'Polyubiquitination of p53 by a ubiquitin ligase activity of p300', *Science*, 300(5617), pp. 342–344.

Gu, W. and Roeder, R. G. (1997) 'Activation of p53 sequence-specific DNA binding by acetylation of the p53 C-terminal domain', *Cell*, 90(4), pp. 595–606. doi: 10.1016/S0092-8674(00)80521-8.

Gudjonsson, T. *et al.* (2012) 'TRIP12 and UBR5 suppress spreading of chromatin ubiquitylation at damaged chromosomes', *Cell*, 150(4), pp. 697–709.

Gupta, A. *et al.* (2013) 'Tip60 degradation by adenovirus relieves transcriptional repression of viral transcriptional activator E1A', *Oncogene*, 32(42), p. 5017.

Halbert, D. N., Cutt, J. R. and Shenk, T. (1985) 'Adenovirus early region 4 encodes functions required for efficient DNA replication, late gene expression, and host cell shutoff', *Journal of Virology*, 56(1), pp. 250–257.

Hanada, K. *et al.* (2007) 'The structure-specific endonuclease Mus81 contributes to replication restart by generating double-strand DNA breaks', *Nature structural & molecular biology*, 14(11), pp. 1096–1104.

Hanahan, D. and Weinberg, R. A. (2000) 'The hallmarks of cancer', *cell*, 100(1), pp. 57–70.

Harada, J. N. *et al.* (2002) 'Analysis of the adenovirus E1B-55K-anchored proteome reveals its link to ubiquitination machinery', *Journal of Virology*, 76(18), pp. 9194–9206. doi: 10.1128/JVI.76.18.9194-9206.2002.

Harbour, J. W. *et al.* (1999) 'Cdk phosphorylation triggers sequential intramolecular interactions that progressively block Rb functions as cells move through G1', *Cell*, 98(6), pp. 859–869.

Harbour, J. W. and Dean, D. C. (2000) 'The Rb/E2F pathway: expanding roles and emerging paradigms', *Genes & development*, 14(19), pp. 2393–2409.

Härtl, B. *et al.* (2008) 'Adenovirus type 5 early region 1B 55-kDa oncoprotein can promote cell transformation by a mechanism independent from blocking p53-activated transcription', *Oncogene*, 27(26), pp. 3673–3684. doi: 10.1038/sj.onc.1211039.

- Hashimoto, Y. *et al.* (2010) 'Rad51 protects nascent DNA from Mre11-dependent degradation and promotes continuous DNA synthesis', *Nature structural & molecular biology*, 17(11), pp. 1305–1311.
- zur Hausen, H. (1967) 'Induction of specific chromosomal aberrations by adenovirus type 12 in human embryonic kidney cells', *Journal of virology*, 1(6), pp. 1174–1185.
- He, G. *et al.* (2005) 'Induction of p21 by p53 following DNA damage inhibits both Cdk4 and Cdk2 activities', *Oncogene*, 24(18), pp. 2929–2943.
- Heffernan, T. P. *et al.* (2007) 'Cdc7-Dbf4 and the human S checkpoint response to UVC', *Journal of Biological Chemistry*, 282(13), pp. 9458–9468.
- Heidenreich, E. *et al.* (2003) 'Non-homologous end joining as an important mutagenic process in cell cycle-arrested cells', *The EMBO journal*, 22(9), pp. 2274–2283.
- Heise, C. *et al.* (1997) 'ONYX-015, an E1B gene-attenuated adenovirus, causes tumor-specific cytolysis and antitumoral efficacy that can be augmented by standard chemotherapeutic agents', *Nature medicine*, 3(6), pp. 639–645.
- Heller, R. C. *et al.* (2011) 'Eukaryotic origin-dependent DNA replication in vitro reveals sequential action of DDK and S-CDK kinases', *Cell*, 146(1), pp. 80–91.
- Hensen, L. C. M., Hoeben, R. C. and Bots, S. T. F. (2020) 'Adenovirus receptor expression in cancer and its multifaceted role in oncolytic adenovirus therapy', *International Journal of Molecular Sciences*, 21(18), p. 6828.
- Hermeking, H. *et al.* (1997) '14-3-3 $\sigma$  is a p53-regulated inhibitor of G2/M progression', *Molecular cell*, 1(1), pp. 3–11.
- Herrmann, C. *et al.* (2020) 'Adenovirus-mediated ubiquitination alters protein–RNA binding and aids viral RNA processing', *Nature microbiology*, 5(10), pp. 1217–1231.
- Van den Heuvel, S. J. *et al.* (1992) 'p53 shares an antigenic determinant with proteins of 92 and 150 kilodaltons that may be involved in senescence of human cells', *Journal of virology*, 66(1), pp. 591–595.
- Hidalgo, P. *et al.* (2019) 'The biology of the adenovirus E1B 55K protein', *FEBS Letters*. Wiley Blackwell, pp. 3504–3517. doi: 10.1002/1873-3468.13694.
- Hillman, M. R. and Werner, J. R. (1954) 'Recovery of a new agent from patients with acute respiratory illness', *Proc. Soc. Exp. Biol. Med*, 85, p. 183.
- Hirao, A. *et al.* (2000) 'DNA damage-induced activation of p53 by the checkpoint kinase Chk2', *Science*, 287(5459), pp. 1824–1827.
- Ho, A. *et al.* (2023) 'Adeno-associated virus 2 infection in children with non-AE hepatitis', *Nature*, pp. 1–5.
- Hoeben, R. C. and Uil, T. G. (2013) 'Adenovirus DNA replication', *Cold Spring Harbor*

*perspectives in biology*, 5(3), p. a013003.

Hollingworth, R. and Grand, R. J. (2015) 'Modulation of DNA damage and repair pathways by human tumour viruses', *Viruses*, pp. 2542–2591. doi: 10.3390/v7052542.

Holm, P. S. *et al.* (2002) 'YB-1 relocates to the nucleus in adenovirus-infected cells and facilitates viral replication by inducing E2 gene expression through the E2 late promoter', *Journal of Biological Chemistry*, 277(12), pp. 10427–10434.

Hoppe, A. *et al.* (2006) 'Interaction of the adenovirus type 5 E4 Orf3 protein with promyelocytic leukemia protein isoform II is required for ND10 disruption', *Journal of virology*, 80(6), pp. 3042–3049.

Horwitz, G. A. *et al.* (2008) 'Adenovirus small e1a alters global patterns of histone modification', *Science*, 321(5892), pp. 1084–1085.

Houweling, A., Van Den Elsen, P. J. and Van Der Eb, A. J. (1980) 'Partial transformation of primary rat cells by the leftmost 4.5% fragment of adenovirus 5 DNA', *Virology*, 105(2), pp. 537–550. doi: 10.1016/0042-6822(80)90054-9.

Howe, J. A. *et al.* (1990) 'Retinoblastoma growth suppressor and a 300-kDa protein appear to regulate cellular DNA synthesis.', *Proceedings of the National Academy of Sciences*, 87(15), pp. 5883–5887.

Hsu, H.-L., Yannone, S. M. and Chen, D. J. (2002) 'Defining interactions between DNA-PK and ligase IV/XRCC4', *DNA repair*, 1(3), pp. 225–235.

Huebner, R. J. *et al.* (1963) 'Specific adenovirus complement-fixing antigens in virus-free hamster and rat tumors', *Proceedings of the National Academy of Sciences*, 50(2), pp. 379–389.

Huen, M. S. Y. *et al.* (2007) 'RNF8 transduces the DNA-damage signal via histone ubiquitylation and checkpoint protein assembly', *Cell*, 131(5), pp. 901–914.

Huertas, P. and Jackson, S. P. (2009) 'Human CtIP mediates cell cycle control of DNA end resection and double strand break repair', *Journal of Biological Chemistry*, 284(14), pp. 9558–9565.

Hung, G. and Flint, S. J. (2017) 'Normal human cell proteins that interact with the adenovirus type 5 E1B 55kDa protein', *Virology*, 504, pp. 12–24. doi: <https://doi.org/10.1016/j.virol.2017.01.013>.

Hupp, T. R. *et al.* (1992) 'Regulation of the specific DNA binding function of p53', *Cell*, 71(5), pp. 875–886.

Hutton, F. G. *et al.* (2000) 'Consequences of disruption of the interaction between p53 and the larger adenovirus early region 1B protein in adenovirus E1 transformed human cells', *Oncogene*, 19(3), pp. 452–462.

Ilves, I. *et al.* (2010) 'Activation of the MCM2-7 helicase by association with Cdc45 and GINS

proteins', *Molecular cell*, 37(2), pp. 247–258.

Ip, S. C. Y. *et al.* (2008) 'Identification of Holliday junction resolvases from humans and yeast', *Nature*, 456(7220), pp. 357–361.

Ip, W. H. and Dobner, T. (2019) 'Cell transformation by the adenovirus oncogenes E1 and E4', *FEBS Letters*, n/a(n/a). doi: 10.1002/1873-3468.13717.

Ira, G., Satory, D. and Haber, J. E. (2006) 'Conservative inheritance of newly synthesized DNA in double-strand break-induced gene conversion', *Molecular and cellular biology*, 26(24), pp. 9424–9429.

Isaacson, M. K. and Ploegh, H. L. (2009) 'Ubiquitination, ubiquitin-like modifiers, and deubiquitination in viral infection', *Cell host & microbe*, 5(6), pp. 559–570.

Izumi, T. and Maller, J. L. (1993) 'Elimination of cdc2 phosphorylation sites in the cdc25 phosphatase blocks initiation of M-phase.', *Molecular biology of the cell*, 4(12), pp. 1337–1350.

Jackson, S. P. and Bartek, J. (2009) 'The DNA-damage response in human biology and disease', *Nature*, 461(7267), pp. 1071–1078.

Javier, R. *et al.* (1991) 'Human adenovirus type 9-induced rat mammary tumors', *Journal of virology*, 65(6), pp. 3192–3202.

Javier, R. T. and Butel, J. S. (2008) 'The history of tumor virology', *Cancer research*, 68(19), pp. 7693–7706.

Jelinek, T. and Graham, F. L. (1992) 'Recombinant human adenoviruses containing hybrid adenovirus type 5 (Ad5)/Ad12 E1A genes: characterization of hybrid E1A proteins and analysis of transforming activity and host range', *Journal of virology*, 66(7), pp. 4117–4125.

Jelinek, T., Pereira, D. S. and Graham, F. L. (1994) 'Tumorigenicity of adenovirus-transformed rodent cells is influenced by at least two regions of adenovirus type 12 early region 1A', *Journal of virology*, 68(2), pp. 888–896.

Jelsma, T. N. *et al.* (1989) 'Sequences in E1A proteins of human adenovirus 5 required for cell transformation, repression of a transcriptional enhancer, and induction of proliferating cell nuclear antigen', *Virology*, 171(1), pp. 120–130.

Johnson, L. *et al.* (2002) 'Selectively replicating adenoviruses targeting deregulated E2F activity are potent, systemic antitumor agents', *Cancer cell*, 1(4), pp. 325–337.

Johnston, J. A., Ward, C. L. and Kopito, R. R. (1998) 'Aggresomes: a cellular response to misfolded proteins', *The Journal of cell biology*, 143(7), pp. 1883–1898.

Jones, N. C. (1990) 'Transformation by the human adenoviruses.', in *Seminars in cancer biology*, pp. 425–435.

de Jong, R. N., van der Vliet, P. C. and Brenkman, A. B. (2003) 'Adenovirus DNA replication:

protein priming, jumping back and the role of the DNA binding protein DBP', in *Adenoviruses: Model and Vectors in Virus-Host Interactions*. Springer, pp. 187–211.

Jordan, A. and Reichard, P. (1998) 'Ribonucleotide reductases', *Annual review of biochemistry*, 67, p. 71.

Juven-Gershon, T. and Oren, M. (1999) 'Mdm2: the ups and downs', *Molecular medicine*, 5(2), pp. 71–83.

Kabeche, L. *et al.* (2018) 'A mitosis-specific and R loop–driven ATR pathway promotes faithful chromosome segregation', *Science*, 359(6371), pp. 108–114.

Kao, C. C., Yew, P. R. and Berk, A. J. (1990) 'Domains required for in vitro association between the cellular p53 and the adenovirus 2 E1B 55k proteins', *Virology*, 179(2), pp. 806–814. doi: 10.1016/0042-6822(90)90148-K.

Karen, K. A. *et al.* (2009) 'Temporal regulation of the Mre11-Rad50-Nbs1 complex during adenovirus infection', *Journal of virology*, 83(9), pp. 4565–4573.

Khanna, K. K. and Jackson, S. P. (2001) 'DNA double-strand breaks: signaling, repair and the cancer connection', *Nature genetics*, 27(3), pp. 247–254.

Kindsmüller, K. *et al.* (2007) 'Intranuclear targeting and nuclear export of the adenovirus E1B-55K protein are regulated by SUMO1 conjugation', *Proceedings of the National Academy of Sciences of the United States of America*, 104(16), pp. 6684–6689. doi: 10.1073/pnas.0702158104.

King, C. R. *et al.* (2018) 'Hacking the cell: network intrusion and exploitation by adenovirus E1A', *MBio*, 9(3), pp. e00390-18.

Kleinberger, T. (2020) 'En Guard! The Interactions between Adenoviruses and the DNA Damage Response', *Viruses*, 12(9), p. 996.

Kleinberger, T. and Shenk, T. (1993) 'Adenovirus E4orf4 protein binds to protein phosphatase 2A, and the complex down regulates E1A-enhanced junB transcription', *Journal of virology*, 67(12), pp. 7556–7560.

Kolas, N. K. *et al.* (2007) 'Orchestration of the DNA-damage response by the RNF8 ubiquitin ligase', *Science*, 318(5856), pp. 1637–1640.

Kress, M. *et al.* (1979) 'Simian virus 40-transformed cells express new species of proteins precipitable by anti-simian virus 40 tumor serum', *Journal of virology*, 31(2), pp. 472–483.

Krupina, K., Goginashvili, A. and Cleveland, D. W. (2021) 'Causes and consequences of micronuclei', *Current Opinion in Cell Biology*, 70, pp. 91–99.

Kulathu, Y. and Komander, D. (2012) 'Atypical ubiquitylation—the unexplored world of polyubiquitin beyond Lys48 and Lys63 linkages', *Nature reviews Molecular cell biology*, 13(8), pp. 508–523.

- Kumagai, A. *et al.* (2006) 'TopBP1 activates the ATR-ATRIP complex', *Cell*, 124(5), pp. 943–955.
- Kumagai, A. *et al.* (2010) 'Treslin collaborates with TopBP1 in triggering the initiation of DNA replication', *Cell*, 140(3), pp. 349–359.
- Kumagai, A. and Dunphy, W. G. (1999) 'Binding of 14-3-3 proteins and nuclear export control the intracellular localization of the mitotic inducer Cdc25', *Genes & development*, 13(9), pp. 1067–1072.
- Lakdawala, S. S. *et al.* (2008) 'Differential requirements of the C terminus of Nbs1 in suppressing adenovirus DNA replication and promoting concatemer formation', *Journal of virology*, 82(17), pp. 8362–8372.
- Lallemand-Breitenbach, V. and de Thé, H. (2018) 'PML nuclear bodies: from architecture to function', *Current opinion in cell biology*, 52, pp. 154–161.
- Lane, D. P. and Crawford, L. V (1979) 'T antigen is bound to a host protein in SY40-transformed cells', *Nature*, 278(5701), pp. 261–263.
- Larson, C. *et al.* (2015) 'Going viral: a review of replication-selective oncolytic adenoviruses', *Oncotarget*, 6(24), p. 19976.
- Lee, C. and Cho, Y. (2002) 'Interactions of SV40 large T antigen and other viral proteins with retinoblastoma tumour suppressor', *Reviews in medical virology*, 12(2), pp. 81–92.
- Lenman, A. *et al.* (2018) 'Polysialic acid is a cellular receptor for human adenovirus 52', *Proceedings of the National Academy of Sciences*, 115(18), pp. E4264–E4273.
- Leppard, K. N. (1993) 'Selective effects on adenovirus late gene expression of deleting the E1b 55K protein', *Journal of general virology*, 74(4), pp. 575–582.
- Leppard, K. N. and Everett, R. D. (1999) 'The adenovirus type 5 E1b 55K and E4 Orf3 proteins associate in infected cells and affect ND10 components.', *Journal of General Virology*, 80(4), pp. 997–1008.
- Leppard, K. N. and Shenk, T. (1989) 'The adenovirus E1B 55 kd protein influences mRNA transport via an intranuclear effect on RNA metabolism.', *The EMBO Journal*, 8(8), pp. 2329–2336.
- Lethbridge, K. J., Scott, G. E. and Leppard, K. N. (2003) 'Nuclear matrix localization and SUMO-1 modification of adenovirus type 5 E1b 55K protein are controlled by E4 Orf6 protein', *Journal of General Virology*, 84(2), pp. 259–268.
- Li, Y. P. *et al.* (1993) 'Generation of a new adenovirus type 12-inducible fragile site by insertion of an artificial U2 locus in the human genome.', *Molecular and cellular biology*, 13(10), pp. 6064–6070.
- Li, Z. *et al.* (1998) 'A Tandem Array of Minimal U1 Small Nuclear RNA Genes Is Sufficient To Generate a New Adenovirus Type 12Inducible Chromosome Fragile Site', *Journal of virology*,



72(5), pp. 4205–4211.

Li, Z. *et al.* (2004) 'Adenoviral E1A targets Mdm4 to stabilize tumor suppressor p53', *Cancer research*, 64(24), pp. 9080–9085.

Liao, D., Yu, A. and Weiner, A. M. (1999) 'Coexpression of the Adenovirus 12 E1B 55 kDa Oncoprotein and Cellular Tumor Suppressor p53 Is Sufficient to Induce Metaphase Fragility of the Human RNU2 Locus', *Virology*, 254(1), pp. 11–23.

Lim, S. and Kaldis, P. (2013) 'Cdks, cyclins and CKIs: roles beyond cell cycle regulation', *Development*, 140(15), pp. 3079–3093.

Limbo, O. *et al.* (2007) 'Ctp1 is a cell-cycle-regulated protein that functions with Mre11 complex to control double-strand break repair by homologous recombination', *Molecular cell*, 28(1), pp. 134–146.

Lin, J. *et al.* (1994) 'Several hydrophobic amino acids in the p53 amino-terminal domain are required for transcriptional activation, binding to mdm-2 and the adenovirus 5 E1B 55-kD protein', *Genes and Development*, 8(10), pp. 1235–1246. doi: 10.1101/gad.8.10.1235.

Lindahl, T. (1993) 'Instability and decay of the primary structure of DNA', *nature*, 362(6422), pp. 709–715.

Lindgren, V. *et al.* (1985) 'Human genes for U2 small nuclear RNA map to a major adenovirus 12 modification site on chromosome 17', *Nature*, 314(6006), pp. 115–116.

Linzer, D. I. H. and Levine, A. J. (1979) 'Characterization of a 54K dalton cellular SV40 tumor antigen present in SV40-transformed cells and uninfected embryonal carcinoma cells', *Cell*, 17(1), pp. 43–52.

Liu, F. *et al.* (1997) 'The human Myt1 kinase preferentially phosphorylates Cdc2 on threonine 14 and localizes to the endoplasmic reticulum and Golgi complex', *Molecular and cellular biology*, 17(2), pp. 571–583.

Liu, Y. *et al.* (2000) 'Adenovirus E1B 55-kilodalton oncoprotein inhibits p53 acetylation by PCAF', *Molecular and cellular biology*, 20(15), pp. 5540–5553.

Liu, Y. *et al.* (2005) 'Adenovirus exploits the cellular aggresome response to accelerate inactivation of the MRN complex', *Journal of virology*, 79(22), pp. 14004–14016.

Löber, C., Lenz-Stöppler, C. and Döbelstein, M. (2002) 'Adenovirus E1-transformed cells grow despite the continuous presence of transcriptionally active p53', *Journal of general virology*, 83(8), pp. 2047–2057.

Lombard, D. B. (2001) 'Nijmegen breakage syndrome disease protein and MRE11 at PML nuclear bodies and meiotic telomeres', in *Biochemistry and Genetics of RecQ-Helicases*. Springer, pp. 59–76.

Lou, Z. *et al.* (2006) 'MDC1 maintains genomic stability by participating in the amplification of ATM-dependent DNA damage signals', *Molecular cell*, 21(2), pp. 187–200.

- Lowe, S. W. *et al.* (1994) 'Abrogation of oncogene-associated apoptosis allows transformation of p53-deficient cells', *Proceedings of the National Academy of Sciences*, 91(6), pp. 2026–2030.
- Lowe, S. W. and Ruley, H. E. (1993) 'Stabilization of the p53 tumor suppressor is induced by adenovirus 5 E1A and accompanies apoptosis.', *Genes & development*, 7(4), pp. 535–545.
- Ludlow, J. W. and Skuse, G. R. (1995) 'Viral oncoprotein binding to pRB, p107, p130, and p300', *Virus research*, 35(2), pp. 113–121.
- Luisoni, S. and Greber, U. F. (2016) 'Biology of adenovirus cell entry: receptors, pathways, mechanisms', in *Adenoviral vectors for gene therapy*. Elsevier, pp. 27–58.
- Lukas, C. *et al.* (2011) '53BP1 nuclear bodies form around DNA lesions generated by mitotic transmission of chromosomes under replication stress', *Nature cell biology*, 13(3), pp. 243–253.
- Luo, H. (2016) 'Interplay between the virus and the ubiquitin–proteasome system: molecular mechanism of viral pathogenesis', *Current opinion in virology*, 17, pp. 1–10.
- Ma, Y. *et al.* (2002) 'Hairpin opening and overhang processing by an Artemis/DNA-dependent protein kinase complex in nonhomologous end joining and V (D) J recombination', *Cell*, 108(6), pp. 781–794.
- Mak, S. *et al.* (1979) 'Tumorigenicity and viral gene expression in rat cells transformed by Ad 12 virions or by the EcoRI c fragment of Ad 12 DNA', *Virology*, 98(2), pp. 456–460.
- Malumbres, M. and Barbacid, M. (2009) 'Cell cycle, CDKs and cancer: a changing paradigm', *Nature reviews cancer*, 9(3), pp. 153–166.
- Mannervik, M. *et al.* (1999) 'Adenovirus E4 open reading frame 4-induced dephosphorylation inhibits E1A activation of the E2 promoter and E2F-1-mediated transactivation independently of the retinoblastoma tumor suppressor protein', *Virology*, 256(2), pp. 313–321.
- de Martel, C. *et al.* (2020) 'Global burden of cancer attributable to infections in 2018: a worldwide incidence analysis', *The Lancet Global Health*, 8(2), pp. e180–e190.
- Martin, M. E. D. and Berk, A. J. (1998) 'Adenovirus E1B 55K represses p53 activation in vitro', *Journal of virology*, 72(4), pp. 3146–3154.
- Martin, M. E. D. and Berk, A. J. (1999) 'Corepressor required for adenovirus E1B 55,000-molecular-weight protein repression of basal transcription', *Molecular and cellular biology*, 19(5), pp. 3403–3414.
- Marttila, M. *et al.* (2005) 'CD46 is a cellular receptor for all species B adenoviruses except types 3 and 7', *Journal of virology*, 79(22), pp. 14429–14436.
- Masai, H. *et al.* (2010) 'Eukaryotic chromosome DNA replication: where, when, and how?', *Annual review of biochemistry*, 79(1), pp. 89–130.

- Maslov, S. and Sneppen, K. (2002) 'Protein interaction networks beyond artifacts', *FEBS letters*, 530(1–3), pp. 255–256.
- Massimi, P. and Banks, L. (1997) 'Repression of p53 transcriptional activity by the HPV E7 proteins', *Virology*, 227(1), pp. 255–259.
- Mathew, S. S. and Bridge, E. (2007) 'The cellular Mre11 protein interferes with adenovirus E4 mutant DNA replication', *Virology*, 365(2), pp. 346–355.
- Mathews, M. B. and Shenk, T. (1991) 'Adenovirus virus-associated RNA and translation control', *Journal of virology*, 65(11), pp. 5657–5662.
- Matsuoka, S. *et al.* (2007) 'ATM and ATR substrate analysis reveals extensive protein networks responsive to DNA damage', *science*, 316(5828), pp. 1160–1166.
- Matsushime, H. *et al.* (1994) 'D-type cyclin-dependent kinase activity in mammalian cells', *Molecular and cellular biology*, 14(3), pp. 2066–2076.
- Matthews, D. A. and Russell, W. C. (1998) 'Adenovirus core protein V interacts with p32--a protein which is associated with both the mitochondria and the nucleus.', *Journal of General Virology*, 79(7), pp. 1677–1685.
- Mattioli, F. *et al.* (2012) 'RNF168 ubiquitinates K13-15 on H2A/H2AX to drive DNA damage signaling', *Cell*, 150(6), pp. 1182–1195.
- McAllister, R. M. *et al.* (1969) 'Transformation of rat embryo cells by adenovirus type 1', *Journal of General Virology*, 4(1), pp. 29–36.
- McDougall, J. K. (1970) 'Effects of adenoviruses on the chromosomes of normal human cells and cells trisomic for an E chromosome', *Nature*, 225(5231), pp. 456–458.
- McDougall, J. K. (1971a) 'Adenovirus-induced chromosome aberrations in human cells', *Journal of General Virology*, 12(1), pp. 43–51.
- McDougall, J. K. (1971b) 'Spontaneous and adenovirus type 12-induced chromosome aberrations in fanconi's anaemia fibroblasts', *International journal of cancer*, 7(3), pp. 526–534.
- McDougall, J. K. *et al.* (1974) 'Cytogenetic studies in permissive and abortive infections by adenovirus type 12', *International journal of cancer*, 14(2), pp. 236–243.
- Meek, D. W. (2004) 'The p53 response to DNA damage', *DNA repair*, 3(8–9), pp. 1049–1056.
- Mellacheruvu, D. *et al.* (2013) 'The CRAPome: a contaminant repository for affinity purification–mass spectrometry data', *Nature methods*, 10(8), pp. 730–736.
- Mennechet, F. J. D. *et al.* (2019) 'A review of 65 years of human adenovirus seroprevalence', *Expert review of vaccines*, 18(6), pp. 597–613.
- Meyerson, M. and Harlow, E. D. (1994) 'Identification of G1 kinase activity for cdk6, a novel

cyclin D partner', *Molecular and cellular biology*, 14(3), pp. 2077–2086.

Mietz, J. A. *et al.* (1992) 'The transcriptional transactivation function of wild-type p53 is inhibited by SV40 large T-antigen and by HPV-16 E6 oncoprotein.', *The EMBO journal*, 11(13), pp. 5013–5020.

Miller, D. L. *et al.* (2007) 'Adenovirus type 5 exerts genome-wide control over cellular programs governing proliferation, quiescence, and survival', *Genome biology*, 8(4), pp. 1–19.

Miller, D. L. *et al.* (2009) 'The adenoviral E1B 55-kilodalton protein controls expression of immune response genes but not p53-dependent transcription', *Journal of virology*, 83(8), pp. 3591–3603.

Miller, M. S. *et al.* (2012) 'Characterization of the 55-residue protein encoded by the 9S E1A mRNA of species C adenovirus', *Journal of virology*, 86(8), pp. 4222–4233.

Mordes, D. A. *et al.* (2008) 'TopBP1 activates ATR through ATRIP and a PIKK regulatory domain', *Genes & development*, 22(11), pp. 1478–1489.

Morfopoulou, S. *et al.* (2022) 'Genomic investigations of acute hepatitis of unknown aetiology in children', *MedRxiv*, pp. 2007–2022.

Mukai, N. *et al.* (1980) 'Retinal tumor induced in the baboon by human adenovirus 12', *Science*, 210(4473), pp. 1023–1025.

Muller, S. and Dobner, T. (2008) 'The adenovirus E1B-55K oncoprotein induces SUMO modification of p53', *Cell Cycle*, 7(6), pp. 754–758.

Münger, K. *et al.* (1989) 'Complex formation of human papillomavirus E7 proteins with the retinoblastoma tumor suppressor gene product.', *The EMBO journal*, 8(13), pp. 4099–4105.

Nazeer, R. *et al.* (2019) 'Adenovirus E1B 55-kilodalton protein targets SMARCA1 for degradation during infection and modulates cellular DNA replication', *Journal of virology*, 93(13), pp. e00402-19.

Nebenzahl-Sharon, K. *et al.* (2019) 'Biphasic functional interaction between the adenovirus E4orf4 protein and DNA-PK', *Journal of Virology*, 93(10), pp. e01365-18.

Nevels, M. *et al.* (1997) 'The adenovirus E4orf6 protein can promote E1A/E1B-induced focus formation by interfering with p53 tumor suppressor function', *Proceedings of the National Academy of Sciences*, 94(4), pp. 1206–1211.

Nevels, M. *et al.* (2001) "'Hit-and-run" transformation by adenovirus oncogenes', *Journal of virology*, 75(7), pp. 3089–3094.

Nieminuszczy, J., Schwab, R. A. and Niedzwiedz, W. (2016) 'The DNA fibre technique—tracking helicases at work', *Methods*, 108, pp. 92–98.

Nilsson, E. C. *et al.* (2011) 'The GD1a glycan is a cellular receptor for adenoviruses causing epidemic keratoconjunctivitis', *Nature medicine*, 17(1), pp. 105–109.

- Nishitani, H. *et al.* (2000) 'The Cdt1 protein is required to license DNA for replication in fission yeast', *Nature*, 404(6778), pp. 625–628.
- Nordqvist, K., Ohman, K. and Akusjärvi, G. (1994) 'Human adenovirus encodes two proteins which have opposite effects on accumulation of alternatively spliced mRNAs', *Molecular and cellular biology*, 14(1), pp. 437–445.
- Norkin, L. C. (2010) *Virology: molecular biology and pathogenesis*. Washington: ASM Press.
- O'Shea, C. C. *et al.* (2004) 'Late viral RNA export, rather than p53 inactivation, determines ONYX-015 tumor selectivity', *Cancer cell*, 6(6), pp. 611–623.
- Ohtani, K., Degregori, J. and Nevins, J. R. (1995) 'Regulation of the cyclin E gene by transcription factor E2F1.', *Proceedings of the National Academy of Sciences*, 92(26), pp. 12146–12150.
- Orazio, N. I. *et al.* (2011) 'The adenovirus E1b55K/E4orf6 complex induces degradation of the Bloom helicase during infection', *Journal of virology*, 85(4), pp. 1887–1892.
- Orlando, J. S. and Ornelles, D. A. (1999) 'An arginine-faced amphipathic alpha helix is required for adenovirus type 5 E4orf6 protein function', *Journal of virology*, 73(6), pp. 4600–4610.
- Ornelles, D. A. and Shenk, T. (1991) 'Localization of the adenovirus early region 1B 55-kilodalton protein during lytic infection: association with nuclear viral inclusions requires the early region 4 34-kilodalton protein.', *Journal of Virology*, 65(1), pp. 424–429.
- Ortiz-Zapater, E., Santis, G. and Parsons, M. (2017) 'CAR: A key regulator of adhesion and inflammation', *The international journal of biochemistry & cell biology*, 89, pp. 1–5.
- Ou, H. D. *et al.* (2012) 'A structural basis for the assembly and functions of a viral polymer that inactivates multiple tumor suppressors', *Cell*, 151(2), pp. 304–319.
- Pancholi, N. J., Price, A. M. and Weitzman, M. D. (2017) 'Take your PIKK: tumour viruses and DNA damage response pathways', *Philosophical Transactions of the Royal Society B: Biological Sciences*, 372(1732), p. 20160269.
- Pancholi, N. J. and Weitzman, M. D. (2018) 'Serotype-specific restriction of wild-type adenoviruses by the cellular Mre11-Rad50-Nbs1 complex', *Virology*, 518, pp. 221–231. doi: 10.1016/j.virol.2018.02.023.
- Pantelidou, C. *et al.* (2016) 'The E1B19K-deleted oncolytic adenovirus mutant AdΔ19K sensitizes pancreatic cancer cells to drug-induced DNA-damage by down-regulating Claspin and Mre11', *Oncotarget*, 7(13), p. 15703.
- Parker, L. L. and Piwnica-Worms, H. (1992) 'Inactivation of the p34 cdc2-cyclin B complex by the human WEE1 tyrosine kinase', *Science*, 257(5078), pp. 1955–1957.
- Patel, D. *et al.* (1999) 'The E6 protein of human papillomavirus type 16 binds to and inhibits co-activation by CBP and p300', *The EMBO journal*, 18(18), pp. 5061–5072.

- Patsalo, V. *et al.* (2012) 'Biophysical and functional analyses suggest that adenovirus E4-ORF3 protein requires higher-order multimerization to function against promyelocytic leukemia protein nuclear bodies', *Journal of Biological Chemistry*, 287(27), pp. 22573–22583.
- Pelka, P. *et al.* (2008) 'Intrinsic structural disorder in adenovirus E1A: a viral molecular hub linking multiple diverse processes', *Journal of virology*, 82(15), pp. 7252–7263.
- Pelka, P. *et al.* (2009) 'Transcriptional control by adenovirus E1A conserved region 3 via p300/CBP', *Nucleic acids research*, 37(4), pp. 1095–1106.
- Pennella, M. A. *et al.* (2010) 'Adenovirus E1B 55-kilodalton protein is a p53-SUMO1 E3 ligase that represses p53 and stimulates its nuclear export through interactions with promyelocytic leukemia nuclear bodies', *Journal of virology*, 84(23), pp. 12210–12225.
- Perricaudet, M. *et al.* (1979) 'Structure of two spliced mRNAs from the transforming region of human subgroup C adenoviruses', *Nature*, 281(5733), pp. 694–696.
- Petermann, E. *et al.* (2010) 'Hydroxyurea-stalled replication forks become progressively inactivated and require two different RAD51-mediated pathways for restart and repair', *Molecular cell*, 37(4), pp. 492–502.
- Petermann, E. and Caldecott, K. W. (2006) 'Evidence that the ATR/Chk1 pathway maintains normal replication fork progression during unperturbed S phase', *Cell cycle*, 5(19), pp. 2203–2209.
- Petersen, B. O. *et al.* (1999) 'Phosphorylation of mammalian CDC6 by cyclin A/CDK2 regulates its subcellular localization', *The EMBO Journal*, 18(2), pp. 396–410.
- Pfeiffer, P., Goedecke, W. and Obe, G. (2000) 'Mechanisms of DNA double-strand break repair and their potential to induce chromosomal aberrations', *Mutagenesis*, 15(4), pp. 289–302.
- Piatti, S., Lengauer, C. and Nasmyth, K. (1995) 'Cdc6 is an unstable protein whose de novo synthesis in G1 is important for the onset of S phase and for preventing a 'reductional'anaphase in the budding yeast *Saccharomyces cerevisiae*.'', *The EMBO Journal*, 14(15), pp. 3788–3799.
- Pilder, S. *et al.* (1986) 'The adenovirus E1B-55K transforming polypeptide modulates transport or cytoplasmic stabilization of viral and host cell mRNAs.', *Molecular and cellular biology*, 6(2), pp. 470–476.
- Pintard, L. *et al.* (2003) 'Neddylation and deneddylation of CUL-3 is required to target MEI-1/Katanin for degradation at the meiosis-to-mitosis transition in *C. elegans*', *Current Biology*, 13(11), pp. 911–921.
- Pomerantz, J. *et al.* (1998) 'The Ink4a tumor suppressor gene product, p19Arf, interacts with MDM2 and neutralizes MDM2's inhibition of p53', *Cell*, 92(6), pp. 713–723.
- Puvion-Dutilleul, F. *et al.* (1995) 'Adenovirus infection induces rearrangements in the

intranuclear distribution of the nuclear body-associated PML protein', *Experimental cell research*, 218(1), pp. 9–16.

Querido, E. *et al.* (1997) 'Regulation of p53 levels by the E1B 55-kilodalton protein and E4orf6 in adenovirus-infected cells.', *Journal of virology*, 71(5), pp. 3788–3798.

Querido, E., Blanchette, P., *et al.* (2001) 'Degradation of p53 by adenovirus E4orf6 and E1B55K proteins occurs via a novel mechanism involving a Cullin-containing complex', *Genes & development*, 15(23), pp. 3104–3117.

Querido, E., Morisson, M. R., *et al.* (2001) 'Identification of three functions of the adenovirus e4orf6 protein that mediate p53 degradation by the E4orf6-E1B55K complex', *Journal of Virology*, 75(2), pp. 699–709.

Querido, E., Teodoro, J. G. and Branton, P. E. (1997) 'Accumulation of p53 induced by the adenovirus E1A protein requires regions involved in the stimulation of DNA synthesis', *Journal of virology*, 71(5), pp. 3526–3533.

Radke, J. R. and Cook, J. L. (2018) 'Human adenovirus infections: Update and consideration of mechanisms of viral persistence', *Current Opinion in Infectious Diseases*, pp. 251–256. doi: 10.1097/QCO.0000000000000451.

Rao, X.-M. *et al.* (2006) 'Gene expression profiles of normal human lung cells affected by adenoviral E1B', *Virology*, 350(2), pp. 418–428.

Rapp, A. and Greulich, K. O. (2004) 'After double-strand break induction by UV-A, homologous recombination and nonhomologous end joining cooperate at the same DSB if both systems are available', *Journal of cell science*, 117(21), pp. 4935–4945.

Rasti, M. *et al.* (2005) 'Recruitment of CBP/p300, TATA-binding protein, and S8 to distinct regions at the N terminus of adenovirus E1A', *Journal of virology*, 79(9), pp. 5594–5605.

Rekosh, D. M. K. *et al.* (1977) 'Identification of a protein linked to the ends of adenovirus DNA', *Cell*, 11(2), pp. 283–295.

Reyes, E. D. *et al.* (2017) 'Identifying host factors associated with DNA replicated during virus infection', *Molecular & cellular proteomics*, 16(12), pp. 2079–2097.

Rogakou, E. P. *et al.* (1998) 'DNA double-stranded breaks induce histone H2AX phosphorylation on serine 139', *Journal of biological chemistry*, 273(10), pp. 5858–5868.

Rotem-Yehudar, R. *et al.* (1996) 'LMP-associated proteolytic activities and TAP-dependent peptide transport for class 1 MHC molecules are suppressed in cell lines transformed by the highly oncogenic adenovirus 12.', *The Journal of experimental medicine*, 183(2), pp. 499–514.

Roth, J. *et al.* (1998) 'Inactivation of p53 but not p73 by adenovirus type 5 E1B 55-kilodalton and E4 34-kilodalton oncoproteins', *Journal of Virology*, 72(11), pp. 8510–8516.

Rous, P. (1911) 'A sarcoma of the fowl transmissible by an agent separable from the tumor

cells', *The Journal of experimental medicine*, 13(4), p. 397.

Rowe, W. P. *et al.* (1953) 'Isolation of a cytopathogenic agent from human adenoids undergoing spontaneous degeneration in tissue culture', *Proceedings of the Society for Experimental Biology and Medicine*, 84(3), pp. 570–573.

Rual, J.-F. *et al.* (2005) 'Towards a proteome-scale map of the human protein–protein interaction network', *Nature*, 437(7062), pp. 1173–1178.

Russell, W. C. (2000) 'Update on adenovirus and its vectors', *Journal of general virology*, 81(11), pp. 2573–2604.

Russell, W. C. (2009) 'Adenoviruses: Update on structure and function', *Journal of General Virology*, pp. 1–20. doi: 10.1099/vir.0.003087-0.

Ryan, E. L. (2016) 'Investigating the role of TAB182 in the DNA damage response and replication stress pathways'. University of Birmingham. Available at: <https://etheses.bham.ac.uk/id/eprint/6741/>.

Ryu, W.-S. (2016) *Molecular virology of human pathogenic viruses*. Academic Press.

Saban, S. D. *et al.* (2006) 'Visualization of  $\alpha$ -helices in a 6-angstrom resolution cryoelectron microscopy structure of adenovirus allows refinement of capsid protein assignments', *Journal of virology*, 80(24), pp. 12049–12059.

Sabbatini, P. *et al.* (1995) 'Essential role for p53-mediated transcription in E1A-induced apoptosis.', *Genes & Development*, 9(17), pp. 2184–2192.

Sancar, A. *et al.* (2004) 'Molecular mechanisms of mammalian DNA repair and the DNA damage checkpoints', *Annual review of biochemistry*, 73(1), pp. 39–85.

Sandler, A. B. and Ketner, G. (1989) 'Adenovirus early region 4 is essential for normal stability of late nuclear RNAs', *Journal of virology*, 63(2), pp. 624–630.

Sarnow, P. *et al.* (1982) 'Adenovirus E1b-58kd tumor antigen and SV40 large tumor antigen are physically associated with the same 54 kd cellular protein in transformed cells', *Cell*, 28(2), pp. 387–394.

Sarnow, P. *et al.* (1984) 'Adenovirus early region 1B 58,000-dalton tumor antigen is physically associated with an early region 4 25,000-dalton protein in productively infected cells', *Journal of virology*, 49(3), pp. 692–700.

Sarnow, P., Sullivan, C. A. and Levine, A. J. (1982) 'A monoclonal antibody detecting the adenovirus type 5 E 1 b-58Kd tumor antigen: Characterization of the E 1 b-58Kd tumor antigen in adenovirus-infected and-transformed cells', *Virology*, 120(2), pp. 510–517.

Schaack, J. *et al.* (1990) 'Adenovirus terminal protein mediates both nuclear matrix association and efficient transcription of adenovirus DNA.', *Genes & development*, 4(7), pp. 1197–1208.



- Schaeper, U. *et al.* (1995) 'Molecular cloning and characterization of a cellular phosphoprotein that interacts with a conserved C-terminal domain of adenovirus E1A involved in negative modulation of oncogenic transformation.', *Proceedings of the National Academy of Sciences*, 92(23), pp. 10467–10471.
- Schaley, J. *et al.* (2000) 'Induction of the cellular E2F-1 promoter by the adenovirus E4-6/7 protein', *Journal of virology*, 74(5), pp. 2084–2093.
- Scheffner, M. *et al.* (1993) 'The HPV-16 E6 and E6-AP complex functions as a ubiquitin-protein ligase in the ubiquitination of p53', *Cell*, 75(3), pp. 495–505.
- Schon, O. *et al.* (2002) 'Molecular mechanism of the interaction between MDM2 and p53', *Journal of molecular biology*, 323(3), pp. 491–501.
- Schramayr, S. *et al.* (1990a) 'Chromosomal damage induced by human adenovirus type 12 requires expression of the E1B 55-kilodalton viral protein.', *Journal of virology*, 64(5), pp. 2090–2095.
- Schramayr, S. *et al.* (1990b) 'Chromosomal damage induced by human adenovirus type 12 requires expression of the E1B 55-kilodalton viral protein', *Journal of virology*, 64(5), pp. 2090–2095.
- Schreiner, S. *et al.* (2010) 'Proteasome-dependent degradation of Daxx by the viral E1B-55K protein in human adenovirus-infected cells', *Journal of virology*, 84(14), pp. 7029–7038.
- Schreiner, S., Bürck, C., *et al.* (2013) 'Control of human adenovirus type 5 gene expression by cellular Daxx/ATRX chromatin-associated complexes', *Nucleic acids research*, 41(6), pp. 3532–3550.
- Schreiner, S., Kinkley, S., *et al.* (2013) 'SPOC1-mediated antiviral host cell response is antagonized early in human adenovirus type 5 infection', *PLoS pathogens*, 9(11), p. e1003775.
- Schreiner, S., Wimmer, P. and Dobner, T. (2012) 'Adenovirus degradation of cellular proteins', *Future microbiology*, 7(2), pp. 211–225.
- Schrier, P. I. *et al.* (1983) 'Expression of class I major histocompatibility antigens switched off by highly oncogenic adenovirus 12 in transformed rat cells', *Nature*, 305(5937), pp. 771–775.
- Schwartz, R. A. *et al.* (2008) 'Distinct requirements of adenovirus E1b55K protein for degradation of cellular substrates', *Journal of virology*, 82(18), pp. 9043–9055.
- Servellita, V. *et al.* (2023) 'Adeno-associated virus type 2 in US children with acute severe hepatitis', *Nature*, pp. 1–3.
- Shah, G. A. and O'Shea, C. C. (2015) 'Viral and Cellular Genomes Activate Distinct DNA Damage Responses', *Cell*, 162(5), pp. 987–1002. doi: 10.1016/j.cell.2015.07.058.
- Shenk, T. E. (2001) 'Adenoviridae: the viruses and their replication', *Fundamental virology*, pp. 1053–1088.

- Sherr, C. J. and Roberts, J. M. (1999) 'CDK inhibitors: positive and negative regulators of G1-phase progression', *Genes & development*, 13(12), pp. 1501–1512.
- Shieh, S.-Y. *et al.* (1997) 'DNA damage-induced phosphorylation of p53 alleviates inhibition by MDM2', *Cell*, 91(3), pp. 325–334.
- Shieh, S.-Y. *et al.* (2000) 'The human homologs of checkpoint kinases Chk1 and Cds1 (Chk2) phosphorylate p53 at multiple DNA damage-inducible sites', *Genes & development*, 14(3), pp. 289–300.
- Shiroki, K. *et al.* (1979) 'Incomplete transformation of rat cells by a small fragment of adenovirus 12 DNA', *Virology*, 95(1), pp. 127–136.
- Shtrichman, R., Sharf, R. and Kleinberger, T. (2000) 'Adenovirus E4orf4 protein interacts with both B $\alpha$  and B' subunits of protein phosphatase 2A, but E4orf4-induced apoptosis is mediated only by the interaction with B $\alpha$ ', *Oncogene*, 19(33), pp. 3757–3765.
- Sieber, T. *et al.* (2011) 'Intrinsic disorder in the common N-terminus of human adenovirus 5 E1B-55K and its related E1BN proteins indicated by studies on E1B-93R', *Virology*, 418(2), pp. 133–143.
- Sieber, T. and Dobner, T. (2007) 'Adenovirus type 5 early region 1B 156R protein promotes cell transformation independently of repression of p53-stimulated transcription', *Journal of virology*, 81(1), pp. 95–105.
- Smith, G. C. M. and Jackson, S. P. (1999) 'The DNA-dependent protein kinase', *Genes & development*, 13(8), pp. 916–934.
- So, S., Davis, A. J. and Chen, D. J. (2009) 'Autophosphorylation at serine 1981 stabilizes ATM at DNA damage sites', *Journal of Cell Biology*, 187(7), pp. 977–990.
- Sohn, S.-Y., Bridges, R. G. and Hearing, P. (2015) 'Proteomic analysis of ubiquitin-like posttranslational modifications induced by the adenovirus E4-ORF3 protein', *Journal of virology*, 89(3), pp. 1744–1755.
- Sohn, S.-Y. and Hearing, P. (2012) 'Adenovirus regulates sumoylation of Mre11-Rad50-Nbs1 components through a paralog-specific mechanism', *Journal of virology*, 86(18), pp. 9656–9665.
- Sohn, S.-Y. and Hearing, P. (2019a) 'Adenoviral strategies to overcome innate cellular responses to infection', *FEBS Letters*, 593(24), pp. 3484–3495. doi: 10.1002/1873-3468.13680.
- Sohn, S.-Y. and Hearing, P. (2019b) 'Mechanism of adenovirus E4-ORF3-mediated SUMO modifications', *MBio*, 10(1), pp. e00022-19.
- Sohn, S. Y. and Hearing, P. (2016) 'Adenovirus early proteins and host sumoylation', *mBio*. doi: 10.1128/mBio.01154-16.
- Sollier, J. *et al.* (2014) 'Transcription-coupled nucleotide excision repair factors promote R-

loop-induced genome instability', *Molecular cell*, 56(6), pp. 777–785.

Sørensen, C. S. *et al.* (2004) 'ATR, Claspin and the Rad9-Rad1-Hus1 complex regulate Chk1 and Cdc25A in the absence of DNA damage', *Cell cycle*, 3(7), pp. 939–943.

Soria, C. *et al.* (2010) 'Heterochromatin silencing of p53 target genes by a small viral protein', *Nature*, 466(7310), pp. 1076–1081.

Speiseder, T. *et al.* (2017) 'Efficient transformation of primary human mesenchymal stromal cells by adenovirus early region 1 oncogenes', *Journal of virology*, 91(1), pp. e01782-16.

de Stanchina, E. *et al.* (1998) 'E1A signaling to p53 involves the p19ARF tumor suppressor', *Genes & development*, 12(15), pp. 2434–2442.

Steegenga, W. T. *et al.* (1995) 'Distinct modulation of p53 activity in transcription and cell-cycle regulation by the large (54 kDa) and small (21 kDa) adenovirus E1B proteins', *Virology*, 212(2), pp. 543–554.

Steegenga, W. T. *et al.* (1998) 'The large E1B protein together with the E4orf6 protein target p53 for active degradation in adenovirus infected cells', *Oncogene*, 16(3), p. 349.

Stelzl, U. *et al.* (2005) 'A human protein-protein interaction network: a resource for annotating the proteome', *Cell*, 122(6), pp. 957–968.

Stewart, G. S. *et al.* (1999) 'The DNA double-strand break repair gene hMRE11 is mutated in individuals with an ataxia-telangiectasia-like disorder', *Cell*, 99(6), pp. 577–587.

Stich, H. F., Van Hoosier, G. L. and Trentin, J. J. (1964) 'Viruses and mammalian chromosomes chromosome aberrations by human adenovirus type 12', *Experimental cell research*, 34(2), pp. 400–403.

Stiff, T. *et al.* (2016) 'ATR promotes cilia signalling: links to developmental impacts', *Human molecular genetics*, 25(8), pp. 1574–1587.

Stillman, B. W. *et al.* (1981) 'Identification of the gene and mRNA for the adenovirus terminal protein precursor', *Cell*, 23(2), pp. 497–508.

Stracker, T. H. *et al.* (2005) 'Serotype-specific reorganization of the Mre11 complex by adenoviral E4orf3 proteins', *Journal of virology*, 79(11), pp. 6664–6673.

Stracker, T. H., Carson, C. T. and Weitzman, M. D. (2002) 'Adenovirus oncoproteins inactivate the Mre11–Rad50–NBS1 DNA repair complex', *Nature*, 418(6895), p. 348.

Sugiyama, T. and Kowalczykowski, S. C. (2002) 'Rad52 protein associates with replication protein A (RPA)-single-stranded DNA to accelerate Rad51-mediated displacement of RPA and presynaptic complex formation', *Journal of Biological Chemistry*, 277(35), pp. 31663–31672.

Sun, Y. *et al.* (2005) 'A role for the Tip60 histone acetyltransferase in the acetylation and activation of ATM', *Proceedings of the National Academy of Sciences*, 102(37), pp. 13182–

13187.

Sundararajan, R. and White, E. (2001) 'E1B 19K blocks Bax oligomerization and tumor necrosis factor alpha-mediated apoptosis', *Journal of virology*, 75(16), pp. 7506–7516.

Surget, S., Khoury, M. P. and Bourdon, J.-C. (2014) 'Uncovering the role of p53 splice variants in human malignancy: a clinical perspective', *OncoTargets and therapy*, 7, p. 57.

Swamy, M. K., Purushotham, B. and Sinniah, U. R. (2021) 'Camptothecin: Occurrence, Chemistry and Mode of Action', in *Bioactive Natural Products for Pharmaceutical Applications*. Springer, pp. 311–327.

Takata, M. *et al.* (1998) 'Homologous recombination and non-homologous end-joining pathways of DNA double-strand break repair have overlapping roles in the maintenance of chromosomal integrity in vertebrate cells', *The EMBO journal*, 17(18), pp. 5497–5508.

Tanimura, S. *et al.* (1999) 'MDM2 interacts with MDMX through their RING finger domains', *FEBS letters*, 447(1), pp. 5–9.

Tauber, B. and Dobner, T. (2001) 'Adenovirus early E4 genes in viral oncogenesis', *Oncogene*, 20(54), pp. 7847–7854.

Täuber, B. and Dobner, T. (2001) 'Molecular regulation and biological function of adenovirus early genes: the E4 ORFs', *Gene*, 278(1–2), pp. 1–23.

Tejera, B. *et al.* (2019) 'The human adenovirus type 5 E1B 55kDa protein interacts with RNA promoting timely DNA replication and viral late mRNA metabolism', *PLoS ONE*, 14(4). doi: 10.1371/journal.pone.0214882.

Telling, G. C. and Williams, J. (1994) 'Constructing chimeric type 12/type 5 adenovirus E1A genes and using them to identify an oncogenic determinant of adenovirus type 12', *Journal of virology*, 68(2), pp. 877–887.

Teodoro, J. G. *et al.* (1994) 'Phosphorylation at the carboxy terminus of the 55-kilodalton adenovirus type 5 E1B protein regulates transforming activity.', *Journal of virology*, 68(2), pp. 776–786.

Teodoro, J. G. and Branton, P. E. (1997) 'Regulation of p53-dependent apoptosis, transcriptional repression, and cell transformation by phosphorylation of the 55-kilodalton E1B protein of human adenovirus type 5.', *Journal of virology*, 71(5), pp. 3620–3627.

Thomas, A. and White, E. (1998) 'Suppression of the p300-dependent mdm2negative-feedback loop induces the p53 apoptotic function', *Genes & development*, 12(13), pp. 1975–1985.

Thomas, D. L. *et al.* (2001) 'Several E4 region functions influence mammary tumorigenesis by human adenovirus type 9', *Journal of virology*, 75(2), pp. 557–568.

Thomas, M. C. and Chiang, C.-M. (2005) 'E6 oncoprotein represses p53-dependent gene activation via inhibition of protein acetylation independently of inducing p53 degradation',

*Molecular cell*, 17(2), pp. 251–264.

Tollefson, A. E. *et al.* (1996) 'The adenovirus death protein (E3-11.6 K) is required at very late stages of infection for efficient cell lysis and release of adenovirus from infected cells.', *Journal of virology*, 70(4), pp. 2296–2306.

Trentin, J. J., Yabe, Y. and Taylor, G. (1962) 'The Quest for Human Cancer Viruses: A new approach to an old problem reveals cancer induction in hamsters by human adenovirus.', *Science*, 137(3533), pp. 835–841.

Trimarchi, J. M. and Lees, J. A. (2002) 'Sibling rivalry in the E2F family', *Nature reviews Molecular cell biology*, 3(1), pp. 11–20.

Tuduri, S. *et al.* (2009) 'Topoisomerase I suppresses genomic instability by preventing interference between replication and transcription', *Nature cell biology*, 11(11), pp. 1315–1324.

Turnell, A. S. *et al.* (2000) 'Regulation of the 26S proteasome by adenovirus E1A', *The EMBO journal*, 19(17), pp. 4759–4773.

Turnell, A. S. and Grand, R. J. (2012) 'DNA viruses and the cellular DNA-damage response', *Journal of General Virology*, pp. 2076–2097. doi: 10.1099/vir.0.044412-0.

Turnell, A. S., Grand, R. J. A. and Gallimore, P. H. (1999) 'The replicative capacities of large E1B-null group A and group C adenoviruses are independent of host cell p53 status', *Journal of virology*, 73(3), pp. 2074–2083.

Uziel, T. *et al.* (2003) 'Requirement of the MRN complex for ATM activation by DNA damage', *The EMBO journal*, 22(20), pp. 5612–5621.

Vaessen, R. T. *et al.* (1986) 'Adenovirus E1A-mediated regulation of class I MHC expression.', *The EMBO Journal*, 5(2), pp. 335–341.

Valentine, R. C. and Pereira, H. G. (1965) 'Antigens and structure of the adenovirus', *Journal of molecular biology*, 13(1), pp. 13–IN13.

Virtanen, A. *et al.* (1984) 'mRNAs from human adenovirus 2 early region 4', *Journal of virology*, 51(3), pp. 822–831.

Vogelstein, B., Lane, D. and Levine, A. J. (2000) 'Surfing the p53 network', *Nature*, 408(6810), pp. 307–310.

Walker, J. R., Corpina, R. A. and Goldberg, J. (2001) 'Structure of the Ku heterodimer bound to DNA and its implications for double-strand break repair', *Nature*, 412(6847), pp. 607–614.

Wang, B. *et al.* (2002) '53BP1, a mediator of the DNA damage checkpoint', *Science*, 298(5597), pp. 1435–1438.

Wang, B. and Elledge, S. J. (2007) 'Ubc13/Rnf8 ubiquitin ligases control foci formation of the Rap80/Abraxas/Brca1/Brcc36 complex in response to DNA damage', *Proceedings of the*

*National Academy of Sciences*, 104(52), pp. 20759–20763.

Wang, H. *et al.* (2011) 'Desmoglein 2 is a receptor for adenovirus serotypes 3, 7, 11 and 14', *Nature medicine*, 17(1), pp. 96–104.

Wang, W. *et al.* (2000) 'Possible association of BLM in decreasing DNA double strand breaks during DNA replication', *The EMBO journal*, 19(13), pp. 3428–3435.

Wang, X. W. *et al.* (1999) 'GADD45 induction of a G2/M cell cycle checkpoint', *Proceedings of the National Academy of Sciences*, 96(7), pp. 3706–3711.

Wang, Y. *et al.* (2000) 'BASC, a super complex of BRCA1-associated proteins involved in the recognition and repair of aberrant DNA structures', *Genes & development*, 14(8), pp. 927–939.

Webster, L. C. and Ricciardi, R. P. (1991) 'trans-dominant mutants of E1A provide genetic evidence that the zinc finger of the trans-activating domain binds a transcription factor', *Molecular and cellular biology*, 11(9), pp. 4287–4296.

Weiden, M. D. and Ginsberg, H. S. (1994) 'Deletion of the E4 region of the genome produces adenovirus DNA concatemers.', *Proceedings of the National Academy of Sciences*, 91(1), pp. 153–157.

Weigel, S. and Dobbstein, M. (2000) 'The nuclear export signal within the E4orf6 protein of adenovirus type 5 supports virus replication and cytoplasmic accumulation of viral mRNA', *Journal of Virology*, 74(2), pp. 764–772.

Weitzman, M. D. *et al.* (2004) 'Interactions of viruses with the cellular DNA repair machinery', *DNA repair*, 3(8–9), pp. 1165–1173.

Weitzman, M. D. and Ornelles, D. A. (2005) 'Inactivating intracellular antiviral responses during adenovirus infection', *Oncogene*, 24(52), pp. 7686–7696.

Welchman, R. L., Gordon, C. and Mayer, R. J. (2005) 'Ubiquitin and ubiquitin-like proteins as multifunctional signals', *Nature reviews Molecular cell biology*, 6(8), pp. 599–609.

Wellinger, R. E., Prado, F. and Aguilera, A. (2006) 'Replication fork progression is impaired by transcription in hyperrecombinant yeast cells lacking a functional THO complex', *Molecular and cellular biology*, 26(8), pp. 3327–3334.

White, E. (2001) 'Regulation of the cell cycle and apoptosis by the oncogenes of adenovirus', *Oncogene*, 20(54), pp. 7836–7846.

Whittaker, J. L. *et al.* (1984) 'Isolation and characterization of four adenovirus type 12-transformed human embryo kidney cell lines', *Molecular and cellular biology*, 4(1), pp. 110–116.

Whyte, P. *et al.* (1988) 'Association between an oncogene and an anti-oncogene: the adenovirus E1A proteins bind to the retinoblastoma gene product', *Nature*, 334(6178), pp. 124–129.

- Wienzek, S., Roth, J. and Dobbelstein, M. (2000) 'E1B 55-kilodalton oncoproteins of adenovirus types 5 and 12 inactivate and relocalize p53, but not p51 or p73, and cooperate with E4orf6 proteins to destabilize p53', *Journal of virology*, 74(1), pp. 193–202.
- Wilhelm, T., Said, M. and Naim, V. (2020) 'DNA replication stress and chromosomal instability: Dangerous liaisons', *Genes*, 11(6), p. 642.
- Williams, J. *et al.* (1995) 'Assessing the role of E1A in the differential oncogenicity of group A and group C human adenoviruses', *The Molecular Repertoire of Adenoviruses III*, pp. 149–175.
- Williams, R. S., Williams, J. S. and Tainer, J. A. (2007) 'Mre11–Rad50–Nbs1 is a keystone complex connecting DNA repair machinery, double-strand break signaling, and the chromatin template This paper is one of a selection of papers published in this Special Issue, entitled 28th International West Coast Chromatin a', *Biochemistry and Cell Biology*, 85(4), pp. 509–520. doi: 10.1139/O07-069.
- Wimmer, P. *et al.* (2010) 'SUMO modification of E1B-55K oncoprotein regulates isoform-specific binding to the tumour suppressor protein PML', *Oncogene*, 29(40), pp. 5511–5522.
- Wimmer, P. *et al.* (2013) 'Cross-talk between phosphorylation and SUMOylation regulates transforming activities of an adenoviral oncoprotein', *Oncogene*, 32(13), p. 1626.
- Wold, W. S. M., Tollefson, A. E. and Hermiston, T. W. (1995) 'E3 transcription unit of adenovirus', *The Molecular Repertoire of Adenoviruses I*, pp. 237–274.
- Woo, J. L. and Berk, A. J. (2007) 'Adenovirus ubiquitin-protein ligase stimulates viral late mRNA nuclear export', *Journal of virology*, 81(2), pp. 575–587.
- Wu, L. and Hickson, I. D. (2003) 'The Bloom's syndrome helicase suppresses crossing over during homologous recombination', *Nature*, 426(6968), pp. 870–874.
- Xu, T. *et al.* (2022) 'A small molecule inhibitor of the UBE2F-CRL5 axis induces apoptosis and radiosensitization in lung cancer', *Signal Transduction and Targeted Therapy*, 7(1), p. 354.
- Yabe, Y., Trentin, J. J. and Taylor, G. (1962) 'Cancer induction in hamsters by human type 12 adenovirus. Effect of age and of virus dose.', *Proceedings of the Society for Experimental Biology and Medicine*, 111(2), pp. 343–344.
- Yatherajam, G., Huang, W. and Flint, S. J. (2011) 'Export of adenoviral late mRNA from the nucleus requires the Nxf1/Tap export receptor', *Journal of virology*, 85(4), pp. 1429–1438.
- Yau, R. and Rape, M. (2016) 'The increasing complexity of the ubiquitin code', *Nature cell biology*, 18(6), pp. 579–586.
- Yew, P. R. and Berk, A. J. (1992) 'Inhibition of p53 transactivation required for transformation by adenovirus early 1B protein', *Nature*, 357(6373), p. 82.
- Yew, P. R., Kao, C. C. and Berk, A. J. (1990) 'Dissection of functional domains in the adenovirus 2 early 1B 55K polypeptide by suppressor-linker insertional mutagenesis',

*Virology*, 179(2), pp. 795–805.

Yew, P. R., Liu, X. and Berk, A. J. (1994) 'Adenovirus E1B oncoprotein tethers a transcriptional repression domain to p53.', *Genes & development*, 8(2), pp. 190–202.

Yousef, A. F., Brandl, C. J. and Mymryk, J. S. (2009) 'Requirements for E1A dependent transcription in the yeast *Saccharomyces cerevisiae*', *BMC molecular biology*, 10(1), pp. 1–10.

Zantema, Schrier, P. I., *et al.* (1985) 'Adenovirus serotype determines association and localization of the large E1B tumor antigen with cellular tumor antigen p53 in transformed cells.', *Molecular and Cellular Biology*, 5(11), pp. 3084–3091.

Zantema, Fransen, J. A. M., *et al.* (1985) 'Localization of the E1 B proteins of adenovirus 5 in transformed cells, as revealed by interaction with monoclonal antibodies', *Virology*, 142(1), pp. 44–58.

Zegerman, P. and Diffley, J. F. X. (2010) 'Checkpoint-dependent inhibition of DNA replication initiation by Sld3 and Dbf4 phosphorylation', *Nature*, 467(7314), pp. 474–478.

Zellweger, R. *et al.* (2015) 'Rad51-mediated replication fork reversal is a global response to genotoxic treatments in human cells', *Journal of Cell Biology*, 208(5), pp. 563–579.

Zeman, M. K. and Cimprich, K. A. (2014) 'Causes and consequences of replication stress', *Nature cell biology*, 16(1), pp. 2–9.

Zhang, Q. *et al.* (2000) 'Acetylation of adenovirus E1A regulates binding of the transcriptional corepressor CtBP', *Proceedings of the National Academy of Sciences*, 97(26), pp. 14323–14328.

Zhang, Y., Xiong, Y. and Yarbrough, W. G. (1998) 'ARF promotes MDM2 degradation and stabilizes p53: ARF-INK4a locus deletion impairs both the Rb and p53 tumor suppression pathways', *Cell*, 92(6), pp. 725–734.

Zhao, H., Watkins, J. L. and Piwnicka-Worms, H. (2002) 'Disruption of the checkpoint kinase 1/cell division cycle 25A pathway abrogates ionizing radiation-induced S and G2 checkpoints', *Proceedings of the National Academy of Sciences*, 99(23), pp. 14795–14800.

Zhao, L. Y. and Liao, D. (2003) 'Sequestration of p53 in the Cytoplasm by Adenovirus Type 12 E1B 55-Kilodalton Oncoprotein Is Required for Inhibition of p53-Mediated Apoptosis', *Journal of virology*, 77(24), pp. 13171–13181.

Zhao, X. (2018) 'SUMO-mediated regulation of nuclear functions and signaling processes', *Molecular cell*, 71(3), pp. 409–418.

Zheng, N. *et al.* (2002) 'Structure of the Cul1–Rbx1–Skp1–F box Skp2 SCF ubiquitin ligase complex', *Nature*, 416(6882), pp. 703–709.

Zheng, X. *et al.* (2008) 'Adenovirus E1B55K region is required to enhance cyclin E expression for efficient viral DNA replication', *Journal of virology*, 82(7), pp. 3415–3427.



Zheng, Z.-M. (2010) 'Viral oncogenes, noncoding RNAs, and RNA splicing in human tumor viruses', *International journal of biological sciences*, 6(7), p. 730.

Zhong, H. *et al.* (2005) 'Rad50 depletion impacts upon ATR-dependent DNA damage responses', *Human molecular genetics*, 14(18), pp. 2685–2693.

Zhou, P. *et al.* (2020) 'A pneumonia outbreak associated with a new coronavirus of probable bat origin', *nature*, 579(7798), pp. 270–273.

Zhu, Z. *et al.* (2008) 'Sgs1 helicase and two nucleases Dna2 and Exo1 resect DNA double-strand break ends', *Cell*, 134(6), pp. 981–994.

Zimmermann, H. *et al.* (1999) 'The human papillomavirus type 16 E6 oncoprotein can down-regulate p53 activity by targeting the transcriptional coactivator CBP/p300', *Journal of virology*, 73(8), pp. 6209–6219.

Zou, L. and Elledge, S. J. (2003) 'Sensing DNA damage through ATRIP recognition of RPA-ssDNA complexes', *Science*, 300(5625), pp. 1542–1548.

# APPENDIX

**Table A1.1** Full lists of proteins immunoprecipitating with HA-E1B55K from HAdVs 16 (group B), 9 (group D), 4 (group E) and 40 (group F).

## HeLa cells

Protein	FDR	Confidence	Accession	Description	Contaminant	Coverage	[%]	# Peptides	# PSMs	# Unique Peptides	# AAs	MW [kDa]	calc. pI	Sequest HT
High			Q07954	Prolow-density lipoprotein receptor-related protein 1 OS=Homo sapiens OX=9606 GN=LRP1 PE=1 SV=2	FALSE	10		33	35	33	4544	504.3	5.39	51.03
High			P04264	Keratin, type II cytoskeletal 1 OS=Homo sapiens OX=9606 GN=KRT1 PE=1 SV=6	TRUE	25		14	23	12	644	66	8.12	35.79
High			P13645	Keratin, type I cytoskeletal 10 OS=Homo sapiens OX=9606 GN=KRT10 PE=1 SV=6	TRUE	26		17	21	16	584	58.8	5.21	45.27
High			O95202	Mitochondrial proton/calcium exchanger protein OS=Homo sapiens OX=9606 GN=LETM1 PE=1 SV=1	FALSE	24		14	18	14	739	83.3	6.7	42
High			P28799	Progranulin OS=Homo sapiens OX=9606 GN=GRN PE=1 SV=2	FALSE	22		11	17	11	593	63.5	6.83	24.26
High			P35527	Keratin, type I cytoskeletal 9 OS=Homo sapiens OX=9606 GN=KRT9 PE=1 SV=3	TRUE	21		9	16	9	623	62	5.24	34.85
High			P38646	Stress-70 protein, mitochondrial OS=Homo sapiens OX=9606 GN=HSPA9 PE=1 SV=2	FALSE	31		15	15	15	679	73.6	6.16	22.22
High			Q14139	Ubiquitin conjugation factor E4 A OS=Homo sapiens OX=9606 GN=UBE4A PE=1 SV=2	FALSE	11		10	14	10	1066	122.5	5.24	20.15
High			P05787	Keratin, type II cytoskeletal 8 OS=Homo sapiens OX=9606 GN=KRT8 PE=1 SV=7	TRUE	23		11	12	10	483	53.7	5.59	19.16
High			P83436	Conserved oligomeric Golgi complex subunit 7 OS=Homo sapiens OX=9606 GN=COG7 PE=1 SV=1	FALSE	12		9	9	9	770	86.3	5.47	4.07
High			O75822	Eukaryotic translation initiation factor 3 subunit J OS=Homo sapiens OX=9606 GN=EIF3J PE=1 SV=2	FALSE	35		7	9	7	258	29	4.83	16.93
High			P02533	Keratin, type I cytoskeletal 14 OS=Homo sapiens OX=9606 GN=KRT14 PE=1 SV=4	TRUE	18		7	8	4	472	51.5	5.16	14.61
High			Q9UHX1	Poly(U)-binding-splicing factor PUF60 OS=Homo sapiens OX=9606 GN=PUF60 PE=1 SV=1	FALSE	13		7	8	7	559	59.8	5.29	13.03
High			Q16630	Cleavage and polyadenylation specificity factor subunit 6 OS=Homo sapiens OX=9606 GN=CPSF6 PE=1 SV=2	FALSE	15		6	7	6	551	59.2	7.15	14.46
High			AA0B4J2	T cell receptor alpha variable 1-1 OS=Homo sapiens OX=9606 GN=TRAV1-1 PE=3 SV=1	FALSE	14		1	7	1	108	11.9	4.59	0
High			P35908	Keratin, type II cytoskeletal 2 epidermal OS=Homo sapiens OX=9606 GN=KRT2 PE=1 SV=2	TRUE	12		7	7	5	639	65.4	8	12.38
High			Q9UP83	Conserved oligomeric Golgi complex subunit 5 OS=Homo sapiens OX=9606 GN=COG5 PE=1 SV=3	FALSE	9		7	7	7	839	92.7	6.6	12.37
High			Q9Y2V7	Conserved oligomeric Golgi complex subunit 6 OS=Homo sapiens OX=9606 GN=COG6 PE=1 SV=2	FALSE	10		6	7	6	657	73.2	5.76	15.23
High			P49756	RNA-binding protein 25 OS=Homo sapiens OX=9606 GN=RBM25 PE=1 SV=3	FALSE	9		6	6	6	483	100.1	6.32	9.99
High			P08779	Keratin, type I cytoskeletal 16 OS=Homo sapiens OX=9606 GN=KRT16 PE=1 SV=4	TRUE	10		5	6	2	473	51.2	5.05	7.72
High			P35637	RNA-binding protein FUS OS=Homo sapiens OX=9606 GN=FUS PE=1 SV=1	FALSE	12		5	6	5	526	53.4	9.36	9.41
High			P13647	Keratin, type II cytoskeletal 5 OS=Homo sapiens OX=9606 GN=KRT5 PE=1 SV=3	TRUE	11		6	6	5	590	62.3	7.74	5.34
High			P11021	Endoplasmic reticulum chaperone BiP OS=Homo sapiens OX=9606 GN=HSPA5 PE=1 SV=2	FALSE	12		6	6	6	654	72.3	5.16	7.89
High			AA0AA0M	Immunoglobulin heavy variable 1-45 OS=Homo sapiens OX=9606 GN=IGHV1-45 PE=3 SV=1	FALSE	9		1	6	1	117	13.5	9.1	9.13
High			Q9ULH0	Kinase D-interacting substrate of 220 kDa OS=Homo sapiens OX=9606 GN=KIDINS220 PE=1 SV=3	FALSE	4		5	5	5	1771	196.4	6.62	8.76
High			Q9BUJ2	Heterogeneous nuclear ribonucleoprotein U-like protein 1 OS=Homo sapiens OX=9606 GN=HNRNPUL1 PE=1 SV=1	FALSE	6		4	4	4	856	95.7	6.92	10.65
High			P05783	Keratin, type I cytoskeletal 18 OS=Homo sapiens OX=9606 GN=KRT18 PE=1 SV=2	FALSE	10		4	4	4	430	48	5.45	8.34
High			P55081	Microfibrillar-associated protein 1 OS=Homo sapiens OX=9606 GN=MFAP1 PE=1 SV=2	FALSE	14		4	4	4	439	51.9	4.98	0
High			P11142	Heat shock cognate 71 kDa protein OS=Homo sapiens OX=9606 GN=HSPA8 PE=1 SV=1	FALSE	7		3	4	3	646	70.9	5.52	4.92
High			Q9Y383	Putative RNA-binding protein Luc7-like 2 OS=Homo sapiens OX=9606 GN=LUC7L2 PE=1 SV=2	FALSE	15		4	4	4	392	46.5	10.01	4.78
High			Q9UKJ3	G patch domain-containing protein 8 OS=Homo sapiens OX=9606 GN=GPATCH8 PE=1 SV=2	FALSE	3		3	4	3	1502	164.1	8.66	4.45
High			P02768	Serum albumin OS=Homo sapiens OX=9606 GN=ALB PE=1 SV=2	TRUE	4		3	4	3	609	69.3	6.28	9.1
High			Q43143	Pre-mRNA-splicing factor ATP-dependent RNA helicase DHX15 OS=Homo sapiens OX=9606 GN=DHX15 PE=1 SV=1	FALSE	4		3	3	3	795	90.9	7.46	5.42
High			O75400	Pre-mRNA-processing factor 40 homolog A OS=Homo sapiens OX=9606 GN=PRPF40A PE=1 SV=2	FALSE	3		3	3	3	957	108.7	7.56	3.77
High			P19338	Nucleolin OS=Homo sapiens OX=9606 GN=NCL PE=1 SV=3	FALSE	4		3	3	3	710	76.6	4.7	2.01
High			Q969Q5	Ras-related protein Rab-24 OS=Homo sapiens OX=9606 GN=RAB24 PE=1 SV=1	FALSE	19		3	3	3	203	23.1	6.23	6.82
High			Q9H9E3	Conserved oligomeric Golgi complex subunit 4 OS=Homo sapiens OX=9606 GN=COG4 PE=1 SV=3	FALSE	4		3	3	3	785	89	5.19	1.78
High			P60709	Actin, cytoplasmic 1 OS=Homo sapiens OX=9606 GN=ACTB PE=1 SV=1	TRUE	10		3	3	3	375	41.7	5.48	1.72
High			P02538	Keratin, type II cytoskeletal 6A OS=Homo sapiens OX=9606 GN=KRT6A PE=1 SV=3	TRUE	5		3	3	1	564	60	8	2.05
High			P62851	40S ribosomal protein S25 OS=Homo sapiens OX=9606 GN=RPS25 PE=1 SV=1	FALSE	15		2	2	2	125	13.7	10.11	3.68
High			P61978	Heterogeneous nuclear ribonucleoprotein K OS=Homo sapiens OX=9606 GN=HNRNPK PE=1 SV=1	FALSE	5		2	2	2	463	50.9	5.54	2.01
High			O76011	Keratin, type I cuticular Ha4 OS=Homo sapiens OX=9606 GN=KRT34 PE=1 SV=2	TRUE	4		2	2	2	436	49.4	5.06	3.88
High			P25705	ATP synthase subunit alpha, mitochondrial OS=Homo sapiens OX=9606 GN=ATP5F1A PE=1 SV=1	FALSE	4		2	2	2	553	59.7	9.13	4.36
High			O15078	Centrosomal protein of 290 kDa OS=Homo sapiens OX=9606 GN=CEP290 PE=1 SV=2	FALSE	0				1	2479	290.2	5.95	0
High			Q66P13	ADP-ribosylation factor-like protein 6-interacting protein 4 OS=Homo sapiens OX=9606 GN=ARL6IP4 PE=1 SV=2	FALSE	7		2	2	2	421	44.9	10.93	2.25
High			P68363	Tubulin alpha-1B chain OS=Homo sapiens OX=9606 GN=TUBA1B PE=1 SV=1	FALSE	4		2	2	2	451	50.1	5.06	2.25
High			P78347	General transcription factor II-I OS=Homo sapiens OX=9606 GN=GTTF2 PE=1 SV=2	FALSE	2		2	2	2	998	112.3	6.39	1.94
High			O75477	Erlin-1 OS=Homo sapiens OX=9606 GN=ERLIN1 PE=1 SV=2	FALSE	7		2	2	2	348	39.1	7.87	3.58
High			P68371	Tubulin beta-4B chain OS=Homo sapiens OX=9606 GN=TUBB4B PE=1 SV=1	FALSE	5		2	2	2	445	49.8	4.89	0
High			Q06830	Peroxiredoxin-1 OS=Homo sapiens OX=9606 GN=PRDX1 PE=1 SV=1	TRUE	11		2	2	2	199	22.1	8.13	3.66
High			Q15287	RNA-binding protein with serine-rich domain 1 OS=Homo sapiens OX=9606 GN=RNPS1 PE=1 SV=1	FALSE	8		2	2	2	305	34.2	11.84	1.92
High			P62826	GTP-binding nuclear protein Ran OS=Homo sapiens OX=9606 GN=RAN PE=1 SV=3	FALSE	10		2	2	2	216	24.4	7.49	0
High			Q00325	Phosphate carrier protein, mitochondrial OS=Homo sapiens OX=9606 GN=SLC25A3 PE=1 SV=2	FALSE	3		1	1	1	362	40.1	9.38	0
High			Q08554	Desmocollin-1 OS=Homo sapiens OX=9606 GN=DSC1 PE=1 SV=2	FALSE	2		1	1	1	894	99.9	5.43	2.33
High			Q5VYY2	Lipase member M OS=Homo sapiens OX=9606 GN=LIPM PE=2 SV=2	FALSE	4		1	1	1	423	48.2	7.12	0

High	Q5T9A4	ATPase family AAA domain-containing protein 3B OS=Homo sapiens OX=9606 GN=ATAD3B PE=1 SV=1	FALSE	1	1	1	1	648	72.5	9.2	0
High	Q7L014	Probable ATP-dependent RNA helicase DDX46 OS=Homo sapiens OX=9606 GN=DDX46 PE=1 SV=2	FALSE	1	1	1	1	1031	117.3	9.29	2.36
High	Q43809	Cleavage and polyadenylation specificity factor subunit 5 OS=Homo sapiens OX=9606 GN=NUDT21 PE=1 SV=1	FALSE	8	1	1	1	227	26.2	8.82	2.58
High	Q15459	Splicing factor 3A subunit 1 OS=Homo sapiens OX=9606 GN=SF3A1 PE=1 SV=1	FALSE	2	1	1	1	793	88.8	5.22	0
High	P36542	ATP synthase subunit gamma, mitochondrial OS=Homo sapiens OX=9606 GN=ATP5F1C PE=1 SV=1	FALSE	3	1	1	1	298	33	9.22	0
High	Q14979	Heterogeneous nuclear ribonucleoprotein D-like OS=Homo sapiens OX=9606 GN=HNRNPDL PE=1 SV=3	FALSE	2	1	1	1	420	46.4	9.57	1.74
High	Q14498	RNA-binding protein 39 OS=Homo sapiens OX=9606 GN=RBM39 PE=1 SV=2	FALSE	3	1	1	1	530	59.3	10.1	0
High	P81605	Dermcidin OS=Homo sapiens OX=9606 GN=DCD PE=1 SV=2	FALSE	10	1	1	1	110	11.3	6.54	2.3
High	Q14746	Conserved oligomeric Golgi complex subunit 2 OS=Homo sapiens OX=9606 GN=COG2 PE=1 SV=1	FALSE	1	1	1	1	738	83.2	6.62	0
High	Q9NZT1	Calmodulin-like protein 5 OS=Homo sapiens OX=9606 GN=CALML5 PE=1 SV=2	FALSE	10	1	1	1	146	15.9	4.44	2.26
High	Q05639	Elongation factor 1-alpha 2 OS=Homo sapiens OX=9606 GN=EEF1A2 PE=1 SV=1	FALSE	2	1	1	1	463	50.4	9.03	0
High	Q01844	RNA-binding protein EWS OS=Homo sapiens OX=9606 GN=EWSR1 PE=1 SV=1	FALSE	4	1	1	1	656	68.4	9.33	2.25
High	Q96MW5	Conserved oligomeric Golgi complex subunit 8 OS=Homo sapiens OX=9606 GN=COG8 PE=1 SV=2	FALSE	1	1	1	1	612	68.4	5.2	1.75
High	Q92734	Protein TFG OS=Homo sapiens OX=9606 GN=TFG PE=1 SV=2	FALSE	3	1	1	1	400	43.4	5.1	1.94
High	Q15393	Splicing factor 3B subunit 3 OS=Homo sapiens OX=9606 GN=SF3B3 PE=1 SV=4	FALSE	1	1	1	1	1217	135.5	5.26	1.65
High	P01861	Immunoglobulin heavy constant gamma 4 OS=Homo sapiens OX=9606 GN=IGHG4 PE=1 SV=1	FALSE	3	1	1	1	327	35.9	7.36	1.78
High	Q92575	UBX domain-containing protein 4 OS=Homo sapiens OX=9606 GN=UBXN4 PE=1 SV=2	FALSE	7	1	1	1	508	56.7	6.38	3.34
High	P31327	Carbamoyl-phosphate synthase [ammonia], mitochondrial OS=Homo sapiens OX=9606 GN=CPS1 PE=1 SV=2	FALSE	1	1	1	1	1500	164.8	6.74	0
High	Q43719	HIV Tat-specific factor 1 OS=Homo sapiens OX=9606 GN=HTATSF1 PE=1 SV=1	FALSE	1	1	1	1	755	85.8	4.4	1.72
High	P62906	60S ribosomal protein L10a OS=Homo sapiens OX=9606 GN=RPL10A PE=1 SV=2	FALSE	4	1	1	1	217	24.8	9.94	0
High	P22061	Protein-L-isoadipate(D-aspartate) O-methyltransferase OS=Homo sapiens OX=9606 GN=PCMT1 PE=1 SV=4	FALSE	6	1	1	1	227	24.6	7.21	3.74
High	Q8N684	Cleavage and polyadenylation specificity factor subunit 7 OS=Homo sapiens OX=9606 GN=CPSF7 PE=1 SV=1	FALSE	3	1	1	1	471	52	8	0
High	P19474	E3 ubiquitin-protein ligase TRIM21 OS=Homo sapiens OX=9606 GN=TRIM21 PE=1 SV=1	FALSE	2	1	1	1	475	54.1	6.38	0
High	P18085	ADP-ribosylation factor 4 OS=Homo sapiens OX=9606 GN=ARF4 PE=1 SV=3	FALSE	6	1	1	1	180	20.5	7.14	1.94
High	P62269	40S ribosomal protein S18 OS=Homo sapiens OX=9606 GN=RP518 PE=1 SV=3	FALSE	7	1	1	1	152	17.7	10.99	2.32
High	O75533	Splicing factor 3B subunit 1 OS=Homo sapiens OX=9606 GN=SF3B1 PE=1 SV=3	FALSE	1	1	1	1	1304	145.7	7.09	0
High	P20648	Potassium-transporting ATPase alpha chain 1 OS=Homo sapiens OX=9606 GN=ATP4A PE=2 SV=5	FALSE	1	1	1	1	1035	114	5.81	0
High	P61353	60S ribosomal protein L27 OS=Homo sapiens OX=9606 GN=RPL27 PE=1 SV=2	FALSE	7	1	1	1	136	15.8	10.56	1.63
High	P22626	Heterogeneous nuclear ribonucleoproteins A2/B1 OS=Homo sapiens OX=9606 GN=HNRNPA2B1 PE=1 SV=2	FALSE	3	1	1	1	353	37.4	8.95	0
High	P62913	60S ribosomal protein L11 OS=Homo sapiens OX=9606 GN=RPL11 PE=1 SV=2	FALSE	5	1	1	1	178	20.2	9.6	1.7
High	P80723	Brain acid soluble protein 1 OS=Homo sapiens OX=9606 GN=BASP1 PE=1 SV=2	FALSE	12	1	1	1	227	22.7	4.63	0
High	Q12874	Splicing factor 3A subunit 3 OS=Homo sapiens OX=9606 GN=SF3A3 PE=1 SV=1	FALSE	2	1	1	1	501	58.8	5.38	0
High	P53999	Activated RNA polymerase II transcriptional coactivator p15 OS=Homo sapiens OX=9606 GN=SUB1 PE=1 SV=3	FALSE	9	1	1	1	127	14.4	9.6	1.78
High	P0DP25	Calmodulin-3 OS=Homo sapiens OX=9606 GN=CALM3 PE=1 SV=1	FALSE	9	1	1	1	149	16.8	4.22	0
High	P08195	4F2 cell-surface antigen heavy chain OS=Homo sapiens OX=9606 GN=SLC3A2 PE=1 SV=3	FALSE	2	1	1	1	630	68	5.01	0
High	P07477	Trypsin-1 OS=Homo sapiens OX=9606 GN=PRSS1 PE=1 SV=1	TRUE	4	1	1	1	247	26.5	6.51	1.93
High	Q02413	Desmoglein-1 OS=Homo sapiens OX=9606 GN=DSG1 PE=1 SV=2	FALSE	1	1	1	1	1049	113.7	5.03	0
High	Q99623	Prohibitin-2 OS=Homo sapiens OX=9606 GN=PHB2 PE=1 SV=2	FALSE	3	1	1	1	299	33.3	9.83	1.94
High	Q01650	Large neutral amino acids transporter small subunit 1 OS=Homo sapiens OX=9606 GN=SLC7A5 PE=1 SV=2	FALSE	3	1	1	1	507	55	7.72	2.1
High	Q96JB2	Conserved oligomeric Golgi complex subunit 3 OS=Homo sapiens OX=9606 GN=COG3 PE=1 SV=3	FALSE	1	1	1	1	828	94	5.57	0
High	P10124	Serglycin OS=Homo sapiens OX=9606 GN=SRGN PE=1 SV=3	FALSE	8	1	1	1	158	17.6	4.96	0
High	P31943	Heterogeneous nuclear ribonucleoprotein H OS=Homo sapiens OX=9606 GN=HNRNPH1 PE=1 SV=4	FALSE	2	1	1	1	449	49.2	6.3	1.73
High	Q9BZF9	Uveal autoantigen with coiled-coil domains and ankyrin repeats OS=Homo sapiens OX=9606 GN=UACA PE=1 SV=1	FALSE	1	1	1	1	1416	162.4	7.03	0

## HAdV16 (group B)

Protein	FDR	Confidence	Accession	Description	Contaminant	Coverage [%]	# Peptides	# PSMs	# Unique Peptides	# AAs	MW [kDa]	calc. pI	Sequest HT
High			P04264	Keratin, type II cytoskeletal 1 OS=Homo sapiens OX=9606 GN=KRT1 PE=1 SV=6	TRUE	49	24	48	21	644	66	8.12	106.85
High			Q07954	Prolow-density lipoprotein receptor-related protein 1 OS=Homo sapiens OX=9606 GN=LRP1 PE=1 SV=2	FALSE	8	31	37	31	4544	504.3	5.39	57.95
High			P35527	Keratin, type I cytoskeletal 9 OS=Homo sapiens OX=9606 GN=KRT9 PE=1 SV=3	TRUE	50	21	36	21	623	62	5.24	87.29
High			P38646	Stress-70 protein, mitochondrial OS=Homo sapiens OX=9606 GN=HSPA9 PE=1 SV=2	FALSE	34	18	28	18	679	73.6	6.16	64.86
High			P13645	Keratin, type I cytoskeletal 10 OS=Homo sapiens OX=9606 GN=KRT10 PE=1 SV=6	TRUE	32	19	28	17	584	58.8	5.21	57.95
High			O95202	Mitochondrial proton/calcium exchanger protein OS=Homo sapiens OX=9606 GN=LETM1 PE=1 SV=1	FALSE	36	21	27	21	739	83.3	6.7	63.57
High			P11142	Heat shock cognate 71 kDa protein OS=Homo sapiens OX=9606 GN=HSPA8 PE=1 SV=1	FALSE	33	18	23	16	646	70.9	5.52	49.52
High			P28799	Progranulin OS=Homo sapiens OX=9606 GN=GRN PE=1 SV=2	FALSE	36	14	19	14	593	63.5	6.83	41.01
High			P11021	Endoplasmic reticulum chaperone BIP OS=Homo sapiens OX=9606 GN=HSPA5 PE=1 SV=2	FALSE	28	15	17	13	654	72.3	5.16	31.08
High			P05787	Keratin, type II cytoskeletal 8 OS=Homo sapiens OX=9606 GN=KRT8 PE=1 SV=7	TRUE	35	14	16	13	483	53.7	5.59	37.78
High			P35908	Keratin, type II cytoskeletal 2 epidermal OS=Homo sapiens OX=9606 GN=KRT2 PE=1 SV=2	TRUE	18	11	16	9	639	65.4	8	27.41
High			Q9UHX1	Poly(U)-binding-splicing factor PUF60 OS=Homo sapiens OX=9606 GN=PUF60 PE=1 SV=1	FALSE	26	11	15	11	559	59.8	5.29	27.14
High			P02533	Keratin, type I cytoskeletal 14 OS=Homo sapiens OX=9606 GN=KRT14 PE=1 SV=4	TRUE	36	14	15	5	472	51.5	5.16	23.71
High			P13647	Keratin, type II cytoskeletal 5 OS=Homo sapiens OX=9606 GN=KRT5 PE=1 SV=3	TRUE	23	12	14	8	590	62.3	7.74	29.4
High			P60709	Actin, cytoplasmic I OS=Homo sapiens OX=9606 GN=ACTB PE=1 SV=1	TRUE	30	8	14	8	375	41.7	5.48	27.56
High			Q5H9R7	Serine/threonine-protein phosphatase 6 regulatory subunit 3 OS=Homo sapiens OX=9606 GN=PPP6R3 PE=1 SV=1	FALSE	15	11	13	11	873	97.6	4.6	26.41
High			P05783	Keratin, type I cytoskeletal 18 OS=Homo sapiens OX=9606 GN=KRT18 PE=1 SV=2	FALSE	30	12	13	11	430	48	5.45	23.25
High			Q14139	Ubiquitin conjugation factor E4 A OS=Homo sapiens OX=9606 GN=UBE4A PE=1 SV=2	FALSE	12	11	12	11	1066	122.5	5.24	23.52
High			P08779	Keratin, type I cytoskeletal 16 OS=Homo sapiens OX=9606 GN=KRT16 PE=1 SV=4	TRUE	25	11	12	4	473	51.2	5.05	18.38
High			P83436	Conserved oligomeric Golgi complex subunit 7 OS=Homo sapiens OX=9606 GN=COG7 PE=1 SV=1	FALSE	16	11	12	11	770	86.3	5.47	20.19
High			Q9ULH0	Kinase D-interacting substrate of 220 kDa OS=Homo sapiens OX=9606 GN=KIDINS220 PE=1 SV=3	FALSE	8	12	12	12	1771	196.4	6.62	18.6
High			O75822	Eukaryotic translation initiation factor 3 subunit J OS=Homo sapiens OX=9606 GN=EIF3J PE=1 SV=2	FALSE	38	9	12	9	258	29	4.83	28.6
High			Q71U36	Tubulin alpha-1A chain OS=Homo sapiens OX=9606 GN=TUBA1A PE=1 SV=1	FALSE	23	8	10	1	451	50.1	5.06	17.77
High			P31943	Heterogeneous nuclear ribonucleoprotein H OS=Homo sapiens OX=9606 GN=HNRNPH1 PE=1 SV=4	FALSE	25	8	10	6	449	49.2	6.3	16.68
High			P35637	RNA-binding protein FUS OS=Homo sapiens OX=9606 GN=FUS PE=1 SV=1	FALSE	16	7	10	5	526	53.4	9.36	17.44
High			P68363	Tubulin alpha-1B chain OS=Homo sapiens OX=9606 GN=TUBA1B PE=1 SV=1	FALSE	23	8	10	1	451	50.1	5.06	17.77
High			P68371	Tubulin beta-4B chain OS=Homo sapiens OX=9606 GN=TUBB4B PE=1 SV=1	FALSE	30	10	10	3	445	49.8	4.89	18.98
High			P49756	RNA-binding protein 25 OS=Homo sapiens OX=9606 GN=RBM25 PE=1 SV=3	FALSE	12	7	9	7	843	100.1	6.32	15.19
High			P07437	Tubulin beta chain OS=Homo sapiens OX=9606 GN=TUBB PE=1 SV=2	FALSE	27	9	9	2	444	49.6	4.89	18.6
High			Q9Y383	Putative RNA-binding protein Luc7-like 2 OS=Homo sapiens OX=9606 GN=LUC7L2 PE=1 SV=2	FALSE	23	7	9	7	392	46.5	10.01	16.7
High			Q9UP83	Conserved oligomeric Golgi complex subunit 5 OS=Homo sapiens OX=9606 GN=COG5 PE=1 SV=3	FALSE	14	9	9	9	839	92.7	6.6	7.57
High			Q16630	Cleavage and polyadenylation specificity factor subunit 6 OS=Homo sapiens OX=9606 GN=CPSF6 PE=1 SV=2	FALSE	18	8	9	8	551	59.2	7.15	20.59
High			P31327	Carbamoyl-phosphate synthase [ammonia], mitochondrial OS=Homo sapiens OX=9606 GN=CPS1 PE=1 SV=2	FALSE	6	8	8	8	1500	164.8	6.74	10.13
High			P02538	Keratin, type II cytoskeletal 6A OS=Homo sapiens OX=9606 GN=KRT6A PE=1 SV=3	TRUE	13	7	8	1	564	60	8	16.67
High			Q9Y2V7	Conserved oligomeric Golgi complex subunit 6 OS=Homo sapiens OX=9606 GN=COG6 PE=1 SV=2	FALSE	13	7	8	7	657	73.2	5.76	13.35
High			P04259	Keratin, type II cytoskeletal 6B OS=Homo sapiens OX=9606 GN=KRT6B PE=1 SV=5	TRUE	12	6	8	0	564	60	8	15.3
High			Q969Q5	Ras-related protein Rab-24 OS=Homo sapiens OX=9606 GN=RAB24 PE=1 SV=1	FALSE	43	6	8	6	203	23.1	6.23	16.53
High			O15084	Serine/threonine-protein phosphatase 6 regulatory ankyrin repeat subunit A OS=Homo sapiens OX=9606 GN=ANKRD6 PE=1 SV=1	FALSE	9	7	7	7	1053	112.9	6.25	12.41
High			P49411	Elongation factor Tu, mitochondrial OS=Homo sapiens OX=9606 GN=TUFM PE=1 SV=2	FALSE	22	7	7	7	452	49.5	7.61	7.23
High			P10809	60 kDa heat shock protein, mitochondrial OS=Homo sapiens OX=9606 GN=HSPD1 PE=1 SV=2	FALSE	18	7	7	7	573	61	5.87	15.95
Medium			Q9NS75	Cysteinyl leukotriene receptor 2 OS=Homo sapiens OX=9606 GN=CYSLTR2 PE=1 SV=1	FALSE	7	1	7	1	346	39.6	9.55	0
High			Q9BUJ2	Heterogeneous nuclear ribonucleoprotein U-like protein 1 OS=Homo sapiens OX=9606 GN=HNRNPUL1 PE=1 SV=1	FALSE	8	6	6	6	856	95.7	6.92	15.76
High			P62241	40S ribosomal protein S8 OS=Homo sapiens OX=9606 GN=RP58 PE=1 SV=2	FALSE	28	5	6	5	208	24.2	10.32	4.14
High			Q7L014	Probable ATP-dependent RNA helicase DDX46 OS=Homo sapiens OX=9606 GN=DDX46 PE=1 SV=2	FALSE	7	6	6	6	1031	117.3	9.29	8.34
High			P14923	Junction plakoglobin OS=Homo sapiens OX=9606 GN=JUP PE=1 SV=3	FALSE	10	5	5	5	745	81.7	6.14	5.49
High			Q92804	TATA-binding protein-associated factor 2N OS=Homo sapiens OX=9606 GN=TAF15 PE=1 SV=1	FALSE	11	5	5	3	592	61.8	8.02	6.96
High			Q5T9A4	ATPase family AAA domain-containing protein 3B OS=Homo sapiens OX=9606 GN=ATAD3B PE=1 SV=1	FALSE	7	5	5	5	648	72.5	9.2	7.99
High			P15924	Desmoplakin OS=Homo sapiens OX=9606 GN=DSP PE=1 SV=3	FALSE	2	5	5	5	2871	331.6	6.81	3.36
High			P02768	Serum albumin OS=Homo sapiens OX=9606 GN=ALB PE=1 SV=2	TRUE	4	3	5	3	609	69.3	6.28	12.52
High			P55081	Microfibrillar-associated protein 1 OS=Homo sapiens OX=9606 GN=MFAP1 PE=1 SV=2	FALSE	19	5	5	5	439	51.9	4.98	8.32
High			P61978	Heterogeneous nuclear ribonucleoprotein K OS=Homo sapiens OX=9606 GN=HNRNPK PE=1 SV=1	FALSE	14	5	5	5	463	50.9	5.54	7.87
High			P52597	Heterogeneous nuclear ribonucleoprotein F OS=Homo sapiens OX=9606 GN=HNRNPF PE=1 SV=3	FALSE	14	4	5	2	415	45.6	5.58	6.39
High			A0A0A0M1	Immunoglobulin heavy variable 1-45 OS=Homo sapiens OX=9606 GN=IGHV1-45 PE=3 SV=1	FALSE	9	1	5	1	117	13.5	9.1	11.87
High			Q04695	Keratin, type I cytoskeletal 17 OS=Homo sapiens OX=9606 GN=KRT17 PE=1 SV=2	TRUE	12	5	5	1	432	48.1	5.02	5.08
High			P62701	40S ribosomal protein S4, X isoform OS=Homo sapiens OX=9606 GN=RP54X PE=1 SV=2	FALSE	21	5	5	5	263	29.6	10.15	4.72
High			O00743	Serine/threonine-protein phosphatase 6 catalytic subunit OS=Homo sapiens OX=9606 GN=PPP6C PE=1 SV=1	FALSE	16	4	4	4	305	35.1	5.69	7.1
High			P25705	ATP synthase subunit alpha, mitochondrial OS=Homo sapiens OX=9606 GN=ATP5F1A PE=1 SV=1	FALSE	10	4	4	4	553	59.7	9.13	9.04

High	Q06830	Peroxisiredoxin-1 OS=Homo sapiens OX=9606 GN=PRDX1 PE=1 SV=1	TRUE	25	4	4	3	199	22.1	8.13	7.89
High	P62750	60S ribosomal protein L23a OS=Homo sapiens OX=9606 GN=RPL23A PE=1 SV=1	FALSE	21	4	4	4	156	17.7	10.45	2.44
High	O43809	Cleavage and polyadenylation specificity factor subunit 5 OS=Homo sapiens OX=9606 GN=NUDT21 PE=1 SV=1	FALSE	21	4	4	4	227	26.2	8.82	3.92
High	P0DMV9	Heat shock 70 kDa protein 1B OS=Homo sapiens OX=9606 GN=HSPA1B PE=1 SV=1	FALSE	11	4	4	3	641	70	5.66	4.12
High	P68104	Elongation factor 1-alpha 1 OS=Homo sapiens OX=9606 GN=EEF1A1 PE=1 SV=1	FALSE	13	4	4	4	462	50.1	9.01	4.33
High	P05141	ADP/ATP translocase 2 OS=Homo sapiens OX=9606 GN=SLC25A5 PE=1 SV=7	FALSE	13	4	4	4	298	32.8	9.69	7.64
High	P19338	Nucleolin OS=Homo sapiens OX=9606 GN=NCL PE=1 SV=3	FALSE	7	4	4	4	710	76.6	4.7	5.93
High	P22061	Protein-L-isoaspartate(D-aspartate) O-methyltransferase OS=Homo sapiens OX=9606 GN=PCMT1 PE=1 SV=4	FALSE	22	3	4	3	227	24.6	7.21	9.36
High	Q15393	Splicing factor 3B subunit 3 OS=Homo sapiens OX=9606 GN=SF3B3 PE=1 SV=4	FALSE	4	4	4	4	1217	135.5	5.26	3.89
High	P62269	40S ribosomal protein S18 OS=Homo sapiens OX=9606 GN=RPS18 PE=1 SV=3	FALSE	18	3	3	3	152	17.7	10.99	4.09
High	O75400	Pre-mRNA-processing factor 40 homolog A OS=Homo sapiens OX=9606 GN=PRPF40A PE=1 SV=2	FALSE	3	2	3	2	957	108.7	7.56	1.9
High	Q93008	Probable ubiquitin carboxyl-terminal hydrolase FAF-X OS=Homo sapiens OX=9606 GN=USP9X PE=1 SV=3	FALSE	1	3	3	3	2570	292.1	5.8	2.45
High	P31942	Heterogeneous nuclear ribonucleoprotein H3 OS=Homo sapiens OX=9606 GN=HNRNPH3 PE=1 SV=2	FALSE	13	3	3	3	346	36.9	6.87	3.25
High	P08195	4F2 cell-surface antigen heavy chain OS=Homo sapiens OX=9606 GN=SLC3A2 PE=1 SV=3	FALSE	7	3	3	3	630	68	5.01	4.69
High	Q14315	Filamin-C OS=Homo sapiens OX=9606 GN=FLNC PE=1 SV=3	FALSE	2	3	3	3	2725	290.8	5.97	5.44
High	P62280	40S ribosomal protein S11 OS=Homo sapiens OX=9606 GN=RPS11 PE=1 SV=3	FALSE	25	3	3	3	158	18.4	10.3	4.19
High	P18621	60S ribosomal protein L17 OS=Homo sapiens OX=9606 GN=RPL17 PE=1 SV=3	FALSE	13	2	3	2	184	21.4	10.17	4.46
High	Q00325	Phosphate carrier protein, mitochondrial OS=Homo sapiens OX=9606 GN=SLC25A3 PE=1 SV=2	FALSE	9	3	3	3	362	40.1	9.38	5.22
High	Q96MW5	Conserved oligomeric Golgi complex subunit 8 OS=Homo sapiens OX=9606 GN=COG8 PE=1 SV=2	FALSE	9	3	3	3	612	68.4	5.2	2.6
Medium	Q9P210	Cleavage and polyadenylation specificity factor subunit 2 OS=Homo sapiens OX=9606 GN=CPSF2 PE=1 SV=2	FALSE	2	1	3	1	782	88.4	5.11	0
High	O14979	Heterogeneous nuclear ribonucleoprotein D-like OS=Homo sapiens OX=9606 GN=HNRNPDL PE=1 SV=3	FALSE	8	3	3	2	420	46.4	9.57	4.08
High	Q01650	Large neutral amino acids transporter small subunit 1 OS=Homo sapiens OX=9606 GN=SLC7A5 PE=1 SV=2	FALSE	8	3	3	3	507	55	7.72	0
High	P26373	60S ribosomal protein L13 OS=Homo sapiens OX=9606 GN=RPL13 PE=1 SV=4	FALSE	14	3	3	3	211	24.2	11.65	5.64
High	P62979	Ubiquitin-40S ribosomal protein S27a OS=Homo sapiens OX=9606 GN=RPS27A PE=1 SV=2	TRUE	24	3	3	3	156	18	9.64	5.57
High	P61247	40S ribosomal protein S3a OS=Homo sapiens OX=9606 GN=RPS3A PE=1 SV=2	FALSE	14	3	3	3	264	29.9	9.73	2.48
High	P11940	Polyadenylate-binding protein 1 OS=Homo sapiens OX=9606 GN=PABPC1 PE=1 SV=2	FALSE	6	3	3	3	636	70.6	9.5	1.98
High	P36578	60S ribosomal protein L4 OS=Homo sapiens OX=9606 GN=RPL4 PE=1 SV=5	FALSE	10	3	3	3	427	47.7	11.06	3.52
High	Q9BZF9	Uveal autoantigen with coiled-coil domains and ankyrin repeats OS=Homo sapiens OX=9606 GN=UACA PE=1 SV=1	FALSE	3	3	3	3	1416	162.4	7.03	0
High	P62851	40S ribosomal protein S25 OS=Homo sapiens OX=9606 GN=RPS25 PE=1 SV=1	FALSE	24	3	3	3	125	13.7	10.11	5.5
High	P61353	60S ribosomal protein L27 OS=Homo sapiens OX=9606 GN=RPL27 PE=1 SV=2	FALSE	22	2	2	2	136	15.8	10.56	1.83
High	P16402	Histone H1.3 OS=Homo sapiens OX=9606 GN=H1-3 PE=1 SV=2	FALSE	10	2	2	2	221	22.3	11.02	3.69
High	P12236	ADP/ATP translocase 3 OS=Homo sapiens OX=9606 GN=SLC25A6 PE=1 SV=4	FALSE	8	2	2	2	298	32.8	9.74	4.03
High	P18124	60S ribosomal protein L7 OS=Homo sapiens OX=9606 GN=RPL7 PE=1 SV=1	FALSE	12	2	2	2	248	29.2	10.65	6.3
High	Q12874	Splicing factor 3A subunit 3 OS=Homo sapiens OX=9606 GN=SF3A3 PE=1 SV=1	FALSE	4	2	2	2	501	58.8	5.38	1.94
High	P50914	60S ribosomal protein L14 OS=Homo sapiens OX=9606 GN=RPL14 PE=1 SV=4	FALSE	11	2	2	2	215	23.4	10.93	4.49
High	P07900	Heat shock protein HSP 90-alpha OS=Homo sapiens OX=9606 GN=HSP90AA1 PE=1 SV=5	FALSE	3	2	2	2	732	84.6	5.02	0
High	P22626	Heterogeneous nuclear ribonucleoproteins A2/B1 OS=Homo sapiens OX=9606 GN=HNRNPA2B1 PE=1 SV=2	FALSE	7	2	2	2	353	37.4	8.95	5.53
High	Q14498	RNA-binding protein 39 OS=Homo sapiens OX=9606 GN=RBM39 PE=1 SV=2	FALSE	5	2	2	2	530	59.3	10.1	4.77
High	O75477	Erlin-1 OS=Homo sapiens OX=9606 GN=ERLIN1 PE=1 SV=2	FALSE	7	2	2	2	348	39.1	7.87	5.2
High	Q14103	Heterogeneous nuclear ribonucleoprotein D0 OS=Homo sapiens OX=9606 GN=HNRNPD PE=1 SV=1	FALSE	7	2	2	1	355	38.4	7.81	2.37
High	P0DOX8	Immunoglobulin lambda-1 light chain OS=Homo sapiens OX=9606 PE=1 SV=1	FALSE	11	2	2	2	216	22.8	6.76	4.02
High	P62249	40S ribosomal protein S16 OS=Homo sapiens OX=9606 GN=RPS16 PE=1 SV=2	FALSE	12	2	2	2	146	16.4	10.21	3.82
High	O95232	Luc7-like protein 3 OS=Homo sapiens OX=9606 GN=LUC7L3 PE=1 SV=2	FALSE	6	2	2	2	432	51.4	9.79	2.53
High	Q9UJZ1	Stomatin-like protein 2, mitochondrial OS=Homo sapiens OX=9606 GN=STOML2 PE=1 SV=1	FALSE	9	2	2	2	356	38.5	7.39	3.52
High	P31040	Succinate dehydrogenase [ubiquinone] flavoprotein subunit, mitochondrial OS=Homo sapiens OX=9606 GN=SDH	FALSE	4	2	2	2	664	72.6	7.39	2
High	P62910	60S ribosomal protein L32 OS=Homo sapiens OX=9606 GN=RPL32 PE=1 SV=2	FALSE	10	1	2	1	135	15.9	11.33	2.36
High	P46781	40S ribosomal protein S9 OS=Homo sapiens OX=9606 GN=RPS9 PE=1 SV=3	FALSE	8	2	2	2	194	22.6	10.65	3.63
High	P78347	General transcription factor II-I OS=Homo sapiens OX=9606 GN=GTF2I PE=1 SV=2	FALSE	2	2	2	2	998	112.3	6.39	0
High	P06576	ATP synthase subunit beta, mitochondrial OS=Homo sapiens OX=9606 GN=ATP5F1B PE=1 SV=3	FALSE	6	2	2	2	529	56.5	5.4	5.19
High	P04843	Dolichyl-diphosphooligosaccharide--protein glycosyltransferase subunit 1 OS=Homo sapiens OX=9606 GN=RPN	FALSE	4	2	2	2	607	68.5	6.38	0
High	P15880	40S ribosomal protein S2 OS=Homo sapiens OX=9606 GN=RPS2 PE=1 SV=2	FALSE	8	2	2	2	293	31.3	10.24	4.44
High	P35232	Prohibitin OS=Homo sapiens OX=9606 GN=PHB PE=1 SV=1	FALSE	11	2	2	2	272	29.8	5.76	4.22
High	P12268	Inosine-5'-monophosphate dehydrogenase 2 OS=Homo sapiens OX=9606 GN=IMPDH2 PE=1 SV=2	FALSE	6	2	2	2	514	55.8	6.9	4.55
High	P32119	Peroxisiredoxin-2 OS=Homo sapiens OX=9606 GN=PRDX2 PE=1 SV=5	FALSE	10	2	2	1	198	21.9	5.97	2.16
High	P17987	T-complex protein 1 subunit alpha OS=Homo sapiens OX=9606 GN=TCP1 PE=1 SV=1	FALSE	4	2	2	2	556	60.3	6.11	0
High	Q96JB2	Conserved oligomeric Golgi complex subunit 3 OS=Homo sapiens OX=9606 GN=COG3 PE=1 SV=3	FALSE	3	2	2	2	828	94	5.57	1.91
High	Q01970	1-phosphatidylinositol 4,5-bisphosphate phosphodiesterase beta-3 OS=Homo sapiens OX=9606 GN=PLCB3 PE=1	FALSE	2	2	2	2	1234	138.7	5.9	0
High	P62826	GTP-binding nuclear protein Ran OS=Homo sapiens OX=9606 GN=RAN PE=1 SV=3	FALSE	11	2	2	2	216	24.4	7.49	3.89



High	Q9UKJ3	G patch domain-containing protein 8 OS=Homo sapiens OX=9606 GN=GPATCH8 PE=1 SV=2	FALSE	2	2	2	2	1502	164.1	8.66	2.04
High	P62829	60S ribosomal protein L23 OS=Homo sapiens OX=9606 GN=RPL23 PE=1 SV=1	FALSE	20	2	2	2	140	14.9	10.51	1.83
High	P62854	40S ribosomal protein S26 OS=Homo sapiens OX=9606 GN=RPS26 PE=1 SV=3	FALSE	21	2	2	2	115	13	11	3.73
High	P05023	Sodium/potassium-transporting ATPase subunit alpha-1 OS=Homo sapiens OX=9606 GN=ATP1A1 PE=1 SV=1	FALSE	2	2	2	2	1023	112.8	5.49	0
High	P25398	40S ribosomal protein S12 OS=Homo sapiens OX=9606 GN=RPS12 PE=1 SV=3	FALSE	13	2	2	2	132	14.5	7.21	2.21
High	P40429	60S ribosomal protein L13a OS=Homo sapiens OX=9606 GN=RPL13A PE=1 SV=2	FALSE	11	2	2	2	203	23.6	10.93	4.24
High	AOA0B4J1	Immunoglobulin heavy variable 3-15 OS=Homo sapiens OX=9606 GN=IGHV3-15 PE=3 SV=1	FALSE	9	1	2	1	119	12.9	8.62	1.91
High	Q05519	Serine/arginine-rich splicing factor 11 OS=Homo sapiens OX=9606 GN=SRSF11 PE=1 SV=1	FALSE	4	1	2	1	484	53.5	10.52	3.93
High	Q02413	Desmoglein-1 OS=Homo sapiens OX=9606 GN=DSG1 PE=1 SV=2	FALSE	3	2	2	2	1049	113.7	5.03	2.88
High	Q07020	60S ribosomal protein L18 OS=Homo sapiens OX=9606 GN=RPL18 PE=1 SV=2	FALSE	12	2	2	2	188	21.6	11.72	5.63
High	Q00839	Heterogeneous nuclear ribonucleoprotein U OS=Homo sapiens OX=9606 GN=HNRNPU PE=1 SV=6	FALSE	2	2	2	2	825	90.5	6	0
High	P62318	Small nuclear ribonucleoprotein Sm D3 OS=Homo sapiens OX=9606 GN=SNRPD3 PE=1 SV=1	FALSE	17	1	2	1	126	13.9	10.32	7.36
High	P06733	Alpha-enolase OS=Homo sapiens OX=9606 GN=ENO1 PE=1 SV=2	FALSE	6	2	2	2	434	47.1	7.39	2.92
High	Q32P28	Prolyl 3-hydroxylase 1 OS=Homo sapiens OX=9606 GN=P3H1 PE=1 SV=2	FALSE	4	2	2	2	736	83.3	5.14	4.87
High	Q8IXB1	DnaJ homolog subfamily C member 10 OS=Homo sapiens OX=9606 GN=DNAJC10 PE=1 SV=2	FALSE	1	1	1	1	793	91	7.18	0
High	P25054	Adenomatous polyposis coli protein OS=Homo sapiens OX=9606 GN=APC PE=1 SV=2	FALSE	0	1	1	1	2843	311.5	7.8	2.26
High	O43813	Glutathione S-transferase LANCL1 OS=Homo sapiens OX=9606 GN=LANCL1 PE=1 SV=1	FALSE	3	1	1	1	399	45.3	7.75	2.12
High	Q9Y285	Phenylalanine--tRNA ligase alpha subunit OS=Homo sapiens OX=9606 GN=FARSA PE=1 SV=3	FALSE	2	1	1	1	508	57.5	7.8	2.29
Medium	P61254	60S ribosomal protein L26 OS=Homo sapiens OX=9606 GN=RPL26 PE=1 SV=1	FALSE	5	1	1	1	145	17.2	10.55	0
High	P14649	Myosin light chain 6B OS=Homo sapiens OX=9606 GN=MYL6B PE=1 SV=1	FALSE	6	1	1	1	208	22.8	5.73	2.31
High	O14684	Prostaglandin E synthase OS=Homo sapiens OX=9606 GN=PTGES PE=1 SV=2	FALSE	7	1	1	1	152	17.1	9.5	0
High	Q8WTW3	Conserved oligomeric Golgi complex subunit 1 OS=Homo sapiens OX=9606 GN=COG1 PE=1 SV=1	FALSE	1	1	1	1	980	108.9	7.31	1.91
Medium	Q15287	RNA-binding protein with serine-rich domain 1 OS=Homo sapiens OX=9606 GN=RNPS1 PE=1 SV=1	FALSE	3	1	1	1	305	34.2	11.84	0
High	Q09028	Histone-binding protein RBBP4 OS=Homo sapiens OX=9606 GN=RBBP4 PE=1 SV=3	FALSE	2	1	1	1	425	47.6	4.89	0
Medium	P13639	Elongation factor 2 OS=Homo sapiens OX=9606 GN=EEF2 PE=1 SV=4	FALSE	1	1	1	1	858	95.3	6.83	0
High	P47914	60S ribosomal protein L29 OS=Homo sapiens OX=9606 GN=RPL29 PE=1 SV=2	FALSE	9	1	1	1	159	17.7	11.66	2.62
High	O43143	Pre-mRNA-splicing factor ATP-dependent RNA helicase DHX15 OS=Homo sapiens OX=9606 GN=DHX15 PE=1 SV=1	FALSE	2	1	1	1	795	90.9	7.46	1.84
High	P08708	40S ribosomal protein S17 OS=Homo sapiens OX=9606 GN=RPS17 PE=1 SV=2	FALSE	16	1	1	1	135	15.5	9.85	0
High	P46776	60S ribosomal protein L27a OS=Homo sapiens OX=9606 GN=RPL27A PE=1 SV=2	FALSE	7	1	1	1	148	16.6	11	2.36
High	O95071	E3 ubiquitin-protein ligase UBR5 OS=Homo sapiens OX=9606 GN=UBR5 PE=1 SV=2	FALSE	1	1	1	1	2799	309.2	5.85	0
High	Q01081	Splicing factor U2AF 35 kDa subunit OS=Homo sapiens OX=9606 GN=U2AF1 PE=1 SV=3	FALSE	5	1	1	1	240	27.9	8.81	1.82
High	P81605	Dermcidin OS=Homo sapiens OX=9606 GN=DCD PE=1 SV=2	FALSE	10	1	1	1	110	11.3	6.54	2.3
High	Q9UNL2	Translocon-associated protein subunit gamma OS=Homo sapiens OX=9606 GN=SSR3 PE=1 SV=1	FALSE	8	1	1	1	185	21.1	9.61	1.86
High	P61313	60S ribosomal protein L15 OS=Homo sapiens OX=9606 GN=RPL15 PE=1 SV=2	FALSE	3	1	1	1	204	24.1	11.62	0
High	P06312	Immunoglobulin kappa variable 4-1 OS=Homo sapiens OX=9606 GN=IGKV4-1 PE=1 SV=1	FALSE	7	1	1	1	121	13.4	5.25	2.09
High	Q15459	Splicing factor 3A subunit 1 OS=Homo sapiens OX=9606 GN=SF3A1 PE=1 SV=1	FALSE	2	1	1	1	793	88.8	5.22	0
Medium	P78527	DNA-dependent protein kinase catalytic subunit OS=Homo sapiens OX=9606 GN=PRKDC PE=1 SV=3	FALSE	0	1	1	1	4128	468.8	7.12	0
High	Q13435	Splicing factor 3B subunit 2 OS=Homo sapiens OX=9606 GN=SF3B2 PE=1 SV=2	FALSE	2	1	1	1	895	100.2	5.67	2.1
Medium	P52272	Heterogeneous nuclear ribonucleoprotein M OS=Homo sapiens OX=9606 GN=HNRNPM PE=1 SV=3	FALSE	2	1	1	1	730	77.5	8.7	1.88
High	P27348	14-3-3 protein theta OS=Homo sapiens OX=9606 GN=YWHAQ PE=1 SV=1	FALSE	6	1	1	1	245	27.7	4.78	0
High	Q9NZ01	Very-long-chain enoyl-CoA reductase OS=Homo sapiens OX=9606 GN=TECR PE=1 SV=1	FALSE	3	1	1	1	308	36	9.45	0
High	O00170	AH receptor-interacting protein OS=Homo sapiens OX=9606 GN=AIP PE=1 SV=2	FALSE	4	1	1	1	330	37.6	6.29	2.04
High	Q06210	Glutamine--fructose-6-phosphate aminotransferase [isomerizing] 1 OS=Homo sapiens OX=9606 GN=GFPT1 PE=1 SV=1	FALSE	2	1	1	1	699	78.8	7.11	0
High	P62857	40S ribosomal protein S28 OS=Homo sapiens OX=9606 GN=RPS28 PE=1 SV=1	FALSE	17	1	1	1	69	7.8	10.7	2.01
High	P62244	40S ribosomal protein S15a OS=Homo sapiens OX=9606 GN=RPS15A PE=1 SV=2	FALSE	7	1	1	1	130	14.8	10.13	2.15
High	Q08554	Desmocollin-1 OS=Homo sapiens OX=9606 GN=DSC1 PE=1 SV=2	FALSE	2	1	1	1	894	99.9	5.43	2.87
High	Q9BRX9	WD repeat domain-containing protein 83 OS=Homo sapiens OX=9606 GN=WDR83 PE=1 SV=1	FALSE	4	1	1	1	315	34.3	5.58	2.46
High	P62306	Small nuclear ribonucleoprotein F OS=Homo sapiens OX=9606 GN=SNRPF PE=1 SV=1	FALSE	15	1	1	1	86	9.7	4.67	2.69
High	Q13200	26S proteasome non-ATPase regulatory subunit 2 OS=Homo sapiens OX=9606 GN=PSMD2 PE=1 SV=3	FALSE	2	1	1	1	908	100.1	5.2	0
High	Q86Y23	Hornrin OS=Homo sapiens OX=9606 GN=HNRN PE=1 SV=2	TRUE	2	1	1	1	2850	282.2	10.04	2.98
High	Q02878	60S ribosomal protein L6 OS=Homo sapiens OX=9606 GN=RPL6 PE=1 SV=3	FALSE	5	1	1	1	288	32.7	10.58	2.83
High	Q16629	Serine/arginine-rich splicing factor 7 OS=Homo sapiens OX=9606 GN=SRSF7 PE=1 SV=1	FALSE	6	1	1	1	238	27.4	11.82	0
Medium	P60866	40S ribosomal protein S20 OS=Homo sapiens OX=9606 GN=RPS20 PE=1 SV=1	FALSE	10	1	1	1	119	13.4	9.94	2.21
High	Q8N684	Cleavage and polyadenylation specificity factor subunit 7 OS=Homo sapiens OX=9606 GN=CPSF7 PE=1 SV=1	FALSE	2	1	1	1	471	52	8	1.63
High	P62314	Small nuclear ribonucleoprotein Sm D1 OS=Homo sapiens OX=9606 GN=SNRPD1 PE=1 SV=1	FALSE	11	1	1	1	119	13.3	11.56	3.34
Medium	P62906	60S ribosomal protein L10a OS=Homo sapiens OX=9606 GN=RPL10A PE=1 SV=2	FALSE	4	1	1	1	217	24.8	9.94	0
High	P62316	Small nuclear ribonucleoprotein Sm D2 OS=Homo sapiens OX=9606 GN=SNRPD2 PE=1 SV=1	FALSE	15	1	1	1	118	13.5	9.91	0
High	P18085	ADP-ribosylation factor 4 OS=Homo sapiens OX=9606 GN=ARF4 PE=1 SV=3	FALSE	4	1	1	1	180	20.5	7.14	0

Medium	Q9Y3U8	60S ribosomal protein L36 OS=Homo sapiens OX=9606 GN=RPL36 PE=1 SV=3	FALSE	9	1	1	1	105	12.2	11.59	1.64
Medium	P62917	60S ribosomal protein L8 OS=Homo sapiens OX=9606 GN=RPL8 PE=1 SV=2	FALSE	4	1	1	1	257	28	11.03	2.04
Medium	P28300	Protein-lysine 6-oxidase OS=Homo sapiens OX=9606 GN=LOX PE=1 SV=2	FALSE	2	1	1	1	417	46.9	8.09	1.65
High	P25205	DNA replication licensing factor MCM3 OS=Homo sapiens OX=9606 GN=MCM3 PE=1 SV=3	FALSE	2	1	1	1	808	90.9	5.77	1.94
High	O95816	BAG family molecular chaperone regulator 2 OS=Homo sapiens OX=9606 GN=BAG2 PE=1 SV=1	FALSE	5	1	1	1	211	23.8	6.7	1.98
High	P16401	Histone H1.5 OS=Homo sapiens OX=9606 GN=H1-5 PE=1 SV=3	FALSE	5	1	1	1	226	22.6	10.92	2.04
High	P62277	40S ribosomal protein S13 OS=Homo sapiens OX=9606 GN=RPS13 PE=1 SV=2	FALSE	10	1	1	1	151	17.2	10.54	0
High	Q5T749	Keratinocyte proline-rich protein OS=Homo sapiens OX=9606 GN=KPRP PE=1 SV=1	FALSE	2	1	1	1	579	64.1	8.27	1.88
High	P04792	Heat shock protein beta-1 OS=Homo sapiens OX=9606 GN=HSPB1 PE=1 SV=2	FALSE	5	1	1	1	205	22.8	6.4	2.53
High	O43719	HIV Tat-specific factor 1 OS=Homo sapiens OX=9606 GN=HTATSF1 PE=1 SV=1	FALSE	1	1	1	1	755	85.8	4.4	1.64
High	P62633	Cellular nucleic acid-binding protein OS=Homo sapiens OX=9606 GN=CNBP PE=1 SV=1	FALSE	8	1	1	1	177	19.5	7.71	1.97
High	Q9BWJ5	Splicing factor 3B subunit 5 OS=Homo sapiens OX=9606 GN=SF3B5 PE=1 SV=1	FALSE	17	1	1	1	86	10.1	6.35	0
High	P08621	U1 small nuclear ribonucleoprotein 70 kDa OS=Homo sapiens OX=9606 GN=SNRNP70 PE=1 SV=2	FALSE	3	1	1	1	437	51.5	9.94	0
High	Q9UBH6	Xenotropic and polytropic retrovirus receptor 1 OS=Homo sapiens OX=9606 GN=XPR1 PE=1 SV=1	FALSE	2	1	1	1	696	81.5	8.44	0
High	Q01844	RNA-binding protein EWS OS=Homo sapiens OX=9606 GN=EWSR1 PE=1 SV=1	FALSE	4	1	1	1	656	68.4	9.33	4.02
High	Q13347	Eukaryotic translation initiation factor 3 subunit I OS=Homo sapiens OX=9606 GN=EIF3I PE=1 SV=1	FALSE	3	1	1	1	325	36.5	5.64	0
High	P17980	26S proteasome regulatory subunit 6A OS=Homo sapiens OX=9606 GN=PSM3 PE=1 SV=3	FALSE	4	1	1	1	439	49.2	5.24	1.97
High	A6NMV6	Putative annexin A2-like protein OS=Homo sapiens OX=9606 GN=ANXA2P2 PE=5 SV=2	FALSE	3	1	1	1	339	38.6	6.95	0
Medium	O00571	ATP-dependent RNA helicase DDX3X OS=Homo sapiens OX=9606 GN=DDX3X PE=1 SV=3	FALSE	2	1	1	1	662	73.2	7.18	0
Medium	Q92734	Protein TFG OS=Homo sapiens OX=9606 GN=TFG PE=1 SV=2	FALSE	3	1	1	1	400	43.4	5.1	0
High	P61204	ADP-ribosylation factor 3 OS=Homo sapiens OX=9606 GN=ARF3 PE=1 SV=2	FALSE	6	1	1	1	181	20.6	7.43	1.64
High	P01861	Immunoglobulin heavy constant gamma 4 OS=Homo sapiens OX=9606 GN=IGHG4 PE=1 SV=1	FALSE	3	1	1	1	327	35.9	7.36	0
Medium	P08670	Vimentin OS=Homo sapiens OX=9606 GN=VIM PE=1 SV=4	FALSE	4	1	1	1	466	53.6	5.12	0
Medium	P04004	Vitronectin OS=Homo sapiens OX=9606 GN=VTN PE=1 SV=1	FALSE	3	1	1	1	478	54.3	5.8	0
High	P55072	Transitional endoplasmic reticulum ATPase OS=Homo sapiens OX=9606 GN=VCP PE=1 SV=4	FALSE	2	1	1	1	806	89.3	5.26	0
High	O15427	Monocarboxylate transporter 4 OS=Homo sapiens OX=9606 GN=SLC16A3 PE=1 SV=1	FALSE	3	1	1	1	465	49.4	7.96	2.24
High	O43684	Mitotic checkpoint protein BUB3 OS=Homo sapiens OX=9606 GN=BUB3 PE=1 SV=1	FALSE	2	1	1	1	328	37.1	6.84	0
High	P62753	40S ribosomal protein S6 OS=Homo sapiens OX=9606 GN=RPS6 PE=1 SV=1	FALSE	5	1	1	1	249	28.7	10.84	2.13
High	O75533	Splicing factor 3B subunit 1 OS=Homo sapiens OX=9606 GN=SF3B1 PE=1 SV=3	FALSE	1	1	1	1	1304	145.7	7.09	2.26
Medium	O00459	Phosphatidylinositol 3-kinase regulatory subunit beta OS=Homo sapiens OX=9606 GN=PIK3R2 PE=1 SV=2	FALSE	3	1	1	1	728	81.5	6.43	2.08
High	P62913	60S ribosomal protein L11 OS=Homo sapiens OX=9606 GN=RPL11 PE=1 SV=2	FALSE	5	1	1	1	178	20.2	9.6	1.71
High	Q6UN15	Pre-mRNA 3'-end-processing factor FIP1 OS=Homo sapiens OX=9606 GN=FIP1P1 PE=1 SV=1	FALSE	2	1	1	1	594	66.5	5.59	2.27
Medium	P62805	Histone H4 OS=Homo sapiens OX=9606 GN=H4C1 PE=1 SV=2	FALSE	8	1	1	1	103	11.4	11.36	0
High	P24534	Elongation factor 1-beta OS=Homo sapiens OX=9606 GN=EEF1B2 PE=1 SV=3	FALSE	7	1	1	1	225	24.7	4.67	2.48
High	Q07021	Complement component 1 Q subcomponent-binding protein, mitochondrial OS=Homo sapiens OX=9606 GN=C1	FALSE	7	1	1	1	282	31.3	4.84	2.09
Medium	P23246	Splicing factor, proline- and glutamine-rich OS=Homo sapiens OX=9606 GN=SFPQ PE=1 SV=2	FALSE	2	1	1	1	707	76.1	9.44	0
High	Q92841	Probable ATP-dependent RNA helicase DDX17 OS=Homo sapiens OX=9606 GN=DDX17 PE=1 SV=2	FALSE	2	1	1	1	729	80.2	8.27	2.01
Medium	P11387	DNA topoisomerase 1 OS=Homo sapiens OX=9606 GN=TOP1 PE=1 SV=2	FALSE	3	1	1	1	765	90.7	9.31	0
High	Q9NZT1	Calmodulin-like protein 5 OS=Homo sapiens OX=9606 GN=CALML5 PE=1 SV=2	FALSE	10	1	1	1	146	15.9	4.44	0
Medium	P35268	60S ribosomal protein L22 OS=Homo sapiens OX=9606 GN=RPL22 PE=1 SV=2	FALSE	10	1	1	1	128	14.8	9.19	1.76
High	Q92901	60S ribosomal protein L3-like OS=Homo sapiens OX=9606 GN=RPL3L PE=2 SV=3	FALSE	3	1	1	1	407	46.3	10.45	2.31
High	P0DP25	Calmodulin-3 OS=Homo sapiens OX=9606 GN=CALM3 PE=1 SV=1	FALSE	9	1	1	1	149	16.8	4.22	0
High	P62263	40S ribosomal protein S14 OS=Homo sapiens OX=9606 GN=RPS14 PE=1 SV=3	FALSE	9	1	1	1	151	16.3	10.05	2.72
High	P26368	Splicing factor U2AF 65 kDa subunit OS=Homo sapiens OX=9606 GN=U2AF2 PE=1 SV=4	FALSE	3	1	1	1	475	53.5	9.09	2.87
High	P35712	Transcription factor SOX-6 OS=Homo sapiens OX=9606 GN=SOX6 PE=1 SV=3	FALSE	1	1	1	1	828	91.9	7.78	0
High	P83731	60S ribosomal protein L24 OS=Homo sapiens OX=9606 GN=RPL24 PE=1 SV=1	FALSE	5	1	1	1	157	17.8	11.25	1.73
High	Q9ULX6	A-kinase anchor protein 8-like OS=Homo sapiens OX=9606 GN=AKAP8L PE=1 SV=4	FALSE	2	1	1	1	646	71.6	5.05	1.6
High	P80723	Brain acid soluble protein 1 OS=Homo sapiens OX=9606 GN=BASP1 PE=1 SV=2	FALSE	12	1	1	1	227	22.7	4.63	2.82
Medium	P67809	Y-box-binding protein 1 OS=Homo sapiens OX=9606 GN=YBX1 PE=1 SV=3	FALSE	6	1	1	1	324	35.9	9.88	0
High	Q8NB46	Serine/threonine-protein phosphatase 6 regulatory ankyrin repeat subunit C OS=Homo sapiens OX=9606 GN=A	FALSE	1	1	1	1	1076	115	6.48	0
High	P62841	40S ribosomal protein S15 OS=Homo sapiens OX=9606 GN=RPS15 PE=1 SV=2	FALSE	8	1	1	1	145	17	10.39	2.5
High	Q99623	Prohibitin-2 OS=Homo sapiens OX=9606 GN=PHB2 PE=1 SV=2	FALSE	6	1	1	1	299	33.3	9.83	3.17
Medium	P56134	ATP synthase subunit f, mitochondrial OS=Homo sapiens OX=9606 GN=ATP5MF PE=1 SV=3	FALSE	14	1	1	1	94	10.9	9.67	0
Medium	P26599	Polypyrimidine tract-binding protein 1 OS=Homo sapiens OX=9606 GN=PTBP1 PE=1 SV=1	FALSE	2	1	1	1	531	57.2	9.17	0
High	P84098	60S ribosomal protein L19 OS=Homo sapiens OX=9606 GN=RPL19 PE=1 SV=1	FALSE	9	1	1	1	196	23.5	11.47	2.98
High	P07477	Trypsin-1 OS=Homo sapiens OX=9606 GN=PRSS1 PE=1 SV=1	TRUE	8	1	1	1	247	26.5	6.51	2.5
High	Q7L412	Arginine/serine-rich coiled-coil protein 2 OS=Homo sapiens OX=9606 GN=RSRC2 PE=1 SV=1	FALSE	4	1	1	1	434	50.5	11.33	0
High	P62899	60S ribosomal protein L31 OS=Homo sapiens OX=9606 GN=RPL31 PE=1 SV=1	FALSE	7	1	1	1	125	14.5	10.54	2.15



Medium	Q09666	Neuroblast differentiation-associated protein AHNK OS=Homo sapiens OX=9606 GN=AHNAK PE=1 SV=2	FALSE	1	1	1	1	5890	628.7	6.15	0
High	P25311	Zinc-alpha-2-glycoprotein OS=Homo sapiens OX=9606 GN=AZGP1 PE=1 SV=2	FALSE	6	1	1	1	298	34.2	6.05	0
High	O60506	Heterogeneous nuclear ribonucleoprotein Q OS=Homo sapiens OX=9606 GN=SYNCRIP PE=1 SV=2	FALSE	2	1	1	1	623	69.6	8.59	2.09
High	Q8NAV1	Pre-mRNA-splicing factor 38A OS=Homo sapiens OX=9606 GN=PRPF38A PE=1 SV=1	FALSE	3	1	1	1	312	37.5	9.96	1.65
High	P62861	40S ribosomal protein S30 OS=Homo sapiens OX=9606 GN=FAU PE=1 SV=1	FALSE	17	1	1	1	59	6.6	12.15	2.31
High	Q9BRL6	Serine/arginine-rich splicing factor 8 OS=Homo sapiens OX=9606 GN=SRSF8 PE=1 SV=1	FALSE	3	1	1	1	282	32.3	11.72	1.99
High	P53999	Activated RNA polymerase II transcriptional coactivator p15 OS=Homo sapiens OX=9606 GN=SUB1 PE=1 SV=3	FALSE	9	1	1	1	127	14.4	9.6	2.31
High	Q9H9E3	Conserved oligomeric Golgi complex subunit 4 OS=Homo sapiens OX=9606 GN=COG4 PE=1 SV=3	FALSE	2	1	1	1	785	89	5.19	0
High	P23396	40S ribosomal protein S3 OS=Homo sapiens OX=9606 GN=RP53 PE=1 SV=2	FALSE	5	1	1	1	243	26.7	9.66	1.81
High	P36542	ATP synthase subunit gamma, mitochondrial OS=Homo sapiens OX=9606 GN=ATP5F1C PE=1 SV=1	FALSE	4	1	1	1	298	33	9.22	0
High	P31483	Nucleolysin TIA-1 isoform p40 OS=Homo sapiens OX=9606 GN=TIA1 PE=1 SV=3	FALSE	3	1	1	1	386	42.9	7.74	2.06

## HAdV9 (group D)

Protein	FDR	Confidence	Accession	Description	Contaminant	Coverage [%]	# Peptides	# PSMs	# Unique Peptides	# AAs	MW [kDa]	calc. pI	Sequest HT
High			O95071	E3 ubiquitin-protein ligase UBR5 OS=Homo sapiens OX=9606 GN=UBR5 PE=1 SV=2	FALSE	28	56	73	56	2799	309.2	5.85	177.17
High			P15924	Desmoplakin OS=Homo sapiens OX=9606 GN=DSP PE=1 SV=3	FALSE	24	53	69	53	2871	331.6	6.81	126.23
High			P78527	DNA-dependent protein kinase catalytic subunit OS=Homo sapiens OX=9606 GN=PRKDC PE=1 SV=3	FALSE	14	49	52	49	4128	468.8	7.12	94.44
High			P35527	Keratin, type I cytoskeletal 9 OS=Homo sapiens OX=9606 GN=KRT9 PE=1 SV=3	TRUE	61	24	51	24	623	62	5.24	142.52
High			Q5T457	E3 ubiquitin-protein ligase UBR4 OS=Homo sapiens OX=9606 GN=UBR4 PE=1 SV=1	FALSE	11	40	43	40	5183	573.5	6.04	96.06
High			P04264	Keratin, type II cytoskeletal 1 OS=Homo sapiens OX=9606 GN=KRT1 PE=1 SV=6	TRUE	43	21	40	18	644	66	8.12	99.9
High			P12268	Inosine-5'-monophosphate dehydrogenase 2 OS=Homo sapiens OX=9606 GN=IMPDH2 PE=1 SV=2	FALSE	43	20	35	20	514	55.8	6.9	104.11
High			P38646	Stress-70 protein, mitochondrial OS=Homo sapiens OX=9606 GN=HSPA9 PE=1 SV=2	FALSE	34	20	32	20	679	73.6	6.16	91.98
High			P48681	Nestin OS=Homo sapiens OX=9606 GN=NES PE=1 SV=2	FALSE	21	26	31	26	1621	177.3	4.36	80.45
High			P31327	Carbamoyl-phosphate synthase [ammonia], mitochondrial OS=Homo sapiens OX=9606 GN=CPS1 PE=1 SV=2	FALSE	30	30	31	28	1500	164.8	6.74	57.19
High			P13645	Keratin, type I cytoskeletal 10 OS=Homo sapiens OX=9606 GN=KRT10 PE=1 SV=6	TRUE	35	22	30	20	584	58.8	5.21	78.94
High			P11142	Heat shock cognate 71 kDa protein OS=Homo sapiens OX=9606 GN=HSPA8 PE=1 SV=1	FALSE	35	20	29	17	646	70.9	5.52	73.97
High			P05787	Keratin, type II cytoskeletal 8 OS=Homo sapiens OX=9606 GN=KRT8 PE=1 SV=7	TRUE	42	19	27	17	483	53.7	5.59	56.2
High			P08670	Vimentin OS=Homo sapiens OX=9606 GN=VIM PE=1 SV=4	FALSE	40	18	24	18	466	53.6	5.12	57.59
High			P28799	Progranulin OS=Homo sapiens OX=9606 GN=GRN PE=1 SV=2	FALSE	30	13	24	13	593	63.5	6.83	70.89
High			O43815	Striatin OS=Homo sapiens OX=9606 GN=STRN PE=1 SV=4	FALSE	41	19	23	18	780	86.1	5.27	60.69
High			P05783	Keratin, type I cytoskeletal 18 OS=Homo sapiens OX=9606 GN=KRT18 PE=1 SV=2	FALSE	45	15	23	14	430	48	5.45	60.7
High			Q148N4	Sarcolemmal membrane-associated protein OS=Homo sapiens OX=9606 GN=SLMAP PE=1 SV=1	FALSE	28	18	23	18	828	95.1	5.47	53.48
High			P60709	Actin, cytoplasmic 1 OS=Homo sapiens OX=9606 GN=ACTB PE=1 SV=1	TRUE	54	14	21	1	375	41.7	5.48	57.3
High			P63261	Actin, cytoplasmic 2 OS=Homo sapiens OX=9606 GN=ACTG1 PE=1 SV=1	FALSE	54	14	21	1	375	41.8	5.48	56.81
High			Q13136	Liprin-alpha-1 OS=Homo sapiens OX=9606 GN=PPFIA1 PE=1 SV=1	FALSE	24	19	20	19	1202	135.7	6.29	58.01
High			Q9BUJ2	Heterogeneous nuclear ribonucleoprotein U-like protein 1 OS=Homo sapiens OX=9606 GN=HNRNPUL1 PE=1 SV=1	FALSE	26	16	20	16	856	95.7	6.92	49.84
High			P49756	RNA-binding protein 25 OS=Homo sapiens OX=9606 GN=RBM25 PE=1 SV=3	FALSE	21	14	19	14	843	100.1	6.32	39.26
High			P07437	Tubulin beta chain OS=Homo sapiens OX=9606 GN=TUBB PE=1 SV=2	FALSE	39	12	18	4	444	49.6	4.89	47.98
High			Q14315	Filamin-C OS=Homo sapiens OX=9606 GN=FLNC PE=1 SV=3	FALSE	10	17	18	15	2725	290.8	5.97	35.86
High			Q93009	Ubiquitin carboxyl-terminal hydrolase 7 OS=Homo sapiens OX=9606 GN=USP7 PE=1 SV=2	FALSE	22	17	18	17	1102	128.2	5.55	38.69
High			P31943	Heterogeneous nuclear ribonucleoprotein H OS=Homo sapiens OX=9606 GN=HNRNP1 PE=1 SV=4	FALSE	33	10	16	5	449	49.2	6.3	49.03
High			Q15149	Plectin OS=Homo sapiens OX=9606 GN=PLEC PE=1 SV=3	FALSE	4	15	16	15	4684	531.5	5.96	31.24
High			Q9UHX1	Poly(U)-binding-splicing factor PUF60 OS=Homo sapiens OX=9606 GN=PUF60 PE=1 SV=1	FALSE	33	12	16	12	559	59.8	5.29	44.39
High			P10809	60 kDa heat shock protein, mitochondrial OS=Homo sapiens OX=9606 GN=HSPD1 PE=1 SV=2	FALSE	40	13	15	13	573	61	5.87	36.97
High			P68371	Tubulin beta-4B chain OS=Homo sapiens OX=9606 GN=TUBB4B PE=1 SV=1	FALSE	38	12	15	4	445	49.8	4.89	32.81
High			P35908	Keratin, type II cytoskeletal 2 epidermal OS=Homo sapiens OX=9606 GN=KRT2 PE=1 SV=2	TRUE	25	13	15	10	639	65.4	8	28.5
High			P11021	Endoplasmic reticulum chaperone BiP OS=Homo sapiens OX=9606 GN=HSPA5 PE=1 SV=2	FALSE	28	13	15	11	654	72.3	5.16	33.2
High			O00571	ATP-dependent RNA helicase DDX3X OS=Homo sapiens OX=9606 GN=DDX3X PE=1 SV=3	FALSE	28	14	15	13	662	73.2	7.18	36.73
High			Q9Y383	Putative RNA-binding protein Luc7-like 2 OS=Homo sapiens OX=9606 GN=LUC7L2 PE=1 SV=2	FALSE	27	10	14	10	392	46.5	10.01	33.38
High			P02533	Keratin, type I cytoskeletal 14 OS=Homo sapiens OX=9606 GN=KRT14 PE=1 SV=4	TRUE	36	13	14	6	472	51.5	5.16	36.09
High			Q71U36	Tubulin alpha-1A chain OS=Homo sapiens OX=9606 GN=TUBA1A PE=1 SV=1	FALSE	37	12	14	5	451	50.1	5.06	31.96
High			P13647	Keratin, type II cytoskeletal 5 OS=Homo sapiens OX=9606 GN=KRT5 PE=1 SV=3	TRUE	24	12	13	7	590	62.3	7.74	27.75
High			O75400	Pre-mRNA-processing factor 40 homolog A OS=Homo sapiens OX=9606 GN=PRPF40A PE=1 SV=2	FALSE	11	9	13	9	957	108.7	7.56	27.22
High			Q9H7D7	WD repeat-containing protein 26 OS=Homo sapiens OX=9606 GN=WDR26 PE=1 SV=3	FALSE	21	11	13	11	661	72.1	6.16	37.37
High			Q16630	Cleavage and polyadenylation specificity factor subunit 6 OS=Homo sapiens OX=9606 GN=CPSF6 PE=1 SV=2	FALSE	23	9	12	9	551	59.2	7.15	21.73
High			Q7L014	Probable ATP-dependent RNA helicase DDX46 OS=Homo sapiens OX=9606 GN=DDX46 PE=1 SV=2	FALSE	15	12	12	12	1031	117.3	9.29	22.26
High			P61978	Heterogeneous nuclear ribonucleoprotein K OS=Homo sapiens OX=9606 GN=HNRNPK PE=1 SV=1	FALSE	24	10	12	10	463	50.9	5.54	30
High			P08779	Keratin, type I cytoskeletal 16 OS=Homo sapiens OX=9606 GN=KRT16 PE=1 SV=4	TRUE	27	11	11	5	473	51.2	5.05	25.36
High			P49411	Elongation factor Tu, mitochondrial OS=Homo sapiens OX=9606 GN=TUFM PE=1 SV=2	FALSE	27	9	11	9	452	49.5	7.61	19.68
High			Q96559	Ran-binding protein 9 OS=Homo sapiens OX=9606 GN=RANBP9 PE=1 SV=1	FALSE	21	10	11	10	729	77.8	6.79	27.49
High			Q13033	Striatin-3 OS=Homo sapiens OX=9606 GN=STRN3 PE=1 SV=3	FALSE	17	10	10	8	797	87.2	5.36	25.23
High			P02538	Keratin, type II cytoskeletal 6A OS=Homo sapiens OX=9606 GN=KRT6A PE=1 SV=3	TRUE	17	9	10	1	564	60	8	19.04
High			P35637	RNA-binding protein FUS OS=Homo sapiens OX=9606 GN=FUS PE=1 SV=1	FALSE	16	8	10	6	526	53.4	9.36	26.37
High			P68366	Tubulin alpha-4A chain OS=Homo sapiens OX=9606 GN=TUBA4A PE=1 SV=1	FALSE	29	9	10	2	448	49.9	5.06	20.45
High			Q6WK24	Rab11 family-interacting protein 1 OS=Homo sapiens OX=9606 GN=RAB11FIP1 PE=1 SV=3	FALSE	9	8	10	8	1283	137.1	5.43	19.78
High			P04259	Keratin, type II cytoskeletal 6B OS=Homo sapiens OX=9606 GN=KRT6B PE=1 SV=5	TRUE	15	8	9	0	564	60	8	16.79
High			Q15459	Splicing factor 3A subunit 1 OS=Homo sapiens OX=9606 GN=SF3A1 PE=1 SV=1	FALSE	12	8	9	8	793	88.8	5.22	15.05
High			P25205	DNA replication licensing factor MCM3 OS=Homo sapiens OX=9606 GN=MCM3 PE=1 SV=3	FALSE	12	8	9	8	808	90.9	5.77	13.44
High			Q92841	Probable ATP-dependent RNA helicase DDX17 OS=Homo sapiens OX=9606 GN=DDX17 PE=1 SV=2	FALSE	13	9	9	8	729	80.2	8.27	18.37

High	P55795	Heterogeneous nuclear ribonucleoprotein H2 OS=Homo sapiens OX=9606 GN=HNRNPH2 PE=1 SV=1	FALSE	20	6	8	2	449	49.2	6.3	17.76
High	Q06830	Peroxisomal protein 1 OS=Homo sapiens OX=9606 GN=PRDX1 PE=1 SV=1	TRUE	37	6	8	5	199	22.1	8.13	21.99
High	P06576	ATP synthase subunit beta, mitochondrial OS=Homo sapiens OX=9606 GN=ATP5F1B PE=1 SV=3	FALSE	24	8	8	8	529	56.5	5.4	17.81
High	Q6VN20	Ran-binding protein 10 OS=Homo sapiens OX=9606 GN=RANBP10 PE=1 SV=1	FALSE	13	5	8	5	620	67.2	6.77	13.22
High	P68032	Actin, alpha cardiac muscle 1 OS=Homo sapiens OX=9606 GN=ACTC1 PE=1 SV=1	FALSE	22	7	8	1	377	42	5.39	18.56
High	P0DMV9	Heat shock 70 kDa protein 1B OS=Homo sapiens OX=9606 GN=HSPA1B PE=1 SV=1	FALSE	17	8	8	6	641	70	5.66	19.5
High	Q9NRL3	Striatin-4 OS=Homo sapiens OX=9606 GN=STRN4 PE=1 SV=2	FALSE	13	8	8	6	753	80.5	5.4	15.64
High	Q13435	Splicing factor 3B subunit 2 OS=Homo sapiens OX=9606 GN=SF3B2 PE=1 SV=2	FALSE	14	8	8	8	895	100.2	5.67	14.01
High	P19338	Nucleolin OS=Homo sapiens OX=9606 GN=NCL PE=1 SV=3	FALSE	12	7	8	7	710	76.6	4.7	18.09
High	Q96ST3	Paired amphipathic helix protein Sin3a OS=Homo sapiens OX=9606 GN=SIN3A PE=1 SV=2	FALSE	6	7	8	7	1273	145.1	7.25	7.72
High	P07355	Annexin A2 OS=Homo sapiens OX=9606 GN=ANXA2 PE=1 SV=2	FALSE	17	5	7	5	339	38.6	7.75	11.45
High	P55081	Microfibrillar-associated protein 1 OS=Homo sapiens OX=9606 GN=MFAP1 PE=1 SV=2	FALSE	21	5	7	5	439	51.9	4.98	15.93
High	P52597	Heterogeneous nuclear ribonucleoprotein F OS=Homo sapiens OX=9606 GN=HNRNPF PE=1 SV=3	FALSE	13	4	7	2	415	45.6	5.58	18.72
High	Q8IUR7	Armado repeat-containing protein 8 OS=Homo sapiens OX=9606 GN=ARMC8 PE=1 SV=2	FALSE	11	6	7	6	673	75.5	6.73	15.85
High	Q09666	Neuroblast differentiation-associated protein AHNK OS=Homo sapiens OX=9606 GN=AHNAK PE=1 SV=2	FALSE	4	6	7	6	5890	628.7	6.15	9.78
High	Q92878	DNA repair protein RAD50 OS=Homo sapiens OX=9606 GN=RAD50 PE=1 SV=1	FALSE	6	5	7	5	1312	153.8	6.89	18.07
High	A0FGR8	Extended synaptotagmin-2 OS=Homo sapiens OX=9606 GN=ESYT2 PE=1 SV=1	FALSE	11	7	7	7	921	102.3	9.26	15.52
High	Q94992	Protein HEXIM1 OS=Homo sapiens OX=9606 GN=HEXIM1 PE=1 SV=1	FALSE	23	7	7	7	359	40.6	4.89	15
High	Q9NWU2	Glucose-induced degradation protein 8 homolog OS=Homo sapiens OX=9606 GN=GID8 PE=1 SV=1	FALSE	44	6	7	6	228	26.7	4.97	24.54
High	P62701	40S ribosomal protein S4, X isoform OS=Homo sapiens OX=9606 GN=RPS4X PE=1 SV=2	FALSE	23	6	7	6	263	29.6	10.15	14.07
High	P25705	ATP synthase subunit alpha, mitochondrial OS=Homo sapiens OX=9606 GN=ATP5F1A PE=1 SV=1	FALSE	17	6	7	6	553	59.7	9.13	15.76
High	P12236	ADP/ATP translocase 3 OS=Homo sapiens OX=9606 GN=SLC25A6 PE=1 SV=4	FALSE	26	7	7	4	298	32.8	9.74	14.75
High	P14923	Junction plakoglobin OS=Homo sapiens OX=9606 GN=JUP PE=1 SV=3	FALSE	10	6	7	6	745	81.7	6.14	11.87
High	Q07666	KH domain-containing, RNA-binding, signal transduction-associated protein 1 OS=Homo sapiens OX=9606 GN=KIF1A PE=1 SV=1	FALSE	13	4	6	4	443	48.2	8.66	16.6
High	O75533	Splicing factor 3B subunit 1 OS=Homo sapiens OX=9606 GN=SF3B1 PE=1 SV=3	FALSE	6	5	6	5	1304	145.7	7.09	15.03
High	Q9Y4B5	Microtubule cross-linking factor 1 OS=Homo sapiens OX=9606 GN=MTCL1 PE=1 SV=5	FALSE	4	6	6	6	1905	209.4	6.43	12.39
High	P06733	Alpha-enolase OS=Homo sapiens OX=9606 GN=ENO1 PE=1 SV=2	FALSE	15	5	6	5	434	47.1	7.39	12.68
High	P05141	ADP/ATP translocase 2 OS=Homo sapiens OX=9606 GN=SLC25A5 PE=1 SV=7	FALSE	22	6	6	3	298	32.8	9.69	12.56
High	Q16576	Histone-binding protein RBBP7 OS=Homo sapiens OX=9606 GN=RBBP7 PE=1 SV=1	FALSE	18	6	6	3	425	47.8	5.05	8.02
High	P27348	14-3-3 protein theta OS=Homo sapiens OX=9606 GN=YWHAQ PE=1 SV=1	FALSE	26	5	6	3	245	27.7	4.78	13.86
High	A0A0A0M5	Immunoglobulin heavy variable 1-45 OS=Homo sapiens OX=9606 GN=IGHV1-45 PE=3 SV=1	FALSE	9	1	6	1	117	13.5	9.1	14.25
High	P13639	Elongation factor 2 OS=Homo sapiens OX=9606 GN=EEF2 PE=1 SV=4	FALSE	11	6	6	6	858	95.3	6.83	10.51
High	P68104	Elongation factor 1-alpha 1 OS=Homo sapiens OX=9606 GN=EEF1A1 PE=1 SV=1	FALSE	19	5	6	5	462	50.1	9.01	16.18
High	P11940	Polyadenylate-binding protein 1 OS=Homo sapiens OX=9606 GN=PABPC1 PE=1 SV=2	FALSE	11	6	6	4	636	70.6	9.5	11.79
High	Q04695	Keratin, type I cytoskeletal 17 OS=Homo sapiens OX=9606 GN=KRT17 PE=1 SV=2	TRUE	13	5	5	2	432	48.1	5.02	11.88
High	O43809	Cleavage and polyadenylation specificity factor subunit 5 OS=Homo sapiens OX=9606 GN=NUDT21 PE=1 SV=1	FALSE	21	5	5	5	227	26.2	8.82	8.29
High	P31942	Heterogeneous nuclear ribonucleoprotein H3 OS=Homo sapiens OX=9606 GN=HNRNPH3 PE=1 SV=2	FALSE	16	4	5	4	346	36.9	6.87	11.32
High	P63167	Dynein light chain 1, cytoplasmic OS=Homo sapiens OX=9606 GN=DYNLL1 PE=1 SV=1	FALSE	49	3	5	3	89	10.4	7.4	13.11
High	P17987	T-complex protein 1 subunit alpha OS=Homo sapiens OX=9606 GN=TCF11 PE=1 SV=1	FALSE	11	5	5	5	556	60.3	6.11	9.42
High	Q9NV17	ATPase family AAA domain-containing protein 3A OS=Homo sapiens OX=9606 GN=ATAD3A PE=1 SV=2	FALSE	8	5	5	5	634	71.3	8.98	9.04
High	Q5VSL9	Striatin-interacting protein 1 OS=Homo sapiens OX=9606 GN=STRI1 PE=1 SV=1	FALSE	7	4	5	3	837	95.5	6.29	9.98
High	Q86Y57	C2 domain-containing protein 5 OS=Homo sapiens OX=9606 GN=C2CD5 PE=1 SV=1	FALSE	6	4	5	4	1000	110.4	5.69	3.91
High	Q96GA3	Protein LTV1 homolog OS=Homo sapiens OX=9606 GN=LTV1 PE=1 SV=1	FALSE	9	3	5	3	475	54.8	4.91	14.33
High	Q5VUA4	Zinc finger protein 318 OS=Homo sapiens OX=9606 GN=ZNF318 PE=1 SV=2	FALSE	3	5	5	5	2279	251	7.2	11.32
High	Q09028	Histone-binding protein RBBP4 OS=Homo sapiens OX=9606 GN=RBBP4 PE=1 SV=3	FALSE	9	4	5	1	425	47.6	4.89	4.32
High	P22626	Heterogeneous nuclear ribonucleoproteins A2/B1 OS=Homo sapiens OX=9606 GN=HNRNPA2B1 PE=1 SV=2	FALSE	17	5	5	5	353	37.4	8.95	10.96
High	O43663	Protein regulator of cytokinesis 1 OS=Homo sapiens OX=9606 GN=PRC1 PE=1 SV=2	FALSE	14	5	5	5	620	71.6	6.68	12.35
High	P02768	Serum albumin OS=Homo sapiens OX=9606 GN=ALB PE=1 SV=2	TRUE	5	4	5	4	609	69.3	6.28	9.86
High	P26368	Splicing factor U2AF 65 kDa subunit OS=Homo sapiens OX=9606 GN=U2AF2 PE=1 SV=4	FALSE	16	5	5	5	475	53.5	9.09	12.62
High	P36578	60S ribosomal protein L4 OS=Homo sapiens OX=9606 GN=RPL4 PE=1 SV=5	FALSE	16	5	5	5	427	47.7	11.06	11.98
High	P30153	Serine/threonine-protein phosphatase 2A 65 kDa regulatory subunit A alpha isoform OS=Homo sapiens OX=9606 GN=PPP2R2A PE=1 SV=1	FALSE	13	5	5	5	589	65.3	5.11	10.79
High	Q9Y5X1	Sorting nexin-9 OS=Homo sapiens OX=9606 GN=SNX9 PE=1 SV=1	FALSE	14	5	5	5	595	66.6	5.58	8.73
High	P63104	14-3-3 protein zeta/delta OS=Homo sapiens OX=9606 GN=YWHAZ PE=1 SV=1	FALSE	26	5	5	3	245	27.7	4.79	9.09
High	Q9Y3A3	MOB-like protein phocein OS=Homo sapiens OX=9606 GN=MOB4 PE=1 SV=1	FALSE	22	4	5	4	225	26	5.78	16.77
High	P08238	Heat shock protein HSP 90-beta OS=Homo sapiens OX=9606 GN=HSP90AB1 PE=1 SV=4	FALSE	7	5	5	5	724	83.2	5.03	7.58
High	P27708	CAD protein OS=Homo sapiens OX=9606 GN=CAD PE=1 SV=3	FALSE	2	5	5	3	2225	242.8	6.46	8.25

High	Q86SQ0	Pleckstrin homology-like domain family B member 2 OS=Homo sapiens OX=9606 GN=PHLDB2 PE=1 SV=2	FALSE	6	4	5	4	1253	142.1	7.43	10.59
High	P22061	Protein-L-isoaspartate(D-aspartate) O-methyltransferase OS=Homo sapiens OX=9606 GN=PCMT1 PE=1 SV=4	FALSE	22	3	5	3	227	24.6	7.21	14.32
High	P18124	60S ribosomal protein L7 OS=Homo sapiens OX=9606 GN=RPL7 PE=1 SV=1	FALSE	23	5	5	5	248	29.2	10.65	4.26
High	O15027	Protein transport protein Sec16A OS=Homo sapiens OX=9606 GN=SEC16A PE=1 SV=4	FALSE	2	4	5	4	2357	251.7	5.8	4.9
High	P67809	Y-box-binding protein 1 OS=Homo sapiens OX=9606 GN=YBX1 PE=1 SV=3	FALSE	25	5	5	2	324	35.9	9.88	6.84
High	P33993	DNA replication licensing factor MCM7 OS=Homo sapiens OX=9606 GN=MCM7 PE=1 SV=4	FALSE	7	4	4	4	719	81.3	6.46	5.31
High	Q8IXB1	DnaJ homolog subfamily C member 10 OS=Homo sapiens OX=9606 GN=DNAJC10 PE=1 SV=2	FALSE	7	4	4	4	793	91	7.18	7.02
High	Q93008	Probable ubiquitin carboxyl-terminal hydrolase FAF-X OS=Homo sapiens OX=9606 GN=USP9X PE=1 SV=3	FALSE	2	4	4	4	2570	292.1	5.8	9.65
High	Q9BUE5	Tubulin beta-6 chain OS=Homo sapiens OX=9606 GN=TUBB6 PE=1 SV=1	FALSE	8	3	4	1	446	49.8	4.88	6.35
High	P23528	Cofilin-1 OS=Homo sapiens OX=9606 GN=CFI1 PE=1 SV=3	FALSE	40	4	4	4	166	18.5	8.09	10
High	P62750	60S ribosomal protein L23a OS=Homo sapiens OX=9606 GN=RPL23A PE=1 SV=1	FALSE	27	4	4	4	156	17.7	10.45	7.74
High	Q13310	Polyadenylate-binding protein 4 OS=Homo sapiens OX=9606 GN=PABPC4 PE=1 SV=1	FALSE	9	4	4	2	644	70.7	9.26	8.05
High	Q05519	Serine/arginine-rich splicing factor 11 OS=Homo sapiens OX=9606 GN=SRSF11 PE=1 SV=1	FALSE	10	3	4	3	484	53.5	10.52	8.6
High	Q6KB66	Keratin, type II cytoskeletal 80 OS=Homo sapiens OX=9606 GN=KRT80 PE=1 SV=2	FALSE	9	4	4	4	452	50.5	5.67	2.24
High	Q14257	Reticulocalbin-2 OS=Homo sapiens OX=9606 GN=RCN2 PE=1 SV=1	FALSE	18	3	4	3	317	36.9	4.4	12.56
High	P62241	40S ribosomal protein S8 OS=Homo sapiens OX=9606 GN=RPS8 PE=1 SV=2	FALSE	25	4	4	4	208	24.2	10.32	10.45
High	P23396	40S ribosomal protein S3 OS=Homo sapiens OX=9606 GN=RPS3 PE=1 SV=2	FALSE	16	4	4	4	243	26.7	9.66	7.84
High	P62979	Ubiquitin-40S ribosomal protein S27a OS=Homo sapiens OX=9606 GN=RPS27A PE=1 SV=2	TRUE	37	4	4	4	156	18	9.64	6.8
High	P08865	40S ribosomal protein SA OS=Homo sapiens OX=9606 GN=RPSA PE=1 SV=4	FALSE	12	4	4	4	295	32.8	4.87	8.02
High	Q96TC7	Regulator of microtubule dynamics protein 3 OS=Homo sapiens OX=9606 GN=RMDN3 PE=1 SV=2	FALSE	17	4	4	4	470	52.1	5.1	6.66
High	Q15393	Splicing factor 3B subunit 3 OS=Homo sapiens OX=9606 GN=SF3B3 PE=1 SV=4	FALSE	4	4	4	4	1217	135.5	5.26	4.36
High	Q00325	Phosphate carrier protein, mitochondrial OS=Homo sapiens OX=9606 GN=SLC25A3 PE=1 SV=2	FALSE	12	4	4	4	362	40.1	9.38	9.84
High	Q9UJZ1	Stomatin-like protein 2, mitochondrial OS=Homo sapiens OX=9606 GN=STOML2 PE=1 SV=1	FALSE	20	4	4	4	356	38.5	7.39	9.1
High	P48729	Casein kinase I isoform alpha OS=Homo sapiens OX=9606 GN=CSNK1A1 PE=1 SV=2	FALSE	13	4	4	4	337	38.9	9.57	4.09
High	Q02878	60S ribosomal protein L6 OS=Homo sapiens OX=9606 GN=RPL6 PE=1 SV=3	FALSE	13	3	4	3	288	32.7	10.58	5.37
High	Q08J23	RNA cytosine C(5)-methyltransferase NSUN2 OS=Homo sapiens OX=9606 GN=NSUN2 PE=1 SV=2	FALSE	6	3	4	3	767	86.4	6.77	4.34
High	P15880	40S ribosomal protein S2 OS=Homo sapiens OX=9606 GN=RPS2 PE=1 SV=2	FALSE	10	3	4	3	293	31.3	10.24	10.01
High	P61247	40S ribosomal protein S3a OS=Homo sapiens OX=9606 GN=RPS3A PE=1 SV=2	FALSE	17	4	4	4	264	29.9	9.73	9.44
High	Q14979	Heterogeneous nuclear ribonucleoprotein D-like OS=Homo sapiens OX=9606 GN=HNRNPDL PE=1 SV=3	FALSE	14	4	4	4	420	46.4	9.57	6.36
High	P16989	Y-box-binding protein 3 OS=Homo sapiens OX=9606 GN=YBX3 PE=1 SV=4	FALSE	14	4	4	1	372	40.1	9.77	5.71
High	P18085	ADP-ribosylation factor 4 OS=Homo sapiens OX=9606 GN=ARF4 PE=1 SV=3	FALSE	19	4	4	4	180	20.5	7.14	7.32
High	Q9ULH0	Kinase D-interacting substrate of 220 kDa OS=Homo sapiens OX=9606 GN=KIDINS220 PE=1 SV=3	FALSE	4	4	4	4	1771	196.4	6.62	7.81
High	Q86VP1	Tax1-binding protein 1 OS=Homo sapiens OX=9606 GN=TAX1BP1 PE=1 SV=2	FALSE	5	4	4	4	789	90.8	5.43	4.38
High	Q9BRV8	Suppressor of IKBKE 1 OS=Homo sapiens OX=9606 GN=SIKE1 PE=1 SV=1	FALSE	18	3	4	3	207	23.7	5.21	12.05
High	P18621	60S ribosomal protein L17 OS=Homo sapiens OX=9606 GN=RPL17 PE=1 SV=3	FALSE	18	3	4	3	184	21.4	10.17	7.2
High	Q9NVK5	FGFR1 oncogene partner 2 OS=Homo sapiens OX=9606 GN=FGFR1OP2 PE=1 SV=1	FALSE	12	3	3	3	253	29.4	6	5.69
High	P62826	GTP-binding nuclear protein Ran OS=Homo sapiens OX=9606 GN=RAN PE=1 SV=3	FALSE	16	3	3	3	216	24.4	7.49	6.37
High	P62269	40S ribosomal protein S18 OS=Homo sapiens OX=9606 GN=RPS18 PE=1 SV=3	FALSE	18	3	3	3	152	17.7	10.99	6.94
High	P48047	ATP synthase subunit O, mitochondrial OS=Homo sapiens OX=9606 GN=ATP5PO PE=1 SV=1	FALSE	16	3	3	3	213	23.3	9.96	5.12
High	P62249	40S ribosomal protein S16 OS=Homo sapiens OX=9606 GN=RPS16 PE=1 SV=2	FALSE	19	3	3	3	146	16.4	10.21	4.19
High	O43823	A-kinase anchor protein 8 OS=Homo sapiens OX=9606 GN=AKAP8 PE=1 SV=1	FALSE	8	3	3	3	692	76.1	5.15	4.9
High	P21333	Filamin-A OS=Homo sapiens OX=9606 GN=FLNA PE=1 SV=4	FALSE	2	3	3	1	2647	280.6	6.06	2.01
High	P28300	Protein-lysine 6-oxidase OS=Homo sapiens OX=9606 GN=LOX PE=1 SV=2	FALSE	9	3	3	3	417	46.9	8.09	3.94
High	O15084	Serine/threonine-protein phosphatase 6 regulatory ankyrin repeat subunit A OS=Homo sapiens OX=9606 GN=AF	FALSE	3	3	3	3	1053	112.9	6.25	5.08
High	Q9Y285	Phenylalanine--tRNA ligase alpha subunit OS=Homo sapiens OX=9606 GN=FARSA PE=1 SV=3	FALSE	5	2	3	2	508	57.5	7.8	5.75
High	P30050	60S ribosomal protein L12 OS=Homo sapiens OX=9606 GN=RPL12 PE=1 SV=1	FALSE	24	3	3	3	165	17.8	9.42	7.45
High	Q9H871	E3 ubiquitin-protein transferase RMND5A OS=Homo sapiens OX=9606 GN=RMND5A PE=1 SV=1	FALSE	14	3	3	3	391	44	6.06	7.51
High	P16403	Histone H1.2 OS=Homo sapiens OX=9606 GN=H1-2 PE=1 SV=2	FALSE	18	3	3	3	213	21.4	10.93	6.2
High	P40429	60S ribosomal protein L13a OS=Homo sapiens OX=9606 GN=RPL13A PE=1 SV=2	FALSE	14	3	3	3	203	23.6	10.93	4.86
High	Q66PJ3	ADP-ribosylation factor-like protein 6-interacting protein 4 OS=Homo sapiens OX=9606 GN=ARL6IP4 PE=1 SV=2	FALSE	9	3	3	3	421	44.9	10.93	7.56
High	P14618	Pyruvate kinase PKM OS=Homo sapiens OX=9606 GN=PKM PE=1 SV=4	FALSE	8	2	3	2	531	57.9	7.84	5.16
High	O43684	Mitotic checkpoint protein BUB3 OS=Homo sapiens OX=9606 GN=BUB3 PE=1 SV=1	FALSE	12	3	3	3	328	37.1	6.84	4.03
High	P52272	Heterogeneous nuclear ribonucleoprotein M OS=Homo sapiens OX=9606 GN=HNRNPM PE=1 SV=3	FALSE	6	3	3	3	730	77.5	8.7	7.69
High	P20839	Inosine-5'-monophosphate dehydrogenase 1 OS=Homo sapiens OX=9606 GN=IMPDH1 PE=1 SV=2	FALSE	7	3	3	3	514	55.4	6.9	8.3
High	Q07020	60S ribosomal protein L18 OS=Homo sapiens OX=9606 GN=RPL18 PE=1 SV=2	FALSE	18	3	3	3	188	21.6	11.72	9.24
High	P08195	4F2 cell-surface antigen heavy chain OS=Homo sapiens OX=9606 GN=SLC3A2 PE=1 SV=3	FALSE	6	3	3	3	630	68	5.01	7.56

High	P61981	14-3-3 protein gamma OS=Homo sapiens OX=9606 GN=YWHAG PE=1 SV=2	FALSE	15	3	3	1	247	28.3	4.89	7.74
High	P46940	Ras GTPase-activating-like protein IQGAP1 OS=Homo sapiens OX=9606 GN=IQGAP1 PE=1 SV=1	FALSE	2	2	3	2	1657	189.1	6.48	8.57
High	Q08380	Galectin-3-binding protein OS=Homo sapiens OX=9606 GN=LGALS3BP PE=1 SV=1	FALSE	7	3	3	3	585	65.3	5.27	4.2
High	Q14192	Four and a half LIM domains protein 2 OS=Homo sapiens OX=9606 GN=FHL2 PE=1 SV=3	FALSE	21	3	3	3	279	32.2	7.55	2.73
High	Q07021	Complement component 1 Q subcomponent-binding protein, mitochondrial OS=Homo sapiens OX=9606 GN=C1	FALSE	12	2	3	2	282	31.3	4.84	10.1
High	Q9B2F9	Uveal autoantigen with coiled-coil domains and ankyrin repeats OS=Homo sapiens OX=9606 GN=UACA PE=1 SV=1	FALSE	3	3	3	3	1416	162.4	7.03	7.4
High	Q8NC51	Plasminogen activator inhibitor 1 RNA-binding protein OS=Homo sapiens OX=9606 GN=SERBP1 PE=1 SV=2	FALSE	8	2	3	2	408	44.9	8.65	9.9
High	Q15654	Thyroid receptor-interacting protein 6 OS=Homo sapiens OX=9606 GN=TRIP6 PE=1 SV=3	FALSE	7	2	3	2	476	50.3	7.37	8.76
High	P62277	40S ribosomal protein S13 OS=Homo sapiens OX=9606 GN=RPS13 PE=1 SV=2	FALSE	21	3	3	3	151	17.2	10.54	4.21
High	P62424	60S ribosomal protein L7a OS=Homo sapiens OX=9606 GN=RPL7A PE=1 SV=2	FALSE	12	3	3	3	266	30	10.61	4.74
High	P62633	Cellular nucleic acid-binding protein OS=Homo sapiens OX=9606 GN=CNBP PE=1 SV=1	FALSE	15	2	3	2	177	19.5	7.71	8.03
High	Q92804	TATA-binding protein-associated factor 2N OS=Homo sapiens OX=9606 GN=TAF15 PE=1 SV=1	FALSE	10	3	3	1	592	61.8	8.02	6.17
High	P35232	Prohibitin OS=Homo sapiens OX=9606 GN=PHB PE=1 SV=1	FALSE	11	2	3	2	272	29.8	5.76	7.45
High	P62841	40S ribosomal protein S15 OS=Homo sapiens OX=9606 GN=RPS15 PE=1 SV=2	FALSE	22	3	3	3	145	17	10.39	7.61
High	Q13162	Peroxisomal protein 4 OS=Homo sapiens OX=9606 GN=PRDX4 PE=1 SV=1	FALSE	11	3	3	2	271	30.5	6.29	6.48
High	Q92499	Double-strand break repair protein DDX1 OS=Homo sapiens OX=9606 GN=DDX1 PE=1 SV=2	FALSE	4	2	3	2	740	82.4	7.23	9.03
High	P49959	Double-strand break repair protein MRE11 OS=Homo sapiens OX=9606 GN=MRE11 PE=1 SV=3	FALSE	5	3	3	3	708	80.5	5.9	6.56
High	P25398	40S ribosomal protein S12 OS=Homo sapiens OX=9606 GN=RPS12 PE=1 SV=3	FALSE	30	3	3	3	132	14.5	7.21	5.16
High	P17812	CTP synthase 1 OS=Homo sapiens OX=9606 GN=CTPS1 PE=1 SV=2	FALSE	4	2	3	2	591	66.6	6.46	1.88
High	P62851	40S ribosomal protein S25 OS=Homo sapiens OX=9606 GN=RPS25 PE=1 SV=1	FALSE	16	2	3	2	125	13.7	10.11	4.53
High	P02545	Prelamin-A/C OS=Homo sapiens OX=9606 GN=LMNA PE=1 SV=1	FALSE	4	3	3	3	664	74.1	7.02	4.1
High	Q6DN12	Multiple C2 and transmembrane domain-containing protein 2 OS=Homo sapiens OX=9606 GN=MCTP2 PE=1 SV=1	FALSE	4	3	3	3	878	99.5	7.56	1.7
High	P78347	General transcription factor II-I OS=Homo sapiens OX=9606 GN=GTF2I PE=1 SV=2	FALSE	4	3	3	3	998	112.3	6.39	5.49
High	P32119	Peroxisomal protein 2 OS=Homo sapiens OX=9606 GN=PRDX2 PE=1 SV=5	FALSE	18	3	3	3	198	21.9	5.97	2.02
High	P62318	Small nuclear ribonucleoprotein Sm D3 OS=Homo sapiens OX=9606 GN=SNRNP3 PE=1 SV=1	FALSE	24	2	3	2	126	13.9	10.32	10.32
High	P46781	40S ribosomal protein S9 OS=Homo sapiens OX=9606 GN=RPS9 PE=1 SV=3	FALSE	12	3	3	3	194	22.6	10.65	5.71
High	Q14498	RNA-binding protein 39 OS=Homo sapiens OX=9606 GN=RBM39 PE=1 SV=2	FALSE	5	3	3	3	530	59.3	10.1	5.51
High	Q15293	Reticulocalbin-1 OS=Homo sapiens OX=9606 GN=RCN1 PE=1 SV=1	FALSE	10	3	3	3	331	38.9	5	4.33
High	O43852	Calumenin OS=Homo sapiens OX=9606 GN=CALU PE=1 SV=2	FALSE	20	3	3	3	315	37.1	4.64	6.61
High	Q5VTL8	Pre-mRNA-splicing factor 38B OS=Homo sapiens OX=9606 GN=PRPF38B PE=1 SV=1	FALSE	7	3	3	3	546	64.4	10.54	5.46
High	Q5J525	Protein PRRC2B OS=Homo sapiens OX=9606 GN=PRRC2B PE=1 SV=2	FALSE	2	3	3	3	2229	242.8	8.34	9.55
High	P80723	Brain acid soluble protein 1 OS=Homo sapiens OX=9606 GN=BASP1 PE=1 SV=2	FALSE	23	2	2	2	227	22.7	4.63	7.77
High	P36542	ATP synthase subunit gamma, mitochondrial OS=Homo sapiens OX=9606 GN=ATP5F1C PE=1 SV=1	FALSE	7	2	2	2	298	33	9.22	4.11
High	Q8TBX8	Phosphatidylinositol 5-phosphate 4-kinase type-2 gamma OS=Homo sapiens OX=9606 GN=PIP4K2C PE=1 SV=3	FALSE	7	2	2	2	421	47.3	6.84	8.04
High	Q15084	Protein disulfide-isomerase A6 OS=Homo sapiens OX=9606 GN=PDIA6 PE=1 SV=1	FALSE	9	2	2	2	440	48.1	5.08	0
High	P06748	Nucleophosmin OS=Homo sapiens OX=9606 GN=NPM1 PE=1 SV=2	FALSE	5	1	2	1	294	32.6	4.78	6.37
High	Q9UJ50	Calcium-binding mitochondrial carrier protein Aralar2 OS=Homo sapiens OX=9606 GN=SLC25A13 PE=1 SV=2	FALSE	4	2	2	2	675	74.1	8.62	4.1
High	P55735	Protein SEC13 homolog OS=Homo sapiens OX=9606 GN=SEC13 PE=1 SV=3	FALSE	12	2	2	2	322	35.5	5.48	2.33
High	P23246	Splicing factor, proline- and glutamine-rich OS=Homo sapiens OX=9606 GN=SFPQ PE=1 SV=2	FALSE	5	2	2	2	707	76.1	9.44	5.01
High	P16615	Sarcoplasmic/endoplasmic reticulum calcium ATPase 2 OS=Homo sapiens OX=9606 GN=ATP2A2 PE=1 SV=1	FALSE	3	2	2	2	1042	114.7	5.34	4.58
High	O95218	Zinc finger Ran-binding domain-containing protein 2 OS=Homo sapiens OX=9606 GN=ZRANB2 PE=1 SV=2	FALSE	9	2	2	2	330	37.4	10.01	2.35
High	P62910	60S ribosomal protein L32 OS=Homo sapiens OX=9606 GN=RPL32 PE=1 SV=2	FALSE	17	2	2	2	135	15.9	11.33	5.15
High	P61353	60S ribosomal protein L27 OS=Homo sapiens OX=9606 GN=RPL27 PE=1 SV=2	FALSE	22	2	2	2	136	15.8	10.56	4.28
High	P85037	Forkhead box protein K1 OS=Homo sapiens OX=9606 GN=FOXK1 PE=1 SV=1	FALSE	3	2	2	2	733	75.4	9.32	0
High	P63173	60S ribosomal protein L38 OS=Homo sapiens OX=9606 GN=RPL38 PE=1 SV=2	FALSE	33	2	2	2	70	8.2	10.1	3.98
High	Q01081	Splicing factor U2AF 35 kDa subunit OS=Homo sapiens OX=9606 GN=U2AF1 PE=1 SV=3	FALSE	9	2	2	2	240	27.9	8.81	4.37
High	O43143	Pre-mRNA-splicing factor ATP-dependent RNA helicase DHX15 OS=Homo sapiens OX=9606 GN=DHX15 PE=1 SV=1	FALSE	3	2	2	2	795	90.9	7.46	4.38
High	P62266	40S ribosomal protein S23 OS=Homo sapiens OX=9606 GN=RPS23 PE=1 SV=3	FALSE	27	2	2	2	143	15.8	10.49	2.92
High	P62913	60S ribosomal protein L11 OS=Homo sapiens OX=9606 GN=RPL11 PE=1 SV=2	FALSE	12	2	2	2	178	20.2	9.6	1.85
High	P04843	Dolichyl-diphosphooligosaccharide--protein glycosyltransferase subunit 1 OS=Homo sapiens OX=9606 GN=RPN1	FALSE	4	2	2	2	607	68.5	6.38	4.96
High	O95817	BAG family molecular chaperone regulator 3 OS=Homo sapiens OX=9606 GN=BAG3 PE=1 SV=3	FALSE	6	2	2	2	575	61.6	6.95	0
High	Q8NBS9	Thioredoxin domain-containing protein 5 OS=Homo sapiens OX=9606 GN=TXNDC5 PE=1 SV=2	FALSE	6	2	2	2	432	47.6	5.97	4.04
High	P31689	DnaJ homolog subfamily A member 1 OS=Homo sapiens OX=9606 GN=DNAJA1 PE=1 SV=2	FALSE	10	2	2	2	397	44.8	7.08	3.44
High	P0DP25	Calmodulin-3 OS=Homo sapiens OX=9606 GN=CALM3 PE=1 SV=1	FALSE	15	1	2	1	149	16.8	4.22	2.55
High	O95232	Luc7-like protein 3 OS=Homo sapiens OX=9606 GN=LUC7L3 PE=1 SV=2	FALSE	6	2	2	2	432	51.4	9.79	2.56
High	Q01813	ATP-dependent 6-phosphofructokinase, platelet type OS=Homo sapiens OX=9606 GN=PFKP PE=1 SV=2	FALSE	3	2	2	2	784	85.5	7.55	3.79



High	P46782	40S ribosomal protein S5 OS=Homo sapiens OX=9606 GN=RP55 PE=1 SV=4	FALSE	16	2	2	2	204	22.9	9.72	6.29
High	Q60716	Catenin delta-1 OS=Homo sapiens OX=9606 GN=CTNND1 PE=1 SV=1	FALSE	3	2	2	2	968	108.1	6.23	4.99
High	P26373	60S ribosomal protein L13 OS=Homo sapiens OX=9606 GN=RPL13 PE=1 SV=4	FALSE	9	2	2	2	211	24.2	11.65	4.27
High	Q9Y450	HBS1-like protein OS=Homo sapiens OX=9606 GN=HBS1L PE=1 SV=1	FALSE	3	1	2	1	684	75.4	6.61	0
High	P62699	Protein yippee-like 5 OS=Homo sapiens OX=9606 GN=YPEL5 PE=1 SV=1	FALSE	21	2	2	2	121	13.8	7.31	4.63
High	P62753	40S ribosomal protein S6 OS=Homo sapiens OX=9606 GN=RP56 PE=1 SV=1	FALSE	11	2	2	2	249	28.7	10.84	4.94
High	P52907	F-actin-capping protein subunit alpha-1 OS=Homo sapiens OX=9606 GN=CAPZA1 PE=1 SV=3	FALSE	9	2	2	2	286	32.9	5.69	2.63
High	P16401	Histone H1.5 OS=Homo sapiens OX=9606 GN=H1-5 PE=1 SV=3	FALSE	10	2	2	2	226	22.6	10.92	1.89
High	P55072	Transitional endoplasmic reticulum ATPase OS=Homo sapiens OX=9606 GN=VCP PE=1 SV=4	FALSE	4	2	2	2	806	89.3	5.26	1.94
High	P33992	DNA replication licensing factor MCM5 OS=Homo sapiens OX=9606 GN=MCM5 PE=1 SV=5	FALSE	4	2	2	2	734	82.2	8.37	0
High	Q9NZ01	Very-long-chain enoyl-CoA reductase OS=Homo sapiens OX=9606 GN=TECR PE=1 SV=1	FALSE	3	1	2	1	308	36	9.45	4.18
High	Q14244	Enscosin OS=Homo sapiens OX=9606 GN=MAP7 PE=1 SV=1	FALSE	3	2	2	2	749	84	9.61	4.76
High	P62917	60S ribosomal protein L8 OS=Homo sapiens OX=9606 GN=RPL8 PE=1 SV=2	FALSE	11	2	2	2	257	28	11.03	5.31
High	Q9H0G5	Nuclear speckle splicing regulatory protein 1 OS=Homo sapiens OX=9606 GN=NSRP1 PE=1 SV=1	FALSE	4	2	2	2	558	66.4	8.84	0
High	P19474	E3 ubiquitin-protein ligase TRIM21 OS=Homo sapiens OX=9606 GN=TRIM21 PE=1 SV=1	FALSE	4	2	2	2	475	54.1	6.38	3.42
High	Q01130	Serine/arginine-rich splicing factor 2 OS=Homo sapiens OX=9606 GN=SRSF2 PE=1 SV=4	FALSE	11	2	2	2	221	25.5	11.85	4.72
High	P62316	Small nuclear ribonucleoprotein Sm D2 OS=Homo sapiens OX=9606 GN=SNRPD2 PE=1 SV=1	FALSE	23	2	2	2	118	13.5	9.91	2.75
High	P08708	40S ribosomal protein S17 OS=Homo sapiens OX=9606 GN=RP517 PE=1 SV=2	FALSE	16	1	2	1	135	15.5	9.85	5.5
High	Q14247	Src substrate cortactin OS=Homo sapiens OX=9606 GN=CTTN PE=1 SV=2	FALSE	5	2	2	2	550	61.5	5.4	2.45
High	Q32P28	Prolyl 3-hydroxylase 1 OS=Homo sapiens OX=9606 GN=P3H1 PE=1 SV=2	FALSE	3	2	2	2	736	83.3	5.14	2.04
Medium	Q3T906	N-acetylglucosamine-1-phosphotransferase subunits alpha/beta OS=Homo sapiens OX=9606 GN=GNPTAB PE=1 SV=1	FALSE	2	1	2	1	1256	143.5	7.17	0
High	P08621	U1 small nuclear ribonucleoprotein 70 kDa OS=Homo sapiens OX=9606 GN=SNRNP70 PE=1 SV=2	FALSE	5	2	2	2	437	51.5	9.94	4.47
High	Q14203	Dynactin subunit 1 OS=Homo sapiens OX=9606 GN=DCTN1 PE=1 SV=3	FALSE	2	2	2	2	1278	141.6	5.81	2.07
High	O60232	Protein ZNRD2 OS=Homo sapiens OX=9606 GN=ZNRD2 PE=1 SV=1	FALSE	15	2	2	2	199	21.5	5.24	1.86
High	P31040	Succinate dehydrogenase [ubiquinone] flavoprotein subunit, mitochondrial OS=Homo sapiens OX=9606 GN=SDH	FALSE	5	2	2	2	664	72.6	7.39	3.5
High	P49368	T-complex protein 1 subunit gamma OS=Homo sapiens OX=9606 GN=CCT3 PE=1 SV=4	FALSE	6	2	2	2	545	60.5	6.49	4.94
High	O94806	Serine/threonine-protein kinase D3 OS=Homo sapiens OX=9606 GN=PRKD3 PE=1 SV=1	FALSE	3	2	2	2	890	100.4	6.87	2.48
High	Q7L5Y9	E3 ubiquitin-protein transferase MAEA OS=Homo sapiens OX=9606 GN=MAEA PE=1 SV=1	FALSE	6	2	2	2	396	45.3	8.69	4.32
High	O75477	Erlin-1 OS=Homo sapiens OX=9606 GN=ERLIN1 PE=1 SV=2	FALSE	7	2	2	2	348	39.1	7.87	4.49
High	P17028	Zinc finger protein 24 OS=Homo sapiens OX=9606 GN=ZNF24 PE=1 SV=4	FALSE	8	1	2	1	368	42.1	6.21	0
High	P19623	Spermidine synthase OS=Homo sapiens OX=9606 GN=SRM PE=1 SV=1	FALSE	6	2	2	2	302	33.8	5.49	1.65
High	P26641	Elongation factor 1-gamma OS=Homo sapiens OX=9606 GN=EEF1G PE=1 SV=3	FALSE	6	2	2	2	437	50.1	6.67	3.7
High	O43290	U4/U6.U5 tri-snRNP-associated protein 1 OS=Homo sapiens OX=9606 GN=SART1 PE=1 SV=1	FALSE	5	2	2	2	800	90.2	6.13	0
High	Q00839	Heterogeneous nuclear ribonucleoprotein U OS=Homo sapiens OX=9606 GN=HNRNPU PE=1 SV=6	FALSE	4	2	2	2	825	90.5	6	5.88
High	Q9UL63	Muskelin OS=Homo sapiens OX=9606 GN=MKLN1 PE=1 SV=2	FALSE	3	2	2	2	735	84.7	6.34	2.51
High	Q14980	Nuclear mitotic apparatus protein 1 OS=Homo sapiens OX=9606 GN=NUMA1 PE=1 SV=2	FALSE	2	2	2	2	2115	238.1	5.78	5.56
High	O15427	Monocarboxylate transporter 4 OS=Homo sapiens OX=9606 GN=SLC16A3 PE=1 SV=1	FALSE	6	2	2	2	465	49.4	7.96	5.65
High	Q9ULQ0	Striatin-interacting protein 2 OS=Homo sapiens OX=9606 GN=STRIP2 PE=1 SV=2	FALSE	3	2	2	2	834	95.3	5.91	2.01
High	P62136	Serine/threonine-protein phosphatase PP1-alpha catalytic subunit OS=Homo sapiens OX=9606 GN=PPP1CA PE=1 SV=1	FALSE	11	2	2	2	330	37.5	6.33	4.44
High	P50914	60S ribosomal protein L14 OS=Homo sapiens OX=9606 GN=RPL14 PE=1 SV=4	FALSE	11	2	2	2	215	23.4	10.93	4.84
High	P11586	C-1-tetrahydrofolate synthase, cytoplasmic OS=Homo sapiens OX=9606 GN=MTHFD1 PE=1 SV=3	FALSE	3	2	2	2	935	101.5	7.3	1.82
High	Q02978	Mitochondrial 2-oxoglutarate/malate carrier protein OS=Homo sapiens OX=9606 GN=SLC25A11 PE=1 SV=3	FALSE	8	2	2	2	314	34	9.91	4.77
High	Q6P2H3	Centrosomal protein of 85 kDa OS=Homo sapiens OX=9606 GN=CEP85 PE=1 SV=1	FALSE	4	2	2	2	762	85.6	6	0
High	P84098	60S ribosomal protein L19 OS=Homo sapiens OX=9606 GN=RPL19 PE=1 SV=1	FALSE	13	2	2	2	196	23.5	11.47	5.61
High	Q9ULW0	Targeting protein for Xklp2 OS=Homo sapiens OX=9606 GN=TPX2 PE=1 SV=2	FALSE	3	2	2	2	747	85.6	9.23	0
High	Q08554	Desmocollin-1 OS=Homo sapiens OX=9606 GN=DSC1 PE=1 SV=2	FALSE	3	2	2	2	894	99.9	5.43	2.55
High	Q5D862	Filaggrin-2 OS=Homo sapiens OX=9606 GN=FLG2 PE=1 SV=1	TRUE	2	2	2	2	2391	247.9	8.31	2.22
High	Q13123	Protein Red OS=Homo sapiens OX=9606 GN=IK PE=1 SV=3	FALSE	6	2	2	2	557	65.6	6.64	5.26
High	Q98XP5	Serrate RNA effector molecule homolog OS=Homo sapiens OX=9606 GN=SRRT PE=1 SV=1	FALSE	4	2	2	2	876	100.6	5.96	4.97
High	P62829	60S ribosomal protein L23 OS=Homo sapiens OX=9606 GN=RPL23 PE=1 SV=1	FALSE	25	2	2	2	140	14.9	10.51	6.79
High	P39023	60S ribosomal protein L3 OS=Homo sapiens OX=9606 GN=RPL3 PE=1 SV=2	FALSE	9	2	2	2	403	46.1	10.18	5.84
High	Q6ZRV2	Protein FAM83H OS=Homo sapiens OX=9606 GN=FAM83H PE=1 SV=3	FALSE	1	1	1	1	1179	127	6.98	0
High	P82930	28S ribosomal protein S34, mitochondrial OS=Homo sapiens OX=9606 GN=MRPS34 PE=1 SV=2	FALSE	6	1	1	1	218	25.6	9.98	0
High	Q9H650	3'-5' RNA helicase YTHDC2 OS=Homo sapiens OX=9606 GN=YTHDC2 PE=1 SV=2	FALSE	1	1	1	1	1430	160.1	8.4	0
High	P62857	40S ribosomal protein S28 OS=Homo sapiens OX=9606 GN=RP528 PE=1 SV=1	FALSE	17	1	1	1	69	7.8	10.7	2.51
High	P47756	F-actin-capping protein subunit beta OS=Homo sapiens OX=9606 GN=CAPZB PE=1 SV=4	FALSE	7	1	1	1	277	31.3	5.59	2.69

High	P46776	60S ribosomal protein L27a OS=Homo sapiens OX=9606 GN=RPL27A PE=1 SV=2	FALSE	7	1	1	1	148	16.6	11	2.37
High	P09622	Dihydrolipoyl dehydrogenase, mitochondrial OS=Homo sapiens OX=9606 GN=DLD PE=1 SV=2	FALSE	3	1	1	1	509	54.1	7.85	2.1
High	P31930	Cytochrome b-c1 complex subunit 1, mitochondrial OS=Homo sapiens OX=9606 GN=UQCRC1 PE=1 SV=3	FALSE	3	1	1	1	480	52.6	6.37	1.79
High	P12004	Proliferating cell nuclear antigen OS=Homo sapiens OX=9606 GN=PCNA PE=1 SV=1	FALSE	8	1	1	1	261	28.8	4.69	2.2
High	P0DOX7	Immunoglobulin kappa light chain OS=Homo sapiens OX=9606 PE=1 SV=1	FALSE	9	1	1	1	214	23.4	7.17	2.95
Medium	Q15652	Probable JmjC domain-containing histone demethylation protein 2C OS=Homo sapiens OX=9606 GN=JMJDC1 PE=1 SV=1	FALSE	1	1	1	1	2540	284.3	7.87	0
High	Q08379	Golgin subfamily A member 2 OS=Homo sapiens OX=9606 GN=GOLGA2 PE=1 SV=3	FALSE	1	1	1	1	1002	113	5.02	2.04
High	Q16891	MICOS complex subunit MIC60 OS=Homo sapiens OX=9606 GN=IMMT PE=1 SV=1	FALSE	2	1	1	1	758	83.6	6.48	1.97
High	P47914	60S ribosomal protein L29 OS=Homo sapiens OX=9606 GN=RPL29 PE=1 SV=2	FALSE	9	1	1	1	159	17.7	11.66	3.03
High	P11387	DNA topoisomerase 1 OS=Homo sapiens OX=9606 GN=TOP1 PE=1 SV=2	FALSE	3	1	1	1	765	90.7	9.31	0
High	Q9Y3F4	Serine-threonine kinase receptor-associated protein OS=Homo sapiens OX=9606 GN=STRAP PE=1 SV=1	FALSE	3	1	1	1	350	38.4	5.12	2.35
High	Q9NNW5	WD repeat-containing protein 6 OS=Homo sapiens OX=9606 GN=WDR6 PE=1 SV=1	FALSE	2	1	1	1	1121	121.6	6.87	1.81
High	P63151	Serine/threonine-protein phosphatase 2A 55 kDa regulatory subunit B alpha isoform OS=Homo sapiens OX=9606 GN=PPP2R2B PE=1 SV=1	FALSE	3	1	1	1	447	51.7	6.2	0
High	P05387	60S acidic ribosomal protein P2 OS=Homo sapiens OX=9606 GN=RPLP2 PE=1 SV=1	FALSE	10	1	1	1	115	11.7	4.54	2.36
High	P20742	Pregnancy zone protein OS=Homo sapiens OX=9606 GN=PZP PE=1 SV=4	FALSE	1	1	1	1	1482	163.8	6.38	0
High	P11166	Solute carrier family 2, facilitated glucose transporter member 1 OS=Homo sapiens OX=9606 GN=SLC2A1 PE=1 SV=1	FALSE	2	1	1	1	492	54	8.72	0
High	Q86XP1	Diacylglycerol kinase eta OS=Homo sapiens OX=9606 GN=DGKH PE=1 SV=1	FALSE	1	1	1	1	1220	134.8	6.54	0
High	Q8WX93	Palladin OS=Homo sapiens OX=9606 GN=PALLD PE=1 SV=3	FALSE	1	1	1	1	1383	150.5	7.09	2.5
Medium	Q6P1L8	39S ribosomal protein L14, mitochondrial OS=Homo sapiens OX=9606 GN=MRPL14 PE=1 SV=1	FALSE	10	1	1	1	145	15.9	10.24	0
High	P25054	Adenomatous polyposis coli protein OS=Homo sapiens OX=9606 GN=APC PE=1 SV=2	FALSE	1	1	1	1	2843	311.5	7.8	2.11
High	Q16543	Hsp90 co-chaperone Cdc37 OS=Homo sapiens OX=9606 GN=CDC37 PE=1 SV=1	FALSE	6	1	1	1	378	44.4	5.25	0
Medium	Q95613	Pericentrin OS=Homo sapiens OX=9606 GN=PCNT PE=1 SV=4	FALSE	0	1	1	1	3336	377.8	5.55	0
High	O75607	Nucleoplasmin-3 OS=Homo sapiens OX=9606 GN=NPM3 PE=1 SV=3	FALSE	10	1	1	1	178	19.3	4.63	3.42
High	Q15287	RNA-binding protein with serine-rich domain 1 OS=Homo sapiens OX=9606 GN=RNPS1 PE=1 SV=1	FALSE	3	1	1	1	305	34.2	11.84	0
High	Q9UKJ3	G patch domain-containing protein 8 OS=Homo sapiens OX=9606 GN=GPATCH8 PE=1 SV=2	FALSE	1	1	1	1	1502	164.1	8.66	0
Medium	P52747	Zinc finger protein 143 OS=Homo sapiens OX=9606 GN=ZNF143 PE=1 SV=2	FALSE	3	1	1	1	638	68.9	6.05	0
High	O15042	U2 snRNP-associated SURP motif-containing protein OS=Homo sapiens OX=9606 GN=U2SURP PE=1 SV=2	FALSE	1	1	1	1	1029	118.2	8.47	2.83
High	Q9Y3B4	Splicing factor 3B subunit 6 OS=Homo sapiens OX=9606 GN=SF3B6 PE=1 SV=1	FALSE	11	1	1	1	125	14.6	9.38	3.02
High	P62244	40S ribosomal protein S15a OS=Homo sapiens OX=9606 GN=RPS15A PE=1 SV=2	FALSE	7	1	1	1	130	14.8	10.13	1.86
High	P06312	Immunoglobulin kappa variable 4-1 OS=Homo sapiens OX=9606 GN=IGKV4-1 PE=1 SV=1	FALSE	7	1	1	1	121	13.4	5.25	2.1
High	O95373	Importin-7 OS=Homo sapiens OX=9606 GN=IPO7 PE=1 SV=1	FALSE	1	1	1	1	1038	119.4	4.82	0
High	P02786	Transferrin receptor protein 1 OS=Homo sapiens OX=9606 GN=TFRC PE=1 SV=2	FALSE	2	1	1	1	760	84.8	6.61	2.33
High	P12270	Nucleoprotein TPR OS=Homo sapiens OX=9606 GN=TPR PE=1 SV=3	FALSE	0	1	1	1	2363	267.1	5.02	1.66
High	O00767	Acyl-CoA desaturase OS=Homo sapiens OX=9606 GN=SCD PE=1 SV=2	FALSE	4	1	1	1	359	41.5	9	2.68
High	O43813	Glutathione S-transferase LANCL1 OS=Homo sapiens OX=9606 GN=LANCL1 PE=1 SV=1	FALSE	3	1	1	1	399	45.3	7.75	1.91
High	Q15428	Splicing factor 3A subunit 2 OS=Homo sapiens OX=9606 GN=SF3A2 PE=1 SV=2	FALSE	2	1	1	1	464	49.2	9.64	2.65
High	Q6R327	Rapamycin-insensitive companion of mTOR OS=Homo sapiens OX=9606 GN=RICTOR PE=1 SV=1	FALSE	1	1	1	1	1708	192.1	7.47	2.89
High	Q53EZ4	Centrosomal protein of 55 kDa OS=Homo sapiens OX=9606 GN=CEP55 PE=1 SV=3	FALSE	2	1	1	1	464	54.1	7.01	2.09
High	P41250	Glycine--tRNA ligase OS=Homo sapiens OX=9606 GN=GARS1 PE=1 SV=3	FALSE	3	1	1	1	739	83.1	7.03	2.39
High	Q9Y4K0	Lysyl oxidase homolog 2 OS=Homo sapiens OX=9606 GN=LOXL2 PE=1 SV=1	FALSE	2	1	1	1	774	86.7	6.38	0
High	P14649	Myosin light chain 6B OS=Homo sapiens OX=9606 GN=MYL6B PE=1 SV=1	FALSE	6	1	1	1	208	22.8	5.73	2.36
High	P06753	Tropomyosin alpha-3 chain OS=Homo sapiens OX=9606 GN=TPM3 PE=1 SV=2	FALSE	5	1	1	1	285	32.9	4.72	1.6
High	P43686	26S proteasome regulatory subunit 6B OS=Homo sapiens OX=9606 GN=PSMC4 PE=1 SV=2	FALSE	3	1	1	1	418	47.3	5.21	0
Medium	Q96MA6	Adenylate kinase 8 OS=Homo sapiens OX=9606 GN=AK8 PE=1 SV=1	FALSE	3	1	1	1	479	54.9	6.15	2.37
High	P61313	60S ribosomal protein L15 OS=Homo sapiens OX=9606 GN=RPL15 PE=1 SV=2	FALSE	7	1	1	1	204	24.1	11.62	2.68
High	Q9UNL2	Translocon-associated protein subunit gamma OS=Homo sapiens OX=9606 GN=SSR3 PE=1 SV=1	FALSE	8	1	1	1	185	21.1	9.61	3.5
High	Q01469	Fatty acid-binding protein 5 OS=Homo sapiens OX=9606 GN=FABP5 PE=1 SV=3	FALSE	7	1	1	1	135	15.2	7.01	2.05
High	O15066	Kinesin-like protein KIF3B OS=Homo sapiens OX=9606 GN=KIF3B PE=1 SV=1	FALSE	2	1	1	1	747	85.1	7.69	2.1
Medium	Q13573	SNW domain-containing protein 1 OS=Homo sapiens OX=9606 GN=SNW1 PE=1 SV=1	FALSE	4	1	1	1	536	61.5	9.52	0
High	P17612	cAMP-dependent protein kinase catalytic subunit alpha OS=Homo sapiens OX=9606 GN=PRKACA PE=1 SV=2	FALSE	5	1	1	1	351	40.6	8.79	1.87
High	Q9H3K6	Bola-like protein 2 OS=Homo sapiens OX=9606 GN=BOLA2 PE=1 SV=1	FALSE	10	1	1	1	86	10.1	6.52	1.94
High	P62906	60S ribosomal protein L10a OS=Homo sapiens OX=9606 GN=RPL10A PE=1 SV=2	FALSE	4	1	1	1	217	24.8	9.94	0
High	Q86VZ3	Hornerin OS=Homo sapiens OX=9606 GN=HRNR PE=1 SV=2	TRUE	1	1	1	1	2850	282.2	10.04	2.79
High	Q86V48	Leucine zipper protein 1 OS=Homo sapiens OX=9606 GN=LUZP1 PE=1 SV=2	FALSE	1	1	1	1	1076	120.2	8.5	0
High	P07858	Cathepsin B OS=Homo sapiens OX=9606 GN=CTSB PE=1 SV=3	FALSE	3	1	1	1	339	37.8	6.3	1.72
High	Q9COD9	Ethanolaminephosphotransferase 1 OS=Homo sapiens OX=9606 GN=SELENOI PE=1 SV=3	FALSE	4	1	1	1	397	45.2	6.6	1.94

High	Q12872	Splicing factor, suppressor of white-apricot homolog OS=Homo sapiens OX=9606 GN=SFSWAP PE=1 SV=3	FALSE	1	1	1	1	951	104.8	8.05	2.78
High	A0A0B4J11	Immunoglobulin heavy variable 3-15 OS=Homo sapiens OX=9606 GN=IGHV3-15 PE=3 SV=1	FALSE	9	1	1	1	119	12.9	8.62	2.37
High	P42766	60S ribosomal protein L35 OS=Homo sapiens OX=9606 GN=RPL35 PE=1 SV=2	FALSE	11	1	1	1	123	14.5	11.05	2.88
High	Q16629	Serine/arginine-rich splicing factor 7 OS=Homo sapiens OX=9606 GN=SRSF7 PE=1 SV=1	FALSE	6	1	1	1	238	27.4	11.82	1.63
High	P60866	40S ribosomal protein S20 OS=Homo sapiens OX=9606 GN=RPS20 PE=1 SV=1	FALSE	10	1	1	1	119	13.4	9.94	2.19
Medium	P49207	60S ribosomal protein L34 OS=Homo sapiens OX=9606 GN=RPL34 PE=1 SV=3	FALSE	6	1	1	1	117	13.3	11.47	1.75
Medium	Q99496	E3 ubiquitin-protein ligase RING2 OS=Homo sapiens OX=9606 GN=RNFE2 PE=1 SV=1	FALSE	4	1	1	1	336	37.6	6.84	0
High	Q8N684	Cleavage and polyadenylation specificity factor subunit 7 OS=Homo sapiens OX=9606 GN=CPSF7 PE=1 SV=1	FALSE	2	1	1	1	471	52	8	1.66
High	P04792	Heat shock protein beta-1 OS=Homo sapiens OX=9606 GN=HSPB1 PE=1 SV=2	FALSE	5	1	1	1	205	22.8	6.4	2.22
High	Q43175	D-3-phosphoglycerate dehydrogenase OS=Homo sapiens OX=9606 GN=PHGDH PE=1 SV=4	FALSE	2	1	1	1	533	56.6	6.71	0
Medium	A0A0B4J2F	Probable serine/threonine-protein kinase SIK1B OS=Homo sapiens OX=9606 GN=SIK1B PE=3 SV=1	FALSE	4	1	1	1	783	84.9	7.2	0
High	P62314	Small nuclear ribonucleoprotein Sm D1 OS=Homo sapiens OX=9606 GN=SNRPD1 PE=1 SV=1	FALSE	17	1	1	1	119	13.3	11.56	0
High	Q5BJF6	Outer dense fiber protein 2 OS=Homo sapiens OX=9606 GN=ODF2 PE=1 SV=1	FALSE	2	1	1	1	829	95.3	7.62	1.91
High	Q9Y3U8	60S ribosomal protein L36 OS=Homo sapiens OX=9606 GN=RPL36 PE=1 SV=3	FALSE	9	1	1	1	105	12.2	11.59	1.97
High	Q53GT1	Kelch-like protein 22 OS=Homo sapiens OX=9606 GN=KLHL22 PE=1 SV=2	FALSE	1	1	1	1	634	71.6	5.49	0
High	P50402	Emerin OS=Homo sapiens OX=9606 GN=EMD PE=1 SV=1	FALSE	7	1	1	1	254	29	5.5	3.34
High	O14545	TRAF-type zinc finger domain-containing protein 1 OS=Homo sapiens OX=9606 GN=TRAFD1 PE=1 SV=1	FALSE	3	1	1	1	582	64.8	5.29	0
Medium	Q9BRK4	Leucine zipper putative tumor suppressor 2 OS=Homo sapiens OX=9606 GN=LZTS2 PE=1 SV=2	FALSE	2	1	1	1	669	72.7	6.51	2
High	P62847	40S ribosomal protein S24 OS=Homo sapiens OX=9606 GN=RPS24 PE=1 SV=1	FALSE	11	1	1	1	133	15.4	10.78	2.39
High	P21291	Cysteine and glycine-rich protein 1 OS=Homo sapiens OX=9606 GN=CSRP1 PE=1 SV=3	FALSE	5	1	1	1	193	20.6	8.57	1.87
High	Q5T749	Keratinocyte proline-rich protein OS=Homo sapiens OX=9606 GN=KPRP PE=1 SV=1	FALSE	2	1	1	1	579	64.1	8.27	0
High	Q9H2U1	ATP-dependent DNA/RNA helicase DHX36 OS=Homo sapiens OX=9606 GN=DHX36 PE=1 SV=2	FALSE	1	1	1	1	1008	114.7	7.68	1.66
High	P20648	Potassium-transporting ATPase alpha chain 1 OS=Homo sapiens OX=9606 GN=ATP4A PE=2 SV=5	FALSE	1	1	1	1	1035	114	5.81	2.58
High	Q96JB2	Conserved oligomeric Golgi complex subunit 3 OS=Homo sapiens OX=9606 GN=COG3 PE=1 SV=3	FALSE	2	1	1	1	828	94	5.57	1.9
High	Q8IWV8	Calcium homeostasis endoplasmic reticulum protein OS=Homo sapiens OX=9606 GN=CHERP PE=1 SV=3	FALSE	2	1	1	1	916	103.6	9.04	2.94
High	P27635	60S ribosomal protein L10 OS=Homo sapiens OX=9606 GN=RPL10 PE=1 SV=4	FALSE	13	1	1	1	214	24.6	10.08	4.14
High	Q15437	Protein transport protein Sec23B OS=Homo sapiens OX=9606 GN=SEC23B PE=1 SV=2	FALSE	2	1	1	1	767	86.4	6.89	2.07
High	P82650	28S ribosomal protein S22, mitochondrial OS=Homo sapiens OX=9606 GN=MRPS22 PE=1 SV=1	FALSE	3	1	1	1	360	41.3	7.9	0
High	Q71RC2	La-related protein 4 OS=Homo sapiens OX=9606 GN=LARP4 PE=1 SV=3	FALSE	2	1	1	1	724	80.5	6.61	0
High	Q9BQ67	Glutamate-rich WD repeat-containing protein 1 OS=Homo sapiens OX=9606 GN=GRWD1 PE=1 SV=1	FALSE	4	1	1	1	446	49.4	4.92	0
High	P61026	Ras-related protein Rab-10 OS=Homo sapiens OX=9606 GN=RAB10 PE=1 SV=1	FALSE	6	1	1	1	200	22.5	8.38	1.79
High	P29692	Elongation factor 1-delta OS=Homo sapiens OX=9606 GN=EEF1D PE=1 SV=5	FALSE	4	1	1	1	281	31.1	5.01	0
High	Q9HAU0	Pleckstrin homology domain-containing family A member 5 OS=Homo sapiens OX=9606 GN=PLEKHA5 PE=1 SV=	FALSE	1	1	1	1	1116	127.4	7.53	0
High	Q12906	Interleukin enhancer-binding factor 3 OS=Homo sapiens OX=9606 GN=ILF3 PE=1 SV=3	FALSE	1	1	1	1	894	95.3	8.76	2.12
High	Q9BWJ5	Splicing factor 3B subunit 5 OS=Homo sapiens OX=9606 GN=SF3B5 PE=1 SV=1	FALSE	17	1	1	1	86	10.1	6.35	2.97
High	Q13888	General transcription factor IIH subunit 2 OS=Homo sapiens OX=9606 GN=GTF2H2 PE=1 SV=1	FALSE	2	1	1	1	395	44.4	6.78	0
High	Q13561	Dynactin subunit 2 OS=Homo sapiens OX=9606 GN=DCTN2 PE=1 SV=4	FALSE	3	1	1	1	401	44.2	5.21	2.33
High	Q9NZM1	Myoferlin OS=Homo sapiens OX=9606 GN=MYOF PE=1 SV=1	FALSE	1	1	1	1	2061	234.6	6.18	0
High	Q92845	Kinesin-associated protein 3 OS=Homo sapiens OX=9606 GN=KIFAP3 PE=1 SV=2	FALSE	3	1	1	1	792	91.1	5.08	4.41
High	Q9UBH6	Xenotropic and polytropic retrovirus receptor 1 OS=Homo sapiens OX=9606 GN=XPR1 PE=1 SV=1	FALSE	4	1	1	1	696	81.5	8.44	0
High	Q9BQA1	Methylosome protein 50 OS=Homo sapiens OX=9606 GN=WDR77 PE=1 SV=1	FALSE	4	1	1	1	342	36.7	5.17	2.94
High	O15479	Melanoma-associated antigen B2 OS=Homo sapiens OX=9606 GN=MAGEB2 PE=1 SV=3	FALSE	5	1	1	1	319	35.3	8.76	3.61
Medium	Q9UDY2	Tight junction protein ZO-2 OS=Homo sapiens OX=9606 GN=TJP2 PE=1 SV=2	FALSE	1	1	1	1	1190	133.9	7.4	0
High	Q01844	RNA-binding protein EWS OS=Homo sapiens OX=9606 GN=EWSR1 PE=1 SV=1	FALSE	4	1	1	1	656	68.4	9.33	6.3
High	P19387	DNA-directed RNA polymerase II subunit RPB3 OS=Homo sapiens OX=9606 GN=POLR2C PE=1 SV=2	FALSE	5	1	1	1	275	31.4	4.92	0
High	P17980	26S proteasome regulatory subunit 6A OS=Homo sapiens OX=9606 GN=PSMC3 PE=1 SV=3	FALSE	4	1	1	1	439	49.2	5.24	1.7
High	Q9H0E3	Histone deacetylase complex subunit SAP130 OS=Homo sapiens OX=9606 GN=SAP130 PE=1 SV=1	FALSE	1	1	1	1	1048	110.3	9.83	2.38
High	P61204	ADP-ribosylation factor 3 OS=Homo sapiens OX=9606 GN=ARF3 PE=1 SV=2	FALSE	6	1	1	1	181	20.6	7.43	1.77
High	P01861	Immunoglobulin heavy constant gamma 4 OS=Homo sapiens OX=9606 GN=IGHG4 PE=1 SV=1	FALSE	3	1	1	1	327	35.9	7.36	0
High	Q9Y3Z3	Deoxynucleoside triphosphate triphosphohydrolase SAMHD1 OS=Homo sapiens OX=9606 GN=SAMHD1 PE=1 SV	FALSE	3	1	1	1	626	72.2	7.14	1.79
High	P50991	T-complex protein 1 subunit delta OS=Homo sapiens OX=9606 GN=CCT4 PE=1 SV=4	FALSE	2	1	1	1	539	57.9	7.83	2.44
High	P09012	U1 small nuclear ribonucleoprotein A OS=Homo sapiens OX=9606 GN=SNRPA PE=1 SV=3	FALSE	3	1	1	1	282	31.3	9.83	1.84
High	P63220	40S ribosomal protein S21 OS=Homo sapiens OX=9606 GN=RPS21 PE=1 SV=1	FALSE	18	1	1	1	83	9.1	8.5	2.47
High	P62714	Serine/threonine-protein phosphatase 2A catalytic subunit beta isoform OS=Homo sapiens OX=9606 GN=PPP2C	FALSE	5	1	1	1	309	35.6	5.43	2.03
High	Q96D15	Reticulocalbin-3 OS=Homo sapiens OX=9606 GN=RCN3 PE=1 SV=1	FALSE	4	1	1	1	328	37.5	4.89	2.57
High	P04004	Vitronectin OS=Homo sapiens OX=9606 GN=VTN PE=1 SV=1	FALSE	3	1	1	1	478	54.3	5.8	2.26



High	Q15758	Neutral amino acid transporter B(0) OS=Homo sapiens OX=9606 GN=SLC1A5 PE=1 SV=2	FALSE	2	1	1	1	541	56.6	5.48	2
High	O43719	HIV Tat-specific factor 1 OS=Homo sapiens OX=9606 GN=HTATS1 PE=1 SV=1	FALSE	2	1	1	1	755	85.8	4.4	2.28
High	P51991	Heterogeneous nuclear ribonucleoprotein A3 OS=Homo sapiens OX=9606 GN=HNRNPA3 PE=1 SV=2	FALSE	4	1	1	1	378	39.6	9.01	0
High	Q9HCE1	Helicase MOV-10 OS=Homo sapiens OX=9606 GN=MOV10 PE=1 SV=2	FALSE	2	1	1	1	1003	113.6	8.82	0
High	O00187	Mannan-binding lectin serine protease 2 OS=Homo sapiens OX=9606 GN=MASP2 PE=1 SV=4	FALSE	2	1	1	1	686	75.7	5.63	0
High	Q96N67	Dedicator of cytokinesis protein 7 OS=Homo sapiens OX=9606 GN=DOCK7 PE=1 SV=4	FALSE	1	1	1	1	2140	242.4	6.8	0
High	Q15637	Splicing factor 1 OS=Homo sapiens OX=9606 GN=SF1 PE=1 SV=4	FALSE	2	1	1	1	639	68.3	8.98	0
High	P05198	Eukaryotic translation initiation factor 2 subunit 1 OS=Homo sapiens OX=9606 GN=EIF2S1 PE=1 SV=3	FALSE	4	1	1	1	315	36.1	5.08	2.16
High	P30101	Protein disulfide-isomerase A3 OS=Homo sapiens OX=9606 GN=PDIA3 PE=1 SV=4	FALSE	3	1	1	1	505	56.7	6.35	0
High	P24534	Elongation factor 1-beta OS=Homo sapiens OX=9606 GN=EEF1B2 PE=1 SV=3	FALSE	7	1	1	1	225	24.7	4.67	1.61
High	P62888	60S ribosomal protein L30 OS=Homo sapiens OX=9606 GN=RPL30 PE=1 SV=2	FALSE	17	1	1	1	115	12.8	9.63	2.41
High	P14678	Small nuclear ribonucleoprotein-associated proteins B and B' OS=Homo sapiens OX=9606 GN=SNRNP PE=1 SV=2	FALSE	3	1	1	1	240	24.6	11.19	0
High	P63208	S-phase kinase-associated protein 1 OS=Homo sapiens OX=9606 GN=SKP1 PE=1 SV=2	FALSE	7	1	1	1	163	18.6	4.54	2.74
High	Q9NZT1	Calmodulin-like protein 5 OS=Homo sapiens OX=9606 GN=CALML5 PE=1 SV=2	FALSE	10	1	1	1	146	15.9	4.44	1.82
Medium	P63241	Eukaryotic translation initiation factor 5A-1 OS=Homo sapiens OX=9606 GN=EIF5A PE=1 SV=2	FALSE	17	1	1	1	154	16.8	5.24	1.77
High	P12956	X-ray repair cross-complementing protein 6 OS=Homo sapiens OX=9606 GN=XRCC6 PE=1 SV=2	FALSE	2	1	1	1	609	69.8	6.64	1.85
High	Q14004	Cyclin-dependent kinase 13 OS=Homo sapiens OX=9606 GN=CDK13 PE=1 SV=2	FALSE	1	1	1	1	1512	164.8	9.69	0
High	P46778	60S ribosomal protein L21 OS=Homo sapiens OX=9606 GN=RPL21 PE=1 SV=2	FALSE	7	1	1	1	160	18.6	10.49	2.54
High	P35268	60S ribosomal protein L22 OS=Homo sapiens OX=9606 GN=RPL22 PE=1 SV=2	FALSE	10	1	1	1	128	14.8	9.19	3.12
High	O00743	Serine/threonine-protein phosphatase 6 catalytic subunit OS=Homo sapiens OX=9606 GN=PPP6C PE=1 SV=1	FALSE	3	1	1	1	305	35.1	5.69	0
High	Q6Q0C0	E3 ubiquitin-protein ligase TRAF7 OS=Homo sapiens OX=9606 GN=TRAF7 PE=1 SV=1	FALSE	1	1	1	1	670	74.6	7.15	2.13
High	Q7Z5K2	Wings apart-like protein homolog OS=Homo sapiens OX=9606 GN=WAPL PE=1 SV=1	FALSE	1	1	1	1	1190	132.9	5.44	0
High	O43920	NADH dehydrogenase [ubiquinone] iron-sulfur protein 5 OS=Homo sapiens OX=9606 GN=NDUF55 PE=1 SV=3	FALSE	11	1	1	1	106	12.5	9.14	2.12
High	P27824	Calnexin OS=Homo sapiens OX=9606 GN=CANX PE=1 SV=2	FALSE	3	1	1	1	592	67.5	4.6	0
High	Q9UG63	ATP-binding cassette sub-family F member 2 OS=Homo sapiens OX=9606 GN=ABCF2 PE=1 SV=2	FALSE	2	1	1	1	623	71.2	7.37	0
High	P00338	L-lactate dehydrogenase A chain OS=Homo sapiens OX=9606 GN=LDHA PE=1 SV=2	FALSE	5	1	1	1	332	36.7	8.27	0
Medium	P82663	28S ribosomal protein S25, mitochondrial OS=Homo sapiens OX=9606 GN=MRPS25 PE=1 SV=1	FALSE	6	1	1	1	173	20.1	8.82	0
Medium	O94913	Pre-mRNA cleavage complex 2 protein Pcf11 OS=Homo sapiens OX=9606 GN=PCF11 PE=1 SV=3	FALSE	1	1	1	1	1555	172.9	8.48	0
High	Q9C0C2	182 kDa tankyrase-1-binding protein OS=Homo sapiens OX=9606 GN=TNKS1BP1 PE=1 SV=4	FALSE	1	1	1	1	1729	181.7	4.86	2.9
High	P62263	40S ribosomal protein S14 OS=Homo sapiens OX=9606 GN=RPS14 PE=1 SV=3	FALSE	9	1	1	1	151	16.3	10.05	0
High	P83731	60S ribosomal protein L24 OS=Homo sapiens OX=9606 GN=RPL24 PE=1 SV=1	FALSE	5	1	1	1	157	17.8	11.25	1.75
High	P62306	Small nuclear ribonucleoprotein F OS=Homo sapiens OX=9606 GN=SNRPF PE=1 SV=1	FALSE	15	1	1	1	86	9.7	4.67	2.55
Medium	Q8N9E0	Protein FAM133A OS=Homo sapiens OX=9606 GN=FAM133A PE=1 SV=1	FALSE	4	1	1	1	248	28.9	10.1	0
High	P60903	Protein S100-A10 OS=Homo sapiens OX=9606 GN=S100A10 PE=1 SV=2	FALSE	18	1	1	1	97	11.2	7.37	2.18
High	P62854	40S ribosomal protein S26 OS=Homo sapiens OX=9606 GN=RPS26 PE=1 SV=3	FALSE	13	1	1	1	115	13	11	2.15
High	P61254	60S ribosomal protein L26 OS=Homo sapiens OX=9606 GN=RPL26 PE=1 SV=1	FALSE	5	1	1	1	145	17.2	10.55	0
High	Q96MH2	Protein HEXIM2 OS=Homo sapiens OX=9606 GN=HEXIM2 PE=1 SV=1	FALSE	5	1	1	1	286	32.4	6.55	2.54
High	P41091	Eukaryotic translation initiation factor 2 subunit 3 OS=Homo sapiens OX=9606 GN=EIF2S3 PE=1 SV=3	FALSE	3	1	1	1	472	51.1	8.4	2.43
High	Q6UN15	Pre-mRNA 3'-end-processing factor FIP1 OS=Homo sapiens OX=9606 GN=FIP1L1 PE=1 SV=1	FALSE	2	1	1	1	594	66.5	5.59	2.56
High	Q9Y265	RuvB-like 1 OS=Homo sapiens OX=9606 GN=RUVBL1 PE=1 SV=1	FALSE	3	1	1	1	456	50.2	6.42	2.06
High	O00148	ATP-dependent RNA helicase DDX39A OS=Homo sapiens OX=9606 GN=DDX39A PE=1 SV=2	FALSE	3	1	1	1	427	49.1	5.68	0
High	Q01650	Large neutral amino acids transporter small subunit 1 OS=Homo sapiens OX=9606 GN=SLC7A5 PE=1 SV=2	FALSE	4	1	1	1	507	55	7.72	2.99
High	P56134	ATP synthase subunit f, mitochondrial OS=Homo sapiens OX=9606 GN=ATP5MF PE=1 SV=3	FALSE	14	1	1	1	94	10.9	9.67	2.19
High	Q9H2D6	TRIO and F-actin-binding protein OS=Homo sapiens OX=9606 GN=TRIOBP PE=1 SV=3	FALSE	1	1	1	1	2365	261.2	8.48	0
High	P55060	Exportin-2 OS=Homo sapiens OX=9606 GN=CSE1L PE=1 SV=3	FALSE	2	1	1	1	971	110.3	5.77	2.5
High	Q02413	Desmoglein-1 OS=Homo sapiens OX=9606 GN=DSG1 PE=1 SV=2	FALSE	1	1	1	1	1049	113.7	5.03	2.39
High	P07477	Trypsin-1 OS=Homo sapiens OX=9606 GN=PRSS1 PE=1 SV=1	TRUE	4	1	1	1	247	26.5	6.51	1.6
High	P62280	40S ribosomal protein S11 OS=Homo sapiens OX=9606 GN=RPS11 PE=1 SV=3	FALSE	11	1	1	1	158	18.4	10.3	2.57
High	P42677	40S ribosomal protein S27 OS=Homo sapiens OX=9606 GN=RPS27 PE=1 SV=3	FALSE	13	1	1	1	84	9.5	9.45	0
High	P33991	DNA replication licensing factor MCM4 OS=Homo sapiens OX=9606 GN=MCM4 PE=1 SV=5	FALSE	1	1	1	1	863	96.5	6.74	0
High	O75446	Histone deacetylase complex subunit SAP30 OS=Homo sapiens OX=9606 GN=SAP30 PE=1 SV=1	FALSE	4	1	1	1	220	23.3	9.17	0
High	Q7L4I2	Arginine/serine-rich coiled-coil protein 2 OS=Homo sapiens OX=9606 GN=RSRC2 PE=1 SV=1	FALSE	4	1	1	1	434	50.5	11.33	2
High	P21127	Cyclin-dependent kinase 11B OS=Homo sapiens OX=9606 GN=CDK11B PE=1 SV=4	FALSE	2	1	1	1	795	92.6	5.54	2.2
High	Q9UQ35	Serine/arginine repetitive matrix protein 2 OS=Homo sapiens OX=9606 GN=SRRM2 PE=1 SV=2	FALSE	0	1	1	1	2752	299.4	12.06	2.74
High	P62899	60S ribosomal protein L31 OS=Homo sapiens OX=9606 GN=RPL31 PE=1 SV=1	FALSE	7	1	1	1	125	14.5	10.54	2.47
High	P47897	Glutamine--tRNA ligase OS=Homo sapiens OX=9606 GN=QARS PE=1 SV=1	FALSE	2	1	1	1	775	87.7	7.15	1.85

High	Q9UPN4	Centrosomal protein of 131 kDa OS=Homo sapiens OX=9606 GN=CEP131 PE=1 SV=3	FALSE	1	1	1	1	1083	122.1	8.69	0
High	O15014	Zinc finger protein 609 OS=Homo sapiens OX=9606 GN=ZNF609 PE=1 SV=2	FALSE	1	1	1	1	1411	151.1	8.03	2.84
High	P22695	Cytochrome b-c1 complex subunit 2, mitochondrial OS=Homo sapiens OX=9606 GN=UQCRC2 PE=1 SV=3	FALSE	4	1	1	1	453	48.4	8.63	2.44
High	Q9PJ07	E3 ubiquitin-protein ligase KCMF1 OS=Homo sapiens OX=9606 GN=KCMF1 PE=1 SV=2	FALSE	4	1	1	1	381	41.9	5.66	2.11
Medium	Q9Y2R9	28S ribosomal protein S7, mitochondrial OS=Homo sapiens OX=9606 GN=MRPS7 PE=1 SV=2	FALSE	6	1	1	1	242	28.1	9.99	0
High	Q12874	Splicing factor 3A subunit 3 OS=Homo sapiens OX=9606 GN=SF3A3 PE=1 SV=1	FALSE	2	1	1	1	501	58.8	5.38	2.71
High	P56270	Myc-associated zinc finger protein OS=Homo sapiens OX=9606 GN=MAZ PE=1 SV=1	FALSE	3	1	1	1	477	48.6	8.95	0
High	Q06210	Glutamine--fructose-6-phosphate aminotransferase [isomerizing] 1 OS=Homo sapiens OX=9606 GN=GFPT1 PE=	FALSE	2	1	1	1	699	78.8	7.11	0
High	Q14596	Next to BRCA1 gene 1 protein OS=Homo sapiens OX=9606 GN=NBR1 PE=1 SV=3	FALSE	2	1	1	1	966	107.3	5.12	0
High	P53999	Activated RNA polymerase II transcriptional coactivator p15 OS=Homo sapiens OX=9606 GN=SUB1 PE=1 SV=3	FALSE	7	1	1	1	127	14.4	9.6	2.05
High	O00471	Exocyst complex component 5 OS=Homo sapiens OX=9606 GN=EXOC5 PE=1 SV=1	FALSE	3	1	1	1	708	81.8	6.71	0
High	P62861	40S ribosomal protein S30 OS=Homo sapiens OX=9606 GN=FAU PE=1 SV=1	FALSE	17	1	1	1	59	6.6	12.15	1.79
High	Q8IWS0	PHD finger protein 6 OS=Homo sapiens OX=9606 GN=PHF6 PE=1 SV=1	FALSE	2	1	1	1	365	41.3	8.68	0
High	O43670	BUB3-interacting and GLEBS motif-containing protein ZNF207 OS=Homo sapiens OX=9606 GN=ZNF207 PE=1 SV=	FALSE	3	1	1	1	478	50.7	9.1	2.08
High	Q9UNS2	COP9 signalosome complex subunit 3 OS=Homo sapiens OX=9606 GN=COPS3 PE=1 SV=3	FALSE	3	1	1	1	423	47.8	6.65	1.81
Medium	Q13813	Spectrin alpha chain, non-erythrocytic 1 OS=Homo sapiens OX=9606 GN=SPTAN1 PE=1 SV=3	FALSE	1	1	1	1	2472	284.4	5.35	0
High	Q6Y7W6	GRB10-interacting GYF protein 2 OS=Homo sapiens OX=9606 GN=GIGYF2 PE=1 SV=1	FALSE	1	1	1	1	1299	150	5.54	1.97

## HAdV4 (group E)

Protein	FDR	Confidence	Accession	Description	Contaminant	Coverage [%]	# Peptides	# PSMs	# Unique Peptides	# AAs	MW [kDa]	calc. pI	Sequest HT
High			Q9ULH0	Kinase D-interacting substrate of 220 kDa OS=Homo sapiens OX=9606 GN=KIDINS220 PE=1 SV=3	FALSE	28	37	45	37	1771	196.4	6.62	88.15
High			O95202	Mitochondrial proton/calcium exchanger protein OS=Homo sapiens OX=9606 GN=LETM1 PE=1 SV=1	FALSE	45	25	40	25	739	83.3	6.7	117.07
High			P11142	Heat shock cognate 71 kDa protein OS=Homo sapiens OX=9606 GN=HSPA8 PE=1 SV=1	FALSE	42	23	33	19	646	70.9	5.52	85.17
High			P38646	Stress-70 protein, mitochondrial OS=Homo sapiens OX=9606 GN=HSPA9 PE=1 SV=2	FALSE	37	20	30	20	679	73.6	6.16	82.43
High			Q07954	Prolow-density lipoprotein receptor-related protein 1 OS=Homo sapiens OX=9606 GN=LRP1 PE=1 SV=2	FALSE	6	22	24	22	4544	504.3	5.39	39.02
High			P11021	Endoplasmic reticulum chaperone BiP OS=Homo sapiens OX=9606 GN=HSPA5 PE=1 SV=2	FALSE	36	19	23	17	654	72.3	5.16	50.8
High			P0DMV9	Heat shock 70 kDa protein 1B OS=Homo sapiens OX=9606 GN=HSPA1B PE=1 SV=1	FALSE	36	18	22	12	641	70	5.66	51.46
High			O75822	Eukaryotic translation initiation factor 3 subunit J OS=Homo sapiens OX=9606 GN=EIF3J PE=1 SV=2	FALSE	47	13	21	13	258	29	4.83	56.18
High			P10809	60 kDa heat shock protein, mitochondrial OS=Homo sapiens OX=9606 GN=HSPD1 PE=1 SV=2	FALSE	43	16	20	16	573	61	5.87	51.25
High			P49756	RNA-binding protein 25 OS=Homo sapiens OX=9606 GN=RBM25 PE=1 SV=3	FALSE	24	15	19	15	843	100.1	6.32	37.63
High			Q9UHX1	Poly(U)-binding-splicing factor PUF60 OS=Homo sapiens OX=9606 GN=PUF60 PE=1 SV=1	FALSE	31	13	16	13	559	59.8	5.29	41.14
High			P07437	Tubulin beta chain OS=Homo sapiens OX=9606 GN=TUBB PE=1 SV=2	FALSE	41	13	16	4	444	49.6	4.89	38.13
High			P28799	Progranulin OS=Homo sapiens OX=9606 GN=GRN PE=1 SV=2	FALSE	28	11	15	11	593	63.5	6.83	47.81
High			Q14139	Ubiquitin conjugation factor E4 A OS=Homo sapiens OX=9606 GN=UBE4A PE=1 SV=2	FALSE	16	14	15	14	1066	122.5	5.24	26.38
High			P17066	Heat shock 70 kDa protein 6 OS=Homo sapiens OX=9606 GN=HSPA6 PE=1 SV=2	FALSE	19	10	15	3	643	71	6.14	28.59
High			Q9UP83	Conserved oligomeric Golgi complex subunit 5 OS=Homo sapiens OX=9606 GN=COG5 PE=1 SV=3	FALSE	18	12	14	12	839	92.7	6.6	30.06
High			P68371	Tubulin beta-4B chain OS=Homo sapiens OX=9606 GN=TUBB4B PE=1 SV=1	FALSE	41	13	14	4	445	49.8	4.89	32.21
High			P60709	Actin, cytoplasmic 1 OS=Homo sapiens OX=9606 GN=ACTB PE=1 SV=1	TRUE	36	9	14	6	375	41.7	5.48	33.91
High			Q9Y2V7	Conserved oligomeric Golgi complex subunit 6 OS=Homo sapiens OX=9606 GN=COG6 PE=1 SV=2	FALSE	21	11	13	11	657	73.2	5.76	28.34
High			P49411	Elongation factor Tu, mitochondrial OS=Homo sapiens OX=9606 GN=TUFM PE=1 SV=2	FALSE	35	12	13	12	452	49.5	7.61	28.77
High			P05787	Keratin, type II cytoskeletal 8 OS=Homo sapiens OX=9606 GN=KRT8 PE=1 SV=7	TRUE	26	11	13	10	483	53.7	5.59	26.75
High			Q9UKJ3	G patch domain-containing protein 8 OS=Homo sapiens OX=9606 GN=GPATCH8 PE=1 SV=2	FALSE	8	9	13	9	1502	164.1	8.66	26.3
High			P83436	Conserved oligomeric Golgi complex subunit 7 OS=Homo sapiens OX=9606 GN=COG7 PE=1 SV=1	FALSE	21	12	13	12	770	86.3	5.47	25.61
High			P05783	Keratin, type I cytoskeletal 18 OS=Homo sapiens OX=9606 GN=KRT18 PE=1 SV=2	FALSE	27	10	12	10	430	48	5.45	28.3
High			Q71U36	Tubulin alpha-1A chain OS=Homo sapiens OX=9606 GN=TUBA1A PE=1 SV=1	FALSE	29	10	12	6	451	50.1	5.06	28.81
High			Q9Y383	Putative RNA-binding protein Luc7-like 2 OS=Homo sapiens OX=9606 GN=LUC7L2 PE=1 SV=2	FALSE	30	11	12	11	392	46.5	10.01	27.21
High			Q92878	DNA repair protein RAD50 OS=Homo sapiens OX=9606 GN=RAD50 PE=1 SV=1	FALSE	9	10	12	10	1312	153.8	6.89	24.41
High			Q14315	Filamin-C OS=Homo sapiens OX=9606 GN=FLNC PE=1 SV=3	FALSE	6	11	11	10	2725	290.8	5.97	17.8
High			P48643	T-complex protein 1 subunit epsilon OS=Homo sapiens OX=9606 GN=CCT5 PE=1 SV=1	FALSE	22	10	11	9	541	59.6	5.66	23.64
High			P13645	Keratin, type I cytoskeletal 10 OS=Homo sapiens OX=9606 GN=KRT10 PE=1 SV=6	TRUE	19	10	11	10	584	58.8	5.21	25.52
High			P35527	Keratin, type I cytoskeletal 9 OS=Homo sapiens OX=9606 GN=KRT9 PE=1 SV=3	TRUE	23	8	11	8	623	62	5.24	26.74
High			P50990	T-complex protein 1 subunit theta OS=Homo sapiens OX=9606 GN=CCT8 PE=1 SV=4	FALSE	22	10	10	10	548	59.6	5.6	20.5
High			P04264	Keratin, type II cytoskeletal 1 OS=Homo sapiens OX=9606 GN=KRT1 PE=1 SV=6	TRUE	18	9	10	7	644	66	8.12	19.24
High			P17987	T-complex protein 1 subunit alpha OS=Homo sapiens OX=9606 GN=TCP1 PE=1 SV=1	FALSE	23	9	10	9	556	60.3	6.11	17.83
High			P31943	Heterogeneous nuclear ribonucleoprotein H OS=Homo sapiens OX=9606 GN=HNRNPH1 PE=1 SV=4	FALSE	25	7	10	5	449	49.2	6.3	20.5
High			P78371	T-complex protein 1 subunit beta OS=Homo sapiens OX=9606 GN=CCT2 PE=1 SV=4	FALSE	26	9	10	9	535	57.5	6.46	21.07
High			P68366	Tubulin alpha-4A chain OS=Homo sapiens OX=9606 GN=TUBA4A PE=1 SV=1	FALSE	20	8	9	4	448	49.9	5.06	18.61
High			Q7L014	Probable ATP-dependent RNA helicase DDX46 OS=Homo sapiens OX=9606 GN=DDX46 PE=1 SV=2	FALSE	10	9	9	9	1031	117.3	9.29	15.2
High			Q16630	Cleavage and polyadenylation specificity factor subunit 6 OS=Homo sapiens OX=9606 GN=CPSP6 PE=1 SV=2	FALSE	18	7	9	7	551	59.2	7.15	20.46
High			O00170	AH receptor-interacting protein OS=Homo sapiens OX=9606 GN=AIP PE=1 SV=2	FALSE	34	8	9	8	330	37.6	6.29	19.63
High			Q9UBH6	Xenotropic and polytropic retrovirus receptor 1 OS=Homo sapiens OX=9606 GN=XPR1 PE=1 SV=1	FALSE	15	7	9	7	696	81.5	8.44	15.18
High			P31327	Carbamoyl-phosphate synthase [ammonia], mitochondrial OS=Homo sapiens OX=9606 GN=CPSP1 PE=1 SV=2	FALSE	8	9	9	8	1500	164.8	6.74	19.16
High			P50991	T-complex protein 1 subunit delta OS=Homo sapiens OX=9606 GN=CCT4 PE=1 SV=4	FALSE	22	8	9	7	539	57.9	7.83	9.95
High			Q99832	T-complex protein 1 subunit eta OS=Homo sapiens OX=9606 GN=CCT7 PE=1 SV=2	FALSE	23	9	9	9	543	59.3	7.65	17.74
High			Q93008	Probable ubiquitin carboxyl-terminal hydrolase FAF-X OS=Homo sapiens OX=9606 GN=USP9X PE=1 SV=3	FALSE	4	9	9	9	2570	292.1	5.8	15.29
High			P35637	RNA-binding protein FUS OS=Homo sapiens OX=9606 GN=FUS PE=1 SV=1	FALSE	14	6	9	4	526	53.4	9.36	18.28
High			P16615	Sarcoplasmic/endoplasmic reticulum calcium ATPase 2 OS=Homo sapiens OX=9606 GN=ATP2A2 PE=1 SV=1	FALSE	8	7	8	7	1042	114.7	5.34	12.73
High			O75533	Splicing factor 3B subunit 1 OS=Homo sapiens OX=9606 GN=SF3B1 PE=1 SV=3	FALSE	9	8	8	8	1304	145.7	7.09	9.32
High			Q9BUJ2	Heterogeneous nuclear ribonucleoprotein U-like protein 1 OS=Homo sapiens OX=9606 GN=HNRNPUL1 PE=1 SV=1	FALSE	7	7	7	7	856	95.7	6.92	15.86
High			P05141	ADP/ATP translocase 2 OS=Homo sapiens OX=9606 GN=SLC25A5 PE=1 SV=7	FALSE	24	7	7	4	298	32.8	9.69	12.82
High			P08238	Heat shock protein HSP 90-beta OS=Homo sapiens OX=9606 GN=HSP90AB1 PE=1 SV=4	FALSE	13	7	7	4	724	83.2	5.03	6.98
High			P27708	CAD protein OS=Homo sapiens OX=9606 GN=CAD PE=1 SV=3	FALSE	4	7	7	6	2225	242.8	6.46	3.69
High			P49368	T-complex protein 1 subunit gamma OS=Homo sapiens OX=9606 GN=CCT3 PE=1 SV=4	FALSE	18	7	7	7	545	60.5	6.49	15.91
High			P12236	ADP/ATP translocase 3 OS=Homo sapiens OX=9606 GN=SLC25A6 PE=1 SV=4	FALSE	24	7	7	4	298	32.8	9.74	13.37
High			O15084	Serine/threonine-protein phosphatase 6 regulatory ankyrin repeat subunit A OS=Homo sapiens OX=9606 GN=AI	FALSE	11	7	7	7	1053	112.9	6.25	11.18

High	P78527	DNA-dependent protein kinase catalytic subunit OS=Homo sapiens OX=9606 GN=PRKDC PE=1 SV=3	FALSE	2	6	6	6	4128	468.8	7.12	8.2
High	O75400	Pre-mRNA-processing factor 40 homolog A OS=Homo sapiens OX=9606 GN=PRPF40A PE=1 SV=2	FALSE	8	5	6	5	957	108.7	7.56	12.99
High	Q9BUF5	Tubulin beta-6 chain OS=Homo sapiens OX=9606 GN=TUBB6 PE=1 SV=1	FALSE	17	6	6	3	446	49.8	4.88	11.91
High	P55081	Microfibrillar-associated protein 1 OS=Homo sapiens OX=9606 GN=MFAP1 PE=1 SV=2	FALSE	16	4	6	4	439	51.9	4.98	15
High	Q06830	Peroxisomal protein 1 OS=Homo sapiens OX=9606 GN=PRDX1 PE=1 SV=1	TRUE	30	5	6	3	199	22.1	8.13	16.14
High	Q00839	Heterogeneous nuclear ribonucleoprotein U OS=Homo sapiens OX=9606 GN=HNRNPU PE=1 SV=6	FALSE	7	4	6	4	825	90.5	6	4.97
High	Q92804	TATA-binding protein-associated factor 2N OS=Homo sapiens OX=9606 GN=TAIF15 PE=1 SV=1	FALSE	17	5	6	3	592	61.8	8.02	13.96
High	POCG39	POTE ankyrin domain family member J OS=Homo sapiens OX=9606 GN=POTEJ PE=3 SV=1	FALSE	5	4	6	1	1038	117.3	5.97	11.71
High	P61978	Heterogeneous nuclear ribonucleoprotein K OS=Homo sapiens OX=9606 GN=HNRNPK PE=1 SV=1	FALSE	16	6	6	6	463	50.9	5.54	14.05
High	Q14498	RNA-binding protein 39 OS=Homo sapiens OX=9606 GN=RBM39 PE=1 SV=2	FALSE	16	6	6	6	530	59.3	10.1	12.72
High	Q969Q5	Ras-related protein Rab-24 OS=Homo sapiens OX=9606 GN=RAB24 PE=1 SV=1	FALSE	36	5	6	5	203	23.1	6.23	15.55
High	P15880	40S ribosomal protein S2 OS=Homo sapiens OX=9606 GN=RPS2 PE=1 SV=2	FALSE	18	5	5	5	293	31.3	10.24	8.82
High	P19338	Nucleolin OS=Homo sapiens OX=9606 GN=NCL PE=1 SV=3	FALSE	8	5	5	5	710	76.6	4.7	9.26
High	P40227	T-complex protein 1 subunit zeta OS=Homo sapiens OX=9606 GN=CCT6A PE=1 SV=3	FALSE	12	5	5	5	531	58	6.68	7.9
High	Q5H9R7	Serine/threonine-protein phosphatase 6 regulatory subunit 3 OS=Homo sapiens OX=9606 GN=PPP6R3 PE=1 SV=1	FALSE	8	5	5	5	873	97.6	4.6	8.37
High	Q15459	Splicing factor 3A subunit 1 OS=Homo sapiens OX=9606 GN=SF3A1 PE=1 SV=1	FALSE	4	3	5	3	793	88.8	5.22	6.77
High	P22061	Protein-L-isoaspartate(D-aspartate) O-methyltransferase OS=Homo sapiens OX=9606 GN=PCMT1 PE=1 SV=4	FALSE	26	4	5	4	227	24.6	7.21	13.68
High	P25597	Heterogeneous nuclear ribonucleoprotein F OS=Homo sapiens OX=9606 GN=HNRNPF PE=1 SV=3	FALSE	12	4	5	2	415	45.6	5.58	8.59
High	P62241	40S ribosomal protein S8 OS=Homo sapiens OX=9606 GN=RPS8 PE=1 SV=2	FALSE	28	5	5	5	208	24.2	10.32	9.7
High	Q00325	Phosphate carrier protein, mitochondrial OS=Homo sapiens OX=9606 GN=SLC25A3 PE=1 SV=2	FALSE	12	4	4	4	362	40.1	9.38	6.96
High	P06576	ATP synthase subunit beta, mitochondrial OS=Homo sapiens OX=9606 GN=ATP5F1B PE=1 SV=3	FALSE	10	4	4	4	529	56.5	5.4	6.76
High	P49959	Double-strand break repair protein MRE11 OS=Homo sapiens OX=9606 GN=MRE11 PE=1 SV=3	FALSE	7	4	4	4	708	80.5	5.9	8.86
High	P07900	Heat shock protein HSP 90-alpha OS=Homo sapiens OX=9606 GN=HSP90AA1 PE=1 SV=5	FALSE	6	4	4	1	732	84.6	5.02	4.28
High	Q15149	Plectin OS=Homo sapiens OX=9606 GN=PLEC PE=1 SV=3	FALSE	1	4	4	4	4684	531.5	5.96	6.56
Medium	P0D0X3	Immunoglobulin delta heavy chain OS=Homo sapiens OX=9606 GN=IGHD PE=1 SV=1	FALSE	4	1	4	1	512	56.2	8.02	0
High	Q96MW5	Conserved oligomeric Golgi complex subunit 8 OS=Homo sapiens OX=9606 GN=COG8 PE=1 SV=2	FALSE	10	3	4	3	612	68.4	5.2	4.26
High	Q13435	Splicing factor 3B subunit 2 OS=Homo sapiens OX=9606 GN=SF3B2 PE=1 SV=2	FALSE	6	4	4	4	895	100.2	5.67	7.31
High	A0A0A0M1	Immunoglobulin heavy variable 1-45 OS=Homo sapiens OX=9606 GN=IGHV1-45 PE=3 SV=1	FALSE	9	1	4	1	117	13.5	9.1	9.89
High	P07477	Trypsin-1 OS=Homo sapiens OX=9606 GN=PRSS1 PE=1 SV=1	TRUE	12	2	4	2	247	26.5	6.51	3.98
High	Q14204	Cytoplasmic dynein 1 heavy chain 1 OS=Homo sapiens OX=9606 GN=DYNC1H1 PE=1 SV=5	FALSE	1	4	4	4	4646	532.1	6.4	1.84
High	P25705	ATP synthase subunit alpha, mitochondrial OS=Homo sapiens OX=9606 GN=ATP5F1A PE=1 SV=1	FALSE	10	4	4	4	553	59.7	9.13	8.64
High	O95232	Luc7-like protein 3 OS=Homo sapiens OX=9606 GN=LUC7L3 PE=1 SV=2	FALSE	9	3	4	3	432	51.4	9.79	2.16
High	O95071	E3 ubiquitin-protein ligase UBR5 OS=Homo sapiens OX=9606 GN=UBR5 PE=1 SV=2	FALSE	2	4	4	4	2799	309.2	5.85	5.48
High	O95816	BAG family molecular chaperone regulator 2 OS=Homo sapiens OX=9606 GN=BAG2 PE=1 SV=1	FALSE	21	4	4	4	211	23.8	6.7	6.24
High	P67809	Y-box-binding protein 1 OS=Homo sapiens OX=9606 GN=YBX1 PE=1 SV=3	FALSE	18	3	3	3	324	35.9	9.88	4.55
High	P08195	4F2 cell-surface antigen heavy chain OS=Homo sapiens OX=9606 GN=SLC3A2 PE=1 SV=3	FALSE	6	3	3	3	630	68	5.01	4.36
High	P62701	40S ribosomal protein S4, X isoform OS=Homo sapiens OX=9606 GN=RPS4X PE=1 SV=2	FALSE	11	3	3	3	263	29.6	10.15	2.33
High	Q9UJ50	Calcium-binding mitochondrial carrier protein Aralar2 OS=Homo sapiens OX=9606 GN=SLC25A13 PE=1 SV=2	FALSE	6	3	3	3	675	74.1	8.62	4.72
High	Q13501	Sequestosome-1 OS=Homo sapiens OX=9606 GN=SQSTM1 PE=1 SV=1	FALSE	10	3	3	3	440	47.7	5.22	5.61
High	P68104	Elongation factor 1-alpha 1 OS=Homo sapiens OX=9606 GN=EEF1A1 PE=1 SV=1	FALSE	4	2	3	2	462	50.1	9.01	6.61
High	P04843	Dolichyl-diphosphooligosaccharide--protein glycosyltransferase subunit 1 OS=Homo sapiens OX=9606 GN=RPN1	FALSE	7	3	3	3	607	68.5	6.38	2.51
High	O95817	BAG family molecular chaperone regulator 3 OS=Homo sapiens OX=9606 GN=BAG3 PE=1 SV=3	FALSE	10	3	3	3	575	61.6	6.95	2.59
High	P16403	Histone H1.2 OS=Homo sapiens OX=9606 GN=H1-2 PE=1 SV=2	FALSE	18	3	3	3	213	21.4	10.93	6.61
High	P18621	60S ribosomal protein L17 OS=Homo sapiens OX=9606 GN=RPL17 PE=1 SV=3	FALSE	13	2	3	2	184	21.4	10.17	8.22
High	P23396	40S ribosomal protein S3 OS=Homo sapiens OX=9606 GN=RPS3 PE=1 SV=2	FALSE	14	3	3	3	243	26.7	9.66	5.78
High	P31689	DnaJ homolog subfamily A member 1 OS=Homo sapiens OX=9606 GN=DNAJA1 PE=1 SV=2	FALSE	9	2	3	2	397	44.8	7.08	5
High	P62280	40S ribosomal protein S11 OS=Homo sapiens OX=9606 GN=RPS11 PE=1 SV=3	FALSE	25	3	3	3	158	18.4	10.3	4.01
High	Q07020	60S ribosomal protein L18 OS=Homo sapiens OX=9606 GN=RPL18 PE=1 SV=2	FALSE	18	3	3	3	188	21.6	11.72	7.68
High	Q9H9E3	Conserved oligomeric Golgi complex subunit 4 OS=Homo sapiens OX=9606 GN=COG4 PE=1 SV=3	FALSE	5	3	3	3	785	89	5.19	2.23
High	P62979	Ubiquitin-40S ribosomal protein S27a OS=Homo sapiens OX=9606 GN=RPS27A PE=1 SV=2	TRUE	24	3	3	3	156	18	9.64	5.37
High	P62851	40S ribosomal protein S25 OS=Homo sapiens OX=9606 GN=RPS25 PE=1 SV=1	FALSE	24	3	3	3	125	13.7	10.11	6.83
High	Q7RTV0	PHD finger-like domain-containing protein 5A OS=Homo sapiens OX=9606 GN=PHF5A PE=1 SV=1	FALSE	26	3	3	3	110	12.4	8.41	6.74
High	P04792	Heat shock protein beta-1 OS=Homo sapiens OX=9606 GN=HSPB1 PE=1 SV=2	FALSE	21	3	3	3	205	22.8	6.4	9.34
High	P26368	Splicing factor U2AF 65 kDa subunit OS=Homo sapiens OX=9606 GN=U2AF2 PE=1 SV=4	FALSE	6	3	3	3	475	53.5	9.09	3.63
High	P35908	Keratin, type II cytoskeletal 2 epidermal OS=Homo sapiens OX=9606 GN=KRT2 PE=1 SV=2	TRUE	6	3	3	2	639	65.4	8	7.05
High	P11940	Polyadenylate-binding protein 1 OS=Homo sapiens OX=9606 GN=PABPC1 PE=1 SV=2	FALSE	5	3	3	3	636	70.6	9.5	3.69

High	O15427	Monocarboxylate transporter 4 OS=Homo sapiens OX=9606 GN=SLC16A3 PE=1 SV=1	FALSE	7	3	3	3	465	49.4	7.96	5.26
High	P23284	Peptidyl-prolyl cis-trans isomerase B OS=Homo sapiens OX=9606 GN=PPIB PE=1 SV=2	FALSE	12	2	3	2	216	23.7	9.41	1.98
High	Q9NZ01	Very-long-chain enoyl-CoA reductase OS=Homo sapiens OX=9606 GN=TECR PE=1 SV=1	FALSE	7	2	3	2	308	36	9.45	4.13
High	O75477	Erlin-1 OS=Homo sapiens OX=9606 GN=ERLIN1 PE=1 SV=2	FALSE	9	3	3	3	348	39.1	7.87	6.75
High	P27348	14-3-3 protein theta OS=Homo sapiens OX=9606 GN=YWHAQ PE=1 SV=1	FALSE	13	3	3	1	245	27.7	4.78	6.24
High	Q9Y230	RuvB-like 2 OS=Homo sapiens OX=9606 GN=RUVBL2 PE=1 SV=3	FALSE	8	3	3	3	463	51.1	5.64	4.57
High	P26373	60S ribosomal protein L13 OS=Homo sapiens OX=9606 GN=RPL13 PE=1 SV=4	FALSE	14	3	3	3	211	24.2	11.65	2.03
High	P39023	60S ribosomal protein L3 OS=Homo sapiens OX=9606 GN=RPL3 PE=1 SV=2	FALSE	12	3	3	3	403	46.1	10.18	2.75
High	P63104	14-3-3 protein zeta/delta OS=Homo sapiens OX=9606 GN=YWHAZ PE=1 SV=1	FALSE	13	3	3	1	245	27.7	4.79	3.65
High	P50914	60S ribosomal protein L14 OS=Homo sapiens OX=9606 GN=RPL14 PE=1 SV=4	FALSE	16	3	3	3	215	23.4	10.93	4.81
High	P62750	60S ribosomal protein L23a OS=Homo sapiens OX=9606 GN=RPL23A PE=1 SV=1	FALSE	21	3	3	3	156	17.7	10.45	4.46
High	Q99615	DnaJ homolog subfamily C member 7 OS=Homo sapiens OX=9606 GN=DNAJC7 PE=1 SV=2	FALSE	8	2	3	2	494	56.4	6.96	4.58
High	Q9Y265	RuvB-like 1 OS=Homo sapiens OX=9606 GN=RUVBL1 PE=1 SV=1	FALSE	8	3	3	3	456	50.2	6.42	2.18
High	Q05519	Serine/arginine-rich splicing factor 11 OS=Homo sapiens OX=9606 GN=SRSF11 PE=1 SV=1	FALSE	5	2	3	2	484	53.5	10.52	5.41
High	P61247	40S ribosomal protein S3a OS=Homo sapiens OX=9606 GN=RPS3A PE=1 SV=2	FALSE	15	3	3	3	264	29.9	9.73	4.88
High	O43143	Pre-mRNA-splicing factor ATP-dependent RNA helicase DHX15 OS=Homo sapiens OX=9606 GN=DHX15 PE=1 SV=1	FALSE	4	3	3	3	795	90.9	7.46	5.77
High	P18124	60S ribosomal protein L7 OS=Homo sapiens OX=9606 GN=RPL7 PE=1 SV=1	FALSE	12	2	3	2	248	29.2	10.65	8.85
High	P46781	40S ribosomal protein S9 OS=Homo sapiens OX=9606 GN=RPS9 PE=1 SV=3	FALSE	12	3	3	3	194	22.6	10.65	2.01
High	Q01970	1-phosphatidylinositol 4,5-bisphosphate phosphodiesterase beta-3 OS=Homo sapiens OX=9606 GN=PLCB3 PE=1 SV=1	FALSE	4	3	3	3	1234	138.7	5.9	3.76
High	Q96J82	Conserved oligomeric Golgi complex subunit 3 OS=Homo sapiens OX=9606 GN=COG3 PE=1 SV=3	FALSE	4	3	3	3	828	94	5.57	3.74
High	P19474	E3 ubiquitin-protein ligase TRIM21 OS=Homo sapiens OX=9606 GN=TRIM21 PE=1 SV=1	FALSE	7	3	3	3	475	54.1	6.38	5.26
High	P18085	ADP-ribosylation factor 4 OS=Homo sapiens OX=9606 GN=ARF4 PE=1 SV=3	FALSE	16	3	3	3	180	20.5	7.14	3.53
High	Q9Y285	Phenylalanine--tRNA ligase alpha subunit OS=Homo sapiens OX=9606 GN=FARSA PE=1 SV=3	FALSE	5	2	2	2	508	57.5	7.8	4.72
High	P62424	60S ribosomal protein L7a OS=Homo sapiens OX=9606 GN=RPL7A PE=1 SV=2	FALSE	8	2	2	2	266	30	10.61	2.35
High	P61353	60S ribosomal protein L27 OS=Homo sapiens OX=9606 GN=RPL27 PE=1 SV=2	FALSE	13	2	2	2	136	15.8	10.56	1.88
High	Q9NV17	ATPase family AAA domain-containing protein 3A OS=Homo sapiens OX=9606 GN=ATAD3A PE=1 SV=2	FALSE	3	2	2	1	634	71.3	8.98	2.06
High	Q07021	Complement component 1 Q subcomponent-binding protein, mitochondrial OS=Homo sapiens OX=9606 GN=C1	FALSE	12	2	2	2	282	31.3	4.84	5.86
High	Q5T9A4	ATPase family AAA domain-containing protein 3B OS=Homo sapiens OX=9606 GN=ATAD3B PE=1 SV=1	FALSE	3	2	2	1	648	72.5	9.2	4.37
High	P32119	Peroxioredoxin-2 OS=Homo sapiens OX=9606 GN=PRDX2 PE=1 SV=5	FALSE	10	2	2	1	198	21.9	5.97	2.44
High	P52272	Heterogeneous nuclear ribonucleoprotein M OS=Homo sapiens OX=9606 GN=HNRNPM PE=1 SV=3	FALSE	4	2	2	2	730	77.5	8.7	4.03
High	Q9H0G5	Nuclear speckle splicing regulatory protein 1 OS=Homo sapiens OX=9606 GN=NSRP1 PE=1 SV=1	FALSE	3	1	2	1	558	66.4	8.84	2.32
High	P62910	60S ribosomal protein L32 OS=Homo sapiens OX=9606 GN=RPL32 PE=1 SV=2	FALSE	10	1	2	1	135	15.9	11.33	4.47
High	Q13162	Peroxioredoxin-4 OS=Homo sapiens OX=9606 GN=PRDX4 PE=1 SV=1	FALSE	7	2	2	1	271	30.5	6.29	3.43
High	Q72627	E3 ubiquitin-protein ligase HUWE1 OS=Homo sapiens OX=9606 GN=HUWE1 PE=1 SV=3	FALSE	1	2	2	2	4374	481.6	5.22	1.67
High	P78347	General transcription factor II-I OS=Homo sapiens OX=9606 GN=GTF2I PE=1 SV=2	FALSE	3	2	2	2	998	112.3	6.39	3.42
High	O60884	DnaJ homolog subfamily A member 2 OS=Homo sapiens OX=9606 GN=DNAJA2 PE=1 SV=1	FALSE	4	2	2	2	412	45.7	6.48	0
High	Q9UG63	ATP-binding cassette sub-family F member 2 OS=Homo sapiens OX=9606 GN=ABCF2 PE=1 SV=2	FALSE	3	2	2	2	623	71.2	7.37	3.33
High	O43809	Cleavage and polyadenylation specificity factor subunit 5 OS=Homo sapiens OX=9606 GN=NUDT21 PE=1 SV=1	FALSE	13	2	2	2	227	26.2	8.82	0
High	Q8WTW3	Conserved oligomeric Golgi complex subunit 1 OS=Homo sapiens OX=9606 GN=COG1 PE=1 SV=1	FALSE	3	2	2	2	980	108.9	7.31	2.38
High	P06733	Alpha-enolase OS=Homo sapiens OX=9606 GN=ENO1 PE=1 SV=2	FALSE	6	2	2	2	434	47.1	7.39	4.7
High	O14979	Heterogeneous nuclear ribonucleoprotein D-like OS=Homo sapiens OX=9606 GN=HNRNPDL PE=1 SV=3	FALSE	4	2	2	2	420	46.4	9.57	2.14
High	P22626	Heterogeneous nuclear ribonucleoproteins A2/B1 OS=Homo sapiens OX=9606 GN=HNRNPA2B1 PE=1 SV=2	FALSE	7	2	2	2	353	37.4	8.95	6.52
High	P25685	DnaJ homolog subfamily B member 1 OS=Homo sapiens OX=9606 GN=DNAJB1 PE=1 SV=4	FALSE	8	2	2	2	340	38	8.63	0
High	Q9Y3U8	60S ribosomal protein L36 OS=Homo sapiens OX=9606 GN=RPL36 PE=1 SV=3	FALSE	18	2	2	2	105	12.2	11.59	1.62
High	O00459	Phosphatidylinositol 3-kinase regulatory subunit beta OS=Homo sapiens OX=9606 GN=PIK3R2 PE=1 SV=2	FALSE	5	2	2	2	728	81.5	6.43	3.68
High	P62829	60S ribosomal protein L23 OS=Homo sapiens OX=9606 GN=RPL23 PE=1 SV=1	FALSE	20	2	2	2	140	14.9	10.51	3.83
High	Q92575	UBX domain-containing protein 4 OS=Homo sapiens OX=9606 GN=UBXN4 PE=1 SV=2	FALSE	7	1	2	1	508	56.7	6.38	2.92
High	Q5J5Z5	Protein PRRC2B OS=Homo sapiens OX=9606 GN=PRRC2B PE=1 SV=2	FALSE	1	2	2	2	2229	242.8	8.34	4.47
High	P62753	40S ribosomal protein S6 OS=Homo sapiens OX=9606 GN=RPS6 PE=1 SV=1	FALSE	11	2	2	2	249	28.7	10.84	5.27
High	P02533	Keratin, type I cytoskeletal 14 OS=Homo sapiens OX=9606 GN=KRT14 PE=1 SV=4	TRUE	5	2	2	2	472	51.5	5.16	2.57
High	P16401	Histone H1.5 OS=Homo sapiens OX=9606 GN=H1-5 PE=1 SV=3	FALSE	9	2	2	2	226	22.6	10.92	3.34
High	Q14257	Reticulocalbin-2 OS=Homo sapiens OX=9606 GN=RCN2 PE=1 SV=1	FALSE	12	2	2	2	317	36.9	4.4	0
High	P62269	40S ribosomal protein S18 OS=Homo sapiens OX=9606 GN=RPS18 PE=1 SV=3	FALSE	11	2	2	2	152	17.7	10.99	3.94
High	P01861	Immunoglobulin heavy constant gamma 4 OS=Homo sapiens OX=9606 GN=IGHG4 PE=1 SV=1	FALSE	10	2	2	2	327	35.9	7.36	1.76
High	P21127	Cyclin-dependent kinase 11B OS=Homo sapiens OX=9606 GN=CDK11B PE=1 SV=4	FALSE	3	2	2	2	795	92.6	5.54	0
High	O00571	ATP-dependent RNA helicase DDX3X OS=Homo sapiens OX=9606 GN=DDX3X PE=1 SV=3	FALSE	3	2	2	2	662	73.2	7.18	4.34



High	P36578	60S ribosomal protein L4 OS=Homo sapiens OX=9606 GN=RPL4 PE=1 SV=5	FALSE	4	2	2	2	427	47.7	11.06	0
High	Q5VTL8	Pre-mRNA-splicing factor 38B OS=Homo sapiens OX=9606 GN=PRPF38B PE=1 SV=1	FALSE	4	2	2	2	546	64.4	10.54	4.4
High	O43823	A-kinase anchor protein 8 OS=Homo sapiens OX=9606 GN=AKAP8 PE=1 SV=1	FALSE	3	1	2	1	692	76.1	5.15	0
High	P35232	Prohibitin OS=Homo sapiens OX=9606 GN=PHB PE=1 SV=1	FALSE	7	1	2	1	272	29.8	5.76	4.54
High	P21333	Filamin-A OS=Homo sapiens OX=9606 GN=FLNA PE=1 SV=4	FALSE	1	2	2	1	2647	280.6	6.06	1.83
High	Q02878	60S ribosomal protein L6 OS=Homo sapiens OX=9606 GN=RPL6 PE=1 SV=3	FALSE	9	2	2	2	288	32.7	10.58	3.29
High	P62277	40S ribosomal protein S13 OS=Homo sapiens OX=9606 GN=RPS13 PE=1 SV=2	FALSE	15	2	2	2	151	17.2	10.54	3.93
High	O75607	Nucleoplasmin-3 OS=Homo sapiens OX=9606 GN=NPM3 PE=1 SV=3	FALSE	10	1	1	1	178	19.3	4.63	0
High	Q8N684	Cleavage and polyadenylation specificity factor subunit 7 OS=Homo sapiens OX=9606 GN=CPSF7 PE=1 SV=1	FALSE	2	1	1	1	471	52	8	0
High	Q15084	Protein disulfide-isomerase A6 OS=Homo sapiens OX=9606 GN=PDIA6 PE=1 SV=1	FALSE	3	1	1	1	440	48.1	5.08	0
High	O15258	Protein RER1 OS=Homo sapiens OX=9606 GN=RER1 PE=1 SV=1	FALSE	10	1	1	1	196	22.9	9.54	2.48
Medium	A6NMY6	Putative annexin A2-like protein OS=Homo sapiens OX=9606 GN=ANXA2P2 PE=5 SV=2	FALSE	5	1	1	1	339	38.6	6.95	0
Medium	P60866	40S ribosomal protein S20 OS=Homo sapiens OX=9606 GN=RPS20 PE=1 SV=1	FALSE	10	1	1	1	119	13.4	9.94	0
High	P62318	Small nuclear ribonucleoprotein Sm D3 OS=Homo sapiens OX=9606 GN=SNRPD3 PE=1 SV=1	FALSE	7	1	1	1	126	13.9	10.32	0
Medium	P62906	60S ribosomal protein L10a OS=Homo sapiens OX=9606 GN=RPL10A PE=1 SV=2	FALSE	4	1	1	1	217	24.8	9.94	1.72
High	P35030	Trypsin-3 OS=Homo sapiens OX=9606 GN=PRSS3 PE=1 SV=2	FALSE	4	1	1	1	304	32.5	7.49	0
Medium	O43852	Calumenin OS=Homo sapiens OX=9606 GN=CALU PE=1 SV=2	FALSE	2	1	1	1	315	37.1	4.64	0
High	P35613	Basigin OS=Homo sapiens OX=9606 GN=BSG PE=1 SV=2	FALSE	4	1	1	1	385	42.2	5.66	0
High	Q16629	Serine/arginine-rich splicing factor 7 OS=Homo sapiens OX=9606 GN=SRSF7 PE=1 SV=1	FALSE	6	1	1	1	238	27.4	11.82	0
High	Q92552	28S ribosomal protein S27, mitochondrial OS=Homo sapiens OX=9606 GN=MRPS27 PE=1 SV=3	FALSE	3	1	1	1	414	47.6	6.18	0
High	P62826	GTP-binding nuclear protein Ran OS=Homo sapiens OX=9606 GN=RAN PE=1 SV=3	FALSE	5	1	1	1	216	24.4	7.49	2.27
High	O43719	HIV Tat-specific factor 1 OS=Homo sapiens OX=9606 GN=HTATSF1 PE=1 SV=1	FALSE	2	1	1	1	755	85.8	4.4	0
High	AA08411	Immunoglobulin heavy variable 3-15 OS=Homo sapiens OX=9606 GN=IGHV3-15 PE=3 SV=1	FALSE	9	1	1	1	119	12.9	8.62	2.43
High	Q9C0D9	Ethanolaminephosphotransferase 1 OS=Homo sapiens OX=9606 GN=SELENOI PE=1 SV=3	FALSE	4	1	1	1	397	45.2	6.6	1.7
High	Q13200	26S proteasome non-ATPase regulatory subunit 2 OS=Homo sapiens OX=9606 GN=PSMD2 PE=1 SV=3	FALSE	2	1	1	1	908	100.1	5.2	0
High	Q7L2H7	Eukaryotic translation initiation factor 3 subunit M OS=Homo sapiens OX=9606 GN=EIF3M PE=1 SV=1	FALSE	5	1	1	1	374	42.5	5.63	0
High	Q15287	RNA-binding protein with serine-rich domain 1 OS=Homo sapiens OX=9606 GN=RNPS1 PE=1 SV=1	FALSE	5	1	1	1	305	34.2	11.84	0
Medium	Q96D15	Reticulocalbin-3 OS=Homo sapiens OX=9606 GN=RCN3 PE=1 SV=1	FALSE	2	1	1	1	328	37.5	4.89	0
High	P06312	Immunoglobulin kappa variable 4-1 OS=Homo sapiens OX=9606 GN=IGKV4-1 PE=1 SV=1	FALSE	7	1	1	1	121	13.4	5.25	2.11
High	P26641	Elongation factor 1-gamma OS=Homo sapiens OX=9606 GN=EEF1G PE=1 SV=3	FALSE	3	1	1	1	437	50.1	6.67	0
High	Q13428	Treacle protein OS=Homo sapiens OX=9606 GN=TCOF1 PE=1 SV=3	FALSE	1	1	1	1	1488	152	9.04	0
High	Q9UJ21	Stomatin-like protein 2, mitochondrial OS=Homo sapiens OX=9606 GN=STOML2 PE=1 SV=1	FALSE	4	1	1	1	356	38.5	7.39	0
High	P61758	Prefoldin subunit 3 OS=Homo sapiens OX=9606 GN=VBP1 PE=1 SV=4	FALSE	5	1	1	1	197	22.6	7.11	0
High	P62857	40S ribosomal protein S28 OS=Homo sapiens OX=9606 GN=RPS28 PE=1 SV=1	FALSE	17	1	1	1	69	7.8	10.7	2.11
High	Q9BWJ5	Splicing factor 3B subunit 5 OS=Homo sapiens OX=9606 GN=SF3B5 PE=1 SV=1	FALSE	17	1	1	1	86	10.1	6.35	1.94
Medium	P08621	U1 small nuclear ribonucleoprotein 70 kDa OS=Homo sapiens OX=9606 GN=SNRNP70 PE=1 SV=2	FALSE	2	1	1	1	437	51.5	9.94	0
High	Q01844	RNA-binding protein EWS OS=Homo sapiens OX=9606 GN=EWSR1 PE=1 SV=1	FALSE	4	1	1	1	656	68.4	9.33	3.66
High	P62249	40S ribosomal protein S16 OS=Homo sapiens OX=9606 GN=RPS16 PE=1 SV=2	FALSE	7	1	1	1	146	16.4	10.21	2.24
High	P0D0X8	Immunoglobulin lambda-1 light chain OS=Homo sapiens OX=9606 GN=IGLC1 PE=1 SV=1	FALSE	4	1	1	1	216	22.8	6.76	2.05
High	P78344	Eukaryotic translation initiation factor 4 gamma 2 OS=Homo sapiens OX=9606 GN=EIF4G2 PE=1 SV=1	FALSE	2	1	1	1	907	102.3	7.14	0
High	P09651	Heterogeneous nuclear ribonucleoprotein A1 OS=Homo sapiens OX=9606 GN=HNRNPA1 PE=1 SV=5	FALSE	4	1	1	1	372	38.7	9.13	2.58
High	P17980	26S proteasome regulatory subunit 6A OS=Homo sapiens OX=9606 GN=PSMC3 PE=1 SV=3	FALSE	2	1	1	1	439	49.2	5.24	0
High	P04004	Vitronectin OS=Homo sapiens OX=9606 GN=VTN PE=1 SV=1	FALSE	3	1	1	1	478	54.3	5.8	0
Medium	P05387	60S acidic ribosomal protein P2 OS=Homo sapiens OX=9606 GN=RPLP2 PE=1 SV=1	FALSE	15	1	1	1	115	11.7	4.54	0
High	Q15393	Splicing factor 3B subunit 3 OS=Homo sapiens OX=9606 GN=SF3B3 PE=1 SV=4	FALSE	1	1	1	1	1217	135.5	5.26	0
High	Q96MA6	Adenylate kinase 8 OS=Homo sapiens OX=9606 GN=AK8 PE=1 SV=1	FALSE	3	1	1	1	479	54.9	6.15	1.61
High	P53985	Monocarboxylate transporter 1 OS=Homo sapiens OX=9606 GN=SLC16A1 PE=1 SV=3	FALSE	2	1	1	1	500	53.9	8.66	3.04
High	P08670	Vimentin OS=Homo sapiens OX=9606 GN=VIM PE=1 SV=4	FALSE	2	1	1	1	466	53.6	5.12	1.95
High	P02768	Serum albumin OS=Homo sapiens OX=9606 GN=ALB PE=1 SV=2	TRUE	2	1	1	1	609	69.3	6.28	3.53
High	P14649	Myosin light chain 6B OS=Homo sapiens OX=9606 GN=MYL6B PE=1 SV=1	FALSE	6	1	1	1	208	22.8	5.73	2.16
Medium	P01241	Somatotropin OS=Homo sapiens OX=9606 GN=GH1 PE=1 SV=2	FALSE	5	1	1	1	217	24.8	5.43	2.03
High	O00767	Acyl-CoA desaturase OS=Homo sapiens OX=9606 GN=SCD PE=1 SV=2	FALSE	4	1	1	1	359	41.5	9	1.72
High	P63244	Receptor of activated protein C kinase 1 OS=Homo sapiens OX=9606 GN=RACK1 PE=1 SV=3	FALSE	3	1	1	1	317	35.1	7.69	1.79
High	P12270	Nucleoprotein TPR OS=Homo sapiens OX=9606 GN=TPR PE=1 SV=3	FALSE	0	1	1	1	2363	267.1	5.02	0
High	P08708	40S ribosomal protein S17 OS=Homo sapiens OX=9606 GN=RPS17 PE=1 SV=2	FALSE	16	1	1	1	135	15.5	9.85	0
Medium	O43175	D-3-phosphoglycerate dehydrogenase OS=Homo sapiens OX=9606 GN=PHGDH PE=1 SV=4	FALSE	2	1	1	1	533	56.6	6.71	0

High	P02786	Transferrin receptor protein 1 OS=Homo sapiens OX=9606 GN=TFRC PE=1 SV=2	FALSE	2	1	1	1	760	84.8	6.61	2.17
High	Q15293	Reticulocalbin-1 OS=Homo sapiens OX=9606 GN=RCN1 PE=1 SV=1	FALSE	4	1	1	1	331	38.9	5	0
Medium	P01859	Immunoglobulin heavy constant gamma 2 OS=Homo sapiens OX=9606 GN=IGHG2 PE=1 SV=2	FALSE	5	1	1	1	326	35.9	7.59	0
High	P22695	Cytochrome b-c1 complex subunit 2, mitochondrial OS=Homo sapiens OX=9606 GN=UQCRC2 PE=1 SV=3	FALSE	4	1	1	1	453	48.4	8.63	0
High	O43390	Heterogeneous nuclear ribonucleoprotein R OS=Homo sapiens OX=9606 GN=HNRNPR PE=1 SV=1	FALSE	2	1	1	1	633	70.9	8.13	1.67
High	Q93009	Ubiquitin carboxyl-terminal hydrolase 7 OS=Homo sapiens OX=9606 GN=USP7 PE=1 SV=2	FALSE	1	1	1	1	1102	128.2	5.55	0
High	P84098	60S ribosomal protein L19 OS=Homo sapiens OX=9606 GN=RPL19 PE=1 SV=1	FALSE	9	1	1	1	196	23.5	11.47	3.38
Medium	P46060	Ran GTPase-activating protein 1 OS=Homo sapiens OX=9606 GN=RANGAP1 PE=1 SV=1	FALSE	2	1	1	1	587	63.5	4.68	1.91
High	Q66PJ3	ADP-ribosylation factor-like protein 6-interacting protein 4 OS=Homo sapiens OX=9606 GN=ARL6IP4 PE=1 SV=2	FALSE	3	1	1	1	421	44.9	10.93	2.21
High	Q02543	60S ribosomal protein L18a OS=Homo sapiens OX=9606 GN=RPL18A PE=1 SV=2	FALSE	7	1	1	1	176	20.7	10.71	1.94
High	O60925	Prefoldin subunit 1 OS=Homo sapiens OX=9606 GN=PFDN1 PE=1 SV=2	FALSE	9	1	1	1	122	14.2	6.81	2.55
High	P40429	60S ribosomal protein L13a OS=Homo sapiens OX=9606 GN=RPL13A PE=1 SV=2	FALSE	5	1	1	1	203	23.6	10.93	2.13
High	Q7L4I2	Arginine/serine-rich coiled-coil protein 2 OS=Homo sapiens OX=9606 GN=RSRC2 PE=1 SV=1	FALSE	4	1	1	1	434	50.5	11.33	3.06
High	P27824	Calnexin OS=Homo sapiens OX=9606 GN=CANX PE=1 SV=2	FALSE	2	1	1	1	592	67.5	4.6	0
High	P62899	60S ribosomal protein L31 OS=Homo sapiens OX=9606 GN=RPL31 PE=1 SV=1	FALSE	7	1	1	1	125	14.5	10.54	2.45
High	Q09666	Neuroblast differentiation-associated protein AHNAK OS=Homo sapiens OX=9606 GN=AHNAK PE=1 SV=2	FALSE	0	1	1	1	5890	628.7	6.15	0
High	P62861	40S ribosomal protein S30 OS=Homo sapiens OX=9606 GN=FAU PE=1 SV=1	FALSE	17	1	1	1	59	6.6	12.15	1.84
High	Q96A08	Histone H2B type 1-A OS=Homo sapiens OX=9606 GN=H2BC1 PE=1 SV=3	FALSE	7	1	1	1	127	14.2	10.32	0
High	O00743	Serine/threonine-protein phosphatase 6 catalytic subunit OS=Homo sapiens OX=9606 GN=PPP6C PE=1 SV=1	FALSE	3	1	1	1	305	35.1	5.69	0
High	Q9NWB6	Arginine and glutamate-rich protein 1 OS=Homo sapiens OX=9606 GN=ARGLU1 PE=1 SV=1	FALSE	3	1	1	1	273	33.2	10.35	1.7
High	Q9BRL6	Serine/arginine-rich splicing factor 8 OS=Homo sapiens OX=9606 GN=SRSF8 PE=1 SV=1	FALSE	3	1	1	1	282	32.3	11.72	2.14
High	P53999	Activated RNA polymerase II transcriptional coactivator p15 OS=Homo sapiens OX=9606 GN=SUB1 PE=1 SV=3	FALSE	9	1	1	1	127	14.4	9.6	0
High	Q9UBX3	Mitochondrial dicarboxylate carrier OS=Homo sapiens OX=9606 GN=SLC25A10 PE=1 SV=2	FALSE	5	1	1	1	287	31.3	9.54	0
High	Q14746	Conserved oligomeric Golgi complex subunit 2 OS=Homo sapiens OX=9606 GN=COG2 PE=1 SV=1	FALSE	3	1	1	1	738	83.2	6.62	2.32
High	P43307	Translocon-associated protein subunit alpha OS=Homo sapiens OX=9606 GN=SSR1 PE=1 SV=3	FALSE	5	1	1	1	286	32.2	4.49	0
High	P47914	60S ribosomal protein L29 OS=Homo sapiens OX=9606 GN=RPL29 PE=1 SV=2	FALSE	9	1	1	1	159	17.7	11.66	2.46
High	Q12874	Splicing factor 3A subunit 3 OS=Homo sapiens OX=9606 GN=SF3A3 PE=1 SV=1	FALSE	2	1	1	1	501	58.8	5.38	2.07
High	P02545	Prelamin-A/C OS=Homo sapiens OX=9606 GN=LMNA PE=1 SV=1	FALSE	2	1	1	1	664	74.1	7.02	2.17
High	P31942	Heterogeneous nuclear ribonucleoprotein H3 OS=Homo sapiens OX=9606 GN=HNRNPH3 PE=1 SV=2	FALSE	4	1	1	1	346	36.9	6.87	1.71
High	Q6Q0C0	E3 ubiquitin-protein ligase TRAF7 OS=Homo sapiens OX=9606 GN=TRAF7 PE=1 SV=1	FALSE	1	1	1	1	670	74.6	7.15	2.03
High	P05187	Alkaline phosphatase, placental type OS=Homo sapiens OX=9606 GN=ALPP PE=1 SV=2	FALSE	3	1	1	1	535	57.9	6.29	3.82
High	Q9ULX6	A-kinase anchor protein 8-like OS=Homo sapiens OX=9606 GN=AKAP8L PE=1 SV=4	FALSE	2	1	1	1	646	71.6	5.05	2.33
High	Q81WX8	Calcium homeostasis endoplasmic reticulum protein OS=Homo sapiens OX=9606 GN=CHERP PE=1 SV=3	FALSE	1	1	1	1	916	103.6	9.04	0
High	P56134	ATP synthase subunit f, mitochondrial OS=Homo sapiens OX=9606 GN=ATP5MF PE=1 SV=3	FALSE	14	1	1	1	94	10.9	9.67	0
High	Q92551	Inositol hexakisphosphate kinase 1 OS=Homo sapiens OX=9606 GN=IP6K1 PE=1 SV=3	FALSE	3	1	1	1	441	50.2	7.24	0
High	P57088	Transmembrane protein 33 OS=Homo sapiens OX=9606 GN=TMEM33 PE=1 SV=2	FALSE	5	1	1	1	247	28	9.7	1.87
High	P62314	Small nuclear ribonucleoprotein Sm D1 OS=Homo sapiens OX=9606 GN=SNRPD1 PE=1 SV=1	FALSE	11	1	1	1	119	13.3	11.56	3.65
High	P62316	Small nuclear ribonucleoprotein Sm D2 OS=Homo sapiens OX=9606 GN=SNRPD2 PE=1 SV=1	FALSE	7	1	1	1	118	13.5	9.91	0
High	Q6UN15	Pre-mRNA 3'-end-processing factor FIP1 OS=Homo sapiens OX=9606 GN=FIP1L1 PE=1 SV=1	FALSE	2	1	1	1	594	66.5	5.59	2.6
High	P62917	60S ribosomal protein L8 OS=Homo sapiens OX=9606 GN=RPL8 PE=1 SV=2	FALSE	4	1	1	1	257	28	11.03	2.26
High	P00403	Cytochrome c oxidase subunit 2 OS=Homo sapiens OX=9606 GN=MT-CO2 PE=1 SV=1	FALSE	4	1	1	1	227	25.5	4.82	0
High	P25205	DNA replication licensing factor MCM3 OS=Homo sapiens OX=9606 GN=MCM3 PE=1 SV=3	FALSE	2	1	1	1	808	90.9	5.77	2.05
High	P18077	60S ribosomal protein L35a OS=Homo sapiens OX=9606 GN=RPL35A PE=1 SV=2	FALSE	8	1	1	1	110	12.5	11.06	1.88
High	P43686	26S proteasome regulatory subunit 6B OS=Homo sapiens OX=9606 GN=PSMC4 PE=1 SV=2	FALSE	2	1	1	1	418	47.3	5.21	1.74
High	Q9UNL2	Translocon-associated protein subunit gamma OS=Homo sapiens OX=9606 GN=SSR3 PE=1 SV=1	FALSE	8	1	1	1	185	21.1	9.61	1.67
High	Q9NZB2	Constitutive coactivator of PPAR-gamma-like protein 1 OS=Homo sapiens OX=9606 GN=FAM120A PE=1 SV=2	FALSE	1	1	1	1	1118	121.8	8.88	0
High	P62847	40S ribosomal protein S24 OS=Homo sapiens OX=9606 GN=RPS24 PE=1 SV=1	FALSE	11	1	1	1	133	15.4	10.78	0
High	P04844	Dolichyl-diphosphooligosaccharide--protein glycosyltransferase subunit 2 OS=Homo sapiens OX=9606 GN=RPNG2	FALSE	2	1	1	1	631	69.2	5.69	1.78
High	P06748	Nucleophosmin OS=Homo sapiens OX=9606 GN=NPM1 PE=1 SV=2	FALSE	5	1	1	1	294	32.6	4.78	2.3
High	P46782	40S ribosomal protein S5 OS=Homo sapiens OX=9606 GN=RPSS5 PE=1 SV=4	FALSE	7	1	1	1	204	22.9	9.72	0
High	Q06210	Glutamine-fructose-6-phosphate aminotransferase [isomerizing] 1 OS=Homo sapiens OX=9606 GN=GFPT1 PE=	FALSE	2	1	1	1	699	78.8	7.11	3.02
High	Q53LP3	Ankyrin repeat domain-containing protein SOWAHC OS=Homo sapiens OX=9606 GN=SOWAHC PE=1 SV=1	FALSE	4	1	1	1	525	55.6	7.03	0
High	Q15427	Splicing factor 3B subunit 4 OS=Homo sapiens OX=9606 GN=SF3B4 PE=1 SV=1	FALSE	6	1	1	1	424	44.4	8.56	0
High	P20648	Potassium-transporting ATPase alpha chain 1 OS=Homo sapiens OX=9606 GN=ATP4A PE=2 SV=5	FALSE	1	1	1	1	1035	114	5.81	2.52
High	P27635	60S ribosomal protein L10 OS=Homo sapiens OX=9606 GN=RPL10 PE=1 SV=4	FALSE	6	1	1	1	214	24.6	10.08	2.1
Medium	P35222	Catenin beta-1 OS=Homo sapiens OX=9606 GN=CTNNB1 PE=1 SV=1	FALSE	1	1	1	1	781	85.4	5.86	0

High	P36542	ATP synthase subunit gamma, mitochondrial OS=Homo sapiens OX=9606 GN=ATP5F1C PE=1 SV=1	FALSE	3	1	1	1	298	33	9.22	1.81
High	P62841	40S ribosomal protein S15 OS=Homo sapiens OX=9606 GN=RPS15 PE=1 SV=2	FALSE	8	1	1	1	145	17	10.39	2.69
High	P62306	Small nuclear ribonucleoprotein F OS=Homo sapiens OX=9606 GN=SNRPF PE=1 SV=1	FALSE	15	1	1	1	86	9.7	4.67	2.69
High	Q14643	Inositol 1,4,5-trisphosphate receptor type 1 OS=Homo sapiens OX=9606 GN=ITPR1 PE=1 SV=3	FALSE	1	1	1	1	2758	313.7	6.04	0
High	Q01650	Large neutral amino acids transporter small subunit 1 OS=Homo sapiens OX=9606 GN=SLC7A5 PE=1 SV=2	FALSE	3	1	1	1	507	55	7.72	2.71
High	P0DOX7	Immunoglobulin kappa light chain OS=Homo sapiens OX=9606 PE=1 SV=1	FALSE	9	1	1	1	214	23.4	7.17	2.05
High	Q9BRX9	WD repeat domain-containing protein 83 OS=Homo sapiens OX=9606 GN=WDR83 PE=1 SV=1	FALSE	4	1	1	1	315	34.3	5.58	0



## HAdV40 (group F)

Protein	FDR	Confidence	Accession	Description	Contaminant	Coverage [%]	# Peptides	# PSMs	# Unique Peptides	# AAs	MW [kDa]	calc. pI	Sequest HT
High			Q14315	Filamin-C OS=Homo sapiens OX=9606 GN=FLNC PE=1 SV=3	FALSE	26	47	55	43	2725	290.8	5.97	123.58
High			P11142	Heat shock cognate 71 kDa protein OS=Homo sapiens OX=9606 GN=HSPA8 PE=1 SV=1	FALSE	50	26	45	18	646	70.9	5.52	113.86
High			O95202	Mitochondrial proton/calcium exchanger protein OS=Homo sapiens OX=9606 GN=LETM1 PE=1 SV=1	FALSE	47	27	37	27	739	83.3	6.7	98.14
High			Q93008	Probable ubiquitin carboxyl-terminal hydrolase FAF-X OS=Homo sapiens OX=9606 GN=USP9X PE=1 SV=3	FALSE	15	32	34	32	2570	292.1	5.8	68.17
High			P38646	Stress-70 protein, mitochondrial OS=Homo sapiens OX=9606 GN=HSPA9 PE=1 SV=2	FALSE	35	18	32	18	679	73.6	6.16	84.34
High			P00MV9	Heat shock 70 kDa protein 1B OS=Homo sapiens OX=9606 GN=HSPA1B PE=1 SV=1	FALSE	40	19	29	13	641	70	5.66	67.64
High			Q07954	Prolow-density lipoprotein receptor-related protein 1 OS=Homo sapiens OX=9606 GN=LRP1 PE=1 SV=2	FALSE	8	28	28	28	4544	504.3	5.39	49.41
High			P11021	Endoplasmic reticulum chaperone BiP OS=Homo sapiens OX=9606 GN=HSPA5 PE=1 SV=2	FALSE	38	19	27	17	654	72.3	5.16	60.19
High			Q5JSZ5	Protein PRRC2B OS=Homo sapiens OX=9606 GN=PRRC2B PE=1 SV=2	FALSE	18	26	27	26	2229	242.8	8.34	60.64
High			Q9ULH0	Kinase D-interacting substrate of 220 kDa OS=Homo sapiens OX=9606 GN=KIDINS220 PE=1 SV=3	FALSE	18	24	27	24	1771	196.4	6.62	50.12
High			P35527	Keratin, type I cytoskeletal 9 OS=Homo sapiens OX=9606 GN=KRT9 PE=1 SV=3	TRUE	25	11	23	11	623	62	5.24	47.97
High			Q15149	Plectin OS=Homo sapiens OX=9606 GN=PLEC PE=1 SV=3	FALSE	6	20	22	20	4684	531.5	5.96	41.08
High			P28799	Progranulin OS=Homo sapiens OX=9606 GN=GRN PE=1 SV=2	FALSE	40	16	22	16	593	63.5	6.83	61.84
High			P05783	Keratin, type I cytoskeletal 18 OS=Homo sapiens OX=9606 GN=KRT18 PE=1 SV=2	FALSE	33	13	21	12	430	48	5.45	39.17
High			P13645	Keratin, type I cytoskeletal 10 OS=Homo sapiens OX=9606 GN=KRT10 PE=1 SV=6	TRUE	26	15	20	13	584	58.8	5.21	38.65
High			P15924	Desmoplakin OS=Homo sapiens OX=9606 GN=DSP PE=1 SV=3	FALSE	8	18	20	18	2871	331.6	6.81	24.5
High			O95817	BAG family molecular chaperone regulator 3 OS=Homo sapiens OX=9606 GN=BAG3 PE=1 SV=3	FALSE	35	13	20	13	575	61.6	6.95	44.58
High			P05787	Keratin, type II cytoskeletal 8 OS=Homo sapiens OX=9606 GN=KRT8 PE=1 SV=7	TRUE	33	14	19	13	483	53.7	5.59	39.84
High			P04264	Keratin, type II cytoskeletal 1 OS=Homo sapiens OX=9606 GN=KRT1 PE=1 SV=6	TRUE	23	14	18	11	644	66	8.12	33.16
High			Q93009	Ubiquitin carboxyl-terminal hydrolase 7 OS=Homo sapiens OX=9606 GN=USP7 PE=1 SV=2	FALSE	19	17	18	17	1102	128.2	5.55	29.84
High			P07437	Tubulin beta chain OS=Homo sapiens OX=9606 GN=TUBB PE=1 SV=2	FALSE	41	13	18	4	444	49.6	4.89	39.84
High			Q71U36	Tubulin alpha-1A chain OS=Homo sapiens OX=9606 GN=TUBA1A PE=1 SV=1	FALSE	41	13	18	1	451	50.1	5.06	40.19
High			P54652	Heat shock-related 70 kDa protein 2 OS=Homo sapiens OX=9606 GN=HSPA2 PE=1 SV=1	FALSE	16	10	17	2	639	70	5.74	41.65
High			P68371	Tubulin beta-4B chain OS=Homo sapiens OX=9606 GN=TUBB4B PE=1 SV=1	FALSE	41	13	17	1	445	49.8	4.89	34.88
High			Q9BQE3	Tubulin alpha-1C chain OS=Homo sapiens OX=9606 GN=TUBA1C PE=1 SV=1	FALSE	35	12	17	2	449	49.9	5.1	35.9
High			P68366	Tubulin alpha-4A chain OS=Homo sapiens OX=9606 GN=TUBA4A PE=1 SV=1	FALSE	39	13	16	5	448	49.9	5.06	33.82
High			Q9UHX1	Poly(U)-binding-splicing factor PUF60 OS=Homo sapiens OX=9606 GN=PUF60 PE=1 SV=1	FALSE	31	12	16	12	559	59.8	5.29	35.22
High			P17066	Heat shock 70 kDa protein 6 OS=Homo sapiens OX=9606 GN=HSPA6 PE=1 SV=2	FALSE	19	10	15	3	643	71	6.14	32.31
High			Q14139	Ubiquitin conjugation factor E4 A OS=Homo sapiens OX=9606 GN=UBE4A PE=1 SV=2	FALSE	17	14	15	14	1066	122.5	5.24	27.94
High			O75822	Eukaryotic translation initiation factor 3 subunit J OS=Homo sapiens OX=9606 GN=EIF3J PE=1 SV=2	FALSE	34	10	14	10	258	29	4.83	39.05
High			P25054	Adenomatous polyposis coli protein OS=Homo sapiens OX=9606 GN=APC PE=1 SV=2	FALSE	7	13	14	13	2843	311.5	7.8	29.63
High			Q7L014	Probable ATP-dependent RNA helicase DDX46 OS=Homo sapiens OX=9606 GN=DDX46 PE=1 SV=2	FALSE	15	14	14	14	1031	117.3	9.29	19.95
High			P04350	Tubulin beta-4A chain OS=Homo sapiens OX=9606 GN=TUBB4A PE=1 SV=2	FALSE	38	12	14	1	444	49.6	4.88	22.01
High			P49756	RNA-binding protein 25 OS=Homo sapiens OX=9606 GN=RBM25 PE=1 SV=3	FALSE	17	10	14	10	843	100.1	6.32	39.73
High			Q9UP83	Conserved oligomeric Golgi complex subunit 5 OS=Homo sapiens OX=9606 GN=COG5 PE=1 SV=3	FALSE	17	13	14	13	839	92.7	6.6	20.92
High			P31943	Heterogeneous nuclear ribonucleoprotein H OS=Homo sapiens OX=9606 GN=HNRNPH1 PE=1 SV=4	FALSE	27	8	14	6	449	49.2	6.3	20.95
High			Q13501	Sequestosome-1 OS=Homo sapiens OX=9606 GN=SQSTM1 PE=1 SV=1	FALSE	46	11	14	11	440	47.7	5.22	40.53
High			P02545	Prelamin-A/C OS=Homo sapiens OX=9606 GN=LMNA PE=1 SV=1	FALSE	22	14	14	14	664	74.1	7.02	36.8
High			P60709	Actin, cytoplasmic 1 OS=Homo sapiens OX=9606 GN=ACTB PE=1 SV=1	TRUE	35	9	13	1	375	41.7	5.48	27.52
High			P49411	Elongation factor Tu, mitochondrial OS=Homo sapiens OX=9606 GN=TUFM PE=1 SV=2	FALSE	32	11	13	11	452	49.5	7.61	29.39
High			P10809	60 kDa heat shock protein, mitochondrial OS=Homo sapiens OX=9606 GN=HSPD1 PE=1 SV=2	FALSE	36	12	13	12	573	61	5.87	29.35
High			P14923	Junction plakoglobin OS=Homo sapiens OX=9606 GN=JUP PE=1 SV=3	FALSE	20	11	12	11	745	81.7	6.14	21.75
High			Q9Y2V7	Conserved oligomeric Golgi complex subunit 6 OS=Homo sapiens OX=9606 GN=COG6 PE=1 SV=2	FALSE	18	10	12	10	657	73.2	5.76	29.81
High			Q9Y383	Putative RNA-binding protein Luc7-like 2 OS=Homo sapiens OX=9606 GN=LUC7L2 PE=1 SV=2	FALSE	27	9	12	9	392	46.5	10.01	29.91
High			P63261	Actin, cytoplasmic 2 OS=Homo sapiens OX=9606 GN=ACTG1 PE=1 SV=1	FALSE	35	9	11	1	375	41.8	5.48	23.82
High			Q15181	Inorganic pyrophosphatase OS=Homo sapiens OX=9606 GN=PPA1 PE=1 SV=2	FALSE	37	8	11	8	289	32.6	5.86	19.8
High			P83436	Conserved oligomeric Golgi complex subunit 7 OS=Homo sapiens OX=9606 GN=COG7 PE=1 SV=1	FALSE	17	10	10	10	770	86.3	5.47	25.92
High			O00170	AH receptor-interacting protein OS=Homo sapiens OX=9606 GN=AIP PE=1 SV=2	FALSE	34	8	10	8	330	37.6	6.29	23.15
High			Q9BUJ2	Heterogeneous nuclear ribonucleoprotein U-like protein 1 OS=Homo sapiens OX=9606 GN=HNRNPUL1 PE=1 SV=1	FALSE	12	9	10	9	856	95.7	6.92	14.52
High			Q09666	Neuroblast differentiation-associated protein AHNAK OS=Homo sapiens OX=9606 GN=AHNAK PE=1 SV=2	FALSE	9	10	10	10	5890	628.7	6.15	11.61
High			P19474	E3 ubiquitin-protein ligase TRIM21 OS=Homo sapiens OX=9606 GN=TRIM21 PE=1 SV=1	FALSE	20	8	9	8	475	54.1	6.38	17.55
High			Q9UBH6	Xenotropic and polytropic retrovirus receptor 1 OS=Homo sapiens OX=9606 GN=XPR1 PE=1 SV=1	FALSE	14	6	9	6	696	81.5	8.44	14.93
High			Q16630	Cleavage and polyadenylation specificity factor subunit 6 OS=Homo sapiens OX=9606 GN=CPSF6 PE=1 SV=2	FALSE	21	8	9	8	551	59.2	7.15	19.46
High			Q9COC2	182 kDa tankyrase-1-binding protein OS=Homo sapiens OX=9606 GN=TNKS1BP1 PE=1 SV=4	FALSE	8	8	9	8	1729	181.7	4.86	9.85
High			P19338	Nucleolin OS=Homo sapiens OX=9606 GN=NCL PE=1 SV=3	FALSE	16	9	9	9	710	76.6	4.7	23.03
High			P08238	Heat shock protein HSP 90-beta OS=Homo sapiens OX=9606 GN=HSP90AB1 PE=1 SV=4	FALSE	17	9	9	9	724	83.2	5.03	18.51
High			P78527	DNA-dependent protein kinase catalytic subunit OS=Homo sapiens OX=9606 GN=PRKDC PE=1 SV=3	FALSE	3	9	9	9	4128	468.8	7.12	8.26

High	P08779	Keratin, type I cytoskeletal 16 OS=Homo sapiens OX=9606 GN=KRT16 PE=1 SV=4	TRUE	16	8	8	2	473	51.2	5.05	15.25
High	P52597	Heterogeneous nuclear ribonucleoprotein F OS=Homo sapiens OX=9606 GN=HNRNPF PE=1 SV=3	FALSE	20	6	8	4	415	45.6	5.58	12.63
High	O75400	Pre-mRNA-processing factor 40 homolog A OS=Homo sapiens OX=9606 GN=PRPF40A PE=1 SV=2	FALSE	10	7	8	7	957	108.7	7.56	18.61
High	P0DOX3	Immunoglobulin delta heavy chain OS=Homo sapiens OX=9606 PE=1 SV=1	FALSE	4	1	8	1	512	56.2	8.02	2.02
High	P12236	ADP/ATP translocase 3 OS=Homo sapiens OX=9606 GN=SLC25A6 PE=1 SV=4	FALSE	27	8	8	4	298	32.8	9.74	14.55
High	P05141	ADP/ATP translocase 2 OS=Homo sapiens OX=9606 GN=SLC25A5 PE=1 SV=7	FALSE	27	8	8	4	298	32.8	9.69	15.14
High	P61247	40S ribosomal protein S3a OS=Homo sapiens OX=9606 GN=RP53A PE=1 SV=2	FALSE	28	7	8	7	264	29.9	9.73	13.79
High	Q06830	Peroxisiredoxin-1 OS=Homo sapiens OX=9606 GN=PRDX1 PE=1 SV=1	TRUE	39	7	8	5	199	22.1	8.13	17.14
High	P21333	Filamin-A OS=Homo sapiens OX=9606 GN=FLNA PE=1 SV=4	FALSE	4	8	8	4	2647	280.6	6.06	13.35
High	P23497	Nuclear autoantigen Sp-100 OS=Homo sapiens OX=9606 GN=SP100 PE=1 SV=3	FALSE	9	7	8	7	879	100.4	8.22	14.63
High	P02533	Keratin, type I cytoskeletal 14 OS=Homo sapiens OX=9606 GN=KRT14 PE=1 SV=4	TRUE	17	8	8	2	472	51.5	5.16	15.98
High	P55081	Microfibrillar-associated protein 1 OS=Homo sapiens OX=9606 GN=MFAP1 PE=1 SV=2	FALSE	23	6	8	6	439	51.9	4.98	19.47
High	P35637	RNA-binding protein FUS OS=Homo sapiens OX=9606 GN=FUS PE=1 SV=1	FALSE	14	6	8	4	526	53.4	9.36	21.03
High	O95816	BAG family molecular chaperone regulator 2 OS=Homo sapiens OX=9606 GN=BAG2 PE=1 SV=1	FALSE	42	6	7	6	211	23.8	6.7	20.65
High	P68104	Elongation factor 1-alpha 1 OS=Homo sapiens OX=9606 GN=EEF1A1 PE=1 SV=1	FALSE	19	5	7	5	462	50.1	9.01	9.7
High	P25705	ATP synthase subunit alpha, mitochondrial OS=Homo sapiens OX=9606 GN=ATP5F1A PE=1 SV=1	FALSE	15	7	7	7	553	59.7	9.13	11.57
High	O75533	Splicing factor 3B subunit 1 OS=Homo sapiens OX=9606 GN=SF3B1 PE=1 SV=3	FALSE	7	7	7	7	1304	145.7	7.09	11.27
High	O43143	Pre-mRNA-splicing factor ATP-dependent RNA helicase DHX15 OS=Homo sapiens OX=9606 GN=DHX15 PE=1 SV=1	FALSE	9	7	7	7	795	90.9	7.46	12.77
High	Q969Q5	Ras-related protein Rab-24 OS=Homo sapiens OX=9606 GN=RAB24 PE=1 SV=1	FALSE	43	6	7	6	203	23.1	6.23	19.6
High	Q92804	TATA-binding protein-associated factor 2N OS=Homo sapiens OX=9606 GN=TAF15 PE=1 SV=1	FALSE	20	6	7	4	592	61.8	8.02	8.24
High	Q9ULX6	A-kinase anchor protein 8-like OS=Homo sapiens OX=9606 GN=AKAP8L PE=1 SV=4	FALSE	9	5	7	5	646	71.6	5.05	10.19
High	Q9UKJ3	G patch domain-containing protein 8 OS=Homo sapiens OX=9606 GN=GPATCH8 PE=1 SV=2	FALSE	3	4	7	4	1502	164.1	8.66	13.84
High	P31689	DnaJ homolog subfamily A member 1 OS=Homo sapiens OX=9606 GN=DNAJ1 PE=1 SV=2	FALSE	18	4	6	4	397	44.8	7.08	13.62
High	P61978	Heterogeneous nuclear ribonucleoprotein K OS=Homo sapiens OX=9606 GN=HNRNPK PE=1 SV=1	FALSE	14	6	6	6	463	50.9	5.54	14.63
High	P11940	Polyadenylate-binding protein 1 OS=Homo sapiens OX=9606 GN=PABPC1 PE=1 SV=2	FALSE	10	6	6	6	636	70.6	9.5	9.05
High	P13647	Keratin, type II cytoskeletal 5 OS=Homo sapiens OX=9606 GN=KRT5 PE=1 SV=3	TRUE	11	6	6	4	590	62.3	7.74	5.53
High	O15027	Protein transport protein Sec16A OS=Homo sapiens OX=9606 GN=SEC16A PE=1 SV=4	FALSE	3	5	6	5	2357	251.7	5.8	6.35
High	P31327	Carbamoyl-phosphate synthase [ammonia], mitochondrial OS=Homo sapiens OX=9606 GN=CPS1 PE=1 SV=2	FALSE	5	6	6	5	1500	164.8	6.74	11.34
High	Q9BUF5	Tubulin beta-6 chain OS=Homo sapiens OX=9606 GN=TUBB6 PE=1 SV=1	FALSE	18	6	6	2	446	49.8	4.88	12.37
High	Q96559	Ran-binding protein 9 OS=Homo sapiens OX=9606 GN=RANBP9 PE=1 SV=1	FALSE	10	5	6	5	729	77.8	6.79	8.64
High	Q14257	Reticulocalbin-2 OS=Homo sapiens OX=9606 GN=RCN2 PE=1 SV=1	FALSE	28	5	6	5	317	36.9	4.4	14.3
High	P22061	Protein-L-isaspartate(D-aspartate) O-methyltransferase OS=Homo sapiens OX=9606 GN=PCMT1 PE=1 SV=4	FALSE	25	4	6	4	227	24.6	7.21	14.35
High	P43243	Matrin-3 OS=Homo sapiens OX=9606 GN=MATR3 PE=1 SV=2	FALSE	8	5	5	5	847	94.6	6.25	5.48
High	Q00325	Phosphate carrier protein, mitochondrial OS=Homo sapiens OX=9606 GN=SLC25A3 PE=1 SV=2	FALSE	16	5	5	5	362	40.1	9.38	7.14
High	P35908	Keratin, type II cytoskeletal 2 epidermal OS=Homo sapiens OX=9606 GN=KRT2 PE=1 SV=2	TRUE	9	5	5	3	639	65.4	8	11.81
High	O95071	E3 ubiquitin-protein ligase UBR5 OS=Homo sapiens OX=9606 GN=UBR5 PE=1 SV=2	FALSE	3	5	5	5	2799	309.2	5.85	7.01
High	Q14498	RNA-binding protein 39 OS=Homo sapiens OX=9606 GN=RBM39 PE=1 SV=2	FALSE	13	5	5	5	530	59.3	10.1	13.78
High	P18085	ADP-ribosylation factor 4 OS=Homo sapiens OX=9606 GN=ARF4 PE=1 SV=3	FALSE	26	5	5	4	180	20.5	7.14	9.41
High	P04259	Keratin, type II cytoskeletal 6B OS=Homo sapiens OX=9606 GN=KRT6B PE=1 SV=5	TRUE	10	5	5	1	564	60	8	6.8
High	O43823	A-kinase anchor protein 8 OS=Homo sapiens OX=9606 GN=AKAP8 PE=1 SV=1	FALSE	10	4	5	4	692	76.1	5.15	7.26
High	Q99615	DnaJ homolog subfamily C member 7 OS=Homo sapiens OX=9606 GN=DNAJC7 PE=1 SV=2	FALSE	14	5	5	5	494	56.4	6.96	13.04
High	P62269	40S ribosomal protein S18 OS=Homo sapiens OX=9606 GN=RP518 PE=1 SV=3	FALSE	30	5	5	5	152	17.7	10.99	8.32
High	P17987	T-complex protein 1 subunit alpha OS=Homo sapiens OX=9606 GN=TCP1 PE=1 SV=1	FALSE	11	5	5	5	556	60.3	6.11	10.99
High	P01130	Low-density lipoprotein receptor OS=Homo sapiens OX=9606 GN=LDLR PE=1 SV=1	FALSE	6	5	5	5	860	95.3	5.05	0
High	P62701	40S ribosomal protein S4, X isoform OS=Homo sapiens OX=9606 GN=RP54X PE=1 SV=2	FALSE	16	5	5	5	263	29.6	10.15	7.23
High	P04792	Heat shock protein beta-1 OS=Homo sapiens OX=9606 GN=HSPB1 PE=1 SV=2	FALSE	25	4	5	4	205	22.8	6.4	12.17
High	P67809	Y-box-binding protein 1 OS=Homo sapiens OX=9606 GN=YBX1 PE=1 SV=3	FALSE	18	4	4	4	324	35.9	9.88	10.28
High	P62424	60S ribosomal protein L7a OS=Homo sapiens OX=9606 GN=RPL7A PE=1 SV=2	FALSE	14	4	4	4	266	30	10.61	6.17
High	P62829	60S ribosomal protein L23 OS=Homo sapiens OX=9606 GN=RPL23 PE=1 SV=1	FALSE	31	3	4	3	140	14.9	10.51	7.37
High	Q00839	Heterogeneous nuclear ribonucleoprotein U OS=Homo sapiens OX=9606 GN=HNRNPU PE=1 SV=6	FALSE	7	4	4	4	825	90.5	6	4.72
High	P23396	40S ribosomal protein S3 OS=Homo sapiens OX=9606 GN=RP53 PE=1 SV=2	FALSE	18	4	4	4	243	26.7	9.66	8.05
High	P16615	Sarcoplasmic/endoplasmic reticulum calcium ATPase 2 OS=Homo sapiens OX=9606 GN=ATP2A2 PE=1 SV=1	FALSE	5	4	4	4	1042	114.7	5.34	10.05
High	P62241	40S ribosomal protein S8 OS=Homo sapiens OX=9606 GN=RP58 PE=1 SV=2	FALSE	23	4	4	4	208	24.2	10.32	4.27
High	P27348	14-3-3 protein theta OS=Homo sapiens OX=9606 GN=YWHAQ PE=1 SV=1	FALSE	22	4	4	3	245	27.7	4.78	7.14
High	P18124	60S ribosomal protein L7 OS=Homo sapiens OX=9606 GN=RPL7 PE=1 SV=1	FALSE	15	3	4	3	248	29.2	10.65	8.55
High	Q02878	60S ribosomal protein L6 OS=Homo sapiens OX=9606 GN=RPL6 PE=1 SV=3	FALSE	12	3	4	3	288	32.7	10.58	8.14
High	P46781	40S ribosomal protein S9 OS=Homo sapiens OX=9606 GN=RP59 PE=1 SV=3	FALSE	16	4	4	4	194	22.6	10.65	5.36
High	P15880	40S ribosomal protein S2 OS=Homo sapiens OX=9606 GN=RP52 PE=1 SV=2	FALSE	15	4	4	4	293	31.3	10.24	6.56

High	P35221	Catenin alpha-1 OS=Homo sapiens OX=9606 GN=CTNNA1 PE=1 SV=1	FALSE	6	4	4	4	906	100	6.29	6.16
High	P39023	60S ribosomal protein L3 OS=Homo sapiens OX=9606 GN=RPL3 PE=1 SV=2	FALSE	12	3	4	3	403	46.1	10.18	5.02
High	P27708	CAD protein OS=Homo sapiens OX=9606 GN=CAD PE=1 SV=3	FALSE	2	4	4	3	2225	242.8	6.46	4.32
High	O00571	ATP-dependent RNA helicase DDX3X OS=Homo sapiens OX=9606 GN=DDX3X PE=1 SV=3	FALSE	6	4	4	4	662	73.2	7.18	5.77
High	O43852	Calumenin OS=Homo sapiens OX=9606 GN=CALU PE=1 SV=2	FALSE	20	4	4	4	315	37.1	4.64	5.55
High	Q8TF72	Protein Shroom3 OS=Homo sapiens OX=9606 GN=SHROOM3 PE=1 SV=2	FALSE	3	4	4	4	1996	216.7	7.8	3.67
High	P10412	Histone H1.4 OS=Homo sapiens OX=9606 GN=H1-4 PE=1 SV=2	FALSE	18	4	4	4	219	21.9	11.03	8.45
High	P62979	Ubiquitin-40S ribosomal protein S27a OS=Homo sapiens OX=9606 GN=RPS27A PE=1 SV=2	TRUE	24	3	4	3	156	18	9.64	6.06
Medium	Q8WVV9	Heterogeneous nuclear ribonucleoprotein L-like OS=Homo sapiens OX=9606 GN=HNRNPPLL PE=1 SV=1	FALSE	6	1	4	1	542	60	7.72	0
High	A0A0A0M1	Immunoglobulin heavy variable 1-45 OS=Homo sapiens OX=9606 GN=IGHV1-45 PE=3 SV=1	FALSE	9	1	4	1	117	13.5	9.1	7.59
High	Q9N201	Very-long-chain enoyl-CoA reductase OS=Homo sapiens OX=9606 GN=TECR PE=1 SV=1	FALSE	7	2	3	2	308	36	9.45	4.05
High	Q9HA65	TBC1 domain family member 17 OS=Homo sapiens OX=9606 GN=TBC1D17 PE=1 SV=2	FALSE	6	3	3	3	648	72.7	5.19	4.77
High	Q6VN20	Ran-binding protein 10 OS=Homo sapiens OX=9606 GN=RANBP10 PE=1 SV=1	FALSE	7	3	3	3	620	67.2	6.77	2.15
High	P52272	Heterogeneous nuclear ribonucleoprotein M OS=Homo sapiens OX=9606 GN=HNRNPM PE=1 SV=3	FALSE	6	3	3	3	730	77.5	8.7	5.72
High	P48643	T-complex protein 1 subunit epsilon OS=Homo sapiens OX=9606 GN=CCT5 PE=1 SV=1	FALSE	8	3	3	3	541	59.6	5.66	2.65
High	P62750	60S ribosomal protein L23a OS=Homo sapiens OX=9606 GN=RPL23A PE=1 SV=1	FALSE	21	3	3	3	156	17.7	10.45	2.2
High	Q07020	60S ribosomal protein L18 OS=Homo sapiens OX=9606 GN=RPL18 PE=1 SV=2	FALSE	18	3	3	3	188	21.6	11.72	7.72
High	Q05519	Serine/arginine-rich splicing factor 11 OS=Homo sapiens OX=9606 GN=SRSF11 PE=1 SV=1	FALSE	8	3	3	3	484	53.5	10.52	6.44
High	Q72627	E3 ubiquitin-protein ligase HUWE1 OS=Homo sapiens OX=9606 GN=HUWE1 PE=1 SV=3	FALSE	1	3	3	3	4374	481.6	5.22	2.19
High	Q15293	Reticulocalbin-1 OS=Homo sapiens OX=9606 GN=RCN1 PE=1 SV=1	FALSE	10	3	3	3	331	38.9	5	4.98
High	Q15459	Splicing factor 3A subunit 1 OS=Homo sapiens OX=9606 GN=SF3A1 PE=1 SV=1	FALSE	4	2	3	2	793	88.8	5.22	0
High	Q9UDY4	DnaJ homolog subfamily B member 4 OS=Homo sapiens OX=9606 GN=DNAJB4 PE=1 SV=1	FALSE	12	3	3	2	337	37.8	8.5	7.07
High	Q07021	Complement component 1 Q subcomponent-binding protein, mitochondrial OS=Homo sapiens OX=9606 GN=C1	FALSE	21	3	3	3	282	31.3	4.84	4.62
High	P07910	Heterogeneous nuclear ribonucleoproteins C1/C2 OS=Homo sapiens OX=9606 GN=HNRNPC PE=1 SV=4	FALSE	12	3	3	3	306	33.7	5.08	4.3
High	Q5T9A4	ATPase family AAA domain-containing protein 3B OS=Homo sapiens OX=9606 GN=ATAD3B PE=1 SV=1	FALSE	4	3	3	3	648	72.5	9.2	1.99
High	P26368	Splicing factor U2AF 65 kDa subunit OS=Homo sapiens OX=9606 GN=U2AF2 PE=1 SV=4	FALSE	6	3	3	3	475	53.5	9.09	3.39
High	P22626	Heterogeneous nuclear ribonucleoproteins A2/B1 OS=Homo sapiens OX=9606 GN=HNRNPA2B1 PE=1 SV=2	FALSE	10	3	3	3	353	37.4	8.95	7.02
High	Q9Y285	Phenylalanine-tRNA ligase alpha subunit OS=Homo sapiens OX=9606 GN=FARSA PE=1 SV=3	FALSE	7	3	3	3	508	57.5	7.8	4.98
High	P61353	60S ribosomal protein L27 OS=Homo sapiens OX=9606 GN=RPL27 PE=1 SV=2	FALSE	28	3	3	3	136	15.8	10.56	3.87
High	O94905	Erlin-2 OS=Homo sapiens OX=9606 GN=ERLIN2 PE=1 SV=1	FALSE	12	3	3	1	339	37.8	5.62	4.54
High	Q9H7D7	WD repeat-containing protein 26 OS=Homo sapiens OX=9606 GN=WDR26 PE=1 SV=3	FALSE	5	3	3	3	661	72.1	6.16	4.25
High	P06576	ATP synthase subunit beta, mitochondrial OS=Homo sapiens OX=9606 GN=ATP5F1B PE=1 SV=3	FALSE	8	3	3	3	529	56.5	5.4	4.82
High	Q13162	Peroxiredoxin-4 OS=Homo sapiens OX=9606 GN=PRDX4 PE=1 SV=1	FALSE	11	3	3	2	271	30.5	6.29	5.94
Medium	Q9NQW6	Anillin OS=Homo sapiens OX=9606 GN=ANLN PE=1 SV=2	FALSE	4	1	3	1	1124	124.1	8.07	0
High	P06733	Alpha-enolase OS=Homo sapiens OX=9606 GN=ENO1 PE=1 SV=2	FALSE	8	3	3	3	434	47.1	7.39	7.04
High	P55735	Protein SEC13 homolog OS=Homo sapiens OX=9606 GN=SEC13 PE=1 SV=3	FALSE	14	3	3	3	322	35.5	5.48	7.33
High	P25685	DnaJ homolog subfamily B member 1 OS=Homo sapiens OX=9606 GN=DNAJB1 PE=1 SV=4	FALSE	11	3	3	2	340	38	8.63	4.99
High	P08195	4F2 cell-surface antigen heavy chain OS=Homo sapiens OX=9606 GN=SLC3A2 PE=1 SV=3	FALSE	5	3	3	3	630	68	5.01	4.75
High	P17980	26S proteasome regulatory subunit 6A OS=Homo sapiens OX=9606 GN=PSMC3 PE=1 SV=3	FALSE	10	3	3	3	439	49.2	5.24	5.39
High	P62841	40S ribosomal protein S15 OS=Homo sapiens OX=9606 GN=RPS15 PE=1 SV=2	FALSE	21	2	3	2	145	17	10.39	4.95
High	Q9NWU2	Glucose-induced degradation protein 8 homolog OS=Homo sapiens OX=9606 GN=GID8 PE=1 SV=1	FALSE	18	3	3	3	228	26.7	4.97	7.47
High	O15427	Monocarboxylate transporter 4 OS=Homo sapiens OX=9606 GN=SLC16A3 PE=1 SV=1	FALSE	7	3	3	3	465	49.4	7.96	5.59
High	Q8TC07	TBC1 domain family member 15 OS=Homo sapiens OX=9606 GN=TBC1D15 PE=1 SV=2	FALSE	4	3	3	3	691	79.4	5.67	1.79
High	Q16576	Histone-binding protein RBBP7 OS=Homo sapiens OX=9606 GN=RBBP7 PE=1 SV=1	FALSE	8	3	3	3	425	47.8	5.05	3.79
High	P19022	Cadherin-2 OS=Homo sapiens OX=9606 GN=CDH2 PE=1 SV=4	FALSE	4	2	3	2	906	99.7	4.81	0
High	P62277	40S ribosomal protein S13 OS=Homo sapiens OX=9606 GN=RPS13 PE=1 SV=2	FALSE	15	2	3	2	151	17.2	10.54	4.16
High	Q96J82	Conserved oligomeric Golgi complex subunit 3 OS=Homo sapiens OX=9606 GN=COG3 PE=1 SV=3	FALSE	4	3	3	3	828	94	5.57	5.56
High	O75477	Erlin-1 OS=Homo sapiens OX=9606 GN=ERLIN1 PE=1 SV=2	FALSE	9	3	3	1	348	39.1	7.87	4.54
High	P02768	Serum albumin OS=Homo sapiens OX=9606 GN=ALB PE=1 SV=2	TRUE	4	3	3	3	609	69.3	6.28	6.38
High	P50914	60S ribosomal protein L14 OS=Homo sapiens OX=9606 GN=RPL14 PE=1 SV=4	FALSE	16	3	3	3	215	23.4	10.93	6.89
High	Q96MW5	Conserved oligomeric Golgi complex subunit 8 OS=Homo sapiens OX=9606 GN=COG8 PE=1 SV=2	FALSE	10	3	3	3	612	68.4	5.2	4.75
High	P16401	Histone H1.5 OS=Homo sapiens OX=9606 GN=H1-5 PE=1 SV=3	FALSE	16	3	3	3	226	22.6	10.92	3.66
High	P26373	60S ribosomal protein L13 OS=Homo sapiens OX=9606 GN=RPL13 PE=1 SV=4	FALSE	13	3	3	3	211	24.2	11.65	5.78
High	Q8IUR7	Armadillo repeat-containing protein 8 OS=Homo sapiens OX=9606 GN=ARMC8 PE=1 SV=2	FALSE	5	2	3	2	673	75.5	6.73	7.34
High	P63104	14-3-3 protein zeta/delta OS=Homo sapiens OX=9606 GN=YWHAZ PE=1 SV=1	FALSE	14	3	3	2	245	27.7	4.79	7.05
High	P62753	40S ribosomal protein S6 OS=Homo sapiens OX=9606 GN=RPS6 PE=1 SV=1	FALSE	11	2	3	2	249	28.7	10.84	8.08
High	Q725K2	Wings apart-like protein homolog OS=Homo sapiens OX=9606 GN=WAPL PE=1 SV=1	FALSE	3	2	2	2	1190	132.9	5.44	4.07
High	P50402	Emerin OS=Homo sapiens OX=9606 GN=EMD PE=1 SV=1	FALSE	10	2	2	2	254	29	5.5	1.77

Medium	Q5VU36	Spermatogenesis-associated protein 31A5 OS=Homo sapiens OX=9606 GN=SPATA31A5 PE=3 SV=1	FALSE	1	1	2	1	1347	148.6	8.72	0
High	P62847	40S ribosomal protein S24 OS=Homo sapiens OX=9606 GN=RP524 PE=1 SV=1	FALSE	20	2	2	2	133	15.4	10.78	2.11
High	P47756	F-actin-capping protein subunit beta OS=Homo sapiens OX=9606 GN=CAPZB PE=1 SV=4	FALSE	9	2	2	2	277	31.3	5.59	4.33
High	Q9UJS0	Calcium-binding mitochondrial carrier protein Aralar2 OS=Homo sapiens OX=9606 GN=SLC25A13 PE=1 SV=2	FALSE	4	2	2	2	675	74.1	8.62	1.95
High	P61204	ADP-ribosylation factor 3 OS=Homo sapiens OX=9606 GN=ARF3 PE=1 SV=2	FALSE	12	2	2	1	181	20.6	7.43	3.47
High	Q9HC44	Vasculin-like protein 1 OS=Homo sapiens OX=9606 GN=GPBP1L1 PE=1 SV=1	FALSE	7	2	2	2	474	52.3	6.84	2.18
High	P36578	60S ribosomal protein L4 OS=Homo sapiens OX=9606 GN=RPL4 PE=1 SV=5	FALSE	4	2	2	2	427	47.7	11.06	3.32
High	Q96PE2	Rho guanine nucleotide exchange factor 17 OS=Homo sapiens OX=9606 GN=ARHGEF17 PE=1 SV=1	FALSE	2	2	2	2	2063	221.5	6.29	2.07
High	P62851	40S ribosomal protein S25 OS=Homo sapiens OX=9606 GN=RP525 PE=1 SV=1	FALSE	15	2	2	2	125	13.7	10.11	4.21
High	P04843	Dolichyl-diphosphooligosaccharide--protein glycosyltransferase subunit 1 OS=Homo sapiens OX=9606 GN=RPN1	FALSE	4	2	2	2	607	68.5	6.38	4.74
High	P49368	T-complex protein 1 subunit gamma OS=Homo sapiens OX=9606 GN=CCT3 PE=1 SV=4	FALSE	4	2	2	2	545	60.5	6.49	2.29
High	Q92841	Probable ATP-dependent RNA helicase DDX17 OS=Homo sapiens OX=9606 GN=DDX17 PE=1 SV=2	FALSE	3	2	2	2	729	80.2	8.27	1.81
High	Q12774	Rho guanine nucleotide exchange factor 5 OS=Homo sapiens OX=9606 GN=ARHGEF5 PE=1 SV=3	FALSE	2	2	2	2	1597	176.7	5.53	0
High	P40227	T-complex protein 1 subunit zeta OS=Homo sapiens OX=9606 GN=CCT6A PE=1 SV=3	FALSE	6	2	2	2	531	58	6.68	0
High	P62910	60S ribosomal protein L32 OS=Homo sapiens OX=9606 GN=RPL32 PE=1 SV=2	FALSE	10	1	2	1	135	15.9	11.33	4.1
High	P25398	40S ribosomal protein S12 OS=Homo sapiens OX=9606 GN=RP512 PE=1 SV=3	FALSE	18	2	2	2	132	14.5	7.21	5.28
High	O95232	Luc7-like protein 3 OS=Homo sapiens OX=9606 GN=LUC7L3 PE=1 SV=2	FALSE	6	2	2	2	432	51.4	9.79	3.42
High	Q9H814	Phosphorylated adapter RNA export protein OS=Homo sapiens OX=9606 GN=PHAX PE=1 SV=1	FALSE	6	2	2	2	394	44.4	5.4	0
High	Q9Y3U8	60S ribosomal protein L36 OS=Homo sapiens OX=9606 GN=RPL36 PE=1 SV=3	FALSE	18	2	2	2	105	12.2	11.59	1.74
High	P18621	60S ribosomal protein L17 OS=Homo sapiens OX=9606 GN=RPL17 PE=1 SV=3	FALSE	8	1	2	1	184	21.4	10.17	4.81
High	P01861	Immunoglobulin heavy constant gamma 4 OS=Homo sapiens OX=9606 GN=IGHG4 PE=1 SV=1	FALSE	10	2	2	2	327	35.9	7.36	1.64
High	O95573	Long-chain-fatty-acid--CoA ligase 3 OS=Homo sapiens OX=9606 GN=ACSL3 PE=1 SV=3	FALSE	4	2	2	2	720	80.4	8.38	1.97
High	P07477	Trypsin-1 OS=Homo sapiens OX=9606 GN=PRSS1 PE=1 SV=1	TRUE	12	2	2	2	247	26.5	6.51	5.06
High	O43809	Cleavage and polyadenylation specificity factor subunit 5 OS=Homo sapiens OX=9606 GN=NUDT21 PE=1 SV=1	FALSE	9	2	2	2	227	26.2	8.82	1.94
High	O14979	Heterogeneous nuclear ribonucleoprotein D-like OS=Homo sapiens OX=9606 GN=HNRNPDL PE=1 SV=3	FALSE	4	2	2	2	420	46.4	9.57	4.09
High	P23528	Cofilin-1 OS=Homo sapiens OX=9606 GN=CFL1 PE=1 SV=3	FALSE	25	2	2	2	166	18.5	8.09	2.49
High	Q9H9E3	Conserved oligomeric Golgi complex subunit 4 OS=Homo sapiens OX=9606 GN=COG4 PE=1 SV=3	FALSE	3	2	2	2	785	89	5.19	3.73
High	Q13200	26S proteasome non-ATPase regulatory subunit 2 OS=Homo sapiens OX=9606 GN=PSMD2 PE=1 SV=3	FALSE	4	2	2	2	908	100.1	5.2	5.14
High	O60884	DnaJ homolog subfamily A member 2 OS=Homo sapiens OX=9606 GN=DNAJA2 PE=1 SV=1	FALSE	8	2	2	2	412	45.7	6.48	2.38
High	P62249	40S ribosomal protein S16 OS=Homo sapiens OX=9606 GN=RP516 PE=1 SV=2	FALSE	12	2	2	2	146	16.4	10.21	3.75
High	P32119	Peroxisomal protein 2 OS=Homo sapiens OX=9606 GN=PRDX2 PE=1 SV=5	FALSE	10	2	2	1	198	21.9	5.97	4.09
High	P42677	40S ribosomal protein S27 OS=Homo sapiens OX=9606 GN=RP527 PE=1 SV=3	FALSE	29	2	2	2	84	9.5	9.45	4.3
High	P06748	Nucleophosmin OS=Homo sapiens OX=9606 GN=NPM1 PE=1 SV=2	FALSE	9	2	2	2	294	32.6	4.78	0
High	O95373	Importin-7 OS=Homo sapiens OX=9606 GN=IPO7 PE=1 SV=1	FALSE	3	2	2	2	1038	119.4	4.82	0
High	P10644	cAMP-dependent protein kinase type I-alpha regulatory subunit OS=Homo sapiens OX=9606 GN=PRKAR1A PE=1	FALSE	8	2	2	2	381	43	5.35	2.54
High	Q9GZR7	ATP-dependent RNA helicase DDX24 OS=Homo sapiens OX=9606 GN=DDX24 PE=1 SV=1	FALSE	3	2	2	2	859	96.3	9.06	2.1
High	Q9UJZ1	Stomatin-like protein 2, mitochondrial OS=Homo sapiens OX=9606 GN=STOML2 PE=1 SV=1	FALSE	9	2	2	2	356	38.5	7.39	5.24
High	P61313	60S ribosomal protein L15 OS=Homo sapiens OX=9606 GN=RPL15 PE=1 SV=2	FALSE	15	2	2	2	204	24.1	11.62	0
High	P43686	26S proteasome regulatory subunit 6B OS=Homo sapiens OX=9606 GN=PSMC4 PE=1 SV=2	FALSE	7	2	2	2	418	47.3	5.21	0
High	P0DOX7	Immunoglobulin kappa light chain OS=Homo sapiens OX=9606 PE=1 SV=1	FALSE	9	1	2	1	214	23.4	7.17	6.05
High	P08670	Vimentin OS=Homo sapiens OX=9606 GN=VIM PE=1 SV=4	FALSE	4	2	2	2	466	53.6	5.12	3.89
High	O14545	TRAF-type zinc finger domain-containing protein 1 OS=Homo sapiens OX=9606 GN=TRAFD1 PE=1 SV=1	FALSE	4	2	2	2	582	64.8	5.29	1.65
High	P31948	Stress-induced-phosphoprotein 1 OS=Homo sapiens OX=9606 GN=STIP1 PE=1 SV=1	FALSE	6	2	2	2	543	62.6	6.8	4.13
High	O15479	Melanoma-associated antigen B2 OS=Homo sapiens OX=9606 GN=MAGEB2 PE=1 SV=3	FALSE	7	2	2	2	319	35.3	8.76	3.29
High	P53985	Monocarboxylate transporter 1 OS=Homo sapiens OX=9606 GN=SLC16A1 PE=1 SV=3	FALSE	6	2	2	2	500	53.9	8.66	2.08
High	Q9Y4B5	Microtubule cross-linking factor 1 OS=Homo sapiens OX=9606 GN=MTCL1 PE=1 SV=5	FALSE	1	2	2	2	1905	209.4	6.43	2.65
High	P61981	14-3-3 protein gamma OS=Homo sapiens OX=9606 GN=YWHAG PE=1 SV=2	FALSE	7	2	2	1	247	28.3	4.89	1.96
High	Q01813	ATP-dependent 6-phosphofructokinase, platelet type OS=Homo sapiens OX=9606 GN=PFKP PE=1 SV=2	FALSE	3	2	2	2	784	85.5	7.55	3.78
High	Q12874	Splicing factor 3A subunit 3 OS=Homo sapiens OX=9606 GN=SF3A3 PE=1 SV=1	FALSE	7	2	2	2	501	58.8	5.38	2.12
High	Q51JC6	APC membrane recruitment protein 1 OS=Homo sapiens OX=9606 GN=AMER1 PE=1 SV=2	FALSE	3	2	2	2	1135	124	4.84	1.73
High	Q14204	Cytoplasmic dynein 1 heavy chain 1 OS=Homo sapiens OX=9606 GN=DYNC1H1 PE=1 SV=5	FALSE	1	2	2	2	4646	532.1	6.4	0
Medium	Q96D15	Reticulocalbin-3 OS=Homo sapiens OX=9606 GN=RCN3 PE=1 SV=1	FALSE	2	1	1	1	328	37.5	4.89	1.68
High	P04004	Vitronectin OS=Homo sapiens OX=9606 GN=VTN PE=1 SV=1	FALSE	3	1	1	1	478	54.3	5.08	0
High	Q92598	Heat shock protein 105 kDa OS=Homo sapiens OX=9606 GN=HSPH1 PE=1 SV=1	FALSE	2	1	1	1	858	96.8	5.39	0
High	Q5VTL8	Pre-mRNA-splicing factor 38B OS=Homo sapiens OX=9606 GN=PRPF38B PE=1 SV=1	FALSE	1	1	1	1	546	64.4	10.54	0
High	O75096	Low-density lipoprotein receptor-related protein 4 OS=Homo sapiens OX=9606 GN=LRP4 PE=1 SV=4	FALSE	1	1	1	1	1905	211.9	5.27	0
High	O43719	HIV Tat-specific factor 1 OS=Homo sapiens OX=9606 GN=HTATSF1 PE=1 SV=1	FALSE	2	1	1	1	755	85.8	4.4	0
High	Q9UBM7	7-dehydrocholesterol reductase OS=Homo sapiens OX=9606 GN=DHCR7 PE=1 SV=1	FALSE	3	1	1	1	475	54.5	8.7	2.17



High	Q15758	Neutral amino acid transporter B(0) OS=Homo sapiens OX=9606 GN=SLC1A5 PE=1 SV=2	FALSE	2	1	1	1	541	56.6	5.48	0
High	P23284	Peptidyl-prolyl cis-trans isomerase B OS=Homo sapiens OX=9606 GN=PPIB PE=1 SV=2	FALSE	6	1	1	1	216	23.7	9.41	2.19
High	Q96EY1	DnaJ homolog subfamily A member 3, mitochondrial OS=Homo sapiens OX=9606 GN=DNAJA3 PE=1 SV=2	FALSE	3	1	1	1	480	52.5	9.26	0
Medium	P62906	60S ribosomal protein L10a OS=Homo sapiens OX=9606 GN=RPL10A PE=1 SV=2	FALSE	4	1	1	1	217	24.8	9.94	0
High	Q15654	Thyroid receptor-interacting protein 6 OS=Homo sapiens OX=9606 GN=TRIP6 PE=1 SV=3	FALSE	4	1	1	1	476	50.3	7.37	2.41
High	Q965T3	Paired amphipathic helix protein Sin3a OS=Homo sapiens OX=9606 GN=SIN3A PE=1 SV=2	FALSE	1	1	1	1	1273	145.1	7.25	0
High	Q15393	Splicing factor 3B subunit 3 OS=Homo sapiens OX=9606 GN=SF3B3 PE=1 SV=4	FALSE	1	1	1	1	1217	135.5	5.26	0
High	O75607	Nucleoplasmin-3 OS=Homo sapiens OX=9606 GN=NPM3 PE=1 SV=3	FALSE	10	1	1	1	178	19.3	4.63	2.18
High	Q5T457	E3 ubiquitin-protein ligase UBR4 OS=Homo sapiens OX=9606 GN=UBR4 PE=1 SV=1	FALSE	0	1	1	1	5183	573.5	6.04	0
Medium	P01241	Somatotropin OS=Homo sapiens OX=9606 GN=GH1 PE=1 SV=2	FALSE	5	1	1	1	217	24.8	5.43	1.77
High	P14649	Myosin light chain 6B OS=Homo sapiens OX=9606 GN=MYL6B PE=1 SV=1	FALSE	6	1	1	1	208	22.8	5.73	2.11
High	P06753	Tropomyosin alpha-3 chain OS=Homo sapiens OX=9606 GN=TPM3 PE=1 SV=2	FALSE	5	1	1	1	285	32.9	4.72	2.21
Medium	P30050	60S ribosomal protein L12 OS=Homo sapiens OX=9606 GN=RPL12 PE=1 SV=1	FALSE	9	1	1	1	165	17.8	9.42	0
Medium	Q96MA6	Adenylate kinase 8 OS=Homo sapiens OX=9606 GN=AK8 PE=1 SV=1	FALSE	3	1	1	1	479	54.9	6.15	2
High	P08621	U1 small nuclear ribonucleoprotein 70 kDa OS=Homo sapiens OX=9606 GN=SNRNP70 PE=1 SV=2	FALSE	3	1	1	1	437	51.5	9.94	2.45
High	Q9BWJ5	Splicing factor 3B subunit 5 OS=Homo sapiens OX=9606 GN=SF3B5 PE=1 SV=1	FALSE	17	1	1	1	86	10.1	6.35	0
High	P05387	60S acidic ribosomal protein P2 OS=Homo sapiens OX=9606 GN=RPLP2 PE=1 SV=1	FALSE	15	1	1	1	115	11.7	4.54	2.64
High	P0DOX8	Immunoglobulin lambda-1 light chain OS=Homo sapiens OX=9606 PE=1 SV=1	FALSE	7	1	1	1	216	22.8	6.76	1.75
Medium	Q9ULM3	YEATS domain-containing protein 2 OS=Homo sapiens OX=9606 GN=YEATS2 PE=1 SV=2	FALSE	1	1	1	1	1422	150.7	8.98	0
High	P62633	Cellular nucleic acid-binding protein OS=Homo sapiens OX=9606 GN=CNBP PE=1 SV=1	FALSE	7	1	1	1	177	19.5	7.71	2.32
High	P62857	40S ribosomal protein S28 OS=Homo sapiens OX=9606 GN=RPS28 PE=1 SV=1	FALSE	17	1	1	1	69	7.8	10.7	2.08
High	O95429	BAG family molecular chaperone regulator 4 OS=Homo sapiens OX=9606 GN=BAG4 PE=1 SV=1	FALSE	3	1	1	1	457	49.6	5.12	1.82
High	P46776	60S ribosomal protein L27a OS=Homo sapiens OX=9606 GN=RPL27A PE=1 SV=2	FALSE	7	1	1	1	148	16.6	11	2.08
High	Q86SQ0	Pleckstrin homology-like domain family B member 2 OS=Homo sapiens OX=9606 GN=PHLDB2 PE=1 SV=2	FALSE	1	1	1	1	1253	142.1	7.43	2.36
High	P47914	60S ribosomal protein L29 OS=Homo sapiens OX=9606 GN=RPL29 PE=1 SV=2	FALSE	9	1	1	1	159	17.7	11.66	2.66
High	Q9BRK5	45 kDa calcium-binding protein OS=Homo sapiens OX=9606 GN=SDP4 PE=1 SV=1	FALSE	4	1	1	1	362	41.8	4.86	0
High	O00767	Acyl-CoA desaturase OS=Homo sapiens OX=9606 GN=SCD PE=1 SV=2	FALSE	4	1	1	1	359	41.5	9	2.24
High	P63244	Receptor of activated protein C kinase 1 OS=Homo sapiens OX=9606 GN=RACK1 PE=1 SV=3	FALSE	3	1	1	1	317	35.1	7.69	1.94
High	P12270	Nucleoprotein TPR OS=Homo sapiens OX=9606 GN=TPR PE=1 SV=3	FALSE	0	1	1	1	2363	267.1	5.02	1.75
High	P12268	Inosine-5'-monophosphate dehydrogenase 2 OS=Homo sapiens OX=9606 GN=IMPDH2 PE=1 SV=2	FALSE	2	1	1	1	514	55.8	6.9	1.84
Medium	Q6UXR4	Putative serpin A13 OS=Homo sapiens OX=9606 GN=SERPINA13 PE=5 SV=1	FALSE	6	1	1	1	307	34.8	6.4	2.46
High	P50991	T-complex protein 1 subunit delta OS=Homo sapiens OX=9606 GN=CCT4 PE=1 SV=4	FALSE	3	1	1	1	539	57.9	7.83	0
High	Q14974	Importin subunit beta-1 OS=Homo sapiens OX=9606 GN=KPNB1 PE=1 SV=2	FALSE	2	1	1	1	876	97.1	4.78	0
High	Q15287	RNA-binding protein with serine-rich domain 1 OS=Homo sapiens OX=9606 GN=RNPS1 PE=1 SV=1	FALSE	5	1	1	1	305	34.2	11.84	2.17
High	P62826	GTP-binding nuclear protein Ran OS=Homo sapiens OX=9606 GN=RAN PE=1 SV=3	FALSE	5	1	1	1	216	24.4	7.49	1.97
High	Q9BQ70	Transcription factor 25 OS=Homo sapiens OX=9606 GN=TCF25 PE=1 SV=1	FALSE	3	1	1	1	676	76.6	6.35	2.21
High	Q9Y3B4	Splicing factor 3B subunit 6 OS=Homo sapiens OX=9606 GN=SF3B6 PE=1 SV=1	FALSE	11	1	1	1	125	14.6	9.38	0
High	Q8WTW3	Conserved oligomeric Golgi complex subunit 1 OS=Homo sapiens OX=9606 GN=COG1 PE=1 SV=1	FALSE	1	1	1	1	980	108.9	7.31	0
High	Q14244	Enscosin OS=Homo sapiens OX=9606 GN=MAP7 PE=1 SV=1	FALSE	2	1	1	1	749	84	9.61	0
High	Q08211	ATP-dependent RNA helicase A OS=Homo sapiens OX=9606 GN=DHX9 PE=1 SV=4	FALSE	1	1	1	1	1270	140.9	6.84	0
High	P63167	Dynein light chain 1, cytoplasmic OS=Homo sapiens OX=9606 GN=DYNLL1 PE=1 SV=1	FALSE	12	1	1	1	89	10.4	7.4	0
High	P52907	F-actin-capping protein subunit alpha-1 OS=Homo sapiens OX=9606 GN=CAPZA1 PE=1 SV=3	FALSE	5	1	1	1	286	32.9	5.69	2.35
Medium	Q7Z333	Probable helicase senataxin OS=Homo sapiens OX=9606 GN=SETX PE=1 SV=4	FALSE	1	1	1	1	2677	302.7	7.17	0
High	P06312	Immunoglobulin kappa variable 4-1 OS=Homo sapiens OX=9606 GN=IGKV4-1 PE=1 SV=1	FALSE	7	1	1	1	121	13.4	5.25	2.08
High	P02786	Transferrin receptor protein 1 OS=Homo sapiens OX=9606 GN=TFRC PE=1 SV=2	FALSE	2	1	1	1	760	84.8	6.61	0
High	P08708	40S ribosomal protein S17 OS=Homo sapiens OX=9606 GN=RPS17 PE=1 SV=2	FALSE	16	1	1	1	135	15.5	9.85	2.82
High	P51991	Heterogeneous nuclear ribonucleoprotein A3 OS=Homo sapiens OX=9606 GN=HNRNPA3 PE=1 SV=2	FALSE	4	1	1	1	378	39.6	9.01	2.62
High	A6NCI4	von Willebrand factor A domain-containing protein 3A OS=Homo sapiens OX=9606 GN=VWA3A PE=2 SV=3	FALSE	1	1	1	1	1184	133.9	8.46	0
High	Q7RTV0	PHD finger-like domain-containing protein 5A OS=Homo sapiens OX=9606 GN=PHF5A PE=1 SV=1	FALSE	12	1	1	1	110	12.4	8.41	2.58
High	P13639	Elongation factor 2 OS=Homo sapiens OX=9606 GN=EEF2 PE=1 SV=4	FALSE	1	1	1	1	858	95.3	6.83	2.31
High	P42766	60S ribosomal protein L35 OS=Homo sapiens OX=9606 GN=RPL35 PE=1 SV=2	FALSE	11	1	1	1	123	14.5	11.05	0
High	Q6ZW76	Ankyrin repeat and SAM domain-containing protein 3 OS=Homo sapiens OX=9606 GN=ANKS3 PE=1 SV=1	FALSE	2	1	1	1	656	72	5.45	2.57
High	P17028	Zinc finger protein 24 OS=Homo sapiens OX=9606 GN=ZNF24 PE=1 SV=4	FALSE	3	1	1	1	368	42.1	6.21	0
Medium	Q15436	Protein transport protein Sec23A OS=Homo sapiens OX=9606 GN=SEC23A PE=1 SV=2	FALSE	2	1	1	1	765	86.1	7.08	0
High	Q96A08	Histone H2B type 1-A OS=Homo sapiens OX=9606 GN=H2BC1 PE=1 SV=3	FALSE	7	1	1	1	127	14.2	10.32	0
High	P35080	Profilin-2 OS=Homo sapiens OX=9606 GN=PFN2 PE=1 SV=3	FALSE	10	1	1	1	140	15	6.99	0
High	Q8NB59	Thioredoxin domain-containing protein 5 OS=Homo sapiens OX=9606 GN=TXNDC5 PE=1 SV=2	FALSE	4	1	1	1	432	47.6	5.97	0
High	P62266	40S ribosomal protein S23 OS=Homo sapiens OX=9606 GN=RPS23 PE=1 SV=3	FALSE	8	1	1	1	143	15.8	10.49	2.81

High	Q9Y265	RuvB-like 1 OS=Homo sapiens OX=9606 GN=RUVBL1 PE=1 SV=1	FALSE	3	1	1	1	456	50.2	6.42	0
Medium	Q6UN15	Pre-mRNA 3'-end-processing factor FIP1 OS=Homo sapiens OX=9606 GN=FIP1L1 PE=1 SV=1	FALSE	2	1	1	1	594	66.5	5.59	0
High	Q8NC51	Plasminogen activator inhibitor 1 RNA-binding protein OS=Homo sapiens OX=9606 GN=SERBP1 PE=1 SV=2	FALSE	4	1	1	1	408	44.9	8.65	0
High	P56134	ATP synthase subunit f, mitochondrial OS=Homo sapiens OX=9606 GN=ATP5MF PE=1 SV=3	FALSE	14	1	1	1	94	10.9	9.67	0
High	P25686	DnaJ homolog subfamily B member 2 OS=Homo sapiens OX=9606 GN=DNAJB2 PE=1 SV=3	FALSE	4	1	1	1	324	35.6	5.95	1.82
High	P04844	Dolichyl-diphosphooligosaccharide--protein glycosyltransferase subunit 2 OS=Homo sapiens OX=9606 GN=RPN2	FALSE	2	1	1	1	631	69.2	5.69	1.61
High	O75190	DnaJ homolog subfamily B member 6 OS=Homo sapiens OX=9606 GN=DNAJB6 PE=1 SV=2	FALSE	4	1	1	1	326	36.1	9.16	0
High	P51153	Ras-related protein Rab-13 OS=Homo sapiens OX=9606 GN=RAB13 PE=1 SV=1	FALSE	5	1	1	1	203	22.8	9.19	0
Medium	P62805	Histone H4 OS=Homo sapiens OX=9606 GN=H4C1 PE=1 SV=2	FALSE	8	1	1	1	103	11.4	11.36	0
Medium	P14678	Small nuclear ribonucleoprotein-associated proteins B and B' OS=Homo sapiens OX=9606 GN=SNRBP PE=1 SV=2	FALSE	3	1	1	1	240	24.6	11.19	0
High	P84098	60S ribosomal protein L19 OS=Homo sapiens OX=9606 GN=RPL19 PE=1 SV=1	FALSE	9	1	1	1	196	23.5	11.47	0
High	Q66PJ3	ADP-ribosylation factor-like protein 6-interacting protein 4 OS=Homo sapiens OX=9606 GN=ARL6IP4 PE=1 SV=2	FALSE	4	1	1	1	421	44.9	10.93	2.51
Medium	O60825	6-phosphofructo-2-kinase/fructose-2,6-bisphosphatase 2 OS=Homo sapiens OX=9606 GN=PFKFB2 PE=1 SV=2	FALSE	2	1	1	1	505	58.4	8.38	0
High	Q15365	Poly(rC)-binding protein 1 OS=Homo sapiens OX=9606 GN=PCBP1 PE=1 SV=2	FALSE	4	1	1	1	356	37.5	7.09	1.74
High	P62899	60S ribosomal protein L31 OS=Homo sapiens OX=9606 GN=RPL31 PE=1 SV=1	FALSE	7	1	1	1	125	14.5	10.54	2.3
High	P49023	Paxillin OS=Homo sapiens OX=9606 GN=PXN PE=1 SV=3	FALSE	3	1	1	1	591	64.5	6.19	2.06
High	P62861	40S ribosomal protein S30 OS=Homo sapiens OX=9606 GN=FAU PE=1 SV=1	FALSE	17	1	1	1	59	6.6	12.15	2.28
High	O00165	HCLS1-associated protein X-1 OS=Homo sapiens OX=9606 GN=HAX1 PE=1 SV=2	FALSE	4	1	1	1	279	31.6	4.92	2.29
High	Q7L412	Arginine/serine-rich coiled-coil protein 2 OS=Homo sapiens OX=9606 GN=RSRC2 PE=1 SV=1	FALSE	4	1	1	1	434	50.5	11.33	0
High	P40429	60S ribosomal protein L13a OS=Homo sapiens OX=9606 GN=RPL13A PE=1 SV=2	FALSE	6	1	1	1	203	23.6	10.93	2.71
High	P07195	L-lactate dehydrogenase B chain OS=Homo sapiens OX=9606 GN=LDHB PE=1 SV=2	FALSE	4	1	1	1	334	36.6	6.05	1.93
High	Q9BRL6	Serine/arginine-rich splicing factor 8 OS=Homo sapiens OX=9606 GN=SRSF8 PE=1 SV=1	FALSE	3	1	1	1	282	32.3	11.72	2.1
Medium	P07919	Cytochrome b-c1 complex subunit 6, mitochondrial OS=Homo sapiens OX=9606 GN=UQCRRH PE=1 SV=2	FALSE	10	1	1	1	91	10.7	4.44	0
High	P53999	Activated RNA polymerase II transcriptional coactivator p15 OS=Homo sapiens OX=9606 GN=SUB1 PE=1 SV=3	FALSE	9	1	1	1	127	14.4	9.6	1.89
High	Q8WWC4	m-AAA protease-interacting protein 1, mitochondrial OS=Homo sapiens OX=9606 GN=MAIP1 PE=1 SV=1	FALSE	3	1	1	1	291	32.5	9.17	0
Medium	P56270	Myc-associated zinc finger protein OS=Homo sapiens OX=9606 GN=MAZ PE=1 SV=1	FALSE	3	1	1	1	477	48.6	8.95	0
High	P35232	Prohibitin OS=Homo sapiens OX=9606 GN=PHB PE=1 SV=1	FALSE	7	1	1	1	272	29.8	5.76	0
High	Q13409	Cytoplasmic dynein 1 intermediate chain 2 OS=Homo sapiens OX=9606 GN=DYNC1I2 PE=1 SV=3	FALSE	3	1	1	1	638	71.4	5.2	2.45
High	Q14746	Conserved oligomeric Golgi complex subunit 2 OS=Homo sapiens OX=9606 GN=COG2 PE=1 SV=1	FALSE	3	1	1	1	738	83.2	6.62	1.79
High	P43307	Translocon-associated protein subunit alpha OS=Homo sapiens OX=9606 GN=SSR1 PE=1 SV=3	FALSE	5	1	1	1	286	32.2	4.49	3.12
High	P62280	40S ribosomal protein S11 OS=Homo sapiens OX=9606 GN=RPS11 PE=1 SV=3	FALSE	11	1	1	1	158	18.4	10.3	3.61
High	P07355	Annexin A2 OS=Homo sapiens OX=9606 GN=ANXA2 PE=1 SV=2	FALSE	4	1	1	1	339	38.6	7.75	1.96
Medium	Q99728	BRCA1-associated RING domain protein 1 OS=Homo sapiens OX=9606 GN=BARD1 PE=1 SV=2	FALSE	2	1	1	1	777	86.6	8.72	0
High	O95831	Apoptosis-inducing factor 1, mitochondrial OS=Homo sapiens OX=9606 GN=AIFM1 PE=1 SV=1	FALSE	2	1	1	1	613	66.9	8.95	2.04
High	P28066	Proteasome subunit alpha type-5 OS=Homo sapiens OX=9606 GN=PSMA5 PE=1 SV=3	FALSE	8	1	1	1	241	26.4	4.79	2.73
High	P27635	60S ribosomal protein L10 OS=Homo sapiens OX=9606 GN=RPL10 PE=1 SV=4	FALSE	6	1	1	1	214	24.6	10.08	2.16
High	P62314	Small nuclear ribonucleoprotein Sm D1 OS=Homo sapiens OX=9606 GN=SNRPD1 PE=1 SV=1	FALSE	11	1	1	1	119	13.3	11.56	3.87
High	Q9UJY1	Heat shock protein beta-8 OS=Homo sapiens OX=9606 GN=HSPB8 PE=1 SV=1	FALSE	6	1	1	1	196	21.6	5.12	0
High	P36542	ATP synthase subunit gamma, mitochondrial OS=Homo sapiens OX=9606 GN=ATP5F1C PE=1 SV=1	FALSE	3	1	1	1	298	33	9.22	1.61
High	P62854	40S ribosomal protein S26 OS=Homo sapiens OX=9606 GN=RPS26 PE=1 SV=3	FALSE	13	1	1	1	115	13	11	2.18
High	P57088	Transmembrane protein 33 OS=Homo sapiens OX=9606 GN=TMEM33 PE=1 SV=2	FALSE	5	1	1	1	247	28	9.7	2.1
Medium	O43390	Heterogeneous nuclear ribonucleoprotein R OS=Homo sapiens OX=9606 GN=HNRNP R PE=1 SV=1	FALSE	2	1	1	1	633	70.9	8.13	0
Medium	Q6ZV73	FYVE, RhoGEF and PH domain-containing protein 6 OS=Homo sapiens OX=9606 GN=FGD6 PE=1 SV=2	FALSE	1	1	1	1	1430	160.7	7.03	0
High	Q9NX63	MICOS complex subunit MIC19 OS=Homo sapiens OX=9606 GN=CHCHD3 PE=1 SV=1	FALSE	5	1	1	1	227	26.1	8.28	2.52
Medium	O43175	D-3-phosphoglycerate dehydrogenase OS=Homo sapiens OX=9606 GN=PHGDH PE=1 SV=4	FALSE	2	1	1	1	533	56.6	6.71	0
High	Q15427	Splicing factor 3B subunit 4 OS=Homo sapiens OX=9606 GN=SF3B4 PE=1 SV=1	FALSE	3	1	1	1	424	44.4	8.56	2.69
High	Q06210	Glutamine--fructose-6-phosphate aminotransferase [isomerizing] 1 OS=Homo sapiens OX=9606 GN=GFPT1 PE=1 SV=1	FALSE	2	1	1	1	699	78.8	7.11	3.13
High	P46782	40S ribosomal protein S5 OS=Homo sapiens OX=9606 GN=RPS5 PE=1 SV=4	FALSE	7	1	1	1	204	22.9	9.72	2.08
High	Q9P209	Centrosomal protein of 72 kDa OS=Homo sapiens OX=9606 GN=CEP72 PE=1 SV=2	FALSE	2	1	1	1	647	71.7	6.52	0
High	Q9Y3F4	Serine-threonine kinase receptor-associated protein OS=Homo sapiens OX=9606 GN=STRAP PE=1 SV=1	FALSE	3	1	1	1	350	38.4	5.12	0
High	Q15773	Myeloid leukemia factor 2 OS=Homo sapiens OX=9606 GN=MLF2 PE=1 SV=1	FALSE	5	1	1	1	248	28.1	6.9	0
High	Q16629	Serine/arginine-rich splicing factor 7 OS=Homo sapiens OX=9606 GN=SRSF7 PE=1 SV=1	FALSE	6	1	1	1	238	27.4	11.82	1.7
High	P81605	Dermcidin OS=Homo sapiens OX=9606 GN=DCD PE=1 SV=2	FALSE	10	1	1	1	110	11.3	6.54	2.25
High	P62306	Small nuclear ribonucleoprotein F OS=Homo sapiens OX=9606 GN=SNRPF PE=1 SV=1	FALSE	15	1	1	1	86	9.7	4.67	2.55
Medium	Q9H6T0	Epithelial splicing regulatory protein 2 OS=Homo sapiens OX=9606 GN=ESRP2 PE=1 SV=1	FALSE	1	1	1	1	727	78.4	6.71	0
High	Q9UPP1	Histone lysine demethylase PHF8 OS=Homo sapiens OX=9606 GN=PHF8 PE=1 SV=3	FALSE	1	1	1	1	1060	117.8	8.72	0
Medium	Q9NX00	Transmembrane protein 160 OS=Homo sapiens OX=9606 GN=TMEM160 PE=1 SV=1	FALSE	4	1	1	1	188	19.6	8.03	0
High	P23246	Splicing factor, proline- and glutamine-rich OS=Homo sapiens OX=9606 GN=SFPQ PE=1 SV=2	FALSE	2	1	1	1	707	76.1	9.44	0




High	P63208	S-phase kinase-associated protein 1 OS=Homo sapiens OX=9606 GN=SKP1 PE=1 SV=2	FALSE	7	1	1	1	163	18.6	4.54	2.6
High	Q01970	1-phosphatidylinositol 4,5-bisphosphate phosphodiesterase beta-3 OS=Homo sapiens OX=9606 GN=PLCB3 PE=1	FALSE	2	1	1	1	1234	138.7	5.9	3.06
High	O95218	Zinc finger Ran-binding domain-containing protein 2 OS=Homo sapiens OX=9606 GN=ZRANB2 PE=1 SV=2	FALSE	6	1	1	1	330	37.4	10.01	0
Medium	P50591	Tumor necrosis factor ligand superfamily member 10 OS=Homo sapiens OX=9606 GN=TNFSF10 PE=1 SV=1	FALSE	5	1	1	1	281	32.5	7.42	0
High	P10124	Serglycin OS=Homo sapiens OX=9606 GN=SRGN PE=1 SV=3	FALSE	8	1	1	1	158	17.6	4.96	2.11
High	P62699	Protein yippee-like 5 OS=Homo sapiens OX=9606 GN=YPEL5 PE=1 SV=1	FALSE	10	1	1	1	121	13.8	7.31	2.8
High	P20648	Potassium-transporting ATPase alpha chain 1 OS=Homo sapiens OX=9606 GN=ATP4A PE=2 SV=5	FALSE	1	1	1	1	1035	114	5.81	2.17
Medium	Q9H7L9	Sin3 histone deacetylase corepressor complex component SDS3 OS=Homo sapiens OX=9606 GN=SUDS3 PE=1 SV=1	FALSE	4	1	1	1	328	38.1	5.66	0
High	P62937	Peptidyl-prolyl cis-trans isomerase A OS=Homo sapiens OX=9606 GN=PPIA PE=1 SV=2	TRUE	5	1	1	1	165	18	7.81	0
High	Q9UG63	ATP-binding cassette sub-family F member 2 OS=Homo sapiens OX=9606 GN=ABCF2 PE=1 SV=2	FALSE	1	1	1	1	623	71.2	7.37	1.64
High	Q12816	Trophinin OS=Homo sapiens OX=9606 GN=TRO PE=1 SV=3	FALSE	1	1	1	1	1431	143.6	9.03	0
High	Q15370	Elongin-B OS=Homo sapiens OX=9606 GN=ELOB PE=1 SV=1	FALSE	8	1	1	1	118	13.1	4.88	1.63
High	P25205	DNA replication licensing factor MCM3 OS=Homo sapiens OX=9606 GN=MCM3 PE=1 SV=3	FALSE	2	1	1	1	808	90.9	5.77	1.93
High	P0DP25	Calmodulin-3 OS=Homo sapiens OX=9606 GN=CALM3 PE=1 SV=1	FALSE	15	1	1	1	149	16.8	4.22	0
Medium	Q9BUN8	Derlin-1 OS=Homo sapiens OX=9606 GN=DERL1 PE=1 SV=1	FALSE	4	1	1	1	251	28.8	9.51	0
High	P00403	Cytochrome c oxidase subunit 2 OS=Homo sapiens OX=9606 GN=MT-CO2 PE=1 SV=1	FALSE	4	1	1	1	227	25.5	4.82	1.61
High	P62263	40S ribosomal protein S14 OS=Homo sapiens OX=9606 GN=RPS14 PE=1 SV=3	FALSE	9	1	1	1	151	16.3	10.05	1.76
High	P27824	Calnexin OS=Homo sapiens OX=9606 GN=CANX PE=1 SV=2	FALSE	3	1	1	1	592	67.5	4.6	2.01
High	Q8WZ19	BTB/POZ domain-containing adapter for CUL3-mediated RhoA degradation protein 1 OS=Homo sapiens OX=9606 GN=BTBD9 PE=1 SV=1	FALSE	2	1	1	1	329	36.3	7.23	0

# ORIGINAL PUBLICATION



## Article

# The Promotion of Genomic Instability in Human Fibroblasts by Adenovirus 12 Early Region 1B 55K Protein in the Absence of Viral Infection

Tareq Abualfaraj, Nafiseh Chalabi Hagkarim, Robert Hollingworth, Laura Grange , Satpal Jhuji ,  
Grant S. Stewart  and Roger J. Grand \*

Institute for Cancer and Genomic Sciences, The Medical School, University of Birmingham, Birmingham B15 2TT, UK; TMA845@student.bham.ac.uk (T.A.); N.ChalabiHagkarim@bham.ac.uk (N.C.H.); r.hollingworth@bham.ac.uk (R.H.); LXG852@student.bham.ac.uk (L.G.); s.s.jhuji@bham.ac.uk (S.J.); g.s.stewart@bham.ac.uk (G.S.S.)

\* Correspondence: r.j.a.grand@bham.ac.uk

**Abstract:** The adenovirus 12 early region 1B55K (Ad12E1B55K) protein has long been known to cause non-random damage to chromosomes 1 and 17 in human cells. These sites, referred to as Ad12 modification sites, have marked similarities to classic fragile sites. In the present report we have investigated the effects of Ad12E1B55K on the cellular DNA damage response and on DNA replication, considering our increased understanding of the pathways involved. We have compared human skin fibroblasts expressing Ad12E1B55K (55K<sup>+</sup>HSF), but no other viral proteins, with the parental cells. Appreciable chromosomal damage was observed in 55K<sup>+</sup>HSFs compared to parental cells. Similarly, an increased number of micronuclei was observed in 55K<sup>+</sup>HSFs, both in cycling cells and after DNA damage. We compared DNA replication in the two cell populations; 55K<sup>+</sup>HSFs showed increased fork stalling and a decrease in fork speed. When replication stress was introduced with hydroxyurea the percentage of stalled forks and replication speeds were broadly similar, but efficiency of fork restart was significantly reduced in 55K<sup>+</sup>HSFs. After DNA damage, appreciably more foci were formed in 55K<sup>+</sup>HSFs up to 48 h post treatment. In addition, phosphorylation of ATM substrates was greater in Ad12E1B55K-expressing cells following DNA damage. Following DNA damage, 55K<sup>+</sup>HSFs showed an inability to arrest in cell cycle, probably due to the association of Ad12E1B55K with p53. To confirm that Ad12E1B55K was targeting components of the double-strand break repair pathways, co-immunoprecipitation experiments were performed which showed an association of the viral protein with ATM, MRE11, NBS1, DNA-PK, BLM, TOPBP1 and p53, as well as with components of the replisome, MCM3, MCM7, ORC1, DNA polymerase  $\delta$ , TICRR and cdc45, which may account for some of the observed effects on DNA replication. We conclude that Ad12E1B55K impacts the cellular DNA damage response pathways and the replisome at multiple points through protein–protein interactions, causing genomic instability.

**Keywords:** adenovirus 12; E1B55K; DNA damage; DNA replication; DNA replication stress; DNA repair; DNA damage response



**Citation:** Abualfaraj, T.; Hagkarim, N.C.; Hollingworth, R.; Grange, L.; Jhuji, S.; Stewart, G.S.; Grand, R.J. The Promotion of Genomic Instability in Human Fibroblasts by Adenovirus 12 Early Region 1B 55K Protein in the Absence of Viral Infection. *Viruses* **2021**, *13*, 2444. <https://doi.org/10.3390/v13122444>

Academic Editor: Cary Moody

Received: 23 November 2021

Accepted: 30 November 2021

Published: 6 December 2021

**Publisher's Note:** MDPI stays neutral with regard to jurisdictional claims in published maps and institutional affiliations.



**Copyright:** © 2021 by the authors. Licensee MDPI, Basel, Switzerland. This article is an open access article distributed under the terms and conditions of the Creative Commons Attribution (CC BY) license (<https://creativecommons.org/licenses/by/4.0/>).

## 1. Introduction

Human adenoviruses comprise a large family of approximately 90 different types divided into seven species (A to G). Normally they cause relatively mild infections of the respiratory and gastrointestinal tracts and the eye, depending on species. However, in immunocompromised patients, adenoviruses constitute a serious health risk, often resulting in high mortality rates [1,2]. In early studies it was shown that viruses from species A, such as adenovirus 12 (Ad12), were able to induce tumors in new-born rodents although viruses from species C (such as the very commonly studied Ad2 and Ad5) could not [3–5]. Injection of Ad12E1-transformed rodent cells into the syngeneic host could also

produce tumors, whereas cells transformed with Ad5 or Ad2 DNA were only tumorigenic in athymic nude mice or immunosuppressed animals [6–9]. These observations allowed adenoviruses to be categorized as ‘DNA tumor viruses’. Consistent with this, Ad12 has also been shown to cause retinoblastoma-like tumors in baboons [10].

In slightly later studies it was shown that Ad12 could cause non-random damage to chromosomes 1 and 17 in human embryo kidney and human embryo lung cells [11–13]. These sites, referred to as Ad12 modification sites, have been mapped to chromosomes 17q21–22, 1p36, 1q21 and 1q42–43 and have marked similarities to classic fragile sites [11,13–17]. The four loci correspond to clusters of genes encoding small abundant structural RNAs. *RNU1* and *RNU2* loci contain tandemly repeated genes encoding U1 and U2 small nuclear RNAs (snRNAs), the *PSU1* locus is a cluster of degenerate U1 genes and the *RN5S* locus comprises tandemly repeated genes encoding 5S rRNA [16,18–20]. Adenovirus 5, on the other hand, appears to cause much more random breaks in human chromosomes [21,22]. Studies using Ad12 viruses with mutations in the E1 genes have demonstrated that expression of E1B55K is essential for chromosomal damage, whereas E1A and E1B19K had relatively little effect [23,24]. The random damage by Ad5, however, has been attributed to expression of E1A [21]. In view of these observations, we considered that further analysis of the ability of Ad12E1B55K to cause DNA damage and its effects on cellular DNA damage response (DDR) would be of considerable interest, particularly in view of our greatly enhanced understanding of DNA damage repair pathways since the original investigations were undertaken.

Expression of Ad12E1B55K is necessary for efficient viral replication, although this requirement appears to be less strict in the case of Ad5. Most functions of AdE1B55K, during viral infection, have previously been linked to its interaction with E4orf6 when it forms a ubiquitin E3 ligase in combination with cellular Cullins, Elongins and Ring box1, reviewed in [25–28]. The ubiquitylation of target E1B55K-binding proteins results in protein degradation in many but not all cases [25–29]. Thus, among the E1B55K-binding proteins already identified (reviewed in [27]), [29] a proportion are degraded while others remain intact [29].

Of the proteins degraded during Ad5 infection, an appreciable number of those studied in detail are involved in the DNA damage response (DDR), such as p53, MRE11, NBS1, BLM, DNA Ligase IV, TOPBP1, TIP60 and TAB182 [30–36]. Following adenovirus infection, there is an inactivation of the DDR which is recognized as a reduction in the activity of DDR kinases and, probably importantly from the virus’s point of view, a reduction in the ability of the cells to produce concatemers of viral genomes [32,37,38]. However, several reports have indicated that DDR proteins are localized to viral replication centers where it is believed that they contribute to replication, although their actual roles are as yet largely unknown. Similarly, DDR proteins have been identified at replication centers of other DNA viruses, such as HPV and KSHV, (reviewed in [39–41]).

Most previous studies of AdE1B55K have concentrated on its role during viral infection, when it is present with its partner, E4orf6, and functions as part of the E3 ligase. However, in the present study we were particularly interested in any unique functions of the protein linked to the DDR but distinct from its E3 ligase activity. Therefore, we have made use of human fibroblast cells expressing Ad12 E1B55K (55K<sup>+</sup>HSF). These cells are not transformed, nor are they immortal, but they do have an extended lifespan in culture [42]. Results have been compared to parental fibroblasts (HSFs) from the same donor. We have shown that Ad12E1B55K expression sensitizes cells to different damaging agents, seen as an increased number of DNA damage foci and increased activation of ATM, and, consistent with historical reports, increased genomic instability, seen as an increase in chromosomal damage and micronuclei occurrence. Furthermore, Ad12E1B55K has a detrimental effect on DNA replication, markedly increasing the number of stalled forks; it also increases the number of R-loops present. We suggest that most of these effects are probably due to the association of the viral protein with various DDR and replication complex proteins.

## 2. Materials and Methods

### 2.1. Cells and Drug Treatments

The derivation of HSFs and Ad12E1B55K-expressing HSFs (55K<sup>+</sup>HSFs) has been described previously [42]. Cells were grown in Dulbecco's modified Eagle's medium (DMEM) (Sigma-Aldrich), supplemented with 8% fetal calf serum (FCS) (Sigma-Aldrich, St. Louis, MO, USA). Adenovirus 12 Early Region 1 Human Embryo Retinal 2 (Ad12E1HER2) cells were also grown in DMEM supplemented with 8% FCS [43]. For various experiments, cells were treated with 1  $\mu$ M camptothecin (CPT) (Cayman Chemicals, Ann Arbor, MI, USA), 2 mM hydroxyurea (HU) (Sigma-Aldrich), 3  $\mu$ M aphidicolin (Sigma-Aldrich) and ionizing radiation (IR). In the CPT and aphidicolin experiments, the drug was left on the cells for the duration of the experiment, but treatment with HU was for 1 h only followed by removal of the drug and replacement with normal medium. Cells were also treated with 50  $\mu$ M mirin or nocodazole (both from Sigma-Aldrich).

### 2.2. Western Blotting and Antibodies

Cells were grown to approximately 70% confluency and then harvested or treated with 2 mM HU, 1  $\mu$ M CPT or ionizing radiation (4 Gy). Cells were washed in ice-cold phosphate buffered saline (PBS) and cell pellets were solubilized in 9 M urea, 40 mM Tris HCl, pH 7.4, 0.15 M  $\beta$ -mercaptoethanol. Cell lysates were fractionated by SDS-PAGE and proteins transferred to nitrocellulose membranes. Membranes were probed with antibodies against the following proteins: Ad12E1B55K (XPH9, raised against an Ad12E1B55K/ $\beta$ -galactosidase fusion protein, or a rabbit antibody raised against purified GST-Ad12E1B55K), p53 (DO1, a gift from David Lane),  $\gamma$ H2AX (Millipore, Burlington, MA, USA), phospho-NBS1 (S343), phospho-KAP1 (S824), KAP1, SMC1, BLM, TOPBP1 and ATM (all from Bethyl Laboratories, Montgomery, TX, USA), phospho-CHK1 (S345) and phospho-CHK2 (T68) (both from Cell Signaling, Danvers, MA, USA), GAPDH, DNA-PK, PARP1, Ku80, CHK1, CHK2, NBS1, MRE11, MCM2, MCM3, MCM5, ORC1, ORC2, ORC3, ORC5, cdc45 and DNA Pol  $\delta$  (all from Santa Cruz Biotechnology, Dallas, TX, USA), phospho-ATM (S1981) (R&D Systems, Minneapolis, MN, USA), H2B (Abcam, Cambridge, UK), TICCR (Sigma-Aldrich) and RPA32 (Calbiochem, San Diego, CA, USA). Antigens were visualized using ECL reagent (GE Healthcare, Chicago, IL, USA) and X-ray film (Kodak, Rochester, NY, USA).

Additional antibodies used in microscopical aspects of this study were raised against 53BP1 (Novus Biologicals, Littleton, CO, USA), Rad51 (Calbiochem), R-loops (S9.6, a gift from Angelo Agathangelou, University of Birmingham, UK), Mitosin (Bethyl Laboratories, Montgomery, TX, USA) and Nucleolin (BD Bioscience, Franklin Lakes, NJ, USA), and BrdU (IdU, Becton Dickinson, Franklin Lakes, NJ, USA) and CldU (AbD SeroTec, Oxford, UK).

### 2.3. Co-Immunoprecipitation

Ad12E1HER2 cells were harvested in ice-cold PBS and lysed in 40 mM Tris HCl, pH 7.4, 1% NP40, 5 mM EDTA, 0.4 M NaCl. Insoluble material was removed by centrifugation at  $100,000 \times g$  for 20 min. Lysates were incubated with appropriate antibodies overnight. Antigen-antibody complexes were isolated with protein G-agarose beads (Generon, Slough, UK) and fractionated by SDS-PAGE. Co-immunoprecipitating proteins were identified by western blotting.

### 2.4. Chromatin Preparation

Chromatin was prepared from 55K<sup>+</sup>HSFs and Ad12E1HER2 cells as described by Mendez and Stillman [44]. Briefly, cells were harvested in ice-cold PBS and resuspended in 0.34 M sucrose, 10% glycerol, 1.5 mM Mg<sub>2</sub>Cl, 10 mM KCl, 10 mM HEPES pH 7.9. Triton X100 was added to a concentration of 0.1% and cells were left on ice for 10 min. The cells were centrifuged for 5 min at  $1300 \times g$  to give a nuclear pellet and a supernatant which was termed the 'cytoplasmic fraction' although it contained other organelles. After washing in the HEPES buffer, the nuclear pellet was resuspended in 3 mM EDTA, 0.5 mM EGTA, left

on ice for 10 min and then centrifuged at  $1700\times g$  for 10 min. The pellet was taken as the chromatin fraction and the supernatant was the nucleoplasm.

### 2.5. Metaphase Spreads

Nocodazole at a final concentration of 200 ng/mL was added to sub-confluent HSFs and 55K<sup>+</sup>HSFs for 16 h. Cells were then harvested and subjected to hypotonic shock in 75 mM KCl for 30 min at 37 °C. Swollen cells were fixed with ethanol:acetic acid (3:1) solution and stored at −20 °C. Cells were dropped onto acetic acid-coated glass slides and allowed to dry overnight. Slides were then immersed in 5% Giemsa stain (Millipore) for 15 min followed by 5 min in water. The following day slides were mounted using Etellan mounting medium (Millipore) before metaphase abnormalities were scored using a Nikon Eclipse Ni microscope.

### 2.6. Immunofluorescence Microscopy

Cells were grown on glass cover slips for 24 h and then treated with 2 mM HU (for 1 h), 1  $\mu$ M CPT or IR (2 Gy or 4 Gy). After the stated times, cells were fixed in 3.6% paraformaldehyde in PBS for 10 min and then permeabilized in 0.5% Triton X100 in PBS for 5 min before washing with PBS. Cells were stained with antibodies overnight, washed three times in PBS, and then stained with secondary antibodies for 1 h. DNA was stained with 4',6-diamidino-2-phenylindole (DAPI). Fluorescence images were taken using a Nikon E600 Eclipse 333 microscope equipped with a 60 $\times$  oil lens, and images were acquired using Volocity software 334 v4.1 (Improvision). Foci were counted in at least 100 cells in 3 separate experiments. Micronuclei were detected in cells fixed and permeabilized as described and stained for 5 min with DAPI. Micronuclei were also counted in at least 100 cells in 3 separate experiments.

### 2.7. Estimation of R-Loops

Cells were fixed and stained as described in the previous section. Cells were stained with the S9.6 antibody which recognizes R-loops and counterstained with an antibody against Nucleolin. Nuclei were stained with DAPI. The intensity of total nuclear staining due to S9.6 was measured and the intensity of the staining in the nucleoli subtracted as described [45]. Data were calculated using ImageJ.

### 2.8. DNA Fiber Analysis

DNA fiber analysis was performed essentially as described by Petermann and colleagues [46]. Briefly, cells were pulse-labelled with 25  $\mu$ M CldU (Sigma-Aldrich) for 40 min, washed twice with medium and pulse-labelled with 250  $\mu$ M IdU (Sigma-Aldrich) for 40 min. When cells were treated with 2 mM HU, it was included with the IdU. Labelled cells were harvested, and DNA fiber spreads were prepared as described [47]. CldU and IdU were detected by incubating acid-treated fibers with rat anti-BrdU antibody and mouse anti-BrdU antibody for 1 h. Slides were fixed with 3.6% PFA and incubated with Alexa Fluor 555 conjugated anti-rat IgG (Molecular Probes, Eugene, OR, USA) and Alexa Fluor 488-conjugated anti-mouse IgG secondary antibodies for 1.5 h. DNA fibers were viewed with a Nikon Eclipse E600 microscope and analyzed using ImageJ software. A summary of the protocol is shown in Supplementary Figure S1.

### 2.9. Statistical Analysis

The dot plot for the DNA fiber assay was performed using GraphPad Prism statistical software; ( $n = 3$  independent experiments; >175 cells analyzed per repeat; Stats: unpaired  $t$ -test, \*  $p < 0.05$ , \*\*  $p < 0.01$ , \*\*\*  $p < 0.001$  and \*\*\*\*  $p < 0.0001$ ). Quantification of cells with micronuclei classified in four categories: 1 micronucleus per cell, 2 micronuclei per cell, 3 micronuclei per cell and >4 micronuclei per cell ( $n = 3$  independent experiments; >100 cells counted per repeat, mean  $\pm$  SD, \*  $p < 0.05$ , \*\*  $p < 0.01$  and \*\*\*  $p < 0.001$ ). Quantification of

foci:  $n = 3$  independent experiments;  $>100$  cells counted per repeat, mean  $\pm$  SD, \*  $p < 0.05$ , \*\*  $p < 0.01$  and \*\*\*  $p < 0.001$ . NS, not significant in all figures.

### 3. Results

To determine to what extent the AdE1B55K protein influences the cellular DNA damage response and DNA replication stress in the absence of E4orf6 and, therefore, the viral E3 ligase activity, we have made use of HSFs expressing Ad12E1B55K (55K<sup>+</sup>HSF) [42]. The cells have an appreciably extended life span but are not immortal or transformed and are similar in appearance to the parental cells (Figure 1A,B). It is notable that they express Ad12E1B55K at an appreciably lower level than Ad12E1 transformed human cells, as shown in Figure 1B.

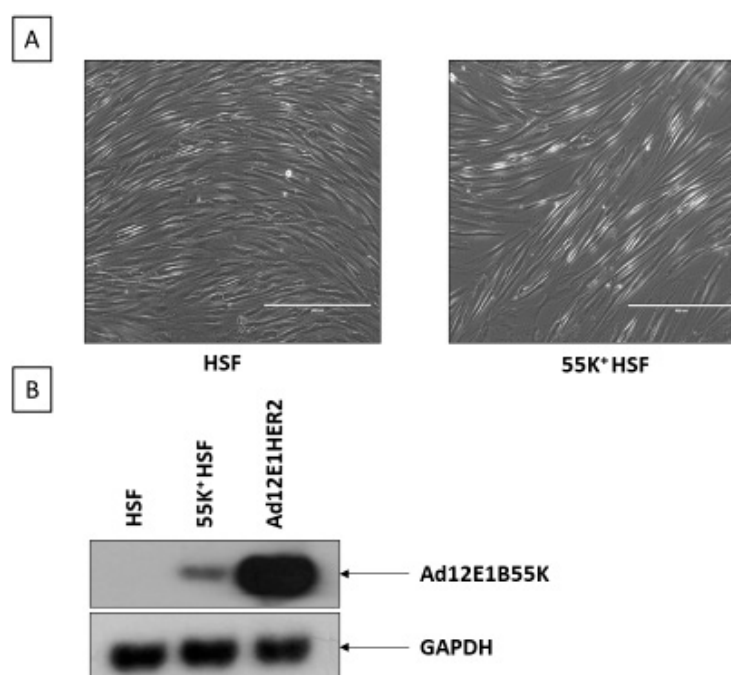


**Figure 1.** The morphology of HSFs expressing Ad12E1B55K (55K<sup>+</sup>HSFs). (A) Phase contrast micrograph of parental HSFs (left-hand panel) and 55K<sup>+</sup>HSFs (right-hand panel). The bar represents 400 μm. (B) Western blot of HSFs, 55K<sup>+</sup>HSFs and Ad12E1HER cells probed with antibodies against Ad12E1B55K and GAPDH.

#### 3.1. Ad12E1B55K Induces Genomic Instability in Human Skin Fibroblasts

Previous studies have indicated that Ad12E1B55K induces chromosomal breaks at specific fragile sites and that these are similar to those induced by exposure to low doses of DNA-damaging agents [11,13,15,17,22,24]. However, these experiments were largely performed in the context of adenovirus 12 infection. To obtain a direct indication of the effect of the viral protein on genomic stability, the number of micronuclei was counted in normally dividing HSFs and in 55K<sup>+</sup>HSFs (Figure 2B). Micronuclei were also counted 24 or 48 h after treatment with HU, camptothecin or IR (Figure 2C–E). Micronuclei are rare in untreated HSFs but can be seen in 5–10% of the cells expressing Ad12E1B55K (Figure 2A,B). The micronuclei tended to be generally similar in size, although an occasional large one was visible, and clustered close to the DAPI-stained nucleus. In cells treated with DNA-damaging agents there are notably higher levels of micronuclei in 55K<sup>+</sup>HSFs, suggesting that Ad12E1B55K interferes with the cellular response to DNA replication stress and to DNA damage quite separately from its well-characterized ability to degrade DDR proteins with E4orf6 (Figure 2C–E).



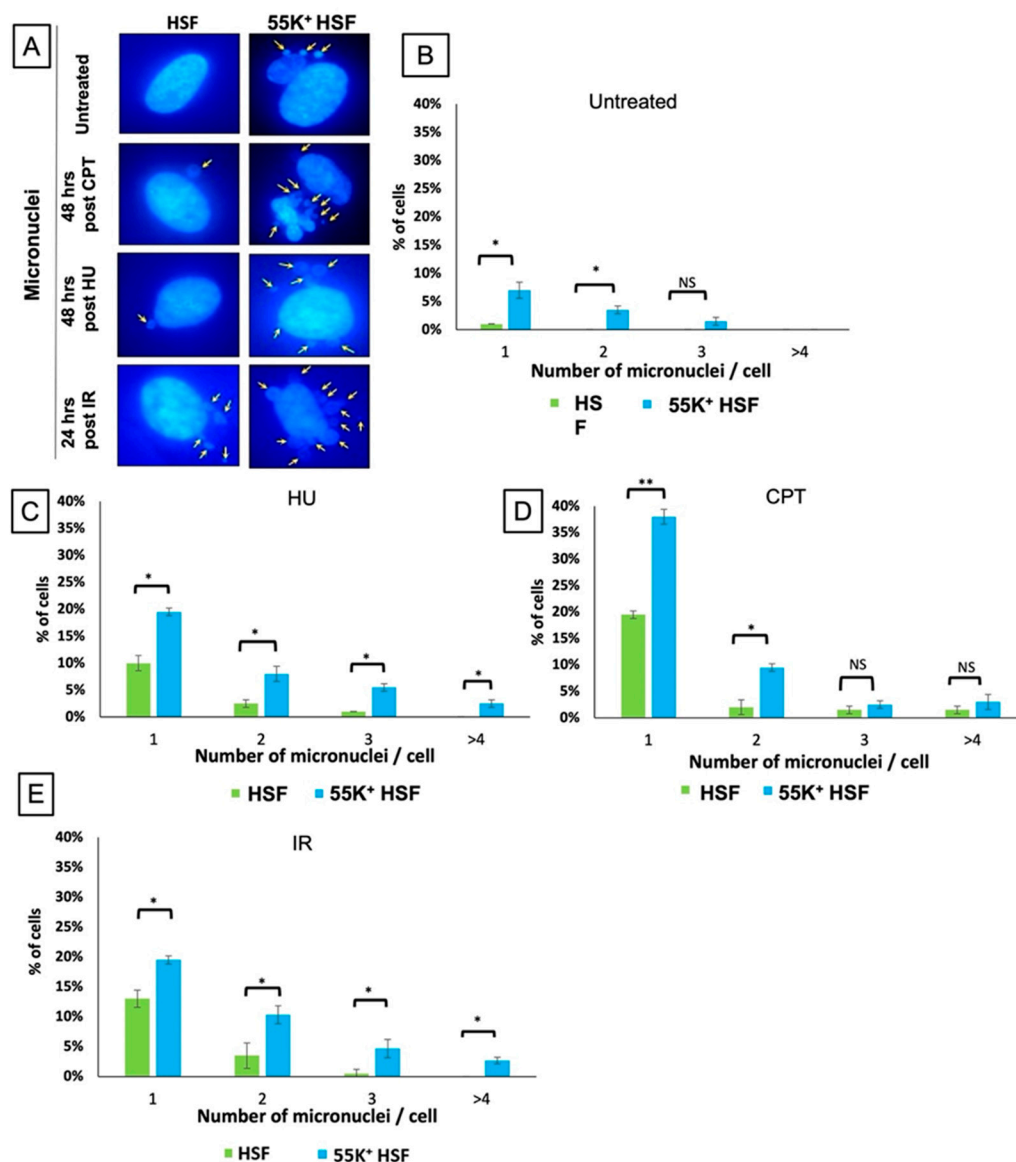


**Figure 2.** Micronuclei present in 55K<sup>+</sup>HSFs. HSFs and 55K<sup>+</sup>HSFs were exposed to DNA damaging agents, fixed after 48 or 24 h, and stained with DAPI. (A) Representative images of HSFs and 55K<sup>+</sup>HSFs (arrows indicate micronuclei). (B) Micronuclei observed in untreated cells. (C) Micronuclei observed 48 h after treatment with 2 mM HU. (D) Micronuclei observed 48 h after treatment with 1  $\mu$ M CPT. (E) Micronuclei observed 24 h after treatment with IR (4 Gy). (100 cells were counted for each treatment:  $n = 3$  independent experiments. Mean  $\pm$  SD, \*  $p < 0.05$ , \*\*  $p < 0.01$  NS, not significant.

In the original investigations of the effects of Ad12 on human chromosomes, gaps and breaks were observed in chromosomes 1 and 17 [11–13]. We were interested to see if there were more chromosomal abnormalities in the 55K<sup>+</sup>HSF cells. In the representative 55K<sup>+</sup>HSF metaphase spread shown in Figure 3, gaps, breaks and radials can be seen. Comparison of spreads from HSFs and 55K<sup>+</sup>HSFs showed appreciably more damage in cells expressing Ad12E1B55K (Figure 3). (No attempt was made to perform a more detailed analysis to see which chromosomes were particularly susceptible to damage.)

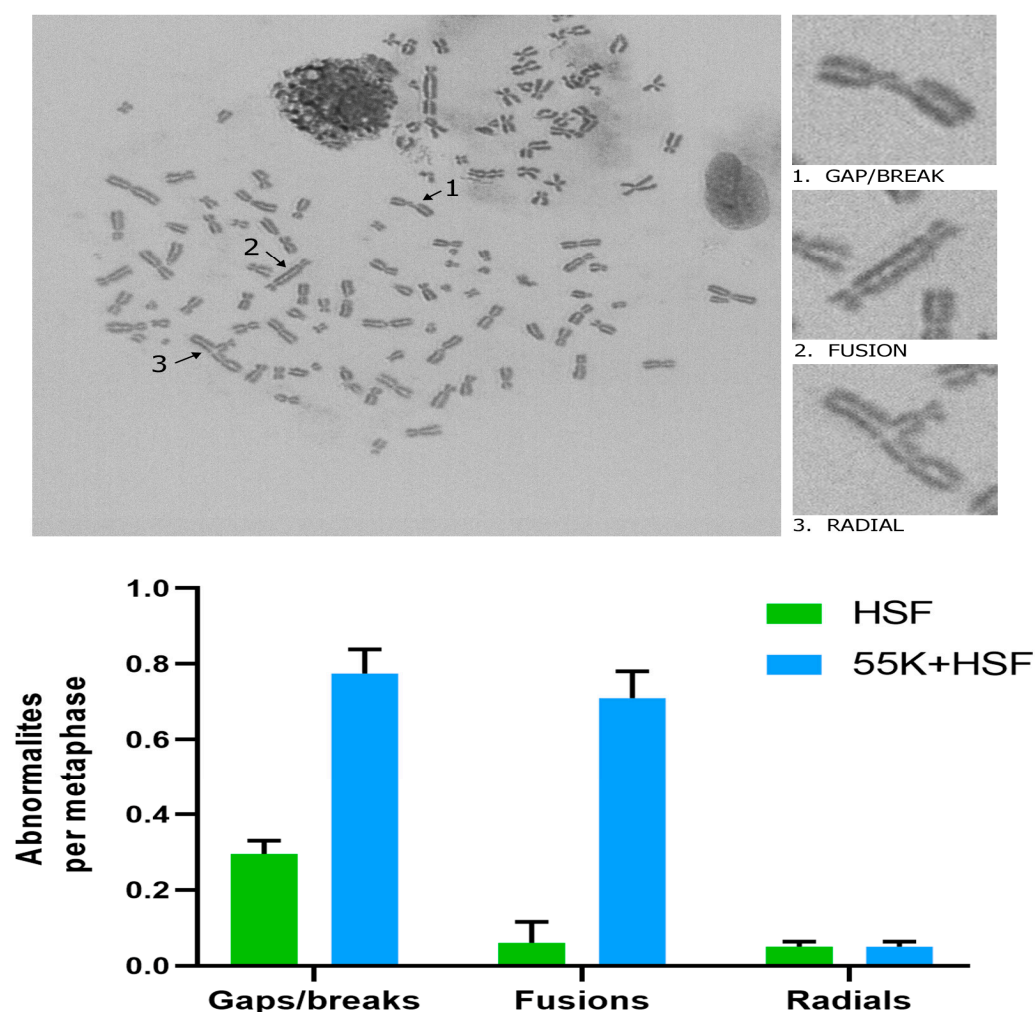


**Figure 3.** Metaphase spreads of 55K<sup>+</sup>HSFs. HSFs and 55K<sup>+</sup>HSFs were processed as described in the Materials and Methods section and the metaphase spreads prepared. A representative spread from 55K<sup>+</sup>HSFs is shown in the upper panel. Average numbers of abnormalities from 50 metaphase spreads from each cell population is shown in the histogram ( $n = 2$ ).

### 3.2. Ad12E1B55K Affects DNA Replication in HSFs and Leads to an Increase in R-Loop Formation

As treatment with the replication inhibitor, HU, has a marked effect on the genomic stability of 55K<sup>+</sup>HSFs (Figure 2C), we have investigated DNA replication in the two sets of cells. To examine DNA replication, use was made of DNA fiber assays [48] as outlined in the Materials and Methods section. Comparing 55K<sup>+</sup>HSFs with ‘normal’ HSFs, it is clear that expression of the viral protein increases the number of stalled replication forks observed, with a slight increase in new origin firing (Figure 4A). The efficiency of fork restart and replication fork speed is also decreased appreciably in 55K<sup>+</sup>HSFs (Figure 4B,C). To examine the effect of Ad12E1B55K on the response to DNA replication stress, cells were treated with 2 mM HU, which causes depletion of the nucleotide pool resulting in global replication fork stalling. In both populations, HU treatment resulted in a similar large increase in the number of stalled forks (Figure 4A), as expected, although the 55K<sup>+</sup>HSFs had a significantly reduced ability to restart replication efficiently (Figure 4B). The increase in stalled forks due to HU in the 55K<sup>+</sup>HSFs was only marginal. Examples of DNA fibers obtained in the study are shown in Supplementary Figure S1.

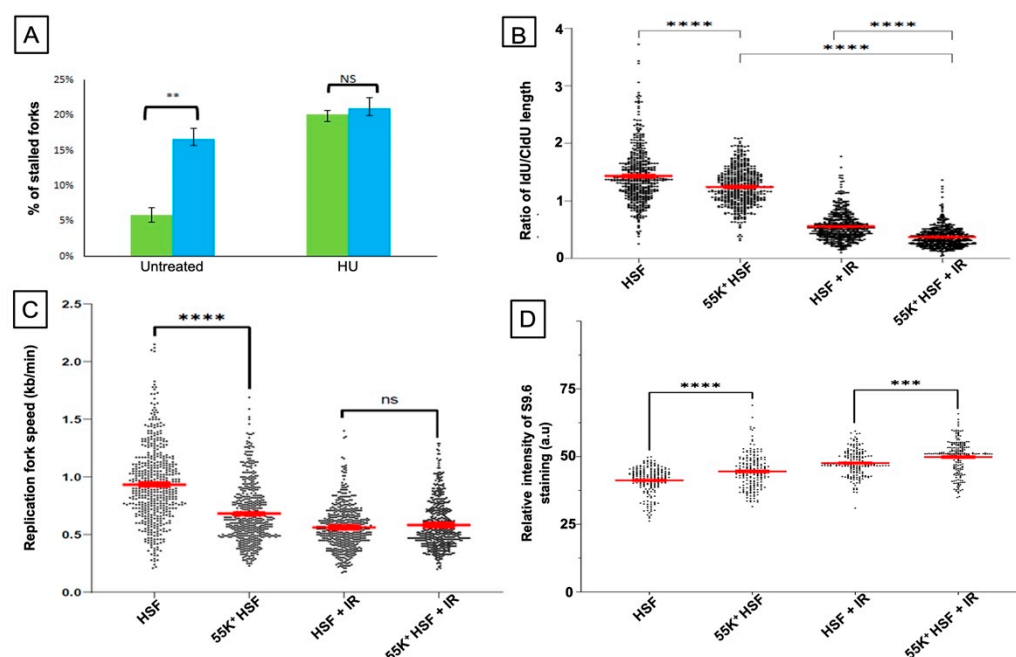


**Figure 4.** Expression of Ad12E1B55K in HSFs affects DNA replication and R-loop formation. (A–C), DNA fiber analysis was carried out on HSFs and 55K+HSFs in the presence or absence of 2mM HU, as described in Materials and Methods. (A) Percentage of HSFs and 55K+HSFs with stalled replication forks, before and after treatment with HU. (B) Ratio of Idu/CldU tract length (taken as a measure of fork restart after fork stalling) before and after HU treatment. (C) Replication fork speeds of HSFs and 55K+HSFs, before and after treatment with HU. (D) Relative level of R-loops in HSFs and 55K+HSFs, before and after treatment with IR (4 Gy). Cells were fixed and stained with antibodies recognizing R-loops (S9.6) and Nucleolin and with DAPI. The intensity of R-loop staining in the nucleus, but outside the nucleoli, was calculated for cells in three separate experiments. For DNA fiber analysis, approximately 175 cells were analyzed for each repeat:  $n = 3$  independent experiments. For the R-loop determination, 200 cells were measured for each repeat:  $n = 3$  independent experiments. Unpaired  $t$ -test, \*\*  $p < 0.01$ , \*\*\*  $p < 0.001$  and \*\*\*\*  $p < 0.0001$ . NS, not significant.

A common cause of DNA replication stress is the presence of DNA–RNA hybrid R-loops. To examine whether Ad12E1B55K affected R-loop formation, cells were stained with the S9.6 antibody [49] and the intensity of staining was calculated as described [45]. (R-loop staining in the nucleoli was subtracted from total nuclear staining.) There were significantly more R-loops, as indicated by the increased intensity of S9.6 staining, in the 55K+HSFs compared to the parental HSFs. In addition, staining with S9.6 was appreciably more intense, following IR, in cells expressing Ad12E1B55K (Figure 4D). Examples of R-loop staining are shown in Supplementary Figure S2.

### 3.3. Ad12E1B55K Protein Sensitises HSFs to DNA Damaging Agents

To understand better how Ad12E1B55K impinges on the DDR, we exposed 55K+HSFs and control cells to HU, camptothecin or IR and examined DNA repair foci formation over a 24- or 48-h time course, looking at recruitment of  $\gamma$ H2AX, 53BP1 and Rad 51. In all cases, a greater number of foci were formed in the 55K+HSFs compared to the parental cells (Figure 5). For example, at 8 h after treatment, for each damaging agent, there are significantly more  $\gamma$ H2AX, Rad51 and 53BP1 foci in the 55K+HSFs (Figure 5). This increased damage is consistent with the observed micronuclei, chromosomal aberrations, and increased replication fork stalling in cycling 55K+HSFs



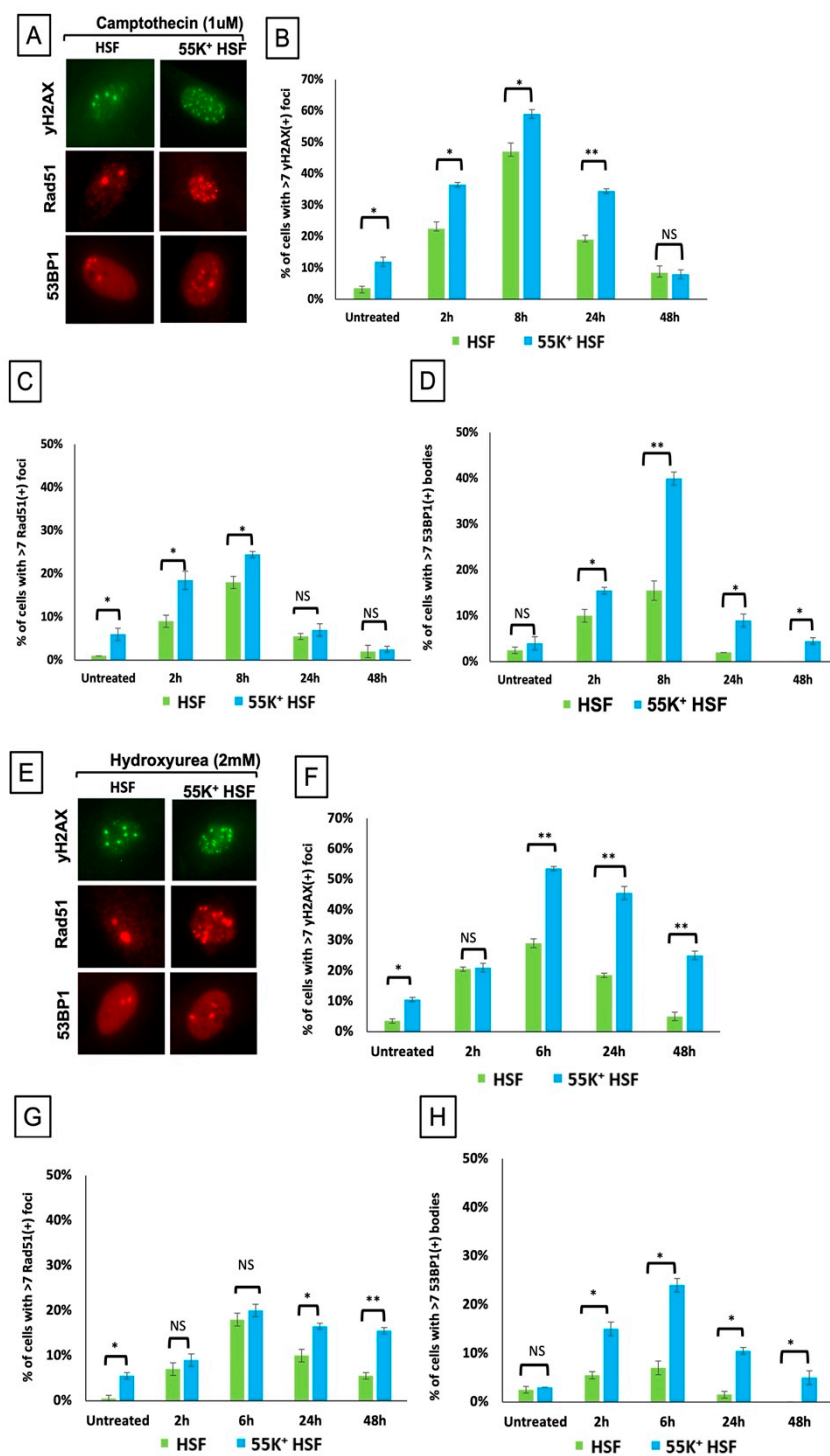
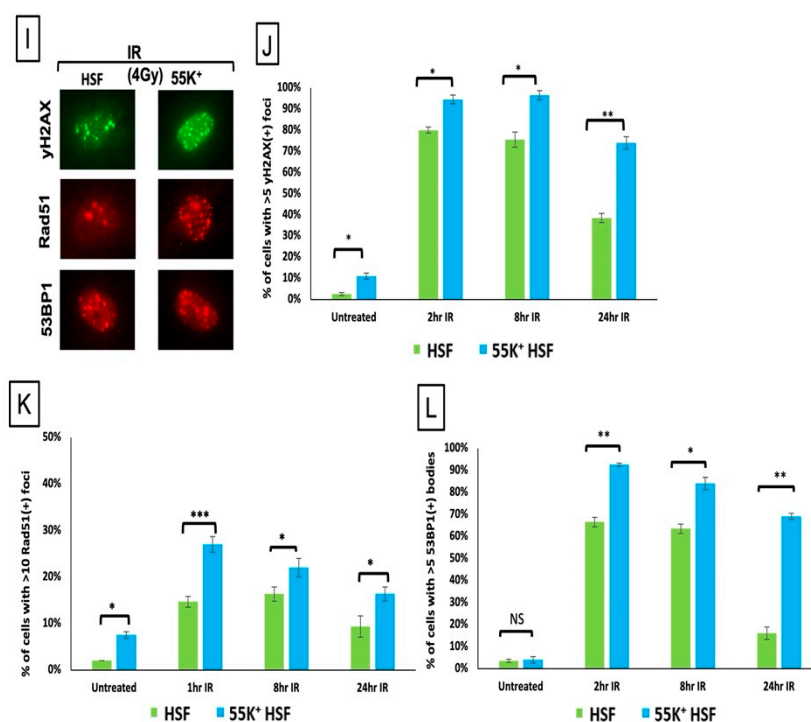


Figure 5. Cont.



**Figure 5.** Expression of Ad12E1B55K in HSFs affects focus formation, following DNA damage. HSFs and 55K<sup>+</sup> HSFs were exposed to DNA-damaging agents and fixed at various times after treatment. Cells were stained with antibodies against Ad12E1B55K,  $\gamma$ H2AX, 53BP1 and Rad51 and with DAPI. Panels (A,E,I) show representative images after exposure to CPT (1  $\mu$ M), HU (2 mM) and IR (4 Gy), respectively. (B–D) cells exposed to CPT and stained for  $\gamma$ H2AX (B), Rad51 (C) and 53BP1 (D). (F–H) Cells exposed to HU and stained for  $\gamma$ H2AX (F), Rad51 (G) and 53BP1 (H). (J–L) Cells exposed to IR and stained for  $\gamma$ H2AX (J), Rad51 (K) and 53BP1 (L). ( $n$  = 3 independent experiments; >100 cells counted per repeat; mean  $\pm$  SD, \*  $p$  < 0.05, \*\*  $p$  < 0.01 and \*\*\*  $p$  < 0.001). NS, not significant.

In a further experiment we have examined DNA damage focus formation in the different phases of the cell cycle. Cells were treated with 3  $\mu$ M aphidicolin for 45 min, irradiated with 2 Gy and fixed after 1 h, 8 h or 24 h. Cells were stained with an antibody against Mitosin, which is expressed during the S, G2 and M phases of the cycle, and counter-stained for  $\gamma$ H2AX (Figure 6), allowing the distinction between foci formed in G1 and those formed in G2 and S phases. In the Mitosin-positive cells it was also possible to distinguish between G2 cells (with a limited number of very distinct  $\gamma$ H2AX foci) and S phase cells (with many more diffuse  $\gamma$ H2AX foci). In the irradiated G1 cells (Mitosis negative), there are a similar number of foci in 55K<sup>+</sup> HSFs and HSFs at 1 h and 8 h post irradiation, although at 24 h there were appreciably more foci in the Ad12E1B55K-expressing cells. However, in the G2 cells there were appreciably more foci at 1 h and 8 h in the 55K<sup>+</sup> HSFs. We suggest that these data are indicative of deficiencies in the homologous recombination (HR) pathway, which is responsible for most DNA repair in G2, in cells expressing Ad12E1B55K.

We considered the possibility that Ad12E1B55K could localize to damaged foci following DNA damage. Generally, there was no co-localization between the viral protein and  $\gamma$ H2AX and 53BP1 (Supplementary Figure S3). However, a few  $\gamma$ H2AX foci appear to localize with more intense concentrations of Ad12E1B55K (marked with arrows in Supplementary Figure S3). It is not possible to say whether this is biologically significant at present. There appeared to be no co-localization with 53BP1.

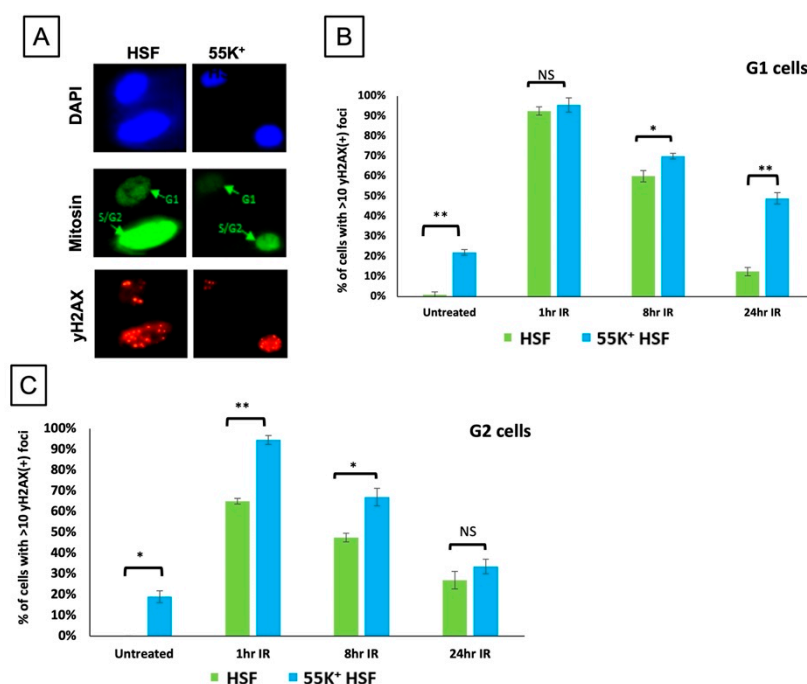


**Figure 6.** Ad12E1B55K affects DNA repair in HSFs in G2. Cells were treated with 3  $\mu$ M aphidicolin for 45 min and then exposed to IR (2 Gy). Cells were fixed after the times shown and stained with antibodies against Mitosin and  $\gamma$ H2AX and DAPI.  $\gamma$ H2AX foci were counted in G1 (Mitosis negative) and G2 cells (Mitosis positive) (A) Representative images of Mitosin and  $\gamma$ H2AX staining. (B)  $\gamma$ H2AX foci in G1 cells. (C)  $\gamma$ H2AX foci in G2 cells. (Approximately 100 cells were counted for each treatment at each time point for each repeat:  $n = 3$  independent experiments; mean  $\pm$  SD, \*  $p < 0.05$ , \*\*  $p < 0.01$ ). NS, not significant.

In a further investigation, we exposed HSFs and 55K<sup>+</sup>HSFs to different DNA-damaging agents and examined the activation of the DDR over a 24-h time course, using western blotting coupled with antibodies recognizing known substrates of the PI-3-kinase-like kinases, ATM and ATR. The replication stress caused by HU will lead to single-strand breaks and ultimately to double-strand breaks in the DNA; similarly, camptothecin, a Topoisomerase 1 inhibitor, also causes double-strand breaks. It can be seen from Figure 7 that all three treatments produce a much more marked activation of the ATM pathway in the 55K<sup>+</sup>HSFs than in the parental cells, with CHK2, KAP1 and  $\gamma$ H2AX being appreciably more highly phosphorylated (Figure 7). These data strongly suggest that Ad12E1B55K impinges on double-strand break repair pathways. This is consistent with previous studies, showing E1B55K/E4orf6-dependent degradation of the MRN complex, BLM, DNA Ligase IV and TIP60 in Ad5 infected cells [30–32,35]. Furthermore, some of these proteins are also degraded following Ad12 infection [50,51] (data not shown), with E1B55K probably acting as the binding component. Only very slight phosphorylation of DNAPK was observed (Figure 7C). Surprisingly, very limited phosphorylation of CHK1 was observed after HU treatment. It was expected that a much more marked response would be seen as the cells will be undergoing replication stress. The reasons for these observations are not clear at present. (In the blots shown in Figure 7, p53 is not obvious in the HSF cells; this is because relatively short exposures of the autoradiographs are shown so that those of 55K<sup>+</sup>HSFs are not too dark to be interpreted.) Interestingly, there does not appear to be an induction of p53 expression in the presence of Ad12E1B55K after DNA damage.

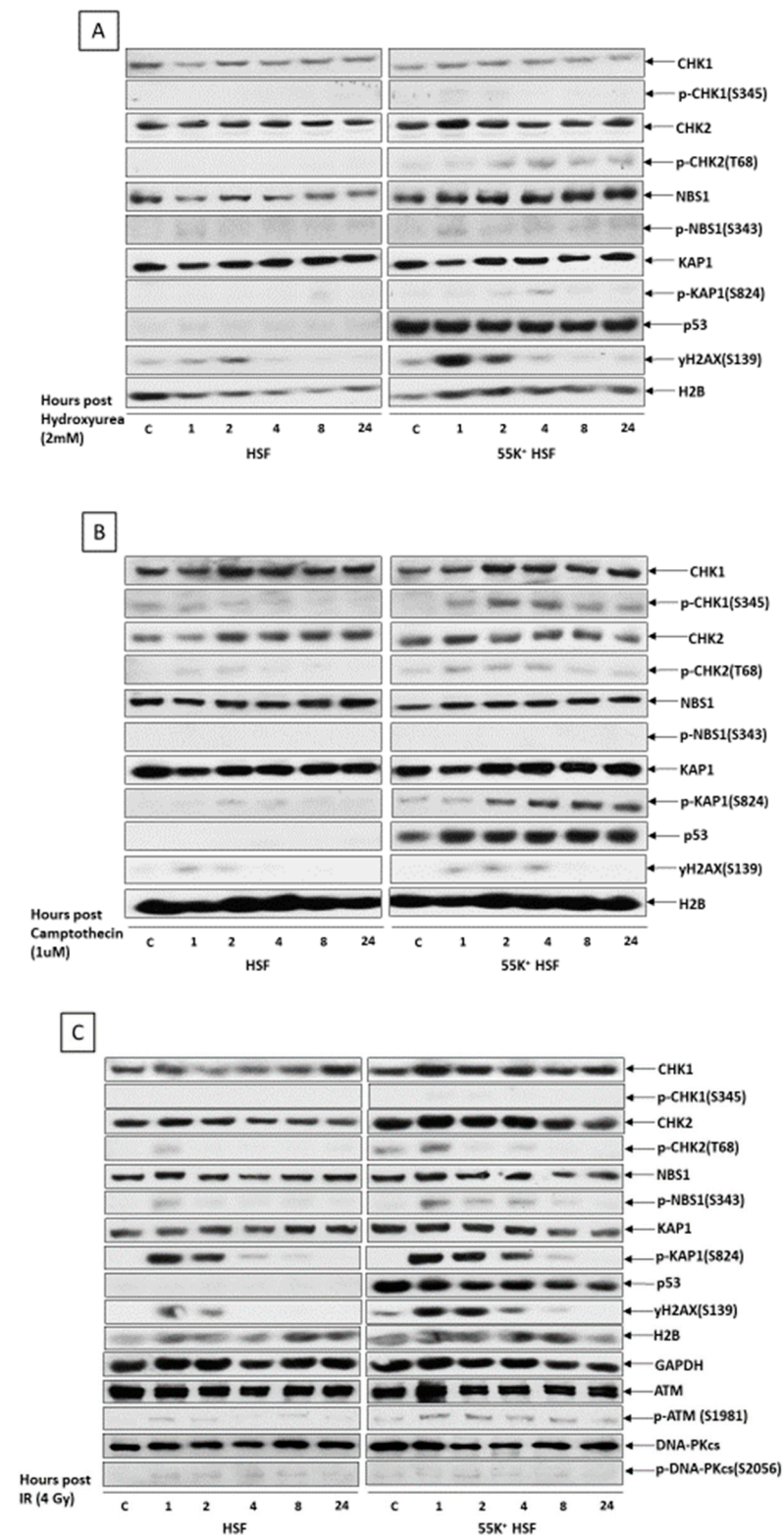


**Figure 7.** Ad12E1B55K sensitizes HSFs to DNA damaging agents. HSFs and 55K<sup>+</sup> HSFs were exposed to various DNA-damaging agents and harvested at the times shown. Cell lysates were fractionated by SDS-PAGE and western blotted using the antibodies shown. (A) HSFs and 55K<sup>+</sup> HSFs treated with 2 mM HU. (B) HSFs and 55K<sup>+</sup> HSFs treated with 1 μM CPT. (C) HSFs and 55K<sup>+</sup> HSFs treated with IR (4 Gy). c, untreated control cells.

It is clear from the data presented in Figures 5 and 7 that Ad12E1B55K has a marked effect on the DDR, probably compromising double-strand break repair and possibly other pathways. To investigate this further, we examined whether inactivation of MRE11 by the inhibitor mirin would duplicate some of the effects of Ad12E1B55K in the parental HSFs. 50  $\mu$ M mirin was added to HSFs and 55K<sup>+</sup>HSFs for 45 min before treatment with 1  $\mu$ M camptothecin. Cells were fixed after 2, 8, 24 and 48 h and  $\gamma$ H2AX foci were counted (Figure 8A). The number of foci in 55K<sup>+</sup>HSFs was not appreciably affected by mirin at the earlier time points, although it was markedly increased at 48 h. However, there were significantly more foci in HSFs. Notably, at 24 h the number of  $\gamma$ H2AX foci were very similar in the two populations in the presence of mirin, but in its absence, there were 1.7 times as many foci in 55K<sup>+</sup>HSFs. We suggest, based on these data, that Ad12E1B55K influences the cellular DDR, at least in part, by inactivation of the MRN complex. In addition, the number of micronuclei observed 48 h after damage was much more similar in the two populations in the presence of mirin than in its absence (Figure 8B). Thus, there were approximately four times as many cells with two micronuclei per cell in the 55K<sup>+</sup>HSFs than in the parental cells in the absence of mirin but a comparable number in each in its presence. Virtually no HSFs were seen with more than three micronuclei in HSFs in the absence of mirin but there were similar numbers in the two populations when MRE11 was inhibited.

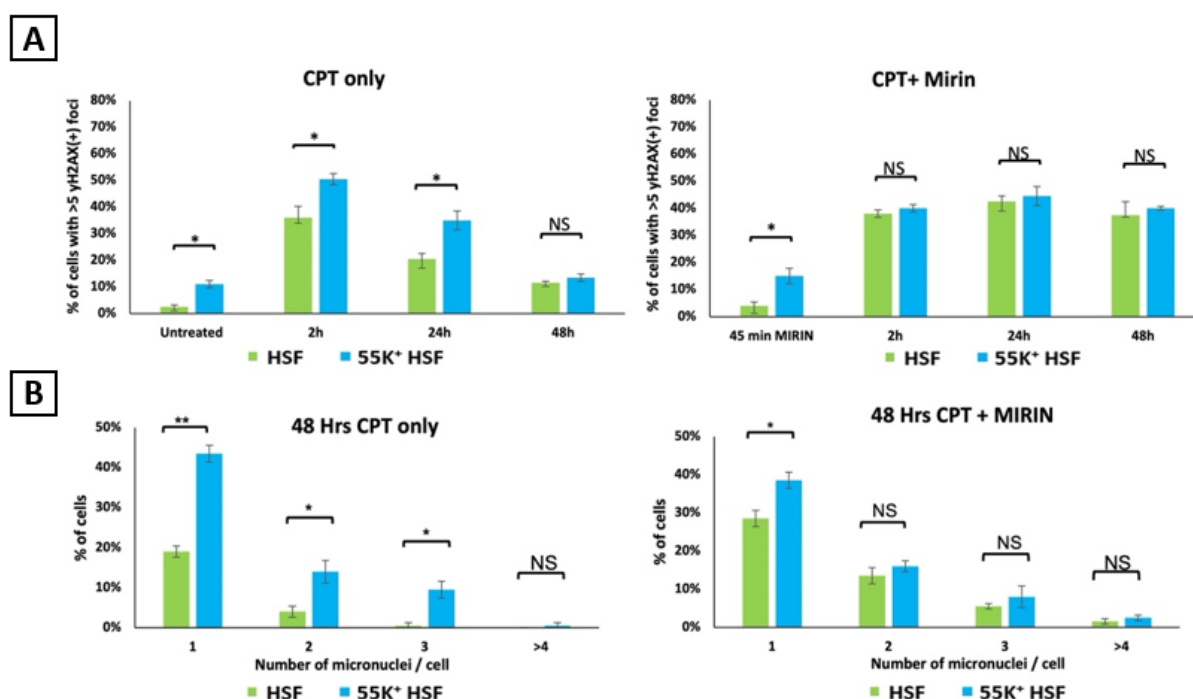


**Figure 8.** The effect of mirin of  $\gamma$ H2AX foci and micronuclei formation in HSFs and 55K<sup>+</sup>HSFs. Cells were grown on glass coverslips for 24 h and treated with 50  $\mu$ M mirin for 45 min. Cells were then treated with 1  $\mu$ M camptothecin in the presence of mirin. (A) cells were fixed at the times shown and then stained for  $\gamma$ H2AX. Foci were counted. (B) DAPI-staining micronuclei were counted after 48 h ( $n = 3$  independent experiments; >100 cells counted per repeat; mean  $\pm$  SD, \*  $p < 0.05$ , \*\*  $p < 0.01$ ). NS, not significant.

### 3.4. Ad12E1B55K Affects the Ability of HSFs to Undergo Cell Cycle Arrest following DNA Damage

In view of the widespread effects of Ad12E1B55K on the DDR and on DNA replication, we examined whether there were differences between both sets of cells in their ability to arrest their cell cycles following DNA damage. HSFs and 55K<sup>+</sup>HSFs were treated with 1  $\mu$ M camptothecin and harvested at times up to 48 h. Cell lysates were western blotted for cyclins to assess progress through the cell cycle (Figure 9). In the HSFs there appears to



be cell cycle arrest soon after DNA damage with a low level of expression of cyclins A, B1 and D1. After 8 h, cyclin D1 expression increases, presumably as cells re-enter cycle. After 24 h, there is an increase in cyclins A and B1 as cells go through S and G2 phases. On the other hand, in the 55K<sup>+</sup>HSFs the expression of cyclins remains high throughout the time course, suggesting that the cells do not undergo arrest, most probably due to inactivation of p53 (even though the expression is much higher than in the parental cells (Supplementary Figure S4)).

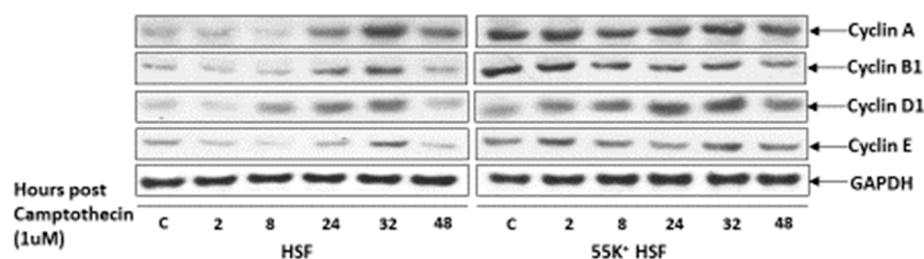


**Figure 9.** Cyclin expression in 55K<sup>+</sup>HSFs and HSFs following DNA damage. HSFs and 55K<sup>+</sup>HSFs were treated with 1  $\mu$ M camptothecin. After 1 h the drug was washed out and the cells incubated in normal medium. Cells were harvested at the times shown and lysates subjected to western blotting using the antibodies shown.

### 3.5. Association of Ad12E1B55K with Replication Machinery and DDR Pathway Components

To examine whether Ad12E1B55K influences DNA replication and the DNA repair pathways by affecting levels of relevant protein expression, samples of the 55K<sup>+</sup>HSFs and parental HSFs were western blotted using a variety of antibodies, as shown in Supplementary Figure S4. There were some differences in the expression of proteins associated with replication, such as reduced levels of MCM2, ORC1, ORC2 and ORC6 in 55K<sup>+</sup>HSFs (Supplementary Figure S4). There is a large overexpression of p53 in the Ad12E1B55K-expressing cells, as has been reported previously; this protein is transcriptionally inactive, presumably due to its association with Ad12E1B55K [52]. There are limited differences in expression for the other DDR proteins examined between the two cell types; for example, BLM is present at an increased level in 55K<sup>+</sup>HSFs (Supplementary Figure S4).

It is clear from the micrographs shown in Supplementary Figure S3 that Ad12E1B55K is predominantly nuclear. Therefore, initially we were interested to see if a proportion of the protein was associated with chromatin. Figure 10 shows that the nuclear fraction of the viral protein is present in the chromatin and not the nucleoplasm. A significant proportion is also present in the cytoplasmic fraction (Figure 10).

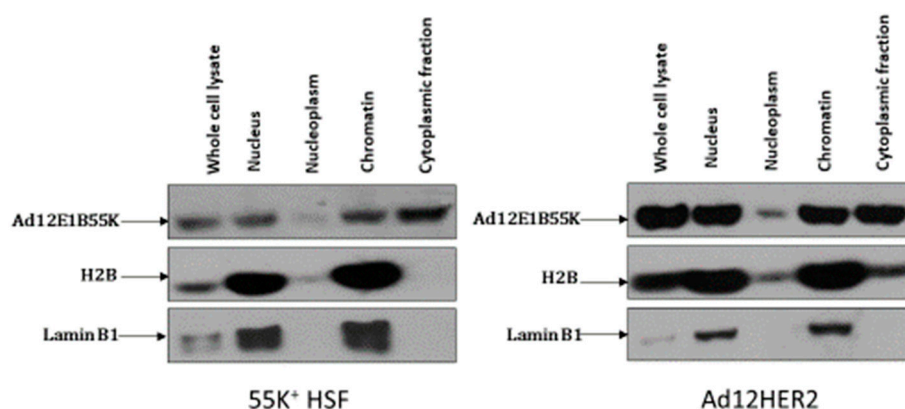


**Figure 10.** Ad12E1B55K localizes to chromatin in 55K<sup>+</sup>HSFs and Ad12E1HER2 cells. Cells were harvested and processed as described in the Materials and Methods. Fractions were western blotted using the antibodies shown. The cytoplasmic fraction also includes some organelles.

During Ad-mediated protein degradation, it has been shown or, in some cases, assumed that the E1B55K protein acts as the binding component for the cellular target to be ubiquitinated by the E3 Ligase [25,27–29]. It is possible, therefore, that the effects of Ad12E1B55K on DNA replication and on the DDR in the 55K<sup>+</sup>HSFs are due to its protein–protein interactions.

In a more detailed analysis, we have carried out a limited series of co-immunoprecipitations, looking at whether Ad12E1B55K associates with various likely replication machinery and DDR pathway components (Figure 11). For this we have used Ad12E1HER2 cells as they can be grown more easily in much greater numbers than the fibroblast line and express E1B55K at a higher level (Figure 1). In Figure 11A, it can be seen that immunoprecipitation of Ad12E1B55K results in co-precipitation of MCM3, MCM7 and ORC3, indicating association between the viral protein and at least some members of the ORC and MCM complexes. No association was seen with ORC2, ORC6, MCM2 or MCM4 (data not shown). In addition, Ad12E1B55K binds strongly to DNA polymerase  $\delta$ , TICRR (also known as Treslin and SLD3) and cdc45 (Figure 11A)—well characterized components of the replisome. No interaction with PCNA could be observed (data not shown). It is possible that binding to the MCM complex, ORC1 and/or DNA Pol  $\delta$  could be responsible for some of the aberrations observed in DNA replication. Ad12E1B55K also associates with p53, as has been observed previously, and MRE11 and NBS1, as might be expected based on the observation that they are targeted for degradation during Ad12 infection [50–52]. Co-immunoprecipitation of Ad12E1B55K with ATM, DNA-PK catalytic subunit, BLM and TOPBP1 was also observed (Figure 11B). It is likely that these interactions could have profound effects on the DDR.

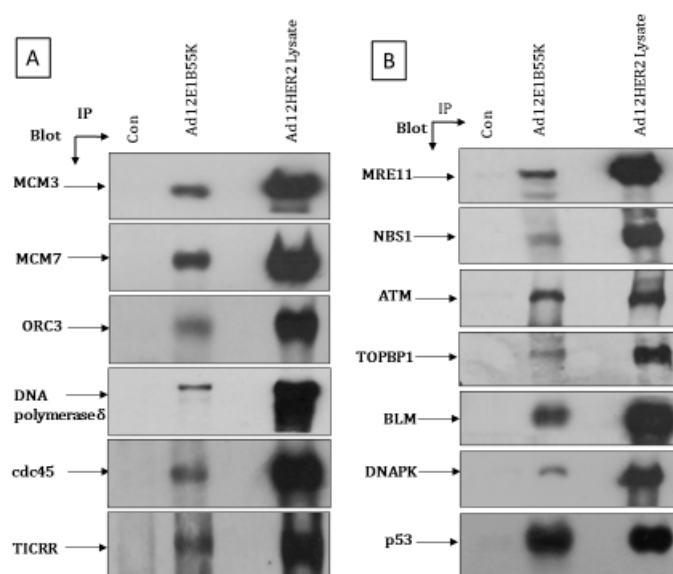


**Figure 11.** Co-immunoprecipitation of Ad12E1B55K with: (A), pre-replication complex and (B), DNA damage-response proteins. Ad12E1HER2 cell lysates (500  $\mu$ g) were incubated with antibodies against Ad12E1B55K and collagen IV (non-specific binding control). Immunocomplexes were isolated with protein G-agarose beads and subsequently resolved by SDS-PAGE and western blotting, using antibodies against the proteins shown. Con: immunoprecipitation with collagen IV antibody.

In the micrographs shown in Supplementary Figure S3 and in the original report [42], it is notable that a proportion of the Ad12E1B55K protein is present as very brightly staining cytoplasmic ‘tracks’ which appear not to be affected by DNA damage. We considered the possibility that these could be sites of interaction with some of the binding proteins identified in Figure 11. Co-staining for some of these, however, showed that only MRE11 had limited co-localization (marked with arrows in the left-hand upper section of Figure 12). We could not detect any of the other binding partners in the ‘tracks’, including NBS1. However, it did appear that there was some co-localization of Ad12E1B55K with NBS1

foci formed after IR treatment (marked with arrows in the right-hand upper section of Figure 12).

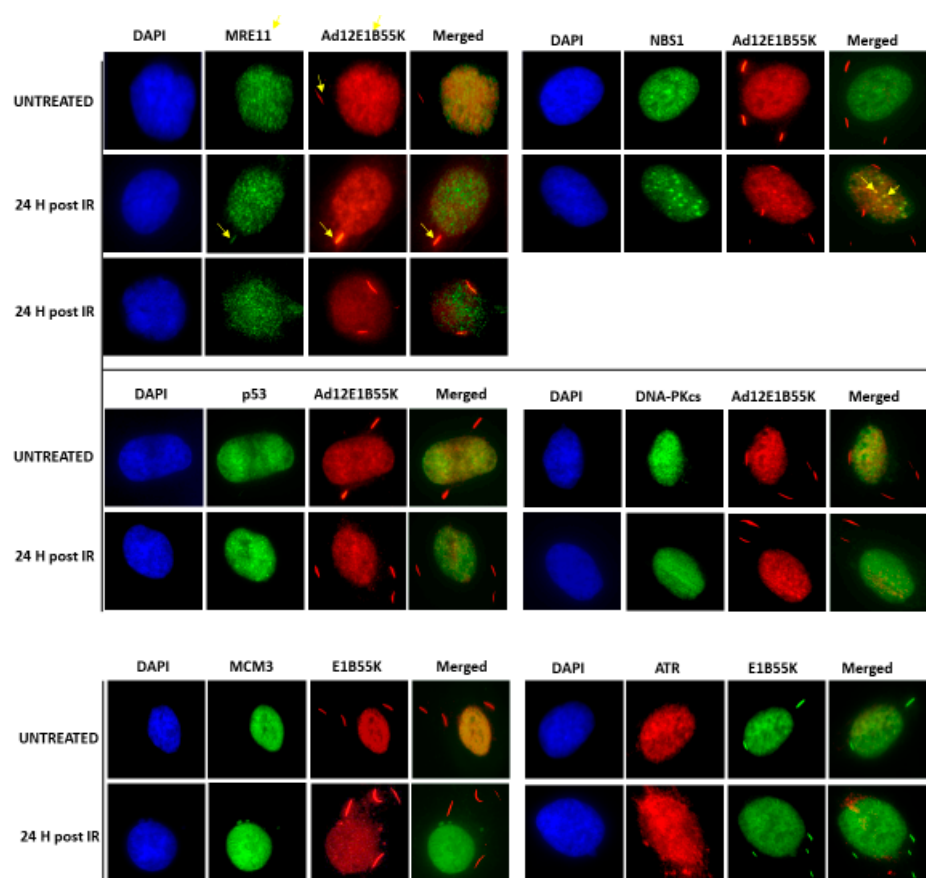


**Figure 12.** Co-localization of Ad12E1B55K with binding partners after DNA damage. 55K<sup>+</sup>HSFs were grown on glass coverslips for 24 h. Cells were treated or mock-treated with IR (3 Gy) and then fixed after 24 h. Cells were stained with the antibodies shown. In the upper left-hand set of images, arrows indicate Ad12E1B55K (red) or MRE11 (green) localizing to cytoplasmic tracks. In the upper right-hand set of images, arrows indicate tentative co-localization of NBS1 and Ad12E1B55K at DNA repair foci.

#### 4. Discussion

It is now well-established that Group A and Group C adenoviruses target multiple key components of the DDR during viral infection (reviewed in [25,27,28]). This has been shown, in most cases, to be achieved through ubiquitylation and proteasome-mediated degradation, initiated by a complex between E1B55K, E4orf6 and cellular Cullins, Elongins and Rbx1. However, we considered the possibility that the E1B55K protein could impact DDR pathways in the absence of E4orf6. This was based on the historic observations that Ad12E1B55K was responsible for non-random damage to chromosomes 1 and 17 at low viral doses and in the absence of other viral proteins [11,13,16,20,24,53,54]. A synergistic effect between Ad12 and a DNA-damaging agent in the induction of these breaks has also been demonstrated [22]. Importantly, expression of the protein is essential for Ad12-mediated transformation of human cells in culture where it is possible that inactivation of the DDR could play a role [43,55]. To examine the relationship between the viral protein and the DDR, we have made use of HSFs expressing Ad12E1B55K (55K<sup>+</sup>HSFs) and compared results with the parental cells [42].

The expression of the Ad12E1B55K protein induces genomic instability in the HSFs, as shown by an appreciable number of micronuclei in growing cells, as well as an enhanced number of micronuclei in cells treated with DNA-damaging agents (Figure 2). Increased



numbers of damaged chromosomes were also observed in metaphase spreads prepared from 55K<sup>+</sup>HSFs (Figure 3), consistent with the original reports [11–15]. As HU increases the number of micronuclei in 55K<sup>+</sup>HSFs to a much greater extent than in the parental cells, we considered it possible that Ad12E1B55K could cause DNA replication stress. From the results presented in Figure 4, it is clear that replication is compromised in the presence of the viral protein in unperturbed cells with a marked increase in stalled forks, reduced efficiency of replication fork restart and a decrease in replication fork speed. Following HU treatment, both populations of cells had a similar number of stalled forks and similar replication fork speed. However, fork restart was significantly more efficient in the parental cells than in 55K<sup>+</sup>HSFs. We suggest that the Ad12E1B55K protein has a major impact on DNA replication in the generation of stalled forks in addition to compromising efficient replication fork restart after stress. All these effects can contribute to genomic instability (reviewed in, for example, [56,57]). It seems likely that the interactions observed between Ad12E1B55K and components of the replisome (ORC1, MCM3, MCM7, DNA polymerase  $\delta$  and cdc45) contribute to these effects (Figure 11).

During viral infection, adenoviruses target multiple aspects of DSB repair, with degradation and/or translocation of MRN components, BLM, DNA Ligase IV and TIP60 [30–32,35,58]. To examine whether the Ad12E1B55K protein in isolation would also affect the cellular response to DSBs, cells were exposed to different damaging agents and repair focus formation and phosphorylation of PI3K-related kinase substrates was monitored. Increased phosphorylation of ATM substrates in 55K<sup>+</sup>HSFs was seen, suggesting problems with the repair of DNA damage and perhaps the presence of additional damage due to checkpoint problems (see below) (Figures 7 and 9). Similarly, an increased number of foci staining positive for  $\gamma$ H2AX, Rad51 and 53BP1 were observed in 55K<sup>+</sup>HSFs, compared to controls at all time points after damage, again suggesting possible inefficiencies in DDR pathways and/or additional damage due to the effects of Ad12E1B55K (Figure 5). Ideally, a more detailed analysis of repair and resolution of DNA damage would have been undertaken to determine the relative contributions of increased damage compared to problems with repair. Interestingly, even in untreated cells an appreciable number of repair foci were visible, consistent with the proposition that Ad12E1B55K contributes to genomic instability in the absence of extraneous DNA-damaging agents (Figures 2 and 3).

To determine which repair pathways were likely to be targeted, we examined  $\gamma$ H2AX focus formation (in response to a low dose of IR) throughout the cell cycle by adding aphidicolin and delineating G1 and G2 cells by staining for Mitosin (Figure 6). Focus formation was similar for both populations of cells in G1 up to 8 h, where repair would be by NHEJ, whereas there were many more foci in the 55K<sup>+</sup>HSF G2 cells, when repair is predominantly by homologous recombination. The observation that there was a greater disparity at 24 h between the control and 55K<sup>+</sup>HSFs in G1 cells (compared to those in G2) is probably due to a breakdown in the aphidicolin cell cycle block (Figure 6). At 8 h, however, there are many more foci in the G2 cells when the cell cycle block is likely to be in place.

Examination of the cell cycle after DNA damage in 55K<sup>+</sup>HSFs suggests that the checkpoints are compromised (Figure 9). This is consistent with inactivation of p53 through direct interaction with Ad12E1B55K [50,52,59]. In the absence of transcriptionally active p53 the G1/S and G2/M checkpoints will not be functional. In the absence of one or more checkpoints, it is likely that more damage to the DNA will be incurred for a given treatment, giving rise to more damage foci and probably more activation of ATM (Figures 5 and 7).

To investigate the effects of Ad12E1B55K further, we have examined the level of expression of several DDR proteins to rule out the possibility that differences seen are due to protein degradation, as it has previously been noted that loss of Daxx during Ad5 infection requires only E1B55K with no contribution from E4orf6 [60]. As Ad12E1B55K also appears to affect DNA replication, the level of expression of some components of the origin recognition complex (ORC) and the pre-replicative complex were examined. Some differences were observed in the expression of ORC proteins and in MCM2, possibly affecting DNA replication. There were some disparities in the expression of some DDR

proteins between the two cell populations, such as BLM. In addition, p53 is massively overexpressed in 55K<sup>+</sup>HSFs, as has been reported previously, although this is likely to be transcriptionally inactive as already discussed [52,59]. We considered that the variations seen in the DDR proteins were probably not sufficient to be responsible for the marked difference in properties observed in the two cell populations, although this would need to be confirmed by further investigation. Moreover, the effects of high levels of transcriptionally inactive p53 are not clear [52].

To pinpoint possible targets of Ad12E1B55K more closely, a series of co-immunoprecipitations was undertaken. It is likely that the observed interaction of Ad12E1B55K with MCM3, MCM7, ORC3, DNA polymerase  $\delta$  and cdc45 could affect ‘normal’ DNA replication and following replication stress. No association with other MCM or ORC proteins or PCNA was observed. In an examination of a limited number of the DNA repair proteins, Ad12E1B55K associated with the MRN complex components, MRE11 and NBS1. This would be expected, as MRE11 is degraded during Ad12 infection [50,51]. Co-immunoprecipitation of p53 has been described previously [52]. Similarly, association between Ad5E1B55K and BLM has been reported [30]. Interactions between AdE1B55K proteins and ATM and DNA-PK, however, represent novel targets which are likely to contribute to the DDR effects reported here. Whether comparable interactions occur with E1B55K proteins from other adenovirus serotypes, such as Ad5, is unknown at present. It seems likely, however, that these associations will be of importance during viral infection.

We have also examined the sub-cellular distribution of E1B55K in the 55K<sup>+</sup>HSFs. Whilst much of the protein is nuclear and associated with chromatin, an appreciable amount is present as ‘tracks’ within the cytoplasm (Figure 12 and Supplementary Figure S3B). Previous studies, particularly of Ad5, have reported the presence of E1B55K in large cytoplasmic juxtanuclear aggresomes in Ad5E1-transformed cells [61–63]. p53 and the MRN complex are also present. During Ad5 infection, similar aggresomes occur, induced by Ad5E4orf3 and/or orf6 and E1B55K [62,63]. These are considered to be the sites of MRN degradation [62,63]. From their location and appearance, we consider it unlikely that the ‘tracks’ seen in 55K<sup>+</sup>HSFs are aggresomes. Furthermore, we could see no co-localization of p53 at these structures (Figure 12). At present, we have no further knowledge of their origin.

The effects of E1B55K on host cell pathways described here may not be very relevant to Ad12 infection since, in that case, E1B55K will be accompanied by E4orf6 and the target proteins will probably be ubiquitinated. Whether this would result in proteasome-mediated degradation remains to be established [29]. However, it is likely that disruption of DNA replication, an increase in R-loop formation and interference with the DNA damage response will all favor AdE1-mediated cellular transformation and tumor formation. It is well known that the interaction of both Ad2/Ad5 and Ad12 E1B55K with p53 inhibits its transcriptional transactivating properties, which is considered to be important for efficient transformation [64]. However, it has also been demonstrated that properties of E1B55K, other than association with p53, contribute to transformation of rodent cells by AdE1 [64–67]. It was suggested that an interaction with the MRN complex, as well as an ability to form multi-protein complexes, could be factors favoring the transformation process [66]. In that study it was not shown whether the mutant E1B55K proteins induced any of the effects on DNA replication or the DDR reported here.

Despite the multiple effects of AdE1B55K on host cells, it cannot transform mammalian cells in isolation; AdE1A is essential for the process [68,69]. However, expression of AdE1A alone results in transformants only very rarely and this probably requires an additional mutational event to occur within the cells to allow immortalization [68,70]. It is not clear whether all the properties of Ad12E1B55K described in this set of experiments apply to E1B55K from other serotypes. There is detailed analysis of the relationship between Ad5E1B55K and components of the MRN complex, as well as other proteins involved in DSB repair, in Ad-infected cells but to what extent the protein itself affects the DDR is much less well understood. It might be supposed that the properties of Ad12 and Ad5E1B55K are broadly similar, since infection of human cells by both viruses results in

degradation of many of the same DDR components, which is not the case for Ads from groups B, D, E and F [50,51]. However, even the Ad5 and Ad12 proteins share only about 50% homology, and so it is quite possible that they have unique features, including the ability of Ad12E1B55K to cause genetic instability. Indeed, it has been shown that the serotype of the E1B55K protein is the determining factor in E1-mediated tumor formation in athymic nude mice, such that rat cells transformed with Ad5E1A/Ad12E1B were as oncogenic as cells transformed with Ad12E1A/Ad12E1B, whereas cells with Ad5E1B55K were appreciably less oncogenic [71,72]. Furthermore, only group A adenoviruses cause tumors in new-born rodents. It is very likely that the genome-destabilizing properties of Ad12E1B55K described here contribute to this process.

The E1B55K interactome extends much more widely than the DDR (reviewed in [27]), and so it is likely that proteins known to associate but not investigated here contribute to some of the observed effects. However, it is probable that the genomic instability originally observed in human cells exposed to Ad12E1B55K could be explained by its effects on DNA replication and its interference with homologous recombination and possibly other DNA repair pathways.

**Supplementary Materials:** The following are available on line at <https://www.mdpi.com/article/10.3390/v13122444/s1>. Supplementary Figure S1. The expression of Ad12E1B55K in HSFs affects DNA replication. Supplementary Figure S2. R-loop detection. Supplementary Figure S3. Co-localization of Ad12E1B55K with repair foci after DNA damage. Supplementary Figure S4. Selected protein expression in HSFs and 55K<sup>+</sup> HSFs.

**Author Contributions:** T.A. performed most of the experiments; R.H. and L.G. performed the metaphase spreads; N.C.H., S.J. and G.S.S. gave detailed advice, oversaw much of the investigation and helped to write the manuscript; R.J.G. planned the investigation, performed some of the experiments and wrote most of the manuscript. All authors have read and agreed to the published version of the manuscript.

**Funding:** GSS and RH are funded by a CR-UK Programme Grant (C17183/A23303). LG is supported by a joint funded University of Birmingham and CR-UK Ph.D studentship (C17422/A25154). TA is funded by a PhD studentship from the Royal Government of Saudi Arabia.

**Institutional Review Board Statement:** Not applicable.

**Informed Consent Statement:** Not applicable.

**Data Availability Statement:** Data available in the published manuscript and in Supporting Material.

**Acknowledgments:** We are most grateful to the Royal Government of Saudi Arabia for a studentship for T.A., to Katie Grand for a charitable donation through the University of Birmingham JustGiving scheme, to Great Ormond Street Hospital Research Fund and to CRUK (for a studentship to L.G. and Program grant to G.S.S.) for financial assistance.

**Conflicts of Interest:** The authors have no conflict of interest.

## References

1. Kajon, A.E.; Lynch, J.P. Adenovirus: Epidemiology, Global Spread of Novel Serotypes, and Advances in Treatment and Prevention. *Semin. Respir. Crit. Care Med.* **2016**, *37*, 586–602. [[CrossRef](#)] [[PubMed](#)]
2. Khanal, S.; Ghimire, P.; Dhamoon, A.S. The Repertoire of Adenovirus in Human Disease: The Innocuous to the Deadly. *Biomedicines* **2018**, *6*, 30. [[CrossRef](#)] [[PubMed](#)]
3. Huebner, R.J.; Rowe, W.P.; Turner, H.C.; Lane, W.T. Specific adenovirus complement-fixing antigens in virus-free hamster and rat tumors. *Proc. Natl. Acad. Sci. USA* **1963**, *50*, 379–389. [[CrossRef](#)] [[PubMed](#)]
4. Yabe, Y.; Trentin, J.J.; Taylor, G. Cancer Induction in Hamsters by Human Type 12 Adenovirus. Effect of Age and of Virus Dose. *Exp. Biol. Med.* **1962**, *111*, 343–344. [[CrossRef](#)] [[PubMed](#)]
5. Trentin, J.J.; Yabe, Y.; Taylor, G. The Quest for Human Cancer Viruses. *Science* **1962**, *137*, 835–841. [[CrossRef](#)]
6. Freeman, A.E.; Black, P.H.; Wolford, R.; Huebner, R.J. Adenovirus type 12-rat embryo transformation system. *J. Virol.* **1967**, *1*, 362–367. [[CrossRef](#)] [[PubMed](#)]
7. Freeman, A.E.; Black, P.H.; Vanderpool, E.A.; Henry, P.H.; Austin, J.B.; Huebner, R.J. Transformation of primary rat embryo cells by adenovirus type 2. *Proc. Natl. Acad. Sci. USA* **1967**, *58*, 1205–1212. [[CrossRef](#)] [[PubMed](#)]

8. Gallimore, P.H. Tumour Production in Immunosuppressed Rats with Cells Transformed in vitro by Adenovirus Type 2. *J. Gen. Virol.* **1972**, *16*, 99–102. [[CrossRef](#)] [[PubMed](#)]
9. Gallimore, P.H.; McDougall, J.K.; Chen, L.B. In vitro traits of adenovirus-transformed cell lines and their relevance to tumorigenicity in nude mice. *Cell* **1977**, *10*, 669–678. [[CrossRef](#)]
10. Mukai, N.; Kalter, S.S.; Cummins, L.B.; Matthews, V.A.; Nishida, T.; Nakajima, T. Retinal Tumor Induced in the Baboon by Human Adenovirus 12. *Science* **1980**, *210*, 1023–1025. [[CrossRef](#)] [[PubMed](#)]
11. Hausen, H.Z. Induction of Specific Chromosomal Aberrations by Adenovirus Type 12 in Human Embryonic Kidney Cells. *J. Virol.* **1967**, *1*, 1174–1185. [[CrossRef](#)] [[PubMed](#)]
12. McDougall, J.K. Effects of Adenoviruses on the Chromosomes of Normal Human Cells and Cells Trisomic for an E Chromosome. *Nature* **1970**, *225*, 456–458. [[CrossRef](#)]
13. McDougall, J.K. Adenovirus-induced Chromosome Aberrations in Human Cells. *J. Gen. Virol.* **1971**, *12*, 43–51. [[CrossRef](#)]
14. Stich, H.; Van Hoosier, G.; Trentin, J. Viruses and mammalian chromosomes chromosome aberrations by human adenovirus type 12. *Exp. Cell Res.* **1964**, *34*, 400–403. [[CrossRef](#)]
15. McDougall, J.K.; Vause, K.E.; Gallimore, P.H.; Dunn, A.R. Cytogenetic studies in permissive and abortive infections by adenovirus type 12. *Int. J. Cancer* **1974**, *14*, 236–243. [[CrossRef](#)] [[PubMed](#)]
16. Lindgren, V.; Ares, M.; Weiner, A.M.; Francke, U. Human genes for U2 small nuclear RNA map to a major adenovirus 12 modification site on chromosome 17. *Nature* **1985**, *314*, 115–116. [[CrossRef](#)] [[PubMed](#)]
17. Durnam, D.M.; Menninger, J.C.; Chandler, S.H.; Smith, P.P.; McDougall, J.K. A fragile site in the human U2 small nuclear RNA gene cluster is revealed by adenovirus type 12 infection. *Mol. Cell Biol.* **1988**, *8*, 1863–1867. [[PubMed](#)]
18. Bailey, A.D.; Li, Z.; Pavelitz, T.; Weiner, A.M. Adenovirus type 12-induced fragility of the human RNU2 locus requires U2 small nuclear RNA transcriptional regulatory elements. *Mol. Cell. Biol.* **1995**, *15*, 6246–6255. [[CrossRef](#)] [[PubMed](#)]
19. Li, Y.P.; Tomanin, R.; Smiley, J.R.; Bacchetti, S. Generation of a new adenovirus type 12-inducible fragile site by insertion of an artificial U2 locus in the human genome. *Mol. Cell. Biol.* **1993**, *13*. [[CrossRef](#)]
20. Li, Z.; Bailey, A.D.; Buchowski, J.; Weiner, A.M. A Tandem Array of Minimal U1 Small Nuclear RNA Genes is Sufficient to Generate a New Adenovirus Type 12Inducible Chromosome Fragile Site. *J. Virol.* **1998**, *72*, 4205–4211. [[CrossRef](#)] [[PubMed](#)]
21. Caporossi, D.; Bacchetti, S.; Kell, B.; Jewers, R.J.; Cason, J.; Pakarian, F.; Kaye, J.N.; Best, J.M. Definition of adenovirus type 5 functions involved in the induction of chromosomal aberrations in human cells. *J. Gen. Virol.* **1990**, *71*, 801–808. [[CrossRef](#)] [[PubMed](#)]
22. Caporossi, D.; Bacchetti, S.; Nicoletti, B. Synergism between aphidicolin and adenoviruses in the induction of breaks at fragile sites on human chromosomes. *Cancer Genet. Cytogenet.* **1991**, *54*, 39–53. [[CrossRef](#)]
23. Durnam, D.M.; Smith, P.P.; Menninger, J.C.; McDougall, J.K. The E1 region of human adenovirus type 12 determines the sites of virally induced chromosomal damage. In *Cancer Cells 4: DNA Tumor Viruses*; Botchan, M., Ed.; Cold Spring Harbor Laboratory: Huntington, NY, USA, 1986; pp. 349–354.
24. Schramayr, S.; Caporossi, D.; Mak, I.; Jelinek, T.; Bacchetti, S. Chromosomal damage induced by human adenovirus type 12 requires expression of the E1B 55-kilodalton viral protein. *J. Virol.* **1990**, *64*, 2090–2095. [[CrossRef](#)] [[PubMed](#)]
25. Blackford, A.N.; Grand, R.J.A. Adenovirus E1B 55-Kilodalton Protein: Multiple Roles in Viral Infection and Cell Transformation. *J. Virol.* **2009**, *83*, 4000–4012. [[CrossRef](#)]
26. Schreiner, S.; Wimmer, P.; Dobner, T. Adenovirus degradation of cellular proteins. *Futur. Microbiol.* **2012**, *7*, 211–225. [[CrossRef](#)] [[PubMed](#)]
27. Hidalgo, P.; Ip, W.H.; Dobner, T.; Gonzalez, R.A. The biology of the adenovirus E1B 55K protein. *FEBS Lett.* **2019**, *593*, 3504–3517. [[CrossRef](#)]
28. Kleinberger, T. En Guard! The Interactions between Adenoviruses and the DNA Damage Response. *Viruses* **2020**, *12*, 996. [[CrossRef](#)]
29. Herrmann, C.; Dybas, J.M.; Liddle, J.C.; Price, A.M.; Hayer, K.E.; Lauman, R.; Purman, C.E.; Charman, M.; Kim, E.T.; Garcia, B.A.; et al. Adenovirus-mediated ubiquitination alters protein–RNA binding and aids viral RNA processing. *Nat. Microbiol.* **2020**, *5*, 1217–1231. [[CrossRef](#)] [[PubMed](#)]
30. Orazio, N.I.; Naeger, C.M.; Karlseder, J.; Weitzman, M.D. The Adenovirus E1b55K/E4orf6 Complex Induces Degradation of the Bloom Helicase during Infection. *J. Virol.* **2010**, *85*, 1887–1892. [[CrossRef](#)] [[PubMed](#)]
31. Baker, A.; Rohleder, K.J.; Hanakahi, L.A.; Ketner, G. Adenovirus E4 34k and E1b 55k Oncoproteins Target Host DNA Ligase IV for Proteasomal Degradation. *J. Virol.* **2007**, *81*, 7034–7040. [[CrossRef](#)]
32. Stracker, T.; Carson, C.T.; Weitzman, M.D. Adenovirus oncoproteins inactivate the Mre11–Rad50–NBS1 DNA repair complex. *Nature* **2002**, *418*, 348–352. [[CrossRef](#)]
33. Sarnow, P.; Ho, Y.S.; Williams, J.; Levine, A.J. Adenovirus E1b-58kd tumor antigen and SV40 large tumor antigen are physically associated with the same 54 kd cellular protein in transformed cells. *Cell* **1982**, *28*, 387–394. [[CrossRef](#)]
34. Hagkarim, N.C.; Ryan, E.L.; Byrd, P.J.; Hollingworth, R.; Shimwell, N.J.; Agathangelou, A.; Vavasseur, M.; Kolbe, V.; Speiseder, T.; Dobner, T.; et al. Degradation of a Novel DNA Damage Response Protein, Tankyrase 1 Binding Protein 1, following Adenovirus Infection. *J. Virol.* **2018**, *92*, e02034–17. [[CrossRef](#)]
35. Gupta, A.; Jha, S.; Engel, D.A.; Ornelles, D.A.; Dutta, A. Tip60 degradation by adenovirus relieves transcriptional repression of viral transcriptional activator E1A. *Oncogene* **2012**, *32*, 5017–5025. [[CrossRef](#)]



36. Blackford, A.N.; Patel, R.N.; Forrester, N.A.; Theil, K.; Groitl, P.; Stewart, G.; Taylor, A.M.R.; Morgan, I.M.; Dobner, T.; Grand, R.J.A.; et al. Adenovirus 12 E4orf6 inhibits ATR activation by promoting TOPBP1 degradation. *Proc. Natl. Acad. Sci. USA* **2010**, *107*, 12251–12256. [[CrossRef](#)] [[PubMed](#)]
37. Carson, C.T.; Schwartz, R.A.; Stracker, T.; Lilley, C.E.; Lee, D.V.; Weitzman, M.D. The Mre11 complex is required for ATM activation and the G2/M checkpoint. *EMBO J.* **2003**, *22*, 6610–6620. [[CrossRef](#)] [[PubMed](#)]
38. Karen, K.A.; Hoey, P.J.; Young, C.S.H.; Hearing, P. Temporal Regulation of the Mre11-Rad50-Nbs1 Complex during Adenovirus Infection. *J. Virol.* **2009**, *83*, 4565–4573. [[CrossRef](#)] [[PubMed](#)]
39. Hollingworth, R.; Grand, R.J. Modulation of DNA Damage and Repair Pathways by Human Tumour Viruses. *Viruses* **2015**, *7*, 2542–2591. [[CrossRef](#)]
40. Weitzman, M.D.; Fradet-Turcotte, A. Virus DNA Replication and the Host DNA Damage Response. *Annu. Rev. Virol.* **2018**, *5*, 141–164. [[CrossRef](#)] [[PubMed](#)]
41. Charman, M.; Weitzman, M.D.; Charman, M.; Weitzman, M.D. Replication Compartments of DNA Viruses in the Nucleus: Location, Location, Location. *Viruses* **2020**, *12*, 151. [[CrossRef](#)] [[PubMed](#)]
42. Gallimore, P.H.; Lecane, P.S.; Roberts, S.; Rookes, S.M.; Grand, R.J.; Parkhill, J. Adenovirus type 12 early region 1B 54K protein significantly extends the life span of normal mammalian cells in culture. *J. Virol.* **1997**, *71*, 6629–6640. [[CrossRef](#)]
43. Byrd, P.; Brown, K.W.; Gallimore, P.H. Malignant transformation of human embryo retinoblasts by cloned adenovirus 12 DNA. *Nature* **1982**, *298*, 69–71. [[CrossRef](#)]
44. Mendez, J.; Stillman, B. Chromatin Association of Human Origin Recognition Complex, Cdc6, and Minichromosome Maintenance Proteins during the Cell Cycle: Assembly of Prereplication Complexes in Late Mitosis. *Mol. Cell. Biol.* **2000**, *20*, 8602–8612. [[CrossRef](#)]
45. Sollier, J.; Stork, C.T.; Garcia-Rubio, M.; Paulsen, R.D.; Aguilera, A.; Cimprich, K.A. Transcription-Coupled Nucleotide Excision Repair Factors Promote R-Loop-Induced Genome Instability. *Mol. Cell* **2014**, *56*, 777–785. [[CrossRef](#)]
46. Petermann, E.; Orta, M.L.; Issaeva, N.; Schultz, N.; Helleday, T. Hydroxyurea-Stalled Replication Forks Become Progressively Inactivated and Require Two Different RAD51-Mediated Pathways for Restart and Repair. *Mol. Cell* **2010**, *37*, 492–502. [[CrossRef](#)]
47. Henry-Mowatt, J.; Jackson, D.; Masson, J.Y.; Johnson, P.A.; Clements, P.M.; Benson, F.E.; Thompson, L.H.; Takeda, S.; West, S.C.; Caldecott, K.W. XRCC3 and Rad51 modulate replication fork progression on damaged vertebrate chromosomes. *Mol. Cell* **2003**, *11*, 1109–1117. [[CrossRef](#)]
48. Nieminuszczy, J.; Schwab, R.A.; Niedzwiedz, W. The DNA fibre technique—tracking helicases at work. *Methods* **2016**, *108*, 92–98. [[CrossRef](#)]
49. Boguslawski, S.J.; Smith, D.E.; Michalak, M.A.; Mickelson, K.E.; Yehle, C.O.; Patterson, W.L.; Carrico, R.J. Characterization of monoclonal antibody to DNA RNA and its application to immunodetection of hybrids. *J. Immunol. Methods* **1986**, *89*, 123–130. [[CrossRef](#)]
50. Forrester, N.A.; Sedgwick, G.G.; Thomas, A.; Blackford, A.; Speiseder, T.; Dobner, T.; Byrd, P.J.; Stewart, G.S.; Turnell, A.S.; Grand, R.J.A. Serotype-Specific Inactivation of the Cellular DNA Damage Response during Adenovirus Infection. *J. Virol.* **2010**, *85*, 2201–2211. [[CrossRef](#)]
51. Cheng, C.Y.; Gilson, T.; Dallaire, F.; Ketner, G.; Branton, P.E.; Blanchette, P. The E4orf6/E1B55K E3 Ubiquitin Ligase Complexes of Human Adenoviruses Exhibit Heterogeneity in Composition and Substrate Specificity. *J. Virol.* **2010**, *85*, 765–775. [[CrossRef](#)] [[PubMed](#)]
52. Grand, R.J.; Owen, D.; Rookes, S.M.; Gallimore, P.H. Control of p53 Expression by Adenovirus 12 Early Region 1A and Early Region 1B 54K Proteins. *Virology* **1996**, *218*, 23–34. [[CrossRef](#)] [[PubMed](#)]
53. Gargano, S.; Wang, P.; Rusanganwa, E.; Bacchetti, S. The transcriptionally competent U2 gene is necessary and sufficient for adenovirus type 12 induction of the fragile site at 17q21-22. *Mol. Cell. Biol.* **1995**, *15*, 6256–6261. [[CrossRef](#)] [[PubMed](#)]
54. Liao, D.; Yu, A.; Weiner, A.M. Coexpression of the Adenovirus 12 E1B 55 kDa Oncoprotein and Cellular Tumor Suppressor p53 Is Sufficient to Induce Metaphase Fragility of the HumanRNU2Locus. *Virology* **1999**, *254*, 11–23. [[CrossRef](#)]
55. Whittaker, J.L.; Byrd, P.J.; Grand, R.J.; Gallimore, P.H. Isolation and characterization of four adenovirus type 12-transformed human embryo kidney cell lines. *Mol. Cell. Biol.* **1984**, *4*. [[CrossRef](#)]
56. Zeman, M.K.; Cimprich, K.A. Causes and consequences of replication stress. *Nat. Cell Biol.* **2014**, *16*, 2–9. [[CrossRef](#)] [[PubMed](#)]
57. Wilhelm, T.; Said, M.; Naim, V. DNA Replication Stress and Chromosomal Instability: Dangerous Liaisons. *Genes* **2020**, *11*, 642. [[CrossRef](#)]
58. Schwartz, R.A.; Lakdawala, S.S.; Eshleman, H.D.; Russell, M.R.; Carson, C.T.; Weitzman, M.D. Distinct Requirements of Adenovirus E1b55K Protein for Degradation of Cellular Substrates. *J. Virol.* **2008**, *82*, 9043–9055. [[CrossRef](#)]
59. Yew, P.R.; Berk, A.J. Inhibition of p53 transactivation required for transformation by adenovirus early 1B protein. *Nature* **1992**, *357*, 82–85. [[CrossRef](#)]
60. Schreiner, S.; Wimmer, P.; Sirma, H.; Everett, R.D.; Blanchette, P.; Groitl, P.; Dobner, T. Proteasome-Dependent Degradation of Daxx by the Viral E1B-55K Protein in Human Adenovirus-Infected Cells. *J. Virol.* **2010**, *84*, 7029–7038. [[CrossRef](#)]
61. Zantema, A.; Fransen, J.; Davis-Olivier, A.; Ramaekers, F.C.; Vooijs, G.P.; Deleys, B.; Van Der Eb, A.J. Localization of the E1 B proteins of adenovirus 5 in transformed cells, as revealed by interaction with monoclonal antibodies. *Virology* **1985**, *142*, 44–58. [[CrossRef](#)]

- 
62. Araujo, F.D.; Stracker, T.H.; Carson, C.T.; Lee, D.V.; Weitzman, M.D. Adenovirus type 5 e4orf3 protein targets the mre11 complex to cytoplasmic aggresomes. *J. Virol.* **2005**, *79*, 11382–11391. [[CrossRef](#)]
  63. Liu, Y.; Shevchenko, A.; Shevchenko, A.; Berk, A.J. Adenovirus Exploits the Cellular Aggresome Response to Accelerate Inactivation of the MRN Complex. *J. Virol.* **2005**, *79*, 14004–14016. [[CrossRef](#)]
  64. Löber, C.; Lenz-Stöppler, C.; Döbelstein, M. Adenovirus E1-transformed cells grow despite the continuous presence of transcriptionally active p53. *J. Gen. Virol.* **2002**, *83*, 2047–2057. [[CrossRef](#)]
  65. Sieber, T.; Dobner, T. Adenovirus Type 5 Early Region 1B 156R Protein Promotes Cell Transformation Independently of Repression of p53-Stimulated Transcription. *J. Virol.* **2007**, *81*, 95–105. [[CrossRef](#)]
  66. Härtl, B.; Zeller, T.; Blanchette, P.; Kremmer, E.; Dobner, T. Adenovirus type 5 early region 1B 55-kDa oncoprotein can promote cell transformation by a mechanism independent from blocking p53-activated transcription. *Oncogene* **2008**, *27*, 3673–3684. [[CrossRef](#)]
  67. Ip, W.H.; Dobner, T. Cell transformation by the adenovirus oncogenes E1 and E4. *FEBS Lett.* **2020**, *594*, 1848–1860. [[CrossRef](#)]
  68. Houweling, A.; van den Elsen, P.J.; Van Der Eb, A.J. Partial transformation of primary rat cells by the leftmost 4.5% fragment of adenovirus 5 DNA. *Virology* **1980**, *105*, 537–550. [[CrossRef](#)]
  69. Van den Elsen, P.; Houweling, A.; Van Der Eb, A. Expression of region E1b of human adenoviruses in the absence of region E1a is not sufficient for complete transformation. *Virology* **1983**, *128*, 377–390. [[CrossRef](#)]
  70. Gallimore, P.H.; Byrd, P.J.; Whittaker, J.L.; Grand, R.J. Properties of rat cells transformed by DNA plasmids containing adenovirus type 12 E1 DNA or specific fragments of the E1 region: Comparison of transforming frequencies. *Cancer Res.* **1985**, *45*, 2670–2680.
  71. Bernards, R.; Houweling, A.; Schrier, P.I.; Bos, J.L.; Van Der Eb, A.J. Characterization of cells transformed by Ad5/Ad12 hybrid early region I plasmids. *Virology* **1982**, *120*, 422–432. [[CrossRef](#)]
  72. Bernards, R.; Schrier, P.I.; Bos, J.L.; Van Der Eb, A.J. Role of adenovirus types 5 and 12 early region 1 b tumor antigens in oncogenic transformation. *Virology* **1983**, *127*, 45–53. [[CrossRef](#)]